



Earth Resources
A Continuing
Bibliography
with Indexes

NASA SP-7041(51)
October 1986

National Aeronautics and
Space Administration

(NASA-SP-7041(51)) EARTH RESOURCES: A
CONTINUING BIBLIOGRAPHY WITH INDEXES (ISSUE
51) (National Aeronautics and Space
Administration) 119 p

N87-13832

CSCL 05B

Unclas

00/43 43926

es Earth Resources
s Earth Resources
Earth Resources E
th Resources Ear
Resources Earth
Resources Earth F
resources Earth Re

ACCESSION NUMBER RANGES

Accession numbers cited in this Supplement fall within the following ranges.

STAR (N-10000 Series) N86-22537 — N86-28047

IAA (A-10000 Series) A86-29843 — A86-40002

EARTH RESOURCES

A CONTINUING BIBLIOGRAPHY WITH INDEXES

Issue 51

A selection of annotated references to unclassified reports and journal articles that were introduced into the NASA scientific and technical information system and announced between July 1 and September 30, 1986 in

- *Scientific and Technical Aerospace Reports (STAR)*
- *International Aerospace Abstracts (IAA).*



This bibliography was prepared by the NASA Scientific and Technical Information Facility operated for the National Aeronautics and Space Administration by RMS Associates.

INTRODUCTION

The technical literature described in this continuing bibliography may be helpful to researchers in numerous disciplines such as agriculture and forestry, geography and cartography, geology and mining, oceanography and fishing, environmental control, and many others. Until recently it was impossible for anyone to examine more than a minute fraction of the Earth's surface continuously. Now vast areas can be observed synoptically, and changes noted in both the Earth's lands and waters, by sensing instrumentation on orbiting spacecraft or on aircraft.

This literature survey lists 382 reports, articles, and other documents announced between July 1 and September 30, 1986 in *Scientific and Technical Aerospace Reports (STAR)*, and *International Aerospace Abstracts (IAA)*.

The coverage includes documents related to the identification and evaluation by means of sensors in spacecraft and aircraft of vegetation, minerals, and other natural resources, and the techniques and potentialities of surveying and keeping up-to-date inventories of such riches. It encompasses studies of such natural phenomena as earthquakes, volcanoes, ocean currents, and magnetic fields; and such cultural phenomena as cities, transportation networks, and irrigation systems. Descriptions of the components and use of remote sensing and geophysical instrumentation, their subsystems, observational procedures, signature and analyses and interpretive techniques for gathering data are also included. All reports generated under NASA's Earth Resources Survey Program for the time period covered in this bibliography are also included. The bibliography does not contain citations to documents dealing mainly with satellites or satellite equipment used in navigation or communication systems, nor with instrumentation not used aboard aerospace vehicles.

The selected items are grouped in nine categories. These are listed in the Table of Contents with notes regarding the scope of each category. These categories were especially chosen for this publication, and differ from those found in *STAR* and *IAA*.

Each entry consists of a standard bibliographic citation accompanied by an abstract. The citations include the original accession numbers from the respective announcement journals.

Under each of the nine categories, the entries are presented in one of two groups that appear in the following order:

IAA entries identified by accession number series A86-10,000 in ascending accession number order;

STAR entries identified by accession number series N86-10,000 in ascending accession number order.

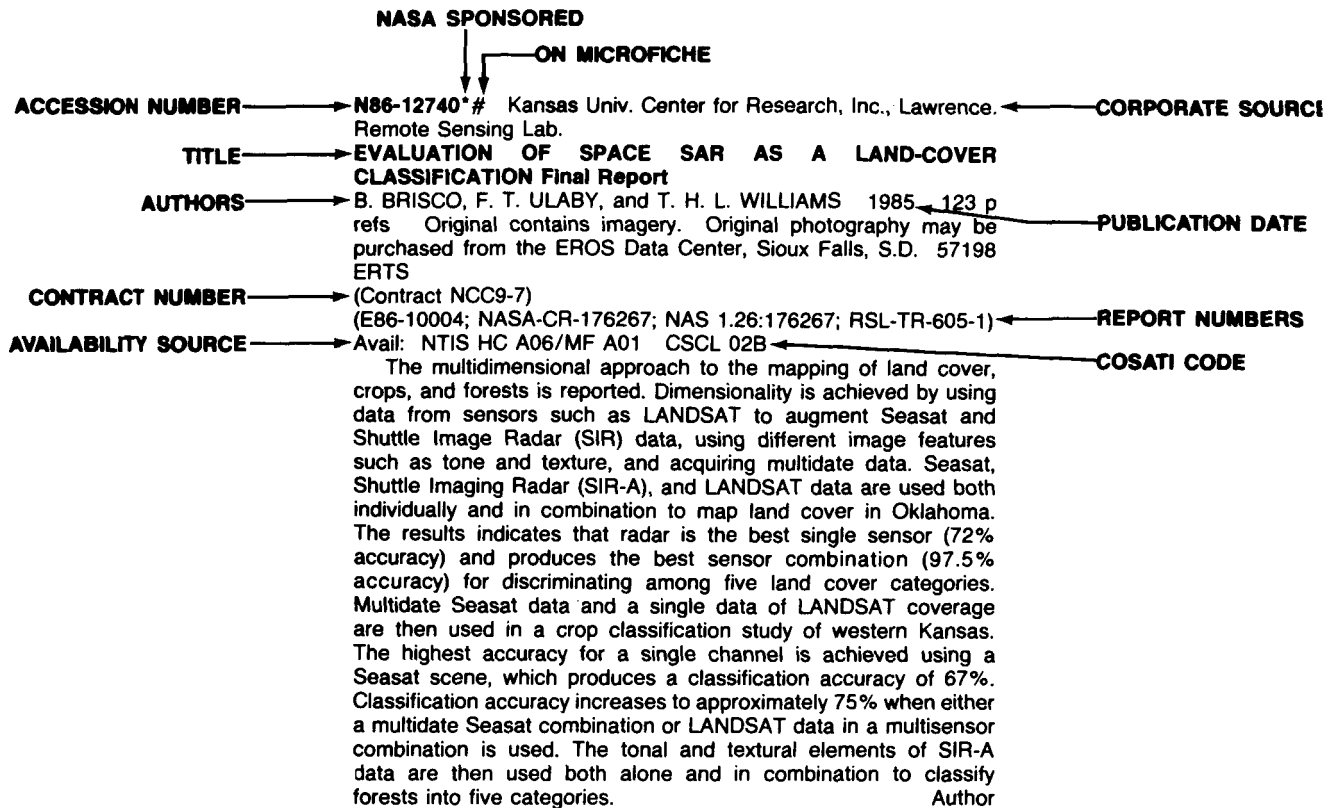
After the abstract section, there are seven indexes:

subject, personal author, corporate source, foreign technology, contract number, report/ accession number, and accession number.

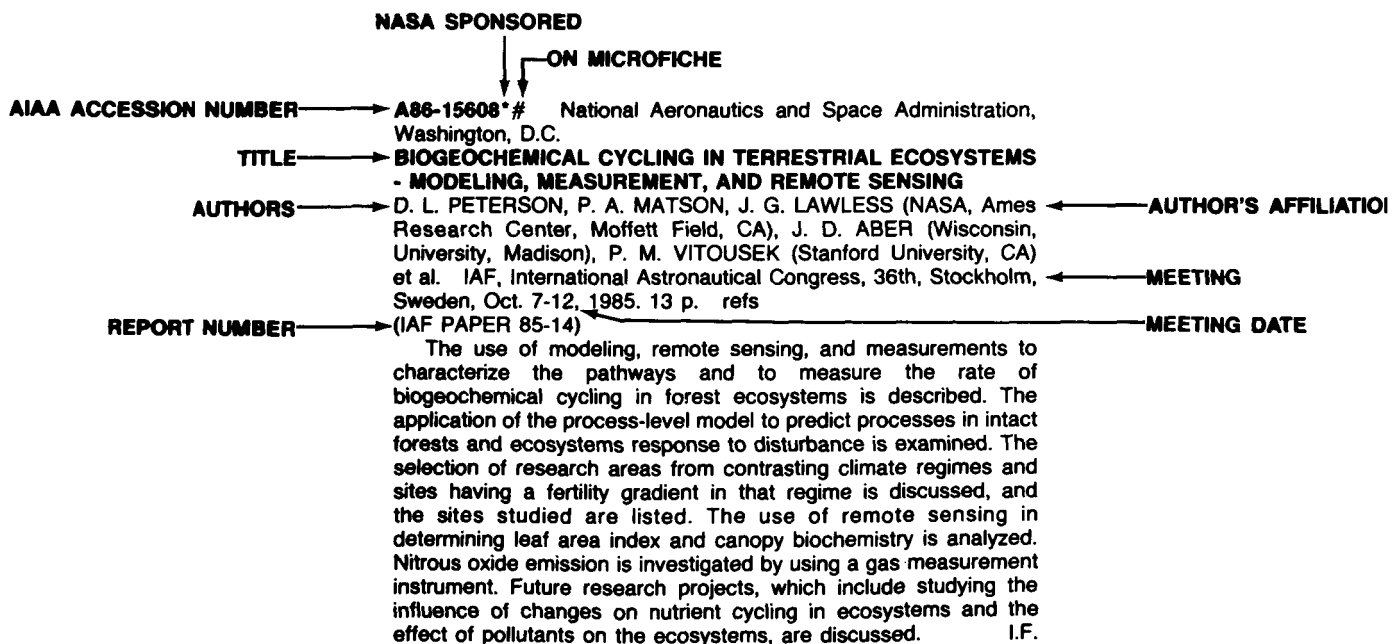
TABLE OF CONTENTS

	Page
Category 01 Agriculture and Forestry Includes crop forecasts, crop signature analysis, soil identification, disease detection, harvest estimates, range resources, timber inventory, forest fire detection, and wildlife migration patterns.	1
Category 02 Environmental Changes and Cultural Resources Includes land use analysis, urban and metropolitan studies, environmental impact, air and water pollution, geographic information systems, and geographic analysis.	15
Category 03 Geodesy and Cartography Includes mapping and topography.	18
Category 04 Geology and Mineral Resources Includes mineral deposits, petroleum deposits, spectral properties of rocks, geological exploration, and lithology.	19
Category 05 Oceanography and Marine Resources Includes sea-surface temperature, ocean bottom surveying imagery, drift rates, sea ice and icebergs, sea state, fish location	24
Category 06 Hydrology and Water Management Includes snow cover and water runoff in rivers and glaciers, saline intrusion, drainage analysis, geomorphology of river basins, land uses, and estuarine studies.	42
Category 07 Data Processing and Distribution Systems Includes film processing, computer technology, satellite and aircraft hardware, and imagery.	44
Category 08 Instrumentation and Sensors Includes data acquisition and camera systems and remote sensors.	52
Category 09 General Includes economic analysis.	58
Subject Index	A-1
Personal Author Index	B-1
Corporate Source Index	C-1
Foreign Technology Index	D-1
Contract Number Index	E-1
Report/Accession Number Index	F-1
Accession Number Index	G-1

TYPICAL REPORT CITATION AND ABSTRACT



TYPICAL JOURNAL ARTICLE CITATION AND ABSTRACT



EARTH RESOURCES

A Continuing Bibliography (Issue 51)

OCTOBER 1986

01

AGRICULTURE AND FORESTRY

Includes crop forecasts, crop signature analysis, soil identification, disease detection, harvest estimates, range resources, timber inventory, forest fire detection, and wildlife migration patterns.

A86-29843

AGRICULTURAL AND SCIENTIFIC SPACE PLATFORMS [NARODNOKHOZIAISTVENNYE I NAUCHNYE KOSMICHESKIE KOMPLEKSY]

V. S. AVDUEVSKII and G. R. USPENSKII Moscow, Izdatel'stvo Mashinostroenie, 1985, 416 p. In Russian. refs

The agricultural and scientific applications of remote sensing platforms in space are discussed, with emphasis given to Soviet Meteor and Salyut programs. The physical principles of a number of remote sensing instruments are briefly described, including lidar, SAR, microwave radiometry, and infrared photography. Numerical techniques for classifying remote sensing data according to the physical characteristics of the object (water, forest land, agricultural areas) are also described. Organizational diagrams describing a typical remote sensing system for agricultural applications are provided. I.H.

A86-30190

MICROWAVE REMOTE SENSING OF AGRICULTURAL CROPS IN CANADA

J. CIHLAR, R. J. BROWN, and B. GUINDON (Canada Centre for Remote Sensing, Ottawa) International Journal of Remote Sensing (ISSN 0143-1161), vol. 7, Feb. 1986, p. 195-212. refs

The objective of this paper is to review current knowledge concerning synthetic aperture radar applications to crops in Canada. Following a brief overview of studies during SURSAT (1978-1980) and RADARSAT (1981 and later) projects, several issues are considered. These include crop-classification accuracies achieved with SAR or SAR and VIR data at various sites, the importance of crop and soil parameters affecting SAR images, the procedures for digital SAR image analysis and the relationship between airborne SAR data and future satellite SAR data. Finally, recent developments of new ground and airborne microwave instruments to be used in agricultural studies are described. Author

A86-30191

MONOTEMPORAL, MULTITEMPORAL, AND MULTIDATE THERMAL INFRARED DATA ACQUISITION FROM SATELLITES FOR SOIL AND SURFACE-MATERIAL SURVEY

D. W. LYNN (Reading, University, England) International Journal of Remote Sensing (ISSN 0143-1161), vol. 7, Feb. 1986, p. 213-231. refs

With the improvement in spatial resolution of thermal sensors over the past decade the employment of thermal infrared satellite data for soil and surface-material survey has become increasingly attractive. The individual orbital characteristics of each satellite provide the opportunity of acquiring monotemporal (same day, one time), multitemporal (same day, different times) and multidate (different days, same time) imagery. The time at which such imagery

is acquired is of great importance since the emitted thermal response of any natural material is a function not only of the material's emissivity, but also of its temperature at the time of imaging. The implications of acquiring monotemporal, multitemporal and multidate thermal infrared data are discussed in relation to thermal sensors in past, current and future satellites. Author

A86-30192

DIURNAL PATTERNS OF BIDIRECTIONAL VEGETATION INDICES FOR WHEAT CANOPIES

M. SHIBAYAMA, C. L. WIEGAND, and A. J. RICHARDSON (USDA, Agricultural Research Service, Weslaco, TX) International Journal of Remote Sensing (ISSN 0143-1161), vol. 7, Feb. 1986, p. 233-246. refs

Solar altitude effects on the perpendicular vegetation index (PVI) and normalized difference vegetation index (NDVI) are examined. Spectral data of two canopies of hard, red spring wheat was collected at A.R.S. South Research Farm in Weslaco, Texas in 1984. Leaf area index (LEA) was measured over plant development and ranged from 4.0-2.5. PVI and NDVI were calculated from radiometer RED (0.63-0.69 microns) and NIR (0.76-0.90 microns) bidirectional radiance observations of wheat canopies; the equation for calculating common solar irradiance (PVIC) from PVI is given. It is observed that PVIC at nadir view increases as the solar zenith angle increases; however, the NDVI remains unchanged. The off-nadir to nadir PVIC ratio increases as the view zenith and solar zenith angles increase and the NDVI is unaffected. It is concluded that PVI, though subjected to bidirectional effects, provides more useful data about wheat canopies at LAI greater than two than does NDVI. I.F.

A86-30193* National Aeronautics and Space Administration. Langley Research Center, Hampton, Va.

ASSESSING IMPACTS OF OFF-NADIR OBSERVATION ON REMOTE SENSING OF VEGETATION - USE OF THE SUITS MODEL

D. S. BARTLETT, R. W. JOHNSON (NASA, Langley Research Center, Hampton, VA), M. A. HARDISKY, and V. KLEMAS (Delaware, University, Newark) International Journal of Remote Sensing (ISSN 0143-1161), vol. 7, Feb. 1986, p. 247-264. NASA-supported research. refs

The use of Suits' (1972a, b) digital radiative transfer model to simulate the effect of nonLambertian canopy reflectance on off-nadir observations of vegetation is discussed. Canopy reflectances of cord grass are calculated using the radiative transfer model, field radiometric measurements, and airborne multispectral scanner data. The effects of varying view angles on canopy reflectance are analyzed and compared. The comparison reveals that the model is effective in simulating the sense and magnitude of reflectance change due to variable angles of observations; however, the model does not reproduce the observed dependence of nadir canopy reflectance on solar zenith angle. It is concluded that the radiative transfer model is applicable for predicting the variation in canopy reflectance due to changing view zenith angles. I.F.

01 AGRICULTURE AND FORESTRY

A86-30194* National Aeronautics and Space Administration. Lyndon B. Johnson Space Center, Houston, Tex.
SATELLITE-DERIVED LEAF-AREA-INDEX AND VEGETATION MAPS AS INPUT TO GLOBAL CARBON CYCLE MODELS - A HIERARCHICAL APPROACH

G. D. BADHWAR, R. B. MACDONALD (NASA, Johnson Space Center, Houston, TX), and N. C. MEHTA (MIT, Lexington, MA) International Journal of Remote Sensing (ISSN 0143-1161), vol. 7, Feb. 1986, p. 265-281. refs

A hierarchical procedure for developing a leaf area index (LAI) map of deciduous boreal forests is studied. The collection of spectral reflectance data from the Boundary Waters Canoe area in Minnesota using helicopter-, high-altitude aircraft-, and Landsat-mounted spectral sensors is described. The relationship between LAI and biomass and the reflectance ratio is analyzed. The sensitivity of canopy reflectance in the visible and infrared to the LAI of the canopy for various boreal forest species is evaluated. The data reveal that Landsat data are useful for producing LAI maps of deciduous forest areas and the maps provide data which clarifies the function of vegetation in the global carbon cycle models. I.F.

A86-30196

THE INFLUENCE OF OBSERVATIONAL INTERDEPENDENCE ON SPECTRAL REFLECTANCE RELATIONSHIPS WITH PLANT AND SOIL VARIABLES

W. J. RIPPLE, B. J. SCHRUMPF, and D. L. ISAACSON (Oregon State University, Corvallis) International Journal of Remote Sensing (ISSN 0143-1161), vol. 7, Feb. 1986, p. 291-294. refs

The relationships between spectral reflectance and plot variables in a desert shrub community were studied by repeated observation as biomass was removed from 2.93 sq m plots. As a result of these repeated observations, interdependence effects were present in the data sets. The spectral/plot relationships were discovered to be weaker with the removal of this observational interdependence. Middle infrared reflectance (2.08-2.35 microns) was found to account for more of the variation in the group of plot variables than did reflectance in the other spectral regions tested, and the variable of total moisture was best for explaining the variability of the spectral data. Author

A86-30197

VEGETATION INDEX AND POSSIBILITY OF COMPLEMENTARY PARAMETERS FROM AVHRR/2

S. M. SINGH (Reading, University, England) International Journal of Remote Sensing (ISSN 0143-1161), vol. 7, Feb. 1986, p. 295-300.

The data from the Advanced Very High Resolution Radiometer are used for calculating atmospherically corrected temperature difference in the split-window channels, the normalized difference vegetation index and the spectral reflectance at channel-1 wavelength. An illustration is presented which shows that when there is significant change (larger than the inherent accuracy) in any one of these three quantities, the other two quantities also change. This qualitative inference indicates the possibility that these three parameters may complement each other. Author

A86-30198

A TEXTURE-ENHANCEMENT PROCEDURE FOR SEPARATING ORCHARD FROM FOREST IN THEMATIC MAPPER DATA

D. K. GORDON and W. R. PHILIPSON (Cornell University, Ithaca, NY) International Journal of Remote Sensing (ISSN 0143-1161), vol. 7, Feb. 1986, p. 301-304. (Contract USDA-58-319T-3-0208X)

A procedure is described for automatically separating temperate fruit tree orchards from mixed deciduous forest in Landsat Thematic Mapper data. A filter is applied to enhance the texture of bands 4 and 3 prior to ratioing, smoothing, and level-slicing to a binary image on the basis of supervised training. Including the binary image in supervised classification of single data imagery has reduced misclassification of forest as orchard from 75 percent of the forest pixels to fewer than 7 percent. Author

A86-32684

DETERMINATION OF THE MOISTURE CONTENT OF NONUNIFORMLY MOISTENED SOILS WITH A SURFACE TRANSITION LAYER ON THE BASIS OF MICROWAVE SPECTRORADIOMETRY [OPREDELЕНИЕ VLAZHNOСТИ NEODNORODNO UVLAZHNNENNYKH POCHVOGRUNTOV S POVERKHNOSTNYM PEREKHODNYM SLOEM PO DANNYM SPEKTRAL'NYKH SVCH-RADIOMETRICHESKIKH IZMERENII]

E. A. REUTOV and A. M. SHUTKO (AN SSSR, Institut Radiotekhniki i Elektroniki, Moscow, USSR) Issledovanie Zemli iz Kosmosa (ISSN 0205-9614), Jan.-Feb. 1986, p. 71-78. In Russian. refs

A86-32689

FORMATION OF A DIGITAL DATA BASE FOR AUTOMATED FOREST MAPPING [FORMIROVANIE TSIFROVOI BAZY DANNYKH PRI AVTOMATIZIROVANNOM KARTOGRAFIROVANII LESOV]

E. D. BODANSKII, D. A. STAROSTENKO, and R. I. ELMAN (Vsesoiuznoe Aerofotolesoustroitel'noe Ob'edinenie Lesproekt, Moscow, USSR) Issledovanie Zemli iz Kosmosa (ISSN 0205-9614), Jan.-Feb. 1986, p. 104-110. In Russian.

The paper examines the content and structure of a digital forest-mapping database, consistent with the content and structure of maps automatically compiled from space remote-sensing images. It is shown how graphic data, in raster and vector formats, can be represented in digital form. The concepts of an elementary graphic feature, a graphic fragment, and a mapping generator are described. B.J.

A86-33503* Department of Agriculture, Washington, D.C.

OVERVIEW OF THE AGRISTARS RESEARCH PROGRAM. I

C. E. CAUDILL (USDA, Statistical Reporting Service, Washington, DC) and R. E. HATCH (NASA, Washington, DC) IN: 1985 International Geoscience and Remote Sensing Symposium (IGARSS '85), Amherst, MA, October 7-9, 1985, Digest. Volume 1. New York, Institute of Electrical and Electronics Engineers, Inc., 1985, p. 9-16.

An account is given of the activities and accomplishments to date of the U.S. Department of Agriculture's Agriculture and Resources Inventory Surveys Through Aerospace Remote Sensing (AgRISTARS) program, which is a cooperative venture with NASA and the Departments of the Interior and of Commerce. AgRISTARS research activities encompass early warning and crop condition assessment, inventory technology development for production forecasting, crop yield model development, soil moisture monitoring, domestic crops and land cover sensing, renewable resources inventory, and conservation and pollution assessment. O.C.

A86-33504* National Aeronautics and Space Administration. Goddard Space Flight Center, Greenbelt, Md.

PASSIVE MICROWAVE SOIL MOISTURE RESEARCH

T. J. SCHMUGGE, P. E. ONEILL, and J. R. WANG (NASA, Goddard Space Flight Center, Greenbelt, MD) IN: 1985 International Geoscience and Remote Sensing Symposium (IGARSS '85), Amherst, MA, October 7-9, 1985, Digest. Volume 1. New York, Institute of Electrical and Electronics Engineers, Inc., 1985, p. 20-25. refs

The AgRISTARS Soil Moisture Project has made significant progress in the quantification of microwave sensor capabilities for soil moisture remote sensing. The 21-cm wavelength has been verified to be the best single channel for radiometric observations of soil moisture. It has also been found that other remote sensing approaches used in conjunction with L-band passive data are more successful than multiple wavelength microwave radiometry in this application. AgRISTARS studies have also improved current understanding of noise factors affecting the interpretability of microwave emission data. The absorption of soil emission by vegetation has been quantified, although this effect is less important than absorption effects for microwave radiometry. O.C.

A86-33506* National Aeronautics and Space Administration. National Space Technology Labs., Bay Saint Louis, Miss.

REMOTE SENSING TECHNIQUES FOR THE DETECTION OF SOIL EROSION AND THE IDENTIFICATION OF SOIL CONSERVATION PRACTICES

R. E. PELLETIER (NASA, National Space Technology Laboratories, Bay St. Louis, MS) and R. H. GRIFFIN (USDA, Fort Worth, TX) IN: 1985 International Geoscience and Remote Sensing Symposium (IGARSS '85), Amherst, MA, October 7-9, 1985, Digest. Volume 1 . New York, Institute of Electrical and Electronics Engineers, Inc., 1985, p. 40-45. refs

The following paper is a summary of a number of techniques initiated under the AgRISTARS (Agriculture and Resources Inventory Surveys Through Aerospace Remote Sensing) project for the detection of soil degradation caused by water erosion and the identification of soil conservation practices for resource inventories. Discussed are methods to utilize a geographic information system to determine potential soil erosion through a USLE (Universal Soil Loss Equation) model; application of the Kauth-Thomas Transform to detect present erosional status; and the identification of conservation practices through visual interpretation and a variety of enhancement procedures applied to digital remotely sensed data. Author

A86-33523* Jet Propulsion Lab., California Inst. of Tech., Pasadena.

RADAR SCATTEROMETER PROBING OF THICK VEGETATION CANOPIES

J. F. PARIS (California Institute of Technology, Jet Propulsion Laboratory, Pasadena) IN: 1985 International Geoscience and Remote Sensing Symposium (IGARSS '85), Amherst, MA, October 7-9, 1985, Digest. Volume 1 . New York, Institute of Electrical and Electronics Engineers, Inc., 1985, p. 161-163.

A86-33524

ESTIMATION OF THE WEIGHT OF VEGETATION USING MICROWAVE TRANSMISSION MEASUREMENTS

W. L. STUTZMAN (Virginia Polytechnic Institute and State University, Blacksburg) and H. S. CRAWFORD (U.S. Forest Service, Orono, ME) IN: 1985 International Geoscience and Remote Sensing Symposium (IGARSS '85), Amherst, MA, October 7-9, 1985, Digest. Volume 1 . New York, Institute of Electrical and Electronics Engineers, Inc., 1985, p. 164-167. refs

Fast, accurate estimation of vegetation weight using microwave transmission measurements is reported, with application to the propagation problem arising in communication. Field tests at 12.25 GHz in 1976 using a 5-m path two first-Fresnel zones wide (35 cm), and one with a cell width of two second-Fresnel zones (49.5 cm), were performed at a site in Virginia containing mostly Virginia pine regrowth. The attenuation least polarized and then compensated for polarization mismatch was found to correlate well with oven-dry weight of vegetation having stems less than 1.25 cm in diameter. Correlation of vegetation to attenuation in controlled field tests from 1977 to 1979 in Maine was significant, though not as good as in previous tests. Results from random sampling testing show similar regeneration coefficients of signal loss to vegetation weight to those of the controlled tests. R.R.

A86-33525* National Aeronautics and Space Administration. National Space Technology Labs., Bay Saint Louis, Miss.

A PRELIMINARY REPORT ON THE MEASUREMENTS OF FOREST CANOPIES WITH C-BAND RADAR SCATTEROMETER AT NASA/NSTL

S. T. WU (NASA, National Space Technology Laboratories, Bay St. Louis, MS) IN: 1985 International Geoscience and Remote Sensing Symposium (IGARSS '85), Amherst, MA, October 7-9, 1985, Digest. Volume 1 . New York, Institute of Electrical and Electronics Engineers, Inc., 1985, p. 168-173.

This paper presents preliminary results of C-band radar scatterometer measurements of forest canopies of southeastern forests in the vicinity of NASA/NSTL. The results are as follows: (1) the radar backscattering coefficients (BSC) of deciduous forests such as oak, maple, blackgum, and cypress are higher than those

of coniferous forests such as slash pine plantation and natural pine; (2) at a large incidence angle, where polarization effect is significant, and by ranging measurement, the VV polarization BSC obtain peak value at the first few meters from the canopy top and decrease rather quickly, while the HH polarization BSC obtain peak value at longer distances from the canopy top and decrease rather slowly through the canopy; and (3) using the active radar calibrator for tree canopy attenuation measurement of a dense and a sparse live oak, it is found that the tree canopies with higher attenuations have higher BSC for all three polarizations, with VV polarization containing the largest differential (2.2 dB).

Author

A86-33538

ONE STEP ABOVE GROUND TRUTH - AIRPHOTO KEYS FOR LARGE-SCALE VEGETATION ANALYSIS

W. BEFORT (New Hampshire, University, Durham) IN: 1985 International Geoscience and Remote Sensing Symposium (IGARSS '85), Amherst, MA, October 7-9, 1985, Digest. Volume 1 . New York, Institute of Electrical and Electronics Engineers, Inc., 1985, p. 278-283. refs

The major requirements for producing an effective pictorial airphoto vegetation key, i.e., a pictorial set of reference material for rapid and accurate analysis of aerial photographs, are discussed. Consideration is given to the reproduction of color stereogram and to the identification and grouping of species, as well as to the cost, publication form, and durability of the key. A modular layout is suggested, which would facilitate making additions and improvements incrementally, without revising the entire work. Publishing the key as a looseleaf, rather than a bound book would enable the user to purchase, in addition to the basic set of pages, only the pages that would suit his specific requirements. Moreover, damaged pages could be replaced individually, and the pages needed in the field could be laminated. I.S.

A86-33539

A CORRELATION AND REGRESSION ANALYSIS OF PRECENT CANOPY CLOSURE VS. TMS SPECTRAL RESPONSE FOR SELECTED FOREST SITES IN THE SAN JUAN NATIONAL FOREST, COLORADO

M. K. BUTERA (Science Applications International Corp., Washington, DC) IN: 1985 International Geoscience and Remote Sensing Symposium (IGARSS '85), Amherst, MA, October 7-9, 1985, Digest. Volume 1 . New York, Institute of Electrical and Electronic Engineers, Inc., 1985, p. 287-302. refs

This investigation tested the correlation of canopy closure with the signal response of individual Thematic Mapper Simulator (TMS) bands for selected forest sites in the San Juan National Forest, Colorado. Ground truth consisted of a photointerpreted determination of percent canopy closure of 0 to 100 percent for 32 sites. The sites selected were situated on plateaus at an elevation of approximately 3 km with slope not greater than 10 percent. The predominant tree species were ponderosa pine and aspen. The mean TMS response per band site was calculated from data acquired by aircraft during mid-September 1981. A correlation analysis of TMS response vs canopy closure resulted in the following correlation coefficients for bands 1 through 7, respectively: -0.757, -0.663, -0.666, -0.088, -0.797, -0.597, -0.763. Two model regressions were applied to the TMS data set to create a map of predicted percent forest canopy closure for the study area. Results indicated percent predictive accuracies of 71, 74, and 57 for percent canopy closure classes of 0-25, 25-75, and 75-100, respectively. Author

01 AGRICULTURE AND FORESTRY

A86-33540* National Aeronautics and Space Administration. Ames Research Center, Moffett Field, Calif.

ANALYSIS OF FOREST/STRUCTURE USING THEMATIC MAPPER SIMULATOR DATA

D. L. PETERSON, J. A. BRASS (NASA, Ames Research Center, Moffett Field, CA), W. E. WESTMAN, V. G. AMBROSIA, M. A. SPANNER (NASA, Ames Research Center; Technicolor Government Services, Inc., Moffett Field, CA) et al. IN: 1985 International Geoscience and Remote Sensing Symposium (IGARSS '85), Amherst, MA, October 7-9, 1985, Digest. Volume 1. New York, Institute of Electrical and Electronics Engineers, Inc., 1985, p. 305-309.

A86-33541* Hunter Coll., New York.

CALIFORNIA TIMBER VOLUME INVENTORY USING LANDSAT

A. H. STRAHLER (Hunter College, New York) IN: 1985 International Geoscience and Remote Sensing Symposium (IGARSS '85), Amherst, MA, October 7-9, 1985, Digest. Volume 1. New York, Institute of Electrical and Electronics Engineers, Inc., 1985, p. 310-312. Research supported by the U.S. Forest Service and California Institute of Technology.
(Contract NAS9-15509; NAS7-100; USDA-53-9158-0-6362)

A86-33542* National Aeronautics and Space Administration. Lyndon B. Johnson Space Center, Houston, Tex.

ESTIMATION OF BIOPHYSICAL PROPERTIES OF FOREST CANOPIES THROUGH INVERSION OF MICROWAVE SCATTEROMETER DATA

D. E. PITTS, G. D. BADHWAR (NASA, Johnson Space Center, Houston, TX), and E. RAYNA (Lockheed Engineering and Management Services Co., Inc., Houston, TX) IN: 1985 International Geoscience and Remote Sensing Symposium (IGARSS '85), Amherst, MA, October 7-9, 1985, Digest. Volume 1. New York, Institute of Electrical and Electronics Engineers, Inc., 1985, p. 313-320.

A method for estimating the biophysical properties of a forest canopy through inversion of microwave scatterometer data is discussed. A C-band scatterometer flown over an aspen site in northern Minnesota during 19 days from May 2 to October 20, 1984, was modified to enable continuous recording of the range of the target. This provided the backscatter cross section as a function of range and was used to study scattering processes within the canopy. The remote estimates of HH, VV, and HV extinction coefficient values agreed well with the estimates obtained with the use of an active radar calibrator. I.S.

A86-33554* California Inst. of Tech., Pasadena.

MODELLING OF BACKSCATTER FROM VEGETATION LAYERS

J. J. VAN ZYL, N. ENGHETA, C. H. PAPAS (California Institute of Technology, Pasadena), C. ELACHI, and H. ZEBKER (California Institute of Technology, Jet Propulsion Laboratory, Pasadena) IN: 1985 International Geoscience and Remote Sensing Symposium (IGARSS '85), Amherst, MA, October 7-9, 1985, Digest. Volume 1. New York, Institute of Electrical and Electronics Engineers, Inc., 1985, p. 389-398. refs

A simple way to build up a library of models which may be used to distinguish between the different types of vegetation and ground surfaces by means of their backscatter properties is presented. The curve of constant power received by the antenna (Gamma sphere) is calculated for the given Stokes Scattering Operator, and model parameters are adopted of the most similar library model Gamma sphere. Results calculated for a single scattering model resembling coniferous trees are compared with the Gamma spheres of a model resembling tropical region trees. The polarization which would minimize the effect of either the ground surface or the vegetation layer can be calculated and used to analyze the backscatter from the ground surface/vegetation layer combination, and enhance the power received from the desired part of the combination. R.R.

A86-33555

BACKSCATTER MEASUREMENTS FROM SIMULATED RESONANT STRUCTURES

D. F. ZOOK and R. J. BLANCHARD (Texas, University, Arlington) IN: 1985 International Geoscience and Remote Sensing Symposium (IGARSS '85), Amherst, MA, October 7-9, 1985, Digest. Volume 1. New York, Institute of Electrical and Electronics Engineers, Inc., 1985, p. 399-404.

A simulation is performed to test the hypothesis that higher nodal dielectric constants in the stalks caused by additional moisture were responsible for increased radar backscatter cross sections in standing corn late in the season. Measurements at L-band were made of 2.5 relative permittivity PUC pipe with metal rings to simulate the moisture laden nodes, using a 20-MHz short pulse radar polarimeter system. Simulation target data from nodal lengths of 0.8, 1.0, and 1.2 wavelengths revealed that the nodal spacing backscatter is dependent on the volume density as well as the nodal spacing of stalk structures. The similarity in the number of scatterers between the rings-only experiments and other experiments suggests that an additional phenomenon must be accounting for the increase in backscatter. R.R.

A86-33556* Jet Propulsion Lab., California Inst. of Tech., Pasadena.

NEAR INFRARED LEAF REFLECTANCE MODELING

J. B. PARRISH (California Institute of Technology, Jet Propulsion Laboratory, Pasadena) IN: 1985 International Geoscience and Remote Sensing Symposium (IGARSS '85), Amherst, MA, October 7-9, 1985, Digest. Volume 1. New York, Institute of Electrical and Electronics Engineers, Inc., 1985, p. 405-409. refs

Near infrared leaf reflectance modeling using Fresnel's equation (Kumar and Silva, 1973) and Snell's Law successfully approximated the spectral curve for a 0.25-mm turgid oak leaf lying on a Halon background. Calculations were made for ten interfaces, air-wax, wax-cellulose, cellulose-water, cellulose-air, air-water, and their inverses. A water path of 0.5 mm yielded acceptable results, and it was found that assignment of more weight to those interfaces involving air versus water or cellulose, and less to those involving wax, decreased the standard deviation of the error for all wavelengths. Data suggest that the air-cell interface is not the only important contributor to the overall reflectance of a leaf. Results also argue against the assertion that the near infrared plateau is a function of cell structure within the leaf. R.R.

A86-33557

LIGHT INTERCEPTION AND LEAF AREA ESTIMATES FROM MEASUREMENTS OF GRASS CANOPY REFLECTANCE

G. ASRAR and E. T. KANEMASU (Kansas State University of Agriculture and Applied Science, Manhattan) IN: 1985 International Geoscience and Remote Sensing Symposium (IGARSS '85), Amherst, MA, October 7-9, 1985, Digest. Volume 1. New York, Institute of Electrical and Electronics Engineers, Inc., 1985, p. 412-417. refs

A procedure for estimating intercepted photosynthetically active radiation (PAR) and the green leaf area index (LAI) from measurements of grass canopy was developed. Spectral measurements were conducted throughout the entire season on the Konza Prairie Research Natural Area (Kansas), using a truck-mounted assembly equipped with Exotech model 100-A and Barnes Modular Multispectral model radiometers. Empirical linear regression equations were derived, based on a simple radiative transfer model and direct field measurements, that can be used to estimate p (the mean daily PAR fraction, corrected for the reflected and transmitted components) from measurements of canopy reflectance by the radiometers that mimic the MSS and TM sensor systems on board Landsat satellites. I.S.

A86-33558

CLASSIFICATION OF SOUTH TEXAS FARM AND RANGE RESOURCES USING NOAA7 AVHRR SATELLITE IMAGERY

A. J. RICHARDSON and J. H. EVERITT (USDA, Agricultural Research Service, Weslaco, TX) IN: 1985 International Geoscience and Remote Sensing Symposium (IGARSS '85), Amherst, MA, October 7-9, 1985, Digest. Volume 1. New York, Institute of Electrical and Electronics Engineers, Inc., 1985, p. 418-425. refs

Polar orbiting meteorological satellite scenes from October 1981 to July 1982 were used to classify south Texas farm and range plant communities using the NOAA7 advanced very high resolution radiometer (AVHRR). Classification results were related to maps of south Texas that contained information about soil, crop, and agronomic resources, and to agronomic resource expertise of local scientists. A table look-up procedure, based on reflective bands 1 and 2, was used to automatically classify AVHRR data into cloud, water, bare soil, and vegetation vigor levels (low, medium, and high). These classified results were found to be related to prominent level I farm and range resources such as oak (*Quercus* spp) trees, improved grasses, unimproved rangeland, dryland cotton and sorghum farming areas, and irrigated cotton and sorghum farming areas. Author

A86-33565* Jet Propulsion Lab., California Inst. of Tech., Pasadena.

FOREST DISCRIMINATION WITH MULTIPOLARIZATION IMAGING RADAR

J. P. FORD and D. E. WICKLAND (California Institute of Technology, Jet Propulsion Laboratory, Pasadena) IN: 1985 International Geoscience and Remote Sensing Symposium (IGARSS '85), Amherst, MA, October 7-9, 1985, Digest. Volume 1. New York, Institute of Electrical and Electronics Engineers, Inc., 1985, p. 462-465. NASA-supported research.

The use of radar polarization diversity for discriminating forest canopy variables on airborne synthetic-aperture radar (SAR) images is evaluated. SAR images were acquired at L-Band (24.6 cm) simultaneously in four linear polarization states (HH, HV, VH, and VV) in South Carolina on March 1, 1984. In order to relate the polarization signatures to biophysical properties, false-color composite images were compared to maps of forest stands in the timber compartment. In decreasing order, the most useful correlative forest data are stand basal area, forest age, site condition index, and forest management type. It is found that multipolarization images discriminate variation in tree density and difference in the amount of understory, but do not discriminate between evergreen and deciduous forest types. R.R.

A86-33566* Jet Propulsion Lab., California Inst. of Tech., Pasadena.

FOREST DISCRIMINATION WITH MULTIPOLARIZATION IMAGING RADAR

J. P. FORD and D. E. WICKLAND (California Institute of Technology, Jet Propulsion Laboratory, Pasadena) IN: 1985 International Geoscience and Remote Sensing Symposium (IGARSS '85), Amherst, MA, October 7-9, 1985, Digest. Volume 1. New York, Institute of Electrical and Electronics Engineers, Inc., 1985, p. 466-469. NASA-supported research.

The relations between polarization signatures and biophysical characteristics through a range of different forest environments were investigated using airborne synthetic-aperture (SAR) images acquired at L-band on March 1, 1984 in South Carolina. SAR data acquired in four linear polarization states with 10-m spatial resolution were encoded as color composite images and compared to US Forest Service forest stand data. The most useful correlative forest data were stand basal area, forest age, site condition index, and forest management type. It is found that the multipolarization images discriminate variation in tree density or difference in the amount of understory, but no evidence has been found for discrimination between evergreen and deciduous forest types. R.R.

A86-33576* Agricultural Research Service, Houston, Tex.

OVERVIEW AND HIGHLIGHTS OF EARLY WARNING AND CROP CONDITION ASSESSMENT PROJECT

G. O. BOATWRIGHT (USDA, Agricultural Research Service, Houston, TX) and V. S. WHITEHEAD (NASA, Johnson Space Center, Houston, TX) IN: 1985 International Geoscience and Remote Sensing Symposium (IGARSS '85), Amherst, MA, October 7-9, 1985, Digest. Volume 2. New York, Institute of Electrical and Electronics Engineers, Inc., 1985, p. 537-546. refs

Work of the Early Warning and Crop Condition Assessment (EW/CCA) project, one of eight projects in the Agriculture and Resources Inventory Surveys Through Aerospace Remote Sensing (AgRISTARS), is reviewed. Its mission, to develop and test remote sensing techniques that enhance operational methodologies for crop condition assessment, was in response to initiatives issued by the Secretary of Agriculture. Meteorologically driven crop stress indicator models have been developed or modified for wheat, maize, grain sorghum, and soybeans. These models provide early warning alerts of potential or actual crop stresses due to water deficits, adverse temperatures, and water excess that could delay planting or harvesting operations. Recommendations are given for future research involving vegetative index numbers and the NOAA and Landsat satellites. D.H.

A86-33577* National Aeronautics and Space Administration, Lyndon B. Johnson Space Center, Houston, Tex.

VEGETATION ASSESSMENT USING A COMBINATION OF VISIBLE, NEAR-IR AND THERMAL-IR AVHRR DATA

V. S. WHITEHEAD (NASA, Johnson Space Center, Houston, TX), W. JOHNSON, and J. BOATRIGT (Lockheed Engineering and Management Services Co., Inc., Houston, TX) IN: 1985 International Geoscience and Remote Sensing Symposium (IGARSS '85), Amherst, MA, October 7-9, 1985, Digest. Volume 2. New York, Institute of Electrical and Electronics Engineers, Inc., 1985, p. 548-555. refs

Twelve hour temperature difference (thermal inertia) maps generated by rectifying and registering ascending (day) passes and descending (night) passes of the NOAA-7 Advanced Very High Resolution Radiometer (AVHRR) are compared to vegetation index maps generated from the visible and near IR data from the day pass of that satellite. There appears to be significant and unique information concerning surface characteristics in the temperature difference data on the 1 km scale of the AVHRR. A scatter diagram is provided which shows the pattern of day-night temperature difference compared to vegetation index for irrigated agriculture, dry rangeland, lakes, wet areas and burned rangeland. A detailed description of the techniques employed to provide the day-night temperature maps is provided. Author

A86-33578

DETECTION AND EVALUATION OF PLANT STRESSES FOR CROP MANAGEMENT DECISIONS

R. D. JACKSON, P. J. PINTER, JR., R. J. REGINATO, and S. B. IDSO (USDA, Water Conservation Laboratory, Phoenix, AZ) IN: 1985 International Geoscience and Remote Sensing Symposium (IGARSS '85), Amherst, MA, October 7-9, 1985, Digest. Volume 2. New York, Institute of Electrical and Electronics Engineers, Inc., 1985, p. 556-561. refs

It is suggested that the ability to quantitatively assess crop conditions using remotely sensed data would not only improve yield forecasts but would also provide information that would be useful to farm managers in making day-to-day management decisions. Experiments were conducted using ground based radiometers to relate spectral response to crop canopy characteristics. It was found that radiometrically measured crop temperature, when compared with a reference temperature, was related to the degree of plant stress and could indicate the onset of stress. Timeliness, frequency of coverage, and resolution are three factors that must be considered when satellite based sensors are used to evaluate crop conditions for farm management applications. D.H.

A86-33579

DEVELOPMENT OF AGROMETEOROLOGICAL CROP MODEL INPUTS FROM REMOTELY SENSED INFORMATION

C. L. WIEGAND, A. J. RICHARDSON (USDA, Agricultural Research Service, Weslaco, TX), R. D. JACKSON, P. J. PINTER, JR. (USDA, Agricultural Research Service, Phoenix, AZ), J. K. AASE (USDA, Agricultural Research Service, Sidney, MT) et al. IN: 1985 International Geoscience and Remote Sensing Symposium (IGARSS '85), Amherst, MA, October 7-9, 1985, Digest. Volume 2. New York, Institute of Electrical and Electronics Engineers, Inc., 1985, p. 564-569.

Efforts at developing agrometeorological crop model inputs from remotely sensed information (AgRISTARS Early Warning/Crop Condition Assessment Project Subtask 5 within USDA) are described. Much effort has gone into developing measurement and interpretation skill, convincing the scientific community of the validity and information content of the spectral measurements, and providing new understanding of the crop scenes viewed as affected by bidirectional, atmospheric, and solid background variations. Vegetation indices are an excellent measure of the amount of green photosynthetically active tissue present in plant stands at any time during the season. They can reliably estimate leaf area index and intercepted photosynthetically active radiation. Newness of the spectral interpretations, combined with continual revisions in the agrometeorological models and lack of feedback capability in them, have prevented the benefits of spectral inputs to agrometeorological models from being fully realized. D.H.

A86-33582

POSSIBLE APPLICATIONS OF THE MICROWAVES SURFACE SOIL MOISTURE REMOTE SENSING

R. BERNARD and D. VIDAL-MADJAR (Centre de Recherches en Physique de l'Environnement Terrestre et Planetaire, Issy-les-Moulineaux, France) IN: 1985 International Geoscience and Remote Sensing Symposium (IGARSS '85), Amherst, MA, October 7-9, 1985, Digest. Volume 2. New York, Institute of Electrical and Electronics Engineers, Inc., 1985, p. 594-600. CNES-supported research. refs

With the development of airborne scatterometers and of microwaves radiometers, it is now possible to map the soil surface water content and its short or long term time variation. It is shown here that this parameter is meaningful to describe the vertical soil water movement in the unsaturated zone and that it can also be used to estimate the drainage properties of bare soils surface.

Author

A86-33583* National Aeronautics and Space Administration. Langley Research Center, Hampton, Va.

AN AIRBORNE MULTIPLE-BEAM 1.4 GHZ PUSHBROOM MICROWAVE RADIOMETER

R. F. HARRINGTON and R. W. LAWRENCE (NASA, Langley Research Center, Hampton, VA) IN: 1985 International Geoscience and Remote Sensing Symposium (IGARSS '85), Amherst, MA, October 7-9, 1985, Digest. Volume 2. New York, Institute of Electrical and Electronics Engineers, Inc., 1985, p. 601-606.

A method is described for providing soil moisture measurements from satellites by performing simultaneous measurements across track (the pushbroom approach). The method has the advantage of obtaining the required swath width without sacrificing sensitivity. A prototype Pushbroom Microwave Radiometer developed at NASA's Langley Research Center is described. It is a multibeam L-Band (1413 MHz) radiometer system providing simultaneous cross track measurements. Results of flight tests onboard a P-3 aircraft are discussed. D.H.

A86-33598

SURFACE MATERIAL CLASSIFICATION BASED ON SPECTRAL SHAPE

M. J. CARLOTTO and V. T. TOM (Analytic Sciences Corp., Reading, MA) IN: 1985 International Geoscience and Remote Sensing Symposium (IGARSS '85), Amherst, MA, October 7-9, 1985, Digest. Volume 2. New York, Institute of Electrical and Electronics Engineers, Inc., 1985, p. 703-708. refs

A method for classifying surface material classes, based on the shape of the spectral signature, is presented. Spectral shape is described in terms of a vector of predicates which specify the relative intensities between all pairs of bands. Spectral signatures are represented as logical expressions of shape predicates which define the classification logic. Preliminary results for Landsat TM image classification are discussed. D.H.

A86-33605

USDA/SRS SOFTWARE FOR LANDSAT MSS-BASED CROP-ACREAGE ESTIMATION

M. OZGA (USDA, Statistical Reporting Service, Washington, DC) IN: 1985 International Geoscience and Remote Sensing Symposium (IGARSS '85), Amherst, MA, October 7-9, 1985, Digest. Volume 2. New York, Institute of Electrical and Electronics Engineers, Inc., 1985, p. 762-772. refs

A description is given of a large software system, known as EDITOR, developed by the Statistical Reporting Service of the USDA to aid in crop acreage estimation. EDITOR is a collection of independent programs operating on data in many different files. Most EDITOR programs are called using relatively simple commands from a main program. Topics covered include: the history and development of EDITOR; the structure and major functions; supercomputer usage; and computer configuration for EDITOR processing. PEDITOR (portable EDITOR) has been developed for use with the smaller machines - including microcomputers - coming into use. To continue to be useful with new types of data, such as Thematic Mapper and SPOT, and the new computers, EDITOR will have to be adapted. D.H.

A86-33606* Houston Univ., Clear Lake, Tex.

EVALUATION OF CROP ACREAGE ESTIMATION METHODS USING LANDSAT DATA AS AUXILIARY INPUT

R. S. CHHIKARA (Houston, University, Clear Lake, TX), A. G. HOUSTON (NASA, Johnson Space Center, Houston, TX), and J. C. LUNDGREN (Lockheed Engineering and Management Services Co., Houston, TX) IN: 1985 International Geoscience and Remote Sensing Symposium (IGARSS '85), Amherst, MA, October 7-9, 1985, Digest. Volume 2. New York, Institute of Electrical and Electronics Engineers, Inc., 1985, p. 778-785. USDA-supported research. refs
(Contract NAS9-15800)

The regression and ratio estimators are studied in the context of improving upon the ground survey estimates of crop acreages by utilizing Landsat data. The approach is to formulate analytically the estimation problem that utilizes ground survey data, as collected by the U.S. Department of Agriculture, and Landsat data, which provide a complete coverage for an area of interest, and then to conduct simulation studies. It is shown over a wide range of conditions that the regression estimator is the most efficient unless there is a low correlation between the actual and estimated crop acreages in the sampled area segments, in which case a ratio type estimator is superior. Estimation of the variance of the regression estimator is also investigated. Author

A86-33622

NONPARAMETRIC MODELS AND CROP CLASSIFICATION

M. L. ARMSTRONG and I. E. ABDOU (Delaware, University, Newark) IN: 1985 International Geoscience and Remote Sensing Symposium (IGARSS '85), Amherst, MA, October 7-9, 1985, Digest. Volume 2. New York, Institute of Electrical and Electronics Engineers, Inc., 1985, p. 892-897. refs

The performance of a nonparametric classifier is compared with that of a Gaussian classifier. Two measures of performance are used: the chi-squared goodness-of-fit test, and the classification

error. The data set used is a Landsat multispectral scanner image, and the classes of interest are corn/soybean fields. The results show that although the Gaussian model did not satisfy the goodness-of-fit measure, the overall classification performance was good. Another conclusion is that the nonparametric classifier error is comparable to the Gaussian error, with more room for improvement. Author

A86-33625
SAR IMAGE SEGMENTATION USING DIGITISED FIELD BOUNDARIES FOR CROP MAPPING AND MONITORING APPLICATIONS

M. G. WOODING (Royal Aircraft Establishment, U.K. National Remote Sensing Centre, Farnborough, England) IN: 1985 International Geoscience and Remote Sensing Symposium (IGARSS '85), Amherst, MA, October 7-9, 1985, Digest. Volume 2 . New York, Institute of Electrical and Electronics Engineers, Inc., 1985, p. 912-918.

An approach to SAR image segmentation (so that areas can be analyzed as separate units) is presented, based on the digitizing of field boundaries from large scale maps and the geometric transformation of SAR images. Following the registration of maps and images, techniques are used for automated backscatter measurement and the generation of segmented images. The approach is seen to be particularly valuable for experimental work in general and for operational crop monitoring. The UK Ordnance Survey has long term plans to digitize fully the preparation of its maps and this could eventually be an important data source of field boundary maps for large area crop mapping. Plans have been made to have a facility to edit field boundaries on a display of the field boundary map superimposed on the image. A segmented image database system is to be developed to exploit and extend the analysis possibilities created by image segmentation. D.H.

A86-33627
SPECTRAL COMPONENTS ANALYSIS - A BRIDGE BETWEEN SPECTRAL OBSERVATIONS AND AGROMETEOROLOGICAL CROP MODELS

C. L. WIEGAND, A. J. RICHARDSON, and P. R. NIXON (USDA, Agricultural Research Service, Weslaco, TX) IN: 1985 International Geoscience and Remote Sensing Symposium (IGARSS '85), Amherst, MA, October 7-9, 1985, Digest. Volume 2 . New York, Institute of Electrical and Electronics Engineers, Inc., 1985, p. 941-946. refs

Two experiments are described that were conducted under AgRISTARS sponsorship, one with cotton and one with spring wheat, specifically to determine the relationships for each term in the 'spectral components analysis' identity, $LAI/VI \times APAR/LAI = APAR/VI$. LAI is leaf area index; VI is vegetation index; and APAR is absorbed photosynthetically active radiation. LAI and APAR were well estimated from vegetation indices such as normalized difference and perpendicular vegetation index. The spectral components analysis results presented lend credence to the information conveyed by spectral canopy observations about plant development and yield, and establish a bridge between remote observations and agrometeorological crop modeling through the variables of mutual concern: LAI, light absorption, and yield. D.H.

A86-33628
COMPARISON BETWEEN LANDSAT MSS AND THEMATIC MAPPER DATA FOR GEOBOTANICAL PROSPECTING IN THE SPANISH-PORTUGUESE PYRITE BELT

C. BANNINGER (Graz, Technische Universitaet und Forschungszentrum; Institut fuer Digitale Bildverarbeitung und Graphik, Austria) IN: 1985 International Geoscience and Remote Sensing Symposium (IGARSS '85), Amherst, MA, October 7-9, 1985, Digest. Volume 2 . New York, Institute of Electrical and Electronics Engineers, Inc., 1985, p. 949-956. refs

Landsat MSS and Thematic Mapper data successfully detected metal-related stress in a pine tree stand growing in copper-lead-zinc rich soils. The far red and near-infrared MSS bands (MSS 3 and

4) and the near-infrared Thematic Mapper band (TM 4) were best in defining metal stress in vegetation, followed closely by the visible (TM 1, 2 and 3) and shortwave infrared (TM 5 and 7) Thematic Mapper bands. Both MSS- and TM-based transformations employing simple band ratios, normalized differences, and principal components generally produced poor to only fair results, with the exception of the first principal component. Author

A86-33629
EVALUATION OF LANDSAT MSS BANDS AND TRANSFORMATIONS FOR DETECTING HEAVY METAL STRESS IN FOREST-COVERED AREAS

C. BANNINGER (Graz, Technische Universitaet und Forschungszentrum; Institut fuer Digitale Bildverarbeitung und Graphik, Austria) IN: 1985 International Geoscience and Remote Sensing Symposium (IGARSS '85), Amherst, MA, October 7-9, 1985, Digest. Volume 2 . New York, Institute of Electrical and Electronics Engineers, Inc., 1985, p. 957-963. refs

Single and transformed band Landsat MSS data from three scene dates of two tree stands growing in metal-rich soils show the first principal component and the Kauth-Thomas green vegetative and, to a lesser extent, the soil brightness indices to be overall best in discriminating heavy metal stress in vegetation. The next most useful, in decreasing order of importance, are Landsat bands 6 and 7, perpendicular vegetation indices, band differences, and simple band ratios (all employing Landsat bands 5, 6, and 7). Landsat bands 4 and 5 and the second principal component are the least useful for metal stress detection. Author

A86-33644* National Aeronautics and Space Administration. Ames Research Center, Moffett Field, Calif.

MULTI-CROP AREA ESTIMATION AND MAPPING ON A MICROPROCESSOR/MAINFRAME NETWORK

E. SHEFFNER (NASA, Ames Research Center; Technicolor Government Services, Inc., Moffett Field, CA) IN: 1985 International Geoscience and Remote Sensing Symposium (IGARSS '85), Amherst, MA, October 7-9, 1985, Digest. Volume 2 . New York, Institute of Electrical and Electronics Engineers, Inc., 1985, p. 1117-1122.

(Contract NAS2-11101)

The data processing system is outlined for a 1985 test aimed at determining the performance characteristics of area estimation and mapping procedures connected with the California Cooperative Remote Sensing Project. The project is a joint effort of the USDA Statistical Reporting Service-Remote Sensing Branch, the California Department of Water Resources, NASA-Ames Research Center, and the University of California Remote Sensing Research Program. One objective of the program was to study performance when data processing is done on a microprocessor/mainframe network under operational conditions. The 1985 test covered the hardware, software, and network specifications and the integration of these three components. Plans for the year - including planned completion of PEDITOR software, testing of software on MIDAS, and accomplishment of data processing on the MIDAS-VAX-CRAY network - are discussed briefly. D.H.

A86-34740
REFLECTANCE MODELLING AND THE DERIVATION OF VEGETATION INDICES FOR AN AUSTRALIAN SEMI-ARID SHRUBLAND

R. P. PECH, R. D. GRAETZ (CSIRO, Div. of Wildlife and Rangelands Research, Lyneham, Australia), and A. W. DAVIS (CSIRO, Div. of Mathematics and Statistics, Glen Osmond, Australia) International Journal of Remote Sensing (ISSN 0143-1161), vol. 7, March 1986, p. 389-403. refs

Indices of vegetation 'cover' and 'greenness' are derived for Landsat MSS digital data for an Australian rangeland type, and their usefulness discussed with reference to the information content of the data and the effect of shadowing as an interaction between landscape components. The indices are related to a class of statistical models called mixture models which provides a formal

01 AGRICULTURE AND FORESTRY

framework for analyzing reflectance data from multicomponent surfaces. Author

A86-34741

FORESTRY INFORMATION CONTENT OF THEMATIC MAPPER DATA

D. N. H. HORLER (Horler Information, Inc., Ottawa, Canada) and F. J. AHERN (Canada Centre for Remote Sensing, Ottawa) *International Journal of Remote Sensing* (ISSN 0143-1161), vol. 7, March 1986, p. 405-428. refs

The spectral and radiometric properties of Thematic Mapper (TM) imagery are studied by principal component analysis. The principal components are: (1) brightness features, (2) greenness-type features, and (3) a contrast between visible and near-infrared regions and the shortwave infrared (SWIR) region. Landsat-4 data of the Dryden-Lac Seul region in western Ontario collected on September 26, 1982 is utilized in this study. The analysis reveals that the spectral data can be reduced to three eigenvectors with a loss of less than 10 percent of the scene variance. TM bands perform well for the three principal components; TM bands 3, 4, and 5 are applicable for general cover-type discrimination and bands 1, 4, and 5 for separating a set of softwood classes. It is observed that the TM bands 5 and 7, which represent the SWIR spectral region, are sensitive to forest vegetation density. I.F.

A86-34742* National Aeronautics and Space Administration. Goddard Space Flight Center, Greenbelt, Md.
IDENTIFYING DEFORESTATION IN BRAZIL USING MULTIREOLUTION SATELLITE DATA

R. NELSON and B. HOLBEN (NASA, Goddard Space Flight Center, Greenbelt, MD) *International Journal of Remote Sensing* (ISSN 0143-1161), vol. 7, March 1986, p. 429-448. refs

The use of multiresolution satellite data to monitor deforestation on a continental/subcontinental scale is examined. MSS, local area coverage (LAC), global area coverage (GAC), and GOES data were applied to the study of deforestation in Rondonia, Brazil; the characteristics of these sensors are described. The probability thresholding and vegetation-index thresholding procedures used to process the data in order to differentiate between forest from nonforest are analyzed. The LAC, GAC, and GOES data are compared to MSS data. It is observed that GOES data is not useful for monitoring colonization projects due to excessive noise in the data; the GAC data is only applicable in large areas of contiguous forest clearing; the MSS data when available is applicable as a ground data reference source for differentiating cleared areas from primary; the LAC data are capable of delineating colonization clearings; and the probability thresholding procedure differentiates forest from nonforest more accurately than the vegetation-index procedure. The data reveal that the LAC data combined with the probability threshold procedure provide the best data-source/classification-procedure combination. I.F.

A86-34744

AN IMPROVED HYBRID CLASSIFIER

J. Y. KOO and M. KIM (Korea Advanced Institute of Science and Technology, Seoul, Republic of Korea) *International Journal of Remote Sensing* (ISSN 0143-1161), vol. 7, March 1986, p. 471-476.

A new hybrid classifier is proposed which utilizes the advantages of the maximum likelihood classifier and the parallelepiped classifier. The new hybrid classifier reduces the processing time more substantially than the conventional one by introducing a lower boundary for each class. The rate of misclassification is comparable to that of maximum likelihood classifier. Performance of the conventional and the new method are compared by an example. Author

A86-35677* National Aeronautics and Space Administration. Lyndon B. Johnson Space Center, Houston, Tex.

SPECTRAL CHARACTERIZATION OF BIOPHYSICAL CHARACTERISTICS IN A BOREAL FOREST - RELATIONSHIP BETWEEN THEMATIC MAPPER BAND REFLECTANCE AND LEAF AREA INDEX FOR ASPEN

G. D. BADHWAR, R. B. MACDONALD, F. G. HALL (NASA, Johnson Space Center, Houston, TX), and J. G. CARNES (Lockheed Engineering and Management Services Co., Houston, TX) (*International Geoscience and Remote Sensing Symposium /IGARSS '84/: From Research toward Operational Use, Strasbourg, France, Aug. 27-30, 1984*) *IEEE Transactions on Geoscience and Remote Sensing* (ISSN 0196-2892), vol. GE-24, May 1986, p. 322-326. Previously announced in STAR as N84-33875. refs

Results from analysis of a data set of simultaneous measurements of Thematic Mapper band reflectance and leaf area index are presented. The measurements were made over pure stands of Aspen in the Superior National Forest of northern Minnesota. The analysis indicates that the reflectance may be sensitive to the leaf area index of the Aspen early in the season. The sensitivity disappears as the season progresses. Based on the results of model calculations, an explanation for the observed relationship is developed. The model calculations indicate that the sensitivity of the reflectance to the Aspen overstory depends on the amount of understory present. ESA

A86-35678

A STABLE ITERATIVE PROCEDURE TO OBTAIN SOIL SURFACE PARAMETERS AND FLUXES FROM SATELLITE DATA

M. RAFFY and F. BECKER (Groupement Scientifique de Teledetection Spatiale, Strasbourg, France) (*International Geoscience and Remote Sensing Symposium /IGARSS '84/: From Research toward Operational Use, Strasbourg, France, Aug. 27-30, 1984*) *IEEE Transactions on Geoscience and Remote Sensing* (ISSN 0196-2892), vol. GE-24, May 1986, p. 327-333. CNRS-supported research. refs

Two general methods recently proposed to obtain the thermal inertia, the sensible heat flux, and the evapotranspiration flux from satellite data are summarized. In these methods, stable algorithms were used, but the stabilization coefficients exist and can lead to an iterative process to calculate the thermal inertia and the fluxes with improved accuracy despite errors of measurements. Some applications using in situ data and theoretically simulated data are given as an example. Author

A86-35679* Texas Univ., Arlington.

UTILIZATION OF ACTIVE MICROWAVE ROUGHNESS MEASUREMENTS TO IMPROVE PASSIVE MICROWAVE SOIL MOISTURE ESTIMATES OVER BARE SOILS

S. W. THEIS (Texas Instruments, Inc., McKinney), A. J. BLANCHARD (Texas University, Arlington), and B. J. BLANCHARD (*International Geoscience and Remote Sensing Symposium /IGARSS '84/: From Research toward Operational Use, Strasbourg, France, Aug. 27-30, 1984*) *IEEE Transactions on Geoscience and Remote Sensing* (ISSN 0196-2892), vol. GE-24, May 1986, p. 334-339. USGS-USDA-supported research. Previously announced in STAR as N84-33898. refs (Contract NSG-5134; DOC-MO-A01-78-004332)

Multisensor aircraft data were used to establish the potential of the active microwave sensor response to be used to compensate for roughness in the passive microwave sensor's response to soil moisture. Only bare fields were used. It is found that the L-band radiometer's capability to estimate soil moisture significantly improves when surface roughness is accounted for with the scatterometers. ESA

A86-35681

MICROWAVE EMISSION FROM ROW CROPS

D. R. BRUNFELDT (Applied Microwave Corp., Lawrence, KS) and F. T. ULABY (Michigan, University, Ann Arbor) (International Geoscience and Remote Sensing Symposium /IGARSS '84/: From Research toward Operational Use, Strasbourg, France, Aug. 27-30, 1984) IEEE Transactions on Geoscience and Remote Sensing (ISSN 0196-2892), vol. GE-24, May 1986, p. 353-359.

In order to examine the emission properties of vegetation without taking into consideration the effects of variations in the soil background, strips of metal screening were used to cover the soil surface between adjacent rows of plants. Temporal measurements were made at 2.7 and 5.1 GHz for soybean, wheat, and corn canopies. Several special experiments were conducted to evaluate the sensitivity of brightness temperature to look direction (relative to row direction), polarization configuration, and incidence angle, and to evaluate the emission contributions of defoliated stalks. In general, the results show that the canopy is highly anisotropic, the emission exhibits a strong dependence on polarization and look direction, and the scattering albedo is typically less than 0.1. Canopy transmissivity was estimated from the radiometric observations and then related empirically to the canopy's integrated water content. Using this relation in a zero-order radiative transfer model led to good agreement between the experimental observations and the model predictions. Author

A86-35687

SEGMENTATION OF A THEMATIC MAPPER IMAGE USING THE FUZZY C-MEANS CLUSTERING ALGORITHM

R. L. CANNON, J. C. BEZDEK (South Carolina, University, Columbia), J. V. DAVE (IBM Palo Alto Scientific Center, CA), and M. M. TRIVEDI (Louisiana State University, Baton Rouge) IEEE Transactions on Geoscience and Remote Sensing (ISSN 0196-2892), vol. GE-24, May 1986, p. 400-408. refs (Contract NSF ECS-82-17191; NSF IST-84-07860)

In this paper, a segmentation procedure that utilizes a clustering algorithm based upon fuzzy set theory is developed. The procedure operates in a nonparametric unsupervised mode. The feasibility of the methodology is demonstrated by segmenting a six-band Landsat-4 digital image with 324 scan lines and 392 pixels per scan line. For this image, 100-percent ground cover information is available for estimating the quality of segmentation. About 80 percent of the imaged area contains corn and soybean fields near the peak of their growing season. The remaining 20 percent of the image contains 12 different types of ground cover classes that appear in regions of different sizes and shapes. The segmentation method uses the fuzzy c-means algorithm in two stages. The large number of clusters resulting from this segmentation process are then merged by use of a similarity measure on the cluster centers. Results are presented to show that this two-stage process leads to separation of corn and soybean, and of several minor classes that would otherwise be overwhelmed in any practical one-stage clustering. Author

A86-35748* National Aeronautics and Space Administration. Ames Research Center, Moffett Field, Calif.

POLARIZATION PHOTOMETER TO MEASURE BIDIRECTIONAL REFLECTANCE FACTOR R(55 DEG, 0 DEG, 55 DEG, 180 DEG) OF LEAVES

V. C. VANDERBILT (NASA, Ames Research Center, Moffett Field, CA; Purdue University, West Lafayette, IN) and L. GRANT (Purdue University, West Lafayette, IN) Optical Engineering (ISSN 0091-3286), vol. 25, April 1986, p. 566-571. refs (Contract NAG5-269; NAS9-16528)

A polarization photometer has been developed for rapidly determining the bidirectional, polarized, and diffuse light-scattering properties of individual leaves illuminated and measured 'in vivo' at an angle of 55 deg (approximately Brewster's angle) in six wavelength bands in the visible and near-IR wavelength regions. The optical performance and data quality of the system are evaluated to estimate the magnitude of the variation in the data attributable to the instrument system and to measurement procedures. The potential to discriminate between three species

of oak is demonstrated using data acquired by the polarization photometer. The instrument is being used to increase understanding of the radiation transfer process in plant canopies and specifically to determine how agronomic information of the physical and chemical processes in leaves, plants, and plant canopies is expressed in these light-scattering properties. Author

A86-36037#

FOREST SIGNATURES IN IMAGING AND NON-IMAGING MICROWAVE SCATTEROMETER DATA

A. J. SIEBER (DFVLR, Institut fuer Hochfrequenztechnik, Oberpfaffenhofen, West Germany) ESA Journal (ISSN 0379-2285), vol. 9, no. 4, 1985, p. 431-448. refs

X-band and L-band radars have been used to determine the signatures of both deciduous and coniferous trees. The information content of the radars is significantly influenced not only by the X- and L-band radar cross-sections of the trees, but also by the spatial resolutions of the measurements. It has been found that selection of the appropriate polarisation allows particular tree species to be identified. Author

A86-36042* National Aeronautics and Space Administration. Earth Resources Lab., Bay St. Louis, Miss.

ANALYSIS OF EFFECTIVE RADIANT TEMPERATURES IN A PACIFIC NORTHWEST FOREST USING THERMAL INFRARED MULTISPECTRAL SCANNER DATA

S. A. SADER (NASA, Earth Resources Laboratory, Bay St. Louis, MS) Remote Sensing of Environment (ISSN 0034-4257), vol. 19, April 1986, p. 105-115. refs

Analysis of Thermal Infrared Multispectral Scanner data collected over H. J. Andrews experimental forest in western Oregon indicated that aspect and slope gradient had a greater effect on the thermal emission of younger reforested clearcuts than of older stands. Older forest stands (older than 25 years) with greater amounts of green biomass and closed canopies, had lower effective radiant temperatures than younger, less dense stands. Aspect and slope had little effect on the effective radiant temperature of these older stands. Canopy temperature recorded at approximately 1:30 pm local time July 29, 1983 were nearly equal to maximum daily air temperature recorded at eight reference stands. The investigation provided some insights into the utility of the thermal sensor for detecting surface temperature differences related to forest composition and green biomass amounts in mountain terrain. Author

A86-36044

SOIL BACKGROUND EFFECTS ON THE SPECTRAL RESPONSE OF A THREE-COMPONENT RANGELAND SCENE

J. L. HEILMAN (Texas A & M University, College Station) and W. E. BOYD (Earth Observation Satellite Co., Lanham, MD) Remote Sensing of Environment (ISSN 0034-4257), vol. 19, April 1986, p. 127-137. refs

Landsat data were simulated for a grass, brush, and soil rangeland scene for active growth and summer dormancy, to evaluate the effect of soil background reflectance on the sensitivity ratio and orthogonal spectral indices to vegetation density. As the density of green vegetation increased, the sensitivities of the ratio vegetation index and the normalized difference decreased for low soil reflectance, and increased for high soil reflectance. Differences were found between some results obtained from published coefficients and those obtained from the simulated data. The results suggest that discrimination of brush and vegetation may not be possible during active growth (when the grass is dormant), and that even if soil-specific calibration and soil lines are used, the accuracy of vegetation density estimates derived from the indices may vary with soil background. R.R.

01 AGRICULTURE AND FORESTRY

A86-36045* Illinois Univ., Chicago.

SCATTERING FROM A RANDOM LAYER EMBEDDED WITH DIELECTRIC NEEDLES

H. J. EOM (Illinois, University, Chicago) and A. K. FUNG (Texas, University, Arlington) Remote Sensing of Environment (ISSN 0034-4257), vol. 19, April 1986, p. 139-149. refs (Contract NAG5-68; NAS9-15421)

Intensity scattering from a random layer imbedded with small dielectric needles is studied for applications to coniferous vegetation. The phase matrix of a thin needle whose length may be appreciable compared to the incident wavelength is presented. The effects of needle orientation on scattering is taken into account by averaging the phase function over angles of orientation. The backscattering coefficient from the layer is computed by solving the radiative transfer equation. The effects of operating frequency, orientation and size of a needle on like- and cross-backscattering are demonstrated. It was found that in backscattering angular trends are mainly controlled by the orientation of the needles. Author

A86-36046* Illinois Univ., Chicago.

REGRESSION MODELS FOR VEGETATION RADAR-BACKSCATTERING AND RADIOMETRIC EMISSION

H. J. EOM (Illinois, University, Chicago) Remote Sensing of Environment (ISSN 0034-4257), vol. 19, April 1986, p. 151-157. refs

(Contract NAG5-486)

Simple regression estimation of radar backscatter and radiometric emission from vegetative terrain is proposed, based on the exact radiative transfer models. A vegetative canopy is modeled as a Rayleigh scattering layer above an irregular Kirchhoff surface. The rms errors between the exact and the estimated ones are found to be less than 5 percent for emission, and 1 dB for the backscattering case, in most practical uses. The proposed formulas are useful in quickly estimating backscattering and emission from the vegetative terrain. Author

A86-36047* Kansas State Univ., Manhattan.

DISTINGUISHING AMONG TALLGRASS PRAIRIE COVER TYPES FROM MEASUREMENTS OF MULTISPECTRAL REFLECTANCE

G. ASRAR, R. L. WEISER, D. E. JOHNSON, E. T. KANEMASU, and J. M. KILLEEN (Kansas State University of Agriculture and Applied Science, Manhattan) Remote Sensing of Environment (ISSN 0034-4257), vol. 19, April 1986, p. 159-169. refs (Contract NAS1-67457)

The heterogeneity in surface cover caused by management practices or natural events complicates monitoring the conditions of grasslands and assessing their productivity by remote sensing techniques. Statistical procedures were sought that would allow different grassland surface cover types (bare soil, senescent vegetation, and green vegetation) to be distinguished by using measurements of grassland multispectral reflectance. Two procedures, discriminant analysis and canonical discriminant analysis, were found suitable for achieving this objective. Linear classification functions and canonical variables were derived, which distinguish between the three cover types. A comparison between two sensor systems, a Barnes multiband radiometer and an Exotech radiometer that simulates the Landsat thematic mapper (TM) and multispectral scanner (MSS) bands, respectively, showed that the separability among the three cover types was substantially improved by the additional and improved spectral features of the Barnes radiometer. Author

A86-36049

EFFECT OF DEW ON CANOPY REFLECTANCE AND TEMPERATURE

P. J. PINTER, JR. (USDA, Water Conservation Laboratory, Phoenix, AZ) Remote Sensing of Environment (ISSN 0034-4257), vol. 19, April 1986, p. 187-205. refs

The diurnal behavior of canopy reflectance and emittance was characterized for six spring wheat cultivars using two ground-based radiometers that had spectral bandpass characteristics similar to the multispectral scanner and thematic mapper radiometers on

Landsats 4 and 5. Nadir measurements of spectral reflectance and emittance were made over well-watered canopies with and without dew to determine its effect on each wavelength interval. The diurnal patterns of reflectances from canopies without dew were symmetric with respect to solar noon. However, when dew was present on canopies, morning reflectances in wavelengths shorter than 0.7 micron and longer than 1.15 microns were significantly different than those observed during the afternoon under similar solar zenith angles. Quantitative measurements of dew density in each cultivar established that moderately high dew levels increased reflectance in visible wavelengths by 40-60 percent and decreased reflectance in wavelengths between 1.15 and 2.35 microns by 25-60 percent. No effect of dew was noted in the near-IR region of the spectrum between 0.7 and 1.1 microns or the thermal IR 10.4-12.5 microns. Author

A86-36084

USE OF MULTITEMPORAL SPECTRAL PROFILES IN AGRICULTURAL LAND-COVER CLASSIFICATION

T. H. C. LO (Alabama, University, University), F. L. SCARPAGE, and T. M. LILLESAND (Wisconsin, University, Madison) Photogrammetric Engineering and Remote Sensing (ISSN 0099-1112), vol. 52, April 1986, p. 535-544. refs

A range of single date and multitemporal classification approaches was compared using Landsat MSS data acquired during the 1979 growing season in the vicinity of Green Bay, WI. In addition to evaluating the traditional supervised and unsupervised classification strategies typically applied in such efforts, an unsupervised multitemporal ratio approach was developed. This involved the use of multitemporal ratioed data in a clustering algorithm sensitive to image texture. A spectral variance threshold for a moving 3 by 3 pixel window in the image data was used to isolate homogeneous areas for cluster center definition. A temporal ratio profile for each cluster center was constructed and then labeled according to the local crop calendar. The paper highlights not only the ease of this procedure, but also its superior accuracy and consistency as compared to the traditional classification procedures tested. The practicality of such multitemporal analyses will be greatly enhanced by the 'on demand' image acquisition features of future satellite systems such as SPOT. Author

A86-36237

EVAPOTRANSPIRATION OVER AN AGRICULTURAL REGION USING A SURFACE FLUX/TEMPERATURE MODEL BASED ON NOAA-AVHRR DATA

O. TACONET, R. BERNARD, and D. VIDAL-MADJAR (Centre de Recherches en Physique de l'Environnement Terrestre et Planetaire, Issy-les-Moulineaux, France) Journal of Climate and Applied Meteorology (ISSN 0733-3021), vol. 25, March 1986, p. 284-307. CNES-supported research. refs

A methodology was developed to infer daily evaporation and soil moisture distribution over large areas. It uses NOAA-7 surface data as input data in a one-dimensional boundary layer/vegetation/soil model based on the formation of Deardorff, which allows the use of a small number of mesoscale surface vegetation parameters. Model sensitivity tests indicate that a single surface temperature measured near midday is sufficient for obtaining the surface energy fluxes over dense vegetation, and for deriving the bulk canopy resistance to evaporation. The ability of the model to predict the area-averaged surface fluxes and canopy resistances over dense vegetation is examined in conjunction with experimental surface flux measurements for three cases over a flat monocultural region (the Beuce in France). Using an empirical expression which relates canopy resistance to root zone water content, an averaged evaluation of the soil moisture can be derived (assuming the absence of a current capability for routine daily soil-moisture observation over an agricultural region). Hence, the spatial gradient of water content between two distinct areas of Beuce is evaluated. K.K.

A86-36697

DETERMINATION OF THE SPECTRAL CHARACTERISTICS OF NATURAL OBJECTS ON TEST RANGES, AND ASPECTS OF THE EFFICIENCY OF SPACE SYSTEMS [OPREDELENIE SPEKTRAL'NYKH KHARAKTERISTIK PRIRODNYKH OB'EKTOV NA POLIGONAKH I VOPROSY EFFEKTIVNOSTI KOSMICHESKIKH SISTEM]

A. M. VOLKOV, ED. and S. G. IAKOVLEV, ED. Leningrad, Gidrometeoizdat (Gosudarstvennyi Nauchno-Issledovatel'skii Tsentr Izucheniia Prirodnykh Resursov, Trudy, No. 24), 1985, 120 p. In Russian. No individual items are abstracted in this volume.

Papers are presented on various aspects of the remote sensing of earth resources. Particular attention is given to the measurement of the reflection characteristics of natural objects using airborne spectrometers; vegetation differentiation according to spectral characteristics; the cost effectiveness of satellite remote-sensing systems; the monitoring of the stability of instruments for measuring the brightness spectral density of natural objects; and the effect of the atmosphere on the spectral brightness of objects during remote sensing in the optical range. B.J.

A86-36783

SMALL FORMAT, OBLIQUE, COLOUR AERIAL PHOTOGRAPHY - AN AID TO THE LOCATION OF METHANE SEEPAGE

P. J. CURRAN (Sheffield, University, England) International Journal of Remote Sensing (ISSN 0143-1161), vol. 7, April 1986, p. 477-479. refs

A86-36789* Lockheed Engineering and Management Services Co., Inc., Houston, Tex.

AN INFORMATION MEASURE FOR CLASS DISCRIMINATION

S. S. SHEN (Lockheed Engineering and Management Services Co., Inc., Houston, TX) and G. D. BADHWAR (NASA, Johnson Space Center, Houston, TX) International Journal of Remote Sensing (ISSN 0143-1161), vol. 7, April 1986, p. 547-556. refs

This article describes a separability measure for class discrimination. This measure is based on the Fisher information measure for estimating the mixing proportion of two classes. The Fisher information measure not only provides a means to assess quantitatively the information content in the features for separating classes, but also gives the lower bound for the variance of any unbiased estimate of the mixing proportion based on observations of the features. Unlike most commonly used separability measures, this measure is not dependent on the form of the probability distribution of the features and does not imply a specific estimation procedure. This is important because the probability distribution function that describes the data for a given class does not have simple analytic forms, such as a Gaussian. Results of applying this measure to compare the information content provided by three Landsat-derived feature vectors for the purpose of separating small grains from other crops are presented. Author

A86-37008* Jet Propulsion Lab., California Inst. of Tech., Pasadena.

FIELD AND AIRBORNE SPECTRAL CHARACTERIZATION OF SUSPECTED DAMAGE IN RED SPRUCE (PICEA RUBENS) FROM VERMONT

B. N. ROCK, J. E. VOGELMANN (California Institute of Technology, Jet Propulsion Laboratory, Pasadena), and D. L. WILLIAMS (NASA, Goddard Space Flight Center, Greenbelt, MD) IN: Machine processing of remotely sensed data - Quantifying global process: Models, sensor systems, and analytical methods; Proceedings of the Eleventh International Symposium, West Lafayette, IN, June 25-27, 1985. New York, Institute of Electrical and Electronics Engineers, 1985, p. 71-81. NASA-supported research. refs

The utilization of remote sensing to monitor forest damage due to acid deposition is investigated. Spectral and water measurements and aircraft radiance data of red spruce and balsam fir, collected in Camels Hump Mountain and Ripton, Vermont between August 13-20, 1984, are analyzed to evaluate the damage levels of the trees. Variations in reflectance features and canopy moisture content are studied. It is observed that damage correlates with elevation (greater damage at higher elevations); xylem water

column tension is greater at higher damage sites; and a 'blue shift' is indicated in the spectral data at high damage sites. I.F.

A86-37014

ADDING SPATIAL CONSIDERATIONS TO THE JABOWA MODEL OF FOREST GROWTH

D. B. BOTKIN, T. E. REYNALES, and K. D. WOODS (California, University, Santa Barbara) IN: Machine processing of remotely sensed data - Quantifying global process: Models, sensor systems, and analytical methods; Proceedings of the Eleventh International Symposium, West Lafayette, IN, June 25-27, 1985. New York, Institute of Electrical and Electronics Engineers, 1985, p. 141-148. refs

Classical ecological questions about the nature of communities and spatial pattern in vegetation may be answered through the integration of data from remote sensing with ecosystem simulation models. JABOWA and related forest growth models have successfully simulated small plots but are not adequate for large-area projections. Study of vegetation pattern requires selection of an appropriate spatial resolution of 'grain size', which should be guided by the ecological phenomena studied and an understanding of the effects of adjacent units on one another. A forest sample plot size of 0.1 hectare is proposed as both ecologically appropriate and consistent with available resolution from remote sensing devices. The rationale and methodology for transforming JABOWA from a non-spatial 'gap' model to a model with the capacity to simulate the growth of spatially-related forest plots are discussed. Author

A86-37015

DETECTION OF BIOMASS BY AN EMPIRIC ALBEDO AND SPECTRAL REFLECTANCE MODEL IN THE SAHARA DESERT FROM LANDSAT-IMAGERY

M. C. MUEKSCH (Bonn, Universitaet, West Germany) IN: Machine processing of remotely sensed data - Quantifying global process: Models, sensor systems, and analytical methods; Proceedings of the Eleventh International Symposium, West Lafayette, IN, June 25-27, 1985. New York, Institute of Electrical and Electronics Engineers, 1985, p. 149-156. refs

A86-37016* Wisconsin Univ., Madison.

MODELING THE CONTROLS OF FOREST PRODUCTIVITY USING CANOPY VARIABLES

J. D. ABER and J. FOWNES (Wisconsin, University, Madison) IN: Machine processing of remotely sensed data - Quantifying global process: Models, sensor systems, and analytical methods; Proceedings of the Eleventh International Symposium, West Lafayette, IN, June 25-27, 1985. New York, Institute of Electrical and Electronics Engineers, 1985, p. 157-161. Research supported by the University of Wisconsin. refs (Contract NCA2-IR-865-401)

A framework is presented by which a generalized, canopy-driven model of biogeochemical cycling in forest ecosystems may be produced. Recent research results demonstrating relationships between canopy characteristics and important ecosystem processes are used to support this approach. Most relationships hold across species groups and suggest that identification of species may not be crucial. Linking this type of model to remote sensing will depend on developing the capability to measure a few key morphological and chemical parameters of whole forest canopies by reflectance characteristics. Author

01 AGRICULTURE AND FORESTRY

A86-37018* National Aeronautics and Space Administration. National Space Technology Labs., Bay Saint Louis, Miss.
ANALYSIS OF DATA ACQUIRED BY SHUTTLE IMAGING RADAR SIR-A AND LANDSAT THEMATIC MAPPER OVER BALDWIN COUNTY, ALABAMA

S.-T. WU (NASA, National Space Technology Laboratories, Bay Saint Louis, MS) IN: Machine processing of remotely sensed data - Quantifying global process: Models, sensor systems, and analytical methods; Proceedings of the Eleventh International Symposium, West Lafayette, IN, June 25-27, 1985. New York, Institute of Electrical and Electronics Engineers, 1985, p. 173-182. refs

Seasonally compatible data collected by SIR-A and by Landsat 4 TM over the lower coastal plain in Alabama were coregistered, forming a SIR-A/TM multichannel data set with 30 m x 30 m pixel size. Spectral signature plots and histogram analysis of the data were used to observe data characteristics. Radar returns from pine forest classes correlated highly with the tree ages, suggesting the potential utility of microwave remote sensing for forest biomass estimation. As compared with the TM-only data set, the use of SIR-A/TM data set improved classification accuracy of the seven land cover types studied. In addition, the SIR-A/TM classified data support previous finding by Engheta and Elachi (1982) that microwave data appear to be correlated with differing bottomland hardwood forest vegetation as associated with varying water regimens (i.e., wet versus dry). I.S.

A86-37020
INTEGRATION OF HIGH AND LOW RESOLUTION SATELLITE DATA FOR CROP CONDITION ASSESSMENT

R. J. BROWN and C. PREVOST (Canada Centre for Remote Sensing, Ottawa) IN: Machine processing of remotely sensed data - Quantifying global process: Models, sensor systems, and analytical methods; Proceedings of the Eleventh International Symposium, West Lafayette, IN, June 25-27, 1985. New York, Institute of Electrical and Electronics Engineers, 1985, p. 189-196. refs

Landsat multispectral scanner (MSS) and NOAA Advanced Very High Resolution Radiometer (AVHRR) imagery were registered and the radiances from several sites were measured. The Landsat data were used to assess which ground cover types were contributing to the AVHRR radiance values and to evaluate the effect nongrain classes would have on estimating grain crop condition. It is seen that great care must be taken in directly comparing areas within one data source with different crop mixes and vegetation classes since the total contribution of the grains to the vegetation index, as measured by the AVHRR, can be less than 40 percent. However, reliable use can be made of the AVHRR data if a comparison is made from year to year for a particular region. Author

A86-37025
SEMI-OPERATIONAL IDENTIFICATION OF AGRICULTURAL CROPS FROM AIRBORNE SLAR-DATA

P. BINNENKADE (Nationaal Lucht- en Ruimtevaartlaboratorium, Amsterdam, Netherlands), H. W. J. VAN KASTEREN, and D. UENK (Centrum voor Agrobiologisch Onderzoek, Wageningen, Netherlands) IN: Machine processing of remotely sensed data - Quantifying global process: Models, sensor systems, and analytical methods; Proceedings of the Eleventh International Symposium, West Lafayette, IN, June 25-27, 1985. New York, Institute of Electrical and Electronics Engineers, 1985, p. 241-247. refs

The 1984-airborne SLAR campaign of the Dutch ROVE-team is discussed. Through preprocessing, segmentation, and pseudohierarchical classification a multitemporal data set of three test sites is treated for identification of potatoes and other agricultural crops. Author

A86-37034* National Aeronautics and Space Administration. National Space Technology Labs., Bay Saint Louis, Miss.
AGRICULTURAL APPLICATIONS FOR THERMAL INFRARED MULTISPECTRAL SCANNER DATA

R. E. PELLETIER, M. C. OCHOA (NASA, National Space Technology Laboratories, Bay Saint Louis, MS), and B. F. HAJEK (Auburn University, AL) IN: Machine processing of remotely sensed data - Quantifying global process: Models, sensor systems, and analytical methods; Proceedings of the Eleventh International Symposium, West Lafayette, IN, June 25-27, 1985. New York, Institute of Electrical and Electronics Engineers, 1985, p. 321-328. refs

The use of the Thermal Infrared Multispectral Scanner (TIMS) data in agricultural landscapes is discussed. The TIMS allows for narrow-band analysis in the 8.2-11.6 micron range at spatial resolutions down to 5 meters in cell size. A coastal plain region in SE Alabama was studied using the TIMS. The crop/plant vigor, canopy density, and thermal response changes for soils obtained from thermal imagery are examined. The application of TIMS data to hydrologic and topographic issues, inventory and conservation monitoring, and the enhancement and extraction of cartographic features is described. I.F.

A86-37035
THE TASSELED CAP - SIZE, SHAPE AND ORIENTATION CHANGES DUE TO SOIL BACKGROUND

A. R. HUETE (Arizona, University, Tucson) and R. D. JACKSON (USDA, Water Conservation Laboratory, Phoenix, AZ) IN: Machine processing of remotely sensed data - Quantifying global process: Models, sensor systems, and analytical methods; Proceedings of the Eleventh International Symposium, West Lafayette, IN, June 25-27, 1985. New York, Institute of Electrical and Electronics Engineers, 1985, p. 329-337. refs

The empirical domain of the Tasseled Cap Graphic Model was examined in the soil brightness-plant greenness plane. Individual, soil-specific tasseled caps were derived for four different soil types with similar plant canopy conditions in order to analyze soil background influences on greenness results. The size, shape and orientation of these tasseled caps were strongly dependent on soil type, and greenness results for identical plant canopy conditions were not reproducible across tasseled caps. Greenness was comparable only when individual tasseled caps were scaled to similar sizes. In contrast to the global tasseled cap, soil-specific models significantly improved vegetation assessment, particularly at low green canopy covers. Author

A86-37036
WAVELENGTH INTENSITY INDICES IN RELATION TO TREE CONDITION AND LEAF-NUTRIENT CONTENT

S.-F. SHIH, D. L. MYHRE, G. J. EDWARDS, C. H. BLAZQUEZ, and J. M. GARDNER (Florida, University, Gainesville) IN: Machine processing of remotely sensed data - Quantifying global process: Models, sensor systems, and analytical methods; Proceedings of the Eleventh International Symposium, West Lafayette, IN, June 25-27, 1985. New York, Institute of Electrical and Electronics Engineers, 1985, p. 350-356. refs

As an alternative to assessing occurrence of citrus blight with conventional techniques, wavelength intensity indices were used to estimate tree health status and the leaf contents of Zn, Na, K, Mg, Ca, P, Cu, and Al. The results of chemical analysis showed that the leaves of declined trees have a tendency to be low in K and Mg and high in Na, Ca, and Al. Photographs made with infrared film were analyzed by densitometry. On the basis of statistical analysis, the parameters of wavelength intensity indices correlating most strongly with either the leaf nutrient content or the tree health status were selected. I.S.

A86-39002* Purdue Univ., West Lafayette, Ind.
SUN ANGLE, VIEW ANGLE, AND BACKGROUND EFFECTS ON SPECTRAL RESPONSE OF SIMULATED BALSAM FIR CANOPIES

K. J. RANSON, C. S. T. DAUGHTRY, and L. L. BIEHL (Purdue University, West Lafayette, IN) Photogrammetric Engineering and Remote Sensing (ISSN 0099-1112), vol. 52, May 1986, p. 649-658. refs

(Contract NAS9-16528)

An experiment is described that examines the effects of solar zenith angle and background reflectance on the composite scene reflectance of small balsam fir (*Abies balsamea* (L.) Mill.) arranged in different densities. In this study, the shape, density, and, consequently, the needle area index and phytomass of the canopies, as well as the background reflectance, were controlled. The effects of sun angle, view angle, and background reflectance on the multispectral response of small balsam fir trees were significant. Regression models relating spectral vegetation indices (i.e., normalized difference (ND) and greenness (GR) to phytomass) showed very poor relationships for balsam fir canopies with a grass background. However, strong linear relationships were found for ND and GR with phytomass for a background that simulated the reflectance of snow. Changing solar zenith angle significantly affected the models relating ND to phytomass for the snow background, but was not significant in the model relating GR to phytomass for the snow background Author

A86-39003* Washington Univ., St. Louis, Mo.
USE OF SIR-A AND LANDSAT MSS DATA IN MAPPING SHRUB AND INTERSHRUB VEGETATION AT KOONAMORE, SOUTH AUSTRALIA

G. M. GREEN (Washington University, St. Louis, MO) Photogrammetric Engineering and Remote Sensing (ISSN 0099-1112), vol. 52, May 1986, p. 659-670. refs
 (Contract JPL-956427; JPL-956515)

Shrublands cover much of the interior of the Australian continent and support a large grazing industry. Distinguishing the woody perennial vegetation from the smaller herbaceous vegetation and soil-encrusting lichen found between the shrubs is critical for range management but is difficult to do using Landsat data alone. In this study Shuttle Imaging Radar-A (SIR-A) and Landsat data acquired over Koonamore Station are examined together. Given the low topography and fine textured soils at Koonamore, radar return should be primarily determined by the percent area occupied by shrubs. During periods when most of the vegetation was non-vigorous and spectrally homogeneous, SIR-A data, as a surrogate measure of shrub cover, allowed the reflectance due to shrubs in Landsat data to be separated from the reflectance due to the intervening ground. This method allows estimation of the intershrub reflectance properties that are related to herbaceous vegetation, lichen, and bare soil exposures. Author

A86-39006
PREDICTING TREE GROUNDLINE DIAMETER FROM CROWN MEASUREMENTS MADE ON 35-MM AERIAL PHOTOGRAPHY

G. F. HAGAN (Purdue University, West Lafayette, IN) and J. L. SMITH (Virginia Polytechnic Institute and State University, Blacksburg) Photogrammetric Engineering and Remote Sensing (ISSN 0099-1112), vol. 52, May 1986, p. 687-690. refs

A86-39146* National Aeronautics and Space Administration. Goddard Space Flight Center, Greenbelt, Md.

DIRECTIONAL REFLECTANCE RESPONSE IN AVHRR RED AND NEAR-IR BANDS FOR THREE COVER TYPES AND VARYING ATMOSPHERIC CONDITIONS

B. HOLBEN, D. KIMES, and R. S. FRASER (NASA, Goddard Space Flight Center, Greenbelt, MD) Remote Sensing of Environment (ISSN 0034-4257), vol. 19, June 1986, p. 213-236. refs

Surface directional red and near-infrared reflectances of bare soil, orchard grass, and fescue were extracted from a multitemporal data set to correspond to NOAA-7 Advanced Very High Resolution Radiometer (AVHRR) scanning and illumination geometry at 30 deg latitude. Radiances were simulated at satellite altitude and a

ratio vegetation index was calculated. The results show that off-nadir directional reflectance measured at the surface in the red and near-IR portions of the spectrum are approximately maintained with AVHRR viewing and illumination characteristics. The two-channel reflectance response is such that the ratio vegetation index is more constant with scan angle and atmospheric conditions than individual channels. It is shown that inclusion of atmospheric and surface reflectance data can greatly improve interpretation of AVHRR data, when knowledge of the range of atmospheric conditions and approximate directional reflectances of major cover types are known. Author

A86-39147
SEPARATION OF SOIL-PLANT SPECTRAL MIXTURES BY FACTOR ANALYSIS

A. R. HUETE (Arizona, University, Tucson) Remote Sensing of Environment (ISSN 0034-4257), vol. 19, June 1986, p. 237-251. refs

A factor-analytic inversion model is presented which enables a data set of spectral mixtures to be decomposed into the sum of unique reflecting components weighted by their corresponding amounts. Spectral mixtures are decomposed into abstract eigenspectra and eigenvector matrices. The eigenspectra are then transformed into pure component spectral signature through a target testing procedure that allows one to individually search for the presence of ground reflecting features. Soil-plant mixtures with variable soil moisture and plant densities were successfully decomposed into dry soil, wet soil, and vegetation components and their respective amounts in all spectral mixtures were determined. Potential uses of factor analysis in soil identification and biomass assessment are discussed. Author

A86-39148* National Aeronautics and Space Administration. Goddard Space Flight Center, Greenbelt, Md.

ANALYSIS OF A RESISTANCE-ENERGY BALANCE METHOD FOR ESTIMATING DAILY EVAPORATION FROM WHEAT PLOTS USING ONE-TIME-OF-DAY INFRARED TEMPERATURE OBSERVATIONS

B. J. CHOUDHURY (NASA, Goddard Space Flight Center, Greenbelt, MD), S. B. IDSO, and R. J. REGINATO (USDA, Water Conservation Laboratory, Phoenix, AZ) Remote Sensing of Environment (ISSN 0034-4257), vol. 19, June 1986, p. 253-268. refs

Accurate estimates of evaporation over field-scale or larger areas are needed in hydrologic studies, irrigation scheduling, and meteorology. Remotely sensed surface temperature might be used in a model to calculate evaporation. A resistance-energy balance model, which combines an energy balance equation, the Penman-Monteith (1981) evaporation equation, and van den Honert's (1948) equation for water extraction by plant roots, is analyzed for estimating daily evaporation from wheat using postnoon canopy temperature measurements. Additional data requirements are half-hourly averages of solar radiation, air and dew point temperatures, and wind speed, along with reasonable estimates of canopy emissivity, albedo, height, and leaf area index. Evaporation fluxes were measured in the field by precision weighing lysimeters for well-watered and water-stressed wheat. Errors in computed daily evaporation were generally less than 10 percent, while errors in cumulative evaporation for 10 clear sky days were less than 5 percent for both well-watered and water-stressed wheat. Some results from sensitivity analysis of the model are also given. Author

A86-39149* Kansas Univ. Center for Research, Inc., Lawrence.
IDENTIFICATION OF MAJOR BACKSCATTERING SOURCES IN TREES AND SHRUBS AT 10 GHZ

R. ZOUGHI, L. K. WU, and R. K. MOORE (University of Kansas Center for Research, Inc., Lawrence) Remote Sensing of Environment (ISSN 0034-4257), vol. 19, June 1986, p. 269-290. refs

(Contract NAG5-271)

A short-range very-fine-resolution FM-CW radar scatterometer has been used to identify the primary contributors to 10-GHz radar

01 AGRICULTURE AND FORESTRY

backscatter from pine, pin oak, American sycamore and sugar maple trees, and from creeping juniper shrubs. This system provided a range resolution of 11 cm and gave a 16-cm diameter illumination area at the target range of about 4 m. For a pine tree, the needles caused the strongest backscatter as well as the strongest attenuation in the radar signal. Cones, although insignificant contributors to the total backscatter, were more important for backscattering than for attenuation. For the rest of the trees, leaves were the strongest cause of backscattering and attenuation. However, in the absence of leaves, the petioles, small twigs, and branches gave relatively strong backscatter. For American sycamore and sugar maple trees, the fruits did not affect the total backscatter unless they were packed in clusters. For creeping juniper the backscattered energy and attenuation in the radar signal were mainly due to the top two layers of the evergreen scales. The contribution of the tree trunks was not determined.

Author

N86-23994*# Delaware Univ., Newark. Coll. of Marine Studies.
REMOTE SENSING INVESTIGATIONS OF WETLAND BIOMASS AND PRODUCTIVITY FOR GLOBAL BIOSYSTEMS RESEARCH Final Technical Report, 1 Nov. 1982 - 1 Apr. 1986
V. KLEMAS 15 Apr. 1986 25 p refs
(Contract NAGW-374)
(NASA-CR-176725; NAS 1.26:176725) Avail: NTIS HC A02/MF A01 CSCL 08B

The relationship between spectral radiance and plant canopy biomass was studied in wetlands. Spectroradiometer data was gathered on Thematic Mapper wavebands 3, 4, and 5, and correlated with canopy and edaphic factors determined by harvesting. The relationship between spectral radiance and plant canopy biomass for major salt and brackish canopy types was determined. Algorithms were developed for biomass measurement in mangrove swamps. The influence of latitudinal variability in canopy structure on biomass assessment of selected plants was investigated. Brackish marsh biomass estimates were obtained from low altitude aircraft and compared with ground measurements. Annual net aerial primary productivity estimates computed from spectral radiance data were compiled for a *Spartina alterniflora* marsh. Spectral radiance data were expressed as vegetation or infrared index values. Biomass estimates computed from models were in close agreement with biomass estimates determined from harvests.

Author

N86-23995*# Operations Research, Inc., Landover, Md.
EOS RADIOMETER CONCEPTS FOR SOIL MOISTURE REMOTE SENSING Final Report
J. CARR 10 Feb. 1986 175 p
(Contract NAS5-28648)
(NASA-CR-177854; NAS 1.26:177854) Avail: NTIS HC A08/MF A01 CSCL 08B

Preliminary work with aperture synthesis concepts for EOS is reported. The effects of nonvanishing bandwidths on image reconstruction in aperture synthesis system was studied. It is found that nonvanishing bandwidths introduce errors in off-axis pixels when naive Fourier processing is used. The net effect is for bandwidth to limit sensor field-of-view. To quantify this effect a computer program was written which is documented. Example runs are included which illustrate the resultant radiometric errors and effective fields-of-view for a plausible simple sensor.

Author

N86-25032# National Aeronautics and Space Administration.
National Space Technology Labs., Bay Saint Louis, Miss.
DUCKS UNLIMITED JOINT RESEARCH PROJECT Final Report
C. L. HILL Dec. 1985 175 p refs
(NASA-TM-88755; NAS 1.15:88755; ERL-238) Avail: NTIS HC A08/MF A01 CSCL 13B

The feasibility of using LANDSAT thematic mapper (TM) data and geographic information system technology as part of a waterfowl habitat inventory and assessment program was determined. The TM data analysis offers interesting results in wetland mapping. The best technique is the one that utilizes a distance derived mask as input to a modified orthogonal

parallelepiped classifier. The classification technique (CLPIPE) and the statistical software module (FIND) are incorporated into a production software runstream (DUCK.CAN). The production runstream allows analysis with geographically referenced raw data, to complete the classification process, develop statistical reports, and produce final output products in the form of maps and tables. It is concluded that the TM has the capability to spectrally identify wetland categories.

E.A.K.

N86-25034*# Jet Propulsion Lab., California Inst. of Tech., Pasadena.
CONCEPTUAL DESIGN STUDY: FOREST FIRE ADVANCED SYSTEM TECHNOLOGY (FFAST)
J. D. NICHOLS and J. R. WARREN (Department of Agriculture, Washington, D.C.) 15 Feb. 1986 132 p refs
(Contract NAS7-918)
(JPL-PUBL-86-5; NAS 1.26:177214; NASA-CR-177214) Avail: NTIS HC A07/MF A01 CSCL 02F

An integrated forest fire detection and mapping system that will be based upon technology available in the 1990s was defined. Uncertainties in emerging and advanced technologies related to the conceptual design were identified and recommended for inclusion as preferred system components. System component technologies identified for an end-to-end system include thermal infrared, linear array detectors, automatic georeferencing and signal processing, geosynchronous satellite communication links, and advanced data integration and display. Potential system configuration options were developed and examined for possible inclusion in the preferred system configuration. The preferred system configuration will provide increased performance and be cost effective over the system currently in use. Forest fire management user requirements and the system component emerging technologies were the basis for the system configuration design. A preferred system configuration was defined that warrants continued refinement and development, examined economic aspects of the current and preferred system, and provided preliminary cost estimates for follow-on system prototype development.

B.G.

N86-25863*# National Aeronautics and Space Administration.
National Space Technology Labs., Bay Saint Louis, Miss.
TIMBER RESOURCES INVENTORY AND MONITORING JOINT RESEARCH PROJECT
C. L. HILL Oct. 1985 35 p refs Prepared in cooperation with International Paper Co., Tuxedo Park, N.Y. Original contains color illustrations
(NASA-TM-88754; NAS 1.15:88754; ERL-237) Avail: NTIS HC A03/MF A01 CSCL 02F

Primary objectives were to develop remote sensing analysis techniques for extracting forest related information from LANDSAT Multispectral Scanner (MMS) and Thematic Mapper data and to determine the extent to which International Paper Company information needs can be addressed with remote sensing information. The company actively manages 8.4 million acres of forest land. Traditionally, their forest inventories, updated on a three year cycle, are conducted through field surveys and aerial photography. The results reside in a digital forest data base containing 240 descriptive parameteres for individual forest stands. The information in the data base is used to develop seasonal and long range management strategies. Forest stand condition assessments (species composition, age, and density stratification) and identification of silvicultural activities (site preparation, planting, thinning, and harvest) are addressed.

B.G.

02 ENVIRONMENTAL CHANGES AND CULTURAL RESOURCES

N86-26666# Instituto de Pesquisas Espaciais, Sao Jose dos Campos (Brazil).

A PROPOSAL FOR A PROJECT ENTITLED ASSESSMENT OF FOREST RESOURCES IN URUGUAY SUBMITTED TO THE UNITED NATIONS INDUSTRIAL DEVELOPMENT ORGANIZATION (UNIDO)

R. A. NOVAES, D. C. L. LEE, P. H. FILHO, A. PACHECODOSSANTOS, and F. J. PONZONI Mar. 1986 13 p (INPE-3828-NTE/255) Avail: NTIS HC A02/MF A01

This project proposal was submitted by request of the United Nations Industrial Development Organization (UNIDO). The main objective is to collect basis forest information for the development, promotion, and utilization of alternative sources of energy through the use of Uruguay's national resources and to define the value of LANDSAT-TM as an aid in efficient management of the country's plantations. An additional objective is to train the Uruguayan technical team. Indications are given as to how each task will be accomplished and what techniques will be employed in performing main tasks such as: forest mapping and development of map legends, map accuracy assessment and forest area correction, stand timber volume evaluation, field sampling, and mensuration procedures. Flow diagrams of the overall project, activity bar diagrams, and list of equipment required for task completion are included. The expected results of the map products and timber volumes are discussed. Author

N86-26667# Instituto de Pesquisas Espaciais, Sao Jose dos Campos (Brazil).

WHEAT AREA ESTIMATION USING DIGITAL LANDSAT MSS DATA AND AERIAL PHOTOGRAPHS

M. A. MOREIRA, S. C. CHEN, and G. T. BATISTA Mar. 1986 28 p Submitted for publication (INPE-3824-PRE/900) Avail: NTIS HC A03/MF A01

A procedure to estimate wheat (*Triticum aestivum* L) area using sampling technique based on aerial photographs and digital LANDSAT MSS data was developed. Aerial photographs covering 720 sq km were visually analyzed. Computer classification of LANDSAT MSS data acquired on Sept. 4, 1979 was done using unsupervised and supervised algorithms and classification results were spatially filtered using a post-processing technique. To estimate wheat area, a regression approach was applied using different sample sizes and various sampling units. Based on four decision criteria proposed in this study, it was concluded that: (1) as the size of sampling unit decreased, the percentage of sample area required to obtain similar estimation performance also decreased; (2) the lowest percentage of the area sampled for wheat estimation under established precision and accuracy criteria through regression estimation was 13.09% using 10 sq km as the sampling unit; and (3) wheat area estimation obtained by regression estimation was more precise and accurate than those obtained by direct expansion method. Author

N86-26674# Institute for Land and Water Management Research, Wageningen (Netherlands). Subfaculteit Wiskunde en Informatica.

A MULTIINDEX MULTITEMPORAL APPROACH TO MAP CROPS IN THE EARLY GROWING SEASON: AN APPLICATION TO TWO ITALIAN IRRIGATION DISTRICTS: EAST SESIA AND GRANDE BONIFIGA FERRARESE

M. S. DOTT and S. AZZALI May 1985 42 p Sponsored by European Economic Commission (ICW-1611; ESA-86-96955) Avail: NTIS HC A03/MF A01

The feasibility of a method to determine quality, quantity, and type of crops and their water stress by LANDSAT images was tested in two irrigation districts in the Po valley, Italy. In spite of striking misestimates, results are promising, 5 out of 11 crops being detected. However, the uncertain number of yearly available images and lack of reference data to tune the method inhibit the operational development of this tool. It is emphasized that the feasibility of mapping individual crops by means of LANDSAT-MSS data is definitely proven in principle. A semioperational use of such data would provide an opportunity to iron out practical details

and assess the amount of needed ancillary and ground-reference data, given the required accuracy of determination. ESA

N86-27698*# Maryland Univ., College Park. Office of Sponsored Programs.

DEPARTMENT OF GEOLOGY/NASA-GSFC GEOBOTANICAL INVESTIGATION Summary Report

26 May 1986 10 p refs (Contract NSG-5423) (NASA-CR-177300; NAS 1.26:177300) Avail: NTIS HC A02/MF A01 CSCL 02F

Geobotanical mapping in the southern Appalachians and soil metal associated changes in vegetation spectral responses in the reflective and emissive portions of the electromagnetic spectrum (EMS) is studied. It is determined whether deciduous forest vegetation reflection and emission characteristics show detectable changes that can be related to residual soil characteristics. Analyses of such related characteristics enhances the ability to discriminate underlying lithologies as well as variances within lithologies associated with natural heavy metal occurrences. An understanding is developed of the factors which contribute to the differing spectral signatures of various lithology/soil types. A combination of field data and remote spectral analysis is studied. E.R.

N86-27704*# Pennsylvania State Univ., University Park. Dept. of Meteorology.

PRELIMINARY ASSESSMENT OF SOIL MOISTURE OVER VEGETATION Final Report, 1 Mar. 1985 - 28 Feb. 1986

T. N. CARLSON Jul. 1986 40 p (Contract NAG5-184) (NASA-CR-177226; NAS 1.26:177226) Avail: NTIS HC A03/MF A01 CSCL 08M

Modeling of surface energy fluxes was combined with in-situ measurement of surface parameters, specifically the surface sensible heat flux and the substrate soil moisture. A vegetation component was incorporated in the atmospheric/substrate model and subsequently showed that fluxes over vegetation can be very much different than those over bare soil for a given surface-air temperature difference. The temperature signatures measured by a satellite or airborne radiometer should be interpreted in conjunction with surface measurements of modeled parameters. Paradoxically, analyses of the large-scale distribution of soil moisture availability shows that there is a very high correlation between antecedent precipitation and inferred surface moisture availability, even when no specific vegetation parameterization is used in the boundary layer model. Preparatory work was begun in streamlining the present boundary layer model, developing better algorithms for relating surface temperatures to substrate moisture, preparing for participation in the French HAPEX experiment, and analyzing aircraft microwave and radiometric surface temperature data for the 1983 French Beauce experiments. B.G.

02

ENVIRONMENTAL CHANGES AND CULTURAL RESOURCES

Includes land use analysis, urban and metropolitan studies, environmental impact, air and water pollution, geographic information systems, and geographic analysis.

A86-30195

REMOTE SENSING FOR DEVELOPING COUNTRIES - A CASE STUDY OF TUNISIA

A. HAMZA (Ministry of Agriculture, Soils Directorate, Tunis, Tunisia) International Journal of Remote Sensing (ISSN 0143-1161), vol. 7, Feb. 1986, p. 283-286.

The use of satellite remote sensing for the technological and economic advancement of developing countries is examined. The

02 ENVIRONMENTAL CHANGES AND CULTURAL RESOURCES

development of a country is achieved by quantitative and qualitative knowledge of resources, exploitation and management of these resources, and control of the resources. Remote sensing data are studied in order to evaluate and control the resources of developing nations. The national and international remote sensing strategies and infrastructures required for developing countries to successfully employ remote sensing technology are described. Examples of remote-sensing application studies in Tunisia are given. I.F.

A86-30974

POSSIBILITY OF SMALL-SCALE PHYSICOGEOGRAPHICAL REGIONALIZATION USING SPACE SPECTROMETRY DATA [O VOZMOZHNOСТИ MELKOMASSHTABNOGO FIZIKO-GEORAFICHESKOGO RAIONIROVANIIA PO DANNYM KOSMICHESKOGO SPEKTROMETRIROVANIIA]

L. I. KISELEVSKII, B. I. BELIAEV, V. E. PLIUTA, and S. G. SINIAKOVICH (AN BSSR, Institut Fiziki, Minsk, Belorussian SSR) Akademiia Nauk SSSR, Doklady (ISSN 0002-3264), vol. 286, no. 5, 1986, p. 1236-1240. In Russian.

Small scale physico-geographical regionalization has been demonstrated using Salyut-4 spectrometry data in the 0.4-0.8 micron range. The study involved boundary definition according to optical-field differences in the case of gradual transitions between physico-geographic zones. The data analyzed covered forest, forest-steppe, steppe, semiarid, and mountainous areas. B.J.

A86-32537

DETECTING DESERT LOCUST BREEDING GROUNDS IN THE SAHEL WITH SATELLITE DATA

P. V. RIGTERINK (Computer Sciences Corp., Silver Spring, MD) IN: EASCON '85: National space strategy - A progress report; Proceedings of the Eighteenth Annual Electronics and Aerospace Systems Conference, Washington, DC, October 28-30, 1985. New York, Institute of Electrical and Electronics Engineers, Inc., 1985, p. 141-143. refs

The problem of detecting desert locust breeding grounds in the Sahel region of Africa with satellite data is reviewed. Early information demonstrated the feasibility of a variety of techniques which were only marginally cost-effective. Recently, a number of scientists have realized that the AVHRR sensor on the NOAA series of satellites will provide appropriate data at a reasonable price. This paper will describe various techniques for processing these data and recommend an approach for future data processing. Author

A86-33595

APPROACHES TO COMPUTER REASONING IN REMOTE SENSING AND GEOGRAPHIC INFORMATION PROCESSING - A SURVEY

P. H. SWAIN (Purdue University, West Lafayette, IN) IN: 1985 International Geoscience and Remote Sensing Symposium (IGARSS '85), Amherst, MA, October 7-9, 1985, Digest. Volume 2. New York, Institute of Electrical and Electronics Engineers, Inc., 1985, p. 687-692. refs (Contract NSF ECS-84-00324)

A survey is given of a number of approaches to computerized reasoning which have been or might be applied to multi-attribute geographic data. Possible low level reasoning methods include: the stacked vector approach, source-specific prior probabilities and a generalization of that approach by Swain et al. (1985), and a contextual classification method. An expert system for change detection represents a possible implementation of higher level reasoning. Possible future directions that such research might take are indicated. D.H.

A86-33643

RESOURCE MONITORING ORIENTED REMOTE SENSING DATA PROCESSING CAPABILITIES

K. STAENZ, E. H. MEIER, D. R. NUESCH, K. I. ITTEN, and H. HAEFNER (Zuerich, Universitaet, Zurich, Switzerland) IN: 1985 International Geoscience and Remote Sensing Symposium (IGARSS '85), Amherst, MA, October 7-9, 1985, Digest. Volume 2. New York, Institute of Electrical and Electronics Engineers, Inc., 1985, p. 1109-1116. refs

Digital image processing capabilities of the University of Zurich are demonstrated with particular emphasis on two image analysis systems, called IBIS and DIPS. In addition, an overview is given over the most important projects (research, development, and applications) conducted in the past as well as currently under way. Further needs in connection with the resource monitoring tasks are discussed. Author

A86-36513

THE POSSIBILITY OF APPLYING DIFFERENT TYPES OF IMAGE-ANALYSIS SOFTWARE TO ENVIRONMENT-PROTECTION PROBLEMS [VOZMOZHNOСТИ PRIMENENIIA RAZNORODNOGO PROGRAMMNOGO OBESPECHENIIA ANALIZA IZOBRAZHENII DLIA ZADACH OKHRANY OKRUZHAIUSHCHEI SREDY]

A. D. KITOV IN: Methods of combined air and space remote-sensing studies of Siberia. Novosibirsk, Izdatel'stvo Nauka, 1985, p. 63-69. In Russian. refs

Software-requirements for an environment-protection approach that employs remote monitoring are formulated for the specific example of pollutant emissions from power plants. Information on existing image-processing software is presented, and the applicability of this software to environment protection is discussed. B.J.

A86-37011

A MEASURING REFERENCE SYSTEM TO QUANTIFY THE DESERTIFICATION PROCESS IN A SEMIARID ECOSYSTEM BASED ON LANDSAT MSS DATA

J. C. DE LA TORRE, J. H. SASSER, and J. LIRA (Direccion General de Geografia, Mexico City, Mexico) IN: Machine processing of remotely sensed data - Quantifying global process: Models, sensor systems, and analytical methods; Proceedings of the Eleventh International Symposium, West Lafayette, IN, June 25-27, 1985. New York, Institute of Electrical and Electronics Engineers, 1985, p. 112-121. refs

Landsat MSS data of a 3600 sq km test site in Mexico, collected over a 9 years period, are used to evaluate the state and rate of change of desertification. A desertification model is derived from the mean albedo and mean information content of the target system. The applicability of the model is verified in three experiments. The first experiment simulated the process of desertification by analyzing a 64 x 64 pixel window, the second utilized a set of 64 x 64 pixel windows, and the third experiment tested the capability of the model to measure the state and progression of desertification. It is observed that albedo and information content are important indicators of desertification. I.F.

A86-38677

ENVIRONMENT AND CLIMATE [OKRUZHAIUSHCHAIIA SREDA I KLIMAT]

K. IA. KONDRATEV Leningrad, Obshchestvo Znanie RSFSR, 1985, 32 p. In Russian. refs

The book is concerned with the effect of the pollution of the atmosphere, water basins, and soil on global climate. It is shown that the most significant changes in climate are associated with an increase in the concentration of carbon dioxide and other optically active small gas components. The increasing carbon dioxide concentration contributes to the greenhouse effect, leading to a general warming of the climate. The discussion also covers space-based observations of environmental changes, global ecological monitoring, and the climate of planets. V.L.

02 ENVIRONMENTAL CHANGES AND CULTURAL RESOURCES

N86-24034# Army Cold Regions Test Center, APO Seattle, Wash. 98733.

VEGETATION AND ENVIRONMENTAL GRADIENTS OF THE PRUDHOE BAY REGION, ALASKA

D. A. WALKER Sep. 1985 238 p
(AD-A162022; CRREL-85-14) Avail: NTIS HC A11/MF A01
CSCL 06C

The following topics are discussed: description of the region (topography, geology, climate, soils, wildlife, oil-field facilities, environmental impacts); microscale gradients; plant communities along the major microscale gradients, aerial analysis of vegetation and other geobotanical units, influence of microscale patterns on soil factors and individual plant taxa; mesoscale gradients; macroscale gradients; floristic analysis; growth of *salix lanata* along the summer temperature gradient; annotated plant checklist for the Prudhoe Bay region; environmental and species data for the permanent study plots; environmental and vegetation data summaries for all stand types; supplementary floristic data. GRA

N86-25036# EG and G Energy Measurements, Inc., Las Vegas, Nev.

COMPREHENSIVE INTEGRATED REMOTE SENSING FOR US DEPARTMENT OF ENERGY APPLICATIONS

L. R. TINNEY and J. G. LACKEY 1985 10 p refs Presented at the International Conference on Man's Role in Changing the Global Environment, Venice, Italy, 21 Oct. 1985
(Contract DE-AC08-83NV-10282)
(DE86-002101; EGG-10282-1096; CONF-8510222-1) Avail:
NTIS HC A02/MF A01

A major remote sensing program of the Department of Energy (DOE) is described and examples of processed data are presented. The program is termed Comprehensive Integrated Remote Sensing, or CIRS, and involves equipment and personnel of the DOE Remote Sensing Laboratory. Data is being collected to support environmental and emergency response functions for large DOE sites. Integration of the data is being enhanced by implementation of a geographic information system. DOE

N86-26669*# Kansas Univ. Center for Research, Inc., Lawrence. Space Technology Center.

RESEARCH ON ENHANCING THE UTILIZATION OF DIGITAL MULTISPECTRAL DATA AND GEOGRAPHIC INFORMATION SYSTEMS IN GLOBAL HABITABILITY STUDIES Final Report, 1985-1986

E. A. MARTINKO and J. W. MERCHANT Feb. 1986 60 p
Sponsored in part by the Kansas Fish and Game Commission
(Contract NGL-17-004-024)
(NASA-CR-177294; NAS 1.26:177294) Avail: NTIS HC A04/MF
A01 CSCL 05B

The University of Kansas Applied Remote Sensing (KARS) program is engaged in a continuing long term research and development effort designed to reveal and facilitate new applications of remote sensing technology for decision makers in governmental agencies and private firms. Some objectives of the program follows. The development of new modes of analyzing multispectral scanner, aerial camera, thermal scanner, and radar data, singly or in concert in order to more effectively use these systems. Merge data derived from remote sensing with data derived from conventional sources in geographic information systems to facilitate better environmental planning. Stimulation of the application of the products of remote sensing systems to problems of resource management and environmental quality now being addressed in NASA's Global Habitability directive. The application of remote sensing techniques and analysis and geographic information systems technology to the solution of significant concerns of state and local officials and private industry. The guidance, assistance and stimulation of faculty, staff and students in the utilization of information from the Earth Resources Satellite (LANDSAT) and Aircraft Programs of NASA in research, education, and public service activities carried at the University of Kansas.

E.R.

N86-26675# Geological Survey, Reston, Va. National Mapping Div.

RESEARCH, INVESTIGATIONS AND TECHNICAL DEVELOPMENTS: NATIONAL MAPPING PROGRAM, 1983-1984

R. B. MCEWEN 1985 134 p
(PB86-166097; USGS-OFR-85-304) Avail: NTIS HC A07/MF
A01 CSCL 08B

Subject areas covered are cartography, photogrammetry and surveying, image mapping, remote sensing, land use and land cover mapping, and geographic information systems. The influence of digital cartographic concepts is found throughout and is leading not only to the automation of map making but to the computer analysis of spatial data, the essence of modern geographic information systems. There are several activities of special interest. These include the 1:100,000-scale digital cartographic data base, the LANDSAT Thematic Mapper image map of Great Salt Lake and Vicinity, the successful testing of the Aerial Profiling of Terrain System, several applications of geographic information systems, and publication of the first chapters of the National Gazetteer of the United States. GRA

N86-27788*# National Aeronautics and Space Administration. Langley Research Center, Hampton, Va.

TRANSPORT PROCESSES AS MANIFESTED IN SATELLITE AND LIDAR AEROSOL MEASUREMENTS

M. P. MCCORMICK /n International Council of Scientific Unions Handbook for MAP, Vol. 18 1 p Dec. 1985
Avail: NTIS HC A23/MF A01; also available from SCOSTEP Secretariat, Illinois Univ., 1406 West Green Street, Urbana, Ill. 61801 CSCL 04A

A large increase in stratospheric aerosol data has become available recently from the SAM II and SAGE satellite sensors and the impetus from increased volcanic perturbations. Six years of SAM II and nearly 3 years of SAGE measurements have been accumulated. The increase in large volcanic eruptions since 1979 has caused an acceleration of new data sets from worldwide lidars and airborne lidar campaigns and from various airborne in situ measurements. The SAM II and SAGE data sets show the tropical stratosphere as a source for background stratospheric aerosols, and midlatitudes as a possible sink. Analyses of SAM II data show that the aerosol within the northern wintertime polar vortex becomes isolated from the outside. Subsidence occurs within the vortex, changing the vertical aerosol distribution over the winter period. SAM II and SAGE data show that the aerosol is transported in the stratosphere from low to high latitudes in wintertime. Entry regions of tropospheric air in the Tropics are also evident in the SAGE data as shown by stratospheric cirrus clouds being formed well above the local tropopause. Nature has provided over the past 5 years a number of large volcanic eruptions which spewed tons of new aerosol into the stratosphere. These eruptions have occurred at various latitudes which allow transport differences to be studied. Satellite and lidar aerosol data will be used to describe the stratospheric motions of aerosols produced after these violent volcanic eruptions. Author

GEODESY AND CARTOGRAPHY

Includes mapping and topography.

A86-33516* Jet Propulsion Lab., California Inst. of Tech., Pasadena.

TOPOGRAPHIC MAPPING FROM INTERFEROMETRIC SYNTHETIC APERTURE RADAR OBSERVATIONS

H. A. ZEBKER and R. M. GOLDSTEIN (California Institute of Technology, Jet Propulsion Laboratory, Pasadena) IN: 1985 International Geoscience and Remote Sensing Symposium (IGARSS '85), Amherst, MA, October 7-9, 1985, Digest. Volume 1. New York, Institute of Electrical and Electronics Engineers, Inc., 1985, p. 113-117. refs

Interferometric SAR observations are a basis for the generation of high resolution topographic maps of a region through the interpretation of interference fringes. The combination of height, along-track, and slant range measurements is sufficient for rectification of the radar imagery for cartographic applications, in addition to furnishing an accurate determination of the scene topography. Topographic maps have been derived on the basis of data recorded by both aircraft and Seasat-A satellite radars. A comparison of the maps obtained with U.S. Geological Survey Contour maps indicates a high degree of correlation between two sets of altitude data. O.C.

A86-36099* Jet Propulsion Lab., California Inst. of Tech., Pasadena.

TOPOGRAPHIC MAPPING FROM INTERFEROMETRIC SYNTHETIC APERTURE RADAR OBSERVATIONS

H. A. ZEBKER and R. M. GOLDSTEIN (California Institute of Technology, Jet Propulsion Laboratory, Pasadena) Journal of Geophysical Research (ISSN 0148-0227), vol. 91, April 10, 1986, p. 4993-4999. NASA-supported research. Previously announced in STAR as N86-10622. refs

The production of high-resolution topographic maps derived from interferometric synthetic aperture radar observations of the earth is reported. Topographic maps are typically determined from stereo-pair optical photographs. Vertical relief causes the same terrain to appear in a slightly different projection for differing look angles, and this shift in appearance is interpreted in terms of the height of the terrain. The radar interferometric approach is related to the stereo technique in that the terrain is viewed at two different angles; however, in this case, the angular separation of the antennas is extremely small, on the order of a milliradian or less, as compared to tens of degrees for the optical case. Thus, the geometrical distortion and subsequent rectification correction algorithms are much less severe in the reduction of interferometric data. R.J.F.

A86-37024* Jet Propulsion Lab., California Inst. of Tech., Pasadena.

LANDSAT THEMATIC MAPPER GEODETIC ACCURACY - IMPLICATIONS FOR GEOCODED MAP COMPATIBILITY

N. A. BRYANT, A. L. ZOBRIST, R. E. WALKER, and B. GOKHMANN (California Institute of Technology, Jet Propulsion Laboratory, Pasadena) IN: Machine processing of remotely sensed data - Quantifying global process: Models, sensor systems, and analytical methods; Proceedings of the Eleventh International Symposium, West Lafayette, IN, June 25-27, 1985. New York, Institute of Electrical and Electronics Engineers, 1985, p. 228-237. refs

(Contract NAS7-918)

The geodetic accuracy and geometric fidelity of corrected thematic mapper (TM) imagery are evaluated. The positional accuracy requirements for the TM are for a single band to within 0.5 pixels of true earth-surface locations at any point over 90 percent of the image and for interband registration to within 0.3 pixel tolerance over 90 percent of the data. Landsat 4 and 5 TM

data are analyzed to investigate: (1) single band geometric integrity, (2) 30 m resolution interband registration; (3) image to image conformity; (4) image to ground conformity; and (5) image projective geometry conformity to a mapped earth geometry. The procedures used to study these characteristics are described. The data reveal that Landsat TM digital data met or exceed map accuracy standards for horizontal control. I.F.

A86-37795* ARCO Oil and Gas Co., Dallas, Tex.
STRUCTURE OF THE SOUTHERN RIO GRANDE RIFT FROM GRAVITY INTERPRETATION

P. H. DAGGETT (ARCO Oil and Gas Co., Exploration and Production Research Dept., Plano, TX), G. R. KELLER, C.-L. WEN (Texas, University, El Paso), and P. MORGAN (Lunar and Planetary Institute, Houston, TX; Purdue University, West Lafayette, IN) Journal of Geophysical Research (ISSN 0148-0227), vol. 91, May 10, 1986, p. 6157-6167. refs

(Contract NSF EAR-70-25371; NASW-3389)

Regional Bouguer gravity anomalies in southern New Mexico have been analyzed by two-dimensional wave number filtering and poly-nomial trend surface analysis of the observed gravity field. A prominent, regional oval-shaped positive gravity anomaly was found to be associated with the southern Rio Grande rift. Computer modeling of three regional gravity profiles suggests that this anomaly is due to crustal thinning beneath the southern Rio Grande rift. These models indicate a 25 to 26-km minimum crustal thickness within the rift and suggest that the rift is underlain by a broad zone of anomalously low-density upper mantle. The southern terminus of the anomalous zone is approximately 50 km southwest of El Paso, Texas. A thinning of the rifted crust of 2-3 km relative to the adjacent Basin and Range province indicates an extension of about 9 percent during the formation of the modern southern Rio Grande rift. This extension estimate is consistent with estimates from other data sources. The crustal thinning and anomalous mantle is thought to result from magmatic activity related to surface volcanism and high heat flow in this area. Author

A86-37797* Cornell Univ., Ithaca, N.Y.
EVIDENCE OF ONGOING CRUSTAL DEFORMATION RELATED TO MAGMATIC ACTIVITY NEAR SOCORRO, NEW MEXICO

S. LARSEN, L. BROWN (Cornell University, Ithaca, NY), and R. REILINGER (USAF, Geophysics Laboratory, Bedford, MA) Journal of Geophysical Research (ISSN 0148-0227), vol. 91, May 10, 1986, p. 6283-6292. refs

(Contract USGS-14-08-0001-20585; NAS5-27232; NAS5-27339)

Leveling measurements conducted in 1980-1981 by the National Geodetic Survey in the Socorro area of the Rio Grande rift are analyzed. Crustal uplift related to magma inflation in the midcrustal magma body is detected; an uplift of 0.18 cm/yr is measured for the time between 1951-1980. The survey data of 1911 and 1959 are compared to the present data and good correlation is observed. The systematic leveling errors including height-dependence and refraction errors are studied. The 30-km-wide subsidence in the area is examined. The spatial correlation between seismic activity, the Socorro magma body, and crustal deformation in Socorro is investigated. The crustal movement from magma reservoir activities is modeled using the formulations of Dieterich and Decker (1975). The modeling of the deformation reveals that the movement in the Socorro area is associated with the 19-km deep Socorro magma body. I.F.

N86-26741*# Massachusetts Inst. of Tech., Cambridge. Dept. of Earth, Atmospheric and Planetary Studies.

PLATE MOTIONS AND DEFORMATIONS FROM GEOLOGIC AND GEODETIC DATA Semiannual Report, 1 Aug. 1984 - 31 Dec. 1985

T. H. JORDAN 30 Jun. 1986 53 p

(Contract NAG5-459)

(NASA-CR-177299; NAS 1.26:177299) Avail: NTIS HC A04/MF A01 CSDL 08G

Research effort on behalf of the Crustal Dynamics Project focused on the development of methodologies suitable for the analysis of space-geodetic data sets for the estimation of crustal

GEOLOGY AND MINERAL RESOURCES

Includes mineral deposits, petroleum deposits, spectral properties of rocks, geological exploration, and lithology.

A86-30189**USE OF SEASAT SAR IMAGERY FOR GEOLOGICAL MAPPING IN A VOLCANIC TERRAIN - ASKJA CALDERA, ICELAND**

J. S. MACKENZIE (Imperial College of Science and Technology, London, England) and P. S. RINGROSE (Strathclyde, University, Glasgow, Scotland) International Journal of Remote Sensing (ISSN 0143-1161), vol. 7, Feb. 1986, p. 181-194. Research supported by the University of Edinburgh and Royal Aircraft Establishment.

Nine distinct surface types have been identified by comparison of Seasat SAR imagery with field observations in the Askja Caldera region of central Iceland. A map of radargeological surface type is presented, together with field descriptions and discussion of the influence of the surface types on radar signal return. Surface relief, surface roughness and clast size were found to have the greatest importance for image interpretation. Author

A86-32680**FEATURES OF THE GEOLOGICAL APPLICATION OF SPACE DATA [OSOBENNOSTI GEOLOGICHESKOGO PRIMENENIIA KOSMICHESKOI INFORMATSII]**

V. G. TRIFONOV (AN SSSR, Geologicheskii Institut, Moscow, USSR) and S. S. SHULTS (Vsesoiuznyi Geologicheskii Institut, Leningrad, USSR) Issledovanie Zemli iz Kosmosa (ISSN 0205-9614), Jan.-Feb. 1986, p. 32-42. In Russian. refs

The information content of spectral signatures is compared to that of geometric signatures with reference to the study of geological formations on the basis of space remote-sensing imagery. The geometric signature of an object includes its shape, structure, and position with respect to other objects on space imagery. Geological formations are characterized by the fact that they are better interpreted by geometric than spectral signature. This calls for a special geology-oriented methodology for the application of space data. B.J.

motions, in conjunction with results derived from land-based geodetic data, neo-tectonic studies, and other geophysical data. These methodologies were used to provide estimates of both global plate motions and intraplate deformation in the western U.S. Results from the satellite ranging experiment for the rate of change of the baseline length between San Diego and Quincy, California indicated that relative motion between the North American and Pacific plates over the course of the observing period during 1972 to 1982 were consistent with estimates calculated from geologic data averaged over the past few million years. This result, when combined with other kinematic constraints on western U.S. deformation derived from land-based geodesy, neo-tectonic studies, and other geophysical data, places limits on the possible extension of the Basin and Range province, and implies significant deformation is occurring west of the San Andreas fault. A new methodology was developed to analyze vector-position space-geodetic data to provide estimates of relative vector motions of the observing sites. The algorithm is suitable for the reduction of large, inhomogeneous data sets, and takes into account the full position covariances, errors due to poorly resolved Earth orientation parameters and vertical positions, and reduces biases due to inhomogeneous sampling of the data. This methodology was applied to the problem of estimating the rate-scaling parameter of a global plate tectonic model using satellite laser ranging observations over a five-year interval. The results indicate that the mean rate of global plate motions for that interval are consistent with those averaged over several million years, and are not consistent with quiescent or greatly accelerated plate motions. This methodology was also used to provide constraints on deformation in the western U.S. using very long baseline interferometry observations over a two-year period. M.G.

N86-26745# Ohio State Univ., Columbus. Dept. of Geodetic Science and Surveying.

THE STUDY OF GRAVITY FIELD ESTIMATION PROCEDURES Final Report, 22 Dec. 1981 - 30 Jun. 1985

R. H. RAPP Sep. 1985 12 p refs

(Contract F19628-82-K-0022)

(AD-A164564; AFGL-TR-85-0278) Avail: NTIS HC A02/MF A01 CSDL 08E

The research described includes the use of high degree potential coefficient expansions, vertical datum corrections, improved gravity fields from satellite altimetry, the computation of the gravity vector in space and the use of digital terrain models for gravimetric computations. GRA

N86-27833*# Massachusetts Inst. of Tech., Cambridge. Dept. of Earth, Atmospheric and Planetary Sciences.

PLATE MOTIONS AND DEFORMATIONS FROM GEOLOGIC AND GEODETIC DATA Semiannual Report, 1 Aug. 1983 - 31 Dec. 1985

T. H. JORDAN 1986 53 p

(Contract NAG5-459)

(NASA-CR-177313; NAS 1.26:177313) Avail: NTIS HC A04/MF A01 CSDL 08E

A satellite laser ranging experiment conducted by NASA since 1972 has measured the relative motion between the North America and Pacific plates in California. Based on these measurements, the 896-km distance between San Diego and Quincy, California, is shortening at 62 ± 9 mm/yr. This geodetic estimate is consistent with the rate of motion between the two plates, calculated from geological data to be 53 ± 3 mm/yr averaged over the past few million years. Author

A86-32681**INTERPRETATION OF RING STRUCTURES ON SPACE IMAGES AND THEIR CORRELATION WITH GEOPHYSICAL FIELDS AND CRUSTAL STRUCTURE IN THE USSR [DESHIFROVANIE KOL'TSEVYKH STRUKTUR NA KOSMICHESKIKH SNIMKAKH I IKH KORELIATSIIA S GEOFIZICHESKIMI POLIAMI I STROENIEM ZEMNOI KORY TERRITORII SSSR]**

A. T. ZVEREV and I. A. G. KATS (Moskovskii Gosudarstvennyi Universitet, Moscow, USSR) Issledovanie Zemli iz Kosmosa (ISSN 0205-9614), Jan.-Feb. 1986, p. 43-50. In Russian. refs

Identified ring structures in the USSR are correlated with geological and geophysical features as well as with the associated lithospheric characteristics. The correlation analysis indicates that the ring structures are deep-lying and have a long evolutionary history. In addition, they are found to exhibit a higher concentration in areas with a thinner and older crust, a higher rock density, and a stronger heat flux. B.J.

A86-32682

APPLICATION OF SPACE IMAGERY TO THE IDENTIFICATION AND GEOLOGICAL-GEOPHYSICAL STUDY OF HIDDEN PLUTONS IN EARLY PROTEROZOIC TROUGHS [ISPOL'ZOVANIE KOSMICHESKIKH SNIMKOV PRI VYIAVLENII I GEOLOGO-GEOFIZICHESKOM IZUCHENII SKRYTYKH PLUTONOV V RANNEPROTEROZOISKIKH TROGAKH]

D. M. TROFIMOV, N. A. STRAKHOVA, V. A. BOGOSLOVSKII, E. B. ILINA, V. A. KAZANTSEV (Moskovskii Gosudarstvennyi Universitet, Moscow, USSR) et al. Issledovanie Zemli iz Kosmosa (ISSN 0205-9614), Jan.-Feb. 1986, p. 51-56. In Russian.

Space imagery was used to identify and examine hidden plutons in the early Proterozoic troughs of the central Kursk Magnetic Anomaly. It is shown that intersections of faults identified on space images are related to sulfide mineralization. It is noted that the method used can be applied to mineral prospecting in the sedimentary cover basement. B.J.

A86-32690

COMPUTER-AIDED INTERPRETATION OF SPACE IMAGES WITH THE AIM OF STRUCTURAL ANALYSIS [AVTOMATIZIROVANNOE DESHIFRIROVANIE KOSMICHESKIKH SNIMKOV S TSEL'IU STRUKTURNOGO ANALIZA]

N. V. KORONOVSKII, A. A. ZLATOPOLSKII, and G. N. IVANCHENKO (Moskovskii Gosudarstvennyi Universitet; Proizvodstvennoe Geologicheskoe Ob'edinenie Aerogeologiya, Moscow, USSR) Issledovanie Zemli iz Kosmosa (ISSN 0205-9614), Jan.-Feb. 1986, p. 111-118. In Russian.

Landsat imagery of the eastern Caucasus was interpreted using special-purpose computer programs to facilitate the structural analysis of the region. Some of the linear elements identified were rejected, while others were combined into lineament zones. Most of the lineaments were found to coincide with those identified by visual interpretation. It is noted that the proposed method can be used for the quick-look assessment of tectonic deformations. B.J.

A86-33517

PHOTGRAMMETRY AND REMOTE SENSING IN PERIGLACIAL GEOMORPHOLOGY

W. G. HOWLAND (Middlebury College, VT) IN: 1985 International Geoscience and Remote Sensing Symposium (IGARSS '85), Amherst, MA, October 7-9, 1985, Digest. Volume 1. New York, Institute of Electrical and Electronics Engineers, Inc., 1985, p. 119-124.

Remote sensing and photogrammetry are seldom effectively applied in geomorphic research. However, instruments, imagery and techniques, which have recently become far more accessible than previously, can provide a quantitative basis for the assessment of terrain morphology, and greatly aid the analysis of geomorphic processes. This paper describes the use of existing technology in ways that directly aid in geomorphic research, and provides an example concerning an Arctic study area. The first part (A) of the paper discusses techniques in the general context of geomorphology, while the second part (B) shows, with a case study, the applicability of these techniques. Author

A86-33518

TOPOGRAPHIC LINEAMENT DOMAINS OF THE APPALACHIANS - SOME NEW METHODS AND TECHNIQUES FOR PALEOSTRESS ANALYSIS

D. U. WISE, L. T. GRADY (Massachusetts, University, Amherst), and F. SALVINI (Pisa, Universita, Italy) IN: 1985 International Geoscience and Remote Sensing Symposium (IGARSS '85), Amherst, MA, October 7-9, 1985, Digest. Volume 1. New York, Institute of Electrical and Electronics Engineers, Inc., 1985, p. 125-130.

The method of Wise et al. (1985) for the analysis of geologic lineaments on remotely sensed images is applied to the Appalachian chain. The technique emphasizes subparallel lineament swarms and their map domains rather than individual lines. The basic data are derived from mosaics of side-lighted

photographs of raised relief maps of the Appalachians. These maps provide a filter, leaving only the most prominent and well developed topographic linears as a subset of the many classes of linear features that are imbedded in a typical Landsat or radar image. Six different mosaics of these maps were produced, illuminated from six different azimuths. Data analyses involved automatic fitting of Gaussian peaks to azimuth-frequency histograms. The origins of the local lineament domains obtained, which represent regional or subregional scale features, and as such must have been created by paleostress fields of at least comparable size, are discussed. I.S.

A86-33519

A PRELIMINARY ANALYSIS OF LANDSAT MSS AND TM DATA IN THE LEVACK AREA, SUDBURY, CANADA

J. K. HORNSBY (Intera Technologies, Ltd., Calgary, Canada) and B. BRUCE (Canada Centre for Remote Sensing, Ottawa, Canada) IN: 1985 International Geoscience and Remote Sensing Symposium (IGARSS '85), Amherst, MA, October 7-9, 1985, Digest. Volume 1. New York, Institute of Electrical and Electronics Engineers, Inc., 1985, p. 131-140. refs

The results of preliminary digital analysis of Landsat's MSS and TM imagery is presented for lineament and lithologic interpretation in the copper-nickel producing Levack area of the Sudbury Basin in Canada. The digital analysis methodology involves the production of a series of band combination enhancements and classification products, used as the bases for comparative visual geological interpretation and feature compilation. The results of the study indicated that the MSS and TM data show more geologic structure within the study area than was previously mapped. Both types of data allow the interpretation of the same major structures, but the TM data reveal more curvilinear and linear features than the MSS data, offer greater detail at points of intersection, and provide a more continuous record of a particular linear across an image. Both the MSS and TM were capable of discriminating the major lithologic units of the Sudbury Igneous Complex, felsic intrusives, and the metavolcanic-metasedimentary belt to the north. Although the TM data display greater spectral variability and provide a more detailed classification, the MSS data yield consistent results and would likely be more cost effective for large area reconnaissance. I.S.

A86-33520

LINEAMENT ANALYSIS IN A TEST AREA OF NORTHERN MOZAMBIQUE

M. POSCOLIERI and S. SALVI (CNR, Istituto di Astrofisica Spaziale, Frascati, Italy) IN: 1985 International Geoscience and Remote Sensing Symposium (IGARSS '85), Amherst, MA, October 7-9, 1985, Digest. Volume 1. New York, Institute of Electrical and Electronics Engineers, Inc., 1985, p. 141-146. refs

Lineament analysis for a test area in northern Mozambique, is presented. The lineaments have been interpreted from a Landsat 2 picture and then digitized. A procedure was developed, based on statistical and analytical methods, for processing large amount of linear data sets, in which the numerical matrices representing the areal density of the structural domains are displayed by contour line maps. These maps allow the identification of regional structural trends suitable for mineral exploration and may be utilized as a check for the precision of the existing geological maps derived by other methods. The results of a comparison of the contour maps with the geological map and the map of the mining districts are discussed. I.S.

A86-33521* Brown Univ., Providence, R. I.
SPECTROSCOPY OF MOSES ROCK DIKE USING REMOTE SENSING

J. F. MUSTARD and C. M. PIETERS (Brown University, Providence, RI) IN: 1985 International Geoscience and Remote Sensing Symposium (IGARSS '85), Amherst, MA, October 7-9, 1985, Digest. Volume 1. New York, Institute of Electrical and Electronics Engineers, Inc., 1985, p. 147-152. refs
 (Contract NASW-4048)

Zeiss IR-photographs, NS0001 (TM simulator) and airborne imaging spectrometer (AIS) data were obtained for the Moses Rock kimberlite dike in southern Utah to identify and characterize the distinctive mafic mineralogy of the dike as well as the surrounding sedimentary rocks. The Zeiss and NS001 images provide information on the regional setting and allow units of the dike to be distinguished from the sediments. The AIS data are narrow images obtained in 128 near-infrared channels and provide characterizing information on the surface composition through. Three distinct spectroscopic units were found which have been tentatively identified as serpentinized olivine-bearing soils found in the dike and two types of gypsum bearing soils found in the surrounding sedimentary soils. Author

A86-33550* Hawaii Univ., Honolulu.
PRELIMINARY GEOLOGIC ANALYSES OF SIR-B RADAR DATA FOR HAWAII

L. R. GADDIS, P. J. MOUGINIS-MARK (Hawaii, University, Honolulu), V. H. KAUPP, H. C. MACDONALD, and W. P. WAITE (Arkansas, University, Fayetteville) IN: 1985 International Geoscience and Remote Sensing Symposium (IGARSS '85), Amherst, MA, October 7-9, 1985, Digest. Volume 1. New York, Institute of Electrical and Electronics Engineers, Inc., 1985, p. 364-369. refs
 (Contract JPL-956925)

A number of distinct topographic and textural units were discerned on SIR-B radar images of the Kilauea/Kau Desert area. The SIR-B enhanced large-scale topographic features, such as the Kahuku Pali and the Koahe Faults (both oriented towards the radar antenna), while it was unable to detect features facing away from the radar antenna such as the Hilina and Kaoiki Pali. Textural units which were identified on the SIR-B images include aa flows of various ages, and several pyroclastic units. The extreme surface roughness of aa flows produced high radar returns on both the 28 deg and 48 deg SIR-B data sets. In contrast, pahoehoe flows produced smooth, low return units which were difficult to distinguish from surrounding radar-dark materials. It is suggested that multilook direction data, acquired at steeper incidence angles during a reflight of SIR-B, may aid in the further identification of pahoehoe flows and subtle topographic features. K.K.

A86-33551
INTRODUCTORY ANALYSES OF SIR-B RADAR DATA FOR HAWAII

B. A. DERRYBERRY, V. H. KAUPP, H. C. MACDONALD, W. P. WAITE (Arkansas, University, Fayetteville), L. R. GADDIS (Hawaii, University, Honolulu) et al. IN: 1985 International Geoscience and Remote Sensing Symposium (IGARSS '85), Amherst, MA, October 7-9, 1985, Digest. Volume 1. New York, Institute of Electrical and Electronics Engineers, Inc., 1985, p. 370-375.

Two synthetic aperture radar (SAR) images of the Kilauea Volcano/Kau Desert were obtained and used, together with surface roughness measurements, to model the interaction between an incident wave and a volcanic surface. An analysis relating lava flow type and age was performed using Shuttle imaging radar (SIR-B) data. Mean, variance, and histogram were used to discriminate between aa and pahoehoe surfaces of differing ages. It was demonstrated that the extreme roughness and blockiness of aa flows produce both distinctively high returns on radar images and histograms characteristic of nonideal scattering surfaces. Pahoehoe flows, by contrast, are smooth low-return features, which are difficult to distinguish from surrounding radar-dark materials, and appear to be nearly ideal scattering surfaces. K.K.

A86-33552* Brown Univ., Providence, R. I.
STRUCTURE OF TERRESTRIAL IMPACT CRATERS FROM SIR-B RADAR DATA - PRELIMINARY RESULTS

P. C. FISHER, J. W. HEAD (Brown University, Providence, RI), S. H. ZISK (Haystack Observatory, Westford, MA), R. A. F. GRIEVE (Department of Energy, Mines, and Resources, Earth Physics Branch, Ottawa, Canada), and K. SULLIVAN (NASA, Johnson Space Center, Houston, TX) IN: 1985 International Geoscience and Remote Sensing Symposium (IGARSS '85), Amherst, MA, October 7-9, 1985, Digest. Volume 1. New York, Institute of Electrical and Electronics Engineers, Inc., 1985, p. 376, 377.

The structure in and around the Charlevoix and Deep Bay impact craters was analyzed by comparing SIR-B radar image lineament maps with maps derived from Landsat data and aerial photography. Relationships revealed include the discovery in the Deep Bay lineament distribution of a mode, of slightly different location and size to that determined by aerial photography, which correlates with the regional glacial trend. The Deep Bay regional glacial trend displays a much more prominent signature in the aerial photography than in the radar data, confirming the influence of radar look direction on the interpretation of lineament distribution and orientation. Effects from the impact event are noted in the radar images of both craters, with lineaments of one km or less appearing to be associated with the rim structure. R.R.

A86-33592* Jet Propulsion Lab., California Inst. of Tech., Pasadena.

WHAT ARE THE BEST RADAR WAVELENGTHS, INCIDENCE ANGLES AND POLARIZATIONS FOR GEOLOGIC APPLICATIONS? A STATISTICAL APPROACH

R. BLOM (California Institute of Technology, Jet Propulsion Laboratory, Pasadena; California, University, Santa Barbara), L. SCHENCK, and R. ALLEY (California Institute of Technology, Jet Propulsion Laboratory, Pasadena) IN: 1985 International Geoscience and Remote Sensing Symposium (IGARSS '85), Amherst, MA, October 7-9, 1985, Digest. Volume 2. New York, Institute of Electrical and Electronics Engineers, Inc., 1985, p. 659-664. NASA-sponsored research.

Linear discriminant analysis of multifrequency and multipolarization radar scatterometer data of lava flows and sedimentary rocks indicates that the lava flows can be separated by age and the sedimentary rocks can be discriminated from one another. The optimum wavelengths, polarizations and incidence angles among those available for these problems was determined by the discriminant analysis program. For separation of the lava flows, shorter wavelengths, smaller incidence angles and horizontal polarization are best. A SIR-C radar configuration could provide nearly complete discrimination of these lava flows. Conversely, the longer wavelengths, larger incidence angles and vertical polarization was preferred for sedimentary rocks, perhaps due to the slight vegetation cover. Satisfactory classification of sedimentary rocks requires more radar data than for the lavas. These results are potentially useful both for radar system configuration and for geological applications. The method developed here may provide a rationale for user specification of imaging system parameters. Author

A86-33593
ANALYSIS OF L-BAND MULTIPOLARIZATION RADAR IMAGES FOR LAVA FLOW MAPPING

V. H. KAUPP, R. E. CHILTON, H. C. MACDONALD, W. P. WAITE (Arkansas, University, Fayetteville), L. R. GADDIS (Hawaii, University, Honolulu) et al. IN: 1985 International Geoscience and Remote Sensing Symposium (IGARSS '85), Amherst, MA, October 7-9, 1985, Digest. Volume 2. New York, Institute of Electrical and Electronics Engineers, Inc., 1985, p. 669-675. refs

Multipolarization radar images of the Medicine Lake Highland, CA, area were obtained in support of the SIR-B (Shuttle imaging radar) program by the JPL aircraft SAR (synthetic aperture radar). These images have been evaluated in an attempt to determine the influences of polarization on lava flow mapping. Images of all four polarizations (HH, HV, VH, and VV) of the region were available. In studying nine flows, the VV images provided the best

04 GEOLOGY AND MINERAL RESOURCES

discrimination in almost all cases. A color composite created from the HH, VV, and VH images was evaluated for each scene, and despite range tonal variations it is seen that discrimination of flows is accomplished more easily using the composites. The incremental value of the cross polarized return cannot be evaluated with this small amount of data, and a more extensive study is needed.

D.H.

A86-35676

STATISTICAL LINEAMENT ANALYSIS IN SOUTH GREENLAND BASED ON LANDSAT IMAGERY

K. CONRADSEN (Danmarks Tekniske Højskole, Lyngby, Denmark), G. NILSSON (Telelogic AB, Malmö, Sweden), and T. THYRSTED (Gronlands Geologiske Undersøgelse, Copenhagen, Denmark) (International Geoscience and Remote Sensing Symposium /IGARSS '84/: From Research toward Operational Use, Strasbourg, France, Aug. 27-30, 1984) IEEE Transactions on Geoscience and Remote Sensing (ISSN 0196-2892), vol. GE-24, May 1986, p. 313-321. refs

Linear features, mapped visually from MSS channel-7 photoprints (1:1,000,000) of Landsat images from South Greenland, were digitized and analyzed statistically. A sinusoidal curve was fitted to the frequency distribution which was then divided into ten significant classes of azimuthal trends. Maps showing the density of linear features for each of the ten classes indicate that many of the classes are distributed in zones defined by elongate maxima or rows of maxima. In cases where the elongate maxima and the linear feature direction of the class in question are parallel, a zone of major crustal discontinuity is inferred. In the area investigated, such zones coincide with geochemical boundaries and graben structures, and the intersections of some zones seem to control intrusion sites. In cases where there is no parallelism between the elongate maxima and the linear feature direction, an en echelon pattern of the lineaments may be inferred. Author

A86-36083* Kansas Univ., Lawrence.
GEOLOGICAL MAPPING POTENTIAL OF COMPUTER-ENHANCED IMAGES FROM THE SHUTTLE IMAGING RADAR - LISBON VALLEY ANTICLINE, UTAH
J. D. CURLIS, V. S. FROST, and L. F. DELLWIG (Kansas, University, Lawrence) Photogrammetric Engineering and Remote Sensing (ISSN 0099-1112), vol. 52, April 1986, p. 525-532. Research supported by Phillips Petroleum Co., American Association of Petroleum Geologists, and University of Kansas. refs (Contract JPL-954946)

Computer-enhancement techniques applied to the SIR-A data from the Lisbon Valley area in the northern portion of the Paradox basin increased the value of the imagery in the development of geologically useful maps. The enhancement techniques include filtering to remove image speckle from the SIR-A data and combining these data with Landsat multispectral scanner data. A method well-suited for the combination of the data sets utilized a three-dimensional domain defined by intensity-hue-saturation (IHS) coordinates. Such a system allows the Landsat data to modulate image intensity, while the SIR-A data control image hue and saturation. Whereas the addition of Landsat data to the SIR-A image by means of a pixel-by-pixel ratio accentuated textural variations within the image, the addition of color to the combined images enabled isolation of areas in which gray-tone contrast was minimal. This isolation resulted in a more precise definition of stratigraphic units. Author

A86-36501

METHODS OF COMBINED AIR AND SPACE REMOTE-SENSING STUDIES OF SIBERIA [METODY KOMPLEKSNYKH AEROKOSMICHESKIKH ISSLEDOVANIY SIBIRI]

L. K. ZIATKOVA, ED. Novosibirsk, Izdatel'stvo Nauka, 1985, 96 p. In Russian. For individual items see A86-36502 to A86-36518.

The use of remote-sensing techniques to solve geological problems is considered along with the computer-aided processing of remote-sensing images. Particular consideration is given to the contribution of remote sensing to the development of structural geomorphology; the quantitative assessment of the information

content of TV images obtained in remote-sensing studies of Siberia; the remote sensing of transition zones of the junction of Siberian platforms and orogens; a combined approach to oil and gas exploration in the southern Permsk region; the application of image-analysis software to environment-protection problems; and the choice of spectral bands for a spaceborne multispectral scanner. B.J.

A86-36502

PROBLEMS AND PRINCIPLES OF THE GEOLOGICAL INTERPRETATION OF REMOTE-SENSING DATA [PROBLEMY I PRINTSIPY GEOLOGICHESKOI INTERPRETATSII REZUL'TATOV DESHFIRIROVANIYA DISTANTSIONNYKH MATERIALOV]

D. M. TROFIMOV IN: Methods of combined air and space remote-sensing studies of Siberia. Novosibirsk, Izdatel'stvo Nauka, 1985, p. 5-8. In Russian.

Principles of the multilevel geological interpretation of aerial and space remote-sensing data are examined. The interpretation is based on the spatial correlation of remote-sensing images of geological objects observed on photographs, as well as on the basis of geological-geophysical data, taking the density of initial information into account. The interpretation involves successive approximation to the object, generating the remote-sensing or landscape image from top to bottom, from the more studied to the less studied 'horizons' of the earth crust. B.J.

A86-36503

COMBINED STRUCTURAL AND GEOMORPHOLOGICAL METHODS FOR THE PROCESSING OF AERIAL AND SPACE PHOTOGRAPHIC REMOTE-SENSING DATA WITH THE AIM OF SOLVING GEOLOGICAL PROBLEMS [KOMPLEKSNYE STRUKTURNO-GEOMORFOLOGICHESKIE METODY OBRABOTKI AEROKOSMICHESKOI FOTOINFORMATSII DLIYA RESHENIYA GEOLOGICHESKIKH ZADACH]

L. K. ZIATKOVA IN: Methods of combined air and space remote-sensing studies of Siberia. Novosibirsk, Izdatel'stvo Nauka, 1985, p. 9-19. In Russian. refs

The paper examines aspects of the development of a combined system for the instrumented, automated processing of aerial and space remote-sensing data with the aim of recognizing various types of tectonic and seismic structures and exploring for fossil fuels and ore deposits. The approach used involves the identification of the interpretation features and morphometric characteristics connected with water divides and river basins. B.J.

A86-36504

INVESTIGATION OF THE EARTH FROM SPACE - A NEW CONTRIBUTION TO THE DEVELOPMENT OF STRUCTURAL GEOMORPHOLOGY [ISSLEDOVANIYA ZEMLI IZ KOSMOSA - NOVYI VKLAD V RAZVITIE STRUKTURNOI GEOMORFOLOGII]

A. P. KULAKOV IN: Methods of combined air and space remote-sensing studies of Siberia. Novosibirsk, Izdatel'stvo Nauka, 1985, p. 19-22. In Russian. refs

It is noted that space remote-sensing data have produced a 'revolution' in morphostructural studies, and have led to a number of new ideas in the area of morphological analysis and synthesis. In particular, the ubiquitous development on the earth of morphostructures of a central type, with diameters up to several thousand kilometers, has been established. In addition, previously undetected transregional fault zones (lineaments) have been observed. B.J.

04 GEOLOGY AND MINERAL RESOURCES

A86-36505

METHOD FOR THE QUANTITATIVE ESTIMATION OF CONVERGENCE IN MAPPING IN THE CASE OF THE INTERPRETATION OF SPACE PHOTOGRAPHS OF OIL-AND-GAS-BEARING REGIONS OF SIBERIA [METOD KOLICHESTVENNOI OTSENKI SKHODIMOSTI V KARTOGRAFICHESKIKH POSTROENIYAKH PRI DESHIFRIROVANII KOSMOSNIMKOV NEFTEGAZONOSNYKH RAIONOV SIBIRI]

A. M. BOROVNIKOV and L. M. SHEMIKIN IN: Methods of combined air and space remote-sensing studies of Siberia . Novosibirsk, Izdatel'stvo Nauka, 1985, p. 22-30. In Russian. refs

A86-36506

QUANTITATIVE ASSESSMENT OF THE INFORMATION CONTENT OF TV IMAGES OF DIFFERENT SCALE ON THE EXAMPLE OF DISJUNCTIVES OF SIBERIA [KOLICHESTVENNAIA OTSENKA INFORMATIVNOSTI RAZNOMASSHTABNYKH TELESNIMKOV NA PRIMERE DIZIUNKTIVOV SIBIRI]

V. I. VITIAZ and V. IA. EROMENKO IN: Methods of combined air and space remote-sensing studies of Siberia . Novosibirsk, Izdatel'stvo Nauka, 1985, p. 30-34. In Russian.

The interpretation of ultrasmall-scale and small-scale TV images of platform regions of Siberia is examined along with the interpretation of small-scale space imagery. Linear, ring-shaped, and arclike elements on interregional and regional scales are identified. The regional features of western and eastern Siberia are manifested in the large relative density of lineaments on the Siberian platform. B.J.

A86-36507

METHODS FOR THE REMOTE SENSING OF TRANSITION ZONES OF THE JUNCTION OF SIBERIAN PLATFORMS AND OROGENS [METODY DISTANTSIONNYKH ISSLEDOVANIY PEREKHODNYKH ZON SOCHLENENIYA PLATFORM I OROGENOV SIBIRI]

L. K. ZIATKOVA IN: Methods of combined air and space remote-sensing studies of Siberia . Novosibirsk, Izdatel'stvo Nauka, 1985, p. 35-41. In Russian. refs

The paper examines the use of space-image interpretation techniques to identify various structures in zones joining Siberian platforms and orogens. It is shown that such junction zones should be considered as a combination of various types of platform and orogenic structures, subjected to endodynamic, exodynamic, hypergenoexodynamic, and technogenoanthropogenic processes. B.J.

A86-36508

THE USE OF REMOTE-SENSING DATA TO PREDICT REGIONAL AND LOCAL OIL-AND-GAS-BEARING STRUCTURES WITHIN THE DNEPROVSK-DONETSK PALEORIFT [OPYT PRIMENENIYA KOSMICHESKOI INFORMATSII DLIA PROGNOZIROVANIYA REGIONAL'NYKH I LOKAL'NYKH NEFTEGAZONOSNYKH STRUKTUR V PREDELAKH DNEPROVSKO-DONETSKOGO PALEORIFTA]

V. K. GAVRISH, A. I. NEDOSHOVENKO, E. S. PETROVA, and V. N. DEMENTEV IN: Methods of combined air and space remote-sensing studies of Siberia . Novosibirsk, Izdatel'stvo Nauka, 1985, p. 42-47. In Russian. refs

A86-36509

COMBINATION OF AIR AND SPACE REMOTE-SENSING METHODS AND GEOLOGICAL-GEOPHYSICAL METHODS FOR THE PURPOSE OF OIL AND GAS EXPLORATION IN THE SOUTHERN PERMSK REGION [KOMPLEKSIROVANIE AERO-KOSMOGEOLOGICHESKIKH I GEOLOGO-GEOFIZICHESKIKH METODOV PRI NEFTEGAZOPOISKOVYKH RABOTAKH NA IUGE PERMSKOI OBLASTI]

IU. A. DULEPOV, V. V. MAKALOVSKII, V. S. KUROCHKIN, and V. G. GATSKOV IN: Methods of combined air and space remote-sensing studies of Siberia . Novosibirsk, Izdatel'stvo Nauka, 1985, p. 48-52. In Russian.

A86-36510

ASPECTS OF THE GEOLOGICAL INTERPRETATION OF GEOPHYSICAL FIELDS AND RESULTS OF AIR AND SPACE REMOTE SENSING OBSERVATIONS OF OIL-AND-GAS-BEARING TERRITORIES [NEKOTORYE VOPROSY GEOLOGICHESKOI INTERPRETATSII GEOFIZICHESKIKH POLEI I REZULTATOV AEROKOSMICHESKIKH NABLIUDENII NEFTEGAZONOSNYKH TERRITORII]

V. V. PANASENKO and V. N. PANASENKO IN: Methods of combined air and space remote-sensing studies of Siberia . Novosibirsk, Izdatel'stvo Nauka, 1985, p. 52-56. In Russian. refs

A86-37009

DIRECTION DEPENDENT INTERPOLATION OF AEROMAGNETIC DATA

L. BRINDT and H. HAUSKA (Lulea, Hogskolan, Sweden) IN: Machine processing of remotely sensed data - Quantifying global process: Models, sensor systems, and analytical methods; Proceedings of the Eleventh International Symposium, West Lafayette, IN, June 25-27, 1985 . New York, Institute of Electrical and Electronics Engineers, 1985, p. 86-95. Sponsorship: Styrelsen for Teknisk Utveckling and Swedish Board for Space Activities. refs

(Contract STU-83-4119; SBSA-63-83; SBSA-56-84)

The paper describes a method for level correction and interpolation of anisotropically sampled aeromagnetic data. The level correction is based on piecewise comparison of adjacent flightlines. The interpolation scheme is based on cubic splines and preserves thin linear structures in anisotropic potential field data. The design of such a method is an important building stone for the design of an image-based information system for geologic applications. Author

A86-37021

LANDSAT MSS AND AIRBORNE GEOPHYSICAL DATA COMBINED FOR MAPPING GRANITE IN SOUTHWEST NOVA SCOTIA

V. R. SLANEY (Geological Survey of Canada, Ottawa) IN: Machine processing of remotely sensed data - Quantifying global process: Models, sensor systems, and analytical methods; Proceedings of the Eleventh International Symposium, West Lafayette, IN, June 25-27, 1985 . New York, Institute of Electrical and Electronics Engineers, 1985, p. 198-206. refs

A86-37865#

APPLICATION OF SPACEBORNE AND AIRBORNE TECHNIQUES IN MINERAL EXPLORATION AT WADI EL ALLAQI AREA, EASTERN DESERT, EGYPT

E. M. EL SHAZLY, M. A. A. HADY, and A. F. EL NASHARTY (Academy of Scientific Research and Technology, Remote Sensing Centre, Cairo, Egypt) IN: International Conference on Space, 25th, Rome, Italy, March 26-28, 1985, Proceedings . Rome, Rassegna Internazionale Elettronica Nucleare ed Aerospaziale, 1985, p. 217-224. refs

04 GEOLOGY AND MINERAL RESOURCES

N86-23030# Office of Technology Assessment, Washington, D.C.

OIL AND GAS TECHNOLOGIES FOR THE ARCTIC AND DEEPWATER

May 1985 235 p

(PB86-119948) Avail: NTIS HC A11/MF A01 CSCL 08I

Nearly 2 billion acres of offshore public domain is owned by the United States adjacent to Alaska and the lower 48 states. Much of the Nation's future domestic petroleum supply is expected to come from this area. Areas of highest potential apparently occur in deeper water and in the Arctic where operating conditions are severe, development costs high, and financial risks immense. As the pace of exploration increases in these frontier regions, questions arise about the technologies needed to safely and efficiently explore and develop oil and gas in harsh environments. The study explores the range of technologies required for exploration and development of offshore energy resources and assesses associated economic factors and financial risks. GRA

N86-25099# Geological Survey, Reston, Va.
REMOTE MONITORING OF PROCESSES THAT SHAPE DESERT SURFACES: THE DESERT WINDS PROJECT

J. F. MCCAULEY, C. S. BREED, P. J. HELM, G. H. BILLINGSLEY, D. J. MACKINNON, M. J. GROLIER, and C. K. MCCAULEY (Museum of Northern Arizona, Flagstaff) 1985 23 p refs (T186-900108; USGS-BULL-1634; LC-84-601115) Avail: NTIS HC A02/MF A01

Investigations of wind as a geologic agent have been hampered by a scarcity of long-term onsite measurements of wind velocity (including peak gusts, direction, and periodicity), precipitation frequency and intensity, relative humidity, and soil and air temperatures in key desert localities. A new long-term study, using data obtained by meteorologic and geologic sensors coupled to nonattended solar-powered data-collector platforms is described. Data obtained from these geometeorologic (Geomet) stations in desert type areas of Arizona are automatically relayed by the Geostationary Operational Environmental Satellite (GOES) to the U.S. Geological Survey in Flagstaff, Ariz., in real time, and converted to graphic form. Preliminary computer analysis of the data indicates strikingly different meteorologic patterns that control, in great part, the local surficial geology of different desert areas. Author

N86-25866*# Lunar and Planetary Inst., Houston, Tex.
THEMATIC MAPPER STUDIES OF ANDEAN VOLCANOES Monthly Report

P. W. FRANCIS 1986 13 p Original contains color illustrations

(Contract NAS5-28759)

(NASA-CR-176807; NAS 1.26:176807; MR-6) Avail: NTIS HC A02/MF A01 CSCL 08K

The primary objective was to identify all the active volcanoes in the Andean region of Bolivia. Morphological features of the Tata Sabaya volcano, Bolivia, were studied with the thematic mapper. Details include marginal levees on lava and pyroclastic flows, and summit crater structure. Valley glacier moraine deposits, not easily identified on the multispectral band scanner, were also unambiguous, and provide useful marker horizons on large volcanic edifices which were built up in preglacial times but which were active subsequently. With such high resolution imagery, it is not only possible to identify potentially active volcanoes, but also to use standard photogeological interpretation to outline the history of individual volcanoes. B.G.

N86-25912*# Nevada Univ., Reno. Dept. of Geological Sciences.

THE NATURE AND ORIGIN OF MINERAL COATINGS ON VOLCANIC ROCKS OF THE BLACK MOUNTAIN, STONEWALL MOUNTAIN AND KANE SPRINGS WASH VOLCANIC CENTERS IN SOUTHERN NEVADA Semiannual Progress Report, Jul. 1985 - Jan. 1986

J. V. TARANIK, D. D. NOBLE, L. C. HSU, and A. HUTSINPILLER Jan. 1986 23 p refs Original contains color illustrations

(Contract NAS5-28765)

(NASA-CR-176805; NAS 1.26:176805) Avail: NTIS HC A02/MF A01 CSCL 08G

Four LANDSAT thematic mapping scenes in southern Nevada were requested at two different acquisition times in order to assess the effect of vegetation on the signature of the volcanic units. The remote sensing data acquisition and analysis portion are nearly completed. The LANDSAT thematic mapping data is of good quality, and image analysis techniques are so far successful in delineating areas with distinct spectral characteristics. Spectrally distinct areas were correlated with variations in surface coating and lithologies of the volcanic rocks. Author

N86-26740*# Bechtel National, Inc., San Francisco, Calif.
THEMATIC MAPPER RESEARCH IN THE EARTH SCIENCES: TECTONIC EVALUATION OF THE NUBIAN SHIELD OF NORTHEASTERN SUDAN/SOUTHEASTERN EGYPT USING THEMATIC MAPPER IMAGERY Interim Report

Feb. 1986 24 p refs Original contains color illustrations

(Contract NAS5-28757)

(NASA-CR-177311; NAS 1.26:177311) Avail: NTIS HC A02/MF A01 CSCL 08G

The tectonic evaluation of the Nubian Shield using the Thematic Mapper (TM) imagery is progressing well and shows great promise. The TM tapes for the six LANDSAT 5 scenes covering the northern portion of the Red Sea hills were received, and preliminary maps and interpretations were made for most of the area. It is apparent that faulting and shearing associated with the major suture zones such as the Sol Hamed are clearly visible and that considerable detail can be seen. An entire quadrant of scene 173,45 was examined in detail using all seven bands, and every band combination was evaluated to best display the geology. A comparison was done with color ratio combinations and color combinations of the eigen vector bands to verify if band combinations of 7-red, 4-green, and 2-blue were indeed superior. There is no single optimum enhancement which provides the greatest detail for every image and no single combination of spectral bands for all cases, although bands 7, 4, and 2 do provide the best overall display. The color combination of the eigen vector bands proved useful in distinguishing fine detailed features. B.G.

05

OCEANOGRAPHY AND MARINE RESOURCES

Includes sea-surface temperature, ocean bottom surveying imagery, drift rates, sea ice and icebergs, sea state, fish location.

A86-31350

INTEGRATED GLOBAL MONITORING OF THE WORLD OCEAN. VOLUMES 1, 2, & 3 [KOMPLEKSNIYI GLOBAL'NYI MONITORING MIROVOGO OKEANA. VOLUMES 1, 2, & 3]

IU. A. IZRAEL, ED. Leningrad, Gidrometeoizdat, 1985, 1134 p. In Russian. No individual items are abstracted in these volumes.

Papers from the First International Symposium on Integrated Global Monitoring of the World Ocean (Tallin, 1983) are presented. Reports from various international organizations are presented. Particular topics include: the scientific foundations of the ecological monitoring of the ocean; methods for the assessment of ocean pollution; the effect of atmospheric transport on ocean pollution; the ecological consequences of ocean pollution; and

biogeochemical cycles and balances of pollutants. Consideration is also given to the monitoring of heat transfer in the ocean and between the atmosphere and the ocean, and to ocean modeling.

B.J.

A86-31976

EVIDENCE FOR SMALL-SCALE MANTLE CONVECTION FROM SEASAT ALTIMETER DATA

W. F. HAXBY and J. K. WEISSEL (Lamont-Doherty Geological Observatory, Palisades, NY) *Journal of Geophysical Research* (ISSN 0148-0227), vol. 91, March 10, 1986, p. 3507-3520. refs (Contract N00014-80-C-0098; N00014-84-C-0132; NSF OCE-82-02454; NSF OCE-82-08927)

The present paper has mainly the objective to draw attention to singular but subtle patterns of gravity undulations, taking into account their association with the younger portions of fast-moving oceanic plates. The explanation is proposed that these gravity features reflect the development, through instability in the thermal boundary layer, of small-scale mantle convection which is organized into longitudinal rolls by shear imparted fast-moving plates. From the crustal age at which the lineated gravity patterns become discernable it is inferred that small-scale convection becomes established within 5-10 m.y. after initiation of plate cooling. Attention is given to new information from Seasat altimeter data, other geophysical data, and implications for convection in the mantle.

G.R.

A86-32267

THE EFFECTIVE ELASTIC LITHOSPHERE UNDER THE COOK-AUSTRAL AND SOCIETY ISLANDS

S. CALMANT and A. CAZENAVE (CNES, Groupe de Recherche de Geodesie Spatiale, Toulouse, France) *Earth and Planetary Science Letters* (ISSN 0012-821X), vol. 77, no. 2, March 1986, p. 187-202. Research supported by the Institut National des Sciences de l'Univers and CNES. refs

The elastic thickness, T_e , of the oceanic lithosphere along the volcanic chains of Cook-Austral and Society islands was determined, using a three-dimensional spatial method to model the lithospheric flexure and assuming a continuous elastic plate. The model was constrained by geoid height data from the Seasat satellite. When the Society and Cook-Austral T_e results versus age of load are plotted together, it becomes obvious that within the first five-million years after loading, T_e decreases significantly while tending rapidly to an equilibrium value. This may be interpreted as the effect of initial stress relaxation which occurs just after loading inside the lower lithosphere and suggests that the presently measured elastic thickness under the very young Tahiti load (about 0.8 Ma) is not yet the equilibrium thickness.

I.S.

A86-32556*# National Aeronautics and Space Administration, Washington, D.C.

THE OCEAN TOPOGRAPHY EXPERIMENT (TOPEX) - SOME QUESTIONS ANSWERED

W. F. TOWNSEND (NASA, Washington, DC) IN: EASCON '85: National space strategy - A progress report; Proceedings to the Eighteenth Annual Electronics and Aerospace Systems Conference, Washington, DC, October 28-30, 1985. New York, Institute of Electrical and Electronics Engineers, Inc., 1985, p. 293-296.

The Ocean Topography Experiment (TOPEX) is to provide a basis for improving the understanding of the general circulation of the global oceans. In the context of this experiment, measurements of the surface topography of the oceans are to be conducted with the aid of radar altimetry. The obtained data, when combined with appropriate in situ observations, will make it possible to determine the three-dimensional structure of the ocean currents. The in situ observations needed are to be provided by the World Ocean Circulation Experiment (WOCE). Information regarding the ocean surface winds obtained with the aid of the NASA Scatterometer (NSCAT) to be flown on the Navy Remote Ocean Sensing System (N-ROSS) can supplement the TOPEX and WOCE data about the oceans. The TOPEX satellite is to be designed for a three year lifetime, but it will carry expendables for two additional

years. Attention is given to TOPEX as an international program, aspects of timing regarding the conduction of the various experiments dealing with the oceans and the global climate, and the special characteristics of the TOPEX mission.

G.R.

A86-32599#

OPEN OCEAN RADAR SEA SCATTER MEASUREMENTS

D. B. TRIZNA (U.S. Navy, Naval Research Laboratory, Washington, DC) IN: International Radar Conference, Arlington, VA, May 6-9, 1985, Record. New York, Institute of Electrical and Electronics Engineers, Inc., 1985, p. 135-140. refs

Measurements are reported of shipboard X-band radar sea scatter for a variety of wind speeds, collected over 360 degrees in azimuth using horizontal polarization. The data were sorted by azimuth and statistics are reported for the upwind aspect. These are fit well by a double Weibull distribution, similar to that reported by Hansen and Cavaleri. The scattering mechanisms responsible for this double distribution are suggested to be Bragg scatter and sea spikes. Results of correlating the parameters of these distributions against environmental parameters which were collected aboard the research vessel are presented.

Author

A86-32635

THE DESIGN, CONSTRUCTION AND EARLY TRIALS OF A NOVEL AIRBORNE SURVEILLANCE RADAR

J. G. SCHOENENBERGER and P. D. L. WILLIAMS (Racal-Decca Advanced Development, Ltd., Walton-on-Thames, England) IN: International Radar Conference, Arlington, VA, May 6-9, 1985, Record. New York, Institute of Electrical and Electronics Engineers, Inc., 1985, p. 372-377. refs

Attention is given to a novel airborne surveillance radar that originated in a conventional pulse radar carried under a variety of test aircraft and which was then upgraded to SLAR equipment incorporating a bandwidth processor for the real time recording of images on an inexpensive audio tape deck. Ocean surface imagery of reasonable quality has been obtained by these means. The system is expected to be useful in searches for patterns of shipping and features such as oil slicks and thermal currents in disturbed water.

O.C.

A86-32676

NEAR-SURFACE WATER CIRCULATION IN THE SUB-ARCTIC FRONTAL ZONE (ACCORDING TO SATELLITE DATA) [O PRIPOVERKHNOSTNOI TSIRKULIATSII VOD V SUBARKTICHESKOI FRONTAL'NOI ZONE /PO DANNYM ISZ/]

A. I. GINZBURG and K. N. FEDOROV (AN SSSR, Institut Okeanologii, Moscow, USSR) *Issledovanie Zemli iz Kosmosa* (ISSN 0205-9614), Jan.-Feb. 1986, p. 8-13. In Russian. refs

Two satellite images, one taken in the IR and the other taken in the visible, of the region bounded by Hokkaido and sub-Arctic waters on the north, Honsu Island on the west, and the main Kuroshio front on the south are analyzed. The IR image was obtained with the NOAA-6 satellite on May 20, 1981, while the visible image was obtained with a Meteor satellite on May 19, 1984. Similar conditions are shown to produce similar circulation patterns, consisting of an anticyclonic eddy and interrelated meridional and zonal jetlike or mushroomlike currents 150-250 km in extent. The possible mechanism for their formation is examined together with the conditions under which this eddy-jet combination is most probable.

B.J.

A86-32677

SOME FEATURES OF SMALL-SCALE OCEAN EDDIES ACCORDING TO AN ANALYSIS OF SATELLITE IMAGES [O NEKOTORYKH OSOBENNOSTIYAKH MELKOMASSHTABNYKH OKEANSKIKH VIKHREI /PO DANNYM ANALIZA SPUTNIKOVYKH IZOBRAZHENII/]

A. S. KAZMIN and N. P. KUZMINA (AN SSSR, Institut Okeanologii, Moscow, USSR) *Issledovanie Zemli iz Kosmosa* (ISSN 0205-9614), Jan.-Feb. 1986, p. 14-19. In Russian. refs

Salyut-6 and Landsat-1 images of several regions of the Gulf Stream and North Atlantic current are analyzed. The analysis yielded a more accurate spatial pattern of small-scale (5-30 km)

05 OCEANOGRAPHY AND MARINE RESOURCES

eddies and improved their correlation and large-scale circulation features. B.J.

A86-32678

SALYUT-6 OBSERVATION OF COLOR AND BRIGHTNESS CONTRASTS CORRELATED WITH OCEAN-BOTTOM RELIEF [NABLIUDENIE S ORBITAL'NOI STANTSII 'SALIUT-6' TSVETOVYKH I IARKOSTNYKH KONTRASTOV, KORRELIROVANNYKH S REL'EFOM DNA OKEANA]

V. T. ISAKOV, V. V. KOVALENOK, A. I. LAZAREV, and T. A. DAMINOVA (Gosudarstvennyi Opticheskii Institut, Leningrad, USSR) *Issledovanie Zemli iz Kosmosa* (ISSN 0205-9614), Jan.-Feb. 1986, p. 20-25. In Russian.

A86-32679

REMOTE SENSING AND MODELING OF THE DYNAMICS OF THE WESTERN PART OF THE BLACK SEA [DISTANTSIONNYE I MODEL'NYE ISSLEDOVANIIA DINAMIKI ZAPADNOI CHASTI CHERNOGO MORIA]

E. V. STANEV, L. I. MILENOVA, V. M. RUSENOV, and E. K. RUMENINA (Natsional'nyi Komitet po Issledovaniiu i Ispol'zovaniiu Kosmicheskogo Prostranstva, Sofia, Bulgaria) *Issledovanie Zemli iz Kosmosa* (ISSN 0205-9614), Jan.-Feb. 1986, p. 26-31. In Russian. refs

The dynamics of the western part of the Black Sea was investigated on the basis of Salyut-Soyuz MSS data and numerical modeling. It is shown that the propagation of Danube waters, frontal zones, the meandering of the main stream, and the formation of off-shore rings in the western Black Sea could be recognized on the space images. The remote-sensing and simulation data are compared for features of different scales. B.J.

A86-32683

DETERMINATION OF SEA SPECTRAL REFLECTANCE FROM AIRBORNE MEASUREMENTS [OPREDELENIE KOEFFITSIENTA SPEKTRAL'NOI IARKOSTI MORIA PO IZMERENIAM S AVIANOSITELIA]

A. P. VASILKOV, O. A. ERSHOV, and A. I. SUDBIN (AN SSSR, Institut Okeanologii, Moscow, USSR) *Issledovanie Zemli iz Kosmosa* (ISSN 0205-9614), Jan.-Feb. 1986, p. 63-70. In Russian. refs

Upward radiance spectra measured by helicopter at 2-5 km over Black Sea coastal areas are analyzed. The data were used to retrieve spectra at sea level; and the spectra were corrected for atmospheric effects using a modified Gordon algorithm and concurrent measurements of atmospheric spectral transpance. The correction method made it possible to retrieve the sea spectral reflectance in the 400-700 nm range with a maximum absolute error of about 0.01 for measurement altitudes up to 5 km. The retrieval accuracy was checked by comparing the spectra obtained with those measured at 100 m. B.J.

A86-33104*# National Aeronautics and Space Administration. Goddard Space Flight Center, Greenbelt, Md.

REDUCTION OF WEATHER EFFECTS IN THE CALCULATION OF SEA ICE CONCENTRATION FROM MICROWAVE RADIANCES

P. GLOERSEN and D. J. CAVALIER (NASA, Goddard Space Flight Center, Greenbelt, MD) *Journal of Geophysical Research* (ISSN 0148-0227), vol. 91, March 15, 1986, p. 3913-3919. NASA-supported research. refs

A technique is presented which improves existing methods of calculating sea ice concentrations from microwave radiances by reducing weather-related effects over open ocean areas and in the vicinity of marginal sea ice zones. Winds, atmospheric water vapor, cloud liquid water, and rain increase the microwave emission over these regions and thus result in erroneous values of computed sea ice concentration. The method described is based on the microwave spectral properties of sea ice and ice-free ocean and utilizes ratios of the polarized radiances at the 0.81-cm (37 GHz) and 1.7-cm (18 GHz) wavelengths. Following a discussion of the physical basis for this technique, examples are provided which demonstrate its utility. While the technique was developed for use

with the Nimbus 7 scanning multichannel microwave radiometer data, it is applicable also to data from other microwave radiometers operating in a similar wavelength range. Author

A86-33105* Jet Propulsion Lab., California Inst. of Tech., Pasadena.

WEDDELL-SCOTIA SEA MARGINAL ICE ZONE OBSERVATIONS FROM SPACE, OCTOBER 1984

F. D. CARSEY, B. HOLT (California Institute of Technology, Jet Propulsion Laboratory, Pasadena), S. MARTIN, D. A. ROTHROCK (Washington, University, Seattle), L. MCNUTT (Radarsat, Ottawa, Canada) et al. *Journal of Geophysical Research* (ISSN 0148-0227), vol. 91, March 15, 1986, p. 3920-3924. NASA-supported research. refs

Imagery from the Shuttle imaging radar-B experiment as well as other satellite and meteorological data are examined to learn more about the open sea ice margin of the Weddell-Scotia Seas region. At the ice edge, the ice forms into bandlike aggregates of small ice floes similar to those observed in the Bering Sea. The radar backscatter characteristics of these bands suggest that their upper surface is wet. Further into the pack, the radar imagery shows a transition to large floes. In the open sea, large icebergs and long surface gravity waves are discernable in the radar images. Author

A86-33120

EVOLUTION OF THE NET SURFACE SHORTWAVE RADIATION OVER THE INDIAN OCEAN DURING SUMMER MONEX (1979) - A SATELLITE DESCRIPTION

C. GAUTIER (California, University, La Jolla) *Monthly Weather Review* (ISSN 0027-0644), vol. 114, March 1986, p. 525-533. NASA-supported research. refs

(Contract NSF ATM-82-05817; NSF OCE-82-14791)

The evolution of the net shortwave (NSW) radiation fields during the monsoon of 1979 was analyzed, using geostationary satellite data, collected before, during, and after the monsoon onset. It is seen, from the time sequence of NSW fields, that during the preonset phase the characteristics of the NSW field are dominated by a strong maximum in the entire Arabian Sea and by a strong minimum in the central and eastern equatorial Indian Ocean, the minimum being associated with the intense convective activity occurring in that region. As the season evolves, the minima of NSW associated with the large scale convective activity propagate westward in the equatorial ocean. During the monsoon onset, there occurs an explosive onset of the convection activity in the Arabian Sea: the maximum has retreated towards the Somalia coast, and most of the sea then experiences a strong minimum of NSW associated with the intense precipitation occurring along the southwestern coast of the Indian subcontinent. I.S.

A86-33315

STRUCTURAL FEATURES OF THE EASTERLY JET STREAM ACCORDING TO SATELLITE DATA [OB OSOBNOSTI AKH STRUKTURY VOSTOCHNOGO STRUINOGO TECHENIIA PO DANNYM ISZ]

T. KH. GEOKHLANIAN IN: Aspects of the processing and interpretation of measurement data from meteorological satellites. Leningrad, Gidrometeoizdat, 1985, p. 19-26. In Russian. refs

Several features of the cloud structure of the easterly jet stream are examined on the basis of a combined analysis of cloud photographs taken by the Meteor and NOAA satellites, and aerosynoptic data. It is noted that these features can serve as the basis of an analysis of weather in the tropical zone of the Indian Ocean. B.J.

A86-33320

ESTIMATION OF THE ACCURACY OF THE REMOTE DETERMINATION OF OCEAN SURFACE TEMPERATURE ON THE BASIS OF SATELLITE MEASUREMENTS OF OUTGOING THERMAL RADIATION IN THE 10.5-12.5 MICRON RANGE [OTSENKI TOCHNOSTI DISTANTSIONNOGO OPREDELENIIA TEMPERATURY POVERKHNOSTI OKEANA PO DANNYM SPUTNIKOVYKH IZMERENII UKHODIASHCHEGO TEPLOVOGO IZLUCHENIIA V DIAPAZONE 10,5-12,5 MKM]

V. M. SUTOVSKII, A. B. USPENSKII, and V. E. TRETIAKOV IN: Aspects of the processing and interpretation of measurement data from meteorological satellites. Leningrad, Gidrometeoizdat, 1985, p. 66-79. In Russian. refs

A86-33392

OBSERVATION OF INTERNAL WAVES AND SEISMIC WAVES IN THE SICILIAN CHANNEL

P. TRIVERO (Torino, Universita; CNR, Istituto di Cosmogeofisica, Turin, Italy) Nuovo Cimento, Lettere, Serie 2, vol. 44, Dec. 16, 1985, p. 658-664. refs

Internal and seismic waves in the Sicilian Channel are studied. The structural features of the internal waves observed in synthetic aperture radar images are examined; internal waves propagating in a circle about 60 km in diameter and about 1 km apart, radar signatures, and volcanic activity are detected. Analysis of the six months of seismographic data reveals low frequency oscillations occurring in groups of decreasing amplitude at 1 hour intervals, which are preceded by intensified signals in the seismograph readings, and a correlation between the occurrence of earthquakes and the shape of the oscillations is observed. I.F.

A86-33481

SATELLITE OCEANIC REMOTE SENSING

B. SALTZMAN, ED. (Yale University, New Haven, CT) Orlando, FL, Academic Press, Inc., 1985, 525 p. For individual items see A86-33482 to A86-33490.

Oceanic remote sensing by several NASA sponsored satellite systems is described, and the results of these measurements are discussed. Papers are presented on the Seasat, Nimbus-7, and TIROS-N observations; analysis and interpretation of altimeter sea echo; oceanic surface winds; surface and internal ocean wave observations; and microwave wind and rain observations in severe tropical and midlatitude marine storms. Consideration is given to sea surface temperature determinations, ocean color measurements, observations of the polar regions from satellites using active and passive microwave techniques, precipitation in tropical cyclones, and living marine resources applications. Additional papers provide details of the remote sensors involved in these oceanic studies, details of the Seasat validation program, and a summary of the data availability. I.S.

A86-33482

THE 1978 OCEANIC TRILOGY - SEASAT, NIMBUS-7, AND TIROS-N

J. W. SHERMAN, III (NOAA, National Environmental Satellite, Data, and Information Service, Washington, DC) IN: Satellite oceanic remote sensing. Orlando, FL, Academic Press, Inc., 1985, p. 11-60. refs

The sensors aboard NASA's Seasat, Nimbus-7, and TIROS-N satellites are described. These include the Seasat-A Scatterometer System (SASS), a radar altimeter, a SAR, the Scanning Multichannel Microwave Radiometer, the Visible and Infrared Radiometer, and the Coastal Zone Color Scanner. Results obtained on ice dynamics, ocean color, sea surface temperature, atmospheric water, wind characteristics, sea current characteristics, and eddy structures, are summarized. I.S.

A86-33483

ANALYSIS AND INTERPRETATION OF ALTIMETER SEA ECHO

D. E. BARRICK (Ocean Surface Research, Boulder, CO) and B. J. LIPA (Ocean Surface Research, Woodside, CA) IN: Satellite oceanic remote sensing. Orlando, FL, Academic Press, Inc., 1985, p. 61-100. refs

Attention is given to Barrick's (1972) mathematical model describing the altimetric echo waveform, using physical optics to represent the scatter from the rough surface. A convolutional form of this model is presented which expresses the sea surface wave-height probability density function. Models are developed to study various factors which bias or distort the altimeter echo, such as antenna errors and rain biases, and the Seasat altimeter data are used to test their application. I.S.

A86-33484

OCEANIC SURFACE WINDS

D. B. ROSS (NOAA, Atlantic Oceanographic and Meteorological Laboratory, Miami, FL), V. J. CARDONE (Oceanweather, Inc., White Plains, NY), J. OVERLAND (NOAA, Pacific Marine Environmental Laboratories, Seattle, WA), R. D. MCPHERSON (NOAA, National Meteorological Center, Washington, DC), and W. J. PIERSON, JR. (City College, New York) IN: Satellite oceanic remote sensing. Orlando, FL, Academic Press, Inc., 1985, p. 101-140. refs

The mechanism of radar backscatter, which provides a foundation for wind measurements by the Seasat-A Scatterometer System (SASS) is examined. Development of a model relating the SASS data to surface wind speed, which accounts for changes of the marine wind field and the effects of the surface roughness and thermodynamic factors, is discussed. The effect produced by including the satellite data into the standard data base on atmospheric circulation is evaluated using an experiment in which global SASS data were compared with the wind data obtained without SASS (NOSASS). In the Northern Hemisphere, there is little difference between SASS and NOSASS analysis, suggesting that SASS winds are at least as useful as ship winds, buoy reports, and low level, cloud-tracked winds. In the Southern Hemisphere, differences in wind and height analyses were quite large. I.S.

A86-33485* National Oceanic and Atmospheric Administration, Boulder, Colo.

SURFACE AND INTERNAL OCEAN WAVE OBSERVATIONS

C. L. RUFENACH, L. S. FEDOR (NOAA, Wave Propagation Laboratory, Boulder, CO), J. R. APEL (Johns Hopkins University, Laurel, MD), and F. I. GONZALEZ (NOAA, Pacific Marine Environmental Laboratories, Seattle, WA) IN: Satellite oceanic remote sensing. Orlando, FL, Academic Press, Inc., 1985, p. 141-196. NOAA-supported research. refs (Contract NASA ORDER W-15084)

The physical characteristics of the ocean surface waves are discussed, together with the principles behind altimetry measurements of the wave height and SAR measurements of surface wave direction and length. In addition, theoretical aspects of oceanic internal gravity waves are presented, and the measurements of oceanic internal wave fields, using the 'surface signatures' accompanying the underlying oscillations, are described. Results of the surface wave measurements obtained by the Seasat altimeter and SAR are presented along with inferred internal wave results obtained by SAR. I.S.

A86-33486* National Oceanic and Atmospheric Administration, Miami, Fla.

SEASAT MICROWAVE WIND AND RAIN OBSERVATIONS IN SEVERE TROPICAL AND MIDLATITUDE MARINE STORMS

P. G. BLACK, J. D. HAWKINS (NOAA, Atlantic Oceanographic and Meteorological Laboratory, Miami, FL), R. C. GENTRY (Clemson University, SC), and V. J. CARDONE (Oceanweather, Inc., White Plains, NY) IN: Satellite oceanic remote sensing. Orlando, FL, Academic Press, Inc., 1985, p. 197-277. NOAA-NASA-sponsored research. refs

Initial results of studies concerning Seasat measurements in and around tropical and severe midlatitude cyclones over the open

05 OCEANOGRAPHY AND MARINE RESOURCES

ocean are presented, together with an assessment of their accuracy and usefulness. Complementary measurements of surface wind speed and direction, rainfall rate, and the sea surface temperature obtained with the Seasat-A Satellite Scatterometer (SASS), the Scanning Multichannel Microwave Radiometer (SMMR), and the Seasat SAR are analyzed. The Seasat data for the Hurricanes Fico, Ella, and Greta and the QE II storm are compared with data obtained from aircraft, buoys, and ships. It is shown that the SASS-derived wind speeds are accurate to within 10 percent, and the directions are accurate to within 20 percent. In general, the SASS estimates tend to measure light winds too high and intense winds too low. The errors of the SMMR-derived measurements of the winds in hurricanes tend to be higher than those of the SASS-derived measurements. I.S.

A86-33487

SEA SURFACE TEMPERATURE DETERMINATIONS

J. C. ALISHOUSE and E. P. MCCLAIN (NOAA, National Environmental Satellite, Data, and Information Service, Washington, DC) IN: Satellite oceanic remote sensing. Orlando, FL, Academic Press, Inc., 1985, p. 279-296. refs

Sea surface temperature (SST) determinations by the use of microwave and infrared sensors aboard Seasat, the Scanning Multichannel Microwave Radiometer (SMMR) and the Advanced Very High Resolution Radiometer (AVHRR), respectively, are discussed. The SMMR data have been screened to avoid rain, sun glint, and land effects, while the AVHRR data have been screened for clouds and sun glint. Comparison of the SMMR data with surface observations on both a point-by-point and a monthly grid basis have shown much better agreement between the averaged and the gridded values than in the case of point-by-point comparison. The point-by-point comparison between the AVHRR-derived SST's and surface observations are better than in the case of the SMMR, possibly because of the much smaller field of view. I.S.

A86-33488* Miami Univ., Fla.

OCEAN COLOR MEASUREMENTS

H. R. GORDON (Miami University, Coral Gables, FL), R. W. AUSTIN (California, University, Scripps Institution of Oceanography, La Jolla), D. K. CLARK, W. A. HOVIS (NOAA, National Environmental Satellite, Data, and Information Service, Washington, DC), and C. S. YENTSCH (Bigelow Laboratory for Ocean Sciences, West Boothbay Harbor, ME) IN: Satellite oceanic remote sensing. Orlando, FL, Academic Press, Inc., 1985, p. 297-333. refs (Contract NAS5-22963; NAS5-26247; NAS5-22948; N00014-78-C-0566; NAGW-273; NOAA-NA-79SA00741; NOAA-NA-80AAD00007)

Ocean color observations by the Coastal Zone color scanner (CZCS) aboard the Nimbus-7 satellite are discussed, together with the factors contributing to the 'apparent' color of the ocean. The CZCS optical systems and the techniques for extraction of the phytoplankton pigment concentration and the diffuse attenuation coefficient K from the 'apparent' water color are described in detail. Special consideration is given to the use of biooptical algorithms and the development of the K algorithm for the CZCS imagery. It is shown that under typical atmospheric conditions, the pigment concentration can be extracted from the satellite imagery to within + or - 30 percent over concentration ranges from 0 to 5 mg/cu m for the Morel case 1 water (Morel and Prieur, 1977), to which the oceanic waters belong as a rule. I.S.

A86-33489* Massachusetts Univ., Amherst.

OBSERVATIONS OF THE POLAR REGIONS FROM SATELLITES USING ACTIVE AND PASSIVE MICROWAVE TECHNIQUES

C. T. SWIFT (Massachusetts University, Amherst), D. J. CAVALIERI (USGS, Tacoma, WA), P. GLOERSEN, H. J. ZWALLY, N. M. MOGNARD (NASA, Goddard Space Flight Center, Greenbelt, MD) et al. IN: Satellite oceanic remote sensing. Orlando, FL, Academic Press, Inc., 1985, p. 335-392. refs

Observations of the ocean ice, ice sheets, ice edges, and ocean waves in the Antarctic, performed by the Seasat and Nimbus-7 satellites are described. Specific features of the Seasat

altimeter, the SAR, the Seasat-A Scatterometer System, and the Scanning Multichannel Microwave Radiometer (SMMR) are discussed, together with the advantages and limitations of each instrument as applied to the study of ice dynamics. The Nimbus-7 SMMR algorithm for calculating sea-ice concentrations is presented. In addition, the Seasat altimeter-derived data on wind speed and wave heights in the Southern Ocean, and on the ice sheets of the Antarctica and Greenland were evaluated. I.S.

A86-33490

PRECIPITATION IN TROPICAL CYCLONES

C. G. GRIFFITH and L. S. FEDOR (NOAA, Environmental Research Laboratories, Boulder, CO) IN: Satellite oceanic remote sensing. Orlando, FL, Academic Press, Inc., 1985, p. 393-417. refs

Using the Griffith-Woodley (Griffith et al., 1978) technique, rain rates were derived from the Seasat Visible and Infrared Radiometer (VIRR)-IR data for selected passes over three 1978 Pacific tropical storms: Fico, Agnes, and Carmen. The Griffith-Woodley technique is described in detail, and its limitations are discussed. The VIRR-derived rain rates, besides being useful for assessing storm rainfall prior to landfall, can also be used to correct for attenuation in microwave channels sensitive to rainfall, such as the altimeter and scatterometer. I.S.

A86-33514

MULTIFREQUENCY OBSERVATIONS OF BRIGHTNESS TEMPERATURE OF ARTIFICIAL NEW AND YOUNG SEA ICE

T. C. GRENFELL (Washington, University, Seattle) IN: 1985 International Geoscience and Remote Sensing Symposium (IGARSS '85), Amherst, MA, October 7-9, 1985, Digest. Volume 1. New York, Institute of Electrical and Electronics Engineers, Inc., 1985, p. 92-98. refs

An effective technique for isolating the influence of individual physical properties of sea ice on microwave emission is to study a horizontally homogeneous ice sheet whose thermal history and physical characteristics are closely monitored. This has been undertaken by a study encompassing radiometric, dielectric and scatterometric properties, whose preliminary results are presently reported. The major variations observed were associated with ice growth to about 50 mm, as well as with subsequent changes in the state of the surface associated with roughness and the distribution of brine. The effects of snow cover were significant, but smaller than modifications in surface roughness. O.C.

A86-33529* Illinois Univ., Urbana.

REMOTE SENSING OF ATMOSPHERIC PRESSURE AND SEA STATE USING LASER ALTIMETERS

C. S. GARDNER (Illinois University, Urbana) IN: 1985 International Geoscience and Remote Sensing Symposium (IGARSS '85), Amherst, MA, October 7-9, 1985, Digest. Volume 1. New York, Institute of Electrical and Electronics Engineers, Inc., 1985, p. 199-206. refs (Contract NSG-5049)

Short-pulse multicolor laser ranging systems are currently being developed for satellite ranging applications. These systems use Q-switched pulsed lasers and streak-tube cameras to provide timing accuracies approaching a few picoseconds. Satellite laser ranging systems have been used to evaluate many important geophysical phenomena such as fault motion, polar motion and solid earth tides, by measuring the orbital perturbations of retroreflector equipped satellites. Some existing operational systems provide range resolution approaching a few millimeters. There is currently considerable interest in adapting these highly accurate systems for use as airborne and satellite based altimeters. Potential applications include the measurement of sea state, ground topography and atmospheric pressure. This paper reviews recent progress in the development of multicolor laser altimeters for use in monitoring sea state and atmospheric pressure. Author

A86-33532* National Aeronautics and Space Administration. Goddard Space Flight Center, Greenbelt, Md.
LIDAR OBSERVATIONS OF THE PLANETARY BOUNDARY LAYER

S. H. MELFI, J. D. SPINHIRNE, and S. P. PALM (NASA, Goddard Space Flight Center, Greenbelt, MD) IN: 1985 International Geoscience and Remote Sensing Symposium (IGARSS '85), Amherst, MA, October 7-9, 1985, Digest. Volume 1. New York, Institute of Electrical and Electronics Engineers, Inc., 1985, p. 218-222. refs

The application of an airborne downward-looking lidar to the study of organized cellular convection in the planetary boundary layer (PBL) over the ocean is described. The lidar consisted of a frequency doubled Nd-YAG 530 mm-wavelength laser whose axis was aligned colinearly with the optical axis of an all-reflecting 40 mm-diameter Newtonian telescope. The airborne lidar provided a unique observation of both microscale and mesoscale variations of the PBL top. The lidar data, presented as constant backscatter isopleth soundings, provide a visual indication of the presence of vertically organized convection cells. Comparisons of the lidar-derived PBL structure with both a conceptual model of the PBL and laboratory simulations of Deardorf et al. (1980) of a developing convective PBL showed that the observations are consistent with a model of mixing in the PBL, which involves a field of organized updrafts separated by downdrafts. I.S.

A86-33560* Washington Univ., Seattle.
EXTRACTING SEA ICE DATA FROM SATELLITE SAR IMAGERY

M. FIFY and D. A. ROTHROCK (Washington, University, Seattle) IN: 1985 International Geoscience and Remote Sensing Symposium (IGARSS '85), Amherst, MA, October 7-9, 1985, Digest. Volume 1. New York, Institute of Electrical and Electronics Engineers, Inc., 1985, p. 432-437. NASA-Navy-supported research. refs

With the prospect operational satellite SAR's by the end of the decade, there is a clear need to develop automated algorithms for the extraction of geophysical data about sea ice from high resolution radar imagery. To this end, techniques were developed for distinguishing ice from open water and for resolving the details of deformation within areas 100 km square imaged by SEASAT SAR. The classification of ice and open water is based on the creation of two bands of lower resolution image data: local average brightness, and the local variance of brightness. In the space of these two variables, ice and open water are separated into two distinct clusters. The deformation is found on a 3.4 km mesh by local cross-correlations of the brightness. Comparison with manually determined deformation shows room for improvement in regions of high deformation by using smaller areas for cross-correlation. The concentration and deformation data are used together to determine localized regions of the scene where open water is produced or lost. Author

A86-33561
SAR REMOTE SENSING DURING MIZEX 84

R. A. SHUCHMAN and B. A. BURNS (Michigan, Environmental Research Institute, Ann Arbor) IN: 1985 International Geoscience and Remote Sensing Symposium (IGARSS '85), Amherst, MA, October 7-9, 1985, Digest. Volume 1. New York, Institute of Electrical and Electronics Engineers, Inc., 1985, p. 439-443. (Contract N00014-81-C-0295; N00014-83-C-0404)

During the summer Marginal Ice Zone Experiment (MIZEX) of 1984, extensive mosaic coverage of the experiment area was obtained by the CV-580 Synthetic Aperture Radar (SAR) system over a period of 10 days. By virtue of the SAR's imaging capabilities, such as all-weather imaging, relatively high resolution, and large dynamic range of backscatter from SAR ice and open ocean, information on important MIZ parameters can be derived from the SAR data. Information on ice edge location and location of ice-edge eddies, for example, can be obtained directly from examination of the imagery as can detection of ocean fronts and internal waves. With machine-assisted manual image analysis, estimates of ice concentration, floe size distributions, and ice field motion can also be derived. Full digital analysis, however, is required to obtain

gravity wave spectral information and backscatter statistics for ice type discrimination and automated ice concentration algorithms.

Author

A86-33562* National Oceanic and Atmospheric Administration, Boulder, Colo.
MEASUREMENT OF SEA ICE BACKSCATTER CHARACTERISTICS AT 36 GHZ USING THE SURFACE CONTOUR RADAR

L. S. FEDOR (NOAA, Wave Propagation Laboratory, Boulder, CO) and E. J. WALSH (NASA, Wallops Flight Center, Wallops Island, VA) IN: 1985 International Geoscience and Remote Sensing Symposium (IGARSS '85), Amherst, MA, October 7-9, 1985, Digest. Volume 1. New York, Institute of Electrical and Electronics Engineers, Inc., 1985, p. 446-451.

Scattering studies of sea ice off the coast of Greenland were performed in January 1984 using the 36-GHz Surface Contour Radar (SCR) aboard the NASA P-3 aircraft. An oscillating mirror scans an actual half-power width of 0.96 degrees laterally to measure the surface at 51 evenly spaced points. By banking the aircraft, real-time topographical mapping and relative backscattered power are obtained at incidence angles between 0 and 30 degrees off-nadir, achieving at 175 m altitude a 2.9 by 4.4 m spatial resolution at nadir. With an aircraft ground speed of 100 m/s, 5-m successive scan line spacing and 1.8-m cross-track direction spacing is provided. By circling the aircraft in the 15 degree bank, the azimuthal anisotropy of the scattering is investigated along with the incidence angle dependence. R.R.

A86-33591* National Aeronautics and Space Administration. Wallops Flight Center, Wallops Island, Va.
DESIGN AND BENEFITS OF A MULTIBEAM EARTH OBSERVING RADAR

C. L. PARSONS, E. J. WALSH (NASA, Wallops Flight Center, Wallops Island, VA), and F. B. BECK (NASA, Langley Research Center, Hampton, VA) IN: 1985 International Geoscience and Remote Sensing Symposium (IGARSS '85), Amherst, MA, October 7-9, 1985, Digest. Volume 2. New York, Institute of Electrical and Electronics Engineers, Inc., 1985, p. 650-656. refs

The oceanographic rationale is described for continuing to advance the state of the art in satellite radar altimetry, and the expected capabilities of a multibeam Earth Observing Radar are noted. At the end of this decade, there is the possibility that altimeters may be in orbit aboard the American TOPEX, the ESA ERS-1, and the French SPOT satellites at the same time. The TOPEX version will be the most precise altimeter yet built. Global ocean circulation will be measured by using TOPEX to monitor the elevation changes across the ocean basins due to oceanic currents. It will then be possible to monitor the 'mean' circulation patterns in the oceans. The multiple beams of EOR might be used to measure the curvature of the topographic surface. The use of curvature is especially beneficial because it is directly related to ocean circulation, which is a function only of the Laplacian of the topographic height field in a given area. With the EOR, that height field will be known and ocean circulation can be immediately computed. D.H.

A86-33601* Jet Propulsion Lab., California Inst. of Tech., Pasadena.

A MEDIAN FILTER APPROACH FOR CORRECTING ERRORS IN A VECTOR FIELD

H. SCHULTZ (California Institute of Technology, Jet Propulsion Laboratory, Pasadena) IN: 1985 International Geoscience and Remote Sensing Symposium (IGARSS '85), Amherst, MA, October 7-9, 1985, Digest. Volume 2. New York, Institute of Electrical and Electronics Engineers, Inc., 1985, p. 724-728.

Techniques are presented for detecting and correcting errors in a vector field. These methods employ median filters which are frequently used in image processing to enhance edges and remove noise. A detailed example is given for wind field maps produced by a spaceborne scatterometer. The error detection and replacement algorithm was tested with simulation data from the NASA Scatterometer (NSCAT) project. Author

A86-33602

THE SPATIAL EVOLUTION OF SAR DERIVED WAVE SPECTRA IN THE VICINITY OF HURRICANE IVA

F. M. MONALDO, D. E. IRVINE (Johns Hopkins University, Laurel, MD), and F. I. GONZALEZ (NOAA, Pacific Marine Environmental Laboratory, Seattle, WA) IN: 1985 International Geoscience and Remote Sensing Symposium (IGARSS '85), Amherst, MA, October 7-9, 1985, Digest. Volume 2 . New York, Institute of Electrical and Electronics Engineers, Inc., 1985, p. 731-736. refs

A swath of Seasat SAR imagery 1200 km long was used to generate a spatial series of SAR ocean image spectra in the vicinity of Hurricane IVA. These spectra were corrected for an instrument transfer function. By using a much longer image strip than previous investigators, it is possible to explain the evolution of SAR measured spectral parameters, dominate wavelength and propagation direction, in terms of simple kinematic parameters of the moving hurricane. Author

A86-33607

THE SIR-B EXTREME WAVES EXPERIMENT IN THE SOUTHERN OCEANS

R. C. BEAL (Johns Hopkins University, Laurel, MD) IN: 1985 International Geoscience and Remote Sensing Symposium (IGARSS '85), Amherst, MA, October 7-9, 1985, Digest. Volume 2 . New York, Institute of Electrical and Electronics Engineers, Inc., 1985, p. 787-791. refs

An account is given of the October 1984 SIR-B Extreme Waves Experiment off the west coast of southern Chile and in the region of the Agulhas Current south and east of South Africa. The experiment was designed to overcome many of the limitations encountered in Seasat by collecting simultaneous and independent estimates of the directional wave spectra from aircraft to verify and calibrate the SAR measurements over a variety of incidence angles and sea states. For the SIR-B reflight, scheduled for March 1987, the intent is to repeat the Chile experiment just to the east and north of St. Johns, Newfoundland where North Atlantic storms are notorious for producing high waves. D.H.

A86-33608

WAVES PREDICTED BY THE GLOBAL SPECTRAL OCEAN WAVE MODEL OFF THE WEST COAST OF CHILE DURING THE SIR-B MISSION

L. F. ZAMBRESKY (U.S. Navy, Fleet Numerical Oceanography Center, Monterey, CA) IN: 1985 International Geoscience and Remote Sensing Symposium (IGARSS '85), Amherst, MA, October 7-9, 1985, Digest. Volume 2 . New York, Institute of Electrical and Electronics Engineers, Inc., 1985, p. 792-797.

The verification of the GSOWM (Global Spectral Ocean Wave Model) of the Fleet Numerical Oceanography Center in the Southern Hemisphere in October 1984 is described. The primary output of GSOWM is directional wave spectra with a resolution of 15 frequencies and 24 directions at every point on a 2.5 degree latitude/longitude grid. From October 8 through October 12, 1984, SIR-B observed directional wave spectra of the southwestern tip of Chile from the Space Shuttle. Two airborne scanning radars made nearly simultaneous measurements. A wave model without any direct initialization through wave observations can predict waves with a reasonable degree of skill. The next step toward improving wave modeling would be to incorporate near real-time wave observations; a spaceborne synthetic aperture radar is one of the few viable instruments for providing the quasi-synoptic observations of directional wave spectra required by GSOWM. D.H.

A86-33609* National Aeronautics and Space Administration. Wallops Flight Center, Wallops Island, Va.

SPECTRAL MEASUREMENTS IN SUPPORT OF SIR-B USING THE SURFACE CONTOUR RADAR

E. J. WALSH, D. W. HANCOCK, III, D. E. HINES (NASA, Wallops Flight Center, Wallops Island, VA), R. N. SWIFT, and J. F. SCOTT (EG & G Washington Analytical Services Center, Inc., Pocomoke City, MD) IN: 1985 International Geoscience and Remote Sensing Symposium (IGARSS '85), Amherst, MA, October 7-9, 1985, Digest. Volume 2 . New York, Institute of Electrical and Electronics Engineers, Inc., 1985, p. 798-803. refs

The use of the Surface Contour Radar (SCR) from an aircraft to obtain spectral information on the seas off the tip of South America, in support of the SIR-B experiment in October 1984, is reported. The SCR is a computer-controlled 36-GHz radar that measures sea surface directional wave spectra and produces a real-time topographical map of the surface below the aircraft. Ground tracks and polar plots of the data obtained are illustrated. D.H.

A86-33611* Environmental Research Inst. of Michigan, Ann Arbor.

SIMULATIONS OF SAR WAVE SPECTRA USING HIGH SPECTRAL RESOLUTION ESTIMATES FROM THE SCR AND ROWS INSTRUMENTS

D. LYZENGA (Michigan, Environmental Research Institute, Ann Arbor) IN: 1985 International Geoscience and Remote Sensing Symposium (IGARSS '85), Amherst, MA, October 7-9, 1985, Digest. Volume 2 . New York, Institute of Electrical and Electronics Engineers, Inc., 1985, p. 812-817. NASA-supported research. (Contract N00014-81-C-0692)

A numerical model for predicting the synthetic aperture radar (SAR) image of a moving ocean surface is described, and results are presented for two SIR-B data sets collected off the coast of Chile. Wave height spectra measured by the NASA radar ocean wave spectrometer (ROWS) and surface contour radar (SCR) were used as inputs to this model, and results are compared with actual SIR-B image spectra from orbits 91 and 106. Author

A86-33612

DIRECTIONAL OCEAN WAVE SPECTRA OBTAINED FROM THE SHUTTLE IMAGING RADAR OFF THE COAST OF CHILE

F. M. MONALDO and D. G. TILLEY (Johns Hopkins University, Laurel, MD) IN: 1985 International Geoscience and Remote Sensing Symposium (IGARSS '85), Amherst, MA, October 7-9, 1985, Digest. Volume 2 . New York, Institute of Electrical and Electronics Engineers, Inc., 1985, p. 818-822. refs

During the Shuttle Imaging Radar Mission (SIR-B) in October 1984, synthetic aperture radar (SAR) ocean wave imagery was acquired coincident with independent measurements of the two-dimensional ocean wave spectrum made by instruments aboard a P-3 aircraft. Preliminary evaluation of SAR image spectra suggest a close correspondence between SAR image spectra and ocean surface slope-variance spectra. Author

A86-33619

RADAR SOUNDING OF ICE MASSES CONTAINING LIQUID WATER

S. M. HODGE (USGS; Puget Sound, University, Tacoma, WA) IN: 1985 International Geoscience and Remote Sensing Symposium (IGARSS '85), Amherst, MA, October 7-9, 1985, Digest. Volume 2 . New York, Institute of Electrical and Electronics Engineers, Inc., 1985, p. 868-873. refs

When frequencies of 1-10 MHz are used, scattering from water-filled cavities found in temperate glaciers is sufficiently reduced that bottom returns are usually detectable. An impulse type of radar, with resistively-loaded antennas, is necessary for acceptable range resolution. Evidence from two independent radar studies, as well as from borehole drilling, suggests that the characteristic dimension of these cavities is of the order of 0.5-1.0 m. Significant potential exists for substantially improving overall system performance and for applying this remote sensing technique

to studies of the internal structure and flow of polar ice sheets as well as temperate glaciers. Author

A86-33631
SATELLITE IMAGING OF COASTAL FLOW CIRCULATION IN RELATION TO NUMERICAL MODELLING

L. JONSSON (Lund, Universitet, Sweden) IN: 1985 International Geoscience and Remote Sensing Symposium (IGARSS '85), Amherst, MA, October 7-9, 1985, Digest. Volume 2. New York, Institute of Electrical and Electronics Engineers, Inc., 1985, p. 979-983.

Flow related problems have been investigated in the area of the coastal waters near southern Sweden, using numerical models and satellite imagery. Different kinds of approximation of flow behavior are examined - the shallow water approach and laterally integrated flow equations. Some of the applications are discussed especially with reference to assumptions made and the remotely sensed flow information. Satellite imaging has demonstrated its potential of providing large-scale synoptic flow information in the coastal waters off Scania, Sweden. Both temperature differences and suspended material were used as indicators. The findings have implications in several respects for numerical modeling.

D.H.

A86-33632
APPLICABILITY OF ATMOSPHERIC CORRECTION ALGORITHM FOR CZCS DATA TO JAPANESE COASTAL AREA

H. FUKUSHIMA (Tokai University, Shimizu, Japan) and T. OGISHIMA (Hokkaido Regional Fisheries Research Laboratory, Kushiro, Japan) IN: 1985 International Geoscience and Remote Sensing Symposium (IGARSS '85), Amherst, MA, October 7-9, 1985, Digest. Volume 2. New York, Institute of Electrical and Electronics Engineers, Inc., 1985, p. 987-992. refs

Several concepts are discussed on which NASA's atmospheric correction algorithm strongly rely, based on the observed chlorophyll and irradiance data for Japanese coastal waters. The assumption that the water-leaving radiance at 670 nm is zero is tested against the observed data and the error due to the assumption is evaluated. It is shown that the error might be significant for areas with high sediment concentrations. The spectral relation of water-leaving radiance for various lambdas (the basis for the iterative procedure used when the radiance at 670 nm is not zero) is also discussed. The regularly observed chlorophyll concentration data from 1979-1983 around Japan are investigated to check the presence, extent, and location of the 'clear water' area which acts as an anchor point for atmospheric correction. Always finding such an area presents some difficulties, and this suggests the necessity for other algorithms that do not rely on this concept.

D.H.

A86-33645
AN OVERVIEW OF THE SAR INTERNAL WAVE SIGNATURE EXPERIMENT

R. F. GASPAROVIC and J. R. APEL (Johns Hopkins University, Laurel, MD) IN: 1985 International Geoscience and Remote Sensing Symposium (IGARSS '85), Amherst, MA, October 7-9, 1985, Digest. Volume 2. New York, Institute of Electrical and Electronics Engineers, Inc., 1985, p. 1123-1128. Navy-supported research.

Activities during SARSEX Phase I (the synthetic aperture radar internal wave signature experiment) from August 27 to September 7, 1984 are summarized. SARSEX is a research program sponsored by the Office of Naval Research to investigate SAR imaging of oceanic internal wave surface effects. The experiment, conducted in the New York Bight south of Long Island was designed to yield calibrated SAR images of internal waves with coincident sea truth data to provide quantitative tests of model predictions for internal wave signatures. Oceanographic measurements were made from two research vessels. Four current meter moorings were implanted to measure internal wave currents. Dual frequency (X-band and L-band) SAR imagery was obtained from a CV-580 aircraft; another CV-580 aircraft flew a laser scatterometer and a third aircraft was used for visual observation of the internal wave surface features.

A large body of data on the hydrodynamic properties and electromagnetic signatures of continental shelf internal waves was obtained under a variety of wind, surface wave, and radar illumination conditions. D.H.

A86-33646
SAR-OBSERVED INTERNAL WAVE SIGNATURES FROM SARSEX - INITIAL OBSERVATIONS

E. S. KASISCHKE, R. A. SHUCHMAN, and D. R. LYZENGA (Michigan, Environmental Research Institute, Ann Arbor) IN: 1985 International Geoscience and Remote Sensing Symposium (IGARSS '85), Amherst, MA, October 7-9, 1985, Digest. Volume 2. New York, Institute of Electrical and Electronics Engineers, Inc., 1985, p. 1129-1134.

(Contract N00014-81-C-0692)

The aircraft SAR data set collected during the 1984 SARSEX experiment is summarized. Digitally-recorded and processed imagery (X- and L-band), collected on August 31, 1984, is presented, along with calibrated radar cross-section scans showing internal wave surface patterns. These scans reveal a distinct difference for the signatures between X- and L-bands, with the L-band signatures having a greater peak-to-background modulation. Also, the scans reveal that the SAR images range-traveling waves more distinctly than azimuth-traveling waves. Author

A86-33647
SAR OBSERVED INTERNAL WAVE SIGNATURES FROM SARSEX-COMPARISONS WITH SAR IMAGING MODELS

R. A. SHUCHMAN, E. S. KASISCHKE, D. R. LYZENGA (Michigan, Environmental Research Institute, Ann Arbor), and D. R. THOMPSON (Johns Hopkins University, Laurel, MD) IN: 1985 International Geoscience and Remote Sensing Symposium (IGARSS '85), Amherst, MA, October 7-9, 1985, Digest. Volume 2. New York, Institute of Electrical and Electronics Engineers, Inc., 1985, p. 1153-1159. refs

(Contract N00014-81-C-0692; N00024-83-C-5301)

This paper discusses comparisons between actual and model predicted SAR intensities from internal waves collected during the 1984 SARSEX experiment. A SAR ocean surface imaging model based upon the spectral perturbation of Bragg scatterers is described. Results from this model are compared with the SAR observations. At L-band, the model predictions compare favorably with the SAR observations for range-traveling internal waves. The model present predicts no surface signature for any X-band cases and for L-band azimuth-traveling waves, whereas the SAR clearly shows signatures for these cases. Other possible imaging mechanisms are suggested. Author

A86-34488
OPTIMAL DISPOSITION OF SATELLITE-TRACKED DRIFTING BUOYS IN THE SOUTH ATLANTIC [OB OPTIMAL'NOM RAZMESHCHENII V IUZHNOI ATLANTIKE DREIFUIUSHCHIKH BUEV, OTSLEZHIVAEMYKH SO SPUTNIKOV]

A. F. TRESHNIKOV, V. V. GURETSKII, A. I. DANILOV, V. N. EREMEEV, L. M. IVANOV (Arkticheskii i Antarkticheskii Nauchno-Issledovatel'skii Institut, Leningrad, USSR) et al. Akademiia Nauk SSSR, Doklady (ISSN 0002-3264), vol. 287, no. 2, 1986, p. 430-434. In Russian. refs

A86-34743
ESTIMATION OF SEA-SURFACE TEMPERATURE FROM AVHRR DATA COMMENTS ON THE PAPER BY SINGH ET AL. (1985)

J. R. EYRE (Oxford University, England) International Journal of Remote Sensing (ISSN 0143-1161), vol. 7, March 1986, p. 465-469. refs

The method proposed by Singh et al. (1985) for estimating sea-surface temperature using one channel of the Advanced Very High Resolution Radiometer is shown to be, in its optimum form, mathematically equivalent to a simple linear regression method. The relationship between single-channel and split-window methods and the reasons for the superiority of the latter over the former are discussed. Author

05 OCEANOGRAPHY AND MARINE RESOURCES

A86-34754

INVESTIGATION OF THE CONTENT OF TRACE ELEMENTS IN SEA AEROSOLS AND THE SURFACE MICROLAYER OFF SEA WATER [ISSLEDOVANIIE SODERZHANIIA MIKROELEMENTOV V MORSKIKH AEROZOLICAKM I POVERKHNOSTNONI MIKROSLOE MORSKOI VPDY]

V. D. KORZH (AN SSSR, Institut Okeanologii, Moscow, USSR) Akademiia Nauk SSSR, Doklady (ISSN 0002-3264), vol. 286, no. 6, 1986, p. 1348-1351. In Russian. refs

A86-35278#

ACCURACY ESTIMATE OF GEOID AND OCEAN TOPOGRAPHY RECOVERED JOINTLY FROM SATELLITE ALTIMETRY

C. A. WAGNER (NOAA, National Geodetic Survey, Rockville, MD) Journal of Geophysical Research (ISSN 0148-0227), vol. 91, Jan. 10, 1986, p. 453-461. refs

Joint determination of the geoid and permanent dynamic sea topography is demonstrated by simulation from direct use of satellite altimetry. The separation is feasible because of the disparities between the error spectra of the geoid and its unique perturbative effects as seen on the orbit. The solution for the components of the permanent topography from 14 cm Seasat altimetry promises to yield accurate results down to half wavelengths of about 1000 km. Present discrimination of this surface from disjoint satellite altimeter results appears to be at a scale near 4000 km. The radial effects of uncertainties in the M2 ocean tide on the Seasat orbit and altimeter measurements will probably be only a minor contaminant of the solution. Author

A86-35531

INTENSITY MODULATION IN SAR IMAGES OF INTERNAL WAVES

D. R. THOMPSON and R. F. GASPAROVIC (Johns Hopkins University, Laurel, MD) Nature (ISSN 0028-0836), vol. 320, March 27, 1986, p. 345-348. Navy-sponsored research. refs

During the SAR Signature Experiment (SARSEX), conducted in 1984 in the New York Bight off the eastern coast of the United States, SAR images of the ocean surface and concurrent ground-truth measurements were collected in order to test quantitatively various imaging theories. These theories predict that the intensity modulations observed in SAR images of internal waves are produced by variations in the internal wave surface roughness induced by spatial variations in the internal wave surface current field. Analysis of the SARSEX data indicates that the imaging theories can explain the observed modulation for L-band SAR wavelengths, but underpredict by almost an order of magnitude the observed X-band modulation. This discrepancy is explained by hypothesizing a two-step mechanism in which the observed X-band modulation results from additional small-scale roughness produced by the strong perturbation of meter-scale surface waves by the internal wave current field. C.D.

A86-35545

SATELLITE OBSERVATIONS OF SEA SURFACE COOLING BY HURRICANES

L. STRAMMA, P. CORNILLON (Rhode Island, University, Narragansett), and J. F. PRICE (Woods Hole Oceanographic Institution, MA) Journal of Geophysical Research (ISSN 0148-0227), vol. 91, April 15, 1986, p. 5031-5035. refs (Contract N00014-81-C-0062; N00014-76-C-0197; NR PROJECT 083-165; NR PROJECT 083-400)

Sea surface cooling associated with 13 hurricanes in the western North Atlantic between September 1981 and December 1984 is examined, using satellite-derived sea surface temperature fields. Some surface cooling is observed in all cases; however, because of cloud cover and the fairly weak signal in some cases, pronounced cooling is seen along an extensive and continuous portion of the storm path for only three strong hurricanes. The persistence of cooling following the passage of a hurricane varies from a few days to at least 16 days. The amplitude of cooling is moderately well correlated with hurricane strength, and is as large as 3.5 C. When the hurricanes move rapidly, the maximum cooling occurs well to the right of the track (approximately 70 km), whereas

for slowly moving hurricanes the maximum cooling occurs near or on the track. Because western North Atlantic hurricanes are often found in close proximity to high pressure systems, daytime satellite images must be made with some care because of diurnal warming. Author

A86-35550* Washington Univ., Seattle.

A SIMPLE, OBJECTIVE ANALYSIS SCHEME FOR SCATTEROMETER DATA

G. LEVY and R. A. BROWN (Washington, University, Seattle) Journal of Geophysical Research (ISSN 0148-0227), vol. 91, April 15, 1986, p. 5153-5158. refs (Contract NAGW-679)

A simple economical objective analysis scheme is devised and tested on real scatterometer data. It is designed to treat dense data such as those of the Seasat A Satellite Scatterometer (SASS) for individual or multiple passes, and preserves subsynoptic scale features. Errors are evaluated with the aid of sampling ('bootstrap') statistical methods. In addition, sensitivity tests have been performed which establish qualitative confidence in calculated fields of divergence and vorticity. The SASS wind algorithm could be improved; however, the data at this point are limited by instrument errors rather than analysis errors. The analysis error is typically negligible in comparison with the instrument error, but amounts to 30 percent of the instrument error in areas of strong wind shear. The scheme is very economical, and thus suitable for large volumes of dense data such as SASS data. Author

A86-35682

MICROWAVE RADIOMETRY FOR OIL POLLUTION MONITORING, MEASUREMENTS, AND SYSTEMS

N. SKOU (Danmarks Tekniske Højskole, Lyngby, Denmark) (International Geoscience and Remote Sensing Symposium /IGARSS '84/: From Research toward Operational Use, Strasbourg, France, Aug. 27-30, 1984) IEEE Transactions on Geoscience and Remote Sensing (ISSN 0196-2892), vol. GE-24, May 1986, p. 360-367. refs

Work is presently carried out in Europe to change the status of the microwave radiometer, namely, to develop it from a research instrument to an operational instrument - especially for measuring oil pollution on the sea surface. The Technical University of Denmark (TUD), with its long experience in airborne microwave radiometry, is heavily involved in this process. The TUD multichannel imaging radiometer system has been flown in several large-scale oil-pollution experiments, the collected data have been analyzed, and they have revealed that care must be exercised to obtain accurate oil volume estimations. Computer simulations of the total measurement situation have shown how the observed difficulties come about and have indicated the countermeasures to apply. Based on the abovementioned exercises, optimum (and practical) systems are being developed. Author

A86-35683*# National Aeronautics and Space Administration, Goddard Space Flight Center, Greenbelt, Md.

AIRCRAFT AND SATELLITE PASSIVE MICROWAVE OBSERVATIONS OF THE BERING SEA ICE COVER DURING MIZEX WEST

D. J. CAVALIERI, P. GLOERSEN, and T. T. WILHEIT, JR. (NASA, Goddard Space Flight Center, Greenbelt, MD) (International Geoscience and Remote Sensing Symposium /IGARSS '84/: From Research toward Operational Use, Strasbourg, France, Aug. 27-30, 1984) IEEE Transactions on Geoscience and Remote Sensing (ISSN 0196-2892), vol. GE-24, May 1986, p. 368-377. NASA-supported research. Previously announced in STAR as N84-33917. refs

Passive microwave measurements of the Bering Sea were made with the NASA CV-990 airborne laboratory during February. Microwave data were obtained with imaging and dual-polarized, fixed-beam radiometers in a range of frequencies from 10 to 183 GHz. The high resolution imagery at 92 GHz provides a particularly good description of the marginal ice zone delineating regions of open water, ice compactness, and ice-edge structure. Analysis of the fixed-beam data shows that spectral differences increase with

a decrease in ice thickness. Polarization at 18 and 37 GHz distinguishes among new, young, and first-year ice types. ESA

A86-35688
RELATIVE VERTICAL POSITIONING USING GROUND-LEVEL TRANSPONDERS WITH THE ERS-1 ALTIMETER

R. J. POWELL (SERC, Rutherford Appleton Laboratory, Didcot, England) IEEE Transactions on Geoscience and Remote Sensing (ISSN 0196-2892), vol. GE-24, May 1986, p. 421-425.

The use of the ERS-1 satellite altimeter to measure the relative vertical position of land-based transponders and the ocean geoid on 2000-km-long segments of the satellite ground track is proposed. The procedures and equations for calculating delay measurements, evaluating their accuracy, and converting the delay data to range measurements are described. The usefulness of this technique is tested by obtaining measurements from aircraft using the RAL altimeter over ground-based corner reflectors; the experiment revealed the accuracy of the vertical positioning data and the validity of the predicted delay resolution. The vertical positioning data are applicable for altimeter calibration, measurements of sea-state bias effects, seismic and geodetic studies, and satellite orbit measurements. I.F.

A86-35860#
WIND DEPENDENCE OF L-BAND RADAR BACKSCATTER

A. SARKAR, L. BHADURI, and R. KUMAR (Indian Space Research Organization, Space Applications Centre, Ahmedabad, India) Defence Science Journal (ISSN 0011-748X), vol. 35, Oct. 1985, p. 383-389.

Like other microwave frequency bands, L-band scattering coefficient measurements have shown a definite dependence on ocean surface wind speed (W). The relationship between the two depends on the observation angle of the radar. The satellite-borne L-band radars Seasat-SAR and SIR-A made observations at fixed incidence angles, while the just completed SIR-B mission has made observations at multiple incidence angles. The present work uses the theory of scattering from a composite surface and generates an analytic function of the relationship between the scattering coefficient and W for varying incidence angle at L-band by the method of empirical curve fitting. Author

A86-36048
SATELLITE THERMAL OBSERVATION OF OIL SLICKS ON THE PERSIAN GULF

I. ASANUMA, K. MUNEYAMA, Y. SASAKI (Japan Marine Science and Technology Center, Yokosuka), J. IISAKA (Canada Centre for Remote Sensing, Ottawa), Y. YASUDA (Chiba, University, Japan) et al. Remote Sensing of Environment (ISSN 0034-4257), vol. 19, April 1986, p. 171-186. refs

A possibility of oil slicks detection is discussed for oil slicks spread in the vicinity of the Nowruz oil fields in the Persian Gulf since March 1983 to July 1983 with considering an apparent thermal inertia. The apparent thermal was computed from continuous observations of sea surface temperature and albedo by the Advanced Very High Resolution Radiometer (AVHRR) on the NOAA-7 through day and night with 12 h interval. The apparent thermal inertia is defined as a function of a temperature difference between the daytime and the nighttime and an apparent albedo. Sea surface temperature used for computing the apparent thermal inertia was obtained through an atmospheric correction with an empirical equation which uses an energy difference between two thermal channels of the AVHRR. Although there was an ambiguity on a selection of same object on water body, the computed apparent thermal inertia showed the possibility of oil slicks detection from sea water. Author

A86-36096
GRAVITY ANOMALIES AND SEA SURFACE HEIGHTS DERIVED FROM A COMBINED GEOS 3/SEASAT ALTIMETER DATA SET
 R. H. RAPP (Ohio State University, Columbus) Journal of Geophysical Research (ISSN 0148-0227), vol. 91, April 10, 1986, p. 4867-4876. refs
 (Contract F19628-82-K-0022)

The development of a set of gravity anomalies and sea surface height (SSH) on a 0.125 deg grid from altimeter data is described. The gravity anomalies and SSH set are estimated using Mortiz's (1980) method of least squares collocation. The point prediction tests performed to evaluate the accuracy of the gravity anomaly predictions are examined. The effect of sea surface topography on the predicted anomalies is studied. The predicted anomalies are compared with ship gravity data. The calculation of power spectra from the point predictions and of geoid undulation power between specified spherical harmonic degrees are discussed. I.F.

A86-36480
PROBABILISTIC MODELING OF FIELDS OF ATMOSPHERIC TURBULENCE AND SEA ROUGHNESS WITH REFERENCE TO THE STUDY OF COMPLEX SYSTEMS [VEROJATNOSTNOE MODELIROVANIE POLEI TURBULENTNOSTI ATMOSFERY I MORSKOGO VOLNENIIA PRI ISSLEDOVANII SLOZHNYKH SISTEM]

I. I. PALAGIN, S. V. FEDOTOV, and A. S. SHALYGIN Radiotekhnika i Elektronika (ISSN 0033-8494), vol. 31, April 1986, p. 721-727. In Russian. refs

Simulation models of atmospheric turbulence and sea roughness are developed on the basis of parametric representations of random fields. The models do not exhibit errors in relation to the spectral-correlation characteristics, require a limited computation volume, and are convenient for implementation on both digital and analog processors. The present approach is applied to the statistical modeling of the motion-control system of a flight vehicle with a radar altimeter. Author

A86-36788
POSITION FIXING AFLOAT

A. E. INGHAM (Meeting on Location-Terrestrial Positioning and Geometric Correction of Imagery, University of Nottingham, England, May 23, 1984) International Journal of Remote Sensing (ISSN 0143-1161), vol. 7, April 1986, p. 541-546.

The utopian notion of position determination at sea is for an unlimited number of users to obtain an unambiguous, extremely accurate positioning facility, not only at the sea surface but also on the seabed or anywhere in between, 24 hours per day, continuously and in all weathers. This has traditionally implied such unattainable standards of technology that the notion has inspired little but cynical laughter. Now however, the notion has become reality for most of the practical situations encountered offshore. The question of how accurate a position should be can still evoke debate, of course, but only remote sensing and, perhaps, geodesy demand, on occasion, higher standards than are attainable by contemporary methods. This paper attempts to set in perspective the various methods employed to determine position offshore and to discuss in general terms the several approaches to the accuracy requirement. Author

A86-36954#
REMOTE SENSING WITH THE JINDALEE SKYWAVE RADAR
 S. J. ANDERSON (Department of Defence, Electronics Research Laboratory, Adelaide, Australia) IN: Conference on the Ionosphere and Radio Wave Propagation, 3rd, Sydney, Australia, February 11-15, 1985, Proceedings. Darlinghurst, Australia, Ionospheric Prediction Service, 1985, 4 p. refs

An account is given of the use of the Jindalee skywave radar to produce a surface wind map that was transmitted over a facsimile link from near Alice Springs to the Bureau of Meteorology Regional Office in Darwin. The event, on February 7, 1985, marked the commencement of what may one day become a routine service - the provision of real-time wind and sea-state information extracted

05 OCEANOGRAPHY AND MARINE RESOURCES

from skywave radar echoes. A concerted effort is under way to establish the viability and utility of employing the radar in this secondary (nonmilitary) role. Direct observables are: Bragg-resonant wave ratio; surface current, dominant wavenumber; swell frequency and direction; sea-state; nondirection spectrum; and directional spectrum. Wind direction and wind speed are inferred. Topics discussed include: the influence of the ionosphere; estimation of ocean surface parameters; validation of estimation procedures; and present and future radar capabilities. D.H.

A86-37013

ASSESSMENT AND TRENDS OF FLORIDA'S MARINE FISHERIES HABITAT AN INTEGRATION OF AERIAL PHOTOGRAPHY AND THEMATIC MAPPER IMAGERY

K. D. HADDAD and B. A. HARRIS (Florida Department of Natural Resources, St. Petersburg) IN: Machine processing of remotely sensed data - Quantifying global process: Models, sensor systems, and analytical methods; Proceedings of the Eleventh International Symposium, West Lafayette, IN, June 25-27, 1985. New York, Institute of Electrical and Electronics Engineers, 1985, p. 130-138. refs

A86-37506

TECHNOLOGICAL IMPROVEMENTS TO NAVAL AVIATION WEATHER SUPPORT

H. E. NICHOLSON (U.S. Navy, Fleet Numerical Oceanography Center, Monterey, CA) IN: International Conference on the Aviation Weather System, 2nd, Montreal, Canada, June 19-21, 1985, Preprints. Boston, MA, American Meteorological Society, 1985, p. 321-324.

Problems unique to US Naval Aviation weather support, the system currently in use, and technological advances for the near future are presented in detail. The Fleet Numerical Oceanography Center (FNOC) in Monterey, California, is the center of the Naval support system as it now exists. Using a real-time data base and weather/ocean prediction models, the FNOC supplies the basic forecast guidance to US Naval forces around the world, noting various drawbacks. The NEDN (Naval Environmental Data Network) Oceanographic Data Distribution and Expansion System/ Satellite Data Processing Display System (NODDES/SPADS), to be installed in oceanography centers this year, is discussed. The NODDES side of the system will provide for communication, storage, manipulation and display of computer products and conventional data, while SPADS will do the same for satellite data. Other improvements to Naval Aviation weather support include the Aviation Support Display Station (ASDS) and the Optimum Path Aircraft Routing System (OPARS). ASDS will condense satellite and radar images, alphanumeric data and computer-generated weather charts into one unit, while OPARS will provide information on the most efficient flight routes. K.K.

A86-38648#

SEA LEVEL TIME SERIES IN THE EQUATORIAL PACIFIC FROM SATELLITE ALTIMETRY

L. MILLER, R. CHENEY, and D. MILBERT (NOAA, National Ocean Service, Rockville, MD) Geophysical Research Letters (ISSN 0094-8276), vol. 13, May 1986, p. 475-478. refs

Geosat, a Navy satellite launched in March 1985, will provide the first long-term, global altimeter data set. These observations will enable construction of monthly sea level maps of the equatorial Pacific, much like those presently derived from island tide gauges, but with greatly improved spatial resolution and coverage. During the first half of the Geosat mission, the satellite ground track will not repeat, requiring time series analyses to be based on altimetric height differences at crossover points. The 3-month Seasat data set was used in the equatorial Pacific to test the feasibility and accuracy of this procedure. Crossover differences were sorted into diamond-shaped areas with zonal and meridional dimensions of 200 and 400 km, respectively. The sea level time series in each of these areas was then determined using objective analysis. These computations show agreement within 5 cm between altimeter and island tide gauge observations on time scales greater than 1 month. Using this technique, it is proposed that monthly maps of

sea level variability in the equatorial Pacific for the duration of the Geosat mission (approximately 3 years) can be constructed.

Author

A86-38718#

ERS-1 - OUR NEW WINDOW ON THE OCEANS FOR THE 1990S

D. T. LLEWELLYN-JONES (SERC, Rutherford Appleton Laboratory, Didcot, England) British Interplanetary Society, Journal (Space Science) (ISSN 0007-084X), vol. 39, May 1986, p. 228-234.

ESA's First Remote Sensing Satellite (ERS-1) due for launch in 1989 will monitor a carefully selected set of geophysical parameters in an effort to describe the state of the sea-surface. The payload instruments of ERS-1, how they make their measurements, and how the data will be dealt with, are described and discussed. The payload consists of three microwave radars: (1) a wind and wave scatterometer, (2) a synthetic aperture radar, and (3) a radar altimeter. These instruments are complemented by an Along Track Scanning Radiometer and a Precise Range and Range-Rate Experiment. The concept of fast delivery data products is an essential element of the ERS-1 system, meaning that the processed ERS-1 data will be distributed to designated points of contact within three hours of being obtained by the spacecraft. It is concluded that these measurements will lead to a better scientific understanding of ocean-atmosphere interactions; moreover, they will pave the way to the application of such data products to a large range of commercial activities. K.K.

N86-15969# Mound Lab., Miamisburg, Ohio.

OPERATIONAL METHODS FOR DATA INTERPOLATION

G. L. SILVER 1 Aug. 1985 37 p

(Contract DE-AC04-76DP-00053)

(DE85-016050; MLM-3277) Avail: NTIS HC A03/MF A01

The operational method for data treatment is illustrated: four, five, six, and seven point echo functions, formulas for extremum evaluation and location, two-dimensional echo functions, equations relating data in two-dimensional configurations, derivative methods, and programs are given. DOE

N86-23017# Joint Publications Research Service, Arlington, Va.

USSR REPORT: EARTH SCIENCES Abstracts Only

31 Mar. 1986 56 p Transl. into ENGLISH from various Russian articles

(JPRS-UES-86-004) Avail: NTIS HC A04/MF A01

Progress is reported in U.S.S.R. earth sciences. Topics discussed include (1) meteorology; (2) oceanography; (3) terrestrial geophysics; (4) atmospheric physics; and (5) arctic and antarctic research.

N86-23203# Naval Ocean Research and Development Activity, Bay St. Louis, Miss.

PROCEEDINGS OF THE ARCTIC OCEANOGRAPHY CONFERENCE AND WORKSHOP HELD AT THE NAVAL OCEAN RESEARCH AND DEVELOPMENT ACTIVITY, NSTL, MS. ON JUNE 11-14, 1985

1985 293 p Conference held in Bay St. Louis, Miss., 11-14 Jun. 1985

(AD-A162578) Avail: NTIS HC A13/MF A01 CSCL 20A

The four general subject areas were: Arctic Operations and acoustics; Buoys; and Sea Ice. Included titles are: MIZEX (Marginal Ice Zone Experiment) Operations; International Ice Patrol Operations; Remote Sensing for Polar Icebreaker Navigation in Sea Ice; Satellite Telemetry Buoys for Collection of Arctic Acoustic and Environmental Data; Arctic Temperature - Conductivity Buoys; Generation and Movement of Ice Islands near the Canadian Arctic Archipelago; Effect of the Physical Properties of Ice on the High Frequency Acoustic Backscatter from an Ice Keel Model; Simulation Model for High-Frequency Underice Acoustic Backscattering; High Frequency Acoustic Reflection from Flat Sea Ice; Use of Penetrators to Estimate the Properties of Ice in Arctic Regions; Acoustic Bottom Interaction Considerations in the Arctic; Horizontal Directionality of Ice Edge Noise; Characteristics of Industrial Sounds in the Shallow Beaufort Sea; A Multi-bounce, Single-scatter, Ray

Theoretic Model for Under-ice Predictions, Frequency-domain Electromagnetic Ice-sounding; Radiometric Imagery of Sea Ice; Remote Sensing of the Marginal Ice Zone During MIZEX 83 and 84; Variations in Bering Sea Ice Coverage Related to Large-scale Atmospheric Circulation Patterns; Determining Sea Ice Type and Inferred Ice Thickness Distributions from Aerial Photographs; Pressure Ridge Morphology and Physical Properties of Sea Ice in the Greenland Sea. GRA

N86-23207# Johns Hopkins Univ., Laurel, Md. Applied Physics Lab.

STRATEGIES FOR THE CALIBRATION AND OPERATIONAL USE OF THE ERS-1 SAR WAVE MODE Final Report

A. D. GOLDFINGER Paris ESA Mar. 1985 126 p refs Original contains color illustrations

(Contract ESTEC-5538/83)

(JHU/APL/SDO-7565; ESA-CR(P)-2097) Avail: NTIS HC A07/MF A01

Algorithms for estimating ocean wave spectra and tracking spectral peaks for ERS-1 Active Microwave instrument were studied. Procedures for calibrating the system and validating the algorithms are proposed. The ocean can be represented by a two-scale model in which random local phenomena cause small uncorrelated variations in the ocean spectrum that are superimposed on slowly changing excursions due to macroscopic effects. Macroscopic phenomena show correlation lengths of 50 to 100 km. Principal error sources in measuring spectral peak positions are: error inherent in measuring a static spectral peak; error due to dynamic tracking effects; and error due to localized ocean excursions. Two bit quantization of the SAR signals is not a significant error source. Spectra should be estimated from multilook imagery. If the number of looks is maximized, it does not matter how the fixed buffer of SAR data is broken up into subimages. Author (ESA)

N86-23208# National Science Foundation, Washington, D.C. Div. of Polar Programs.

ICE SHELVES OF ANTARCTICA

N. I. BARKOV 1985 272 p Transl. into ENGLISH from the mono. "Shelfove Ledniki Antarktidi" Leningrad, USSR, Gidrometeorologicheskoe, 1971

(PB86-106986; TT-75-52081) Avail: NTIS HC A12/MF A01 CSCL 08L

The vast areas occupied by ice shelves and their peripheral location in Antarctica have attracted the attention of investigators for long. Their special features have been studied and their role in the mass budget of the continent's ice cover examined. Information on the ice shelves, published till 1968, has been examined in the monograph. The author describes the special conditions of existence of ice shelves, their movement, morphology, charging, the structure of the thermal regime, and their contribution to the development of glaciation on the continent. In this respect, particular attention has been paid to the study of the floating, most representative, part of such ice formations. GRA

N86-23209# National Science Foundation, Washington, D.C. Div. of Polar Programs.

PROBLEMS OF THE ARCTIC AND THE ANTARCTIC, COLLECTION OF ARTICLES, VOLUME 56, 1981

A. F. TRESHNIKOV 1985 167 p Transl. into ENGLISH of Problemy Arktiki i Antarktiki (USSR), Sbornik Statei, v. 56, 1981 p 1-159

(PB86-107109; TT-82-00-102) Avail: NTIS HC A08/MF A01 CSCL 08C

Many articles included in this volume deal with various aspects of the studies on sea ice, viz., conditions of regelation, thermal displacement, deformation and stresses, hummocking, morphology, and techniques of thickness measurements. Another group of articles deals with hydrometeorological forecasts, subsurface currents, water density fields, etc. GRA

N86-23211# National Environmental Satellite Service, Washington, D. C.

ENVIRONMENTAL DATA SOURCES FOR THE CHESAPEAKE BAY AREA

Jun. 1985 66 p

(PB86-110640; NESDIS-ENVIRON-INVENT-3) Avail: NTIS HC A04/MF A01 CSCL 08C

Chesapeake Bay is one of the largest and most productive estuaries in the world. It is a unique, irreplaceable natural--as well as national--resource. Declining harvests of fish and shellfish, however, have served notice that the Bay's renewable living resources are endangered by deteriorating water quality and habitat destruction. The primary purpose of this publication is to provide information about environmental data for the Chesapeake Bay area that is available from the National Environmental Satellite, Data, and Information Service. GRA

N86-23213# National Oceanic and Atmospheric Administration, Miami, Fla. Oceanographic and Meteorological Labs.

HEAT BUDGET AND CLIMATIC ATLAS OF THE EQUATORIAL ATLANTIC OCEAN DURING FGGE (FIRST GARP GLOBAL EXPERIMENT, 1979)

E. MARMOEJO, J. F. FESTA, and R. L. MOLINAN Aug. 1985 82 p

(PB86-111622; NOAA-TM-ERL-AOML-61) Avail: NTIS HC A05/MF A01 CSCL 08J

Observations of surface oceanographic and meteorological fields collected during the first GARP Global Experiment (FGGE) in the equatorial Atlantic Ocean have been combined and averaged by month onto a 2 degree by 2 degree grid. Monthly distributions of sea-surface temperature, wind speed and direction, air temperature, specific humidity, and cloud cover have been generated for the period from December 1978 through November 1979. Net short-wave and long-wave radiation, and sensible and latent heat flux distributions have been generated from surface data using the bulk aerodynamic formulas. Standard errors of the mean values have been computed along with monthly contoured plots of each oceanographic and meteorological variable. GRA

N86-24002# Deutsche Forschungs- und Versuchsanstalt fuer Luft- und Raumfahrt, Oberpfaffenhofen (West Germany). Abt. Hochfrequenzverfahren.

ARCHIMEDES PROJECT REMOTE SENSING OF OIL SPILLS NORTH SEA EXPERIMENT, OCTOBER 1983. REPORT ON DFVLR (SIDE-LOOKING AIRBORNE RADAR (SLAR) CONTRIBUTION

F. WITTE Sep. 1985 30 p

(DFVLR-FB-85-54; ISSN-0171-1342) Avail: NTIS HC A03/MF A01; DFVLR, Cologne DM 13

Oil pollution monitoring by SLAR was assessed in flight tests using specially created slicks. The SLAR-system demonstrates its ability to detect and image oil slicks even on a smooth water surface. The received radar backscatter as a function of surface roughness and angle of incidence fluctuates considerably, so the probability to detect oil slicks increases by using steeper depression angles than normal to obtain a large swath width. An important tool to improve the accuracy of classification is the data correction algorithm. The classification quality strongly depends on viewing direction (best perpendicular to the waves) and on the sea state. As expected VV-polarization is the preferable solution for oil slick monitoring with a SLAR. Author (ESA)

N86-24112# National Oceanic and Atmospheric Administration, Seattle, Wash. Marine Environmental Lab.

RELATIONSHIPS BETWEEN SURFACE OBSERVATIONS OVER THE GLOBAL OCEANS AND THE SOUTHERN OSCILLATION

P. B. WRIGHT, T. P. MITCHELL, and J. M. WALLACE Jan. 1985 70 p Prepared in cooperation with Washington Univ., Seattle

(PB86-110038; NOAA-DR-ERL-PMEL-12) Avail: NTIS HC A04/MF A01 CSCL 04B

The atlas contains maps of correlation and regression coefficients between seasonal anomalies of surface meteorological

05 OCEANOGRAPHY AND MARINE RESOURCES

fields over the global oceans and Darwin, Australia annual-mean sea-level pressure anomalies. The statistics were calculated for six consecutive seasons defined relative to the Darwin index. The resulting charts provide a description of the time evolution of meteorological anomalies associated with the Southern Oscillation over the global oceans. GRA

N86-24120* # National Academy of Sciences - National Research Council, Washington, D. C. Commission on Physical Sciences, Mathematics and Resources.

PROCEEDINGS OF THE FIRST NATIONAL WORKSHOP ON THE GLOBAL WEATHER EXPERIMENT: CURRENT ACHIEVEMENTS AND FUTURE DIRECTIONS, VOLUME 1 Final Report

Oct. 1985 89 p refs Workshop held in Woods Hole, Mass., 9-20 Jul. 1984

(Contract NSF ATM-80-25329)

(NASA-CR-176720; NAS 1.26:176720) Avail: NTIS HC A05/MF A01 CSCL 04B

A summary of the proceedings in which the most important findings stemming from the Global Weather Experiment (GWE) are highlighted, additional key results and recommendations are covered, and the presentations and discussion are summarized. Detailed achievements, unresolved problems, and recommendations are included. Author

N86-24142* # National Academy of Sciences - National Research Council, Washington, D. C. Commission on Physical Sciences, Mathematics, and Resources.

PROCEEDINGS OF THE FIRST NATIONAL WORKSHOP ON THE GLOBAL WEATHER EXPERIMENT: CURRENT ACHIEVEMENTS AND FUTURE DIRECTIONS, VOLUME 2, PART 2 Final Report

Oct. 1985 414 p refs Workshop held in Woods Hole, Mass., 9-20 Jul. 1984 Sponsored in cooperation with NASA and NOAA 3 Vol.

(Contract NSF ATM-80-25329)

(NASA-CR-176722; NAS 1.26:176722; PB86-139177) Avail: NTIS HC A18/MF A01 CSCL 04B

An assessment of the status of research using Global Weather Experiment (GWE) data and of the progress in meeting the objectives of the GWE, i.e., better knowledge and understanding of the atmosphere in order to provide more useful weather prediction services. Volume Two consists of a compilation of the papers presented during the workshop. These cover studies that addressed GWE research objectives and utilized GWE information. The titles in Part 2 of this volume include General Circulation Planetary Waves, Interhemispheric, Cross-Equatorial Exchange, Global Aspects of Monsoons, Midlatitude-Tropical Interactions During Monsoons, Stratosphere, Southern Hemisphere, Parameterization, Design of Observations, Oceanography, Future Possibilities, Research Gaps, with an Appendix.

N86-24161* # Scripps Institution of Oceanography, La Jolla, Calif.

SEA SURFACE TEMPERATURE FROM SATELLITES: THE IMPACT OF FGGE Final Report

R. L. BERNSTEIN /n NAS-NRC Proceedings of the First National Workshop on the Global Weather Experiment, Vol. 2, Pt. 2 p 761-764 Oct. 1985 refs

Avail: NTIS HC A18/MF A01 CSCL 04B

Spacecraft instruments first launched at the beginning of the FGGE year are now producing sea surface temperature data accurate to about 1 C. At larger scales, the errors are dominated by systematic effects, some of which are instrumental, but most are geophysical, i.e., correlated with volcanic aerosols, atmospheric water vapor, clouds, and surface wind. Progress is being made to identify and eliminate such errors and thereby provide sea surface temperature data on a global basis consistently accurate to 0.5 C, which will be needed for studies of climate variability. Author

N86-24166# Instituto de Pesquisas Espaciais, Sao Jose dos Campos (Brazil).

DEVELOPMENT OF A SATELLITE-TRACKED OCEANOGRAPHIC DRIFTING BUOY FOR THE BRAZILIAN ANTARCTIC PROGRAM, PART 1

M. R. STEVENSON and E. M. B. ALONSO Feb. 1986 24 p refs Submitted for publication

(INPE-3793-PRE/888) Avail: NTIS HC A02/MF A01

The project Measurement of the Antarctic Current (MEDICA) which was to develop, build and launch drifting oceanographic buoys, located by System ARGOS, in Antarctica is presented. The basis of the drifting buoy was to use a data collection platform (DCP). A biconic geometry was used for the buoy hull to provide good vertical stability and resistance to entrapment by ice. Fiberglass was used for its high strength to weight ratio, and the facility to use molds for production of the hulls. Sandwich construction was incorporated and provided for outer and inner hulls of fiberglass with polyurethane foam between the walls. Within the hull, the DCP unit and its interface box are mounted within a metal conical rack. The transmitting antenna is mounted on a metal base-plane disc and, in turn, is secured atop the rack. A power supply, consisting of several hundred alkaline dry cells, suitably interconnected and sealed within a plastic housing, resides below the rack for maximum buoy stability. An additional thermistor is mounted in a housing on the conical cover of the buoy and provides air temperature readings. The physical specifications and measuring capabilities of the sensors. E.A.K.

N86-24168# Instituto de Pesquisas Espaciais, Sao Jose dos Campos (Brazil).

COMPARISON OF CIRCULATION ESTIMATES AND WINDS BASED ON SHIPBOARD AND SATELLITE-TRACKED BUOY DATA IN BRANSFIELD STRAIT, 9-14 MARCH, 1985, PART 3

M. R. STEVENSON, H. M. INOSTROZAV, J. L. STECH, and E. M. B. ALONSO Feb. 1986 21 p refs Submitted for publication

(INPE-3795-PRE/890) Avail: NTIS HC A02/MF A01

The INPE freely drifting prototype oceanographic buoy (System ARGOS) was launched successfully on 9 March at 19:31 GMT, for a several day test experiment. During the 9 to 14 March, 1985, interval, a set of 7 hydrographic stations was made in the Bransfield Strait to obtain information about temperature, salinity and density. Results of the several day drifter trajectory are presented together with a comparison with geostrophic circulation, surface winds and air and sea temperatures. Mean drifter velocity was 27.0 cm/s toward 042 deg and confirmed a predicted NE movement for the surface water layer. The surface geostrophic current was toward 020 deg at 4 cm/s, at 10 m depth the current was toward 045 deg at 5 cm/s. Best agreement was found between the drifter trajectory and the geostrophic current at 10 m depth. At the time of buoy launch and for about one day thereafter, winds were weak and toward 090 deg; after another day, however, the surface winds changed and blew generally toward 250 deg at speeds that gradually increased up to 16 kts, in opposition to the surface water motion. Air and water temperatures measured from the buoy are also discussed and compared with measurements made at the hydrographic stations. Author

N86-24170# SACLANT ASW Research Center, La Spezia (Italy).

AN ATLAS OF ORIGINAL AND MERCATOR-TRANSFORMED SATELLITE-DATA IMAGES OF THE ALBORAN SEA, AUGUST-OCTOBER 1983

E. NACINI 1 Aug. 1985 132 p

(AD-A161898; SACLANTCEN-SR-89) Avail: NTIS HC A07/MF A01 CSCL 14E

A collection of satellite (NOAA7) images of the Alboran Sea in High Resolution Picture Transmission (HRPT) and Automatic Picture Transmission (APT) format in the visible, near-infrared, and thermal infrared fields is presented. Some of them have been transformed to Mercator projection in order to show how the use of such images can aid in the preparation and conduct of oceanographic and other operations. The contents include: image

collection and processing, transformation to Mercator projection, application to oceanographic studies, water masses, temperature profiling, comparison with synoptic weather charts, and tidal data.

GRA

N86-24172# Naval Ocean Research and Development Activity, Bay St. Louis, Miss.

OCEAN WAVE SLOPE STATISTICS FROM AUTOMATED ANALYSIS OF SUN GLITTER PHOTOGRAPHS Final Report

M. LYBANON Jun. 1985 65 p
(AD-A161995; NORDA-103) Avail: NTIS HC A04/MF A01
CSCL 08C

The image of the Sun reflected from the rough surface of the sea forms a diffuse pattern, whose details depend on the nature of the surface waves and swell. Consequently, statistics of the slope distribution of the sea surface are related to the statistics of the Sun's glitter on the sea surface. Aerial photographs are a convenient medium for recording the glitter pattern. The mathematical relationship to derive the sea surface slope statistics can be determined from an analysis of the imaging geometry. However, analysis of the photographs can be a labor-intensive procedure. The problem was first studied over thirty years ago. Now, there are modern digital image processing systems and techniques that greatly increase the practicality of the analysis. This report derives the relevant equations and describes an implementation on the Interactive Digital Satellite Image Processing System (IDSIPS). The IDSIPS system is operated by the Remote Sensing Branch of the Naval Ocean Research and Development Activity (NORDA). The report includes full formal documentation of the computer software. Author (GRA)

N86-24173# Naval Ocean Research and Development Activity, Bay St. Louis, Miss.

CONTRIBUTIONS TO THE OCEANOGRAPHY OF THE WESTERN ALBORAN SEA Final Report

R. ARNONE, R. BARCALA, G. DAWSON, F. FIEDLER, and G. HEBURN Apr. 1985 120 p Presented at the 29th Congress and Plenary Session of the International Commission for the Scientific Exploration of the Mediterranean Sea, Lucerne, Switzerland, 11-19 Oct. 1984

(AD-A162019; NORDA-TN-315) Avail: NTIS HC A06/MF A01
CSCL 08C

This compilation includes the following articles: Donde Va? An Oceanographic Experiment in the Alboran Sea. The Donde Va Group; The Hydrographic Structure of the Alboran Sea Gyre, June and October 1982; NIMBUS-7/CZCS Derived Maps of Near-Surface Chlorophyll; The Flow of Atlantic Water into the Alboran Sea During Donde Va; A Time Series Station at the Eastern Entrance of the Strait of Gibraltar; A Preliminary Study of a Standing Internal Wave in the Western Approaches to the Strait of Gibraltar; Effects of Wind Versus Hydraulic Forcing on the Dynamics of the Western Mediterranean Sea; and Computational Methods for Two Problems in Air-Sea Interaction. Author (GRA)

N86-24176# Naval Postgraduate School, Monterey, Calif.
HYDROGRAPHIC DATA FROM THE OPTOMA PROGRAM, OPTOMA17: OPTOMA17 P, 21 JULY 1985, OPTOMA17 LEG DI, 10-22 AUGUST 1985, OPTOMA17 LEG DII, 23 AUGUST - 5 SEPTEMBER 1985 Report, Oct. 1982 - Sep. 1985

P. A. WITTMANN, E. A. KELLEY, JR., and C. N. K. MOOERS
Oct. 1985 133 p
(AD-A162067; NPS68-85-026) Avail: NTIS HC A07/MF A01
CSCL 08C

The Ocean Prediction Through Observations, Modeling and Analysis (OPTOMA) Program seeks to understand the mesoscale (fronts, eddies, and jets) variability and dynamics of the California Current System and to determine the scientific limits to practical mesoscale ocean forecasting. To help carry out the aims of this project, a series of cruises has been planned in two subdomains, NOCAL and CENCAL. The two cruises and one AXBT flight comprising OPTOMA17 were undertaken in the USNS DE STEIGUER and a Reserve Patrol Wing P3B aircraft. Hydrographic data were acquired off the coast of California in an area which

covered and extended the NOCAL region. On each of these cruises, hydrographic stations were occupied at approximately 19 km along the track. For the AXBT flight, the along-track station spacing varied between about 28 km and about 46 km. Data acquired during Legs DI and DII include XBT and CTD profiles; whereas data acquired during Leg P are AXBT profiles. Bucket surface temperatures were taken at all CTD stations. A Rosette sampler was used to acquire deep salinity samples. These salinity samples were used for calibration purposes as well as contributions to the data base. Author (GRA)

N86-24180# Lamont-Doherty Geological Observatory, Palisades, N. Y.

MARGINAL ICE ZONE EXPERIMENT - 1984, PHYSICAL OCEANOGRAPHY REPORT: USNS LYNCH AND HELICOPTER-BASED STD DATA

T. O. MANLEY Dec. 1985 291 p

(Contract N00014-84-C-0132)
(AD-A163096; LDGO-85-7) Avail: NTIS HC A13/MF A01
CSCL 08J

During the summer of 1984, the Arctic Oceanography Department of Lamont-Doherty Geological Observatory acquired a total of 222 helicopter-based C/STD stations within the ice-covered region of the Fram Strait to a nominal depth of 500 m. This program was accomplished as part of an international experiment known as MIZEX East 1984. The two ships used in helicopter operations the F/S Polarstern and the M/V Polarqueen. The USNS Lynch was also used to obtain 26 CTD stations from two separate legs into the Fram Strait. The first leg primarily consisted of an open water transect of the strait at a latitude of 79 N. Stations were typically taken to within 10 m of the bottom and extended from the ice edge onto the shelf of Svalbard. The second leg was more acoustically oriented and confined to the southern region of the Yermak Plateau. During this leg, 11 stations to a nominal depth of 450 m were taken. Standard level listings of temperature, potential temperature, salinity, sigma-t, specific volume anomaly, dynamic height, and sound velocity are given for each cast along with profiles of temperature, salinity and sigma-t. Author (GRA)

N86-24181# Lamont-Doherty Geological Observatory, Palisades, N. Y.

PHYSICAL OCEANOGRAPHY REPORT: CAMP-BASED AND HELICOPTER-BASED STD DATA FROM THE DRIFTING ICE STATION FRAM 3

T. O. MANLEY and D. B. CAMP Dec. 1985 339 p

(Contract N00014-84-C-0132)
(AD-A163097; LDGO-85-8) Avail: NTIS HC A15/MF A01
CSCL 08J

During the spring of 1981, a manned camp was established on a drifting ice floe north of Spitzbergen. During the 61 days of occupation, the Arctic Oceanography Department of Lamont-Doherty Geological Observatory obtained a total of 194 STD stations from the combined efforts of personnel in charge of camp-based and helicopter-based operations. This report describes the methods used in the acquisition and processing of the data and provides output for each case. The output consists of standard level listings of temperature, potential temperature, salinity, sigma-t, specific volume anomaly, dynamic height, and sound velocity, along with corresponding profiles of temperature, salinity and sigma-t. Author (GRA)

N86-24182# National Science Foundation, Washington, D.C. Div. of Polar Programs.

PROBLEMS OF THE ARCTIC AND THE ANTARCTIC, COLLECTION OF ARTICLES, VOL. 57, 1981

A. F. TRESHNIKOV, ed. 1985 151 p Transl. into ENGLISH of Sbornik Statei (USSR), v. 57, 1981 p 1-142
(PB86-106994; TT-82-00-104) Avail: NTIS HC A08/MF A01
CSCL 08C

Problems of polar oceanography; hydrochemical studies in the Arctic Ocean; general distribution variability of ice in the World Ocean as a climate-forming factor; air-sea interaction in the Arctic

05 OCEANOGRAPHY AND MARINE RESOURCES

basin and the North Atlantic; physics of ice and the ocean; long-range meteorological forecasts are reported. GRA

N86-25100*# Applied Science Associates, Inc., Apex, N.C.
STUDIES RELATED TO OCEAN DYNAMICS. TASK 3.2: AIRCRAFT FIELD TEST PROGRAM TO INVESTIGATE THE ABILITY OF REMOTE SENSING METHODS TO MEASURE CURRENT/WIND-WAVE INTERACTIONS Final Report
N. E. HUANG, W. A. FLOOD, and G. S. BROWN May 1975
74 p refs
(Contract NAS6-2520)
(NASA-CR-168349; NAS 1.26:168439) Avail: NTIS HC A04/MF A01 CSCL 08C

The feasibility of remote sensing of current flows in the ocean and the remote sensing of ocean currents by backscattering cross section techniques was studied. It was established that for capillary waves, small scale currents could be accurately measured through observation of wave kinematics. Drastic modifications of waves by changing currents were noted. The development of new methods for the measurement of capillary waves are discussed. Improvement methods to resolve data processing problems are suggested.

E.A.K.

N86-25104# Hawaii Inst. of Geophysics, Honolulu.
MONTHLY MAPS OF SEA LEVEL ANOMALIES IN THE PACIFIC, 1975 1981. REPORT ON THE IGOSS (INTEGRATED GLOBAL OCEAN SERVICES SYSTEM) SEA LEVEL PILOT PROJECT
K. WYRTKI and S. NAKAHARA Aug. 1984 96 p
(Contract NA80RA-H-00002)
(AD-A163061; HIG-84-3; JIMAR-84-0085) Avail: NTIS HC A05/MF A01 CSCL 08C

Sea level data obtained on islands in the tropical and subtropical Pacific Ocean are used to compile maps of the sea level anomaly for each month of the period January 1975 to December 1981. The maps reveal the large horizontal coherence of sea level anomalies with space scales of several thousand kilometers. Coherence scales are larger in the east-west than in the north-south direction. The anomalies are also coherent over many months indicating a dominance of low-frequency variations. GRA

N86-25106# National Oceanic and Atmospheric Administration, Boulder, Colo. Wave Propagation Lab.
MANAGEMENT INFORMATION (WAVE PROPAGATION LABORATORY, BOULDER, COLORADO)
Oct. 1985 50 p
(PB86-139524) Avail: NTIS HC A03/MF A01 CSCL 08C

The nation's geophysical research and service is to be improved through creation and application of new remote measurement systems. Essential functions include: Wave propagation studies; Technique development; Atmospheric and Oceanic research; Technology transfer. GRA

N86-25939# National Oceanic and Atmospheric Administration, Seattle, Wash. Marine Environmental Lab.
SEA ICE DYNAMICS AND REGIONAL METEOROLOGY FOR THE ARCTIC POLYNIA EXPERIMENT (APEX)-BERING SEA 1985
C. H. PEASE, M. REYNOLDS, G. A. GALASSO, V. L. LONG, and S. A. SALO Oct. 1985 129 p
(PB86-148038; NOAA-TM-ERL-PMEL-64) Avail: NTIS HC A07/MF A01 CSCL 04B

The purpose of the Arctic Polynya Experiment (APEX) is to investigate physical processes and thermodynamics in the atmosphere, sea ice, and ocean in the vicinity of St. Lawrence Island in the northern Bering Sea. The relative importance on sea ice motion of baroclinic currents due to brine rejection during the freezing of ice in the polynya, barotropic currents due to set-up on the shelf, internal ice stress due to the presence of St. Lawrence Island, wind stress and Coriolis force are being considered through a measurement and modeling program. GRA

N86-25962# Marine Research Inst., Helsinki (Finland).
INVESTIGATION OF ICE DYNAMICS IN THE MARGINAL ICE ZONE Interim Report, 16 May - 30 Sep. 1985
M. LEPPAERANTA 30 Sep. 1985 11 p refs
(Contract DAJ445-83-C-0034)

(AD-A164364; IR-6) Avail: NTIS HC A02/MF A01 CSCL 08L
MIZEX-83 was a pilot study program in the Greenland Sea where ice kinematics data could be collected for about ten days. Ocean current measurements were simultaneously made beneath the same ice floes as we had transponders for the ice kinematics at three stations. The currents were measured with Aanderaa current recorders giving the mean absolute speed and instantaneous direction at ten-minute intervals. The ice kinematics data describe relative motion between the stations. Thus in comparing ice and current kinematics we consider the relative motion, i.e., spatial fluctuations of velocity between two stations and the rate of deformation given by the three stations. The active role of ice in the ice-ocean system has a consequence that an ocean dynamics model for the ice margin problems should have an advanced ice dynamics model coupled with it. The ice motion was also measured with Argos satellite buoys. They are very good for measuring trajectories. GRA

N86-26313# Pacific Missile Test Center, Point Mugu, Calif.
NAVSTAR GPS (GLOBAL POSITIONING SYSTEM) ACCURACY WHILE SURVEYING ARRAYS OF DEEP OCEAN TRANSPONDERS
L. A. ANDERSON Dec. 1985 21 p
(AD-A163364; PMTC-TP-000037) Avail: NTIS HC A02/MF A01 CSCL 17G

The observed accuracy of the Navstar GPS Global Positioning System when used with acoustic data to geodetically locate arrays of bottom-mounted ocean transponders is presented. Two arrays were to be located, and each was surveyed on several separate occasions. In addition to GPS with dual frequency precise P-code, the arrays were located by using Argo, Syledis, Transit satellites, and by several other tracking methods. Because the array positions have been well determined, the data is now able to reveal the absolute GPS fix error while at sea. For one survey, ground truth information from the Yuma GPS facility, 263 nautical miles (487 km) away, was used to reduce measurement bias. GRA

N86-26517# Louisiana State Univ., Baton Rouge. Coastal Studies Inst.
METHODS OF OBTAINING OFFSHORE WIND DIRECTION AND SEA-STATE DATA FROM X-BAND AIRCRAFT SAR (SYNTHETIC APERTURE RADAR) IMAGERY OF COASTAL WATERS
G. A. MASTIN, C. A. HARLOW, O. K. HUH, and S. A. HSU Apr. 1985 18 p
(Contract N00014-83-C-0150)
(AD-A165552; TR-410) Avail: NTIS HC A02/MF A01 CSCL 17I

X-band synthetic aperture radar (SAR) imagery of the Goto Islands of Japan was digitally analyzed to extract air-sea interaction parameters and to assess the potential of texture measures in analysis of SAR ocean imagery. Wind direction is extracted from wind rows, wind streaks, and random turbulence patterns observed in the SAR imagery. Sea-state parameters are either extracted directly from the imagery or estimated using the extracted information in previously established empirical formulas. A convenient method of digitally presenting imagery, local power spectra, and the extracted/estimated parameters is presented. Texture analysis based on gray-level co-occurrence (GLC) matrices is applied to SAR ocean imagery. The inertia measure is shown to extract similar information to the power spectrum. The cluster-shade measure is shown to be sensitive to image phase. GRA

N86-26670* # University of South Florida, St. Petersburg. Dept. of Marine Science.

A SIMULATION ANALYSIS OF THE FATE OF PHYTOPLANKTON WITHIN THE MID-ATLANTIC BIGHT

J. J. WALSH, D. A. DIETERLE, and M. B. MEYERS 1986 62 p (Contract NAGW-678) (NASA-CR-177265; NAS 1.26:177265) Avail: NTIS HC A04/MF A01 CSCL 08A

A time-dependent, three-dimensional simulation model of wind-induced changes of the circulation field, of light and nutrient regulation of photosynthesis, of vertical mixing as well as algal sinking, and of herbivore grazing stress, is used to analyze the seasonal production, consumption, and transport of the spring bloom within the mid-Atlantic Bight. The particular case (c) of a 58-day period in February-April 1979, simulated primary production, based on both nitrate and recycled nitrogen, with a mean of 0.62 g C sq m/day over the whole model domain, and an export at the shelf-break off Long Island of 2.60 g ch1 sq m/day within the lower third of the water column. About 57% of the carbon fixation was removed by herbivores, with 21% lost as export, either downshelf or offshore to slope waters, after the first 58 days of the spring bloom. Extension of the model for another 22 days of case (c) increased the mean export to 27%, while variation of the model's parameters in 8 other cases led to a range in export from 8% to 38% of the average primary production. Spatial and temporal variations of the simulated algal biomass, left behind in the shelf water column, reproduced chlorophyll fields sensed by satellite, shipboard, and in situ instruments. Author

N86-26716# Coast Guard, Washington, D.C.

A REVIEW OF METHODS TO TRACK OIL IN ARCTIC WATERS Final Report

J. W. ST. MARTIN Jun. 1985 25 p refs (AD-A164679; USCG-D-28-85) Avail: NTIS HC A02/MF A01 CSCL 13B

A review of available literature on the tracking of oil in Arctic environments was conducted. The effectiveness of satellite and aircraft mounted detection devices used in locating oil-on-water, ice or in an ice/water mixture was examined. Oil spill tracking buoys and devices, both micro and macro scale, were also reviewed with their applicability to the Arctic environment detailed. Recommendations were made for the U.S. Coast Guard to use ARGOS system buoys on Arctic oil spills for long term tracking of movement. An additional recommendation was made for the future testing of the HU-25A mounted AIREYE surveillance system or an HC-130 mounted sensor package on oil spilled in an Arctic environment. Author (GRA)

N86-26758* # Florida State Univ., Tallahassee. Dept. of Meteorology.

AN INVESTIGATION OF THE MARINE BOUNDARY LAYER DURING COLD AIR OUTBREAK Final Report

S. A. STAGE Jul. 1986 26 p refs (Contract NAG5-332) (NASA-CR-177287; NAS 1.26:177287) Avail: NTIS HC A03/MF A01 CSCL 04B

Methods for use in the remote estimation of ocean surface sensible and latent heat fluxes were developed and evaluated. Three different techniques were developed for determining these fluxes. These methods are: (1) Obtaining surface sensible and latent heat fluxes from satellite measurements; (2) Obtaining surface sensible and latent heat fluxes from an MABL model; (3) A method using horizontal transfer coefficients. These techniques are not very sensitive to errors in the data and therefore appear to hold promise of producing useful answers. Questions remain about how closely the structure of the real atmosphere agrees with the assumptions made for each of these techniques, and, therefore about how well these techniques can perform in actual use. The value of these techniques is that they promise to provide methods for the determination of fluxes over regions where very few traditional measurement exist. E.R.

N86-26782* # National Aeronautics and Space Administration. Goddard Space Flight Center, Greenbelt, Md.

OBJECTIVE ANALYSIS OF TIDAL FIELDS IN THE ATLANTIC AND INDIAN OCEANS

B. V. SANCHEZ, D. B. RAO (National Meteorological Center, Washington, D.C.), and S. D. STEENROD (Applied Research Corp., Landover, Md.) Jun. 1986 25 p refs (NASA-TM-87773; NAS 1.15:87773; REPT-86B0195) Avail: NTIS HC A02/MF A01 CSCL 08C

An objective analysis technique has been developed to extrapolate tidal amplitudes and phases over entire ocean basins using existing gauge data and the altimetric measurements which are now beginning to be provided by satellite oceanography. The technique was previously tested in the Lake Superior basin. The method has now been developed and applied in the Atlantic-Indian ocean basins using a 6 deg x 6 deg grid to test its essential features. The functions used in the interpolation are the eigenfunctions of the velocity potential (Proudman functions) which are computed numerically from a knowledge of the basin's bottom topography, the horizontal plan form and the necessary boundary conditions. These functions are characteristic of the particular basin. The gravitational normal modes of the basin are computed as part of the investigation, they are used to obtain the theoretical forced solutions for the tidal constituents, the latter provide the simulated data for the testing of the method and serve as a guide in choosing the most energetic modes for the objective analysis. The results of the objective analysis of the M2 and K1 tidal constituents indicate the possibility of recovering the tidal signal with a degree of accuracy well within the error bounds of present day satellite techniques. Author

N86-26783* # Alaska Univ., Anchorage.

INFLUENCE OF THE YUKON RIVER ON THE BERING SEA Progress Report

K. DEAN and C. P. MCROY 1986 12 p refs Original contains color illustrations (Contract NAS5-28769) (NASA-CR-177310; NAS 1.26:177310) Avail: NTIS HC A02/MF A01 CSCL 10C

The relationships between the discharge of the Yukon River to the currents and biological productivity in the northern Bering Sea were studied. Specific objectives were: to develop thermal, sediment, and chlorophyll surface maps using Thematic Mapper (TM) data of the discharge of the Yukon River and the Alaskan Coastal Current during the ice free season; to develop a historical model of the distribution of the Yukon River discharge and the Alaskan Coastal Current using LANDSAT Multispectral band scanner (MSS) and NOAA satellite imagery; and to use high resolution TM data to define the surface dynamics of the front between the Alaskan Coastal Current and the Bering Shelf/Anadyr Current. LANDSAT MSS, TM, and Advanced Very High Resolution Radiometer (AVHRR) data were recorded during the 1985 ice free period. The data coincided with shipboard measurements acquired by Inner Shelf Transfer and Recycling (ISTAR) project scientists. An integrated model of the distribution of turbid water discharged from the Yukon River was compiled. A similar model is also being compiled for the Alaskan Coastal and Bering Shelf/Anadyr water masses based on their thermal expressions seen on AVHRR imagery. B.G.

N86-26788# Science Applications International Corp., College Station, Tex.

A STUDY OF SEA ICE KINEMATICS AND THEIR RELATIONSHIP TO ARCTIC AMBIENT NOISE. PART 3, SECTION 1: AMBIENT NOISE. SECTION 2: AMBIENT NOISE Final Report, Mar. 1985 - Feb. 1986

J. K. LEWIS and W. W. DENNER Feb. 1986 327 p (Contract N00014-85-C-0531) (AD-A165304; AD-E301922; SAIC-85/1950-PT-3; SAIC-1-425-07-356-10-PT-3-SE) Avail: NTIS HC A15/MF A01 CSCL 08L

This report details the kinematic analysis of sea ice motion data collected during the Arctic Ice Dynamics Joint Experiment

05 OCEANOGRAPHY AND MARINE RESOURCES

(AIDJEX) in the Beaufort Sea. In addition, relationships between the ice kinematic parameters and associated ambient noise are presented. These relationships were determined by an extensive correlation process between the noise and ice motion time histories. Time scales of the various modes of ice motion were calculated by season. Also, seasonal time and space scales were calculated for ambient noise at 10 Hz, 32 Hz, and 1000 Hz. Contents of this section include: Seasonal Arctic Ambient Noise Variations, Beaufort Sea, 1975-1976; Two-Dimensional Contour Maps of Arctic Ambient Noise Variations, 8-9 August 1975 (Summer); and Two-Dimensional Contour Maps of Arctic Ambient Noise Variations, 16-17 November 1975 (Fall). GRA

N86-26789# Science Applications International Corp., College Station, Tex.

A STUDY OF SEA ICE KINEMATICS AND THEIR RELATIONSHIP TO ARCTIC AMBIENT NOISE. PART 3, SECTION 3: AMBIENT NOISE Final Report, Mar. 1985 - Feb. 1986

J. K. LEWIS and W. W. DENNER Feb. 1986 107 p
(Contract N00014-85-C-0531)
(AD-A165305; AD-E301922; SAIC-85/1950-PT-3-SEC-3;
SAIC-1-425-07-356-10-PT-3-2) Avail: NTIS HC A06/MF A01
CSCL 08L

This report details the kinetic analysis of sea ice motion data collected during the Arctic Ice Dynamics Joint Experiment (AIDJEX) in the Beaufort Sea. In addition, relationships between the ice kinematic parameters and associated ambient noise are presented. These relationships were determined by an extensive correlation process between the noise and ice motion time histories. Time scales of the various modes of ice motion were calculated by season. Also, seasonal time and space scales were calculated for ambient noise at 10 Hz, 32 Hz, and 1000 Hz. Contents of this section include: Seasonal Arctic Ambient Noise Temporal Autocorrelations, Beaufort Sea, 1975-1976; Seasonal Arctic Ambient Noise Spatial Autocorrelations, Beaufort Sea, 1975-1976; Seasonal Arctic Ambient Noise Power Spectra, Beaufort Sea, 1975-1976. GRA

N86-26791# Massachusetts Inst. of Tech., Cambridge. Marine Industry Advisory Services.

REMOTE SENSING AND OCEANOGRAPHIC EQUIPMENT TECHNOLOGY: SOME PRESENT SYSTEMS AND FUTURE NEEDS, REVISED

1 Aug. 1985 24 p Sponsored by NOAA
(Contract NAB4AA-D-00046)
(PB86-156502; MITSG-85-21; OPPORTUNITY-BRIEF-41) Avail:
NTIS HC A02/MF A01 CSCL 08C

Satellite sensing systems offer new capabilities for obtaining synoptic data which can be used for understanding the dynamics of the ocean. While satellites have expanded our potential for exploring the ocean, they have also increased the demand for extensive in situ measurements (footprints or 'ground truth') to calibrate the remotely observed data. Used together with computer models, in situ measurements and satellite measurements provide new insights into the dynamics of the ocean, such as the motions of warm core rings north of the Gulf Stream. Modelling, satellite imagery and in situ measurements are being combined in ways which promise very significant advances in studying natural phenomena. GRA

N86-27414# National Oceanic and Atmospheric Administration, Washington, D. C.

NOAA SATELLITE REQUIREMENTS FORECAST Final Report
D. COTTER, L. FISHER, D. MONTGOMERY, T. PYLE, and F. ZBAR May 1985 119 p
(AD-A165244) Avail: NTIS HC A06/MF A01 CSCL 22B

Environmental satellites have been an essential component of NOAA's global observing system for 25 years. This report offers a projection of NOAA's requirements for satellite data and services covering the next 15 years. These requirements derive from the mission responsibilities of NOAA's public service and research agencies; the National Weather Service, the National Ocean Service, the National Marine Fisheries Service, and the Office of

Oceanic and Atmospheric Research. The National Environmental Satellite, Data, and Information Service operates the Polar-orbiting Operational Environmental Satellite (POES) and Geostationary Operational Environmental Satellite (GOES) systems and provides data archive and distribution services to the public and private sectors. The satellite support needed to help meet their mission goals through the end of this century are presented as they have been identified by each agency. The requirements specified in this report will be a major factor in the long-range planning for NOAA's future satellite programs. Author (GRA)

N86-27694# Meteorological Satellite Center, Tokyo (Japan).

METEOROLOGICAL SATELLITE CENTER TECHNICAL NOTE, NO. 13, 1986

Mar. 1986 73 p In ENGLISH and JAPANESE
(ISSN-0388-9653) Avail: NTIS HC A04/MF A01

Two articles are presented, one addressing the land-sea contrast in the Earth radiation budget and the other discussing the Cb cloud vortical pattern apart from a typhoon pressure center. In addition, a bibliography of references dealing with the use of satellite data in practical work and research is given.

N86-27695# Meteorological Satellite Center, Tokyo (Japan).

ON LAND-SEA CONTRAST IN THE EARTH RADIATION BUDGET

I. KUBOTA and H. IMAI *In its* Meteorological Satellite Center Technical Note, no. 13, 1986 (ISSN-0388-9653) p 1-31 Mar. 1986 In JAPANESE; ENGLISH summary
Avail: NTIS HC A04/MF A01

In order to make clear the difference between the Earth's radiation budget over land and over sea, three components of the budget; absorbed solar radiation, emitted terrestrial radiation, and net total radiation N on the Earth-atmosphere system measured by the wide field of view sensor aboard NIMBUS 7 were analyzed for the period during November 1978 to October 1979. The resultant zonal averages over each land and sea showed following facts. Both S and N in the latitudinal range 40 degrees around the solar declination are above 40 W/sq m larger over the sea than over land. The excess of S over sea beyond land stems mainly from differences of both clear-sky albedo and cloud amount between over land and over sea. In the latitudinal range 30 degrees centered 60N or 60S, S over land in summer is above 15 W/sq m greater than over sea contrary to the low latitudes. Finally, examination of latitudinal variation of T all the year round shows that there are a minimum zone near the equator corresponding to ITCZ, and a maximum zone in the subtropical area of each hemisphere corresponding to the subtropical high pressures or the downward stream branches of the direct circulation. The minimum in the zonal monthly average over land tends to be lower than over sea and the both maximums over land tend to be greater than over sea. These facts show that the direct circulation over land looks more active than over sea. Author

N86-27697 GKSS-Forschungszentrum Geesthacht (West Germany).

ON THE INFORMATION CONTENT OF MULTISPECTRAL RADIANCE MEASUREMENTS OVER AN OCEAN

J. FISCHER 1985 16 p Repr. from International Journal of Remote Sensing, v. 6, no. 5, 1985 p 773-786 In GERMAN
(GKSS-85/E/43; ISSN-0344-9629; ESA-86-96898) Avail: Issuing Activity

An eigenvalue analysis and a multivariate significance test are applied to the problem of measuring suspended matter, phytoplankton, and yellow substance from ship, aircraft, or satellite. The number of linearly independent pieces of information is inferred from multispectral radiance measurements at six wavelengths within the visible part of the spectrum. The radiances analyzed are calculated with a radiative transfer model (matrix operator method) for an atmosphere-ocean system and realistic variations of scattering and absorption by hydrosols in ocean waters, as well as maritime atmospheric aerosols. Instrumental errors and errors in atmospheric correction strongly determine the information content. The wavelength dependence of both errors is taken into

05 OCEANOGRAPHY AND MARINE RESOURCES

account. Depending on atmospheric and oceanic turbidity, at most 2 independent optical parameters of water substances can be derived with an accuracy of a factor of 2 from multispectral radiance measurements made at a height of 10 km. ESA

N86-27699*# National Aeronautics and Space Administration. Goddard Space Flight Center, Greenbelt, Md.
SATELLITE DETECTION OF PHYTOPLANKTON EXPORT FROM THE MID-ATLANTIC BIGHT DURING THE 1979 SPRING BLOOM

J. J. WALSH (University of South Florida, St. Petersburg.), D. A. DIETERLE, and W. E. ESAIAS Feb. 1986 53 p Sponsored in part by DOE and NOAA

(NASA-TM-88782; NAS 1.15:88782) Avail: NTIS HC A04/MF A01 CSCL 08A

Analysis of Coastal Zone Color Scanner (CZCS) imagery confirms shipboard and in situ moored fluorometer observations of resuspension of near-bottom chlorophyll within surface waters (1 to 10 m) by northwesterly wind events in the mid-Atlantic Bight. As much as 8 to 16 micrograms chl/l are found during these wind events from March to May, with a seasonal increase of algal biomass until onset of stratification of the water column. Rapid sinking or downwelling apparently occurs after subsequent wind events, however, such that the predominant surface chlorophyll pattern is approx. 0.5 to 1.5 micrograms/l over the continental shelf during most of the spring bloom. Perhaps half of the chlorophyll increase observed by satellite during a wind resuspension event represents in-situ production during the 4 to 5 day interval, with the remainder attributed to accumulation of algal biomass previously produced and temporarily stored within near-bottom water. Present calculations suggest that about 10% of the primary production of the spring bloom may be exported as ungrazed phytoplankton carbon from mid-Atlantic shelf waters to those of the continental slope. Author

N86-27700*# National Aeronautics and Space Administration. Wallops Flight Center, Wallops Island, Va.

HIGH FREQUENCY SAMPLING OF THE 1984 SPRING BLOOM WITHIN THE MID-ATLANTIC BIGHT: SYNOPTIC SHIPBOARD, AIRCRAFT, AND IN SITU PERSPECTIVES OF THE SEEP-I EXPERIMENT

J. J. WALSH (University of South Florida, St. Petersburg), C. D. WIRICK (Brookhaven National Lab., Upton, N. Y.), L. J. PIETRAFESA (North Carolina State Univ., Raleigh.), T. E. WHITLEDGE (Texas Univ., Port Aransas), F. E. HOGE, and R. N. SWIFT (EG and G Washington Analytical Services Center, Inc., Pocomoke City, Md.) 1986 56 p

(NASA-TM-88765; NAS 1.15:88765) Avail: NTIS HC A04/MF A01 CSCL 08A

Moorings of current meters, thermistors, transmissometers, and fluorometers on the mid-Atlantic shelf, south of Long Island, suggest a cumulative seaward export of perhaps 0.35 g C/sq m/day between the 80 and 120 m isobaths during February-April 1984. Such a horizontal loss of algal carbon over the lower third of the water column would be 23 to 78% of the March-April 1984 primary production. This physical carbon loss is similar to daily grazing losses from zooplankton of 32-40% of the algal fixation of carbon. Metabolic demands of the benthos could be met by just the estimated fecal pellet flux, without direct consumption of algal carbon, while bacterioplankton needs could be served by excretory release of dissolved organic matter during photosynthesis. Sediment traps tethered 10 m off the bottom at the 120 m isobath and 50 m above the 500 m isobath caught as much as 0.16 to 0.26 g C /sq m/day during March-April 1984, in reasonable agreement with the flux estimated from the other moored instruments. Author

N86-27837*# Florida State Univ., Gainesville. Dept. of Meteorology.

A MODEL FOR THE ESTIMATION OF THE SURFACE FLUXES OF MOMENTUM, HEAT AND MOISTURE OF THE CLOUD TOPPED MARINE ATMOSPHERIC BOUNDARY LAYER FROM SATELLITE MEASURABLE PARAMETERS M.S. Thesis

D. E. ALLISON Aug. 1984 73 p

(Contract NAG5-332)

(NASA-CR-177283; NAS 1.26:177283) Avail: NTIS HC A04/MF A01 CSCL 04A

A model is developed for the estimation of the surface fluxes of momentum, heat, and moisture of the cloud topped marine atmospheric boundary layer by use of satellite remotely sensed parameters. The parameters chosen for the problem are the integrated liquid water content, $q_{sub li}$, the integrated water vapor content, $q_{sub vi}$, the cloud top temperature, and either a measure of the 10 meter neutral wind speed or the friction velocity at the surface. Under the assumption of a horizontally homogeneous, well-mixed boundary layer, the model calculates the equivalent potential temperature and total water profiles of the boundary layer along with the boundary layer height from inputs of $q_{sub li}$, $q_{sub vi}$, and cloud top temperature. These values, along with the 10m neutral wind speed or friction velocity and the sea surface temperature are then used to estimate the surface fluxes. The development of a scheme to parameterize the integrated water vapor outside of the boundary layer for the cases of cold air outbreak and California coastal stratus is presented. Author

N86-27838*# Florida State Univ., Tallahassee. Dept. of Meteorology.

AN INVESTIGATION OF THE MARINE BOUNDARY LAYER DURING COLD AIR OUTBREAK Final Report

S. A. STAGE Jul. 1986 26 p

(Contract NAG5-332)

(NASA-CR-177249; NAS 1.26:177249) Avail: NTIS HC A03/MF A01 CSCL 04A

Three techniques were developed and tested for use in the remote estimation of ocean surface heat and vapor fluxes. Methods for measurement of surface sensible and latent heat fluxes discussed include: satellite measurement, marine atmospheric boundary layer (MABL) model, and horizontal transfer coefficients. The accuracy and applicability of the methods are examined. Publications and papers are listed. B.G.

N86-27853*# Florida State Univ., Tallahassee. Coll. of Arts and Sciences.

A MODEL FOR THE ESTIMATION OF THE SURFACE FLUXES OF MOMENTUM, HEAT, AND MOISTURE OF THE CLOUD-TOPPED MARINE ATMOSPHERIC BOUNDARY LAYER FROM SATELLITE MEASURABLE PARAMETERS M.S. Thesis

D. E. ALLISON Aug. 1984 74 p

(Contract NAG5-332)

(NASA-CR-177290; NAS 1.26:177290) Avail: NTIS HC A04/MF A01 CSCL 04B

A model for the estimation of the surface fluxes of momentum, heat, and moisture of the cloud topped marine atmospheric boundary layer was developed by use of satellite remotely sensed parameters. The parameters chosen for the problem were the integrated liquid water content, the integrated water vapor content, the cloud top temperature, the sea surface temperature, and either a measure of the 10 meter neutral wind speed or the friction velocity at the surface. Under the assumptions of a horizontally homogeneous, well-mixed boundary layer, the model calculates the equivalent potential temperature and total water profiles of the boundary layer along with the boundary layer height. The development of a scheme to parameterize the integrated water vapor outside of the boundary layer for the cases of cold air outbreak and California coastal stratus is presented. Sensitivity studies are presented showing the potential accuracy of this technique. With improvements of current technology, the model will provide reasonable estimates of the surface fluxes. Author

HYDROLOGY AND WATER MANAGEMENT

Includes snow cover and water runoff in rivers and glaciers, saline intrusion, drainage analysis, geomorphology of river basins, land uses, and estuarine studies.

A86-33505**LARGE AREA SNOWMELT RUNOFF SIMULATIONS BASED ON LANDSAT-MSS DATA**

M. F. BAUMGARTNER (Zuerich, Eidgenoessische Technische Hochschule; Zuerich, Universitaet, Zurich, Switzerland), K. SEIDEL, H. HAEFNER, K. I. ITTEN (Zuerich, Universitaet, Zurich, Switzerland), and J. MARTINEC (Eidgenoessisches Institut fuer Schneeund Lawinenforschung, Weissfluhjoch-Davos, Switzerland) IN: 1985 International Geoscience and Remote Sensing Symposium (IGARSS '85), Amherst, MA, October 7-9, 1985, Digest. Volume 1. New York, Institute of Electrical and Electronics Engineers, Inc., 1985, p. 30-38. refs

Attention is given to a method for the processing of satellite remote sensing images, as well as to a snowmelt runoff simulation by the Matinec-Rango (1983) model on the basis of such data. The primary problems addressed were those of (1) the morphological and climatological complexity of basins in the Swiss Alps, and (2) the requirement of at least four snow cover evaluations during the snowmelt period, which requires the use of incomplete satellite scenes. The changing extent of seasonal snow cover is an important variable for the snowmelt-runoff model. O.C.

A86-33613**100 MHZ DIELECTRIC CONSTANT MEASUREMENTS OF SNOW COVER DEPENDENCE ON ENVIRONMENTAL AND SNOW PACK PARAMETERS**

B. A. BURNS, R. W. LARSON (Michigan, Environmental Research Institute, Ann Arbor), R. G. ONSTOTT (Kansas, University, Lawrence), and D. J. FISK (U.S. Army, Cold Regions Research and Engineering Laboratory, Hanover, NH) IN: 1985 International Geoscience and Remote Sensing Symposium (IGARSS '85), Amherst, MA, October 7-9, 1985, Digest. Volume 2. New York, Institute of Electrical and Electronics Engineers, Inc., 1985, p. 829-834.

(Contract N00014-81-C-0295)

Research is reported aimed at determining the relationship between the dielectric constant and environmental parameters including physical properties of snow cover and local meteorological variables. It is necessary to understand how snow properties affect remote sensing signatures in order to use microwave remote sensors to find snow depth, snow water equivalent, and coverage. For a given frequency, the dielectric constant of snow is a function of the temperature, density and grain size of the snow and its liquid water content. Results presented are based on measurements made in SE Michigan and at CRREL, during MIZEX '84 and the 1985 USGS-NASA passive microwave study of the Colorado snow pack. Both the masking and the information aspect of the snow cover problem are represented by the experiments. All dielectric constant measurements were made with a 100 MHz Q-meter system developed at ERIM. An alcohol calorimetry technique developed at CRREL (Fisk, 1983) was used to measure liquid water content. D.H.

A86-33615**MILLIMETER-WAVE BACKSCATTER FROM SNOWCOVER**

L. D. WILLIAMS (Aberdeen, University, Scotland), R. V. BIRNIE (Macaulay Institute for Soil Research, Aberdeen, Scotland), and J. G. GALLAGHER (Royal Signals and Radar Establishment, Malvern, England) IN: 1985 International Geoscience and Remote Sensing Symposium (IGARSS '85), Amherst, MA, October 7-9, 1985, Digest. Volume 2. New York, Institute of Electrical and Electronics Engineers, Inc., 1985, p. 842-847. refs

Ground-truth measurements of snowcover properties were made in Bavaria in 1984 in support of helicopter-mounted radar measurements of 80 GHz and 94 GHz backscattering from the snowcover. The variation of the backscattering coefficient with surface snow properties is investigated in this paper by stepwise multiple regression. Similar qualitative results are obtained for 80 GHz and for six polarization combinations of 94 GHz. For wet snow, the backscattering coefficient increased by 4-7 dB per mm surface roughness increase, and decreased by 0.2-1.1 dB per 1 percent increase in volumetric liquid water content. For dry snow, the backscattering coefficient decreased with increasing grain size (contrary to expectation) by 1-2 dB per mm, and did not depend on surface roughness. In a few cases (both wet and dry), porosity makes a small but statistically significant contribution to the regression, the backscattering coefficient increasing by 0.1 dB per 1 percent increase in porosity. Author

A86-33616**REMOTE SENSING OF SNOW WATER EQUIVALENT USING NIMBUS-7 SMMR DATA**

M. HALLIKAINEN and P. JOLMA (Helsinki University of Technology, Espoo, Finland) IN: 1985 International Geoscience and Remote Sensing Symposium (IGARSS '85), Amherst, MA, October 7-9, 1985, Digest. Volume 2. New York, Institute of Electrical and Electronics Engineers, Inc., 1985, p. 850-855.

Nimbus-7 Scanning Multichannel Microwave Radiometer (SMMR) data have been applied to remote sensing studies of seasonal snow cover in Finland. An algorithm has been developed to retrieve the water equivalent of dry snow cover from SMMR data. The algorithm takes into account the influence of land-cover categories (forest, etc.) on the brightness temperature of snow-covered terrain. SMMR data for two winters show that three distinct classes can be observed in the microwave behavior of snow-covered terrain: early and mid-winter, spring (after several melt-freeze cycles), and melting period (wet snow). Substantial differences in the behavior between consecutive winters may occur. Author

A86-33617**ICE CONDITIONS ON THE OHIO AND ILLINOIS RIVERS, 1972-1985**

L. W. GATTO (U.S. Army, Cold Regions Research and Engineering Laboratory, Hanover, NH) IN: 1985 International Geoscience and Remote Sensing Symposium (IGARSS '85), Amherst, MA, October 7-9, 1985, Digest. Volume 2. New York, Institute of Electrical and Electronics Engineers, Inc., 1985, p. 856-861. Army-supported research.

A part of the Corps of Engineers' River Ice Management (RIM) program is discussed, with objectives to document ice conditions along the Ohio and Illinois Rivers from 1972 to 1985. The ice data are required for developing an ice forecasting model, for evaluating remote sensing systems, and for other projects in the RIM program. Images obtained using the Landsat Multispectral Scanner (MSS), Return Beam Vidicon (RBV) and Thematic Mapper (TM) were studied. Despite problems of cloud cover and orbital configurations that limited image taking opportunities, Landsat imagery analysis provides a historical view of general ice conditions. For many rivers this may be the only source of data on past ice conditions. Because of the shortcomings of the Landsat imagery and the success of mapping ice on the Ohio during the winter of 1984-85 with video, ice conditions will be mapped in the future from videotapes taken from a low-flying aircraft. D.H.

A86-33630

PHYSICAL INTERPRETATION OF ESTUARINE WATER COLOR USING VECTOR ANALYSIS OF SATELLITE DATA

R. P. STUMPF (NOAA, Assessment and Information Services Center, Washington, DC) IN: 1985 International Geoscience and Remote Sensing Symposium (IGARSS '85), Amherst, MA, October 7-9, 1985, Digest, Volume 2. New York, Institute of Electrical and Electronics Engineers, Inc., 1985, p. 971-976. refs

An approximately linear relationship between the spectral bands is found in viewing satellite data of estuarine water in spectral space. The relationship may be treated in vector form. By applying a turbid water expression for the irradiant reflectance, one can obtain expressions that explain the spectral relationship, i.e., the vector orientation, in terms of absorption. Changes in vector orientation depend on variations in pigment concentrations, whereas sediment concentration determines the vector's magnitude. The technique provides a physical separation between sediment and pigments in turbid water. By using the unit vector, one can estimate relative quantities of pigments in Chesapeake and Delaware Bays and identify blooms. D.H.

A86-36193* National Aeronautics and Space Administration, Goddard Space Flight Center, Greenbelt, Md.

OPTIMIZED RETRIEVALS OF PRECIPITABLE WATER FIELDS FROM COMBINATIONS OF VAS SATELLITE AND CONVENTIONAL SURFACE OBSERVATIONS

W. D. ROBINSON, D. CHESTERS, and L. W. UCCELLINI (NASA, Goddard Space Flight Center, Greenbelt, MD) Journal of Geophysical Research (ISSN 0148-0227), vol. 91, April 20, 1986, p. 5305-5318. NASA-supported research. refs

VISSR (visible and infrared spin-scan radiometer) atmospheric sounder (VAS) radiances and conventional surface temperature and dewpoint data are used in several combinations within a regression approach to determine the optimum resolution and accuracy of precipitable water (PW) fields retrieved from satellite observations. Point retrievals at radiosonde stations are used to determine the numerical accuracy of each retrieval technique, and image sequences of the retrieved PW fields are used to determine the temporal stability and spatial coherence of mesoscale PW features. VAS channels 5, 6, 7, and 8 and the surface dewpoint contribute the most information to regression-based retrievals of PW. The most accurate PW retrievals are obtained when radiances are averaged to a resolution of 15 to 60 km. A physical 'split-window' approach provides better PW estimates than regression when only the 11- and 12-micron VAS channels are available or when radiosonde-based training is limited to only one time period. Author

A86-36234#

ESTIMATION OF MONTHLY RAINFALL FROM SATELLITE-OBSERVED CLOUD AMOUNT IN THE TROPICAL WESTERN PACIFIC

T. MARUYAMA, T. NITTA, and Y. TSUNEOKA (Meteorological Research Institute, Tsukuba, Japan) Meteorological Society of Japan, Journal (ISSN 0026-1165), vol. 64, Feb. 1986, p. 147-153. refs

A86-37010

HYDROLOGIC MODELING USING LANDSAT MSS DATA

D. P. ALEXANDER (Rural Water Commission, East Doncaster, Australia) and A. RAMACHANDRA RAO (Purdue University, West Lafayette, IN) IN: Machine processing of remotely sensed data - Quantifying global process: Models, sensor systems, and analytical methods; Proceedings of the Eleventh International Symposium, West Lafayette, IN, June 25-27, 1985. New York, Institute of Electrical and Electronics Engineers, 1985, p. 103-111. refs

A hydrologic analysis procedure for simulating the rainfall-runoff process is described. Landsat data are employed to define land cover classes. The development of a data bank to store land use classification data and the utilization of the HEC-1 Flood Hydrograph Package computer program to calculate flood hydrographs and the Hydrolic Parameters program to access the data bank are examined. This procedure is applied to the Sugar

Creek Watershed in Indiana. It is observed that land cover classifications developed from satellite or airborne scanner digital data are useful for classifying land use characteristics. I.F.

A86-37012

THE STUDY OF THE NATURAL GEOGRAPHIC DIFFERENCES IN THE COASTAL AREAS OF WATER COVERED PARTS OF MARMARA REGION IN TURKEY WITH THE HELP OF LANDSAT-4 MSS DATA USING AN UNSUPERVISED CLASSIFICATION ALGORITHM WITH EUCLIDEAN DISTANCE

D. MAKTAV (Istanbul, Technical University, Turkey) IN: Machine processing of remotely sensed data - Quantifying global process: Models, sensor systems, and analytical methods; Proceedings of the Eleventh International Symposium, West Lafayette, IN, June 25-27, 1985. New York, Institute of Electrical and Electronics Engineers, 1985, p. 122-127. refs

A86-39004

USE OF THEMATIC MAPPER DATA TO ASSESS WATER QUALITY IN GREEN BAY AND CENTRAL LAKE MICHIGAN

R. G. LATHROP, JR. and T. M. LILLESAND (Wisconsin, University, Madison) Photogrammetric Engineering and Remote Sensing (ISSN 0099-1112), vol. 52, May 1986, p. 671-680. refs (Contract NOAA-NA-84AAD00065; NOAA PROJECT 144-U824)

N86-23027# Sandia National Labs., Albuquerque, N. Mex. STABLE-ISOTOPE STUDIES OF GROUNDWATERS IN SOUTHEASTERN NEW MEXICO

S. J. LAMBERT 1985 23 p refs Presented at the Conference on the Rustler Formation, Carlsbad, N. Mex., 7 Mar. 1985 (Contract DE-AC04-76DP-00789) (DE86-002590; SAND-85-1978C; CONF-8503189-1) Avail: NTIS HC A02/MF A01

Oxygen-18/16 and deuterium/hydrogen ratio measurements have been made on groundwaters sampled according to specific field criteria applied during pump tests of the Rustler Formation (the uppermost Permian evaporite unit) in Nash Draw, a solution-subsidence valley west of the WIPP site in the northern Delaware Basin of southeastern New Mexico. Comparison of these data with similar measurements on other groundwaters from the northern Delaware Basin indicates two nonoverlapping populations of meteoric groundwaters in delta-0-18/delta-D space. Most of the Rustler waters in Nash Draw and at the WIPP site and older waters from the eastern two-thirds of the Capitan Limestone constitute one population, while unconfined groundwaters originating as observable modern surface recharge to alluvium, the near-surface Rustler in southwestern Nash Draw, and the Capitan in the Guadalupe Mountains (Carlsbad Caverns) constitute the other. The isotopic distinction suggests that Rustler groundwater in most of Nash Draw and at the WIPP site is not receiving significant modern meteoric recharge. A likely explanation for this distinction is that meteoric recharge to most of the Rustler and Capitan took place in the geologic past under climate conditions significantly different from the present. DOE

N86-23993# National Oceanic and Atmospheric Administration, Washington, D. C. National Environmental Satellite, Data, and Information Service.

HYDROLOGIC AND LAND SCIENCES APPLICATIONS OF NOAA POLAR-ORBITING SATELLITE DATA

M. MATSON and F. PARMENTER-HOLT 1985 24 p refs Original document contains color illustrations Avail: NTIS HC A02/MF A01

Hydrologic and land sciences applications of NOAA polar orbiting satellites presented include: continental snow cover; river basin snow mapping and flood monitoring; soil moisture analysis; vegetation progress and seasonal changes; fire detection and monitoring; urban effects; volcanoes; and geologic assessment. B.G.

06 HYDROLOGY AND WATER MANAGEMENT

N86-24075 National Oceanic and Atmospheric Administration, Washington, D. C.

NOAA ATLAS: AN ATLAS OF SATELLITE-DERIVED NORTHERN HEMISPHERIC SNOW COVER FREQUENCY

M. MATSON, C. F. ROPELEWSKI, and M. S. VARNADORE Mar. 1986 149 p

Avail: NTIS HC A07/MF A01

This atlas presents 15 years (1967 to 1981) of satellite derived snow cover data in the form of monthly and midmonth to midmonth snow cover frequency maps. The maps are in two general formats: frequency of snow cover incremented in 10 percent intervals and contour maps incremented in 25 percent intervals. In addition to the maps, tables and time series of Eurasian and North American snow cover are presented. Author

N86-26665*# South Carolina Univ., Columbia. Inst. for Marine Biology and Coastal Research.

APPLICATION OF LANDSAT TM IMAGES TO ASSESS CIRCULATION AND DISPERSION IN COASTAL LAGOONS Progress Report

B. KJERFVE, J. R. JENSEN, and K. E. MAGILL 15 Feb. 1986 38 p refs

(Contract NAS5-28741)

(NASA-CR-177315; NAS 1.26:177315) Avail: NTIS HC A03/MF A01 CSCL 08C

The main objectives are formulated around a four pronged work approach, consisting of tasks related to: image processing and analysis of LANDSAT thematic mapping; numerical modeling of circulation and dispersion; hydrographic and spectral radiation field sampling/ground truth data collection; and special efforts to focus the investigation on turbid coastal/estuarine fronts. Author

N86-26668# National Environmental Satellite Service, Suitland, Md. Satellite Applications Lab.

CHARACTERISTICS OF WESTERN REGION FLASH FLOOD EVENTS IN GOES IMAGERY AND CONVENTIONAL DATA

E. L. FLEMING and L. E. SPAYD, JR. Mar. 1986 87 p refs (NOAA-TM-NESDIS-13) Avail: NTIS HC A05/MF A01

Characteristics of western region convective and extratropical cyclone flash flood events as observed in (VIS and IR) GOES imagery and conventional surface and upper air data are presented. One hundred and thirty-seven convective heavy rainfall events from 1981 to 1983 were examined and categorized into time of year, time of day of maximum precipitation, minimum cloud top temperature at time of maximum precipitation, and type of satellite-observed convective system. Detailed analysis of conventional data for the largest flash flood producing mesoscale convective systems (MCS) yielded four distinct atmospheric patterns at the surface, 700, and 500 mb levels. Twenty-four flash flood events produced by extratropical cyclones from 1981 to 1983 were classified into three main types of satellite observed cloud patterns. These atmospheric composites and satellite observed cloud patterns were designed to aid operational meteorologists in recognizing and forecasting flash flood events in the western region of the United States. M.G.

N86-27703# National Oceanic and Atmospheric Administration, Washington, D. C.

SATELLITE-DERIVED MOISTURE PROFILES

A. TIMCHALK Apr. 1986 70 p

(NOAA-NESDIS-24) Avail: NTIS HC A04/MF A01

An evaluation of relative humidity and mixing ratio profiles determined by two different satellite methods is presented. One method (bogus), which is used operationally, uses GOES cloud imagery to prescribe vertical moisture profiles. The second method (TOVS) uses a 15-channel algorithm with polar orbiting satellite data. The accuracies of both methods, although inferior to moisture profiles obtained from rawinsondes, show sufficient accuracy to be useful as input into forecast models whose domain includes large oceanic areas. TOVS moisture profiles were more accurate in clear and partly cloudy areas, whereas the bogus profiles were more accurate in the broken cloud cover areas. An advantage of the TOVS method is that it is fully automated and can be applied

globally; however, some accompanying disadvantages are that the retrievals are synoptic and that they are made only in clear and partly cloudy areas. The major advantage of the bogus method is that profiles are available at synoptic times and over areas where no TOVS moisture values are retrieved. The disadvantage of the bogus method is that the moisture values are less accurate than the TOVS values in clear and partly cloudy areas. Furthermore, the method is only partially automated and requires subjective interpretation of cloud imagery. Author

07

DATA PROCESSING AND DISTRIBUTION SYSTEMS

Includes film processing, computer technology, satellite and aircraft hardware, and imagery.

A86-32333

IMAGE PROCESSING SYSTEM INTERFACES

W. B. GREEN (System Development Corp., Camarillo, CA) IN: Digital image processing; Proceedings of the Tenth Critical Reviews of Technology Conference, Los Angeles, CA, January 22, 23, 1985 . Bellingham, WA, Society of Photo-Optical Instrumentation Engineers, 1985, p. 103-109.

An image processing architecture is described that provides isolation of external interfaces from image processing applications software modules. The architecture allows development of a variety of specialized user interfaces, each of which utilizes the same basic set of image processing software routines. The architecture also allows development of interfaces to external non-imaging data bases, and other software (such as commercially available Data Base Management Systems) without requiring modification of the image processing software routines. Examples of a user interface developed on a personal workstation and of the correlation of weather satellite imagery with georeferenced data bases are presented. Author

A86-32337

TECHNIQUES FOR MULTISPECTRAL IMAGE CLASSIFICATION

M. J. CARLOTTO (Analytic Sciences Corp., Reading, MA) IN: Digital image processing; Proceedings of the Tenth Critical Reviews of Technology Conference, Los Angeles, CA, January 22, 23, 1985 . Bellingham, WA, Society of Photo-Optical Instrumentation Engineers, 1985, p. 174-191. refs

The state of the art in multispectral classifiers is reviewed by examining current multispectral techniques within the context of the overall classification process. An overview of the classification process is given, addressing such activities as scene and sensor preprocessing requirements, signal vs. semantic considerations in feature extraction, and issues relating to classifier training. Statistical classification theory is reviewed, discussing the use of spatial and contextual information, multitemporal classification techniques, hierarchical classifiers, and methods for incorporating collateral information sources to improve classification accuracy and efficiency. Post-processing techniques for extracting and interpreting spatial and structural information in the thematic map are described. Current trends in applying multispectral classification techniques are summarized, and future directions in the technology are outlined. C.D.

A86-32368

ON-BOARD DATA COMPRESSION FOR ADVANCED LANDSAT
C. SCHUELER, C. DE BOER, B. MARKS, and M. STEGALL
(Hughes Santa Barbara Research Center, Goleta, CA) IN: Architectures and algorithms for digital image processing II; Proceedings of the Meeting, Los Angeles, CA, January 24, 25, 1985. Bellingham, WA, Society of Photo-Optical Instrumentation Engineers, 1985, p. 135-146. refs

Advanced Landsat Sensor (ALS) technology has produced requirements for increasing data rates that may exceed space to ground data link capacity, so that identification of appropriate data compression techniques is of interest. Unlike many other applications, Landsat requires information lossless compression. DPCM, Interpolated DPCM, and error-correcting successive-difference PCM (ESPCM) are compared, leading to the conclusion that ESPCM is a practical, real-time (on-board) compression algorithm. ESPCM offers compression ratios approaching DPCM with no information loss and little or no increase in complexity. Moreover, adaptive ESPCM (AESPCM) yields an average compression efficiency of 84 percent relative to successive difference entropy, and 97 percent relative to scene entropy. Compression ratios vary from a low of 1.18 for a high entropy (6.64 bits/pixel) mountain scene to a high of 2.38 for low entropy (2.54 bits/pixel) ocean data. The weighted average lossless compression ratio to be expected, using a representative selection of Landsat Thematic Mapper eight-bit data as a basis, appears to be approximately 2.1, for an average compressed data rate of about 3.7 bits/pixel. Author

A86-32370

IMAGE SEGMENTATION ALGORITHMS

T. W. RYAN (Science Applications International Corp., Tucson, AZ) IN: Architectures and algorithms for digital image processing II; Proceedings of the Meeting, Los Angeles, CA, January 24, 25, 1985. Bellingham, WA, Society of Photo-Optical Instrumentation Engineers, 1985, p. 172-178. refs

The paper describes a sequence of algorithms used to perform segmentation of aerial images of natural terrain for the purpose of extracting features pertinent to cartographic applications. Topics include image filtering, labeling, automated editing and refinement of the segmentation within a resolution pyramid. These techniques are considered to be preprocessing activities which will, in general, require some editing by trained cartographers. The objective of this work is to minimize the tedium of feature extraction using algorithms that do not require excessive computational overhead. Author

A86-32688

A HISTOGRAM AS THE BASIS OF THE STATISTICAL CLASSIFICATION OF IMAGES [GISTOGRAMMA KAK OSNOVA STATISTICHESKOI KLASSIFIKATSII IZOBRAZHENII]

D. A. USIKOV and T. V. PIATIBRAT (AN SSSR, Institut Kosmicheskikh Issledovaniy, Moscow, USSR) Issledovanie Zemli iz Kosmosa (ISSN 0205-9614), Jan.-Feb. 1986, p. 99-103. In Russian. refs

The concept of statistical image classification (as applied to remote-sensing images, e.g., in crop monitoring, forest inventory, and geological survey) is defined. In this classification, a histogram can have a fundamental role as a complete system of functionals expressing all the other statistical characteristics of the images. Histogram-based procedures for calculating Mahalanobis distances are proposed. B.J.

A86-33515

PRELIMINARY ANALYSIS OF SIR-B IMAGES FOR STEREO APPLICATIONS

V. H. KAUPP, H. C. MACDONALD, W. P. WAITE (Arkansas, University, Fayetteville), and M. A. PISARUCK (Boeing Airplane Co., Seattle, WA) IN: 1985 International Geoscience and Remote Sensing Symposium (IGARSS '85), Amherst, MA, October 7-9, 1985, Digest. Volume 1. New York, Institute of Electrical and Electronics Engineers, Inc., 1985, p. 105-110. refs

Space Shuttle Imaging Radar (SIR-B) SAR images of a single region in South America that were obtained at several different illumination angles have been evaluated to determine the illumination angle combination that best generates a three-dimensional stereo model of a terrain type for human perception. After such parameters as resolution and image scale are taken into account, rankings obtained with the images are found to compare favorably with earlier analyses and with the model of an equation here presented. O.C.

A86-33522

LITHOLOGIC SIGNATURES IN MULTI-CHANNEL SAR IMAGERY

B. A. BURNS, K. I. BARTELS, and R. W. LARSON (Michigan, Environmental Research Institute, Ann Arbor) IN: 1985 International Geoscience and Remote Sensing Symposium (IGARSS '85), Amherst, MA, October 7-9, 1985, Digest. Volume 1. New York, Institute of Electrical and Electronics Engineers, Inc., 1985, p. 153-157. refs
(Contract NSF ECS-82-13418)

Dual polarization, dual frequency SAR data of semiarid terrain in north-central Arizona is found to provide good discrimination between a variety of volcanic and sedimentary units in the area. These data allow not only manipulation of multichannel composite images to enhance scattering differences between units, but also derivation of radiometrically rectified relative backscatter cross sections. Based on these cross section values, dielectric constant measurements of field samples, and surface roughness profiles, the relative importance of surface and volume scattering for the different units are evaluated. Three-color composite images revealed that the 23-cm L-band wave is sensitive to unit contacts, producing high contrast for forested areas and rivers banks, and that the 3-cm X-band wavelength picks up more of the textural details in the units. Experimental results indicate that for two surfaces of similar roughness, differences in dielectric constant alone are sufficient to explain the observed X-band signatures. R.R.

A86-33526

DESCRIPTION OF A DATABANK OF NORMALIZED RADAR CROSS SECTION OF TERRAIN

C. C. BOREL, R. M. NARAYANAN, and R. E. MCINTOSH (Massachusetts, University, Amherst) IN: 1985 International Geoscience and Remote Sensing Symposium (IGARSS '85), Amherst, MA, October 7-9, 1985, Digest. Volume 1. New York, Institute of Electrical and Electronics Engineers, Inc., 1985, p. 176-182.
(Contract F19628-84-K-0018)

A computer program called FINRACS which allows users access to published NRCS data on a variety of terrain conditions is described. The rationale, terrain classification system, and main features of the program are described with examples. Possible applications of the databank are also indicated. Author

A86-33534

AUTOMATIC CLOUD CLASSIFICATION

B. M. MEHTRE, N. N. MURTHY (CMC, Ltd., Secunderabad, India), B. LIPOVSKAK (Hidrometeoroloski Zavod SR Hrvatske, Zagreb, Yugoslavia), and B. CHATTERJEE (Indian Institute of Technology, Kharagpur, India) IN: 1985 International Geoscience and Remote Sensing Symposium (IGARSS '85), Amherst, MA, October 7-9, 1985, Digest. Volume 1 . New York, Institute of Electrical and Electronics Engineers, Inc., 1985, p. 233-241. refs

In this paper design and implementation of an automatic cloud classifier is discussed. It is assumed that the pattern classes obey the multivariate normal distribution. Maximum likelihood with threshold and penalized misclassification algorithms have been implemented both on host computer VAX-11/750 and Array Processor FPS/100. This technique classifies not only different cloud types but land, sea and snow as well. The result of classification and the time required on host as well as on array processor for various picture complexities has been tested. The array processor results are found to approach real time performance. NOAA satellite pictures have been used for testing.

Author

A86-33535

CONTEXT CLASSIFIER

R. M. HARALICK and H. JOO (Machine Vision International, Ann Arbor, MI) IN: 1985 International Geoscience and Remote Sensing Symposium (IGARSS '85), Amherst, MA, October 7-9, 1985, Digest. Volume 1 . New York, Institute of Electrical and Electronics Engineers, Inc., 1985, p. 247-254.

A pixel can have certain properties when viewed in isolation, which change when viewed in the entire context of the image. A theory, and an algorithm are presented for a context classifier which gives each pixel the highest probability label, given some substantially sized context neighboring the pixel. The algorithm takes the form of a recursive neighborhood operator, first applied in a top-down scan of the image, and then in a bottom-up scan of the image. Applied to a simulated image generated from a real Landsat image, the context classifier showed better accuracy than the Bayes classifier. On real images, the context classifier showed a 4 to 8 percent increase in overall classification accuracy over the context-free Bayes classifier under a Gaussian-distribution assumption. I.S.

A86-33594* National Aeronautics and Space Administration. National Space Technology Labs., Bay Saint Louis, Miss.

MULTIPOLARIZATION SAR DATA FOR SURFACE FEATURE DELINEATION

S. T. WU (NASA, National Space Technology Laboratories, Bay St. Louis, MS) IN: 1985 International Geoscience and Remote Sensing Symposium (IGARSS '85), Amherst, MA, October 7-9, 1985, Digest. Volume 2 . New York, Institute of Electrical and Electronics Engineers, Inc., 1985, p. 678-683. refs

This paper presents the techniques and the utility of multipolarization Synthetic Aperture Radar (SAR) data for surface feature delineation. Three channels of ratioed data (VV/HH, VH/HH, and VH/VV) are generated from the HH, VV, and VH polarization data (V = vertical, H = horizontal). The technique assumes redundancy of the VH and HV polarization and only VH polarization is used. The ratioed data are linearly stretched to yield a digital number within a range of 0 to 255. Based on the separability measure for two-class delineation, it was found that (1) the ratioed data resulted in a better delineation of surface features with high like (HH or VV) polarization digital number, and (2) the use of ratioed data provided further information not available from the original three-polarization data. The results suggest an advantage in using the ratioed data and the original three-polarization data for surface feature delineation. Author

A86-33596* National Aeronautics and Space Administration. Ames Research Center, Moffett Field, Calif.

THE DEVELOPMENT OF AN MSS SATELLITE IMAGERY CLASSIFICATION EXPERT SYSTEM

S. W. ENGLE (NASA, Ames Research Center; Informatics General Corp., Moffett Field, CA) IN: 1985 International Geoscience and Remote Sensing Symposium (IGARSS '85), Amherst, MA, October 7-9, 1985, Digest. Volume 2 . New York, Institute of Electrical and Electronics Engineers, Inc., 1985, p. 693-696.

Unsupervised image classification of Landsat MSS imagery entails a significant part of the remote sensing, image analysis effort. Expert systems, a technology developed in the field of artificial intelligence, offers the potential to automate this process, thus greatly increasing the efficiency with which an analyst can perform unsupervised image classification and making the knowledge of the image analyst available to a community of nonexperts. Such a system, under development at the NASA/Ames Research Center, is described and planned enhancements are discussed. Author

A86-33597

A STEPWISE HIERARCHICAL MULTI-BINARY APPROACH IN TM LANDUSE CLASSIFICATION

K. I. ITTEN, K. STAENZ, M. F. BAUMGARTNER, and TH. JOHNSON (Zuerich, Universitaet, Zurich, Switzerland) IN: 1985 International Geoscience and Remote Sensing Symposium (IGARSS '85), Amherst, MA, October 7-9, 1985, Digest. Volume 2 . New York, Institute of Electrical and Electronics Engineers, Inc., 1985, p. 697-702. refs

In Thematic Mapper landuse classification, a stepwise procedure is suggested as an alternative to the usual practice of classifying the total scene content in one expensive swath. Binary decisions in a hierarchically structured model lead to the degree of separation and classification level that is predefined by the customer and that can be obtained, so control is not lost in a multidimensional, multiproblem compromise. Thematic Mapper data will not completely solve all classification problems, but even with a medium technology approach it permits landuse classifications better than any previous sensor. D.H.

A86-33600

SLOPE-INTERCEPT-DENSITY PLOTS - A NEW METHOD FOR LINE DETECTION IN IMAGES

F. SALVINI (Pisa, Universita, Italy) IN: 1985 International Geoscience and Remote Sensing Symposium (IGARSS '85), Amherst, MA, October 7-9, 1985, Digest. Volume 2 . New York, Institute of Electrical and Electronics Engineers, Inc., 1985, p. 715-720.

A new approach to the problem of line detection is announced, going back to the first principles of lines to define slopes and intercepts with the X or Y axes. Most plotting and calculations are then done in slope-intercept space in which a line is represented as a point and a line in slope-intercept space represents all possible lines passing through a point in XY space. If a pixel has something distinctive about it that might help to define a line in the image, then all possible lines through that pixel can be represented by a line in slope-intercept space. In this way a grid can be prepared representing all possible lines through all distinctive pixels in the image. The number of calculations required increases approximately linearly with the number of pixels, rather than exponentially as with other methods. If the size or shape of the counting circle is allowed to vary, the sharpness of the detected lines can be made greater or less. D.H.

A86-33621

A NON-STATIONARY CONTEXTUAL CLASSIFIER WITH IMPROVED ACCURACY

J. K. RHO and K. H. PARK (Korea Advanced Institute of Science and Technology, Seoul, Republic of Korea) IN: 1985 International Geoscience and Remote Sensing Symposium (IGARSS '85), Amherst, MA, October 7-9, 1985, Digest. Volume 2. New York, Institute of Electrical and Electronics Engineers, Inc., 1985, p. 886-891.

A modified contextual classifier - called a nonstationary contextual classifier - is proposed. In the new method, the context distribution function is considered as the context probability. It is shown by real Landsat II data for the Seoul area and simulated data that the method offers substantial improvement in classification accuracy. Results are compared with a classify-and-count contextual classifier and the Bayes classifier. As the raw speed of computer components improve, it is expected that the proposed classifier will be useful in various applications where classification accuracy is very important. D.H.

A86-33624* National Aeronautics and Space Administration. Ames Research Center, Moffett Field, Calif.

LAND USE MAPPING USING EDGE DENSITY TEXTURE MEASURES ON THEMATIC MAPPER SIMULATOR DATA

C. A. HLAVKA (NASA, Ames Research Center, Moffett Field, CA) IN: 1985 International Geoscience and Remote Sensing Symposium (IGARSS '85), Amherst, MA, October 7-9, 1985, Digest. Volume 2. New York, Institute of Electrical and Electronics Engineers, Inc., 1985, p. 906-911. refs

Texture analysis was performed as part of an investigation of the information content of Thematic Mapper (TM) imagery. High altitude aircraft scanner imagery from the Airborne Thematic Mapper (ATM) instrument was acquired over central California and used to simulate TM data. Edge density texture images were constructed by computation of proportions of edge pixels in a 31 x 31 moving window on a near infrared ATM band. A training technique was employed to select computational parameters to maximize the difference between edge density measurements in urban and in rural areas. The results of classification of the texture images showed that urban and rural areas could be distinguished with texture alone, indicating that inclusion of texture in automated classification procedures could significantly improve their accuracy. Author

A86-33626

CLASSIFICATION OF GEOPHYSICAL PARAMETERS USING PASSIVE MICROWAVE SATELLITE MEASUREMENTS

R. R. FERRARO, JR., J. A. KOGUT (Research and Data Systems, Inc., Lanham, MD), and N. C. GRODY (NOAA, National Environmental Satellite, Data, and Information Service, Washington, DC) IN: 1985 International Geoscience and Remote Sensing Symposium (IGARSS '85), Amherst, MA, October 7-9, 1985, Digest. Volume 2. New York, Institute of Electrical and Electronics Engineers, Inc., 1985, p. 919-924. refs

A method using the 18 and 37 GHz vertically polarized brightness temperatures from the Nimbus-7 Scanning Multichannel Microwave Radiometer (SMMR) to classify six different geophysical parameters is presented. These parameters are: dry snow, sea ice, dry land, flooded land, precipitation, and open water. The microwave theory and classification algorithm are briefly discussed, and the method is illustrated with an example. C.D.

A86-33638* Boston Univ., Mass.

VARIOGRAMS AND SPATIAL VARIATION IN REMOTELY SENSED IMAGES

C. WOODCOCK (Boston University, MA) IN: 1985 International Geoscience and Remote Sensing Symposium (IGARSS '85), Amherst, MA, October 7-9, 1985, Digest. Volume 2. New York, Institute of Electrical and Electronics Engineers, Inc., 1985, p. 1078-1083. NASA-supported research.

Research is presented that is aimed at developing a link or connection between ground scenes and spatial variation in images. The link is established through the use of models of scenes and

a measure of spatial variation - the variogram. The approach used to explore the nature of spatial variation in remotely sensed images can be thought of as a 'bottom up' approach because it starts with a model of the scene and works toward the characteristics of a remotely sensed image derived from the scene. To date, observed images at two resolutions for each of three kinds of environment have been used to evaluate the use of variograms in real images. The images are from forests, residential, and agricultural environments. One resolution used is 30 m from the Thematic Mapper or Thematic Mapper Simulator. For each environment also there is fine resolution data from the range of 0.15-2.5 m. It is noted that variograms from these images show considerable structure. Work continues on checking the validity of the disk model (a way of representing trees and their shadows). D.H.

A86-33639

SPATIAL ENHANCEMENT TECHNIQUES FOR MULTICHANNEL SATELLITE IMAGERY

V. T. TOM and M. J. CARLOTTO (Analytic Sciences Corp., Reading, MA) IN: 1985 International Geoscience and Remote Sensing Symposium (IGARSS '85), Amherst, MA, October 7-9, 1985, Digest. Volume 2. New York, Institute of Electrical and Electronics Engineers, Inc., 1985, p. 1084-1090.

Global and local multiband spatial enhancement techniques for digital imagery are described. The techniques are based on a least-squares approach, and utilize correlation between a low resolution image of one spectral wavelength and a high resolution reference image of a different wavelength in order to augment the high spatial frequency content of the low resolution image. The limitations of the global approach motivate a local approach based on a sliding window technique. Using the local enhancement approach, the apparent ground resolution for TM thermal imagery and SPOT multispectral imagery is improved from 120 to 30 meters and 20 to 10 meters, respectively. Author

A86-33640* Du Pont de Nemours (E. I.) and Co., Wilmington, Del.

MODIFIED CUBIC CONVOLUTION RESAMPLING FOR LANDSAT

A. PRAKASH (Du Pont de Nemours and Co., Wilmington, DE) and B. MCKEE (General Electric Co., Philadelphia, PA) IN: 1985 International Geoscience and Remote Sensing Symposium (IGARSS '85), Amherst, MA, October 7-9, 1985, Digest. Volume 2. New York, Institute of Electrical and Electronics Engineers, Inc., 1985, p. 1091-1096. (Contract NAS-5-25300)

An overview is given of Landsat Thematic Mapper resampling technique, including a modification of the well-known cubic convolution interpolator (nearest neighbor interpolation) used to provide geometric correction for TM data. Post launch study has shown that the modified cubic convolution interpolator can selectively enhance or suppress frequency bands in the output image. This selectivity is demonstrated on TM Band 3 imagery. D.H.

A86-34738

THE ESTIMATION OF ATMOSPHERIC EFFECTS FOR SPOT USING AVHRR CHANNEL-1 DATA

S. M. SINGH and A. P. CRACKNELL (Dundee, University, Scotland) International Journal of Remote Sensing (ISSN 0143-1161), vol. 7, March 1986, p. 361-377. Sponsorship: Ministry of Defence. refs (Contract MOD-2205/24S)

The aim of this paper is to estimate the effect of atmospheric contamination on SPOT satellite data for stereoscopic modelling by using data from the AVHRR instrument carried on the NOAA satellite series. This paper includes the development of an atmospheric correction algorithm for the visible spectral channel data from the AVHRR instrument, and an analysis of the atmospherically corrected AVHRR data from many successive days, bearing in mind that the SPOT data for stereoscopic modelling

07 DATA PROCESSING AND DISTRIBUTION SYSTEMS

will be from two orbits which will be separated by several days.

Author

A86-34739

THE APPLICABILITY OF LOWTRAN 5 COMPUTER CODE TO AERIAL THERMOGRAPHIC DATA CORRECTION

S. B. WILSON and J. M. ANDERSON (Dundee, University, Scotland) *International Journal of Remote Sensing* (ISSN 0143-1161), vol. 7, March 1986, p. 379-388. refs

The data available in the LOWTRAN 5 computer code are applied to short path lengths for radiation in the thermal infrared range during a particular survey. The resulting calculated value for the atmospheric transmittance is compared with an experimentally derived value.

Author

A86-35111

PROBLEMS WITH GLOBAL MAPPING

K. RAWER (Freiburg, Universitaet, Freiburg im Breisgau, West Germany) *Acta Astronautica* (ISSN 0094-5765), vol. 13, March 1986, p. 131, 132. refs

The empirical and orthogonal functions mapping techniques are described. The incorrect mapping characteristics obtained with these techniques and various methods of correcting these problems are examined. The relationship between coordinates and the mapping procedures is studied. Various examples of global mapping by empirical and orthogonal functions methods are provided. I.F.

A86-35292

EXAMPLES OF THE AUTOMATED DERIVATION OF DIGITAL SURFACE MODELS [BEISPIELE ZUR AUTOMATISCHEN ERFASSUNG VON DIGITALEN OBERFLAECHEMODELLEN]

W. FOERSTNER (Stuttgart, Universitaet, West Germany) *Bildmessung und Luftbildwesen* (ISSN 0006-2421), vol. 54, March 1986, p. 71-79. In German. refs

The power and heterogeneity of existing approaches to the automated derivation of digital surface models are shown using three examples of feature-based stereo matching algorithms. The automated measurement of digital surface models is discussed, examining criteria for the selection of control points, suitable features for surface measurement, and available information suitable for interpolation.

C.D.

A86-36079

SATELLITE ORIENTATION AND POSITION FOR GEOMETRIC CORRECTION OF SCANNER IMAGERY

P. H. SALAMONOWICZ (USGS, Reston, VA) *Photogrammetric Engineering and Remote Sensing* (ISSN 0099-1112), vol. 52, April 1986, p. 491-499. refs

The U.S. Geological Survey (USGS) Mini Image Processing System currently relies on a polynomial method for geometric correction of Landsat multispectral scanner (MSS) data. A large number of ground control points are required because polynomials do not model the sources of error. In order to reduce the number of necessary points, a set of mathematical equations modeling the Landsat satellite motions and MSS scanner has been derived and programmed. A best fit to the equations is obtained by using a least-squares technique that permits computation of the satellite orientation and position parameters based on only a few control points. The parameters thus derived serve as a basis for geometric correction of the whole image. A preliminary test shows that the model permits pixel location to be predicted to approximately 100 meters based on six control points.

Author

A86-36082

ECONOMICAL MAINTENANCE OF A NATIONAL TOPOGRAPHIC DATA BASE USING LANDSAT IMAGES

A. F. GREGORY and H. D. MOORE (Gregory Geoscience, Ltd., Ottawa, Canada) *Photogrammetric Engineering and Remote Sensing* (ISSN 0099-1112), vol. 52, April 1986, p. 519-524. refs

An operational program to detect changes for 1:50,000 mapping and to provide information for the revision of 1:250,000 maps has been developed and implemented. A specialized projection-compositor (PROCOM-2) is used to register a recent

Landsat MSS image onto a 1:50,000 topographic map. Experience to date indicates that the average relative error in positioning of linear features is about 30 m at a scale of 1:50,000. A recent program of 2700 maps, representing an area of about 2 million sq km, was completed in nine months including selected field verification. The average cost for this combined program of change detection and map revision was \$0.15 (U.S.) per sq km or \$150 (U.S.) per 1:50,000 map. Relevant experience suggests that these techniques can be transferred with minimal training and capital cost for use in other parts of the world; some modification may be required for arid areas and rainforest.

Author

A86-36227#

INTRASEASONAL VARIATIONS OF OLR IN THE TROPICS DURING THE FGGE YEAR

T. NAKAZAWA (Meteorological Research Institute, Tsukuba, Japan) *Meteorological Society of Japan, Journal* (ISSN 0026-1165), vol. 64, Feb. 1986, p. 17-34. refs

NOAA satellite data collected during the FGGE experiment are analyzed to model the seasonal characteristics of the intraseasonal variations and the relationship with shorter period fluctuations and tropical cyclone activities in the Northern and Southern Hemisphere tropics. The satellite data encompassed twice-daily outgoing longwave radiation (OLR), a measure of the convective activity over the tropics. A harmonic analysis with a least squares approach was applied to 11 months of data to study the annual mean, yearly and half-yearly cycles, as well as any periodicity in 3-10 day periods. The latter periods exhibited amplitude modulations that had a 30-60 day period. The short-period fluctuations had amplitudes that were large during the active phase of the intraseasonal variations and small during the lapse in the variations. The data only covered a period of 11 months and need to be supplemented with data from several more years to test the validity of the observed relationships.

M.S.K.

A86-36511

TECHNICAL AND SOFTWARE FACILITIES AT A CENTER FOR THE PROCESSING OF REMOTE-SENSING DATA [TEKHNICHESKOE I PROGRAMMNOE OBESPECHENIE TSENTRA OBRABOTKI AEROKOSMICHESKOI INFORMATSII]

A. S. ALEKSEEV, S. T. VASKOV, V. N. DEMENTEV, B. K. KOZHEVNIKOV, E. G. MIKHALTSOV et al. IN: *Methods of combined air and space remote-sensing studies of Siberia*. Novosibirsk, Izdatel'stvo Nauka, 1985, p. 57-60. In Russian.

The structure of technical and software facilities at TsOGI, the Soviet center for the processing of remote-sensing data, is examined. Particular attention is given to: (1) the main tasks toward which the technical facilities are oriented; and (2) the multilevel organization of the software system for image processing. The user-oriented character of the center is emphasized, and prospects for the further development of the facilities are discussed.

B.J.

A86-36515

STATISTICAL APPROACH TO THE CLASSIFICATION OF OBJECTS ON AIR AND SPACE REMOTE-SENSING IMAGES [STATISTICHESKII PODKHOD K KLASSIFIKATSII OB'EKTOV NA AEROKOSMICHESKIKH IZOBRAZHENIIAKH]

B. A. GORBUNOV IN: *Methods of combined air and space remote-sensing studies of Siberia*. Novosibirsk, Izdatel'stvo Nauka, 1985, p. 75-79. In Russian.

A86-36517

CERTAIN TRANSFORMATIONS IN A QUANTITATIVE APPROACH TO IMAGE PROCESSING [NEKOTORYE PREEBRAZOVANIIA V KOLICHESTVENNOM PODKHODE PRI OBRABOTKE IZOBRAZHENII]

V. A. ZABELIN and V. P. PIATKIN IN: *Methods of combined air and space remote-sensing studies of Siberia*. Novosibirsk, Izdatel'stvo Nauka, 1985, p. 84-87. In Russian. refs

A quantitative image-synthesis approach for remote-sensing images is examined. The development of quantitative methods for the processing of spectrally superposed data is considered with

emphasis on the choice of spectral band for the image synthesis.
B.J.

A86-36518
COMPUTER PROCESSING OF SPECTRALLY SUPERPOSED DATA [OBRABOTKA SPEKTROSOVMESHCHENNOI INFORMATSII NA EVM]

V. A. ZABELIN IN: Methods of combined air and space remote-sensing studies of Siberia. Novosibirsk, Izdatel'stvo Nauka, 1985, p. 87-90. In Russian. refs

An interactive technique for the processing of multispectral remote-sensing data is described. Particular attention is given to the subprograms in the appropriate software package, intended for the processing of spectrally superposed data. B.J.

A86-36784
ESTIMATION OF ATMOSPHERIC CORRECTIONS FROM MULTIPLE AIRCRAFT IMAGERY

M. D. STEVEN and E. M. ROLLIN (Nottingham University, England) (Workshop on Atmospheric Corrections, University of Nottingham, England, May 22, 1985) International Journal of Remote Sensing (ISSN 0143-1161), vol. 7, April 1986, p. 481-497. NERC-supported research. refs

Remote-sensing techniques measure the radiance of the surface through a layer of atmosphere which both attenuates the signal and adds a path radiance. One class of solution can be found using the known dependence of transmittance on atmospheric path length. Multiheight measurements from aircraft enable the determination of transmittance and path radiance by linear regression. Multiangle measurements from overlapping aircraft scans have also been applied, but the difference of path lengths offered by the range of aircraft scan angles is insufficient to determine the atmospheric parameters with accuracy, especially with the uncertainties introduced by reflection from non-Lambertian surfaces. The atmosphere is not horizontally homogeneous in the presence of cloud or dense haze. Significant variations occur even at a distance from clouds and, on cloudless days, variations in optical depth can occur in dense haze layers. The variations are most significant at shorter wavelengths but have a coherent spatial distribution which can be applied to distinguish zones of different atmospheric characteristics. Author

A86-36790
LANDSAT TM IMAGE FORWARD/REVERSE SCAN BANDING CHARACTERIZATION AND CORRECTION

L. FUSCO, U. FREI, D. TREVESE (ESA, European Space Research Institute, Frascati, Italy), P. N. BLONDA, G. PASQUARIELLO (CNR, Istituto Elaborazione Segnali ed Immagini, Bari, Italy) et al. International Journal of Remote Sensing (ISSN 0143-1161), vol. 7, April 1986, p. 557-575. refs

Cross-scan averages of forward and reverse scan are analysed to model the within-line sample-position-dependent noise of Landsat Thematic Mapper images, in cases where no radiometric saturation is present. Two sources of banding are discussed: the droop, already mentioned by other authors, and the so-called radiometric hysteresis. The defined models are used to generate a correction algorithm which has been tested with real data. Author

A86-37003
HIGH ACCURACY CLUSTERING USING RESIDUAL IMAGE

K. FUKUE, H. SHIMODA, and T. SAKATA (Tokai University, Tokyo, Japan) IN: Machine processing of remotely sensed data - Quantifying global process: Models, sensor systems, and analytical methods; Proceedings of the Eleventh International Symposium, West Lafayette, IN, June 25-27, 1985. New York, Institute of Electrical and Electronics Engineers, 1985, p. 17-25.

The minimum residual clustering procedures used to classify remote sensing data is described. Training data problems, which include the number of training classes and training data, and the effect of subclasses on training classes, are examined. Two simulations were conducted in order to evaluate the characteristics of the minimum residual clustering. The applicability of the minimum

residual clustering is examined in two case studies: one case is the land cover classification of the Osaka district and the second is the forest classification of the Mount Fuji area using Landsat MSS data. The data reveal that the minimum residual clustering has a higher classification accuracy and a shorter processing time than conventional clustering procedures. I.F.

A86-37004
MULTISPECTRAL CHANGE DETECTION USING DIFFERENCE CLASSIFICATION AND BITEMPORAL CLASSIFICATION

G. M. HALEY (Santa Barbara Research Center, CA) IN: Machine processing of remotely sensed data - Quantifying global process: Models, sensor systems, and analytical methods; Proceedings of the Eleventh International Symposium, West Lafayette, IN, June 25-27, 1985. New York, Institute of Electrical and Electronics Engineers, 1985, p. 26-33.

The development of a boundary change detection technique is discussed. The technique is applicable for agriculture, building construction, military surveillance, and glacier movement observations. The gradient methods for boundary indications and the global histogram and region growing classification techniques are examined. The procedures for two methods of boundary change detection are described and compared in terms of accuracy and computational requirements. One method uses gradient operators and difference classifications to observe spectral changes and the second technique employs bitemporal classification to detect spatial variations. It is noted that the second technique is more accurate than the first; however, it requires more computational time. Author

A86-37006
ESTIMATION OF THE LOCATION PARAMETER OF A MULTISPECTRAL DISTRIBUTION BY A MEDIAN OPERATOR

C. A. POMALAZA-RAEZ and Y.-S. FONG (Clarkson University, Potsdam, NY) IN: Machine processing of remotely sensed data - Quantifying global process: Models, sensor systems, and analytical methods; Proceedings of the Eleventh International Symposium, West Lafayette, IN, June 25-27, 1985. New York, Institute of Electrical and Electronics Engineers, 1985, p. 41-48. refs

Three different kinds of median type estimators for use in applications where the underlying probability distribution is multivariable are proposed and analyzed. Such applications arise in the area of remote sensing classification, problems, multispectral edges filtering, and computer vision systems. Both aspects, the numerical complexity, and the statistical characteristics of the estimators are studied and discussed. From the numerical results obtained by analytical and computer simulation methods there is evidence that a simple extension of the scalar median estimator has an overall performance (in the mean square error sense) that is the same or better than the other two proposed estimators. The computational requirements of this estimator are not excessive making it attractive for applications where large amounts of data are present. Author

A86-37017
HIERARCHICAL CLASSIFICATION OF MULTITEMPORAL/MULTISPECTRAL SCANNER DATA

D. F. LOZANO-GARCIA and R. M. HOFFER (Purdue University, West Lafayette, IN) IN: Machine processing of remotely sensed data - Quantifying global process: Models, sensor systems, and analytical methods; Proceedings of the Eleventh International Symposium, West Lafayette, IN, June 25-27, 1985. New York, Institute of Electrical and Electronics Engineers, 1985, p. 162-169. refs

To evaluate the classification accuracy of hierarchical classifiers, the results obtained by the use of the layered hierarchical classifier were compared to those of a single stage classifier, using Landsat-1 MSS data obtained in June 1973 and February 1974 over two central Indiana areas. Four procedures were used: (1) a standard single stage maximum likelihood classification employing an eight-channel training statistics, and (4) the layered classifier, but treating the data from the two dates independently. It has been

07 DATA PROCESSING AND DISTRIBUTION SYSTEMS

found that the classification accuracies were relatively high for all four procedures, but that the layered classifier was more efficient, requiring only one third of the CPU time used in the single stage classification. I.S.

A86-37019

PROCESSING OF MULTI-SENSOR REMOTELY SENSED DATA TO A STANDARD GEOCODED FORMAT

T. A. FISHER (Canada Centre for Remote Sensing, Ottawa) and N. MINIALLY (MacDonald Dettwiler and Associates, Ltd., Vancouver, Canada) IN: Machine processing of remotely sensed data - Quantifying global process: Models, sensor systems, and analytical methods; Proceedings of the Eleventh International Symposium, West Lafayette, IN, June 25-27, 1985. New York, Institute of Electrical and Electronics Engineers, 1985, p. 183-188.

To realize the full potential of remotely sensed data, it must be corrected and converted to a standard format. The Canada Centre for Remote Sensing (CCRS) has defined a standard geocoded format (Guertin et al.) which is compatible with the Canadian National Topographic System (NTS) series of maps. This paper gives the characteristics of the CCRS geocoded products, describes some of the benefits that will be derived from the application of geocoded products, and gives a brief overview of the Multi-Observational Satellite Image Correction System (MOSAICS) which is being developed to create these products. MOSAICS will correct and convert imagery from a number of different satellites and sensors into CCRS geocoded format, producing a large number of high accuracy CCT and film products. Author

A86-37022

MULTISOURCE DATA ANALYSIS IN REMOTE SENSING AND GEOGRAPHIC INFORMATION PROCESSING

P. H. SWAIN (Purdue University, West Lafayette, IN), J. A. RICHARDS, and T. LEE (New South Wales, University, Kensington, Australia) IN: Machine processing of remotely sensed data - Quantifying global process: Models, sensor systems, and analytical methods; Proceedings of the Eleventh International Symposium, West Lafayette, IN, June 25-27, 1985. New York, Institute of Electrical and Electronics Engineers, 1985, p. 211-218. (Contract NSF ECS-84-00324)

A general approach is presented for the computer analysis, using quantitative multivariate methods, of remote sensing data combined with other sources of data in geographic information systems. A method is proposed by which inferences can be drawn systematically from multiple observations having significant but unknown interactions. A simple classification experiment with Landsat MSS data is undertaken to illustrate the use of this method. Author

A86-37026

RADAR IMAGE SIMULATION AS A TOOL TO ANALYZE TOPOGRAPHIC EFFECTS ON GEOMETRY AND RADIOMETRY OF RADAR IMAGERY

G. DOMIK (Graz, Technische Universitaet und Forschungszentrum, Austria) IN: Machine processing of remotely sensed data - Quantifying global process: Models, sensor systems, and analytical methods; Proceedings of the Eleventh International Symposium, West Lafayette, IN, June 25-27, 1985. New York, Institute of Electrical and Electronics Engineers, 1985, p. 248-253. refs (Contract ESA-5443/83/D/IM(SC))

Radar image simulation was used to create a relationship between radar image coordinates and corresponding terrain properties as a means of analyzing radar radiometry and geometry. Using a digital elevation model, and flight and image parameters extracted from SIR-A data of Sardegna collected in November 1981, the simulator models all geometric aspects of the SIR-A sensor, and the image is then registered and geometrically rectified to yield a radar ortho image of the digital terrain model geometry. Radiometric correction of the radar image, removing the effects of topographic slopes, enabled lithological mapping, and for the given example, two thematic classes were differentiated. An

additional simulation study indicated that the loss of image information due to layover, foreshortening and radar shadow would be minimized using an elevation angle as high as 60 degrees at the average Space Shuttle altitude of 260 km. R.R.

A86-37027*

Jet Propulsion Lab., California Inst. of Tech., Pasadena.

PRELIMINARY SCIENCE RESULTS FROM THE SHUTTLE IMAGING RADAR-B

M. RUZEK (California Institute of Technology, Jet Propulsion Laboratory, Pasadena) IN: Machine processing of remotely sensed data - Quantifying global process: Models, sensor systems, and analytical methods; Proceedings of the Eleventh International Symposium, West Lafayette, IN, June 25-27, 1985. New York, Institute of Electrical and Electronics Engineers, 1985, p. 254-265. NASA-supported research. refs

Preliminary results of analyzing digital radar imagery data obtained by the SIR-B aboard the Space Shuttle Challenger STS 41-G are presented. The data cover 5 million square kilometers of the earth surface between 57 deg north and south latitudes. Radar imagery of the same target at different incidence angles was used to classify surfaces by their backscatter response as a function of incidence angle. The SIR-B proved to be useful for collecting multiple incidence angle data sets over a broad range of targets, providing information in the areas of geology, archeology, forestry, agriculture, oceanography, geography, and hydrology. The analysis is also used to optimize radar parameters such as look angle for future missions. I.S.

A86-37028*

Jet Propulsion Lab., California Inst. of Tech., Pasadena.

THE SIR-C EXPERIMENT - MEASURING NEW VARIABLES FROM SPACE WITH SAR

S. D. WALL (California Institute of Technology, Jet Propulsion Laboratory, Pasadena) IN: Machine processing of remotely sensed data - Quantifying global process: Models, sensor systems, and analytical methods; Proceedings of the Eleventh International Symposium, West Lafayette, IN, June 25-27, 1985. New York, Institute of Electrical and Electronics Engineers, 1985, p. 268-270. NASA-supported research.

SIR-C is a continuation of the Shuttle Imaging Radar (SIR) series of synthetic aperture radar (SAR) imaging systems flown by the Jet Propulsion Laboratory aboard the Space Shuttle. SIR-A, flown in 1981, showed that SAR can be a useful remote sensing tool in the fields of geology, hydrology, and oceanography. SIR-B added the capability of moving the radar's antenna in 1984, showing that multiple incidence angle images add materially to the usefulness of SAR. SIR-C will add the dimensions of wavelength and polarization, providing the most powerful system ever flown for SAR scientific studies of the earth. Author

A86-37032*

National Aeronautics and Space Administration.

Ames Research Center, Moffett Field, Calif.

MEASUREMENT OF THEMATIC MAPPER DATA QUALITY

R. C. WRIGLEY, C. A. HLAVKA, D. H. CARD (NASA, Ames Research Center, Moffett Field, CA), J. S. BUIS (Technicolor Government Services, Inc., Moffett Field, CA), R. A. SCHOWENGERDT (Arizona, University, Tucson) et al. IN: Machine processing of remotely sensed data - Quantifying global process: Models, sensor systems, and analytical methods; Proceedings of the Eleventh International Symposium, West Lafayette, IN, June 25-27, 1985. New York, Institute of Electrical and Electronics Engineers, 1985, p. 303-314. refs

Thematic Mapper data from Landsat-4 and Landsat-5 were examined for band-to-band registration, absolute geodetic registration, periodic noise and spatial resolution. Between focal planes, appreciable misregistrations existed in early data products but were corrected in later data products. The analysis of absolute geodetic registration used only system-corrected data because ground control point-corrected data were unavailable. Geodetic registration errors averaged only 9.7 pixels, less than expected for system-corrected data. Periodic noise at four spatial frequencies was observed in Landsat-5 Thematic Mapper data by using Fourier

analysis on small areas over water. Magnitudes of periodic noise components were consistent within a scene. The modulation transfer function was determined for two Landsat-4 scenes. The effective instantaneous field of view was 40.8 meters in one case, and 48.6 meters in the other. Author

A86-37033
A CLUSTERING ALGORITHM FOR REMOTE SENSING MULTISPECTRAL DATA

L. I. DAWEI (Zhanjiang Electronic Industrial Co., People's Republic of China) IN: Machine processing of remotely sensed data - Quantifying global process: Models, sensor systems, and analytical methods; Proceedings of the Eleventh International Symposium, West Lafayette, IN, June 25-27, 1985. New York, Institute of Electrical and Electronics Engineers, 1985, p. 315-318. refs

A clustering algorithm, named SORT, used for classification of remote sensing multispectral data is described. The program involves the scanning of the entire image and the construction of a cluster table. The SORT program operates in the IRAS II image processing system and is applicable for geoscience studies. I.F.

A86-37864#
DESIGN OF THE EUROPEAN SPACE AGENCY THEMATIC MAPPER PROCESSING CHAINS

G. TREVISIOL (Advanced Computer Systems, Italy) IN: International Conference on Space, 25th, Rome, Italy, March 26-28, 1985, Proceedings. Rome, Rassegna Internazionale Elettronica Nucleare ed Aerospaziale, 1985, p. 207-215.

A data processing system is described that is designed to process the data acquired from Landsats 4 and 5 (Multispectral Scanner and Thematic Mapper data) and SPOT (HVR1 and HVR2 data). The data are received by the SSX Acquisition System and recorded on a high density digital recorder during a satellite pass. User products, or output products, are available as images stored on computer compatible tapes (CCT) and as images stored on film. The processing subsystem provides quick-look images on CCT or film and raw/system-corrected images on CCT or 240-mm film. The data management subsystem provides for automatic order handling of output products, monitoring of the production process, and management of the Image Catalogue. Design criteria and hardware and software subsystem overviews are discussed. The project was completely successful. D.H.

A86-39150
APPLICATION OF SHUTTLE IMAGING RADAR DATA FOR LAND USE INVESTIGATIONS

J. LIU (Chinese Academy of Sciences, Institute of Remote Sensing Application, Beijing, People's Republic of China), X. TENG (Chinese Academy of Sciences, Changchun Physics Institute, People's Republic of China), and J. XIAO (Chinese Academy of Sciences, Institute of Geochemistry, Guiyang, People's Republic of China) Remote Sensing of Environment (ISSN 0034-4257), vol. 19, June 1986, p. 291-301.

A Shuttle Imaging Radar (SIR)-A image in the south of Tianjin acquired by the SIR-A in November 1981 was interpreted manually and with the aid of a computer system. The methods of processing involved density slicing with statistical training, producing normalized false color composite images through coregistration of the SIR-A and Landsat MSS image data sets, and unsupervised clustering. The interpretation keys for the SIR-A image were established after investigation in situ and analysis of soil dielectric and moisture properties. The interpretation accuracy for various images were determined by using a combination of color infrared and aerial photography and land use maps acquired recently. The research indicates that the SIR-A data can remedy some defects of Landsat MSS data due to the SIR-A's better response to residential areas and linear features. The SIR-A/Landsat MSS normalized composite image incorporated the strong points of both. The interpretation accuracy, therefore was increased. Author

A86-39545
A TECHNIQUE FOR ASSESSING THE SEVERITY OF TERRAIN SHADOWING IN MOBILE SATELLITE SERVICE

A. HILLS (Alaska, University, Fairbanks) and D. C. ROGERS (Chugach Electric Association, Anchorage, AK) IEEE Transactions on Antennas and Propagation (ISSN 0018-926X), vol. AP-34, April 1986, p. 601-603.

A graphical analysis technique is presented that produces an estimate of the severity of terrain shadowing of a particular geosynchronous satellite. The technique can be used to analyze the coverage provided by a new group of satellites capable of direct communication with mobile and transportable units. Application of the technique to a number of highways in Alaska is described. Author

N86-23028# National Aerospace Lab., Amsterdam (Netherlands). Informatics Div.

MAP DIGITIZATION OFFERS NEW POSSIBILITIES

F. A. GERRITSEN and H. J. BOS 6 Aug. 1984 13 p Repr. from De Ingenieur (Utrecht, Netherlands), v. 96, no. 94, Apr. 1984 p 26-29 In DUTCH; ENGLISH summary Presented at Royal Netherlands Institute of Engineering (KLVl) Digital Maps Symposium, The Hague, Netherlands, 8 Feb. 1984 Original contains color illustrations

(NLR-MP-84061-U; B8571449) Avail: NTIS HC A02/MF A01

Alternatives for the digitization of map information, its application possibilities, costs, and required efforts are discussed. Structured geographic data bases for map production offer a large range of possibilities, but require large personnel efforts. Simple interactive use for presentation purposes demands a less complicated way of digitization, but requires relatively expensive apparatus. An automated system for flight route planning is mentioned.

Author (ESA)

N86-25919# National Geophysical Data Center, Boulder, Colo.
EARTHQUAKE AND TSUNAMI DATA SERVICES AND PUBLICATIONS

Dec. 1985 15 p

(PB86-156254; KGRD-15-REV) Avail: NTIS HC A02/MF A01 CSCL 08G

The National Environmental Satellite, Data, and Information Service (NESDIS) collects, manages, and disseminates the great mass of information produced by the scientific observation of interplanetary space and the physical world. Data activities in seismology, gravity, geomagnetism, marine geology and geophysics, geothermics, and solar-terrestrial physics are directed by the NESDIA National Geophysical Data Center (NGDC) in Boulder, CO. NGDC also provides facilities for World Data Center-A (including the disciplines of Solid Earth Geophysics, Marine Geology and Geophysics, Solar-Terrestrial Physics, and Glaciology). The products and services in seismology are briefly described. NGDC is a focal point for disseminating historical earthquake data and information to both technical and general users. Author

N86-27749# Colorado Univ., Boulder. Dept. of Astrophysics, Planetary and Atmospheric Science.

TRANSIENT RESPONSE TO LOCALIZED EPISODIC HEATING IN THE TROPICS

M. L. SALBY and R. R. GARCIA (National Center for Atmospheric Research, Boulder, Colo.) In International Council of Scientific Unions Handbook for MAP, Vol. 18 8 p Dec. 1985

Avail: NTIS HC A23/MF A01; also available from SCOSTEP Secretariat, Illinois Univ., 1406 West Green Street, Urbana, Ill. 61801 CSCL 04A

It is generally recognized that equatorial disturbances in the lower stratosphere are excited by convective latent heat release associated with the Internal Tropical Convergence Zone (ITCZ). Recently, attention has also focused on tropical convection with regard to extratropical teleconnection patterns. Unlike equatorial waves which are trapped about the equator but propagate vertically, the latter extend well out of the tropics but are barotropic. They have been most widely discussed in connection with long-term climatological features. Both types of disturbances have been

examined largely from the standpoint of steady monochromatic forcing, in the latter case zero frequency or time-mean heating. However, tropical convection as revealed by recent geostationary satellite imagery is anything but regular, surely not steady. Much of the heating variance is concentrated spatially within three localized convective centers: Indonesia, the Amazon, and the Congo. Convective activity within these regions undergoes an irregular evolution over the span of a couple of days. It involves a rather broad spectrum of spatial and temporal scales. The analysis of cloud brightness over the Eastern Atlantic and Africa suggests a characteristic time scale of 3-4 days and correlations scales in latitude and longitude of approximately 30 deg. Author

08

INSTRUMENTATION AND SENSORS

Includes data acquisition and camera systems and remote sensors.

A86-31222

SPOT - A HIGH-PRECISION VIEW OF THE EARTH

S. COMPARD Revue Aerospatiale (ISSN 0065-3780), March 1986, p. 34-37. In English and French.

The design of SPOT which travels in a near-polar, sun-synchronous orbit 822 km above the earth is examined. The capabilities of the two high-resolution-visible imaging instruments that scan an area 117 km wide with a resolution of 10 m or 20 m are studied. The noncontinuous imaging process is described. The benefits SPOT provides to its customers including ecologists, geologists, and oceanographers are discussed. I.F.

A86-33317

AN ALGORITHM FOR THE IDENTIFICATION OF CLOUD COVER AND THE ESTIMATION OF SPECTRAL BRIGHTNESSES OF THE CLOUDLESS ATMOSPHERE ACCORDING TO SATELLITE SCANNING MEASUREMENTS OF OUTGOING IR RADIATION [OB ODNOM ALGORITME IDENTIFIKATSII OBLACHNOI I OTSENKI SPEKTRAL'NYKH IARKOSTEI BEZOBLACHNOI ATMOSFERY PO DANNYM SPUTNIKOVYKH SKANIRUIUSHCHIKH IZMERENII UKHODIASHCHEGO IK IZLUCHENIIA]

IU. V. PLOKHENKO and V. E. TRETIAKOV IN: Aspects of the processing and interpretation of measurement data from meteorological satellites. Leningrad, Gidrometeoizdat, 1985, p. 36-41. In Russian.

A86-33318

EXPERIMENTS ON THE REMOTE TEMPERATURE SOUNDING OF THE ATMOSPHERE ON THE BASIS OF NOAA-SATELLITE RADIOMETER MEASUREMENTS [EKSPERIMENTY PO DISTANTSIONNOMU TEMPERATURNOMU ZONDIROVANIU ATMOSFERY NA OSNOVE RADIOMETRICHESKIKH IZMERENII S ISZ NOAA]

IU. M. TUMOFEEV, IU. V. PLOKHENKO, and A. B. USPENSKII IN: Aspects of the processing and interpretation of measurement data from meteorological satellites. Leningrad, Gidrometeoizdat, 1985, p. 42-49. In Russian. refs

A description is given of algorithms and programs for the secondary processing of measurements of outgoing radiation of the ground-atmosphere system, measured with the NOAA HIRS/2 radiometer of the TOVS system with the aim of atmospheric-temperature sounding. Results are presented of numerical experiments on temperature sounding based on HIRS/2 archive data prepared during the ALPEx experiment. B.J.

A86-33501* Massachusetts Univ., Amherst.

1985 INTERNATIONAL GEOSCIENCE AND REMOTE SENSING SYMPOSIUM (IGARSS '85), UNIVERSITY OF MASSACHUSETTS, AMHERST, OCTOBER 7-9, 1985, DIGEST. VOLUMES 1 & 2

K. R. CARVER, ED. (Massachusetts, University, Amherst) Symposium sponsored by IEEE, NASA, Navy, et al. New York, Institute of Electrical and Electronics Engineers, Inc., 1985. Vol. 1, 577 p.; vol. 2, 661 p. For individual items see A86-33502 to A86-33603, A86-33605 to A86-33647.

The present conference on remote sensing instrumentation considers topics in water resources research, planetary remote sensing and mathematical geophysics, sea ice behavior in view of the Cold Regions Research and Engineering Laboratories pond measurements, Shuttle Imaging Radar-B (SIR-B) system performance and calibration results, geological applications of remote sensing, and microwave scattering from vegetation. Further attention is given to atmospheric probing with lasers, image processing for remote sensing, forest inventory and condition assessment, atmospheric remote sensing, SIR-B geological results, the reflectance, emission, and scattering characteristics of vegetation, sea ice sensing, multipolarization SAR results, the theoretical modeling of surfaces and volumes, crop condition assessment and productivity estimates, and SIR-B results for vegetation cover. Also considered are the microwave remote sensing of soil moisture, advanced sensors, advanced information extraction, wind and wave remote observations, results from the ESA Remote Sensing satellite, large area crop and land cover statistics, SIR-B results for directional ocean wave spectra, seasonal snow cover, ice sheets, and lake ice, fundamental research in terrain remote sensing, image classification methods, vegetation stress detection, remote sensing of coastal processes, SAR systems and calibration, electromagnetic geophysical methods and signal processing, image processing techniques, and SAR internal wave measurements. O.C.

A86-33502

NOAA PLANS FOR REMOTE SENSING OF THE EARTH, OCEANS AND ATMOSPHERE

G. OHRING (NOAA, National Environmental Satellite, Data, and Information Service, Washington, DC) IN: 1985 International Geoscience and Remote Sensing Symposium (IGARSS '85), Amherst, MA, October 7-9, 1985, Digest. Volume 1. New York, Institute of Electrical and Electronics Engineers, Inc., 1985, p. 2-8.

The National Oceanographic and Atmospheric Administration (NOAA) operates a multisatellite system, capable of continuous global coverage of the earth, which employs two polar-orbit Advanced Tiros-N (ATN) satellites, two Geostationary Operational Environmental Satellites (GOES), and two Landsats. Although the ATN and GOES satellites were designed for atmospheric observations, they furnish additional data on the land and ocean components of the earth system. Attention is presently given to NOAA plans for the improvement of this earth remote sensing satellite system in the near-term period ending in 1992 and in the long term period extending from there to the year 2000. O.C.

A86-33533

REMOTE SENSING OF CLOUDS

J. A. COAKLEY, JR. (National Center for Atmospheric Research, Boulder, CO) IN: 1985 International Geoscience and Remote Sensing Symposium (IGARSS '85), Amherst, MA, October 7-9, 1985, Digest. Volume 1. New York, Institute of Electrical and Electronics Engineers, Inc., 1985, p. 227-232. refs

An approach is described to the retrieval of cloud cover information from the imagery data of the Tiros-N Advanced Very High Resolution Radiometer, making it possible to probe the physical properties of clouds. The 65,000-pixel visible and IR images for a 1000 km x 1000 km area of the Pacific Ocean were constructed from data with a spatial resolution of 4 km x 4 km. To treat only partially cloud-covered pixels the spatial coherence method of Coakley and Bretherton (1982) was used. The method takes advantage of the fact that for many large-scale cloud systems, the clouds lie in distinct well-defined layers and are often

opaque at infrared wavelengths. A plot of the reflected 3.7-micron radiance data versus emitted 11-micron radiance for a single-layered cloud system observed during the day shows that cloud-covered pixels reflect less of the 3.7-micron radiation than do some of the pixels that are only partially cloud-covered. The reflectivity is greater for small, finite clouds because these clouds allow photons that enter the cloud top to escape through a side, while large extensive clouds would absorb the same photons.

I.S.

A86-33545* Jet Propulsion Lab., California Inst. of Tech., Pasadena.

PASSIVE REMOTE SENSING OF STRATOSPHERIC AND MESOSPHERIC WINDS

D. J. MCCLEESE and J. S. MARGOLIS (California Institute of Technology, Jet Propulsion Laboratory, Pasadena) IN: 1985 International Geoscience and Remote Sensing Symposium (IGARSS '85), Amherst, MA, October 7-9, 1985, Digest. Volume 1. New York, Institute of Electrical and Electronics Engineers, Inc., 1985, p. 333-338. NASA-supported research.

A passive infrared sensor for remote sounding of the wind field in the stratosphere and mesosphere from near earth orbital spacecraft is described. The sensor utilizes gas correlation spectroscopy and electrooptic phase-modulation techniques to measure winds in the 20-120 km altitude range, temperature, and atmospheric species concentrations. The operation of the sensor is examined. The sensitivity of the sensor is small Doppler shifts in an observed spectrum and the performance of the instrument were evaluated using laboratory simulation and numerical modeling. The data reveal that the sensor's wind measurements should have an accuracy better than 5 m/s and a spatial resolution of 5 km vertical by 150 km horizontal.

I.F.

A86-33547

REMOTE SENSING OF VERTICAL MOISTURE PROFILES AND CLOUD PROPERTIES FROM SIMULATED MILLIMETER WAVE SOUNDER AND MICROWAVE IMAGER DATA

R. G. ISAACS and G. DEBLONDE (Atmospheric and Environmental Research Inc., Cambridge, MA) IN: 1985 International Geoscience and Remote Sensing Symposium (IGARSS '85), Amherst, MA, October 7-9, 1985, Digest. Volume 1. New York, Institute of Electrical and Electronics Engineers, Inc., 1985, p. 345-350. refs (Contract F19628-83-C-0027; F19628-84-C-0134)

A86-33584* National Aeronautics and Space Administration. Goddard Space Flight Center, Greenbelt, Md.

MICROWAVE BACKSCATTER AND EMISSION OBSERVED FROM SHUTTLE IMAGING RADAR B AND AN AIRBORNE 1.4 GHZ RADIOMETER

J. R. WANG, J. C. SCHIUE, T. J. SCHMUGGE (NASA, Goddard Space Flight Center, Greenbelt, MD), E. T. ENGMAN (USDA, Agricultural Research Center, Beltsville, MD), T. MO (Computer Sciences Corp., Beltsville, MD), and R. W. LAWRENCE (NASA, Langley Research Center, Hampton, VA) IN: 1985 International Geoscience and Remote Sensing Symposium (IGARSS '85), Amherst, MA, October 7-9, 1985, Digest. Volume 2. New York, Institute of Electrical and Electronics Engineers, Inc., 1985, p. 607-612. refs

A soil moisture experiment conducted with the Shuttle Imaging Radar B (SIR-B) is reported. SIR-B operated at 1.28 GHz provided the active microwave measurements, while a 4-beam pushbroom 1.4 GHz radiometer gave the complementary passive microwave measurements. The aircraft measurements were made at an altitude of 330 m, resulting in a ground resolution cell of about 100 m diameter. SIR-B ground resolution from 225 km was about 35 m. More than 150 agricultural fields in the San Joaquin Valley of California were examined in the experiment. The effect of surface roughness height on radar backscatter and radiometric measurements was studied.

D.H.

A86-33586* Jet Propulsion Lab., California Inst. of Tech., Pasadena.

SPACEBORNE IMAGING RADAR (SIR) PROJECT

C. ELACHI, N. HERMAN (California Institute of Technology, Jet Propulsion Laboratory, Pasadena), and K. CARVER (Massachusetts, University, Amherst) IN: 1985 International Geoscience and Remote Sensing Symposium (IGARSS '85), Amherst, MA, October 7-9, 1985, Digest. Volume 2. New York, Institute of Electrical and Electronics Engineers, Inc., 1985, p. 625-628.

An overview is given of elements of the SIR (Shuttle Imaging Radar) project, covering the coming decade. The project is intended to develop the scientific basis and the required technology of the Earth Orbiting Satellite (EOS) Synthetic Aperture Radar (SAR). Plans are ongoing for a SIR-B reflight in 1987, a dual SIR-C flight in 1989 and a SIR-D flight in 1992 leading to an advanced multispectral multipolarization imaging sensor for flight on EOS in 1994. The conventional and distributed radar approaches are compared.

D.H.

A86-33588* Massachusetts Univ., Amherst.

ELECTRONICALLY STEERED THINNED ARRAY RADIOMETER (ESTAR) SYSTEM DESIGN, CALIBRATION, AND SENSITIVITY

C. RUF, C. T. SWIFT (Massachusetts, University, Amherst), and D. LEVINE (NASA, Goddard Space Flight Center, Greenbelt, MD) IN: 1985 International Geoscience and Remote Sensing Symposium (IGARSS '85), Amherst, MA, October 7-9, 1985, Digest. Volume 2. New York, Institute of Electrical and Electronics Engineers, Inc., 1985, p. 635-640. refs

The ESTAR system, an imaging L-band radiometer designed to provide measurements of soil moisture from space, is described. The large aperture size dictated by the resolution requirement (10 km or less) suggests the use of aperture synthesis, and plans to have ESTAR operate in low earth orbit require that the synthesis be performed in the short data acquisition time permitted by satellite motion. Two forms of ESTAR are described. ESTAR-0 is to be an airborne prototype designed for proof of concept; it will image a line of eight adjacent pixels with 8 degree spatial resolution of 0.1 degree Kelvin temperature resolution, given 1 sec integration time. ESTAR-1 is the satellite version to operate from space. A tentative sensor design will image a line of 128 0.5 degree pixels with 2.0 degree K resolution assuming 0.7 sec integration at 700 km altitude.

D.H.

A86-33589

PUSH-BROOM MICROWAVE RADIOMETER SYSTEMS FOR SPACE APPLICATIONS

N. SKOU (Danmarks Tekniske Højskole, Lyngby, Denmark) IN: 1985 International Geoscience and Remote Sensing Symposium (IGARSS '85), Amherst, MA, October 7-9, 1985, Digest. Volume 2. New York, Institute of Electrical and Electronics Engineers, Inc., 1985, p. 641-646. ESA-supported research. refs

A comparison is given between the conventional method of imaging the earth's surface by scanning a single beam antenna carried by a satellite and the pushbroom approach which does not use a scanning antenna. In the pushbroom approach, a multiple beam antenna covers the swath while the satellite moves forward; numbers of radiometer receivers are connected to an equal number of antenna feeds to sense the earth simultaneously. Relationships between swath width, footprint, integration time, satellite height, frequency AO are presented for earth oriented imaging systems. Three specific examples of geophysical measurement situations calling for the pushbroom solution are dealt with: sea ice mapping, coastal salinity, and soil moisture measurements.

D.H.

A86-33590* Jet Propulsion Lab., California Inst. of Tech., Pasadena.

HIGH RESOLUTION MILLIMETER-WAVE IMAGING SENSOR

W. J. WILSON, R. J. HOWARD, and G. S. PARKS (California Institute of Technology, Jet Propulsion Laboratory, Pasadena) IN: 1985 International Geoscience and Remote Sensing Symposium (IGARSS '85), Amherst, MA, October 7-9, 1985, Digest. Volume 2 . New York, Institute of Electrical and Electronics Engineers, Inc., 1985, p. 647-649. Army-supported research.

A scanning 3-mm radiometer is described that has been built for use on a small aircraft to produce real time high resolution images of the ground when atmospheric conditions such as smoke, dust, and clouds make IR and visual sensors unusable. The sensor can be used for a variety of remote sensing applications such as measurements of snow cover and snow water equivalent, precipitation mapping, vegetation type and extent, surface moisture and temperature, and surface thermal inertia. The advantages of millimeter waves for cloud penetration and the ability to observe different physical phenomena make this system an attractive supplement to visible and IR remote sensing systems. D.H.

A86-33623* National Aeronautics and Space Administration. Goddard Space Flight Center, Greenbelt, Md.

EXTENDED TESTING OF A GENERAL CONTEXTUAL CLASSIFIER USING THE MASSIVELY PARALLEL PROCESSOR - PRELIMINARY RESULTS AND TEST PLANS

J. C. TILTON (NASA, Goddard Space Flight Center, Greenbelt, MD) IN: 1985 International Geoscience and Remote Sensing Symposium (IGARSS '85), Amherst, MA, October 7-9, 1985, Digest. Volume 2 . New York, Institute of Electrical and Electronics Engineers, Inc., 1985, p. 900-905. refs

Earlier encouraging test results of a contextual classifier that combines spatial and spectral information employing a general statistical approach are expanded. The earlier results were of limited meaning because they were produced from small (50-by-50 pixel) data sets. An implementation of the contextual classifier on NASA Goddard's Massively Parallel Processor (MPP) is presented; for the first time the MPP makes feasible the testing of the classifier on large data sets (a 12-hour test on a VAX-11/780 minicomputer now takes 5 minutes on the MPP). The MPP is a Single-Instruction, Multiple Data Stream computer, consisting of 16,384 bit serial microprocessors connected in a 128-by-128 mesh array with each element having data transfer connections with its four nearest neighbors so that the MPP is capable of billions of operations per second. Preliminary results are given (with more expected for the conference) and plans are mentioned for extended testing of the contextual classifier on Thematic Mapper data sets. D.H.

A86-33633

SNR IN SAR

R. K. RANEY (RADARSAT, Ottawa, Canada) IN: 1985 International Geoscience and Remote Sensing Symposium (IGARSS '85), Amherst, MA, October 7-9, 1985, Digest. Volume 2 . New York, Institute of Electrical and Electronics Engineers, Inc., 1985, p. 994-999. refs

The issue of signal-to-noise ratio for a synthetic aperture radar (SAR) observing extended natural terrain is readdressed. The generally accepted form of the SNR equation (providing the design basis of famous SARs) is only 'almost correct' and actually depends on two offsetting errors for its success. It is not appropriate to substitute an area increment of average reflectivity for peak point target reflectivity, nor is it correct phenomenologically to apply coherent gain to mean power measures. An expression is given that retains the minimum parameters essential to describe SAR sensitivity to uniform natural scatterers and is based on more appropriate application of SAR operation. D.H.

A86-33634* Environmental Research Inst. of Michigan, Ann Arbor.

VERIFICATION OF L-BAND SAR CALIBRATION

R. W. LARSON, P. L. JACKSON, and E. KASISCHKE (Michigan, Environmental Research Institute, Ann Arbor) IN: 1985 International Geoscience and Remote Sensing Symposium (IGARSS '85), Amherst, MA, October 7-9, 1985, Digest. Volume 2 . New York, Institute of Electrical and Electronics Engineers, Inc., 1985, p. 1001-1006. NASA-supported research. (Contract N00014-81-C-0692)

Absolute calibration of a digital L-band SAR system to an accuracy of better than 3 dB has been verified. This was accomplished with a calibration signal generator that produces the phase history of a point target. This signal relates calibration values to various SAR data sets. Values of radar cross-section (RCS) of reference reflectors were obtained using a derived calibration relationship for the L-band channel on the ERIM/CCRS X-C-L SAR system. Calibrated RCS values were compared to known RCS values of each reference reflector for verification and to obtain an error estimate. The calibration was based on the radar response to 21 calibrated reference reflectors. Author

A86-33636

RESEARCH AND DEVELOPMENT OF THE SYNTHETIC APERTURE RADAR TRANSMITTER AND RECEIVER SUBSYSTEM DESIGN AND SOME COMPONENT TEST RESULTS

I. IZUMI, K. NISHIKOWA, Y. UENO, M. FUKAI, K. TANAKA (NEC Corp., Tokyo, Japan) et al. IN: 1985 International Geoscience and Remote Sensing Symposium (IGARSS '85), Amherst, MA, October 7-9, 1985, Digest. Volume 2 . New York, Institute of Electrical and Electronics Engineers, Inc., 1985, p. 1014-1017.

An account is given of research and development work on synthetic aperture radar for earth observation satellites, with reference to the Japanese Earth Resources Satellite-1, to be launched in FY 1990. The subsystem design to establish the functions, configuration, and main design parameters for this equipment is described. Test results are given for some key components of the SAR transmitter and receiver. D.H.

A86-33641

HIGH SPEED IMAGE PROCESSING SYSTEM WITH CUSTOM VLSI FOR DSP

M. KUBO, Y. KUNIIYASU, S. HORII, A. KANUMA, M. SUGAI (Toshiba Corp., Kawasaki, Japan) et al. IN: 1985 International Geoscience and Remote Sensing Symposium (IGARSS '85), Amherst, MA, October 7-9, 1985, Digest. Volume 2 . New York, Institute of Electrical and Electronics Engineers, Inc., 1985, p. 1097-1102. refs

The error in the sum of products operation caused by the underflow in the accumulator of the VLSI is analyzed and avoided by its sizing. The effect of word length constraint in FFT and inverse FFT in series is measured by simulation to size the VLSI. The outlook for the precise and fast image processing is examined; 100 km x 100 km SAR image formation is done within six minutes with 16 VLSIs in parallel. Author

A86-34112#

COMMERCIAL APPLICATIONS OF THE NAVSTAR GLOBAL POSITIONING SYSTEM

M. W. MILLER (Rockwell International Corp., Satellite Systems Div., Washington, DC) IN: U.S. Opportunities in Space Conference; Proceedings of the Second Annual Space Business Conference, Washington, DC, October 30-November 1, 1985 . London, Space Consultants International, Ltd., 1985, 10 p.

The characteristics and operation of the Global Positioning System (GPS) are described. The benefits GPS will provide to civilian air, sea, land, and space travel are discussed. Specific commercial applications for the satellite system, which include air traffic control, time synchronization, and oil exploration, are analyzed. I.F.

A86-34736

TERRAIN HEIGHT MEASUREMENT BY SYNTHETIC APERTURE RADAR WITH AN INTERFEROMETER

H. HIROSAWA and N. KOBAYASHI (Tokyo, University, Japan)
International Journal of Remote Sensing (ISSN 0143-1161), vol. 7, March 1986, p. 339-348. refs

This paper describes the terrain height measurement capability of synthetic aperture radar with an interferometer assuming the radar operates on a satellite. The interferometer phase measurement uncertainty due to additive thermal noise and multiplicative speckle noise, which determine the upper limit of the height measurement accuracies of this radar system, has been obtained by numerical simulation. The height measurement accuracies attainable on relatively flat terrain areas are of roughly the same order as range resolution when C- or X-band radar is operated at an altitude of 300 km. Author

A86-34737

AN INTEGRATED APPROACH TO GEOMETRIC PRECISION PROCESSING OF SPACEBORNE HIGH-RESOLUTION SENSORS

A. MOCCIA and S. VETRELLA (Napoli, Universita, Naples, Italy)
International Journal of Remote Sensing (ISSN 0143-1161), vol. 7, March 1986, p. 349-359. Research supported by the Ministero della Pubblica Istruzione and CNR. refs

The planimetric errors due to terrain relief and atmospheric refraction must be considered when high geometric resolution sensors and off-nadir viewing angles are used. This paper presents an approach to correct these errors using an integrated procedure that takes into account geometric and radiometric effects, connected to simulations of future remote-sensing systems or precision data processing. A diagram shows the relation between the root mean square error of the digital elevation model necessary to correct the terrain relief effect and the achievable scale of the output image map. The procedure is currently applied to the SPOT simulation on the Basilicata test site in southern Italy. A short example is given to analyse the geometric errors involved. Author

A86-35425

ASIAN CONFERENCE ON REMOTE SENSING, 5TH, KATHMANDU, NEPAL, NOVEMBER 15-18, 1984, PROCEEDINGS

Conference sponsored by the Ministry of Forest and Soil Conservation of Nepal, Japan Association of Remote Sensing, Tokai University, et al. Tokyo, University of Tokyo, 1985, 503 p. No individual items are abstracted in this volume.

Papers are presented on remote sensing activities in Bangladesh, China, India, Japan, Sri Lanka, Singapore, Nepal, and Asia; airborne radar system use in topographic mapping; photometric camera mission on Spacelab 1; and the use of remote sensing technique in archaeology. Topics discussed include the application of remote sensing to agriculture/forestry, landuse/cartography, water resources/oceanography, and geology and geomorphology. Consideration is given to the utilization of continuation methods is enhancement of satellite/low flying MSS digital imagery; three dimensional measurement by stereo Landsat MSS CCT data; tachometry by a nonmetric camera in a model plane; print plotted false color imageries and its use in remote sensing studies; application of airborne multispectral scanners; remote sensing inputs to resource data management system for developing countries; photogrammetric accuracy of stereo space photographs taken by metric camera from Spacelab 1; remotely sensed canopy temperature based models for estimating evapotranspiration; and the use of color plotter to generate high resolution image pixels. I.F.

A86-36080

PRACTICAL PHOTOGRAMMETRY FROM 35-MM AERIAL PHOTOGRAPHY

A. ROBERTS and L. GRISWOLD (Simon Fraser University, Burnaby, Canada) Photogrammetric Engineering and Remote Sensing (ISSN 0099-1112), vol. 52, April 1986, p. 501-508. refs

To date, photogrammetry has been primarily concerned with the analysis of 240-mm photographs or transparencies taken with metric cameras. With advances in microcomputer controlled analytical stereoplotters, 35-mm aerial photography can achieve acceptable levels of accuracy. The photogrammetric accuracy of 35-mm aerial photography was analyzed using a modified Zeiss G-2 Stereocord. The imagery distortions were corrected using the analytical orientation procedures of the stereoplotting hardware-software system. Vertical measurements deviated not more than + or - 0.001 of the flying height from ground truth values. These results are within precision standards for many practical photogrammetry applications. Author

A86-36514

CHOICE OF SPECTRAL BANDS FOR A SPACEBORNE MULTISPECTRAL SCANNER [VYBOR ZON SPEKTRA PRI KOSMICHESKOI S'EMKE]

N. A. TEPLIAKOV and V. M. CHERNIN IN: Methods of combined air and space remote-sensing studies of Siberia. Novosibirsk, Izdatel'stvo Nauka, 1985, p. 72-75. In Russian.

A graph-analytical method based on the simultaneous analysis of the parameters of the scanning objects is presented for determining the optimal spectral bands for a multispectral scanner. Recommendations are given on the improvement of remote-sensing optical filters and on the compilation of a spectral-contrast catalog for remote-sensing objects. B.J.

A86-36785

SATELLITE REMOTE SENSING OF ATMOSPHERIC OPTICAL DEPTH SPECTRUM

S. ARANUVACHAPUN (Exeter, University, England) (Workshop on Atmospheric Corrections, University of Nottingham, England, May 22, 1985) International Journal of Remote Sensing (ISSN 0143-1161), vol. 7, April 1986, p. 499-514. refs

Satellite radiance data are applied to the study of optical depth and aerosol radiative transfer in the atmosphere. The collection of the coastal zone color scanner (CZCS) radiance data and measured aerosol size distribution data utilized in this analysis is described. The equations for computing the radiance of the aerosol size distribution and oceanic surface albedo are presented. The variability of the aerosol phase function, which represents the aerosol radiative transfer in the atmosphere, is examined. CZCS and the computed radiance data are compared and an optical depth spectrum is derived. The results reveal that there is a strong dependence of optical depth on the wavelength. It is noted that ocean color remote-sensing data is useful for estimating the optical depth spectrum of the earth's atmosphere. I.F.

A86-36838*# National Aeronautics and Space Administration. Langley Research Center, Hampton, Va.

SAGE OBSERVATIONS OF STRATOSPHERIC NITROGEN DIOXIDE

W. P. CHU and M. P. MCCORMICK (NASA, Langley Research Center, Hampton, VA) Journal of Geophysical Research (ISSN 0148-0227), vol. 91, April 30, 1986, p. 5465-5476. refs

The global distribution of nitrogen dioxide in the middle to upper stratosphere (25-45 km altitude) for the period February 1979 to November 1981 has been determined from observations of attenuated solar radiation in the visible region 0.385-0.45 micron by the Stratospheric Aerosol and Gas Experiment (SAGE) satellite instrument. The SAGE-derived NO₂ vertical profiles compare well with observations by balloon- and aircraft-borne sensors. The global SAGE NO₂ distributions generally show a maximum in mixing ratio of 8 parts per billion by volume at about 35 km altitude near the equatorial latitudes at local sunset. The location of the mixing ratio peak moves synchronously with the overhead sun for the four different seasons. High-latitude NO₂ column content shows

strong seasonal variation, with a maximum in local summer and a minimum in local winter. Selected data at high-latitude winter seasons are presented, suggesting that the large variation shown could be explained by the coupling of both dynamics and photochemistry of the NO(x) species. Finally, profiles of the ratio of sunset to sunrise NO₂ mixing ratios, peaking at about a factor of two at 30 km, are shown. Author

A86-37001

MACHINE PROCESSING OF REMOTELY SENSED DATA - QUANTIFYING GLOBAL PROCESS: MODELS, SENSOR SYSTEMS, AND ANALYTICAL METHODS; PROCEEDINGS OF THE ELEVENTH INTERNATIONAL SYMPOSIUM, PURDUE UNIVERSITY, WEST LAFAYETTE, IN, JUNE 25-27, 1985

S. K. MENGEL, ED. and D. B. MORRISON, ED. Symposium sponsored by the American Society of Agronomy, Crop Science Society of America, IEEE, et al. New York, Institute of Electrical and Electronics Engineers, 1985, 380 p. For individual items see A86-37002 to A86-37036.

Consideration is given to global biogeochemical issues, image processing, remote sensing of tropical environments, global processes, geology, landcover hydrology, and ecosystems modeling. Topics discussed include multisensor remote sensing strategies, geographic information systems, radars, and agricultural remote sensing. Papers are presented on fast feature extraction; a computational approach for adjusting TM imagery terrain distortions; the segmentation of a textured image by a maximum likelihood classifier; analysis of MSS Landsat data; sun angle and background effects on spectral response of simulated forest canopies; an integrated approach for vegetation/landcover mapping with digital Landsat images; geological and geomorphological studies using an image processing technique; and wavelength intensity indices in relation to tree conditions and leaf-nutrient content. I.F.

A86-37007

THE EMERGENCE OF AIRBORNE VIDEO TECHNIQUES AS AN ALTERNATIVE FOR ACCESSING TROPICAL ENVIRONMENTS - A HISTORICAL PERSPECTIVE

R. D. MOWER (North Dakota, University, Grand Forks) IN: Machine processing of remotely sensed data - Quantifying global process: Models, sensor systems, and analytical methods; Proceedings of the Eleventh International Symposium, West Lafayette, IN, June 25-27, 1985. New York, Institute of Electrical and Electronics Engineers, 1985, p. 59-64. refs

The development of remote sensing systems is discussed. The use of video technology to acquire airborne video data and techniques for analyzing the data are described. The application of airborne video technology to tropical areas in developing countries is examined. Examples of remote sensing projects that employed airborne video technology are presented. I.F.

A86-37343

APPLICATIONS OF SENSOR PAYLOADS

J. W. JACK (Ferranti Defence Systems, Ltd., Electro-Optics Dept., Edinburgh, Scotland) IN: Remotely piloted vehicles; International Conference, 5th, Bristol, England, September 9-11, 1985, Supplementary Papers. Bristol, England, University of Bristol, 1985, p. 17.1-17.7.

An account is given of the availability and performance capabilities of TV, intensified TV, pyroelectric vidicon, and thermal imaging systems applicable to visible to far-IR sensing tasks aboard RPV platforms. Attention is given to a number of payload configurations which, while conceived to meet a military requirement for the detection and recognition of a military vehicle, are not restricted to military applications. Civilian applications include thermal emission surveys for local governments and industrial concerns, traffic flow pattern surveillance, and pipeline and transmission line surveys. O.C.

A86-39559

THE ARGOS SYSTEM FOR POSITIONING AND DATA COLLECTION BY SATELLITE - CHARACTERISTICS AND PERFORMANCE LEVELS [LE SYSTEME ARGOS DE LOCALISATION ET DE COLLECTE DE DONNEES PAR SATELLITE CARACTERISTIQUES ET PERFORMANCES]

R. ROSSO (CNES, Paris, France) Navigation (Paris) (ISSN 0028-1530), vol. 34, April 1986, p. 187-195. In French.

The ARGOS system was developed jointly by CNES, NASA and NOAA for positioning and data collection purposes after the success of the Eole satellite in relaying meteorological balloon data. The system has three segments: data collection stations, two meteorological satellites, and a ground system for receiving, storing and processing the data. The data gathering equipment is located at 750 sites in 24 countries and on ships at sea. Transmissions to the satellites for relay are performed at 401.650 MHz. The satellites fly an 850 km altitude polar orbit, each having 250 data collection platforms in line-of-sight link at all times. Each data stream received is marked to identify the transmitting station, time and frequency of the transmission. The central data treatment facility is at Toulouse; receiving stations are also located in Alaska, Virginia and Lannion. The data is stored for remote interrogation through telephone links. The satellites transmit signals at 401.650 MHz, which permits positioning by measurement of the Doppler effect so long as precise orbital predictions for the spacecraft are available. M.S.K.

A86-39969

THE EFFECT OF THE ATMOSPHERE ON THE SATELLITE REMOTE SENSING OF EARTH RESOURCES [VLIANIE ATMOSFERY NA ISSLEDOVANIYA PRIRODNYKH RESURSOV IZ KOSMOSA]

K. IA. KONDRATEV, O. I. SMOKTII, and V. V. KOZODEROV Moscow, Izdatel'stvo Mashinostroenie, 1985, 272 p. In Russian. refs

The work examines the development of algorithms and schemes for the atmospheric radiation correction of satellite remote-sensing data. Attention is given to theoretical aspects of the solution of direct and inverse problems connected with the analysis of outgoing-radiation fields of the system consisting of the atmosphere and a horizontal inhomogeneous underlying surface. Computing systems are described which make possible the real-time correction of spectral-band photographs and spectrograms of earth resources. B.J.

N86-23025# Sherbrooke Univ. (Quebec). Dept. de Geographie. THE FUNDAMENTALS OF MICROWAVE REMOTE SENSING [LES MICRO-ONDES EN TELEDETECTION]

P. DESFOSSÉS, J. M. M. DUBOIS, and F. BONN Oct. 1985 126 p refs IN FRENCH; ENGLISH summary (SU-84; SU-85; ISSN-0710-0868) Avail: NTIS HC A07/MF A01

Fundamentals of microwave remote sensing are presented. It is noted that there is a need for a simple introduction to this specialized subject. The fundamentals of microwave physics are introduced. Radar systems, wave interaction with natural surfaces and interpretation of radar imagery are discussed. E.A.K.

N86-23159*# Oklahoma Univ., Norman. National Severe Storms Lab.

ANALYSIS OF AIRBORNE DOPPLER LIDAR, DOPPLER RADAR AND TALL TOWER MEASUREMENTS OF ATMOSPHERIC FLOWS IN QUIESCENT AND STORMY WEATHER Contractor Report, 27 Apr. 1982 - 31 Jul. 1985

H. B. BLUESTEIN, R. J. DOVIK, M. D. EILTS, E. W. MCCAUL, R. RABIN, A. SUNDARA-RAJAN, and D. S. ZRNIC Washington NASA Feb. 1986 178 p refs (Contract NAS8-34749) (NAS-CR-3960; NAS 1.26:3960) Avail: NTIS HC A09/MF A01 CSDL 04B

The first experiment to combine airborne Doppler Lidar and ground-based dual Doppler Radar measurements of wind to detail the lower tropospheric flows in quiescent and stormy weather was conducted in central Oklahoma during four days in June-July 1981.

Data from these unique remote sensing instruments, coupled with data from conventional in-situ facilities, i.e., 500-m meteorological tower, rawinsonde, and surface based sensors, were analyzed to enhance understanding of wind, waves and turbulence. The purposes of the study were to: (1) compare winds mapped by ground-based dual Doppler radars, airborne Doppler lidar, and anemometers on a tower; (2) compare measured atmospheric boundary layer flow with flows predicted by theoretical models; (3) investigate the kinematic structure of air mass boundaries that precede the development of severe storms; and (4) study the kinematic structure of thunderstorm phenomena (downdrafts, gust fronts, etc.) that produce wind shear and turbulence hazardous to aircraft operations. The report consists of three parts: Part 1, Intercomparison of Wind Data from Airborne Lidar, Ground-Based Radars and Instrumented 444 m Tower; Part 2, The Structure of the Convective Atmospheric Boundary Layer as Revealed by Lidar and Doppler Radars; and Part 3, Doppler Lidar Observations in Thunderstorm Environments. Author

N86-23160*# National Aeronautics and Space Administration. Langley Research Center, Hampton, Va.
SITE SELECTION AND DIRECTIONAL MODELS OF DESERTS USED FOR ERBE VALIDATION TARGETS
 W. F. STAYLOR Apr. 1986 15 p refs
 (NASA-TP-2540; L-16041; NAS 1.60:2540) Avail: NTIS HC A02/MF A01 CSCL 04B

Broadband shortwave and longwave radiance measurements obtained from the Nimbus 7 Earth Radiation Budget scanner were used to develop reflectance and emittance models for the Sahara, Gibson, and Saudi Deserts. These deserts will serve as in-flight validation targets for the Earth Radiation Budget Experiment being flown on the Earth Radiation Budget Satellite and two National Oceanic and Atmospheric Administration polar satellites. The directional reflectance model derived for the deserts was a function of the sum and product of the cosines of the solar and viewing zenith angles, and thus reciprocity existed between these zenith angles. The emittance model was related by a power law of the cosine of the viewing zenith angle. Author

N86-23992 Deutsche Geodaetische Kommission, Munich (West Germany).
RECTIFICATION OF SCANNER IMAGES USING PREDICTION APPROACHES Ph.D. Thesis - Bonn Univ. [ENTZERRUNG VON SCANNERBILDERN MIT PRAEDIKTIONSANSAETZEN]
 A. ROSE Bayerischen Akademie der Wissenschaften 1984 85 p refs In GERMAN
 (SER-C-303; ISBN-3-7696-9353-1; ISSN-0065-5325) Avail: Issuing Activity

The rectification of airborne scanner data was investigated. The concept on which the covariance estimation is based, and the resulting prediction formulas are explained; the common ground and differences with the Ebner method are discussed. The developed method was tested on airborne scanner images. The prediction of the image rectification results from the prediction of orientation parameters; the model combines interpolation and parametric methods. A modular programming system was developed to conduct the rectification work; the programming package consists of a prediction and an image processing part. The test results satisfy expectations; a substantial increase in accuracy is obtained. The improvements depend on the number and the quality of the control points. Author (ESA)

N86-24000# Deutsche Forschungs- und Versuchsanstalt fuer Luft- und Raumfahrt, Oberpfaffenhofen (West Germany). Inst. fuer Hochfrequenztechnik.
SATELLITE-BORNE 90 GHZ RADIOMETER EXPERIMENT (SABREX), PHASE A1
 D. SALZER, H. KIETZMANN, P. SLIWINSKI, B. AUMILLER, H. BLOETSCHER, and R. SCHMID Jun. 1985 174 p refs
 (DFVLR-MITT-85-13; ISSN-0176-7739) Avail: NTIS HC A08/MF A01; DFVLR, Cologne DM 51

Flight configurations for a 90 GHz satellite radiometer on a Stretched ROHINI Satellite bus are discussed. The satellite can

be flown with its longitudinal symmetry axis in nadir direction (configuration 1) and with its longitudinal symmetry axis in direction of the velocity vector (configuration 2). Configuration 2 has a longer feeding system, lower overall noise due to lower feed system sidelobes, and better scanning possibilities. The main scientific objective of this experiment is the analysis of the capabilities of a 90 GHz satellite radiometer to determine the fluid water content of clouds, to measure low rain rates, to map the cloud cover and extended targets (diameter 1 km) and to map snow cover. Instrument design, radiometer calibration, data processing, ground support, and development schedule are considered.

Author (ESA)

N86-24003# Messerschmitt-Boelkow-Blohm G.m.b.H., Ottobrunn (West Germany). Systems Space Group.

MOMS-01 (MODULAR OPTOELECTRONIC MULTISPECTRAL SCANNER) FOR EARTH OBSERVATION: FIRST RESULTS OF STS-7 MISSION

D. MEISSNER, H. LAUCHT, J. BODECHTEL, and R. HAYDN 1985 15 p refs Presented at 1983 Joint International Geoscience and Remote Sensing Symposium (IGARSS 83) and National Radio Science-Commission F Meeting, FA-4, San Francisco, Calif., 31 Aug. - 2 Sep. 1983 Previously announced in IAA as A85-35050 Original contains color illustrations
 Avail: NTIS HC A02/MF A01

The MOMS design is outlined and results from STS-7 are described. The mission included mapping of different ground targets with low to high contrast and albedo in visible and near infrared part of the spectrum over arid areas, areas with dense and sparse natural vegetation, coastal zones, mountainous regions and open ocean islands. System verification was achieved under space conditions for a 2-channel version to demonstrate the capability for scan line extension and the ability to combine pixel-coincident modules. Author (ESA)

N86-24128*# National Aeronautics and Space Administration. Goddard Space Flight Center, Greenbelt, Md.
GLAS EXPERIMENTS ON THE IMPACT OF FGGE SATELLITE DATA ON NUMERICAL WEATHER PREDICTION
 E. KALNAY, R. ATLAS, W. E. BAKER, and J. SUSSKIND In NAS-NRC Proceedings of the First National Workshop on the Global Weather Experiment, Vol. 2, Pt. 1 p 121-145 Oct. 1985 refs

Avail: NTIS HC A17/MF A01 CSCL 04B

Simulation studies and pre-FGGE data impact studies were briefly reviewed. Impact of Goddard Laboratory for Atmospheric Science temperature soundings and cloud tracked winds was also examined. B.G.

N86-24160*# National Aeronautics and Space Administration. Goddard Space Flight Center, Greenbelt, Md.
SIMULATION STUDIES RELATED TO THE DESIGN OF POST-FGGE OBSERVING SYSTEMS Final Report
 M. HALEM, R. ATLAS, and J. SUSSKIND In NAS-NRC Proceedings of the First National Workshop on the Global Weather Experiment, Vol. 2, Pt. 2 p 727-760 Oct. 1985 refs
 Avail: NTIS HC A18/MF A01 CSCL 04B

The results of three detailed simulation studies are presented. The first study consists of a comparative assessment of the performance of an advanced moisture/temperature sounder (AMTS) being proposed by NASA as a follow-on replacement to the current HIRS-2 operational sounder aboard the NOAA weather satellites. The second study was concerned with assessing the relative accuracies of inferred atmospheric states for idealized lidar wind profiling systems, temperature profiling systems, temperature profiling systems, surface pressure systems, and composite systems. The third study incorporated the above systems into a highly realistic data analysis/forecast cycle from which a series of forecast impact studies were conducted. These studies, taken together, give us a picture of the potential that emerging technologies can offer in the determination of the basic atmospheric variables required for long-range numerical weather and climate prediction.

Author

N86-25084# Naval Postgraduate School, Monterey, Calif.
SATELLITE CLOUD AND PRECIPITATION ANALYSIS USING A MINICOMPUTER Technical Report, Oct. 1983 - Oct. 1985
 C. H. WASH, L. A. SPRAY, and L. C. CHOU Nov. 1985 94 p refs
 (AD-A163821; NPS63-85-003) Avail: NTIS HC A05/MF A01 CSCL 04B

A satellite-derived cloud and precipitation analysis program has been developed for an interactive mini-computer system. The program utilizes geostationary infrared and visual data with operational upper air and surface temperature analyses to specify cloud-type, cloud amount, cloud-top temperature, cloud-top height and estimated precipitation intensity. Five cases of GOES-East data (2 x 2 n mi visual and 2 x 4 n mi infrared) for an approximately 1600 x 1600 n mi area over the eastern United States and western North Atlantic Ocean are used in evaluating the model's performance. Each satellite-derived, cloud and precipitation analysis is evaluated subjectively, using conventional synoptic data, radar measurements and manual nephanalysis for verification, and objectively, using surface synoptic observations for verification. Successful estimates of cloud amount for overcast and clear skies were obtained; however, broken and scattered conditions were underestimated. The majority of stratiform cloud types and multi-layered clouds were analyzed correctly by the model. Classification errors occurred with cumuliform clouds and thin cirrus. Reasonable precipitation intensity and cloud-top temperature/height analyses were produced by the NPS model.

GRA

N86-25925# Lawrence Livermore National Lab., Calif.
STUDIES OF COMPLEX TERRAIN WIND FLOWS USING ACOUSTIC SOUNDER AND OPTICAL CROSS-WIND REMOTE SENSORS
 W. M. PORCH, W. NEFF, and C. KING Aug. 1985 26 p refs
 (Contract W-7405-ENG-48)
 (DE86-002993; UCID-20519; ASCOT-85-2) Avail: NTIS HC A03/MF A01

Remote sensing instrumentation has played an important role in the Atmospheric Studies in Complex Terrain (ASCOT) field experimental program. The goal of this program is to better understand transport and diffusion processes in complex terrain with an emphasis focused on nighttime drainage wind conditions. Two aspects of the instrumentation are discussed: acoustic sounders (doppler and monostatic) and space averaging optical crosswind sensors. Data from these two sources are discussed and compared with data from conventional tower and tethered sonde instrumentation.

DOE

N86-27705*# Arizona Univ., Tucson. Optical Sciences Center.
SPECTRORADIOMETRIC CONSIDERATIONS FOR ADVANCED LAND OBSERVING SYSTEMS Final Report
 P. N. SLATER Jul. 1986 101 p
 (Contract NAG5-196)
 (NASA-CR-177205; NAS 1.26:177205) Avail: NTIS HC A06/MF A01 CSCL 08B

Research aimed at improving the inflight absolute radiometric calibration of advanced land observing systems was initiated. Emphasis was on the satellite sensor calibration program at White Sands. Topics addressed include: absolute radiometric calibration of advanced remote sensing; atmospheric effects on reflected radiation; inflight radiometric calibration; field radiometric methods for reflectance and atmospheric measurement; and calibration of field reflectance radiometers.

B.G.

GENERAL

Includes economic analysis.

A86-34111#
A MULTI-NATIONAL CONSORTIUM OPPORTUNITY FOR REMOTE SENSING

P. M. MAUGHAN (Space Development Services, Washington, DC) IN: U.S. Opportunities in Space Conference; Proceedings of the Second Annual Space Business Conference, Washington, DC, October 30-November 1, 1985. London, Space Consultants International, Ltd., 1985, 10 p.

The development of a multinational consortium for remote sensing is proposed. Problems that could result, such as data censorship, as multiple sensing systems compete for commercial success are examined. The advantages a consortium would provide to remote sensing data users are discussed. The consortium is to be composed of public or private space-related organizations and to construct, launch, and operate satellite systems. The control each member country would have over the operation of the consortium and the access to data is described. I.F.

A86-34118#
'NEW OPPORTUNITIES IN REMOTE SENSING'

L. P. MITCHELL (Eastman Kodak Co., Rochester, NY) IN: U.S. Opportunities in Space Conference; Proceedings of the Second Annual Space Business Conference, Washington, DC, October 30-November 1, 1985. London, Space Consultants International, Ltd., 1985, 11 p.

Technical and business activities in remote sensing are described. The need for improvements in satellite sensors and computer hardware necessary for the acquisition of higher spatial and spectral resolution data, the storage of more information, and faster retrieval of the data is examined. The development of software, algorithms, and techniques which will improve the processing and enhance the data is studied. The teaching and training of customers on the applications of the remote sensing data and the proper marketing of the information are discussed. I.F.

A86-37002
THE EVOLUTION OF REMOTE SENSING SCIENCE AND APPLICATIONS

J. H. MCELROY (NOAA, National Environmental Satellite, Data, and Information Service, Washington, DC) IN: Machine processing of remotely sensed data - Quantifying global process: Models, sensor systems, and analytical methods; Proceedings of the Eleventh International Symposium, West Lafayette, IN, June 25-27, 1985. New York, Institute of Electrical and Electronics Engineers, 1985, p. 4-11. refs

The development of space observation systems and their applications are examined. The satellite systems that provide meteorological, oceanographic, land-science, and atmospheric data are described. The use of NASA's Polar Platform for observational missions is proposed. The need for data systems which process and distribute data quickly and accurately is discussed. I.F.

N86-25076# National Academy of Sciences - National Research Council, Washington, D. C.
EARTH SCIENCE INVESTIGATIONS IN THE UNITED STATES ANTARCTIC RESEARCH PROGRAM (USARP) FOR THE PERIOD JULY 1, 1984 - JUNE 30, 1985

1985 87 p Sponsored in part by the National Science Foundation, Washington, D.C.

(Contract NSF DPP-82-07098)
 (PB86-143773) Avail: NTIS HC A05/MF A01 CSCL 08G

A listing of earth science research activities was conducted as part of the U.S. Antarctic Research Program for the year July 1, 1984, through June 30, 1985. Publications resulting from the research are also listed. Information was obtained by a survey of

participants in the U.S. Antarctic Program, with respondents providing the data on their work in camera-ready format. GRA

N86-26355*# National Aeronautics and Space Administration, Washington, D.C.

ENVIROSAT-2000 REPORT: FEDERAL AGENCY SATELLITE REQUIREMENTS

D. COTTER, ed., I. WOLZER, ed., N. BLAKE, J. JARMAN, D. LICHY, T. PANGBURN, R. MCARDLE, C. PAUL, L. SHAFFER, G. THORLEY et al. NOAA Jul. 1985 156 p refs (NASA-TM-88752; NAS 1.15:88752) Avail: NTIS HC A08/MF A01 CSCL 22B

The requirement of Federal agencies, other than NOAA, for the data and services of civil operational environmental satellites (both polar orbiting and geostationary) are summarized. Agency plans for taking advantage of proposed future Earth sensing space systems, domestic and foreign, are cited also. Current data uses and future requirements are addressed as identified by each agency. B.G.

N86-27410# National Oceanic and Atmospheric Administration, Washington, D. C. Natl. Environ. Satellite Data and Inform. Service.

FEDERAL AGENCY SATELLITE REQUIREMENTS Final Report

D. COTTER and I. WOLZER Jul. 1985 160 p (AD-A165071) Avail: NTIS HC A08/MF A01 CSCL 04B

This report summarizes the requirements of Federal agencies for the data and services of NOAA's civil operational environmental satellites--both polar-orbiting and geostationary. The Federal agencies contributing to this document have described their current and planned use of the data and services provided by NOAA's environmental satellite and Landsat systems, as well as those provided by the systems of others. Agency plans for taking advantage of proposed future Earth-sensing space systems, domestic and foreign, are cited also. The report emphasizes requirements for direct and indirect support from NOAA's environmental satellite systems. In the direct case, the agencies process, interpret, or use NOAA's satellite data, products, or services as inputs to in-house activities. In the indirect case, NOAA provides the agencies with support products, such as weather forecasts, that depend on satellite operations to various degrees. This report focuses on the direct requirements served by the National Environmental Satellite Data, and Information Service (NESDIS). Described here are the satellite needs of the Department of Agriculture, the Army Corps of Engineers, the Department of Transportation (which includes the Federal Aviation Administration and the Coast Guard), the Agency for International Development, the Department of Defense, the Department of the Interior, and the National Aeronautics and Space Administration. Current data uses and future requirements are addressed. GRA

N86-27411# National Oceanic and Atmospheric Administration, Washington, D. C. Natl. Environ. Satellite Data and Inform. Service.

GOES (GEOSTATIONARY OPERATIONAL ENVIRONMENTAL SATELLITE)-NEXT OVERVIEW Final Report

A. SCHWALB, D. COTTER, and J. HUSSEY Sep. 1985 76 p (AD-A165080) Avail: NTIS HC A05/MF A01 CSCL 22B

This report describes, in summary form, the current National Oceanic and Atmospheric Administration (NOAA) Geostationary Operational Environmental Satellite (GOES) system and the scientific rationale used to develop specifications for the next generation of satellites of this series. The payload instruments of the current satellites are reviewed in conjunction with the products prepared from their data outputs. The rationale used by the National Weather Service (NWS) in developing top-level requirements for GOES-Next stresses the projected use of data within the restructured NWS organization expected in the 1990's. NOAA-certified requirements used by the National Aeronautics and Space Administration (NASA) to develop the Request for Proposal, issued to industry in June 1984, are also provided. Finally, a brief description of the satellite system that will be built for launch in the 1990's is provided. This final section has been abstracted

from the winning proposal submitted by Ford Aerospace and Communications Corporation and is a glimpse at what the future has in store for GOES. Author (GRA)

N86-27412# National Oceanic and Atmospheric Administration, Washington, D. C. Natl. Environ. Satellite Data and Inform. Service.

OPERATIONAL SATELLITE SUPPORT TO SCIENTIFIC PROGRAMS Final Report

H. W. YATES, D. J. COTTER, and G. OHRING Mar. 1985 57 p (AD-A165081) Avail: NTIS HC A04/MF A01 CSCL 22B

The role of operational environmental satellites in science programs undertaken to study the Earth system is examined. It centers on the satellite systems operated by the National Oceanic and Atmospheric Administration (NOAA). Other satellite systems are referenced as appropriate. NOAA's operational satellites are serving the research community extensively. Research programs such as climate studies, ocean dynamics investigations, and global vegetation surveys benefit from the special characteristics of operational satellites. Among these characteristics are routine global coverage in many spectral intervals; reliability, resulting from a commitment to continue the service; speed in data access because of real-time applications; repeatability of measurements because of matched, calibrated instruments; and data handling methods that provide output products in conventional, usable formats and with traceable histories. Author (GRA)

N86-27413# National Oceanic and Atmospheric Administration, Washington, D. C.

COMPARISON OF THE DEFENSE METEOROLOGICAL SATELLITE PROGRAM (DMSP) AND THE NOAA POLAR-ORBITING OPERATIONAL ENVIRONMENTAL SATELLITE (POES) PROGRAM

D. COTTER, A. RAMSEY, E. HEACOCK, J. BAILEY, and Q. WILKES Oct. 1985 416 p (AD-A165118) Avail: NTIS HC A18/MF A01 CSCL 22B

This report offers technical comparison of the two United States operational space programs that are based on the capabilities of polar-orbiting environmental satellites. The U.S. Air Force manages and conducts the operations of the Defense Meteorological Satellite Program (DMSP); the National Oceanic and Atmospheric Administration has the same responsibilities with respect to the NOAA Polar-orbiting Operational Environmental Satellite (POES) program. The report examines the major missions and goals of the two programs, the management and operational procedures that they follow, and the support they extend to each other and to other Federal agencies. Detailed discussions are provided about the specifications and performance characteristics of the spacecraft, sensors, onboard systems, command and control systems, and communications systems employed by the two programs. An extensive relative analysis of the operation and uses of the DMSP and POES imaging and atmospheric sounding instruments is provided. Other sensors and systems are discussed, as is the joint agreement between DOD and NOAA for sharing their satellite data and data processing load. Nonmeteorological users of DMSP and POES data are described. The organization and content of the satellite data archive are presented. Near-future system improvements and longer-term mission requirements are also discussed. Author (GRA)

N86-28007# National Oceanic and Atmospheric Administration, Washington, D. C.

OPTIMUM MANAGEMENT STRATEGIES FOR THE NOAA (NATIONAL OCEANIC AND ATMOSPHERIC ADMINISTRATION) POLAR-ORBITING OPERATIONAL ENVIRONMENTAL SATELLITES, 1985-2000. VOLUME 1 Final Report

W. H. ESKITE and W. P. BISHOP Apr. 1985 70 p (AD-A165143) Avail: NTIS HC A04/MF A01 CSCL 05A

The experience of the past 15 years was used as a basis to establish the best management principles to apply to the POES for the next 15 years. This was done for both a two-satellite configuration and a one-satellite configuration. The principles

09 GENERAL

include always having a spare available, a 4-month call-up capability, taking advantage of satellites that live longer than their design life, and taking advantage of early indications of imminent failure. These principles must be applied in different ways to the two configurations. Applying these principles to several scenarios for the future leads to the conclusion that we should plan for 12 satellites for the next 15 years for either the one-satellite or the two-satellite system. Author (GRA)

N86-28016# National Oceanic and Atmospheric Administration, Washington, D. C.

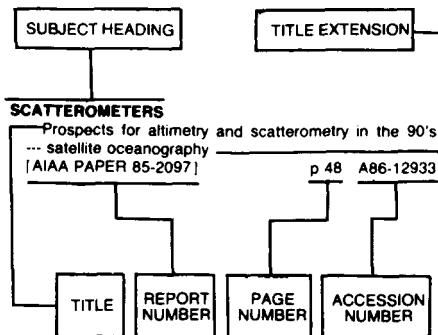
INTERNATIONAL COORDINATION OF AND CONTRIBUTIONS TO ENVIRONMENTAL SATELLITE PROGRAMS Final Report

P. UHLIR and L. SHAFFER Jun. 1985 65 p

(AD-A165142) Avail: NTIS HC A04/MF A01 CSCL 22B

The paper begins with an overview of U.S. policy on remote sensing. Next, the extensive international cooperation in U.S. Polar-orbiting Operational Environmental Satellites (POES) is described. This includes participation in the POES direct readout services program, and existing instrument contributions and commitments to the POES system. The opportunities and mechanisms for future contributions to POES, or to the polar platform component of the U.S. Space Station, are also examined. Geostationary environmental satellites are operated by the United States, the European Space Agency, Japan, and India. These systems are described, and the Coordination on Geostationary Meteorological Satellites is discussed. Other international organizations used for cooperation and coordination in remote-sensing activities are outlined. These include the World Meteorological Organization, the Intergovernmental Oceanographic Commission, the International Council of Scientific Unions, and the Committee on Earth Observations Satellites. Contributions by the United States to planned foreign remote-sensing programs are addressed as well. Finally, the report identifies and discusses three trends in remote sensing, and makes some concluding observations about the future of international remote-sensing activities. Appendix A lists the dates of all relevant documents, such as Memoranda of Understanding, Terms of Reference for international committees, and Minutes of Meetings. GRA

Typical Subject Index Listing



The subject heading is a key to the subject content of the document. The title is used to provide a description of the subject matter. When the title is insufficiently descriptive of the document content, the title extension is added, separated from the title by three hyphens. The (NASA or AIAA) accession number and the page number are included in each entry to assist the user in locating the abstract in the abstract section. If applicable, a report number is also included as an aid in identifying the document. Under any one subject heading, the accession numbers are arranged in sequence with the AIAA accession numbers appearing first.

A

ACCURACY

- Site selection and directional models of deserts used for ERBE validation targets
[NASA-TP-2540] p 57 N86-23160
- Navstar GPS (Global Positioning System) accuracy while surveying arrays of deep ocean transponders
[AD-A163364] p 38 N86-26313

ACID RAIN

- Field and airborne spectral characterization of suspected damage in red spruce (*pinea rubens*) from Vermont
p 11 A86-37008

ACOUSTIC PROPERTIES

- Navstar GPS (Global Positioning System) accuracy while surveying arrays of deep ocean transponders
[AD-A163364] p 38 N86-26313
- A study of sea ice kinematics and their relationship to arctic ambient noise. Part 3, Section 1: Ambient noise. Section 2: Ambient noise
[AD-A165304] p 39 N86-26788
- A study of sea ice kinematics and their relationship to arctic ambient noise. Part 3, section 3: Ambient noise
[AD-A165305] p 40 N86-26789

ACOUSTIC VELOCITY

- Marginal ice zone experiment - 1984, physical oceanography report: USNS Lynch and helicopter-based STD data
[AD-A163096] p 37 N86-24180
- Physical oceanography report: Camp-based and helicopter-based STD data from the drifting ice station FRAM 3
[AD-A163097] p 37 N86-24181

ACOUSTICS

- Proceedings of the Arctic Oceanography Conference and Workshop held at the Naval Ocean Research and Development Activity, NSTL, MS. on June 11-14, 1985
[AD-A162578] p 34 N86-23203

Studies of complex terrain wind flows using acoustic sounder and optical cross-wind remote sensors
[DE86-002993] p 58 N86-25925

AERIAL PHOTOGRAPHY

- Assessing impacts of off-nadir observation on remote sensing of vegetation - Use of the Suits model
p 1 A86-30193
- Image segmentation algorithms p 45 A86-32370
- Determination of sea spectral reflectance from airborne measurements p 26 A86-32683
- One step above ground truth - Airphoto keys for large-scale vegetation analysis p 3 A86-33538
- The applicability of LOWTRAN 5 computer code to aerial thermographic data correction p 48 A86-34739
- Practical photogrammetry from 35-mm aerial photography p 55 A86-36080
- Methods of combined air and space remote-sensing studies of Siberia p 22 A86-36501
- Combined structural and geomorphological methods for the processing of aerial and space photographic remote-sensing data with the aim of solving geological problems p 22 A86-36503
- Statistical approach to the classification of objects on air and space remote-sensing images p 48 A86-36515

Small format, oblique, colour aerial photography - An aid to the location of methane seepage
p 11 A86-36783

- Estimation of atmospheric corrections from multiple aircraft imagery p 49 A86-36784
- Assessment and trends of Florida's marine fisheries habitat An integration of aerial photography and Thematic Mapper imagery p 34 A86-37013
- Wavelength intensity indices in relation to tree condition and leaf-nutrient content p 12 A86-37036
- Application of spaceborne and airborne techniques in mineral exploration at Wadi El Allaqi area, Eastern Desert, Egypt p 23 A86-37865
- Predicting tree groundline diameter from crown measurements made on 35-mm aerial photography p 13 A86-39006

Ocean wave slope statistics from automated analysis of sun glitter photographs
[AD-A161995] p 37 N86-24172

- Wheat area estimation using digital LANDSAT MSS data and aerial photographs
[INPE-3824-PRE/900] p 15 N86-26667
- High frequency sampling of the 1984 spring bloom within the mid-Atlantic Bight: Synoptic shipboard, aircraft, and in situ perspectives of the SEEP-I experiment
[NASA-TM-88765] p 41 N86-27700

AERIAL RECONNAISSANCE

- A review of methods to track oil in arctic waters
[AD-A164679] p 39 N86-26716

AEROMAGNETISM

- Direction dependent interpolation of aeromagnetic data p 23 A86-37009

AEROSOLS

- Investigation of the content of trace elements in sea aerosols and the surface microlayer off sea water p 32 A86-34754
- Transport processes as manifested in satellite and lidar aerosol measurements p 17 N86-27788

AEROSPACE SYSTEMS

- Agricultural and scientific space platforms --- Russian book p 1 A86-29843

AGREEMENTS

- Comparison of the Defense Meteorological Satellite Program (DMSP) and the NOAA Polar-orbiting Operational Environmental Satellite (POES) program
[AD-A165118] p 59 N86-27413

AGRICULTURE

- Agricultural and scientific space platforms --- Russian book p 1 A86-29843
- Use of multitemporal spectral profiles in agricultural land-cover classification p 10 A86-36084
- Agricultural applications for thermal infrared multispectral scanner data p 12 A86-37034
- Federal agency satellite requirements
[AD-A165071] p 59 N86-27410

AGRISTARS PROJECT

- Overview of the AgRISTARS research program. I --- Agriculture and Resources Inventory Surveys Through Aerospace Remote Sensing p 2 A86-33503
- Passive microwave soil moisture research p 2 A86-33504
- Remote sensing techniques for the detection of soil erosion and the identification of soil conservation practices p 3 A86-33506
- Overview and highlights of Early Warning and Crop Condition Assessment project p 5 A86-33576
- Development of agrometeorological crop model inputs from remotely sensed information p 6 A86-33579

AGROMETEOROLOGY

- Development of agrometeorological crop model inputs from remotely sensed information p 6 A86-33579
- Spectral components analysis - A bridge between spectral observations and agrometeorological crop models p 7 A86-33627

AIR SEA ICE INTERACTIONS

- Reduction of weather effects in the calculation of sea ice concentration from microwave radiances p 26 A86-33104

AIR WATER INTERACTIONS

- Lidar observations of the planetary boundary layer p 29 A86-33532
- Comparison of Circulation estimates and winds based on shipboard and satellite-tracked buoy data in Bransfield Strait, 9-14 March, 1985, part 3
[INPE-3795-PRE/890] p 36 N86-24168
- Contributions to the oceanography of the western Alboran Sea
[AD-A162019] p 37 N86-24173
- Sea ice dynamics and regional meteorology for the Arctic polynya experiment (APEX)-Bering Sea 1985
[PB86-148038] p 38 N86-25939
- An investigation of the marine boundary layer during cold air outbreak
[NASA-CR-177287] p 39 N86-26758
- A model for the estimation of the surface fluxes of momentum, heat, and moisture of the cloud-topped marine atmospheric boundary layer from satellite measurable parameters
[NASA-CR-177290] p 41 N86-27853

AIRBORNE EQUIPMENT

- Measurement of sea ice backscatter characteristics at 36 GHz using the surface contour radar p 29 A86-33562
- An airborne multiple-beam 1.4 GHz pushbroom microwave radiometer p 6 A86-33583
- Microwave backscatter and emission observed from Shuttle Imaging Radar B and an airborne 1.4 GHz radiometer p 53 A86-33584
- Electronically Steered Thinned Array Radiometer (ESTAR) system design, calibration, and sensitivity p 53 A86-33588
- High resolution millimeter-wave imaging sensor p 54 A86-33590
- Spectral measurements in support of SIR-B using the Surface Contour Radar --- for South Pacific p 30 A86-33609
- The emergence of airborne video techniques as an alternative for accessing tropical environments - A historical perspective p 56 A86-37007
- Semi-operational identification of agricultural crops from airborne SLAR-data p 12 A86-37025
- Applications of sensor payloads p 56 A86-37343
- Analysis of airborne Doppler lidar, Doppler radar and tall tower measurements of atmospheric flows in quiescent and stormy weather
[NASA-CR-3960] p 56 N86-23159
- Rectification of scanner images using prediction approaches --- airborne scanners
[SER-C-303] p 57 N86-23992
- Archimedes project remote sensing of oil spills North Sea experiment, October 1983. Report on DFVLR (Side-Looking Airborne Radar (SLAR) contribution
[DFVLR-FB-85-54] p 35 N86-24002

AIRBORNE SURVEILLANCE RADAR

- The design, construction and early trials of a novel airborne surveillance radar p 25 A86-32635

SUBJECT

ALASKA

- Influence of the Yukon River on the Bering Sea
[NASA-CR-177310] p 39 N86-26783

ALGAE

- A simulation analysis of the fate of phytoplankton within the mid-Atlantic bight
[NASA-CR-177265] p 39 N86-26670
Satellite detection of phytoplankton export from the mid-Atlantic Bight during the 1979 spring bloom
[NASA-TM-88782] p 41 N86-27699
High frequency sampling of the 1984 spring bloom within the mid-Atlantic Bight: Synoptic shipboard, aircraft, and in situ perspectives of the SEEP-I experiment
[NASA-TM-88765] p 41 N86-27700

ALGORITHMS

- Image segmentation algorithms p 45 A86-32370

ALTIMETERS

- Sea level time series in the equatorial Pacific from satellite altimetry p 34 A86-38648
The study of gravity field estimation procedures
[AD-A164564] p 19 N86-26745

AMBIENCE

- A study of sea ice kinematics and their relationship to arctic ambient noise. Part 3, Section 1: Ambient noise. Section 2: Ambient noise
[AD-A165304] p 39 N86-26788
A study of sea ice kinematics and their relationship to arctic ambient noise. Part 3, section 3: Ambient noise
[AD-A165305] p 40 N86-26789

AMPLITUDES

- Objective analysis of tidal fields in the Atlantic and Indian Oceans
[NASA-TM-87773] p 39 N86-26782

ANDES MOUNTAINS (SOUTH AMERICA)

- Thematic mapper studies of Andean volcanoes
[NASA-CR-176807] p 24 N86-25866

ANNUAL VARIATIONS

- Intraseasonal variations of OLR in the tropics during the FGGE year --- outgoing long wave radiation
p 48 A86-36227
Relationships between surface observations over the global oceans and the southern oscillation
[PB86-110038] p 35 N86-24112
Monthly maps of sea level anomalies in the Pacific, 1975-1981. Report on the IGOSS (Integrated Global Ocean Services System) Sea Level Pilot Project
[AD-A163061] p 38 N86-25104
A study of sea ice kinematics and their relationship to arctic ambient noise. Part 3, Section 1: Ambient noise. Section 2: Ambient noise
[AD-A165304] p 39 N86-26788

ANOMALIES

- Relationships between surface observations over the global oceans and the southern oscillation
[PB86-110038] p 35 N86-24112
Monthly maps of sea level anomalies in the Pacific, 1975-1981. Report on the IGOSS (Integrated Global Ocean Services System) Sea Level Pilot Project
[AD-A163061] p 38 N86-25104

ANTARCTIC REGIONS

- Observations of the polar regions from satellites using active and passive microwave techniques
p 28 A86-33489
USSR report: Earth sciences
[JPRS-UES-86-004] p 34 N86-23017
Ice shelves of Antarctica
[PB86-106986] p 35 N86-23208
Problems of the Arctic and the Antarctic, Collection of Articles, Volume 56, 1981
[PB86-107109] p 35 N86-23209
Development of a satellite-tracked oceanographic drifting buoy for the Brazilian Antarctic Program, part 1
[INPE-3793-PRE/888] p 36 N86-24166
Comparison of Circulation estimates and winds based on shipboard and satellite-tracked buoy data in Bransfield Strait, 9-14 March, 1985, part 3
[INPE-3795-PRE/890] p 36 N86-24168
Problems of the Arctic and the Antarctic, collection of articles, vol. 57, 1981
[PB86-106994] p 37 N86-24182
Earth science investigations in the United States Antarctic Research Program (USARP) for the period July 1, 1984 - June 30, 1985
[PB86-143773] p 58 N86-25076

APPALACHIAN MOUNTAINS (NORTH AMERICA)

- Topographic lineament domains of the Appalachians - Some new methods and techniques for paleostress analysis
p 20 A86-33518

AQUIFERS

- Stable-isotope studies of groundwaters in southeastern New Mexico
[DE86-002590] p 43 N86-23027

ARCHITECTURE (COMPUTERS)

- Image processing system interfaces
p 44 A86-32333

ARCTIC OCEAN

- Proceedings of the Arctic Oceanography Conference and Workshop held at the Naval Ocean Research and Development Activity, NSTL, MS. on June 11-14, 1985
[AD-A162578] p 34 N86-23203
Marginal ice zone experiment - 1984, physical oceanography report: USNS Lynch and helicopter-based STD data
[AD-A163096] p 37 N86-24180
Physical oceanography report: Camp-based and helicopter-based STD data from the drifting ice station FRAM 3
[AD-A163097] p 37 N86-24181
Problems of the Arctic and the Antarctic, collection of articles, vol. 57, 1981
[PB86-106994] p 37 N86-24182
A review of methods to track oil in arctic waters
[AD-A164679] p 39 N86-26716

ARCTIC REGIONS

- Photogrammetry and remote sensing in periglacial geomorphology p 20 A86-33517
Proceedings of the Arctic Oceanography Conference and Workshop held at the Naval Ocean Research and Development Activity, NSTL, MS. on June 11-14, 1985
[AD-A162578] p 34 N86-23203
Problems of the Arctic and the Antarctic, Collection of Articles, Volume 56, 1981
[PB86-107109] p 35 N86-23209
Problems of the Arctic and the Antarctic, collection of articles, vol. 57, 1981
[PB86-106994] p 37 N86-24182
Sea ice dynamics and regional meteorology for the Arctic polynya experiment (APEX)-Bering Sea 1985
[PB86-148038] p 38 N86-25939
A study of sea ice kinematics and their relationship to arctic ambient noise. Part 3, Section 1: Ambient noise. Section 2: Ambient noise
[AD-A165304] p 39 N86-26788
A study of sea ice kinematics and their relationship to arctic ambient noise. Part 3, section 3: Ambient noise
[AD-A165305] p 40 N86-26789

ARID LANDS

- Reflectance modelling and the derivation of vegetation indices for an Australian semi-arid shrubland
p 7 A86-34740
Remote monitoring of processes that shape desert surfaces: The Desert Winds Project
[TI86-900108] p 24 N86-25099

ARRAYS

- Navstar GPS (Global Positioning System) accuracy while surveying arrays of deep ocean transponders
[AD-A163364] p 38 N86-26313

ARTIFICIAL INTELLIGENCE

- Approaches to computer reasoning in remote sensing and geographic information processing - A survey
p 16 A86-33595

ARTIFICIAL SATELLITES

- Operational satellite support to scientific programs
[AD-A165081] p 59 N86-27412

ASIA

- Asian Conference on Remote Sensing, 5th, Kathmandu, Nepal, November 15-18, 1984, Proceedings
p 55 A86-35425

ATLANTIC OCEAN

- Some features of small-scale ocean eddies according to an analysis of satellite images p 25 A86-32677
Heat budget and climatic atlas of the equatorial Atlantic Ocean during FGGE (First GARP Global Experiment, 1979)
[PB86-111622] p 35 N86-23213
A simulation analysis of the fate of phytoplankton within the mid-Atlantic bight
[NASA-CR-177265] p 39 N86-26670
High frequency sampling of the 1984 spring bloom within the mid-Atlantic Bight: Synoptic shipboard, aircraft, and in situ perspectives of the SEEP-I experiment
[NASA-TM-88765] p 41 N86-27700

ATMOSPHERIC ATTENUATION

- The effect of the atmosphere on the satellite remote sensing of earth resources --- Russian book
p 56 A86-39969

ATMOSPHERIC BOUNDARY LAYER

- Analysis of airborne Doppler lidar, Doppler radar and tall tower measurements of atmospheric flows in quiescent and stormy weather
[NASA-CR-3960] p 56 N86-23159
An investigation of the marine boundary layer during cold air outbreak
[NASA-CR-177287] p 39 N86-26758
A model for the estimation of the surface fluxes of momentum, heat and moisture of the cloud topped marine atmospheric boundary layer from satellite measurable parameters
[NASA-CR-177283] p 41 N86-27837

- A model for the estimation of the surface fluxes of momentum, heat, and moisture of the cloud-topped marine atmospheric boundary layer from satellite measurable parameters
[NASA-CR-177290] p 41 N86-27853

ATMOSPHERIC CIRCULATION

- Estimation of monthly rainfall from satellite-observed cloud amount in the tropical western Pacific
p 43 A86-36234
Proceedings of the First National Workshop on the Global Weather Experiment: Current Achievements and Future Directions, volume 2, part 2
[NASA-CR-176722] p 36 N86-24142

ATMOSPHERIC COMPOSITION

- SAGE observations of stratospheric nitrogen dioxide
p 55 A86-36838
Satellite-derived moisture profiles
[NOAA-NESDIS-24] p 44 N86-27703

ATMOSPHERIC CORRECTION

- Reduction of weather effects in the calculation of sea ice concentration from microwave radiances
p 26 A86-33104
Applicability of atmospheric correction algorithm for CZCS data to Japanese coastal area --- Coastal Zone Color Scanner
p 31 A86-33632
The estimation of atmospheric effects for SPOT using AVHRR channel-1 data
p 47 A86-34738
Estimation of atmospheric corrections from multiple aircraft imagery
p 49 A86-36784

ATMOSPHERIC DIFFUSION

- Transport processes as manifested in satellite and lidar aerosol measurements
p 17 N86-27788

ATMOSPHERIC EFFECTS

- Reduction of weather effects in the calculation of sea ice concentration from microwave radiances
p 26 A86-33104
Direct reflectance response in AVHRR red and near-IR bands for three cover types and varying atmospheric conditions
p 13 A86-39146
The effect of the atmosphere on the satellite remote sensing of earth resources --- Russian book
p 56 A86-39969
Spectroradiometric considerations for advanced land observing systems
[NASA-CR-177205] p 58 N86-27705

ATMOSPHERIC HEAT BUDGET

- Heat budget and climatic atlas of the equatorial Atlantic Ocean during FGGE (First GARP Global Experiment, 1979)
[PB86-111622] p 35 N86-23213

ATMOSPHERIC MODELS

- Evapotranspiration over an agricultural region using a surface flux/temperature model based on NOAA-AVHRR data
p 10 A86-36237
Probabilistic modeling of fields of atmospheric turbulence and sea roughness with reference to the study of complex systems --- for flight control
p 33 A86-36480

- Proceedings of the First National Workshop on the Global Weather Experiment: Current Achievements and Future Directions, volume 1
[NASA-CR-176720] p 36 N86-24120

- An investigation of the marine boundary layer during cold air outbreak
[NASA-CR-177249] p 41 N86-27838

- A model for the estimation of the surface fluxes of momentum, heat, and moisture of the cloud-topped marine atmospheric boundary layer from satellite measurable parameters
[NASA-CR-177290] p 41 N86-27853

ATMOSPHERIC MOISTURE

- Remote sensing of vertical moisture profiles and cloud properties from simulated millimeter wave sounder and microwave imager data
p 53 A86-33547

ATMOSPHERIC OPTICS

- Satellite remote sensing of atmospheric optical depth spectrum
p 55 A86-36785

ATMOSPHERIC PHYSICS

- USSR report: Earth sciences
[JPRS-UES-86-004] p 34 N86-23017

ATMOSPHERIC PRESSURE

- Remote sensing of atmospheric pressure and sea state using laser altimeters
p 28 A86-33529

ATMOSPHERIC RADIATION

- Meteorological Satellite Center Technical Note, no. 13, 1986
[ISSN-0388-9653] p 40 N86-27694
On land-sea contrast in the Earth radiation budget
p 40 N86-27695

ATMOSPHERIC SCATTERING

- Estimation of atmospheric corrections from multiple aircraft imagery
p 49 A86-36784

ATMOSPHERIC SOUNDING

- Satellite-borne 90 GHz radiometer experiment (SABREX), phase A1
[DFVLR-MITT-85-13] p 57 N86-24000

ATMOSPHERIC TEMPERATURE

An algorithm for the identification of cloud cover and the estimation of spectral brightnesses of the cloudless atmosphere according to satellite scanning measurements of outgoing IR radiation p 52 A86-33317
 Experiments on the remote temperature sounding of the atmosphere on the basis of NOAA-satellite radiometer measurements p 52 A86-33318

ATMOSPHERIC TURBULENCE

Probabilistic modeling of fields of atmospheric turbulence and sea roughness with reference to the study of complex systems --- for flight control p 33 A86-36480

AUSTRALIA

Relationships between surface observations over the global oceans and the southern oscillation [PB86-110038] p 35 N86-24112

AUTOMATIC CONTROL

An atlas of original and mercator-transformed satellite-data images of the Alboran Sea, August-October 1983 [AD-A161898] p 36 N86-24170

AUTOMATION

Automatic cloud classification p 46 A86-33534

B

BACKSCATTERING

Lithologic signatures in multi-channel SAR imagery p 45 A86-33522
 Modelling of backscatter from vegetation layers p 4 A86-33554
 Backscatter measurements from simulated resonant structures p 4 A86-33555
 Measurement of sea ice backscatter characteristics at 36 GHz using the surface contour radar p 29 A86-33562

Microwave backscatter and emission observed from Shuttle Imaging Radar B and an airborne 1.4 GHz radiometer p 53 A86-33584
 Millimeter-wave backscatter from snowcover p 42 A86-33615

Wind dependence of L-band radar backscatter p 33 A86-35860
 Scattering from a random layer embedded with dielectric needles --- for applications to coniferous vegetation p 10 A86-36045

Regression models for vegetation radar-backscattering and radiometric emission p 10 A86-36046
 Identification of major backscattering sources in trees and shrubs at 10 GHz p 13 A86-39149

Studies related to ocean dynamics. Task 3.2: Aircraft Field Test Program to investigate the ability of remote sensing methods to measure current/wind-wave interactions [NASA-CR-168349] p 38 N86-25100

BANDWIDTH

EOS radiometer concepts for soil moisture remote sensing [NASA-CR-177854] p 14 N86-23995

BATHY THERMOGRAPHS

Hydrographic data from the OPTOMA program, OPTOMA17: OPTOMA17 P, 21 July 1985, OPTOMA17 leg DI, 10-22 August 1985, OPTOMA17 leg DII, 23 August - 5 September 1985 [AD-A162067] p 37 N86-24176

BAYS (TOPOGRAPHIC FEATURES)

Satellite detection of phytoplankton export from the mid-Atlantic Bight during the 1979 spring bloom [NASA-TM-88782] p 41 N86-27699
 High frequency sampling of the 1984 spring bloom within the mid-Atlantic Bight: Synoptic shipboard, aircraft, and in situ perspectives of the SEEP-I experiment [NASA-TM-88765] p 41 N86-27700

BEAUFORT SEA (NORTH AMERICA)

Proceedings of the Arctic Oceanography Conference and Workshop held at the Naval Ocean Research and Development Activity, NSTL, MS. on June 11-14, 1985 [AD-A162578] p 34 N86-23203

A study of sea ice kinematics and their relationship to arctic ambient noise. Part 3, Section 1: Ambient noise. Section 2: Ambient noise [AD-A165304] p 39 N86-26788

A study of sea ice kinematics and their relationship to arctic ambient noise. Part 3, section 3: Ambient noise [AD-A165305] p 40 N86-26789

BERING SEA

Aircraft and satellite passive microwave observations of the Bering Sea ice cover during MIZEX West p 32 A86-35683

Proceedings of the Arctic Oceanography Conference and Workshop held at the Naval Ocean Research and Development Activity, NSTL, MS. on June 11-14, 1985 [AD-A162578] p 34 N86-23203

Influence of the Yukon River on the Bering Sea [NASA-CR-177310] p 39 N86-26783

BIAS

Navstar GPS (Global Positioning System) accuracy while surveying arrays of deep ocean transponders [AD-A163364] p 38 N86-26313

BIBLIOGRAPHIES

Ice shelves of Antarctica [PB86-106986] p 35 N86-23208
 Earth science investigations in the United States Antarctic Research Program (USARP) for the period July 1, 1984 - June 30, 1985 [PB86-143773] p 58 N86-25076

BIOGEOCHEMISTRY

Modeling the controls of forest productivity using canopy variables p 11 A86-37016

BIOMASS

The influence of observational interdependence on spectral reflectance relationships with plant and soil variables p 2 A86-30196
 Estimation of the weight of vegetation using microwave transmission measurements p 3 A86-33524
 Detection of biomass by an empiric albedo and spectral reflectance model in the Sahara Desert from Landsat imagery p 11 A86-37015
 Separation of soil-plant spectral mixtures by factor analysis p 13 A86-39147

Remote sensing investigations of wetland biomass and productivity for global biosystems research [NASA-CR-176725] p 14 N86-23994

Satellite detection of phytoplankton export from the mid-Atlantic Bight during the 1979 spring bloom [NASA-TM-88782] p 41 N86-27699

BLACK SEA

Remote sensing and modeling of the dynamics of the western part of the Black Sea p 26 A86-32679

BLIGHT

Wavelength intensity indices in relation to tree condition and leaf-nutrient content p 12 A86-37036

BOLIVIA

Thematic mapper studies of Andean volcanoes [NASA-CR-176807] p 24 N86-25866

BOUNDARY LAYERS

Preliminary assessment of soil moisture over vegetation [NASA-CR-177226] p 15 N86-27704

BRAZIL

Wheat area estimation using digital LANDSAT MSS data and aerial photographs [INPE-3824-PRE/900] p 15 N86-26667

BRIGHTNESS

Salyut-6 observation of color and brightness contrasts correlated with ocean-bottom relief p 26 A86-32678
 Determination of sea spectral reflectance from airborne measurements p 26 A86-32683

The tasseled cap - Size, shape and orientation changes due to soil background --- in soil brightness-plant greenness plane p 12 A86-37035

BRIGHTNESS TEMPERATURE

Multifrequency observations of brightness temperature of artificial new and young sea ice p 28 A86-33514

BUOYS

Optimal disposition of satellite-tracked drifting buoys in the South Atlantic p 31 A86-34488
 Development of a satellite-tracked oceanographic drifting buoy for the Brazilian Antarctic Program, part 1 [INPE-3793-PRE/888] p 36 N86-24166

Comparison of Circulation estimates and winds based on shipboard and satellite-tracked buoy data in Bransfield Strait, 9-14 March, 1985, part 3 [INPE-3795-PRE/890] p 36 N86-24168
 A review of methods to track oil in arctic waters [AD-A164679] p 39 N86-26716

C

C BAND

A preliminary report on the measurements of forest canopies with C-band radar scatterometer at NASA/NSTL p 3 A86-33525

The SIR-C experiment - Measuring new variables from space with SAR p 50 A86-37028

CALDERAS

Use of Seasat SAR imagery for geological mapping in a volcanic terrain - Askja Caldera, Iceland p 19 A86-30189

CALIBRATING

Verification of L-band SAR calibration p 54 A86-33634
 Strategies for the calibration and operational use of the ERS-1 SAR wave mode [JHU/APL/SDO-7565] p 35 N86-23207

Spectroradiometric considerations for advanced land observing systems [NASA-CR-177205] p 58 N86-27705

CALIFORNIA

Plate motions and deformations from geologic and geodetic data [NASA-CR-177299] p 18 N86-26741

A model for the estimation of the surface fluxes of momentum, heat, and moisture of the cloud-topped marine atmospheric boundary layer from satellite measurable parameters [NASA-CR-177290] p 41 N86-27853

CANOPIES (VEGETATION)

Microwave remote sensing of agricultural crops in Canada p 1 A86-30190
 Diurnal patterns of bidirectional vegetation indices for wheat canopies p 1 A86-30192

Assessing impacts of off-nadir observation on remote sensing of vegetation - Use of the Suits model p 1 A86-30193

Radar scatterometer probing of thick vegetation canopies p 3 A86-33523

A preliminary report on the measurements of forest canopies with C-band radar scatterometer at NASA/NSTL p 3 A86-33525

A correlation and regression analysis of present canopy closure vs. TMS spectral response for selected forest sites in the San Juan National Forest, Colorado p 3 A86-33539

Estimation of biophysical properties of forest canopies through inversion of microwave scatterometer data p 4 A86-33542

Microwave emission from row crops p 9 A86-35681
 Regression models for vegetation radar-backscattering and radiometric emission p 10 A86-36046

Effect of dew on canopy reflectance and temperature p 10 A86-36049
 Modeling the controls of forest productivity using canopy variables p 11 A86-37016

Sun angle, view angle, and background effects on spectral response of simulated balsam fir canopies p 13 A86-39002

Remote sensing investigations of wetland biomass and productivity for global biosystems research [NASA-CR-176725] p 14 N86-23994

Department of Geology/NASA-GSFC geobotanical investigation [NASA-CR-177300] p 15 N86-27698

Preliminary assessment of soil moisture over vegetation [NASA-CR-177226] p 15 N86-27704

CAPILLARY WAVES

Studies related to ocean dynamics. Task 3.2: Aircraft Field Test Program to investigate the ability of remote sensing methods to measure current/wind-wave interactions [NASA-CR-168349] p 38 N86-25100

CARBON

High frequency sampling of the 1984 spring bloom within the mid-Atlantic Bight: Synoptic shipboard, aircraft, and in situ perspectives of the SEEP-I experiment [NASA-TM-88765] p 41 N86-27700

CARBON CYCLE

Satellite-derived leaf-area-index and vegetation maps as input to global carbon cycle models - A hierarchical approach p 2 A86-30194

CARBON DIOXIDE CONCENTRATION

Environment and climate --- Russian book p 16 A86-38677

CHANGE DETECTION

Multispectral change detection using difference classification and bitemporal classification p 49 A86-37004

CHESAPEAKE BAY (US)

Environmental data sources for the Chesapeake Bay Area [PB86-110640] p 35 N86-23211

CHLOROPHYLLS

Influence of the Yukon River on the Bering Sea [NASA-CR-177310] p 39 N86-26783

Satellite detection of phytoplankton export from the mid-Atlantic Bight during the 1979 spring bloom [NASA-TM-88782] p 41 N86-27699

High frequency sampling of the 1984 spring bloom within the mid-Atlantic Bight: Synoptic shipboard, aircraft, and in situ perspectives of the SEEP-I experiment [NASA-TM-88765] p 41 N86-27700

CIRRUS CLOUDS

Satellite cloud and precipitation analysis using a minicomputer [AD-A163821] p 58 N86-25084

CITRUS TREES

Wavelength intensity indices in relation to tree condition and leaf-nutrient content p 12 A86-37036

CLASSIFICATIONS

Techniques for multispectral image classification p 44 A86-32337

A histogram as the basis of the statistical classification of images p 45 A86-32688

- Automatic cloud classification p 46 A86-33534
Context classifier --- pixel classification theory and algorithms p 46 A86-33535
Classification of south Texas farm and range resources using NOAA7 AVHRR satellite imagery p 5 A86-33558
A stepwise hierarchical multi-binary approach in TM landuse classification --- Thematic Mapping p 46 A86-33597
A non-stationary contextual classifier with improved accuracy --- for multispectral data p 47 A86-33621
Extended testing of a general contextual classifier using the massively parallel processor - Preliminary results and test plans --- for thematic mapping p 54 A86-33623
Classification of geophysical parameters using passive microwave satellite measurements p 47 A86-33626
An improved hybrid classifier --- for remote sensing p 8 A86-34744
Use of multitemporal spectral profiles in agricultural land-cover classification p 10 A86-36084
Statistical approach to the classification of objects on air and space remote-sensing images p 48 A86-36515
Multispectral change detection using difference classification and bitemporal classification p 49 A86-37004
Estimation of the location parameter of a multispectral distribution by a median operator p 49 A86-37006
A clustering algorithm for remote sensing multispectral data p 51 A86-37033
- CLASSIFIERS**
Ducks Unlimited Joint Research Project [NASA-TM-88755] p 14 N86-25032
- CLIMATE**
Heat budget and climatic atlas of the equatorial Atlantic Ocean during FGGE (First GARP Global Experiment, 1979 [PB86-111622] p 35 N86-23213
Operational satellite support to scientific programs [AD-A165081] p 59 N86-27412
- CLIMATOLOGY**
Environment and climate --- Russian book p 16 A86-38677
Sea surface temperature from satellites: The impact of FGGE p 36 N86-24161
- CLOSURE LAW**
A correlation and regression analysis of present canopy closure vs. TMS spectral response for selected forest sites in the San Juan National Forest, Colorado p 3 A86-33539
- CLOUD COVER**
Remote sensing of clouds p 52 A86-33533
Estimation of monthly rainfall from satellite-observed cloud amount in the tropical western Pacific p 43 A86-36234
Satellite cloud and precipitation analysis using a minicomputer [AD-A163821] p 58 N86-25084
On land-sea contrast in the Earth radiation budget p 40 N86-27695
- CLOUD PHOTOGRAPHY**
Remote sensing of clouds p 52 A86-33533
Satellite-derived moisture profiles [NOAA-NESDIS-24] p 44 N86-27703
- CLOUD PHYSICS**
Satellite-borne 90 GHz radiometer experiment (SABREX), phase A1 [DFVLR-MITT-85-13] p 57 N86-24000
- CLOUDS**
A model for the estimation of the surface fluxes of momentum, heat and moisture of the cloud topped marine atmospheric boundary layer from satellite measurable parameters [NASA-CR-177283] p 41 N86-27837
- CLOUDS (METEOROLOGY)**
Automatic cloud classification p 46 A86-33534
- CLUSTER ANALYSIS**
High accuracy clustering using residual image --- from Landsat satellite p 49 A86-37003
A clustering algorithm for remote sensing multispectral data p 51 A86-37033
- COASTAL CURRENTS**
Influence of the Yukon River on the Bering Sea [NASA-CR-177310] p 39 N86-26783
- COASTAL PLAINS**
The study of the natural geographic differences in the coastal areas of water covered parts of Marmara region in Turkey with the help of Landsat-4 MSS data using an unsupervised classification algorithm with Euclidean distance p 43 A86-37012
- COASTAL WATER**
Satellite imaging of coastal flow circulation in relation to numerical modelling p 31 A86-33631
- Methods of obtaining offshore wind direction and sea-state data from X-band aircraft SAR (Synthetic Aperture Radar) imagery of coastal waters [AD-A165552] p 38 N86-26517
A simulation analysis of the fate of phytoplankton within the mid-Atlantic bight [NASA-CR-177265] p 39 N86-26670
- COASTAL ZONE COLOR SCANNER**
Ocean color measurements p 28 A86-33488
Applicability of atmospheric correction algorithm for CZCS data to Japanese coastal area --- Coastal Zone Color Scanner p 31 A86-33632
A simulation analysis of the fate of phytoplankton within the mid-Atlantic bight [NASA-CR-177265] p 39 N86-26670
- COASTS**
Methods of obtaining offshore wind direction and sea-state data from X-band aircraft SAR (Synthetic Aperture Radar) imagery of coastal waters [AD-A165552] p 38 N86-26517
A model for the estimation of the surface fluxes of momentum, heat, and moisture of the cloud-topped marine atmospheric boundary layer from satellite measurable parameters [NASA-CR-177290] p 41 N86-27853
- CODES**
The applicability of LOWTRAN 5 computer code to aerial thermographic data correction p 48 A86-34739
- COLD FRONTS**
A model for the estimation of the surface fluxes of momentum, heat, and moisture of the cloud-topped marine atmospheric boundary layer from satellite measurable parameters [NASA-CR-177290] p 41 N86-27853
- COLOR PHOTOGRAPHY**
Small format, oblique, colour aerial photography - An aid to the location of methane seepage p 11 A86-36783
- COLORIMETRY**
Salyut-6 observation of color and brightness contrasts correlated with ocean-bottom relief p 26 A86-32678
- COMMAND AND CONTROL**
Comparison of the Defense Meteorological Satellite Program (DMSP) and the NOAA Polar-orbiting Operational Environmental Satellite (POES) program [AD-A165118] p 59 N86-27413
- COMMUNICATION SATELLITES**
A technique for assessing the severity of terrain shadowing in mobile satellite service p 51 A86-39545
- COMPARISON**
Comparison of the Defense Meteorological Satellite Program (DMSP) and the NOAA Polar-orbiting Operational Environmental Satellite (POES) program [AD-A165118] p 59 N86-27413
- COMPUTER AIDED MAPPING**
Computer-aided interpretation of space images with the aim of structural analysis p 20 A86-32690
Map digitization offers new possibilities [NLR-MP-84061-U] p 51 N86-23028
- COMPUTER PROGRAMS**
Description of a databank of normalized radar cross section of terrain p 45 A86-33526
Ocean wave slope statistics from automated analysis of sun glint photographs [AD-A161995] p 37 N86-24172
- COMPUTER TECHNIQUES**
Approaches to computer reasoning in remote sensing and geographic information processing - A survey p 16 A86-33595
The possibility of applying different types of image-analysis software to environment-protection problems --- in remote sensing p 16 A86-36513
Certain transformations in a quantitative approach to image processing --- computer techniques for satellite photography p 48 A86-36517
Computer processing of spectrally superposed data --- subroutines for MSS remote sensing p 49 A86-36518
Operational methods for data interpolation [DE85-016050] p 34 N86-15969
Map digitization offers new possibilities [NLR-MP-84061-U] p 51 N86-23028
The study of gravity field estimation procedures [AD-A164564] p 19 N86-26745
- COMPUTERIZED SIMULATION**
Radar image simulation as a tool to analyze topographic effects on geometry and radiometry of radar imagery p 50 A86-37026
Simulation studies related to the design of post-FGGE observing systems p 57 N86-24160
Remote sensing and oceanographic equipment technology: Some present systems and future needs, revised [PB86-156502] p 40 N86-26791
- CONFERENCES**
Integrated global monitoring of the world ocean. Volumes 1, 2, & 3 --- Russian book p 24 A86-31350
- 1985 International Geoscience and Remote Sensing Symposium (IGARSS '85), University of Massachusetts, Amherst, October 7-9, 1985, Digest. Volumes 1 & 2 p 52 A86-33501
Asian Conference on Remote Sensing, 5th, Kathmandu, Nepal, November 15-18, 1984, Proceedings p 55 A86-35425
Machine processing of remotely sensed data - Quantifying global process: Models, sensor systems, and analytical methods; Proceedings of the Eleventh International Symposium, Purdue University, West Lafayette, IN, June 25-27, 1985 p 56 A86-37001
Proceedings of the Arctic Oceanography Conference and Workshop held at the Naval Ocean Research and Development Activity, NSTL, MS. on June 11-14, 1985 [AD-A162578] p 34 N86-23203
- CONIFERS**
Forest signatures in imaging and non-imaging microwave scatterometer data p 9 A86-36037
Scattering from a random layer embedded with dielectric needles --- for applications to coniferous vegetation p 10 A86-36045
Field and airborne spectral characterization of suspected damage in red spruce (*Picea rubens*) from Vermont p 11 A86-37008
Sun angle, view angle, and background effects on spectral response of simulated balsam fir canopies p 13 A86-39002
- CONTINENTAL SHELVES**
Satellite detection of phytoplankton export from the mid-Atlantic Bight during the 1979 spring bloom [NASA-TM-88782] p 41 N86-27699
High frequency sampling of the 1984 spring bloom within the mid-Atlantic Bight: Synoptic shipboard, aircraft, and in situ perspectives of the SEEP-I experiment [NASA-TM-88765] p 41 N86-27700
- CONVECTION**
Characteristics of western region flash flood events in GOES imagery and conventional data [NOAA-TM-NESDIS-13] p 44 N86-26668
- CONVECTION CURRENTS**
Lidar observations of the planetary boundary layer p 29 A86-33532
- CONVECTIVE HEAT TRANSFER**
Transient response to localized episodic heating in the tropics p 51 N86-27749
- COOLING**
Satellite observations of sea surface cooling by hurricanes p 32 A86-35545
- CORRELATION**
A correlation and regression analysis of present canopy closure vs. TMS spectral response for selected forest sites in the San Juan National Forest, Colorado p 3 A86-33539
- CRACKING (FRACTURING)**
A study of sea ice kinematics and their relationship to arctic ambient noise. Part 3, Section 1: Ambient noise. Section 2: Ambient noise p 39 N86-26788
A study of sea ice kinematics and their relationship to arctic ambient noise. Part 3, section 3: Ambient noise [AD-A165305] p 40 N86-26789
- CROP IDENTIFICATION**
Nonparametric models and crop classification p 6 A86-33622
Multi-crop area estimation and mapping on a microprocessor/mainframe network p 7 A86-33644
An information measure for class discrimination --- in remote sensing of crop observation p 11 A86-36789
Semi-operational identification of agricultural crops from airborne SLAR-data p 12 A86-37025
Agricultural applications for thermal infrared multispectral scanner data p 12 A86-37034
A multindex multitemporal approach to map crops in the early growing season: An application to two Italian irrigation districts: East Sesia and Grande Bonifica Ferrarese --- flue gases [ICW-1611] p 15 N86-26674
- CROP INVENTORIES**
Microwave remote sensing of agricultural crops in Canada p 1 A86-30190
Diurnal patterns of bidirectional vegetation indices for wheat canopies p 1 A86-30192
Overview of the AgRISTARS research program. I --- Agriculture and Resources Inventory Surveys Through Aerospace Remote Sensing p 2 A86-33503
Classification of south Texas farm and range resources using NOAA7 AVHRR satellite imagery p 5 A86-33558
Overview and highlights of Early Warning and Crop Condition Assessment project p 5 A86-33576
Development of agrometeorological crop model inputs from remotely sensed information p 6 A86-33579
USDA/SRS software for Landsat MSS-based crop-acreage estimation p 6 A86-33605

- Evaluation of crop acreage estimation methods using Landsat data as auxiliary input p 6 A86-33606
 Wheat area estimation using digital LANDSAT MSS data and aerial photographs [INPE-3824-PRE/900] p 15 N86-26667
- CROP VIGOR**
 Overview and highlights of Early Warning and Crop Condition Assessment project p 5 A86-33576
 Detection and evaluation of plant stresses for crop management decisions p 5 A86-33578
- CRUSTAL FRACTURES**
 Evidence of ongoing crustal deformation related to magmatic activity near Socorro, New Mexico p 18 A86-37797
- CUMULONIMBUS CLOUDS**
 Meteorological Satellite Center Technical Note, no. 13, 1986 [ISSN-0388-9653] p 40 N86-27694
- CUMULUS CLOUDS**
 Satellite cloud and precipitation analysis using a minicomputer [AD-A163821] p 58 N86-25084
- CV-990 AIRCRAFT**
 Aircraft and satellite passive microwave observations of the Bering Sea ice cover during MIZEX West p 32 A86-35683
- CYCLONES**
 Seasat microwave wind and rain observations in severe tropical and midlatitude marine storms p 27 A86-33486
 Precipitation in tropical cyclones p 28 A86-33490
 Characteristics of western region flash flood events in GOES imagery and conventional data [NOAA-TM-NESDIS-13] p 44 N86-26668
- D**
- DATA ACQUISITION**
 ENVIROSAT-2000 report: Federal agency satellite requirements [NASA-TM-88752] p 59 N86-26355
- DATA BASES**
 Formation of a digital data base for automated forest mapping p 2 A86-32689
 Description of a databank of normalized radar cross section of terrain p 45 A86-33526
 Economical maintenance of a national topographic data base using Landsat images p 48 A86-36082
 Operational satellite support to scientific programs [AD-A165081] p 59 N86-27412
- DATA COLLECTION PLATFORMS**
 The ARGOS system for positioning and data collection by satellite - Characteristics and performance levels p 56 A86-39559
 Development of a satellite-tracked oceanographic drifting buoy for the Brazilian Antarctic Program, part 1 [INPE-3793-PRE/888] p 36 N86-24166
- DATA COMPRESSION**
 On-board data compression for advanced Landsat p 45 A86-32368
- DATA PROCESSING**
 Multi-crop area estimation and mapping on a microprocessor/mainframe network p 7 A86-33644
 Machine processing of remotely sensed data - Quantifying global process: Models, sensor systems, and analytical methods; Proceedings of the Eleventh International Symposium, Purdue University, West Lafayette, IN, June 25-27, 1985 p 56 A86-37001
 Design of the European Space Agency Thematic Mapper processing chains p 51 A86-37864
 Operational methods for data interpolation [DEBS-016050] p 34 N86-15969
 GOES (Geostationary Operational Environmental Satellite)-next overview [AD-A165080] p 59 N86-27411
- DATA REDUCTION**
 A simple, objective analysis scheme for scatterometer data --- Seasat A satellite observation of wind over ocean p 32 A86-35550
- DATA SAMPLING**
 Modified cubic convolution resampling for Landsat p 47 A86-33640
- DATA SYSTEMS**
 Technological improvements to naval aviation weather support p 34 A86-37506
- DECIDUOUS TREES**
 Forest signatures in imaging and non-imaging microwave scatterometer data p 9 A86-36037
- DEFORESTATION**
 Identifying deforestation in Brazil using multiresolution satellite data p 8 A86-34742
- DEFORMATION**
 Plate motions and deformations from geologic and geodetic data [NASA-CR-177299] p 18 N86-26741
- DEPTH**
 Marginal ice zone experiment - 1984, physical oceanography report: USNS Lynch and helicopter-based STD data [AD-A163096] p 37 N86-24180
- DESERTIFICATION**
 A measuring reference system to quantify the desertification process in a semiarid ecosystem based on Landsat MSS data p 16 A86-37011
- DESERTS**
 The influence of observational interdependence on spectral reflectance relationships with plant and soil variables p 2 A86-30196
 Detecting desert locust breeding grounds in the Sahel with satellite data p 16 A86-32537
 Site selection and directional models of deserts used for ERBE validation targets [NASA-TP-2540] p 57 N86-23160
 Remote monitoring of processes that shape desert surfaces: The Desert Winds Project [T186-900108] p 24 N86-25099
- DETERIORATION**
 Environmental data sources for the Chesapeake Bay Area [PB86-110640] p 35 N86-23211
- DEVELOPING NATIONS**
 Remote sensing for developing countries - A case study of Tunisia p 15 A86-30195
- DEW**
 Effect of dew on canopy reflectance and temperature p 10 A86-36049
- DIAMETERS**
 Predicting tree groundline diameter from crown measurements made on 35-mm aerial photography p 13 A86-39006
- DIFFERENTIAL PULSE CODE MODULATION**
 On-board data compression for advanced Landsat p 45 A86-32368
- DIGITAL DATA**
 Variograms and spatial variation in remotely sensed images p 47 A86-33638
 Examples of the automated derivation of digital surface models p 48 A86-35292
- DIGITAL RADAR SYSTEMS**
 Verification of L-band SAR calibration p 54 A86-33634
- DIGITAL SYSTEMS**
 Ocean wave slope statistics from automated analysis of sun glitter photographs [AD-A161995] p 37 N86-24172
- DIGITAL TECHNIQUES**
 Formation of a digital data base for automated forest mapping p 2 A86-32689
 Map digitization offers new possibilities [NLR-MP-84061-U] p 51 N86-23028
- DISCRIMINANT ANALYSIS (STATISTICS)**
 Distinguishing among tallgrass prairie cover types from measurements of multispectral reflectance p 10 A86-36047
 An information measure for class discrimination --- in remote sensing of crop observation p 11 A86-36789
- DISCRIMINATION**
 Forest discrimination with multipolarization imaging radar p 5 A86-33566
- DIURNAL VARIATIONS**
 Diurnal patterns of bidirectional vegetation indices for wheat canopies p 1 A86-30192
- DMSP SATELLITES**
 Comparison of the Defense Meteorological Satellite Program (DMSP) and the NOAA Polar-orbiting Operational Environmental Satellite (POES) program [AD-A165118] p 59 N86-27413
- DOPPLER RADAR**
 Analysis of airborne Doppler lidar, Doppler radar and tall tower measurements of atmospheric flows in quiescent and stormy weather [NASA-CR-3960] p 56 N86-23159
- DYNAMIC CHARACTERISTICS**
 A study of sea ice kinematics and their relationship to arctic ambient noise. Part 3, Section 1: Ambient noise. Section 2: Ambient noise [AD-A165304] p 39 N86-26788
 A study of sea ice kinematics and their relationship to arctic ambient noise. Part 3, section 3: Ambient noise [AD-A165305] p 40 N86-26789
- E**
- EARTH (PLANET)**
 Operational satellite support to scientific programs [AD-A165081] p 59 N86-27412
 International coordination of and contributions to environmental satellite programs [AD-A165142] p 60 N86-28016
- EARTH ALBEDO**
 On land-sea contrast in the Earth radiation budget p 40 N86-27695
- EARTH CRUST**
 Structure of the southern Rio Grande rift from gravity interpretation p 18 A86-37795
 Evidence of ongoing crustal deformation related to magmatic activity near Socorro, New Mexico p 18 A86-37797
 Plate motions and deformations from geologic and geodetic data [NASA-CR-177313] p 19 N86-27833
- EARTH MANTLE**
 Evidence for small-scale mantle convection from Seasat altimeter data p 25 A86-31976
- EARTH MOVEMENTS**
 Plate motions and deformations from geologic and geodetic data [NASA-CR-177299] p 18 N86-26741
- EARTH OBSERVATIONS (FROM SPACE)**
 Agricultural and scientific space platforms --- Russian book p 1 A86-29843
 Possibility of small-scale physiogeographical regionalization using space spectrometry data p 16 A86-30974
 Weddell-Scotia sea marginal ice zone observations from space, October 1984 p 26 A86-33105
 NOAA plans for remote sensing of the earth, oceans and atmosphere p 52 A86-33502
 Passive remote sensing of stratospheric and mesospheric winds p 53 A86-33545
 Design and benefits of a multibeam Earth Observing Radar p 29 A86-33591
 Investigation of the earth from space - A new contribution to the development of structural geomorphology p 22 A86-36504
 Estimation of atmospheric corrections from multiple aircraft imagery p 49 A86-36784
 The evolution of remote sensing science and applications p 58 A86-37002
 Analysis of data acquired by Shuttle Imaging Radar SIR-A and Landsat Thematic Mapper over Baldwin County, Alabama p 12 A86-37018
 Plate motions and deformations from geologic and geodetic data [NASA-CR-177313] p 19 N86-27833
- EARTH ORBITS**
 The study of gravity field estimation procedures [AD-A164564] p 19 N86-26745
- EARTH RADIATION BUDGET EXPERIMENT**
 Site selection and directional models of deserts used for ERBE validation targets [NASA-TP-2540] p 57 N86-23160
- EARTH RESOURCES**
 Remote sensing for developing countries - A case study of Tunisia p 15 A86-30195
 Resource monitoring oriented remote sensing data processing capabilities p 16 A86-33643
 Determination of the spectral characteristics of natural objects on test ranges, and aspects of the efficiency of space systems --- Russian book p 11 A86-36697
 The effect of the atmosphere on the satellite remote sensing of earth resources --- Russian book p 56 A86-39969
 USSR report: Earth sciences [JPRS-UES-86-004] p 34 N86-23017
 Earth science investigations in the United States Antarctic Research Program (USARP) for the period July 1, 1984 - June 30, 1985 [PB86-143773] p 58 N86-25076
- EARTH SURFACE**
 Structure of terrestrial impact craters from SIR-B radar data - Preliminary results p 21 A86-33552
 Multipolarization SAR data for surface feature delineation p 46 A86-33594
 Examples of the automated derivation of digital surface models p 48 A86-35292
 A stable iterative procedure to obtain soil surface parameters and fluxes from satellite data p 8 A86-35678
 Small format, oblique, colour aerial photography - An aid to the location of methane seepage p 11 A86-36783
- EARTHQUAKES**
 Earthquake and tsunami data services and publications [PB86-156254] p 51 N86-25919
- ECOSYSTEMS**
 Modeling the controls of forest productivity using canopy variables p 11 A86-37016
 Ducks Unlimited Joint Research Project [NASA-TM-88755] p 14 N86-25032
 A simulation analysis of the fate of phytoplankton within the mid-Atlantic bight [NASA-CR-177265] p 39 N86-26670

EGYPT

Application of spaceborne and airborne techniques in mineral exploration at Wadi El Allaqi area, Eastern Desert, Egypt p 23 A86-37865

Thematic mapper research in the Earth sciences: Tectonic evaluation of the Nubian Shield of northeastern Sudan/southeastern Egypt using thematic mapper imagery [NASA-CR-177311] p 24 N86-26740

EIGENVALUES

On the information content of multispectral radiance measurements over an ocean --- ESA programs [GKSS-85/E/43] p 40 N86-27697

EIGENVECTORS

Thematic mapper research in the Earth sciences: Tectonic evaluation of the Nubian Shield of northeastern Sudan/southeastern Egypt using thematic mapper imagery [NASA-CR-177311] p 24 N86-26740

Objective analysis of tidal fields in the Atlantic and Indian Oceans [NASA-TM-87773] p 39 N86-26782

ELASTIC MEDIA

The effective elastic lithosphere under the Cook-Austral and Society islands p 25 A86-32267

ELECTROMAGNETIC RADIATION

The fundamentals of microwave remote sensing [SU-84] p 56 N86-23025

ELECTROMAGNETIC SPECTRA

Thematic mapper research in the Earth sciences: Tectonic evaluation of the Nubian Shield of northeastern Sudan/southeastern Egypt using thematic mapper imagery [NASA-CR-177311] p 24 N86-26740

Department of Geology/NASA-GSFC geobotanical investigation [NASA-CR-177300] p 15 N86-27698

ELECTROMAGNETIC WAVE TRANSMISSION

Position fixing afloat --- coordinate determination at sea p 33 A86-36788

ENERGY BUDGETS

On land-sea contrast in the Earth radiation budget p 40 N86-27695

ENVIRONMENTAL EFFECTS

100 MHz dielectric constant measurements of snow cover Dependence on environmental and snow pack parameters p 42 A86-33613

Environment and climate --- Russian book p 16 A86-38677

Comprehensive integrated remote sensing for US Department of Energy applications [DE86-002101] p 17 N86-25036

ENVIRONMENTAL POLLUTION

Environment and climate --- Russian book p 16 A86-38677

ENVIRONMENTAL ENGINEERING

Research on enhancing the utilization of digital multispectral data and geographic information systems in global habitability studies [NASA-CR-177294] p 17 N86-26669

ENVIRONMENTAL MONITORING

Integrated global monitoring of the world ocean. Volumes 1, 2, & 3 --- Russian book p 24 A86-31350

Detecting desert locust breeding grounds in the Sahel with satellite data p 16 A86-32537

The Ocean Topography Experiment (TOPEX) - Some questions answered p 25 A86-32556

1985 International Geoscience and Remote Sensing Symposium (IGARSS '85), University of Massachusetts, Amherst, October 7-9, 1985, Digest. Volumes 1 & 2 p 52 A86-33501

Remote sensing techniques for the detection of soil erosion and the identification of soil conservation practices p 3 A86-33506

Resource monitoring oriented remote sensing data processing capabilities p 16 A86-33643

Identifying deforestation in Brazil using multiresolution satellite data p 8 A86-34742

Methods of combined air and space remote-sensing studies of Siberia p 22 A86-36501

The possibility of applying different types of image-analysis software to environment-protection problems --- in remote sensing p 16 A86-36513

A measuring reference system to quantify the desertification process in a semiarid ecosystem based on Landsat MSS data p 16 A86-37011

Assessment and trends of Florida's marine fisheries habitat An integration of aerial photography and Thematic Mapper imagery p 34 A86-37013

Use of Thematic Mapper data to assess water quality in Green Bay and central Lake Michigan p 43 A86-39004

Environmental data sources for the Chesapeake Bay Area [PB86-110640] p 35 N86-23211

ENVIRONMENTAL RESEARCH SATELLITES

ENVIROSAT-2000 report: Federal agency satellite requirements [NASA-TM-88752] p 59 N86-26355

ENVIRONMENTAL SURVEYS

Vegetation and environmental gradients of the Prudhoe Bay region, Alaska [AD-A162022] p 17 N86-24034

EQUATORIAL ATMOSPHERE

Transient response to localized episodic heating in the tropics p 51 N86-27749

EQUATORIAL REGIONS

Heat budget and climatic atlas of the equatorial Atlantic Ocean during FGGE (First GARP Global Experiment, 1979 [PB86-111622] p 35 N86-23213

Transient response to localized episodic heating in the tropics p 51 N86-27749

ERROR ANALYSIS

Hierarchical classification of multitemporal/multispectral scanner data p 49 A86-37017

ERROR CORRECTING DEVICES

A median filter approach for correcting errors in a vector field p 29 A86-33601

ERRORS

Navstar GPS (Global Positioning System) accuracy while surveying arrays of deep ocean transponders [AD-A163364] p 38 N86-26313

ERS-1 (ESA SATELLITE)

Relative vertical positioning using ground-level transponders with the ERS-1 altimeter p 33 A86-35688

ERS-1 - Our new window on the oceans for the 1990s p 34 A86-38718

Strategies for the calibration and operational use of the ERS-1 SAR wave mode [JHU/APL/SDO-7565] p 35 N86-23207

ESTIMATING

Wheat area estimation using digital LANDSAT MSS data and aerial photographs [INPE-3824-PRE/900] p 15 N86-26667

ESTUARIES

Physical interpretation of estuarine water color using vector analysis of satellite data p 43 A86-33630

Environmental data sources for the Chesapeake Bay Area [PB86-110640] p 35 N86-23211

Application of LANDSAT TM images to assess circulation and dispersion in coastal lagoons [NASA-CR-177315] p 44 N86-26665

EUROPEAN SPACE AGENCY

Design of the European Space Agency Thematic Mapper processing chains p 51 A86-37864

EVAPORATION

Analysis of a resistance-energy balance method for estimating daily evaporation from wheat plots using one-time-of-day infrared temperature observations p 13 A86-39148

EVAPOTRANSPIRATION

A stable iterative procedure to obtain soil surface parameters and fluxes from satellite data p 8 A86-35678

Evapotranspiration over an agricultural region using a surface flux/temperature model based on NOAA-AVHRR data p 10 A86-36237

EXPERT SYSTEMS

The development of an MSS satellite imagery classification expert system p 46 A86-33596

EXTREMELY HIGH FREQUENCIES

Satellite-borne 90 GHz radiometer experiment (SABREX), phase A1 [DFVLR-MITT-85-13] p 57 N86-24000

F

FACTOR ANALYSIS

Separation of soil-plant spectral mixtures by factor analysis p 13 A86-39147

FARM CROPS

Microwave remote sensing of agricultural crops in Canada p 1 A86-30190

Overview of the AgRISTARS research program. I --- Agriculture and Resources Inventory Surveys Through Aerospace Remote Sensing p 2 A86-33503

Overview and highlights of Early Warning and Crop Condition Assessment project p 5 A86-33576

Detection and evaluation of plant stresses for crop management decisions p 5 A86-33578

Development of agrometeorological crop model inputs from remotely sensed information p 6 A86-33579

USDA/SRS software for Landsat MSS-based crop-acreage estimation p 6 A86-33605

Evaluation of crop acreage estimation methods using Landsat data as auxiliary input p 6 A86-33606

Nonparametric models and crop classification

p 6 A86-33622

SAR image segmentation using digitised field boundaries for crop mapping and monitoring applications p 7 A86-33625

Spectral components analysis - A bridge between spectral observations and agrometeorological crop models p 7 A86-33627

Multi-crop area estimation and mapping on a microprocessor/mainframe network p 7 A86-33644

Microwave emission from row crops p 9 A86-35681

Integration of high and low resolution satellite data for crop condition assessment p 12 A86-37020

FARMLANDS

Classification of south Texas farm and range resources using NOAA7 AVHRR satellite imagery p 5 A86-33558

FIELD OF VIEW

EOS radiometer concepts for soil moisture remote sensing [NASA-CR-177854] p 14 N86-23995

FILTERS

A median filter approach for correcting errors in a vector field p 29 A86-33601

FISHERIES

Assessment and trends of Florida's marine fisheries habitat An integration of aerial photography and Thematic Mapper imagery p 34 A86-37013

NOAA satellite requirements forecast [AD-A165244] p 40 N86-27414

FLIGHT CONDITIONS

Technological improvements to naval aviation weather support p 34 A86-37506

FLIGHT CONTROL

Probabilistic modeling of fields of atmospheric turbulence and sea roughness with reference to the study of complex systems --- for flight control p 33 A86-36480

FLIGHT PLANS

Map digitization offers new possibilities [NLR-MP-84061-U] p 51 N86-23028

FLIGHT TESTS

Archimedes project remote sensing of oil spills North Sea experiment, October 1983. Report on DFVLR (Side-Looking Airborne Radar (SLAR) contribution [DFVLR-FB-85-54] p 35 N86-24002

FLOOD PREDICTIONS

Characteristics of western region flash flood events in GOES imagery and conventional data [NOAA-TM-NESDIS-13] p 44 N86-26668

FLORIDA

Assessment and trends of Florida's marine fisheries habitat An integration of aerial photography and Thematic Mapper imagery p 34 A86-37013

FLOW VELOCITY

Application of LANDSAT TM images to assess circulation and dispersion in coastal lagoons [NASA-CR-177315] p 44 N86-26665

FOREST FIRE DETECTION

Conceptual design study: Forest Fire Advanced System Technology (FFAST) [JPL-PUBL-86-5] p 14 N86-25034

FOREST FIRES

Conceptual design study: Forest Fire Advanced System Technology (FFAST) [JPL-PUBL-86-5] p 14 N86-25034

FOREST MANAGEMENT

Formation of a digital data base for automated forest mapping p 2 A86-32689

Analysis of forest/structure using thematic mapper simulator data p 4 A86-33540

Field and airborne spectral characterization of suspected damage in red spruce (picea rubens) from Vermont p 11 A86-37008

Adding spatial considerations to the JABOWA model of forest growth p 11 A86-37014

Timber Resources Inventory and Monitoring Joint Research Project [NASA-TM-88754] p 14 N86-25863

FORESTS

A texture-enhancement procedure for separating orchard from forest in Thematic Mapper data p 2 A86-30198

A preliminary report on the measurements of forest canopies with C-band radar scatterometer at NASA/NSTL p 3 A86-33525

A correlation and regression analysis of precanopy closure vs. TMS spectral response for selected forest sites in the San Juan National Forest, Colorado p 3 A86-33539

Forest discrimination with multipolarization imaging radar p 5 A86-33565

Forest discrimination with multipolarization imaging radar p 5 A86-33566

- Comparison between Landsat MSS and Thematic Mapper data for geobotanical prospecting in the Spanish-Portuguese Pyrite Belt p 7 A86-33628
- Evaluation of Landsat MSS bands and transformations for detecting heavy metal stress in forest-covered areas p 7 A86-33629
- Forestry information content of Thematic Mapper data p 8 A86-34741
- Spectral characterization of biophysical characteristics in a boreal forest - Relationship between Thematic Mapper band reflectance and leaf area index for Aspen p 8 A86-35677
- Forest signatures in imaging and non-imaging microwave scatterometer data p 9 A86-36037
- Analysis of effective radiant temperatures in a Pacific Northwest forest using Thermal Infrared Multispectral Scanner data p 9 A86-36042
- Modeling the controls of forest productivity using canopy variables p 11 A86-37016
- Analysis of data acquired by Shuttle Imaging Radar SIR-A and Landsat Thematic Mapper over Baldwin County, Alabama p 12 A86-37018
- A proposal for a project entitled Assessment of Forest Resources in Uruguay submitted to the United Nations Industrial Development Organization (UNIDO) [INPE-3828-NTE/255] p 15 N86-26666
- FUZZY SETS**
- Segmentation of a Thematic Mapper image using the fuzzy c-means clustering algorithm p 9 A86-35687
- G**
- GARP ATLANTIC TROPICAL EXPERIMENT**
- Heat budget and climatic atlas of the equatorial Atlantic Ocean during FGGE (First GARP Global Experiment, 1979) [PB86-111622] p 35 N86-23213
- GAS SPECTROSCOPY**
- Passive remote sensing of stratospheric and mesospheric winds p 53 A86-33545
- GEBOTANY**
- Comparison between Landsat MSS and Thematic Mapper data for geobotanical prospecting in the Spanish-Portuguese Pyrite Belt p 7 A86-33628
- Department of Geology/NASA-GSFC geobotanical investigation [NASA-CR-177300] p 15 N86-27698
- GEODESY**
- Plate motions and deformations from geologic and geodetic data [NASA-CR-177299] p 18 N86-26741
- The study of gravity field estimation procedures [AD-A164564] p 19 N86-26745
- GEODETIC ACCURACY**
- Accuracy estimate of geoid and ocean topography recovered jointly from satellite altimetry p 32 A86-35278
- Landsat Thematic Mapper geodetic accuracy - Implications for geocoded map compatibility p 18 A86-37024
- GEODETIC SURVEYS**
- Measurement of Thematic Mapper data quality p 50 A86-37032
- Evidence of ongoing crustal deformation related to magmatic activity near Socorro, New Mexico p 18 A86-37797
- GEODYNAMICS**
- Plate motions and deformations from geologic and geodetic data [NASA-CR-177299] p 18 N86-26741
- GEOGRAPHIC INFORMATION SYSTEMS**
- Image processing system interfaces p 44 A86-32333
- Approaches to computer reasoning in remote sensing and geographic information processing - A survey p 16 A86-33595
- Economical maintenance of a national topographic data base using Landsat images p 48 A86-36082
- Technical and software facilities at a center for the processing of remote-sensing data p 48 A86-36511
- Multisource data analysis in remote sensing and geographic information processing p 50 A86-37022
- Research on enhancing the utilization of digital multispectral data and geographic information systems in global habitability studies [NASA-CR-177294] p 17 N86-26669
- Research, investigations and technical developments: National mapping program, 1983-1984 [PB86-166097] p 17 N86-26675
- GEOGRAPHY**
- Possibility of small-scale physiogeographical regionalization using space spectrometry data p 16 A86-30974
- Stable-isotope studies of groundwaters in southeastern New Mexico [DE86-002590] p 43 N86-23027
- Operational satellite support to scientific programs [AD-A165081] p 59 N86-27412
- GEOIDS**
- Accuracy estimate of geoid and ocean topography recovered jointly from satellite altimetry p 32 A86-35278
- GEOLOGICAL FAULTS**
- Structure of the southern Rio Grande rift from gravity interpretation p 18 A86-37795
- Plate motions and deformations from geologic and geodetic data [NASA-CR-177313] p 19 N86-27833
- GEOLOGICAL SURVEYS**
- Use of Seasat SAR imagery for geological mapping in a volcanic terrain - Askja Caldera, Iceland p 19 A86-30189
- Features of the geological application of space data p 19 A86-32680
- Application of space imagery to the identification and geological-geophysical study of hidden plutons in early Proterozoic troughs p 20 A86-32682
- Lineament analysis in a test area of northern Mozambique p 20 A86-33520
- Preliminary geologic analyses of SIR-B radar data for Hawaii p 21 A86-33550
- What are the best radar wavelengths, incidence angles and polarizations for geologic applications? A statistical approach p 21 A86-33592
- Analysis of L-band multipolarization radar images for lava flow mapping p 21 A86-33593
- Problems and principles of the geological interpretation of remote-sensing data p 22 A86-36502
- Method for the quantitative estimation of convergence in mapping in the case of the interpretation of space photographs of oil-and-gas-bearing regions of Siberia p 23 A86-36505
- Quantitative assessment of the information content of TV images of different scale on the example of disjunctives of Siberia p 23 A86-36506
- Methods for the remote sensing of transition zones of the junction of Siberian platforms and orogens p 23 A86-36507
- The use of remote-sensing data to predict regional and local oil-and-gas-bearing structures within the Dneprovsk-Donetsk paleorift p 23 A86-36508
- Combination of air and space remote-sensing methods and geological-geophysical methods for the purpose of oil and gas exploration in the southern Permsk region p 23 A86-36509
- Aspects of the geological interpretation of geophysical fields and results of air and space remote-sensing observations of oil-and-gas-bearing territories p 23 A86-36510
- Landsat MSS and airborne geophysical data combined for mapping granite in southwest Nova Scotia p 23 A86-37021
- GEOLOGY**
- Vegetation and environmental gradients of the Prudhoe Bay region, Alaska [AD-A162022] p 17 N86-24034
- GEOMETRIC DILUTION OF PRECISION**
- An integrated approach to geometric precision processing of spaceborne high-resolution sensors p 55 A86-34737
- GEOMETRIC RECTIFICATION (IMAGERY)**
- Modified cubic convolution resampling for Landsat p 47 A86-33640
- Satellite orientation and position for geometric correction of scanner imagery p 48 A86-36079
- Processing of multi-sensor remotely sensed data to a standard geocoded format p 50 A86-37019
- Radar image simulation as a tool to analyze topographic effects on geometry and radiometry of radar imagery p 50 A86-37026
- Rectification of scanner images using prediction approaches - airborne scanners [SER-C-303] p 57 N86-23992
- GEOMETRY**
- Ocean wave slope statistics from automated analysis of sun glitter photographs [AD-A161995] p 37 N86-24172
- GEOMORPHOLOGY**
- Photogrammetry and remote sensing in periglacial geomorphology p 20 A86-33517
- Structure of terrestrial impact craters from SIR-B radar data - Preliminary results p 21 A86-33552
- Combined structural and geomorphological methods for the processing of aerial and space photographic remote-sensing data with the aim of solving geological problems p 22 A86-36503
- Investigation of the earth from space - A new contribution to the development of structural geomorphology p 22 A86-36504
- GEOPHYSICS**
- USSR report: Earth sciences [JPRS-UES-86-004] p 34 N86-23017
- GEOS 3 SATELLITE**
- Gravity anomalies and sea surface heights derived from a combined GEOS 3/Seasat altimeter data set p 33 A86-36096
- GLOBAL ATMOSPHERIC RESEARCH PROGRAM**
- Intraseasonal variations of OLR in the tropics during the FGGE year --- outgoing long wave radiation p 48 A86-36227
- Proceedings of the First National Workshop on the Global Weather Experiment: Current Achievements and Future Directions, volume 1 [NASA-CR-176720] p 36 N86-24120
- GLAS experiments on the impact of FGGE satellite data on numerical weather prediction p 57 N86-24128
- Proceedings of the First National Workshop on the Global Weather Experiment: Current Achievements and Future Directions, volume 2, part 2 [NASA-CR-176722] p 36 N86-24142
- Simulation studies related to the design of post-FGGE observing systems p 57 N86-24160
- Sea surface temperature from satellites: The impact of FGGE p 36 N86-24161
- GLOBAL POSITIONING SYSTEM**
- Commercial applications of the Navstar Global Positioning System p 54 A86-34112
- Navstar GPS (Global Positioning System) accuracy while surveying arrays of deep ocean transponders [AD-A163364] p 38 N86-26313
- GOES SATELLITES**
- GOES (Geostationary Operational Environmental Satellite)-next overview [AD-A165080] p 59 N86-27411
- NOAA satellite requirements forecast [AD-A165244] p 40 N86-27414
- GRADIENTS**
- Vegetation and environmental gradients of the Prudhoe Bay region, Alaska [AD-A162022] p 17 N86-24034
- GRANITE**
- Landsat MSS and airborne geophysical data combined for mapping granite in southwest Nova Scotia p 23 A86-37021
- GRASSLANDS**
- Light interception and leaf area estimates from measurements of grass canopy reflectance p 4 A86-33557
- Distinguishing among tallgrass prairie cover types from measurements of multispectral reflectance p 10 A86-36047
- GRAVITATIONAL FIELDS**
- The study of gravity field estimation procedures [AD-A164564] p 19 N86-26745
- GRAVITY ANOMALIES**
- Evidence for small-scale mantle convection from Seasat altimeter data p 25 A86-31976
- Gravity anomalies and sea surface heights derived from a combined GEOS 3/Seasat altimeter data set p 33 A86-36096
- Structure of the southern Rio Grande rift from gravity interpretation p 18 A86-37795
- GREENLAND**
- Statistical lineament analysis in South Greenland based on Landsat imagery p 22 A86-35676
- GROUND STATIONS**
- Design of the European Space Agency Thematic Mapper processing chains p 51 A86-37864
- GROUND TRUTH**
- One step above ground truth - Airphoto keys for large-scale vegetation analysis p 3 A86-33538
- Analysis of airborne Doppler lidar, Doppler radar and tall tower measurements of atmospheric flows in quiescent and stormy weather [NASA-CR-3960] p 56 N86-23159
- Application of LANDSAT TM images to assess circulation and dispersion in coastal lagoons [NASA-CR-177315] p 44 N86-26665
- Remote sensing and oceanographic equipment technology: Some present systems and future needs, revised [PB86-156502] p 40 N86-26791
- GROUND WATER**
- Stable-isotope studies of groundwaters in southeastern New Mexico [DE86-002590] p 43 N86-23027
- GULF STREAM**
- Remote sensing and oceanographic equipment technology: Some present systems and future needs, revised [PB86-156502] p 40 N86-26791

H

HABITATS

- Ducks Unlimited Joint Research Project
[NASA-TM-88755] p 14 N86-25032

HARMONICS

- The study of gravity field estimation procedures
[AD-A164564] p 19 N86-26745

HAWAII

- Preliminary geologic analyses of SIR-B radar data for Hawaii p 21 A86-33550
Introductory analyses of SIR-B radar data for Hawaii p 21 A86-33551

HAZARDS

- Comprehensive integrated remote sensing for US Department of Energy applications
[DE86-002101] p 17 N86-25036

HEAT FLUX

- A stable iterative procedure to obtain soil surface parameters and fluxes from satellite data p 8 A86-35678

- Evapotranspiration over an agricultural region using a surface flux/temperature model based on NOAA-AVHRR data p 10 A86-36237

- Heat budget and climatic atlas of the equatorial Atlantic Ocean during FGGE (First GARP Global Experiment, 1979

- [PB86-111622] p 35 N86-23213

- An investigation of the marine boundary layer during cold air outbreak

- [NASA-CR-177287] p 39 N86-26758

- Preliminary assessment of soil moisture over vegetation

- [NASA-CR-177226] p 15 N86-27704

- A model for the estimation of the surface fluxes of momentum, heat and moisture of the cloud topped marine atmospheric boundary layer from satellite measurable parameters

- [NASA-CR-177283] p 41 N86-27837

- An investigation of the marine boundary layer during cold air outbreak

- [NASA-CR-177249] p 41 N86-27838

- A model for the estimation of the surface fluxes of momentum, heat, and moisture of the cloud-topped marine atmospheric boundary layer from satellite measurable parameters

- [NASA-CR-177290] p 41 N86-27853

HIERARCHIES

- Hierarchical classification of multitemporal/multispectral scanner data p 49 A86-37017

HIGH RESOLUTION

- An atlas of original and mercator-transformed satellite-data images of the Alboran Sea, August-October 1983

- [AD-A161898] p 36 N86-24170

HIGH SPEED

- High speed image processing system with custom VLSI for DSP --- Digital Signal Processor p 54 A86-33641

HUMIDITY MEASUREMENT

- Satellite-derived moisture profiles
[NOAA-NESDIS-24] p 44 N86-27703

HURRICANES

- The spatial evolution of SAR derived wave spectra in the vicinity of Hurricane IVA p 30 A86-33602

- Satellite observations of sea surface cooling by hurricanes p 32 A86-35545

HYDRODYNAMICS

- Problems of the Arctic and the Antarctic, collection of articles, vol. 57, 1981

- [PB86-106994] p 37 N86-24182

HYDROGRAPHY

- Contributions to the oceanography of the western Alboran Sea

- [AD-A162019] p 37 N86-24173

- Hydrographic data from the OPTOMA program, OPTOMA17: OPTOMA17 P, 21 July 1985, OPTOMA17 leg DI, 10-22 August 1985, OPTOMA17 leg DII, 23 August - 5 September 1985

- [AD-A162067] p 37 N86-24176

HYDROLOGY

- The influence of observational interdependence on spectral reflectance relationships with plant and soil variables p 2 A86-30196

- Physical interpretation of estuarine water color using vector analysis of satellite data p 43 A86-33630

- Optimized retrievals of precipitable water fields from combinations of VAS satellite and conventional surface observations p 43 A86-36193

- Hydrologic and land sciences applications of NOAA polar-orbiting satellite data p 43 N86-23993

HYDROLOGY MODELS

- Large area snowmelt runoff simulations based on Landsat-MSS data p 42 A86-33505

- Hydrologic modeling using Landsat MSS data p 43 A86-37010

HYDROMETEOROLOGY

- Satellite-borne 90 GHz radiometer experiment (SABREX), phase A1 [DFVLR-MITT-85-13] p 57 N86-24000

HYDROPHONES

- Navstar GPS (Global Positioning System) accuracy while surveying arrays of deep ocean transponders [AD-A163364] p 38 N86-26313

ICE

- Marginal ice zone experiment - 1984, physical oceanography report: USNS Lynch and helicopter-based STD data [AD-A163096] p 37 N86-24180

ICE ENVIRONMENTS

- Ice shelves of Antarctica [PB86-106986] p 35 N86-23208

- Problems of the Arctic and the Antarctic, Collection of Articles, Volume 56, 1981 [PB86-107109] p 35 N86-23209

- A review of methods to track oil in arctic waters [AD-A164679] p 39 N86-26716

ICE MAPPING

- SAR remote sensing during MIZEX 84 p 29 A86-33561

- Measurement of sea ice backscatter characteristics at 36 GHz using the surface contour radar p 29 A86-33562

- Aircraft and satellite passive microwave observations of the Bering Sea ice cover during MIZEX West p 32 A86-35683

- Ice shelves of Antarctica [PB86-106986] p 35 N86-23208

ICE REPORTING

- Observations of the polar regions from satellites using active and passive microwave techniques p 28 A86-33489

- Multifrequency observations of brightness temperature of artificial new and young sea ice p 28 A86-33514

- Extracting sea ice data from satellite SAR imagery p 29 A86-33560

- SAR remote sensing during MIZEX 84 p 29 A86-33561

- Ice conditions on the Ohio and Illinois Rivers, 1972-1985 p 42 A86-33617

- Radar sounding of ice masses containing liquid water p 30 A86-33619

ICEBERGS

- Investigation of ice dynamics in the marginal ice zone [AD-A164364] p 38 N86-25962

ICELAND

- Use of Seasat SAR imagery for geological mapping in a volcanic terrain - Askja Caldera, Iceland p 19 A86-30189

IMAGE ANALYSIS

- Techniques for multispectral image classification p 44 A86-32337

- A histogram as the basis of the statistical classification of images p 45 A86-32688

- Weddell-Scotia sea marginal ice zone observations from space, October 1984 p 26 A86-33105

- Context classifier --- pixel classification theory and algorithms p 46 A86-33535

- Analysis of forest/structure using thematic mapper simulator data p 4 A86-33540

- Preliminary geologic analyses of SIR-B radar data for Hawaii p 21 A86-33550

- Forest discrimination with multipolarization imaging radar p 5 A86-33566

- Analysis of L-band multipolarization radar images for lava flow mapping p 21 A86-33593

- The development of an MSS satellite imagery classification expert system p 46 A86-33596

- Slope-intercept-density plots - A new method for line detection in images --- in pixels p 46 A86-33600

- Classification of geophysical parameters using passive microwave satellite measurements p 47 A86-33626

- Variograms and spatial variation in remotely sensed images p 47 A86-33638

- Statistical lineament analysis in South Greenland based on Landsat imagery p 22 A86-35676

- Segmentation of a Thematic Mapper image using the fuzzy c-means clustering algorithm p 9 A86-35687

- The possibility of applying different types of image-analysis software to environment-protection problems --- in remote sensing p 16 A86-36513

- Estimation of atmospheric corrections from multiple aircraft imagery p 49 A86-36784

- Landsat TM image forward/reverse scan banding Characterization and correction p 49 A86-36790

- Estimation of the location parameter of a multispectral distribution by a median operator p 49 A86-37006

- Hierarchical classification of multitemporal/multispectral scanner data p 49 A86-37017

- Multisource data analysis in remote sensing and geographic information processing p 50 A86-37022

- Radar image simulation as a tool to analyze topographic effects on geometry and radiometry of radar imagery p 50 A86-37026

- Measurement of Thematic Mapper data quality p 50 A86-37032

- Wheat area estimation using digital LANDSAT MSS data and aerial photographs [INPE-3824-PRE/900] p 15 N86-26667

- On the information content of multispectral radiance measurements over an ocean --- ESA programs [GKSS-85/E/43] p 40 N86-27697

IMAGE CONTRAST

- Salyut-6 observation of color and brightness contrasts correlated with ocean-bottom relief p 26 A86-32678

IMAGE ENHANCEMENT

- A texture-enhancement procedure for separating orchard from forest in Thematic Mapper data p 2 A86-30198

- Spatial enhancement techniques for multichannel satellite imagery p 47 A86-33639

- Geological mapping potential of computer-enhanced images from the Shuttle Imaging Radar - Lisbon Valley Anticline, Utah p 22 A86-36083

IMAGE PROCESSING

- Image processing system interfaces p 44 A86-32333

- Image segmentation algorithms p 45 A86-32370

- High speed image processing system with custom VLSI for DSP --- Digital Signal Processor p 54 A86-33641

- Resource monitoring oriented remote sensing data processing capabilities p 16 A86-33643

- Satellite orientation and position for geometric correction of scanner imagery p 48 A86-36079

- Certain transformations in a quantitative approach to image processing --- computer techniques for satellite photography p 48 A86-36517

- Computer processing of spectrally superposed data --- subroutines for MSS remote sensing p 49 A86-36518

- Machine processing of remotely sensed data - Quantifying global process: Models, sensor systems, and analytical methods; Proceedings of the Eleventh International Symposium, Purdue University, West Lafayette, IN, June 25-27, 1985 p 56 A86-37001

- High accuracy clustering using residual image --- from Landsat satellite p 49 A86-37003

- An atlas of original and mercator-transformed satellite-data images of the Alboran Sea, August-October 1983 [AD-A161898] p 36 N86-24170

- Ocean wave slope statistics from automated analysis of sun glitter photographs [AD-A161995] p 37 N86-24172

- Application of LANDSAT TM images to assess circulation and dispersion in coastal lagoons [NASA-CR-177315] p 44 N86-26665

- Thematic mapper research in the Earth sciences: Tectonic evaluation of the Nubian Shield of northeastern Sudan/southeastern Egypt using thematic mapper imagery [NASA-CR-177311] p 24 N86-26740

- Spectroradiometric considerations for advanced land observing systems [NASA-CR-177205] p 58 N86-27705

IMAGE RESOLUTION

- Measurement of Thematic Mapper data quality p 50 A86-37032

IMAGING RADAR

- Lithologic signatures in multi-channel SAR imagery p 45 A86-33522

- Forest discrimination with multipolarization imaging radar p 5 A86-33566

IMAGING TECHNIQUES

- Influence of the Yukon River on the Bering Sea [NASA-CR-177310] p 39 N86-26783

INDIAN OCEAN

- Evolution of the net surface shortwave radiation over the Indian Ocean during summer MONEX (1979) - A satellite description p 26 A86-33120

INDIAN SPACE PROGRAM

- Satellite-borne 90 GHz radiometer experiment (SABREX), phase A1 [DFVLR-MITT-85-13] p 57 N86-24000

INDUSTRIAL AREAS

- A preliminary analysis of Landsat MSS and TM data in the Leveck area, Sudbury, Canada p 20 A86-33519

INFORMATION DISSEMINATION

- Ducks Unlimited Joint Research Project [NASA-TM-88755] p 14 N86-25032

- Earthquake and tsunami data services and publications [PB86-156254] p 51 N86-25919

INFORMATION MANAGEMENT

- Economical maintenance of a national topographic data base using Landsat images p 48 A86-36082
- Multisource data analysis in remote sensing and geographic information processing p 50 A86-37022

INFORMATION THEORY

- On the information content of multispectral radiance measurements over an ocean --- ESA programs [GKSS-85/E/43] p 40 N86-27697

INFRARED DETECTORS

- Conceptual design study: Forest Fire Advanced System Technology (FFAST) [JPL-PUBL-86-5] p 14 N86-25034

INFRARED IMAGERY

- Monotemporal, multitemporal, and multirate thermal infrared data acquisition from satellites for soil and surface-material survey p 1 A86-30191
- An algorithm for the identification of cloud cover and the estimation of spectral brightnesses of the cloudless atmosphere according to satellite scanning measurements of outgoing IR radiation p 52 A86-33317
- Estimation of the accuracy of the remote determination of ocean surface temperature on the basis of satellite measurements of outgoing thermal radiation in the 10.5-12.5 micron range p 27 A86-33320
- Spectroscopy of Moses Rock dike using remote sensing p 21 A86-33521
- Vegetation assessment using a combination of visible, near-IR and thermal-IR AVHRR data p 5 A86-33577
- Analysis of effective radiant temperatures in a Pacific Northwest forest using Thermal Infrared Multispectral Scanner data p 9 A86-36042
- Agricultural applications for thermal infrared multispectral scanner data p 12 A86-37034
- An atlas of original and mercator-transformed satellite-data images of the Alboran Sea, August-October 1983 [AD-A161898] p 36 N86-24170

INFRARED INSTRUMENTS

- Passive remote sensing of stratospheric and mesospheric winds p 53 A86-33545
- Analysis of a resistance-energy balance method for estimating daily evaporation from wheat plots using one-time-of-day infrared temperature observations p 13 A86-39148

INFRARED RADIATION

- An atlas of original and mercator-transformed satellite-data images of the Alboran Sea, August-October 1983 [AD-A161898] p 36 N86-24170

INFRARED RADIOMETERS

- Vegetation index and possibility of complementary parameters from AVHRR/2 p 2 A86-30197
- Sea surface temperature determinations p 28 A86-33487
- Precipitation in tropical cyclones p 28 A86-33490

INFRARED REFLECTION

- Near infrared leaf reflectance modeling p 4 A86-33556

INFRARED SIGNATURES

- Near infrared leaf reflectance modeling p 4 A86-33556

INFRARED SPECTROSCOPY

- Possibility of small-scale physiogeographical regionalization using space spectrometry data p 16 A86-30974
- Spectroscopy of Moses Rock dike using remote sensing p 21 A86-33521

INLAND WATERS

- Ice conditions on the Ohio and Illinois Rivers, 1972-1985 p 42 A86-33617

INSTRUMENT ERRORS

- An integrated approach to geometric precision processing of spaceborne high-resolution sensors p 55 A86-34737

INTERFEROMETRY

- Topographic mapping from interferometric synthetic aperture radar observations p 18 A86-36099

INTERNAL WAVES

- Observation of internal waves and seismic waves in the Sicilian Channel p 27 A86-33392
- Surface and internal ocean wave observations p 27 A86-33485
- An overview of the SAR internal wave signature experiment p 31 A86-33645
- SAR-observed internal wave signatures from SARSEX - Initial observations p 31 A86-33646
- SAR observed internal wave signatures from SARSEX-comparisons with SAR imaging models p 31 A86-33647

INTERNATIONAL COOPERATION

- A multi-national consortium opportunity for remote sensing p 58 A86-34111
- International coordination of and contributions to environmental satellite programs [AD-A165142] p 60 N86-28016

INTERPOLATION

- Direction dependent interpolation of aeromagnetic data p 23 A86-37009
- Operational methods for data interpolation [DE85-016050] p 34 N86-15969

ISLANDS

- Methods of obtaining offshore wind direction and sea-state data from X-band aircraft SAR (Synthetic Aperture Radar) imagery of coastal waters [AD-A165552] p 38 N86-26517

ISOTOPES

- Stable-isotope studies of groundwaters in southeastern New Mexico [DE86-002590] p 43 N86-23027

ITERATIVE SOLUTION

- A stable iterative procedure to obtain soil surface parameters and fluxes from satellite data p 8 A86-35678

J**JET STREAMS (METEOROLOGY)**

- Structural features of the easterly jet stream according to satellite data p 26 A86-33315

K**KINEMATICS**

- Investigation of ice dynamics in the marginal ice zone [AD-A164364] p 38 N86-25962
- A study of sea ice kinematics and their relationship to arctic ambient noise. Part 3, Section 1: Ambient noise. Section 2: Ambient noise [AD-A165304] p 39 N86-26788
- A study of sea ice kinematics and their relationship to arctic ambient noise. Part 3, section 3: Ambient noise [AD-A165305] p 40 N86-26789

L**LAGOONS**

- Application of LANDSAT TM images to assess circulation and dispersion in coastal lagoons [NASA-CR-177315] p 44 N86-26665

LAKE MICHIGAN

- Use of Thematic Mapper data to assess water quality in Green Bay and central Lake Michigan p 43 A86-39004

LAND ICE

- Radar sounding of ice masses containing liquid water p 30 A86-33619
- Ice shelves of Antarctica [PB86-106986] p 35 N86-23208

LAND MANAGEMENT

- Remote sensing techniques for the detection of soil erosion and the identification of soil conservation practices p 3 A86-33506

LAND USE

- A stepwise hierarchical multi-binary approach in TM landuse classification --- Thematic Mapping p 46 A86-33597

- Land use mapping using edge density texture measures on Thematic Mapper simulator data p 47 A86-33624

- Use of multitemporal spectral profiles in agricultural land-cover classification p 10 A86-36084
- Application of Shuttle imaging radar data for land use investigations p 51 A86-39150

- Hydrologic and land sciences applications of NOAA polar-orbiting satellite data p 43 N86-23993
- Comprehensive integrated remote sensing for US Department of Energy applications [DE86-002101] p 17 N86-25036

- Research, investigations and technical developments: National mapping program, 1983-1984 [PB86-166097] p 17 N86-26675

LANDSAT SATELLITES

- On-board data compression for advanced Landsat p 45 A86-32368

- Large area snowmelt runoff simulations based on Landsat-MSS data p 42 A86-33505

- Lineament analysis in a test area of northern Mozambique p 20 A86-33520
- California timber volume inventory using Landsat p 4 A86-33541

- Modified cubic convolution resampling for Landsat p 47 A86-33640

- Landsat TM image forward/reverse scan banding Characterization and correction p 49 A86-36790

- High accuracy clustering using residual image --- from Landsat satellite p 49 A86-37003
- Hydrologic modeling using Landsat MSS data p 43 A86-37010

- A measuring reference system to quantify the desertification process in a semiarid ecosystem based on Landsat MSS data p 16 A86-37011

- Detection of biomass by an empiric albedo and spectral reflectance model in the Sahara Desert from Landsat-imagery p 11 A86-37015

- Processing of multi-sensor remotely sensed data to a standard geocoded format p 50 A86-37019

- Integration of high and low resolution satellite data for crop condition assessment p 12 A86-37020

- Use of SIR-A and Landsat MSS data in mapping shrub and intershrub vegetation at Koonamore, South Australia p 13 A86-39003

- EOS radiometer concepts for soil moisture remote sensing [NASA-CR-177854] p 14 N86-23995

- A multidex multitemporal approach to map crops in the early growing season: An application to two Italian irrigation districts: East Sesia and Grande Bonifica Ferrarese --- flue gases [ICW-1811] p 15 N86-26674

LANDSAT 4

- The study of the natural geographic differences in the coastal areas of water covered parts of Marmara region in Turkey with the help of Landsat-4 MSS data using an unsupervised classification algorithm with Euclidean distance p 43 A86-37012

LASER ALTIMETERS

- Remote sensing of atmospheric pressure and sea state using laser altimeters p 28 A86-33529

LAVA

- Introductory analyses of SIR-B radar data for Hawaii p 21 A86-33551

- Analysis of L-band multipolarization radar iamgges for lava flow mapping p 21 A86-33593

- Thematic mapper studies of Andean volcanoes [NASA-CR-176807] p 24 N86-25866

LEAVES

- Satellite-derived leaf-area-index and vegetation maps as input to global carbon cycle models - A hierarchical approach p 2 A86-30194

- Near infrared leaf reflectance modeling p 4 A86-33556

- Spectral characterization of biophysical characteristics in a boreal forest - Relationship between Thematic Mapper band reflectance and leaf area index for Aspen p 8 A86-35677

- Polarization photometer to measure bidirectional reflectance factor R(55 deg, 0 deg, 55 deg, 180 deg) of leaves p 9 A86-35748

LIGHT SCATTERING

- Polarization photometer to measure bidirectional reflectance factor R(55 deg, 0 deg, 55 deg, 180 deg) of leaves p 9 A86-35748

LINEAR POLARIZATION

- Forest discrimination with multipolarization imaging radar p 5 A86-33566

LITHOLOGY

- Lithologic signatures in multi-channel SAR imagery p 45 A86-33522

- The nature and origin of mineral coatings on volcanic rocks of the Black Mountain, Stonewall Mountain and Kane Springs Wash volcanic centers in southern Nevada [NASA-CR-176805] p 24 N86-25912

LITHOSPHERE

- The effective elastic lithosphere under the Cook-Austral and Society islands p 25 A86-32267

LOCUSTS

- Detecting desert locust breeding grounds in the Sahel with satellite data p 16 A86-32537

LONG RANGE WEATHER FORECASTING

- Problems of the Arctic and the Antarctic, collection of articles, vol. 57, 1981 [PB86-106994] p 37 N86-24182

LONG WAVE RADIATION

- Intraseasonal variations of OLR in the tropics during the FGGE year --- outgoing long wave radiation p 48 A86-36227

LOSSLESS EQUIPMENT

- On-board data compression for advanced Landsat p 45 A86-32368

LOUISIANA

- Application of LANDSAT TM images to assess circulation and dispersion in coastal lagoons [NASA-CR-177315] p 44 N86-26665

M**MAGMA**

- Evidence of ongoing crustal deformation related to magmatic activity near Socorro, New Mexico p 18 A86-37797

MAPPING

- Use of SIR-A and Landsat MSS data in mapping shrub and intershrub vegetation at Koonamore, South Australia p 13 A86-39003
- An atlas of original and mercator-transformed satellite-data images of the Alboran Sea, August-October 1983 [AD-A161898] p 36 N86-24170
- Conceptual design study: Forest Fire Advanced System Technology (FFAST) [JPL-PUBL-86-5] p 14 N86-25034
- ENVIROSAT-2000 report: Federal agency satellite requirements [NASA-TM-88752] p 59 N86-26355

MAPS

- Relationships between surface observations over the global oceans and the southern oscillation [PB86-110038] p 35 N86-24112
- Monthly maps of sea level anomalies in the Pacific, 1975-1981. Report on the IGOSS (Integrated Global Ocean Services System) Sea Level Pilot Project [AD-A163061] p 38 N86-25104

MARINE BIOLOGY

- A simulation analysis of the fate of phytoplankton within the mid-Atlantic bight [NASA-CR-177265] p 39 N86-26670

MARINE CHEMISTRY

- Investigation of the content of trace elements in sea aerosols and the surface microlayer off sea water p 32 A86-34754

MARINE ENVIRONMENTS

- The Ocean Topography Experiment (TOPEX) - Some questions answered p 25 A86-32556
- Position fixing afloat --- coordinate determination at sea p 33 A86-36788
- Ducks Unlimited Joint Research Project [NASA-TM-88755] p 14 N86-25032
- An investigation of the marine boundary layer during cold air outbreak [NASA-CR-177287] p 39 N86-26758

MARINE METEOROLOGY

- Structural features of the easterly jet stream according to satellite data p 26 A86-33315
- Seasat microwave wind and rain observations in severe tropical and midlatitude marine storms p 27 A86-33486
- Precipitation in tropical cyclones p 28 A86-33490
- A median filter approach for correcting errors in a vector field p 29 A86-33601
- Waves predicted by the Global Spectral Ocean Wave model off the west coast of Chile during the SIR-B mission p 30 A86-33608
- A simple, objective analysis scheme for scatterometer data --- Seasat A satellite observation of wind over ocean p 32 A86-35550
- Estimation of monthly rainfall from satellite-observed cloud amount in the tropical western Pacific p 43 A86-36234

MARSHLANDS

- The study of the natural geographic differences in the coastal areas of water covered parts of Marmara region in Turkey with the help of Landsat-4 MSS data using an unsupervised classification algorithm with Euclidean distance p 43 A86-37012

MATHEMATICAL MODELS

- Spectral characterization of biophysical characteristics in a boreal forest - Relationship between Thematic Mapper band reflectance and leaf area index for Aspen p 8 A86-35677
- Preliminary assessment of soil moisture over vegetation [NASA-CR-177226] p 15 N86-27704
- An investigation of the marine boundary layer during cold air outbreak [NASA-CR-177249] p 41 N86-27838

MAXIMUM LIKELIHOOD ESTIMATES

- An improved hybrid classifier --- for remote sensing p 8 A86-34744

MEDITERRANEAN SEA

- An atlas of original and mercator-transformed satellite-data images of the Alboran Sea, August-October 1983 [AD-A161898] p 36 N86-24170
- Contributions to the oceanography of the western Alboran Sea [AD-A162019] p 37 N86-24173

MESOSCALE PHENOMENA

- Hydrographic data from the OPTOMA program, OPTOMA17: OPTOMA17 P, 21 July 1985, OPTOMA17 leg D1, 10-22 August 1985, OPTOMA17 leg D11, 23 August - 5 September 1985 [AD-A162067] p 37 N86-24176
- Characteristics of western region flash flood events in GOES imagery and conventional data [NOAA-TM-NESDIS-13] p 44 N86-26668

METEOROLOGICAL INSTRUMENTS

- Passive remote sensing of stratospheric and mesospheric winds p 53 A86-33545

METEOROLOGICAL PARAMETERS

- 100 MHz dielectric constant measurements of snow cover Dependence on environmental and snow pack parameters p 42 A86-33613
- Relationships between surface observations over the global oceans and the southern oscillation [PB86-110038] p 35 N86-24112

METEOROLOGICAL RADAR

- A median filter approach for correcting errors in a vector field p 29 A86-33601

METEOROLOGICAL SATELLITES

- The ARGOS system for positioning and data collection by satellite - Characteristics and performance levels p 56 A86-39559
- Satellite cloud and precipitation analysis using a minicomputer [AD-A163821] p 58 N86-25084
- Federal agency satellite requirements [AD-A165071] p 59 N86-27410
- Comparison of the Defense Meteorological Satellite Program (DMSP) and the NOAA Polar-orbiting Operational Environmental Satellite (POES) program [AD-A165118] p 59 N86-27413
- NOAA satellite requirements forecast [AD-A165244] p 40 N86-27414
- Satellite-derived moisture profiles [NOAA-NESDIS-24] p 44 N86-27703
- Optimum management strategies for the NOAA (National Oceanic and Atmospheric Administration) polar-orbiting operational environmental satellites, 1985-2000. Volume 1 [AD-A165143] p 59 N86-28007

METEOROLOGICAL SERVICES

- Technological improvements to naval aviation weather support p 34 A86-37506
- The ARGOS system for positioning and data collection by satellite - Characteristics and performance levels p 56 A86-39559

METEOROLOGY

- USSR report: Earth sciences [JPRS-UES-86-004] p 34 N86-23017
- Relationships between surface observations over the global oceans and the southern oscillation [PB86-110038] p 35 N86-24112
- Sea ice dynamics and regional meteorology for the Arctic polynya experiment (APEX)-Bering Sea 1985 [PB86-148038] p 38 N86-25939

METHANE

- Small format, oblique, colour aerial photography - An aid to the location of methane seepage p 11 A86-36783

MEXICO

- Application of LANDSAT TM images to assess circulation and dispersion in coastal lagoons [NASA-CR-177315] p 44 N86-26665

MICROWAVE EMISSION

- Microwave emission from row crops p 9 A86-35681

MICROWAVE IMAGERY

- Microwave remote sensing of agricultural crops in Canada p 1 A86-30190
- Multifrequency observations of brightness temperature of artificial new and young sea ice p 28 A86-33514
- Classification of geophysical parameters using passive microwave satellite measurements p 47 A86-33626

MICROWAVE RADIOMETERS

- Determination of the moisture content of nonuniformly moistened soils with a surface transition layer on the basis of microwave spectroradiometry p 2 A86-32684
- Reduction of weather effects in the calculation of sea ice concentration from microwave radiances p 26 A86-33104
- Sea surface temperature determinations p 28 A86-33487
- Possible applications of the microwaves surface soil moisture remote sensing p 6 A86-33582
- An airborne multiple-beam 1.4 GHz pushbroom microwave radiometer p 6 A86-33583
- Microwave backscatter and emission observed from Shuttle Imaging Radar B and an airborne 1.4 GHz radiometer p 53 A86-33584
- Electronically Steered Thinned Array Radiometer (ESTAR) system design, calibration, and sensitivity p 53 A86-33588
- Push-broom microwave radiometer systems for space applications p 53 A86-33589
- High resolution millimeter-wave imaging sensor p 54 A86-33590
- Remote sensing of snow water equivalent using Nimbus-7 SMRR data p 42 A86-33616
- The estimation of atmospheric effects for SPOT using AVHRR channel-1 data p 47 A86-34738

- Estimation of sea-surface temperature from AVHRR data Comments on the paper by Singh et al. (1985) p 31 A86-34743

- Microwave radiometry for oil pollution monitoring, measurements, and systems p 32 A86-35682
- Regression models for vegetation radar-backscattering and radiometric emission p 10 A86-36046
- Satellite-borne 90 GHz radiometer experiment (SABREX), phase A1 [DFVLR-MITT-85-13] p 57 N86-24000

MICROWAVE SCATTERING

- Estimation of biophysical properties of forest canopies through inversion of microwave scatterometer data p 4 A86-33542
- Measurement of sea ice backscatter characteristics at 36 GHz using the surface contour radar p 29 A86-33562
- Millimeter-wave backscatter from snowcover p 42 A86-33615

MICROWAVE SENSORS

- Observations of the polar regions from satellites using active and passive microwave techniques p 28 A86-33489
- Passive microwave soil moisture research p 2 A86-33504
- The fundamentals of microwave remote sensing [SU-84] p 56 N86-23025
- Strategies for the calibration and operational use of the ERS-1 SAR wave mode [JHU/APL/SDO-7565] p 35 N86-23207

MICROWAVE SOUNDING

- Remote sensing of vertical moisture profiles and cloud properties from simulated millimeter wave sounder and microwave imager data p 53 A86-33547

MICROWAVE TRANSMISSION

- Estimation of the weight of vegetation using microwave transmission measurements p 3 A86-33524

MINERAL DEPOSITS

- Lineament analysis in a test area of northern Mozambique p 20 A86-33520

MINERAL EXPLORATION

- Comparison between Landsat MSS and Thematic Mapper data for geobotanical prospecting in the Spanish-Portuguese Pyrite Belt p 7 A86-33628
- Statistical lineament analysis in South Greenland based on Landsat imagery p 22 A86-35676
- Aspects of the geological interpretation of geophysical fields and results of air and space remote-sensing observations of oil-and-gas-bearing territories p 23 A86-36510
- Application of spaceborne and airborne techniques in mineral exploration at Wadi El Allaqi area, Eastern Desert, Egypt p 23 A86-37865

MISSION PLANNING

- ENVIROSAT-2000 report: Federal agency satellite requirements [NASA-TM-88752] p 59 N86-26355

MIXING

- An investigation of the marine boundary layer during cold air outbreak [NASA-CR-177249] p 41 N86-27838

MOBILE COMMUNICATION SYSTEMS

- A technique for assessing the severity of terrain shadowing in mobile satellite service p 51 A86-39545

MODELS

- Site selection and directional models of deserts used for ERBE validation targets [NASA-TP-2540] p 57 N86-23160

MOISTURE

- A model for the estimation of the surface fluxes of momentum, heat and moisture of the cloud topped marine atmospheric boundary layer from satellite measurable parameters [NASA-CR-177283] p 41 N86-27837

MOISTURE CONTENT

- Determination of the moisture content of nonuniformly moistened soils with a surface transition layer on the basis of microwave spectroradiometry p 2 A86-32684
- Utilization of active microwave roughness measurements to improve passive microwave soil moisture estimates over bare soils p 8 A86-35679
- Satellite-derived moisture profiles [NOAA-NESDIS-24] p 44 N86-27703
- Preliminary assessment of soil moisture over vegetation [NASA-CR-177226] p 15 N86-27704
- A model for the estimation of the surface fluxes of momentum, heat, and moisture of the cloud-topped marine atmospheric boundary layer from satellite measurable parameters [NASA-CR-177290] p 41 N86-27853

MOMENTUM

A model for the estimation of the surface fluxes of momentum, heat and moisture of the cloud topped marine atmospheric boundary layer from satellite measurable parameters
[NASA-CR-177283] p 41 N86-27837

MONSOONS

Evolution of the net surface shortwave radiation over the Indian Ocean during summer MONEX (1979) - A satellite description p 26 A86-33120

MORPHOLOGY

Thematic mapper studies of Andean volcanoes
[NASA-CR-176807] p 24 N86-25866

MULTISENSOR APPLICATIONS

Processing of multi-sensor remotely sensed data to a standard geocoded format p 50 A86-37019

MULTISPECTRAL BAND SCANNERS

Techniques for multispectral image classification p 44 A86-32337

Evaluation of Landsat MSS bands and transformations for detecting heavy metal stress in forest-covered areas p 7 A86-33629

Analysis of effective radiant temperatures in a Pacific Northwest forest using Thermal Infrared Multispectral Scanner data p 9 A86-36042

Distinguishing among tallgrass prairie cover types from measurements of multispectral reflectance p 10 A86-36047

Choice of spectral bands for a spaceborne multispectral scanner p 55 A86-36514

An information measure for class discrimination --- in remote sensing of crop observation p 11 A86-36789
Multispectral change detection using difference classification and bitemporal classification p 49 A86-37004

Estimation of the location parameter of a multispectral distribution by a median operator p 49 A86-37006
Hydrologic modeling using Landsat MSS data p 43 A86-37010

A measuring reference system to quantify the desertification process in a semiarid ecosystem based on Landsat MSS data p 16 A86-37011
Hierarchical classification of multitemporal/multispectral scanner data p 49 A86-37017

Processing of multi-sensor remotely sensed data to a standard geocoded format p 50 A86-37019
Integration of high and low resolution satellite data for crop condition assessment p 12 A86-37020

Landsat MSS and airborne geophysical data combined for mapping granite in southwest Nova Scotia p 23 A86-37021
Agricultural applications for thermal infrared multispectral scanner data p 12 A86-37034

Use of SIR-A and Landsat MSS data in mapping shrub and intershrub vegetation at Koonamore, South Australia p 13 A86-39003
Rectification of scanner images using prediction approaches --- airborne scanners p 57 N86-23992

MOMS-01 (Modular Optoelectronic Multispectral Scanner) for Earth observation: First results of STS-7 mission p 57 N86-24003

MULTISPECTRAL LINEAR ARRAYS

Processing of multi-sensor remotely sensed data to a standard geocoded format p 50 A86-37019

MULTISPECTRAL PHOTOGRAPHY

A non-stationary contextual classifier with improved accuracy --- for multispectral data p 47 A86-33621

Spatial enhancement techniques for multichannel satellite imagery p 47 A86-33639

Computer processing of spectrally superposed data --- subroutines for MSS remote sensing p 49 A86-36518

A clustering algorithm for remote sensing multispectral data p 51 A86-37033

MULTIVARIATE STATISTICAL ANALYSIS

Multisource data analysis in remote sensing and geographic information processing p 50 A86-37022

On the information content of multispectral radiance measurements over an ocean --- ESA programs [GKSS-85/E/43] p 40 N86-27697

N**NASA PROGRAMS**

Spaceborne Imaging Radar (SIR) project p 53 A86-33586

NAVIGATION AIDS

Map digitization offers new possibilities [NLR-MP-84061-U] p 51 N86-23028

NAVSTAR SATELLITES

Commercial applications of the Navstar Global Positioning System p 54 A86-34112

NAVY

Technological improvements to naval aviation weather support p 34 A86-37506

NEARSHORE WATER

Determination of sea spectral reflectance from airborne measurements p 26 A86-32683

Directional ocean wave spectra obtained from the Shuttle Imaging Radar off the coast of Chile p 30 A86-33612

NEVADA

The nature and origin of mineral coatings on volcanic rocks of the Black Mountain, Stonewall Mountain and Kane Springs Wash volcanic centers in southern Nevada [NASA-CR-176805] p 24 N86-25912

NEW MEXICO

Stable-isotope studies of groundwaters in southeastern New Mexico [DE86-002590] p 43 N86-23027

NIMBUS 7 SATELLITE

The 1978 oceanic trilogy - Seasat, Nimbus-7, and TIROS-N p 27 A86-33482

NITROGEN DIOXIDE

SAGE observations of stratospheric nitrogen dioxide p 55 A86-36838

NOAA SATELLITES

Experiments on the remote temperature sounding of the atmosphere on the basis of NOAA-satellite radiometer measurements p 52 A86-33318

NOAA plans for remote sensing of the earth, oceans and atmosphere p 52 A86-33502

Integration of high and low resolution satellite data for crop condition assessment p 12 A86-37020

Hydrologic and land sciences applications of NOAA polar-orbiting satellite data p 43 N86-23993

Federal agency satellite requirements [AD-A165071] p 59 N86-27410

Operational satellite support to scientific programs [AD-A165081] p 59 N86-27412

Comparison of the Defense Meteorological Satellite Program (DMSP) and the NOAA Polar-orbiting Operational Environmental Satellite (POES) program [AD-A165118] p 59 N86-27413

NOAA satellite requirements forecast [AD-A165244] p 40 N86-27414

Optimum management strategies for the NOAA (National Oceanic and Atmospheric Administration) polar-orbiting operational environmental satellites, 1985-2000. Volume 1 [AD-A165143] p 59 N86-28007

NOISE (SOUND)

A study of sea ice kinematics and their relationship to arctic ambient noise. Part 3, Section 1: Ambient noise. Section 2: Ambient noise [AD-A165304] p 39 N86-26788

A study of sea ice kinematics and their relationship to arctic ambient noise. Part 3, section 3: Ambient noise [AD-A165305] p 40 N86-26789

NONPARAMETRIC STATISTICS

Nonparametric models and crop classification p 6 A86-33622

NORTH SEA

Archimedes project remote sensing of oil spills North Sea experiment, October 1983. Report on DFVLR (Side-Looking Airborne Radar (SLAR) contribution [DFVLR-FB-85-54] p 35 N86-24002

NORTHERN HEMISPHERE

NOAA Atlas: An atlas of satellite-derived Northern Hemisphere snow cover frequency p 44 N86-24075

NOVA SCOTIA

Landsat MSS and airborne geophysical data combined for mapping granite in southwest Nova Scotia p 23 A86-37021

NUMERICAL ANALYSIS

Application of LANDSAT TM images to assess circulation and dispersion in coastal lagoons [NASA-CR-177315] p 44 N86-26665

NUMERICAL WEATHER FORECASTING

GLAS experiments on the impact of FGGE satellite data on numerical weather prediction p 57 N86-24128

Proceedings of the First National Workshop on the Global Weather Experiment: Current Achievements and Future Directions, volume 2, part 2 [NASA-CR-176722] p 36 N86-24142

NUTRIENTS

Wavelength intensity indices in relation to tree condition and leaf-nutrient content p 12 A86-37036

O**OCEAN BOTTOM**

Evidence for small-scale mantle convection from Seasat altimeter data p 25 A86-31976

The effective elastic lithosphere under the Cook-Austral and Society islands p 25 A86-32267

Salyut-6 observation of color and brightness contrasts correlated with ocean-bottom relief p 26 A86-32678

Objective analysis of tidal fields in the Atlantic and Indian Oceans [NASA-TM-87773] p 39 N86-26782

OCEAN CURRENTS

Near-surface water circulation in the sub-Arctic frontal zone (according to satellite data) p 25 A86-32676

Some features of small-scale ocean eddies according to an analysis of satellite images p 25 A86-32677

Remote sensing and modeling of the dynamics of the western part of the Black Sea p 26 A86-32679

Optimal disposition of satellite-tracked drifting buoys in the South Atlantic p 31 A86-34488

Development of a satellite-tracked oceanographic drifting buoy for the Brazilian Antarctic Program, part 1 (INPE-3793-PRE/888) p 36 N86-24166

Hydrographic data from the OPTOMA program, OPTOMA17: OPTOMA17 P, 21 July 1985, OPTOMA17 leg DI, 10-22 August 1985, OPTOMA17 leg DII, 23 August - 5 September 1985 [AD-A162067] p 37 N86-24176

Studies related to ocean dynamics. Task 3.2: Aircraft Field Test Program to investigate the ability of remote sensing methods to measure current/wind-wave interactions [NASA-CR-168349] p 38 N86-25100

Investigation of ice dynamics in the marginal ice zone [AD-A164364] p 38 N86-25962

OCEAN DATA ACQUISITIONS SYSTEMS

Technological improvements to naval aviation weather support p 34 A86-37506

Strategies for the calibration and operational use of the ERS-1 SAR wave mode [JHU/APL/SDO-7565] p 35 N86-23207

OCEAN DYNAMICS

Remote sensing and modeling of the dynamics of the western part of the Black Sea p 26 A86-32679

Observation of internal waves and seismic waves in the Sicilian Channel p 27 A86-33392

Marginal ice zone experiment - 1984, physical oceanography report: USNS Lynch and helicopter-based STD data [AD-A163096] p 37 N86-24180

Physical oceanography report: Camp-based and helicopter-based STD data from the drifting ice station FRAM 3 [AD-A163097] p 37 N86-24181

Investigation of ice dynamics in the marginal ice zone [AD-A164364] p 38 N86-25962

Remote sensing and oceanographic equipment technology: Some present systems and future needs, revised [PB86-156502] p 40 N86-26791

Operational satellite support to scientific programs [AD-A165081] p 59 N86-27412

OCEAN MODELS

Waves predicted by the Global Spectral Ocean Wave model off the west coast of Chile during the SIR-B mission p 30 A86-33608

Probabilistic modeling of fields of atmospheric turbulence and sea roughness with reference to the study of complex systems --- for flight control p 33 A86-36480

Investigation of ice dynamics in the marginal ice zone [AD-A164364] p 38 N86-25962

OCEAN SURFACE

The design, construction and early trials of a novel airborne surveillance radar p 25 A86-32635

Determination of sea spectral reflectance from airborne measurements p 26 A86-32683

Evolution of the net surface shortwave radiation over the Indian Ocean during summer MONEX (1979) - A satellite description p 26 A86-33120

The 1978 oceanic trilogy - Seasat, Nimbus-7, and TIROS-N p 27 A86-33482

Analysis and interpretation of altimeter sea echo p 27 A86-33483

Oceanic surface winds p 27 A86-33484

Surface and internal ocean wave observations p 27 A86-33485

Spectral measurements in support of SIR-B using the Surface Contour Radar --- for South Pacific p 30 A86-33609

Simulations of SAR wave spectra using high spectral resolution estimates from the SCR and ROWS instruments p 30 A86-33611

Investigation of the content of trace elements in sea aerosols and the surface microlayer off sea water p 32 A86-34754

Intensity modulation in SAR images of internal waves p 32 A86-35531

Microwave radiometry for oil pollution monitoring, measurements, and systems p 32 A86-35682

Gravity anomalies and sea surface heights derived from a combined GEOS 3/Seasat altimeter data set p 33 A86-36096

Position fixing afloat --- coordinate determination at sea p 33 A86-36788
 Remote sensing with the Jindalee skywave radar p 33 A86-36954
 ERS-1 - Our new window on the oceans for the 1990s p 34 A86-38718
 Monthly maps of sea level anomalies in the Pacific, 1975-1981. Report on the IGOSS (Integrated Global Ocean Services System) Sea Level Pilot Project [AD-A163061] p 38 N86-25104
 On land-sea contrast in the Earth radiation budget p 40 N86-27695

OCEANOGRAPHIC PARAMETERS

Integrated global monitoring of the world ocean. Volumes 1, 2, & 3 --- Russian book p 24 A86-31350
 The Ocean Topography Experiment (TOPEX) - Some questions answered p 25 A86-32556
 Some features of small-scale ocean eddies according to an analysis of satellite images p 25 A86-32677
 NOAA plans for remote sensing of the earth, oceans and atmosphere p 52 A86-33502
 Design and benefits of a multibeam Earth Observing Radar p 29 A86-33591
 The spatial evolution of SAR derived wave spectra in the vicinity of Hurricane IVA p 30 A86-33602
 The SIR-B Extreme Waves Experiment in the southern oceans p 30 A86-33607
 Spectral measurements in support of SIR-B using the Surface Contour Radar --- for South Pacific p 30 A86-33609
 Satellite imaging of coastal flow circulation in relation to numerical modelling p 31 A86-33631
 Optimal disposition of satellite-tracked drifting buoys in the South Atlantic p 31 A86-34488
 Estimation of sea-surface temperature from AVHRR data. Comments on the paper by Singh et al. (1985) p 31 A86-34743
 ERS-1 - Our new window on the oceans for the 1990s p 34 A86-38718
 Marginal ice zone experiment - 1984, physical oceanography report: USNS Lynch and helicopter-based STD data [AD-A163096] p 37 N86-24180
 Physical oceanography report: Camp-based and helicopter-based STD data from the drifting ice station FRAM 3 [AD-A163097] p 37 N86-24181
 Problems of the Arctic and the Antarctic, collection of articles, vol. 57, 1981 [PB86-106994] p 37 N86-24182
 On the information content of multispectral radiance measurements over an ocean --- ESA programs [GKSS-85/E/43] p 40 N86-27697

OCEANOGRAPHY

Satellite oceanic remote sensing p 27 A86-33481
 The 1978 oceanic trilogy - Seasat, Nimbus-7, and TIROS-N p 27 A86-33482
 Accuracy estimate of geoid and ocean topography recovered jointly from satellite altimetry p 32 A86-35278
 USSR report: Earth sciences [JPRS-UES-86-004] p 34 N86-23017
 Proceedings of the Arctic Oceanography Conference and Workshop held at the Naval Ocean Research and Development Activity, NSTL, MS. on June 11-14, 1985 [AD-A162578] p 34 N86-23203
 An atlas of original and mercator-transformed satellite-data images of the Alboran Sea, August-October 1983 [AD-A161898] p 36 N86-24170
 Contributions to the oceanography of the western Alboran Sea [AD-A162019] p 37 N86-24173
 Management information (Wave Propagation Laboratory, Boulder, Colorado) [PB86-139524] p 38 N86-25106
 Sea ice dynamics and regional meteorology for the Arctic polynya experiment (APEX)-Bering Sea 1985 [PB86-148038] p 38 N86-25939
 International coordination of and contributions to environmental satellite programs [AD-A165142] p 60 N86-28016

OCEANS

Navstar GPS (Global Positioning System) accuracy while surveying arrays of deep ocean transponders [AD-A163364] p 38 N86-26313
 Objective analysis of tidal fields in the Atlantic and Indian Oceans [NASA-TM-87773] p 39 N86-26782

OFFSHORE ENERGY SOURCES

Oil and gas technologies for the Arctic and deepwater [PB86-119948] p 24 N86-23030

OIL EXPLORATION

Method for the quantitative estimation of convergence in mapping in the case of the interpretation of space photographs of oil-and-gas-bearing regions of Siberia p 23 A86-36505
 The use of remote-sensing data to predict regional and local oil-and-gas-bearing structures within the Dneprovsk-Donetsk paleorift p 23 A86-36508
 Combination of air and space remote-sensing methods and geological-geophysical methods for the purpose of oil and gas exploration in the southern Permsk region p 23 A86-36509
 Oil and gas technologies for the Arctic and deepwater [PB86-119948] p 24 N86-23030

OIL FIELDS

Oil and gas technologies for the Arctic and deepwater [PB86-119948] p 24 N86-23030

OIL POLLUTION

Microwave radiometry for oil pollution monitoring, measurements, and systems p 32 A86-35682
 Archimedes project remote sensing of oil spills North Sea experiment, October 1983. Report on DFVLR (Side-Looking Airborne Radar (SLAR) contribution [DFVLR-FB-85-54] p 35 N86-24002

OIL SLICKS

Satellite thermal observation of oil slicks on the Persian Gulf p 33 A86-36048
 A review of methods to track oil in arctic waters [AD-A164679] p 39 N86-26716

ONBOARD DATA PROCESSING

On-board data compression for advanced Landsat p 45 A86-32368

ONBOARD EQUIPMENT

International coordination of and contributions to environmental satellite programs [AD-A165142] p 60 N86-28016

OPERATIONAL CALCULUS

Operational methods for data interpolation [DE85-016050] p 34 N86-15969

OPTICAL MEASURING INSTRUMENTS

Studies of complex terrain wind flows using acoustic sounder and optical cross-wind remote sensors [DE86-002993] p 58 N86-25925

OPTICAL RADAR

Lidar observations of the planetary boundary layer p 29 A86-33532
 Analysis of airborne Doppler lidar, Doppler radar and tall tower measurements of atmospheric flows in quiescent and stormy weather [NASA-CR-3960] p 56 N86-23159
 Transport processes as manifested in satellite and lidar aerosol measurements p 17 N86-27788

ORCHARDS

A texture-enhancement procedure for separating orchard from forest in Thematic Mapper data p 2 A86-30198

ORGANIZATIONS

A multi-national consortium opportunity for remote sensing p 58 A86-34111

OSCILLATIONS

Relationships between surface observations over the global oceans and the southern oscillation [PB86-110038] p 35 N86-24112

P

PACIFIC OCEAN

The effective elastic lithosphere under the Cook-Austral and Society islands p 25 A86-32267
 Near-surface water circulation in the sub-Arctic frontal zone (according to satellite data) p 25 A86-32676
 Hydrographic data from the OPTOMA program, OPTOMA17: OPTOMA17 P, 21 July 1985, OPTOMA17 leg D1, 10-22 August 1985, OPTOMA17 leg DII, 23 August - 5 September 1985 [AD-A162067] p 37 N86-24176

PALEONTOLOGY

Topographic lineament domains of the Appalachians - Some new methods and techniques for paleostress analysis p 20 A86-33518

PARALLEL PROCESSING (COMPUTERS)

Extended testing of a general contextual classifier using the massively parallel processor - Preliminary results and test plans --- for thematic mapping p 54 A86-33623

PARAMETER IDENTIFICATION

Estimation of the location parameter of a multispectral distribution by a median operator p 49 A86-37006

PASSIVE L-BAND RADIOMETERS

Utilization of active microwave roughness measurements to improve passive microwave soil moisture estimates over bare soils p 8 A86-35679
 Aircraft and satellite passive microwave observations of the Bering Sea ice cover during MIZEX West p 32 A86-35683

PERMITTIVITY

100 MHz dielectric constant measurements of snow cover Dependence on environmental and snow pack parameters p 42 A86-33613

PETROLOGY

What are the best radar wavelengths, incidence angles and polarizations for geologic applications? A statistical approach p 21 A86-33592
 Thematic mapper studies of Andean volcanoes [NASA-CR-176807] p 24 N86-25866

PHOTO GEOLOGY

Use of Seasat SAR imagery for geological mapping in a volcanic terrain - Askja Caldera, Iceland p 19 A86-30189
 Features of the geological application of space data p 19 A86-32680

Interpretation of ring structures on space images and their correlation with geophysical fields and crustal structure in the USSR p 19 A86-32681

Application of space imagery to the identification and geological-geophysical study of hidden plutons in early Proterozoic troughs p 20 A86-32682

Computer-aided interpretation of space images with the aim of structural analysis p 20 A86-32690

A preliminary analysis of Landsat MSS and TM data in the Levack area, Sudbury, Canada p 20 A86-33519

Spectroscopy of Moses Rock dike using remote sensing p 21 A86-33521

Geological mapping potential of computer-enhanced images from the Shuttle Imaging Radar - Lisbon Valley Anticline, Utah p 22 A86-36083

Methods of combined air and space remote-sensing studies of Siberia p 22 A86-36501

Problems and principles of the geological interpretation of remote-sensing data p 22 A86-36502

Combined structural and geomorphological methods for the processing of aerial and space photographic remote-sensing data with the aim of solving geological problems p 22 A86-36503

Method for the quantitative estimation of convergence in mapping in the case of the interpretation of space photographs of oil-and-gas-bearing regions of Siberia p 23 A86-36505

Quantitative assessment of the information content of TV images of different scale on the example of disjunctives of Siberia p 23 A86-36506

Methods for the remote sensing of transition zones of the junction of Siberian platforms and orogens p 23 A86-36507

The use of remote-sensing data to predict regional and local oil-and-gas-bearing structures within the Dneprovsk-Donetsk paleorift p 23 A86-36508

Combination of air and space remote-sensing methods and geological-geophysical methods for the purpose of oil and gas exploration in the southern Permsk region p 23 A86-36509

Aspects of the geological interpretation of geophysical fields and results of air and space remote-sensing observations of oil-and-gas-bearing territories p 23 A86-36510

Application of spaceborne and airborne techniques in mineral exploration at Wadi El Allaqi area, Eastern Desert, Egypt p 23 A86-37865

PHOTOGRAMMETRY

Photogrammetry and remote sensing in periglacial geomorphology p 20 A86-33517

Slope-intercept-density plots - A new method for line detection in images --- in pixels p 46 A86-33600

Practical photogrammetry from 35-mm aerial photography p 55 A86-36080

Research, investigations and technical developments: National mapping program, 1983-1984 [PB86-166097] p 17 N86-26675

PHOTOINTERPRETATION

A texture-enhancement procedure for separating orchard from forest in Thematic Mapper data p 2 A86-30198

Interpretation of ring structures on space images and their correlation with geophysical fields and crustal structure in the USSR p 19 A86-32681

Application of space imagery to the identification and geological-geophysical study of hidden plutons in early Proterozoic troughs p 20 A86-32682

A histogram as the basis of the statistical classification of images p 45 A86-32688

Computer-aided interpretation of space images with the aim of structural analysis p 20 A86-32690

Context classifier --- pixel classification theory and algorithms p 46 A86-33535

Forest discrimination with multipolarization imaging radar p 5 A86-33565
 Approaches to computer reasoning in remote sensing and geographic information processing - A survey p 16 A86-33595
 The development of an MSS satellite imagery classification expert system p 46 A86-33596

- Surface material classification based on spectral shape p 6 A86-33598
- Evaluation of crop acreage estimation methods using Landsat data as auxiliary input p 6 A86-33606
- A non-stationary contextual classifier with improved accuracy --- for multispectral data p 47 A86-33621
- Nonparametric models and crop classification p 6 A86-33622
- Extended testing of a general contextual classifier using the massively parallel processor - Preliminary results and test plans --- for thematic mapping p 54 A86-33623
- Land use mapping using edge density texture measures on Thematic Mapper simulator data p 47 A86-33624
- An improved hybrid classifier --- for remote sensing p 8 A86-34744
- Problems and principles of the geological interpretation of remote-sensing data p 22 A86-36502
- Method for the quantitative estimation of convergence in mapping in the case of the interpretation of space photographs of oil-and-gas-bearing regions of Siberia p 23 A86-36505
- Combination of air and space remote-sensing methods and geological-geophysical methods for the purpose of oil and gas exploration in the southern Permsk region p 23 A86-36509
- Aspects of the geological interpretation of geophysical fields and results of air and space remote-sensing observations of oil-and-gas-bearing territories p 23 A86-36510
- Statistical approach to the classification of objects on air and space remote-sensing images p 48 A86-36515
- A clustering algorithm for remote sensing multispectral data p 51 A86-37033
- Thematic mapper research in the Earth sciences: Tectonic evaluation of the Nubian Shield of northeastern Sudan/southeastern Egypt using thematic mapper imagery [NASA-CR-177311] p 24 N86-26740
- PHOTOMAPPING**
- Vegetation index and possibility of complementary parameters from AVHRR/2 p 2 A86-30197
- Possibility of small-scale physiogeographical regionalization using space spectrometry data p 16 A86-30974
- Formation of a digital data base for automated forest mapping p 2 A86-32689
- Slope-intercept-density plots - A new method for line detection in images --- in pixels p 46 A86-33600
- Problems with global mapping p 48 A86-35111
- Geological mapping potential of computer-enhanced images from the Shuttle Imaging Radar - Lisbon Valley Anticline, Utah p 22 A86-36083
- Topographic mapping from interferometric synthetic aperture radar observations p 18 A86-36099
- Landsat Thematic Mapper geodetic accuracy - Implications for geocoded map compatibility p 18 A86-37024
- PHOTOMETERS**
- Polarization photometer to measure bidirectional reflectance factor R(55 deg, 0 deg, 55 deg, 180 deg) of leaves p 9 A86-35748
- PLAN POSITION INDICATORS**
- The design, construction and early trials of a novel airborne surveillance radar p 25 A86-32635
- PLANETARY BOUNDARY LAYER**
- Lidar observations of the planetary boundary layer p 29 A86-33532
- PLANETARY CRATERS**
- Structure of terrestrial impact craters from SIR-B radar data - Preliminary results p 21 A86-33552
- PLANETARY WAVES**
- Transient response to localized episodic heating in the tropics p 51 N86-27749
- PLANKTON**
- Ocean color measurements p 28 A86-33488
- A simulation analysis of the fate of phytoplankton within the mid-Atlantic bight [NASA-CR-177265] p 39 N86-26670
- Satellite detection of phytoplankton export from the mid-Atlantic Bight during the 1979 spring bloom [NASA-TM-88782] p 41 N86-27699
- High frequency sampling of the 1984 spring bloom within the mid-Atlantic Bight: Synoptic shipboard, aircraft, and in situ perspectives of the SEEP-I experiment [NASA-TM-88765] p 41 N86-27700
- PLANNING**
- NOAA satellite requirements forecast [AD-A165244] p 40 N86-27414
- PLANT STRESS**
- Detection and evaluation of plant stresses for crop management decisions p 5 A86-33578
- Comparison between Landsat MSS and Thematic Mapper data for geobotanical prospecting in the Spanish-Portuguese Pyrite Belt p 7 A86-33628
- Evaluation of Landsat MSS bands and transformations for detecting heavy metal stress in forest-covered areas p 7 A86-33629
- PLANTS (BOTANY)**
- The influence of observational interdependence on spectral reflectance relationships with plant and soil variables p 2 A86-30196
- The tasseled cap - Size, shape and orientation changes due to soil background --- in soil brightness-plant greenness plane p 12 A86-37035
- Separation of soil-plant spectral mixtures by factor analysis p 13 A86-39147
- Vegetation and environmental gradients of the Prudhoe Bay region, Alaska [AD-A162022] p 17 N86-24034
- PLATES (TECTONICS)**
- Evidence for small-scale mantle convection from Seasat altimeter data p 25 A86-31976
- Plate motions and deformations from geologic and geodetic data [NASA-CR-177299] p 18 N86-26741
- Plate motions and deformations from geologic and geodetic data [NASA-CR-177313] p 19 N86-27833
- POLAR METEOROLOGY**
- International coordination of and contributions to environmental satellite programs [AD-A165142] p 60 N86-28016
- POLAR NAVIGATION**
- Proceedings of the Arctic Oceanography Conference and Workshop held at the Naval Ocean Research and Development Activity, NSTL, MS. on June 11-14, 1985 [AD-A162578] p 34 N86-23203
- POLAR ORBITS**
- Hydrologic and land sciences applications of NOAA polar-orbiting satellite data p 43 N86-23993
- Optimum management strategies for the NOAA (National Oceanic and Atmospheric Administration) polar-orbiting operational environmental satellites, 1985-2000. Volume 1 [AD-A165143] p 59 N86-28007
- POLARIZATION (WAVES)**
- Polarization photometer to measure bidirectional reflectance factor R(55 deg, 0 deg, 55 deg, 180 deg) of leaves p 9 A86-35748
- POLARIZATION CHARACTERISTICS**
- Forest discrimination with multipolarization imaging radar p 5 A86-33585
- POLLUTION MONITORING**
- Microwave radiometry for oil pollution monitoring, measurements, and systems p 32 A86-35682
- Satellite thermal observation of oil slicks on the Persian Gulf p 33 A86-36048
- Field and airborne spectral characterization of suspected damage in red spruce (*Picea rubens*) from Vermont p 11 A86-37008
- Archimedes project remote sensing of oil spills North Sea experiment, October 1983. Report on DFVLR (Side-Looking Airborne Radar (SLAR) contribution [DFVLR-FB-85-54] p 35 N86-24002
- POROSITY**
- Stable-isotope studies of groundwaters in southeastern New Mexico [DE86-002590] p 43 N86-23027
- POSITION (LOCATION)**
- Position fixing afloat --- coordinate determination at sea p 33 A86-36788
- POSITIONING**
- Navstar GPS (Global Positioning System) accuracy while surveying arrays of deep ocean transponders [AD-A163364] p 38 N86-26313
- POWER SPECTRA**
- Methods of obtaining offshore wind direction and sea-state data from X-band aircraft SAR (Synthetic Aperture Radar) imagery of coastal waters [AD-A165552] p 38 N86-26517
- PRECIPITATION (METEOROLOGY)**
- Optimized retrievals of precipitable water fields from combinations of VAS satellite and conventional surface observations p 43 A86-36193
- Satellite cloud and precipitation analysis using a minicomputer [AD-A163821] p 58 N86-25084
- PREDICTION ANALYSIS TECHNIQUES**
- Waves predicted by the Global Spectral Ocean Wave model off the west coast of Chile during the SIR-B mission p 30 A86-33608
- Rectification of scanner images using prediction approaches --- airborne scanners [SER-C-303] p 57 N86-23992
- Spectroradiometric considerations for advanced land observing systems [NASA-CR-177205] p 58 N86-27705
- PRODUCTIVITY**
- Modeling the controls of forest productivity using canopy variables p 11 A86-37016
- Remote sensing investigations of wetland biomass and productivity for global biosystems research [NASA-CR-176725] p 14 N86-23994
- PULSE RADAR**
- Topographic mapping from interferometric synthetic aperture radar observations p 18 A86-36099
- PUSHBROOM SENSOR MODES**
- An airborne multiple-beam 1.4 GHz pushbroom microwave radiometer p 6 A86-33583
- Push-broom microwave radiometer systems for space applications p 53 A86-33589
- R**
- RADAR CROSS SECTIONS**
- Open ocean radar sea scatter measurements p 25 A86-32599
- Lithologic signatures in multi-channel SAR imagery p 45 A86-33522
- Description of a databank of normalized radar cross section of terrain p 45 A86-33526
- RADAR DATA**
- Application of Shuttle imaging radar data for land use investigations p 51 A86-39150
- RADAR DETECTION**
- Radar sounding of ice masses containing liquid water p 30 A86-33619
- RADAR ECHOES**
- Analysis and interpretation of altimeter sea echo p 27 A86-33483
- Remote sensing with the Jindalee skywave radar p 33 A86-36954
- RADAR EQUIPMENT**
- The design, construction and early trials of a novel airborne surveillance radar p 25 A86-32635
- RADAR GEOLOGY**
- Evidence for small-scale mantle convection from Seasat altimeter data p 25 A86-31976
- Observation of internal waves and seismic waves in the Sicilian Channel p 27 A86-33392
- RADAR IMAGERY**
- Use of Seasat SAR imagery for geological mapping in a volcanic terrain - Askja Caldera, Iceland p 19 A86-30189
- Microwave remote sensing of agricultural crops in Canada p 1 A86-30190
- Preliminary analysis of SIR-B images for stereo applications p 45 A86-33515
- Structure of terrestrial impact craters from SIR-B radar data - Preliminary results p 21 A86-33552
- Forest discrimination with multipolarization imaging radar p 5 A86-33565
- Spaceborne Imaging Radar (SIR) project p 53 A86-33586
- What are the best radar wavelengths, incidence angles and polarizations for geologic applications? A statistical approach p 21 A86-33592
- Analysis of L-band multipolarization radar images for lava flow mapping p 21 A86-33593
- Multipolarization SAR data for surface feature delineation p 46 A86-33594
- Simulations of SAR wave spectra using high spectral resolution estimates from the SCR and ROWS instruments p 30 A86-33611
- Directional ocean wave spectra obtained from the Shuttle Imaging Radar off the coast of Chile p 30 A86-33612
- SAR image segmentation using digitized field boundaries for crop mapping and monitoring applications p 7 A86-33625
- High speed image processing system with custom VLSI for DSP --- Digital Signal Processor p 54 A86-33641
- Intensity modulation in SAR images of internal waves p 32 A86-33531
- Geological mapping potential of computer-enhanced images from the Shuttle Imaging Radar - Lisbon Valley Anticline, Utah p 22 A86-36083
- Analysis of data acquired by Shuttle Imaging Radar SIR-A and Landsat Thematic Mapper over Baldwin County, Alabama p 12 A86-37018
- Radar image simulation as a tool to analyze topographic effects on geometry and radiometry of radar imagery p 50 A86-37026
- Preliminary science results from the Shuttle Imaging Radar-B p 50 A86-37027
- The fundamentals of microwave remote sensing [SU-84] p 56 N86-23025
- Archimedes project remote sensing of oil spills North Sea experiment, October 1983. Report on DFVLR (Side-Looking Airborne Radar (SLAR) contribution [DFVLR-FB-85-54] p 35 N86-24002
- Methods of obtaining offshore wind direction and sea-state data from X-band aircraft SAR (Synthetic Aperture Radar) imagery of coastal waters [AD-A165552] p 38 N86-26517

RADAR MAPS

RADAR MAPS

- Topographic mapping from interferometric synthetic aperture radar observations p 18 A86-33516
 Extracting sea ice data from satellite SAR imagery p 29 A86-33560

RADAR MEASUREMENT

- Open ocean radar sea scatter measurements p 25 A86-32599
 A preliminary report on the measurements of forest canopies with C-band radar scatterometer at NASA/NSTL p 3 A86-33525
 Measurement of sea ice backscatter characteristics at 36 GHz using the surface contour radar p 29 A86-33562

- Design and benefits of a multibeam Earth Observing Radar p 29 A86-33591
 The SIR-B Extreme Waves Experiment in the southern oceans p 30 A86-33607
 Spectral measurements in support of SIR-B using the Surface Contour Radar --- for South Pacific p 30 A86-33609

- Millimeter-wave backscatter from snowcover p 42 A86-33615
 Satellite cloud and precipitation analysis using a minicomputer [AD-A163821] p 58 N86-25084

RADAR SCATTERING

- Open ocean radar sea scatter measurements p 25 A86-32599
 Radar scatterometer probing of thick vegetation canopies p 3 A86-33523
 A preliminary report on the measurements of forest canopies with C-band radar scatterometer at NASA/NSTL p 3 A86-33525
 Modelling of backscatter from vegetation layers p 4 A86-33554
 Backscatter measurements from simulated resonant structures p 4 A86-33555
 Wind dependence of L-band radar backscatter p 33 A86-35860
 Scattering from a random layer embedded with dielectric needles --- for applications to coniferous vegetation p 10 A86-36045
 Regression models for vegetation radar-backscattering and radiometric emission p 10 A86-36046
 Identification of major backscattering sources in trees and shrubs at 10 GHz p 13 A86-39149

RADAR SIGNATURES

- Backscatter measurements from simulated resonant structures p 4 A86-33555
 An overview of the SAR internal wave signature experiment p 31 A86-33645
 SAR-observed internal wave signatures from SARSEX - Initial observations p 31 A86-33646
 SAR observed internal wave signatures from SARSEX-comparisons with SAR imaging models p 31 A86-33647
 Forest signatures in imaging and non-imaging microwave scatterometer data p 9 A86-36037

RADAR TRACKING

- Lidar observations of the planetary boundary layer p 29 A86-33532
 Remote sensing with the Jindalee skywave radar p 33 A86-36954

RADAR TRANSMITTERS

- Research and development of the synthetic aperture radar transmitter and receiver subsystem design and some component test results p 54 A86-33636

RADIANCE

- Site selection and directional models of deserts used for ERBE validation targets [NASA-TP-2540] p 57 N86-23160
 Remote sensing investigations of wetland biomass and productivity for global biosystems research [NASA-CR-176725] p 14 N86-23994

RADIATION MEASUREMENT

- Estimation of the accuracy of the remote determination of ocean surface temperature on the basis of satellite measurements of outgoing thermal radiation in the 10.5-12.5 micron range p 27 A86-33320

RADIATIVE TRANSFER

- Assessing impacts of off-nadir observation on remote sensing of vegetation - Use of the Suits model p 1 A86-30193
 Satellite remote sensing of atmospheric optical depth spectrum p 55 A86-36785
 Spectroradiometric considerations for advanced land observing systems [NASA-CR-177205] p 58 N86-27705

RADIO ALTIMETERS

- Analysis and interpretation of altimeter sea echo p 27 A86-33483
 Design and benefits of a multibeam Earth Observing Radar p 29 A86-33591

- Relative vertical positioning using ground-level transponders with the ERS-1 altimeter p 33 A86-35688

- Gravity anomalies and sea surface heights derived from a combined GEOS 3/Seasat altimeter data set p 33 A86-36096

- Probabilistic modeling of fields of atmospheric turbulence and sea roughness with reference to the study of complex systems --- for flight control p 33 A86-36480

RADIO ANTENNAS

- Development of a satellite-tracked oceanographic drifting buoy for the Brazilian Antarctic Program, part 1 [INPE-3793-PRE/888] p 36 N86-24166

RADIO INTERFEROMETERS

- Topographic mapping from interferometric synthetic aperture radar observations p 18 A86-33516
 Terrain height measurement by synthetic aperture radar with an interferometer p 55 A86-34736

RADIO WAVES

- Remote sensing with the Jindalee skywave radar p 33 A86-36954

RADIOMETERS

- Vegetation assessment using a combination of visible, near-IR and thermal-IR AVHRR data p 5 A86-33577
 EOS radiometer concepts for soil moisture remote sensing [NASA-CR-177854] p 14 N86-23995

RADIOMETRIC CORRECTION

- Landsat TM image forward/reverse scan banding Characterization and correction p 49 A86-36790
 Radar image simulation as a tool to analyze topographic effects on geometry and radiometry of radar imagery p 50 A86-37026
 Spectroradiometric considerations for advanced land observing systems [NASA-CR-177205] p 58 N86-27705

RADIOMETRIC RESOLUTION

- Classification of south Texas farm and range resources using NOAA7 AVHRR satellite imagery p 5 A86-33558
 Integration of high and low resolution satellite data for crop condition assessment p 12 A86-37020

RAIN

- Seasat microwave wind and rain observations in severe tropical and midlatitude marine storms p 27 A86-33486
 Precipitation in tropical cyclones p 28 A86-33490
 Estimation of monthly rainfall from satellite-observed cloud amount in the tropical western Pacific p 43 A86-36234

RAINSTORMS

- Characteristics of western region flash flood events in GOES imagery and conventional data [NOAA-TM-NESDIS-13] p 44 N86-26668

RANGE RESOURCES

- Classification of south Texas farm and range resources using NOAA7 AVHRR satellite imagery p 5 A86-33558

RANGELANDS

- Soil background effects on the spectral response of a three-component rangeland scene p 9 A86-36044

REAL TIME OPERATION

- On-board data compression for advanced Landsat p 45 A86-32368
 Operational satellite support to scientific programs [AD-A165081] p 59 N86-27412

REFERENCE SYSTEMS

- One step above ground truth - Airphoto keys for large-scale vegetation analysis p 3 A86-33538
 A measuring reference system to quantify the desertification process in a semiarid ecosystem based on Landsat MSS data p 16 A86-37011

REFLECTANCE

- Spectral characterization of biophysical characteristics in a boreal forest - Relationship between Thematic Mapper band reflectance and leaf area index for Aspen p 8 A86-35677
 Polarization photometer to measure bidirectional reflectance factor $R(55 \text{ deg}, 0 \text{ deg}, 55 \text{ deg}, 180 \text{ deg})$ of leaves p 9 A86-35748

REForestation

- Timber Resources Inventory and Monitoring Joint Research Project [NASA-TM-88754] p 14 N86-25863

REGIONAL PLANNING

- Timber Resources Inventory and Monitoring Joint Research Project [NASA-TM-88754] p 14 N86-25863

REGIONS

- Possibility of small-scale physiogeographical regionalization using space spectrometry data p 16 A86-30974

REGRESSION ANALYSIS

- A correlation and regression analysis of present canopy closure vs. TMS spectral response for selected forest sites in the San Juan National Forest, Colorado p 3 A86-33539

- Wheat area estimation using digital LANDSAT MSS data and aerial photographs [INPE-3824-PRE/900] p 15 N86-26667

RELIABILITY

- Operational satellite support to scientific programs [AD-A165081] p 59 N86-27412

REMOTE SENSING

- Agricultural and scientific space platforms --- Russian book p 1 A86-29843
 Microwave remote sensing of agricultural crops in Canada p 1 A86-30190
 Remote sensing for developing countries - A case study of Tunisia p 15 A86-30195
 SPOT - A high-precision view of the earth p 52 A86-31222

- Techniques for multispectral image classification p 44 A86-32337

- The design, construction and early trials of a novel airborne surveillance radar p 25 A86-32635

- Remote sensing and modeling of the dynamics of the western part of the Black Sea p 26 A86-32679
 Features of the geological application of space data p 19 A86-32680

- Determination of the moisture content of nonuniformly moistened soils with a surface transition layer on the basis of microwave spectroradiometry p 2 A86-32684

- A histogram as the basis of the statistical classification of images p 45 A86-32688
 Formation of a digital data base for automated forest mapping p 2 A86-32689

- Experiments on the remote temperature sounding of the atmosphere on the basis of NOAA-satellite radiometer measurements p 52 A86-33318

- Estimation of the accuracy of the remote determination of ocean surface temperature on the basis of satellite measurements of outgoing thermal radiation in the 10.5-12.5 micron range p 27 A86-33320

- Satellite oceanic remote sensing p 27 A86-33481
 Sea surface temperature determinations p 28 A86-33487

- 1985 International Geoscience and Remote Sensing Symposium (IGARSS '85), University of Massachusetts, Amherst, October 7-9, 1985, Digest. Volumes 1 & 2 p 52 A86-33501

- NOAA plans for remote sensing of the earth, oceans and atmosphere p 52 A86-33502

- Remote sensing techniques for the detection of soil erosion and the identification of soil conservation practices p 3 A86-33506

- Photogrammetry and remote sensing in periglacial geomorphology p 20 A86-33517

- Topographic lineament domains of the Appalachians - Some new methods and techniques for paleostress analysis p 20 A86-33518

- Spectroscopy of Moses Rock dike using remote sensing p 21 A86-33521

- Radar scatterometer probing of thick vegetation canopies p 3 A86-33523

- Estimation of the weight of vegetation using microwave transmission measurements p 3 A86-33524

- Remote sensing of atmospheric pressure and sea state using laser altimeters p 28 A86-33529

- Lidar observations of the planetary boundary layer p 29 A86-33532

- Context classifier --- pixel classification theory and algorithms p 46 A86-33535

- Analysis of forest/structure using thematic mapper simulator data p 4 A86-33540

- California timber volume inventory using Landsat p 4 A86-33541

- Passive remote sensing of stratospheric and mesospheric winds p 53 A86-33545

- Remote sensing of vertical moisture profiles and cloud properties from simulated millimeter wave sounder and microwave imager data p 53 A86-33547

- Modelling of backscatter from vegetation layers p 4 A86-33554

- Backscatter measurements from simulated resonant structures p 4 A86-33555

- Near infrared leaf reflectance modeling p 4 A86-33556

- Detection and evaluation of plant stresses for crop management decisions p 5 A86-33578
 Development of agrometeorological crop model inputs from remotely sensed information p 6 A86-33579

- Possible applications of the microwaves surface soil moisture remote sensing p 6 A86-33582
 Push-broom microwave radiometer systems for space applications p 53 A86-33589

- What are the best radar wavelengths, incidence angles and polarizations for geologic applications? A statistical approach p 21 A86-33592
- Multipolarization SAR data for surface feature delineation p 46 A86-33594
- Approaches to computer reasoning in remote sensing and geographic information processing - A survey p 16 A86-33595
- Surface material classification based on spectral shape p 6 A86-33598
- Slope-intercept-density plots - A new method for line detection in images --- in pixels p 46 A86-33600
- Ice conditions on the Ohio and Illinois Rivers, 1972-1985 p 42 A86-33617
- Radar sounding of ice masses containing liquid water p 30 A86-33619
- Classification of geophysical parameters using passive microwave satellite measurements p 47 A86-33626
- Spectral components analysis - A bridge between spectral observations and agrometeorological crop models p 7 A86-33627
- Comparison between Landsat MSS and Thematic Mapper data for geobotanical prospecting in the Spanish-Portuguese Pyrite Belt p 7 A86-33628
- Variograms and spatial variation in remotely sensed images p 47 A86-33638
- Resource monitoring oriented remote sensing data processing capabilities p 16 A86-33643
- A multi-national consortium opportunity for remote sensing p 58 A86-34111
- 'New opportunities in remote sensing' p 58 A86-34118
- An improved hybrid classifier --- for remote sensing p 8 A86-34744
- Examples of the automated derivation of digital surface models p 48 A86-35292
- Asian Conference on Remote Sensing, 5th, Kathmandu, Nepal, November 15-18, 1984, Proceedings p 55 A86-35425
- Spectral characterization of biophysical characteristics in a boreal forest - Relationship between Thematic Mapper band reflectance and leaf area index for Aspen p 8 A86-35677
- Microwave emission from row crops p 9 A86-35681
- Microwave radiometry for oil pollution monitoring, measurements, and systems p 32 A86-35682
- Polarization photometer to measure bidirectional reflectance factor R(55 deg, 0 deg, 55 deg, 180 deg) of leaves p 9 A86-35748
- Soil background effects on the spectral response of a three-component rangeland scene p 9 A86-36044
- Scattering from a random layer embedded with dielectric needles --- for applications to coniferous vegetation p 10 A86-36045
- Regression models for vegetation radar-backscattering and radiometric emission p 10 A86-36046
- Distinguishing among tallgrass prairie cover types from measurements of multispectral reflectance p 10 A86-36047
- Effect of dew on canopy reflectance and temperature p 10 A86-36049
- Methods of combined air and space remote-sensing studies of Siberia p 22 A86-36501
- Problems and principles of the geological interpretation of remote-sensing data p 22 A86-36502
- Technical and software facilities at a center for the processing of remote-sensing data p 48 A86-36511
- The possibility of applying different types of image-analysis software to environment-protection problems --- in remote sensing p 16 A86-36513
- Certain transformations in a quantitative approach to image processing --- computer techniques for satellite photography p 48 A86-36517
- Computer processing of spectrally superposed data --- subroutines for MSS remote sensing p 49 A86-36518
- Determination of the spectral characteristics of natural objects on test ranges, and aspects of the efficiency of space systems --- Russian book p 11 A86-36697
- Estimation of atmospheric corrections from multiple aircraft imagery p 49 A86-36784
- Satellite remote sensing of atmospheric optical depth spectrum p 55 A86-36785
- An information measure for class discrimination --- in remote sensing of crop observation p 11 A86-36789
- Remote sensing with the Jindalee skywave radar p 33 A86-36954
- Machine processing of remotely sensed data - Quantifying global process: Models, sensor systems, and analytical methods; Proceedings of the Eleventh International Symposium, Purdue University, West Lafayette, IN, June 25-27, 1985 p 56 A86-37001
- The evolution of remote sensing science and applications p 58 A86-37002
- Multispectral change detection using difference classification and bipartite classification p 49 A86-37004
- Estimation of the location parameter of a multispectral distribution by a median operator p 49 A86-37006
- The emergence of airborne video techniques as an alternative for accessing tropical environments - A historical perspective p 56 A86-37007
- Field and airborne spectral characterization of suspected damage in red spruce (*Picea rubens*) from Vermont p 11 A86-37008
- Direction dependent interpolation of aeromagnetic data p 23 A86-37009
- Hydrologic modeling using Landsat MSS data p 43 A86-37010
- The study of the natural geographic differences in the coastal areas of water covered parts of Marmara region in Turkey with the help of Landsat-4 MSS data using an unsupervised classification algorithm with Euclidean distance p 43 A86-37012
- Adding spatial considerations to the JABOWA model of forest growth p 11 A86-37014
- Modeling the controls of forest productivity using canopy variables p 11 A86-37016
- Hierarchical classification of multitemporal/multispectral scanner data p 49 A86-37017
- Processing of multi-sensor remotely sensed data to a standard geocoded format p 50 A86-37019
- Landsat MSS and airborne geophysical data combined for mapping granite in southwest Nova Scotia p 23 A86-37021
- Multisource data analysis in remote sensing and geographic information processing p 50 A86-37022
- Semi-operational identification of agricultural crops from airborne SLAR-data p 12 A86-37025
- Preliminary science results from the Shuttle Imaging Radar-B p 50 A86-37027
- The SIR-C experiment - Measuring new variables from space with SAR p 50 A86-37028
- Measurement of Thematic Mapper data quality p 50 A86-37032
- Application of spaceborne and airborne techniques in mineral exploration at Wadi El Allaqi area, Eastern Desert, Egypt p 23 A86-37865
- ERS-1 - Our new window on the oceans for the 1990s p 34 A86-38718
- Sun angle, view angle, and background effects on spectral response of simulated balsam fir canopies p 13 A86-39002
- Use of SIR-A and Landsat MSS data in mapping shrub and intershrub vegetation at Koonamore, South Australia p 13 A86-39003
- Use of Thematic Mapper data to assess water quality in Green Bay and central Lake Michigan p 43 A86-39004
- Predicting tree groundline diameter from crown measurements made on 35-mm aerial photography p 13 A86-39006
- Directional reflectance response in AVHRR red and near-IR bands for three cover types and varying atmospheric conditions p 13 A86-39146
- Separation of soil-plant spectral mixtures by factor analysis p 13 A86-39147
- Analysis of a resistance-energy balance method for estimating daily evaporation from wheat plots using one-time-of-day infrared temperature observations p 13 A86-39148
- Identification of major backscattering sources in trees and shrubs at 10 GHz p 13 A86-39149
- The effect of the atmosphere on the satellite remote sensing of earth resources --- Russian book p 56 A86-39969
- The fundamentals of microwave remote sensing [SU-84] p 56 N86-23025
- Analysis of airborne Doppler lidar, Doppler radar and tall tower measurements of atmospheric flows in quiescent and stormy weather [NASA-CR-3960] p 56 N86-23159
- EOS radiometer concepts for soil moisture remote sensing [NASA-CR-177854] p 14 N86-23995
- Comprehensive integrated remote sensing for US Department of Energy applications [DE86-002101] p 17 N86-25036
- Remote monitoring of processes that shape desert surfaces: The Desert Winds Project [T186-900108] p 24 N86-25099
- Studies related to ocean dynamics. Task 3.2: Aircraft Field Test Program to investigate the ability of remote sensing methods to measure current/wind-wave interactions [NASA-CR-168349] p 38 N86-25100
- Management information (Wave Propagation Laboratory, Boulder, Colorado) [PB86-139524] p 38 N86-25106
- A proposal for a project entitled Assessment of Forest Resources in Uruguay submitted to the United Nations Industrial Development Organization (UNIDO) [INPE-3828-NTE/255] p 15 N86-26666
- Research on enhancing the utilization of digital multispectral data and geographic information systems in global habitability studies [NASA-CR-177294] p 17 N86-26669
- Research, investigations and technical developments: National mapping program, 1983-1984 [PB86-166097] p 17 N86-26675
- An investigation of the marine boundary layer during cold air outbreak [NASA-CR-177287] p 39 N86-26758
- Objective analysis of tidal fields in the Atlantic and Indian Oceans [NASA-TM-87773] p 39 N86-26782
- Remote sensing and oceanographic equipment technology: Some present systems and future needs, revised [PB86-156502] p 40 N86-26791
- On the information content of multispectral radiance measurements over an ocean --- ESA programs [GKSS-85/E/43] p 40 N86-27697
- Spectroradiometric considerations for advanced land observing systems [NASA-CR-177205] p 58 N86-27705
- A model for the estimation of the surface fluxes of momentum, heat and moisture of the cloud topped marine atmospheric boundary layer from satellite measurable parameters [NASA-CR-177283] p 41 N86-27837
- An investigation of the marine boundary layer during cold air outbreak [NASA-CR-177249] p 41 N86-27838
- REMOTE SENSORS**
- High resolution millimeter-wave imaging sensor p 54 A86-33590
- Research and development of the synthetic aperture radar transmitter and receiver subsystem design and some component test results p 54 A86-33636
- Applications of sensor payloads p 56 A86-37343
- Proceedings of the Arctic Oceanography Conference and Workshop held at the Naval Ocean Research and Development Activity, NSTL, MS. on June 11-14, 1985 [AD-A162578] p 34 N86-23203
- Studies of complex terrain wind flows using acoustic sounder and optical cross-wind remote sensors [DE86-002993] p 58 N86-25925
- International coordination of and contributions to environmental satellite programs [AD-A165142] p 60 N86-28016
- REMOTELY PILOTTED VEHICLES**
- Applications of sensor payloads p 56 A86-37343
- REQUIREMENTS**
- Federal agency satellite requirements [AD-A165071] p 59 N86-27410
- GOES (Geostationary Operational Environmental Satellite)-next overview [AD-A165080] p 59 N86-27411
- RESEARCH MANAGEMENT**
- Earth science investigations in the United States Antarctic Research Program (USARP) for the period July 1, 1984 - June 30, 1985 [PB86-143773] p 58 N86-25076
- Management information (Wave Propagation Laboratory, Boulder, Colorado) [PB86-139524] p 38 N86-25106
- RESOURCES MANAGEMENT**
- Research on enhancing the utilization of digital multispectral data and geographic information systems in global habitability studies [NASA-CR-177294] p 17 N86-26669
- RING STRUCTURES**
- Interpretation of ring structures on space images and their correlation with geophysical fields and crustal structure in the USSR p 19 A86-32681
- RIO GRANDE (NORTH AMERICA)**
- Structure of the southern Rio Grande rift from gravity interpretation p 18 A86-37795
- RIVERS**
- Influence of the Yukon River on the Bering Sea [NASA-CR-177310] p 39 N86-26783
- ROCK INTRUSIONS**
- Spectroscopy of Moses Rock dike using remote sensing p 21 A86-33521
- ROCKS**
- The nature and origin of mineral coatings on volcanic rocks of the Black Mountain, Stonewall Mountain and Kane Springs Wash volcanic centers in southern Nevada [NASA-CR-176805] p 24 N86-25912

S

S MATRIX THEORY

- Remote sensing with the Jindalee skywave radar p 33 A86-36954

SAGE SATELLITE

SAGE observations of stratospheric nitrogen dioxide
p 55 A86-36838

SAHARA DESERT (AFRICA)

Detection of biomass by an empiric albedo and spectral reflectance model in the Sahara Desert from Landsat-imagery p 11 A86-37015

SALINITY

Comparison of Circulation estimates and winds based on shipboard and satellite-tracked buoy data in Bransfield Strait, 9-14 March, 1985, part 3
[INPE-3795-PRE/890] p 36 N86-24168

Hydrographic data from the OPTOMA program, OPTOMA17: OPTOMA17 P, 21 July 1985, OPTOMA17 leg DI, 10-22 August 1985, OPTOMA17 leg DII, 23 August - 5 September 1985
[AD-A162067] p 37 N86-24176

Marginal ice zone experiment - 1984, physical oceanography report: USNS Lynch and helicopter-based STD data
[AD-A163096] p 37 N86-24180

Physical oceanography report: Camp-based and helicopter-based STD data from the drifting ice station FRAM 3
[AD-A163097] p 37 N86-24181

Application of LANDSAT TM images to assess circulation and dispersion in coastal lagoons
[NASA-CR-177315] p 44 N86-26665

SALYUT SPACE STATION

Possibility of small-scale physiogeographical regionalization using space spectrometry data
p 16 A86-30974

SATELLITE DESIGN

Satellite-borne 90 GHz radiometer experiment (SABREX), phase A1
[DFVLR-MITT-85-13] p 57 N86-24000

SATELLITE DOPPLER POSITIONING

Plate motions and deformations from geologic and geodetic data
[NASA-CR-177299] p 18 N86-26741

SATELLITE IMAGERY

Use of Seasat SAR imagery for geological mapping in a volcanic terrain - Askja Caldera, Iceland
p 19 A86-30189

Monotemporal, multitemporal, and multidecade thermal infrared data acquisition from satellites for soil and surface-material survey
p 1 A86-30191

Assessing impacts of off-nadir observation on remote sensing of vegetation - Use of the Suits model
p 1 A86-30193

Satellite-derived leaf-area-index and vegetation maps as input to global carbon cycle models - A hierarchical approach
p 2 A86-30194

Remote sensing for developing countries - A case study of Tunisia
p 15 A86-30195

Vegetation index and possibility of complementary parameters from AVHRR/2
p 2 A86-30197

Detecting desert locust breeding grounds in the Sahel with satellite data
p 16 A86-32537

Near-surface water circulation in the sub-Arctic frontal zone (according to satellite data)
p 25 A86-32676

Some features of small-scale ocean eddies according to an analysis of satellite images
p 25 A86-32677

Salyut-6 observation of color and brightness contrasts correlated with ocean-bottom relief
p 26 A86-32678

Features of the geological application of space data
p 19 A86-32680

Interpretation of ring structures on space images and their correlation with geophysical fields and crustal structure in the USSR
p 19 A86-32681

Computer-aided interpretation of space images with the aim of structural analysis
p 20 A86-32690

Weddell-Scotia sea marginal ice zone observations from space, October 1984
p 26 A86-33105

Ocean color measurements
p 28 A86-33488

1985 International Geoscience and Remote Sensing Symposium (IGARSS '85), University of Massachusetts, Amherst, October 7-9, 1985, Digest, Volumes 1 & 2
p 52 A86-33501

NOAA plans for remote sensing of the earth, oceans and atmosphere
p 52 A86-33502

Overview of the AgRISTARS research program. I --- Agriculture and Resources Inventory Surveys Through Aerospace Remote Sensing
p 2 A86-33503

Large area snowmelt runoff simulations based on Landsat-MSS data
p 42 A86-33505

A preliminary analysis of Landsat MSS and TM data in the Levack area, Sudbury, Canada
p 20 A86-33519

Remote sensing of clouds
p 52 A86-33533

California timber volume inventory using Landsat
p 4 A86-33541

Structure of terrestrial impact craters from SIR-B radar data - Preliminary results
p 21 A86-33552

Classification of south Texas farm and range resources using NOAA7 AVHRR satellite imagery
p 5 A86-33558

Extracting sea ice data from satellite SAR imagery

p 29 A86-33560

Vegetation assessment using a combination of visible, near-IR and thermal-IR AVHRR data
p 5 A86-33577

The development of an MSS satellite imagery classification expert system
p 46 A86-33596

A stepwise hierarchical multi-binary approach in TM landuse classification --- Thematic Mapping
p 46 A86-33597

USDA/SRS software for Landsat MSS-based crop-acreage estimation
p 6 A86-33605

Evaluation of crop acreage estimation methods using Landsat data as auxiliary input
p 6 A86-33606

Remote sensing of snow water equivalent using Nimbus-7 SMMR data
p 42 A86-33616

Ice conditions on the Ohio and Illinois Rivers, 1972-1985
p 42 A86-33617

Classification of geophysical parameters using passive microwave satellite measurements
p 47 A86-33626

Evaluation of Landsat MSS bands and transformations for detecting heavy metal stress in forest-covered areas
p 7 A86-33629

Physical interpretation of estuarine water color using vector analysis of satellite data
p 43 A86-33630

Satellite imaging of coastal flow circulation in relation to numerical modelling
p 31 A86-33631

Applicability of atmospheric correction algorithm for CZCS data to Japanese coastal area --- Coastal Zone Color Scanner
p 31 A86-33632

Spatial enhancement techniques for multichannel satellite imagery
p 47 A86-33639

An integrated approach to geometric precision processing of spaceborne high-resolution sensors
p 55 A86-34737

The estimation of atmospheric effects for SPOT using AVHRR channel-1 data
p 47 A86-34738

Reflectance modelling and the derivation of vegetation indices for an Australian semi-arid shrubland
p 7 A86-34740

Forestry information content of Thematic Mapper data
p 8 A86-34741

Identifying deforestation in Brazil using multiresolution satellite data
p 8 A86-34742

Statistical lineament analysis in South Greenland based on Landsat imagery
p 22 A86-35676

Segmentation of a Thematic Mapper image using the fuzzy c-means clustering algorithm
p 9 A86-35687

Satellite orientation and position for geometric correction of scanner imagery
p 48 A86-36079

Economical maintenance of a national topographic data base using Landsat images
p 48 A86-36082

Use of multitemporal spectral profiles in agricultural land-cover classification
p 10 A86-36084

Optimized retrievals of precipitable water fields from combinations of VAS satellite and conventional surface observations
p 43 A86-36193

Evapotranspiration over an agricultural region using a surface flux/temperature model based on NOAA-AVHRR data
p 10 A86-36237

Combined structural and geomorphological methods for the processing of aerial and space photographic remote-sensing data with the aim of solving geological problems
p 22 A86-36503

Investigation of the earth from space - A new contribution to the development of structural geomorphology
p 22 A86-36504

The use of remote-sensing data to predict regional and local oil-and-gas-bearing structures within the Dneprovsk-Donetsk paleorift
p 23 A86-36508

Technical and software facilities at a center for the processing of remote-sensing data
p 48 A86-36511

Choice of spectral bands for a spaceborne multispectral scanner
p 55 A86-36514

Statistical approach to the classification of objects on air and space remote-sensing images
p 48 A86-36515

Determination of the spectral characteristics of natural objects on test ranges, and aspects of the efficiency of space systems --- Russian book
p 11 A86-36697

Landsat TM image forward/reverse scan banding Characterization and correction
p 49 A86-36790

The evolution of remote sensing science and applications
p 58 A86-37002

High accuracy clustering using residual image --- from Landsat satellite
p 49 A86-37003

Hydrologic modeling using Landsat MSS data
p 43 A86-37010

A measuring reference system to quantify the desertification process in a semiarid ecosystem based on Landsat MSS data
p 16 A86-37011

The study of the natural geographic differences in the coastal areas of water covered parts of Marmara region in Turkey with the help of Landsat-4 MSS data using an unsupervised classification algorithm with Euclidean distance
p 43 A86-37012

Assessment and trends of Florida's marine fisheries habitat An integration of aerial photography and Thematic Mapper imagery
p 34 A86-37013

Detection of biomass by an empiric albedo and spectral reflectance model in the Sahara Desert from Landsat-imagery
p 11 A86-37015

Analysis of data acquired by Shuttle Imaging Radar SIR-A and Landsat Thematic Mapper over Baldwin County, Alabama
p 12 A86-37018

Integration of high and low resolution satellite data for crop condition assessment
p 12 A86-37020

Landsat Thematic Mapper geodetic accuracy - Implications for geocoded map compatibility
p 18 A86-37024

Design of the European Space Agency Thematic Mapper processing chains
p 51 A86-37864

Application of spaceborne and airborne techniques in mineral exploration at Wadi El Allaqi area, Eastern Desert, Egypt
p 23 A86-37865

A proposal for a project entitled Assessment of Forest Resources in Uruguay submitted to the United Nations Industrial Development Organization (UNIDO)
[INPE-3828-NTE/255] p 15 N86-26666

Wheat area estimation using digital LANDSAT MSS data and aerial photographs
[INPE-3824-PRE/900] p 15 N86-26667

Characteristics of western region flash flood events in GOES imagery and conventional data
[NOAA-TM-NESDIS-13] p 44 N86-26668

A multindex multitemporal approach to map crops in the early growing season: An application to two Italian irrigation districts: East Sesia and Grande Bonifica Ferrarese --- flue gases
[ICW-1611] p 15 N86-26674

Satellite detection of phytoplankton export from the mid-Atlantic Bight during the 1979 spring bloom
[NASA-TM-88782] p 41 N86-27699

Transient response to localized episodic heating in the tropics
p 51 N86-27749

SATELLITE NETWORKS

The ARGOS system for positioning and data collection by satellite - Characteristics and performance levels
p 56 A86-39559

SATELLITE OBSERVATION

Evolution of the net surface shortwave radiation over the Indian Ocean during summer MONEX (1979) - A satellite description
p 26 A86-33120

Satellite oceanic remote sensing
p 27 A86-33481

Observations of the polar regions from satellites using active and passive microwave techniques
p 28 A86-33489

Light interception and leaf area estimates from measurements of grass canopy reflectance
p 4 A86-33557

A multi-national consortium opportunity for remote sensing
p 58 A86-34111

Accuracy estimate of geoid and ocean topography recovered jointly from satellite altimetry
p 32 A86-35278

Satellite observations of sea surface cooling by hurricanes
p 32 A86-35545

A stable iterative procedure to obtain soil surface parameters and fluxes from satellite data
p 8 A86-35678

Satellite thermal observation of oil slicks on the Persian Gulf
p 33 A86-36048

Gravity anomalies and sea surface heights derived from a combined GEOS 3/Seasat altimeter data set
p 33 A86-36096

Intraseasonal variations of OLR in the tropics during the FGGE year --- outgoing long wave radiation
p 48 A86-36227

Estimation of monthly rainfall from satellite-observed cloud amount in the tropical western Pacific
p 43 A86-36234

Satellite remote sensing of atmospheric optical depth spectrum
p 55 A86-36785

An information measure for class discrimination --- in remote sensing of crop observation
p 11 A86-36789

SAGE observations of stratospheric nitrogen dioxide
p 55 A86-36838

Preliminary science results from the Shuttle Imaging Radar-B
p 50 A86-37027

Sea level time series in the equatorial Pacific from satellite altimetry
p 34 A86-38648

The effect of the atmosphere on the satellite remote sensing of earth resources --- Russian book
p 56 A86-39969

NOAA Atlas: An atlas of satellite-derived Northern Hemispheric snow cover frequency
p 44 N86-24075

Proceedings of the First National Workshop on the Global Weather Experiment: Current Achievements and Future Directions, volume 2, part 2
[NASA-CR-176722] p 36 N86-24142

Simulation studies related to the design of post-FGGE observing systems
p 57 N86-24160

- Sea surface temperature from satellites: The impact of FGGE p 36 N86-24161
- Characteristics of western region flash flood events in GOES imagery and conventional data [NOAA-TM-NESDIS-13] p 44 N86-26668
- A simulation analysis of the fate of phytoplankton within the mid-Atlantic bight [NASA-CR-177265] p 39 N86-26670
- A review of methods to track oil in arctic waters [AD-A164679] p 39 N86-26716
- Meteorological Satellite Center Technical Note, no. 13, 1986 [ISSN-0388-9653] p 40 N86-27694
- On land-sea contrast in the Earth radiation budget p 40 N86-27695
- Transport processes as manifested in satellite and lidar aerosol measurements p 17 N86-27788
- A model for the estimation of the surface fluxes of momentum, heat and moisture of the cloud topped marine atmospheric boundary layer from satellite measurable parameters [NASA-CR-177283] p 41 N86-27837
- SATELLITE ORBITS**
- ENVIROSAT-2000 report: Federal agency satellite requirements [NASA-TM-88752] p 59 N86-26355
- SATELLITE ORIENTATION**
- Satellite orientation and position for geometric correction of scanner imagery p 48 N86-36079
- SATELLITE PERTURBATION**
- The study of gravity field estimation procedures [AD-A164564] p 19 N86-26745
- SATELLITE SOUNDING**
- The Ocean Topography Experiment (TOPEX) - Some questions answered p 25 A86-32556
- Structural features of the easterly jet stream according to satellite data p 26 A86-33315
- An algorithm for the identification of cloud cover and the estimation of spectral brightnesses of the cloudless atmosphere according to satellite scanning measurements of outgoing IR radiation p 52 A86-33317
- Estimation of the accuracy of the remote determination of ocean surface temperature on the basis of satellite measurements of outgoing thermal radiation in the 10.5-12.5 micron range p 27 A86-33320
- Satellite oceanic remote sensing p 27 A86-33481
- Optimal disposition of satellite-tracked drifting buoys in the South Atlantic p 31 A86-34488
- SATELLITE TRACKING**
- Development of a satellite-tracked oceanographic drifting buoy for the Brazilian Antarctic Program, part 1 [INPE-3793-PRE/888] p 36 N86-24166
- SATELLITE-BORNE INSTRUMENTS**
- The 1978 oceanic trilogy - Seasat, Nimbus-7, and TIROS-N p 27 A86-33482
- Analysis and interpretation of altimeter sea echo p 27 A86-33483
- Electronically Steered Thinned Array Radiometer (ESTAR) system design, calibration, and sensitivity p 53 A86-33588
- Push-broom microwave radiometer systems for space applications p 53 A86-33589
- Research and development of the synthetic aperture radar transmitter and receiver subsystem design and some component test results p 54 A86-33636
- Terrain height measurement by synthetic aperture radar with an interferometer p 55 A86-34736
- A simple, objective analysis scheme for scatterometer data --- Seasat A satellite observation of wind over ocean p 32 A86-35550
- Relative vertical positioning using ground-level transponders with the ERS-1 altimeter p 33 A86-35688
- Satellite-borne 90 GHz radiometer experiment (SABREX), phase A1 [DFVLR-MITT-85-13] p 57 N86-24000
- SATELLITE-BORNE PHOTOGRAPHY**
- Application of space imagery to the identification and geological-geophysical study of hidden plutons in early Proterozoic troughs p 20 A86-32682
- Methods of combined air and space remote-sensing studies of Siberia p 22 A86-36501
- Certain transformations in a quantitative approach to image processing --- computer techniques for satellite photography p 48 A86-36517
- An atlas of original and mercator-transformed satellite-data images of the Alboran Sea, August-October 1983 [AD-A161898] p 36 N86-24170
- SATELLITES**
- Federal agency satellite requirements [AD-A165071] p 59 N86-27410
- SCATTERING CROSS SECTIONS**
- Backscatter measurements from simulated resonant structures p 4 A86-33555
- Studies related to ocean dynamics. Task 3.2: Aircraft Field Test Program to investigate the ability of remote sensing methods to measure current/wind-wave interactions [NASA-CR-168349] p 38 N86-25100
- SCATTEROMETERS**
- Oceanic surface winds p 27 A86-33484
- Radar scatterometer probing of thick vegetation canopies p 3 A86-33523
- Estimation of biophysical properties of forest canopies through inversion of microwave scatterometer data p 4 A86-33542
- Possible applications of the microwaves surface soil moisture remote sensing p 6 A86-33582
- What are the best radar wavelengths, incidence angles and polarizations for geologic applications? A statistical approach p 21 A86-33592
- A simple, objective analysis scheme for scatterometer data --- Seasat A satellite observation of wind over ocean p 32 A86-35550
- Forest signatures in imaging and non-imaging microwave scatterometer data p 9 A86-36037
- SCENE ANALYSIS**
- Variograms and spatial variation in remotely sensed images p 47 A86-33638
- Multispectral change detection using difference classification and bitemporal classification p 49 A86-37004
- SCIENTIFIC SATELLITES**
- Agricultural and scientific space platforms --- Russian book p 1 A86-29843
- Federal agency satellite requirements [AD-A165071] p 59 N86-27410
- GOES (Geostationary Operational Environmental Satellite)-next overview [AD-A165080] p 59 N86-27411
- Operational satellite support to scientific programs [AD-A165081] p 59 N86-27412
- Comparison of the Defense Meteorological Satellite Program (DMSP) and the NOAA Polar-orbiting Operational Environmental Satellite (POES) program [AD-A165118] p 59 N86-27413
- NOAA satellite requirements forecast [AD-A165244] p 40 N86-27414
- International coordination of and contributions to environmental satellite programs [AD-A165142] p 60 N86-28016
- SEA ICE**
- Weddell-Scotia sea marginal ice zone observations from space, October 1984 p 26 A86-33105
- Observations of the polar regions from satellites using active and passive microwave techniques p 28 A86-33489
- Multifrequency observations of brightness temperature of artificial new and young sea ice p 28 A86-33514
- Extracting sea ice data from satellite SAR imagery p 29 A86-33560
- SAR remote sensing during MIZEX 84 p 29 A86-33561
- Measurement of sea ice backscatter characteristics at 36 GHz using the surface contour radar p 29 A86-33562
- Radar sounding of ice masses containing liquid water p 30 A86-33619
- Aircraft and satellite passive microwave observations of the Bering Sea ice cover during MIZEX West p 32 A86-35683
- Proceedings of the Arctic Oceanography Conference and Workshop held at the Naval Ocean Research and Development Activity, NSTL, MS. on June 11-14, 1985 [AD-A162578] p 34 N86-23203
- Ice shelves of Antarctica [PB86-106986] p 35 N86-23208
- Problems of the Arctic and the Antarctic, Collection of Articles, Volume 56, 1981 [PB86-107109] p 35 N86-23209
- Sea ice dynamics and regional meteorology for the Arctic polynya experiment (APEX)-Bering Sea 1985 [PB86-148038] p 38 N86-25939
- A study of sea ice kinematics and their relationship to arctic ambient noise. Part 3, Section 1: Ambient noise. Section 2: Ambient noise [AD-A165304] p 39 N86-26788
- A study of sea ice kinematics and their relationship to arctic ambient noise. Part 3, section 3: Ambient noise [AD-A165305] p 40 N86-26789
- SEA LEVEL**
- Sea level time series in the equatorial Pacific from satellite altimetry p 34 A86-38648
- Monthly maps of sea level anomalies in the Pacific, 1975 1981. Report on the IGOSS (Integrated Global Ocean Services System) Sea Level Pilot Project [AD-A163061] p 38 N86-25104
- SEA ROUGHNESS**
- Open ocean radar sea scatter measurements p 25 A86-32599
- Probabilistic modeling of fields of atmospheric turbulence and sea roughness with reference to the study of complex systems --- for flight control p 33 A86-36480
- SEA STATES**
- Remote sensing of atmospheric pressure and sea state using laser altimeters p 28 A86-33529
- The SIR-B Extreme Waves Experiment in the southern oceans p 30 A86-33607
- Waves predicted by the Global Spectral Ocean Wave model off the west coast of Chile during the SIR-B mission p 30 A86-33608
- Relative vertical positioning using ground-level transponders with the ERS-1 altimeter p 33 A86-35688
- Methods of obtaining offshore wind direction and sea-state data from X-band aircraft SAR (Synthetic Aperture Radar) imagery of coastal waters [AD-A165552] p 38 N86-26517
- SEA SURFACE TEMPERATURE**
- Estimation of the accuracy of the remote determination of ocean surface temperature on the basis of satellite measurements of outgoing thermal radiation in the 10.5-12.5 micron range p 27 A86-33320
- Sea surface temperature determinations p 28 A86-33487
- Estimation of sea-surface temperature from AVHRR data Comments on the paper by Singh et al. (1985) p 31 A86-34743
- Satellite observations of sea surface cooling by hurricanes p 32 A86-35545
- Heat budget and climatic atlas of the equatorial Atlantic Ocean during FGGE (First GARP Global Experiment, 1979 [PB86-111622] p 35 N86-23213
- Sea surface temperature from satellites: The impact of FGGE p 36 N86-24161
- Sea ice dynamics and regional meteorology for the Arctic polynya experiment (APEX)-Bering Sea 1985 [PB86-148038] p 38 N86-25939
- An investigation of the marine boundary layer during cold air outbreak [NASA-CR-177249] p 41 N86-27838
- SEA WATER**
- Investigation of the content of trace elements in sea aerosols and the surface microlayer off sea water p 32 A86-34754
- A review of methods to track oil in arctic waters [AD-A164679] p 39 N86-26716
- SEASAT SATELLITES**
- Evidence for small-scale mantle convection from Seasat altimeter data p 25 A86-31976
- Observation of internal waves and seismic waves in the Sicilian Channel p 27 A86-33392
- The 1978 oceanic trilogy - Seasat, Nimbus-7, and TIROS-N p 27 A86-33482
- Analysis and interpretation of altimeter sea echo p 27 A86-33483
- Oceanic surface winds p 27 A86-33484
- Surface and internal ocean wave observations p 27 A86-33485
- Seasat microwave wind and rain observations in severe tropical and midlatitude marine storms p 27 A86-33486
- Sea surface temperature determinations p 28 A86-33487
- Precipitation in tropical cyclones p 28 A86-33490
- SEDIMENTS**
- Application of LANDSAT TM images to assess circulation and dispersion in coastal lagoons [NASA-CR-177315] p 44 N86-26665
- Influence of the Yukon River on the Bering Sea [NASA-CR-177310] p 39 N86-26783
- SEGMENTS**
- Image segmentation algorithms p 45 A86-32370
- SEISMIC WAVES**
- Observation of internal waves and seismic waves in the Sicilian Channel p 27 A86-33392
- SEISMOLOGY**
- Earthquake and tsunami data services and publications [PB86-156254] p 51 N86-25919
- SENSITIVITY**
- Methods of obtaining offshore wind direction and sea-state data from X-band aircraft SAR (Synthetic Aperture Radar) imagery of coastal waters [AD-A165552] p 38 N86-26517
- SET THEORY**
- Segmentation of a Thematic Mapper image using the fuzzy c-means clustering algorithm p 9 A86-35687
- SHADOWS**
- A technique for assessing the severity of terrain shadowing in mobile satellite service p 51 A86-39545

SHORT WAVE RADIATION

Evolution of the net surface shortwave radiation over the Indian Ocean during summer MONEX (1979) - A satellite description p 26 A86-33120

SHUTTLE IMAGING RADAR

Preliminary analysis of SIR-B images for stereo applications p 45 A86-33515
Preliminary geologic analyses of SIR-B radar data for Hawaii p 21 A86-33550
Introductory analyses of SIR-B radar data for Hawaii p 21 A86-33551
Microwave backscatter and emission observed from Shuttle Imaging Radar B and an airborne 1.4 GHz radiometer p 53 A86-33584
Spaceborne Imaging Radar (SIR) project p 53 A86-33586
The SIR-B Extreme Waves Experiment in the southern oceans p 30 A86-33607
Spectral measurements in support of SIR-B using the Surface Contour Radar --- for South Pacific p 30 A86-33609
Directional ocean wave spectra obtained from the Shuttle Imaging Radar off the coast of Chile p 30 A86-33612
Geological mapping potential of computer-enhanced images from the Shuttle Imaging Radar - Lisbon Valley Anticline, Utah p 22 A86-36083
Analysis of data acquired by Shuttle Imaging Radar SIR-A and Landsat Thematic Mapper over Baldwin County, Alabama p 12 A86-37018
Preliminary science results from the Shuttle Imaging Radar-B p 50 A86-37027
The SIR-C experiment - Measuring new variables from space with SAR p 50 A86-37028
Use of SIR-A and Landsat MSS data in mapping shrub and intershrub vegetation at Koonamore, South Australia p 13 A86-39003
Application of Shuttle imaging radar data for land use investigations p 51 A86-39150

SIBERIA

Methods of combined air and space remote-sensing studies of Siberia p 22 A86-36501

SICILY

Observation of internal waves and seismic waves in the Sicilian Channel p 27 A86-33392

SIDE-LOOKING RADAR

The design, construction and early trials of a novel airborne surveillance radar p 25 A86-32635
Semi-operational identification of agricultural crops from airborne SLAR-data p 12 A86-37025
Archimedes project remote sensing of oil spills North Sea experiment, October 1983. Report on DFVLR (Side-Looking Airborne Radar (SLAR) contribution [DFVLR-FB-85-54] p 35 N86-24002

SIGNAL ANALYSIS

Analysis and interpretation of altimeter sea echo p 27 A86-33483
Topographic lineament domains of the Appalachians - Some new methods and techniques for paleostress analysis p 20 A86-33518

SIGNAL DETECTORS

Studies of complex terrain wind flows using acoustic sounder and optical cross-wind remote sensors [DE86-002993] p 58 N86-25925

SIGNAL TO NOISE RATIOS

SNR in SAR --- sensitivity in natural terrain sensing p 54 A86-33633

SIGNATURE ANALYSIS

Preliminary assessment of soil moisture over vegetation [NASA-CR-177226] p 15 N86-27704

SILVICULTURE

Timber Resources Inventory and Monitoring Joint Research Project [NASA-TM-88754] p 14 N86-25863

SITE SELECTION

Site selection and directional models of deserts used for ERBE validation targets [NASA-TP-2540] p 57 N86-23160

SKY BRIGHTNESS

An algorithm for the identification of cloud cover and the estimation of spectral brightnesses of the cloudless atmosphere according to satellite scanning measurements of outgoing IR radiation p 52 A86-33317

SNOW COVER

Large area snowmelt runoff simulations based on Landsat-MSS data p 42 A86-33505
100 MHz dielectric constant measurements of snow cover Dependence on environmental and snow pack parameters p 42 A86-33613
Millimeter-wave backscatter from snowcover p 42 A86-33615
Remote sensing of snow water equivalent using Nimbus-7 SMMR data p 42 A86-33616
NOAA Atlas: An atlas of satellite-derived Northern Hemispheric snow cover frequency p 44 N86-24075

SOFTWARE TOOLS

Image processing system interfaces p 44 A86-32333
USDA/SRS software for Landsat MSS-based crop-acreage estimation p 6 A86-33605

The applicability of LOWTRAN 5 computer code to aerial thermographic data correction p 48 A86-34739
Technical and software facilities at a center for the processing of remote-sensing data p 48 A86-36511
The possibility of applying different types of image-analysis software to environment-protection problems --- in remote sensing p 16 A86-36513

SOIL EROSION

Remote sensing techniques for the detection of soil erosion and the identification of soil conservation practices p 3 A86-33506

SOIL MAPPING

Monotemporal, multitemporal, and multirate thermal infrared data acquisition from satellites for soil and surface-material survey p 1 A86-30191

Soil background effects on the spectral response of a three-component rangeland scene p 9 A86-36044
Small format, oblique, colour aerial photography - An aid to the location of methane seepage p 11 A86-36783

The tasseled cap - Size, shape and orientation changes due to soil background --- in soil brightness-plant greenness plane p 12 A86-37035

SOIL MOISTURE

Determination of the moisture content of nonuniformly moistened soils with a surface transition layer on the basis of microwave spectroradiometry p 2 A86-32684
Passive microwave soil moisture research p 2 A86-33504

Possible applications of the microwaves surface soil moisture remote sensing p 6 A86-33582
An airborne multiple-beam 1.4 GHz pushbroom microwave radiometer p 6 A86-33583

Electronically Steered Thinned Array Radiometer (ESTAR) system design, calibration, and sensitivity p 53 A86-33588

EOS radiometer concepts for soil moisture remote sensing [NASA-CR-177854] p 14 N86-23995

SOILS

Utilization of active microwave roughness measurements to improve passive microwave soil moisture estimates over bare soils p 8 A86-35679

Separation of soil-plant spectral mixtures by factor analysis p 13 A86-39147
Vegetation and environmental gradients of the Prudhoe Bay region, Alaska [AD-A162022] p 17 N86-24034

Preliminary assessment of soil moisture over vegetation [NASA-CR-177226] p 15 N86-27704

SOUTHERN HEMISPHERE

Relationships between surface observations over the global oceans and the southern oscillation [PB86-110038] p 35 N86-24112

SPACE COMMERCIALIZATION

Commercial applications of the Navstar Global Positioning System p 54 A86-34112
'New opportunities in remote sensing' p 58 A86-34118

SPACE SHUTTLE MISSION 31-C

MOMS-01 (Modular Optoelectronic Multispectral Scanner) for Earth observation: First results of STS-7 mission p 57 N86-24003

SPACE STATIONS

International coordination of and contributions to environmental satellite programs [AD-A165142] p 60 N86-28016

SPACEBORNE EXPERIMENTS

Spaceborne Imaging Radar (SIR) project p 53 A86-33586

SPACEBORNE PHOTOGRAPHY

Problems with global mapping p 48 A86-35111
MOMS-01 (Modular Optoelectronic Multispectral Scanner) for Earth observation: First results of STS-7 mission p 57 N86-24003

SPACECRAFT COMMUNICATION

Comparison of the Defense Meteorological Satellite Program (DMSP) and the NOAA Polar-orbiting Operational Environmental Satellite (POES) program [AD-A165118] p 59 N86-27413

SPACECRAFT DEFENSE

Comparison of the Defense Meteorological Satellite Program (DMSP) and the NOAA Polar-orbiting Operational Environmental Satellite (POES) program [AD-A165118] p 59 N86-27413

SPECTRAL BANDS

Choice of spectral bands for a spaceborne multispectral scanner p 55 A86-36514

SPECTRAL EMISSION

Department of Geology/NASA-GSFC geobotanical investigation [NASA-CR-177300] p 15 N86-27698

SPECTRAL METHODS

Determination of the moisture content of nonuniformly moistened soils with a surface transition layer on the basis of microwave spectroradiometry p 2 A86-32684
Spectral components analysis - A bridge between spectral observations and agrometeorological crop models p 7 A86-33627

SPECTRAL REFLECTANCE

Assessing impacts of off-nadir observation on remote sensing of vegetation - Use of the Suits model p 1 A86-30193

The influence of observational interdependence on spectral reflectance relationships with plant and soil variables p 2 A86-30196

Determination of sea spectral reflectance from airborne measurements p 26 A86-32683
Near infrared leaf reflectance modeling p 4 A86-33556

Light interception and leaf area estimates from measurements of grass canopy reflectance p 4 A86-33557

Reflectance modelling and the derivation of vegetation indices for an Australian semi-arid shrubland p 7 A86-34740

Soil background effects on the spectral response of a three-component rangeland scene p 9 A86-36044
Distinguishing among tallgrass prairie cover types from measurements of multispectral reflectance p 10 A86-36047

Effect of dew on canopy reflectance and temperature p 10 A86-36049

Determination of the spectral characteristics of natural objects on test ranges, and aspects of the efficiency of space systems --- Russian book p 11 A86-36697

Field and airborne spectral characterization of suspected damage in red spruce (*Picea rubens*) from Vermont p 11 A86-37008

Detection of biomass by an empiric albedo and spectral reflectance model in the Sahara Desert from Landsat-imagery p 11 A86-37015

The tasseled cap - Size, shape and orientation changes due to soil background --- in soil brightness-plant greenness plane p 12 A86-37035

Sun angle, view angle, and background effects on spectral response of simulated balsam fir canopies p 13 A86-39002

Directional reflectance response in AVHRR red and near-IR bands for three cover types and varying atmospheric conditions p 13 A86-39146

Separation of soil-plant spectral mixtures by factor analysis p 13 A86-39147

Department of Geology/NASA-GSFC geobotanical investigation [NASA-CR-177300] p 15 N86-27698

SPECTRAL SIGNATURES

Surface material classification based on spectral shape p 6 A86-33598

SPECTRUM ANALYSIS

A correlation and regression analysis of precent canopy closure vs. TMS spectral response for selected forest sites in the San Juan National Forest, Colorado p 3 A86-33539

SPILLING

A review of methods to track oil in arctic waters [AD-A164679] p 39 N86-26716

SPOT (FRENCH SATELLITE)

SPOT - A high-precision view of the earth p 52 A86-31222

The estimation of atmospheric effects for SPOT using AVHRR channel-1 data p 47 A86-34738

SPRING (SEASON)

High frequency sampling of the 1984 spring bloom within the mid-Atlantic Bight: Synoptic shipboard, aircraft, and in situ perspectives of the SEEP-I experiment [NASA-TM-88765] p 41 N86-27700

STATISTICAL ANALYSIS

Lineament analysis in a test area of northern Mozambique p 20 A86-33520

Statistical lineament analysis in South Greenland based on Landsat imagery p 22 A86-35676

Statistical approach to the classification of objects on air and space remote-sensing images p 48 A86-36515

Wavelength intensity indices in relation to tree condition and leaf-nutrient content p 12 A86-37036

STEREOPHOTOGRAPHY

Preliminary analysis of SIR-B images for stereo applications p 45 A86-33515

STRATOSPHERE

SAGE observations of stratospheric nitrogen dioxide p 55 A86-36838

- Transient response to localized episodic heating in the tropics p 51 N86-27749
- STRATUS CLOUDS**
Satellite cloud and precipitation analysis using a minicomputer [AD-A163821] p 58 N86-25084
- STRESS ANALYSIS**
Topographic lineament domains of the Appalachians - Some new methods and techniques for paleostress analysis p 20 A86-33518
- STRUCTURAL BASINS**
Objective analysis of tidal fields in the Atlantic and Indian Oceans [NASA-TM-87773] p 39 N86-26782
- STRUCTURAL PROPERTIES (GEOLOGY)**
Computer-aided interpretation of space images with the aim of structural analysis p 20 A86-32690
Topographic lineament domains of the Appalachians - Some new methods and techniques for paleostress analysis p 20 A86-33518
Lineament analysis in a test area of northern Mozambique p 20 A86-33520
Statistical lineament analysis in South Greenland based on Landsat imagery p 22 A86-36576
Combined structural and geomorphological methods for the processing of aerial and space photographic remote-sensing data with the aim of solving geological problems p 22 A86-36503
Investigation of the earth from space - A new contribution to the development of structural geomorphology p 22 A86-36504
Quantitative assessment of the information content of TV images of different scale on the example of disjunctives of Siberia p 23 A86-36506
Methods for the remote sensing of transition zones of the junction of Siberian platforms and orogens p 23 A86-36507
Thematic mapper studies of Andean volcanoes [NASA-CR-176807] p 24 N86-25866
The nature and origin of mineral coatings on volcanic rocks of the Black Mountain, Stonewall Mountain and Kane Springs Wash volcanic centers in southern Nevada [NASA-CR-176805] p 24 N86-25912
Thematic mapper research in the Earth sciences: Tectonic evaluation of the Nubian Shield of northeastern Sudan/southeastern Egypt using thematic mapper imagery [NASA-CR-177311] p 24 N86-26740
- SUDAN**
Thematic mapper research in the Earth sciences: Tectonic evaluation of the Nubian Shield of northeastern Sudan/southeastern Egypt using thematic mapper imagery [NASA-CR-177311] p 24 N86-26740
- SUMMER**
Evolution of the net surface shortwave radiation over the Indian Ocean during summer MONEX (1979) - A satellite description p 26 A86-33120
Vegetation and environmental gradients of the Prudhoe Bay region, Alaska [AD-A162022] p 17 N86-24034
- SUPERHIGH FREQUENCIES**
Methods of obtaining offshore wind direction and sea-state data from X-band aircraft SAR (Synthetic Aperture Radar) imagery of coastal waters [AD-A165552] p 38 N86-26517
- SURFACE NAVIGATION**
Position fixing afloat --- coordinate determination at sea p 33 A86-36788
- SURFACE PROPERTIES**
Surface material classification based on spectral shape p 6 A86-33598
The nature and origin of mineral coatings on volcanic rocks of the Black Mountain, Stonewall Mountain and Kane Springs Wash volcanic centers in southern Nevada [NASA-CR-176805] p 24 N86-25912
- SURFACE ROUGHNESS EFFECTS**
Utilization of active microwave roughness measurements to improve passive microwave soil moisture estimates over bare soils p 8 A86-35679
- SURFACE TEMPERATURE**
Evapotranspiration over an agricultural region using a surface flux/temperature model based on NOAA-AVHRR data p 10 A86-36237
Preliminary assessment of soil moisture over vegetation [NASA-CR-177226] p 15 N86-27704
- SURFACE WATER**
Relationships between surface observations over the global oceans and the southern oscillation [PB86-110038] p 35 N86-24112
- SURFACE WAVES**
Surface and internal ocean wave observations p 27 A86-33485
- SYNCHRONOUS METEOROLOGICAL SATELLITE**
International coordination of and contributions to environmental satellite programs [AD-A165142] p 60 N86-28016
- SYNCHRONOUS SATELLITES**
GOES (Geostationary Operational Environmental Satellite)-next overview [AD-A165080] p 59 N86-27411
NOAA satellite requirements forecast [AD-A165244] p 40 N86-27414
Transient response to localized episodic heating in the tropics p 51 N86-27749
- SYNOPTIC METEOROLOGY**
Remote sensing and oceanographic equipment technology: Some present systems and future needs, revised [PB86-156502] p 40 N86-26791
- SYNTHETIC APERTURE RADAR**
Surface and internal ocean wave observations p 27 A86-33485
Topographic mapping from interferometric synthetic aperture radar observations p 18 A86-33516
Lithologic signatures in multi-channel SAR imagery p 45 A86-33522
Introductory analyses of SIR-B radar data for Hawaii p 21 A86-33551
SAR remote sensing during MIZEX 84 p 29 A86-33561
Forest discrimination with multipolarization imaging radar p 5 A86-33565
Forest discrimination with multipolarization imaging radar p 5 A86-33566
Multipolarization SAR data for surface feature delineation p 46 A86-33594
The spatial evolution of SAR derived wave spectra in the vicinity of Hurricane IVA p 30 A86-33602
Simulations of SAR wave spectra using high spectral resolution estimates from the SCR and ROWS instruments p 30 A86-33611
Directional ocean wave spectra obtained from the Shuttle Imaging Radar off the coast of Chile p 30 A86-33612
SAR image segmentation using digitized field boundaries for crop mapping and monitoring applications p 7 A86-33625
SNR in SAR --- sensitivity in natural terrain sensing p 54 A86-33633
Verification of L-band SAR calibration p 54 A86-33634
Research and development of the synthetic aperture radar transmitter and receiver subsystem design and some component test results p 54 A86-33636
High speed image processing system with custom VLSI for DSP --- Digital Signal Processor p 54 A86-33641
An overview of the SAR internal wave signature experiment p 31 A86-33645
SAR-observed internal wave signatures from SARSEX - Initial observations p 31 A86-33646
SAR observed internal wave signatures from SARSEX-comparisons with SAR imaging models p 31 A86-33647
Terrain height measurement by synthetic aperture radar with an interferometer p 55 A86-34736
Intensity modulation in SAR images of internal waves p 32 A86-35531
Topographic mapping from interferometric synthetic aperture radar observations p 18 A86-36099
The SIR-C experiment - Measuring new variables from space with SAR p 50 A86-37028
Methods of obtaining offshore wind direction and sea-state data from X-band aircraft SAR (Synthetic Aperture Radar) imagery of coastal waters [AD-A165552] p 38 N86-26517
- SYNTHETIC APERTURES**
EOS radiometer concepts for soil moisture remote sensing [NASA-CR-177854] p 14 N86-23995
- SYSTEMS ENGINEERING**
Simulation studies related to the design of post-FGGE observing systems p 57 N86-24160
Conceptual design study: Forest Fire Advanced System Technology (FFAST) [JPL-PUBL-86-5] p 14 N86-25034
- T**
- TABLES (DATA)**
International coordination of and contributions to environmental satellite programs [AD-A165142] p 60 N86-28016
- TECHNOLOGY ASSESSMENT**
Conceptual design study: Forest Fire Advanced System Technology (FFAST) [JPL-PUBL-86-5] p 14 N86-25034
- A multindex multitemporal approach to map crops in the early growing season: An application to two Italian irrigation districts: East Sesia and Grande Bonifica Ferrarese --- flue gases [ICW-1611] p 15 N86-26674
- TECHNOLOGY TRANSFER**
Research on enhancing the utilization of digital multispectral data and geographic information systems in global habitability studies [NASA-CR-177294] p 17 N86-26669
- TECHNOLOGY UTILIZATION**
Applications of sensor payloads p 56 A86-37343
- TECTONICS**
Evidence of ongoing crustal deformation related to magmatic activity near Socorro, New Mexico p 18 A86-37797
Plate motions and deformations from geologic and geodetic data [NASA-CR-177299] p 18 N86-26741
Plate motions and deformations from geologic and geodetic data [NASA-CR-177313] p 19 N86-27833
- TELECOMMUNICATION**
GOES (Geostationary Operational Environmental Satellite)-next overview [AD-A165080] p 59 N86-27411
- TELEMETRY**
Proceedings of the Arctic Oceanography Conference and Workshop held at the Naval Ocean Research and Development Activity, NSTL, MS. on June 11-14, 1985 [AD-A162578] p 34 N86-23203
- TEMPERATURE**
Physical oceanography report: Camp-based and helicopter-based STD data from the drifting ice station FRAM 3 [AD-A163097] p 37 N86-24181
- TEMPERATURE GRADIENTS**
Vegetation and environmental gradients of the Prudhoe Bay region, Alaska [AD-A162022] p 17 N86-24034
- TEMPERATURE MEASUREMENT**
Experiments on the remote temperature sounding of the atmosphere on the basis of NOAA-satellite radiometer measurements p 52 A86-33318
Estimation of sea-surface temperature from AVHRR data Comments on the paper by Singh et al. (1985) p 31 A86-34743
Analysis of a resistance-energy balance method for estimating daily evaporation from wheat plots using one-time-of-day infrared temperature observations p 13 A86-39148
Comparison of Circulation estimates and winds based on shipboard and satellite-tracked buoy data in Bransfield Strait, 9-14 March, 1985, part 3 [INPE-3795-PRE/890] p 36 N86-24168
Influence of the Yukon River on the Bering Sea [NASA-CR-177310] p 39 N86-26783
- TEMPORAL RESOLUTION**
Hierarchical classification of multitemporal/multispectral scanner data p 49 A86-37017
- TERRAIN**
A technique for assessing the severity of terrain shadowing in mobile satellite service p 51 A86-39545
Studies of complex terrain wind flows using acoustic sounder and optical cross-wind remote sensors [DE86-002993] p 58 N86-25925
- TERRAIN ANALYSIS**
Preliminary analysis of SIR-B images for stereo applications p 45 A86-33515
Description of a databank of normalized radar cross section of terrain p 45 A86-33526
SNR in SAR --- sensitivity in natural terrain sensing p 54 A86-33633
Terrain height measurement by synthetic aperture radar with an interferometer p 55 A86-34736
An integrated approach to geometric precision processing of spaceborne high-resolution sensors p 55 A86-34737
- TERRESTRIAL RADIATION**
Meteorological Satellite Center Technical Note, no. 13, 1986 [ISSN-0388-9653] p 40 N86-27694
On land-sea contrast in the Earth radiation budget p 40 N86-27695
- TEXTBOOKS**
The fundamentals of microwave remote sensing [SU-84] p 56 N86-23025
- TEXTURES**
Land use mapping using edge density texture measures on Thematic Mapper simulator data p 47 A86-33624
Methods of obtaining offshore wind direction and sea-state data from X-band aircraft SAR (Synthetic Aperture Radar) imagery of coastal waters [AD-A165552] p 38 N86-26517

THEMATIC MAPPING

- Satellite-derived leaf-area-index and vegetation maps as input to global carbon cycle models - A hierarchical approach p 2 A86-30194
- A texture-enhancement procedure for separating orchard from forest in Thematic Mapper data p 2 A86-30198
- Detecting desert locust breeding grounds in the Sahel with satellite data p 16 A86-32537
- Formation of a digital data base for automated forest mapping p 2 A86-32689
- A preliminary analysis of Landsat MSS and TM data in the Levack area, Sudbury, Canada p 20 A86-33519
- A correlation and regression analysis of present canopy closure vs. TMS spectral response for selected forest sites in the San Juan National Forest, Colorado p 3 A86-33539
- Analysis of forest/structure using thematic mapper simulator data p 4 A86-33540
- Analysis of L-band multipolarization radar images for lava flow mapping p 21 A86-33593
- A stepwise hierarchical multi-binary approach in TM landuse classification --- Thematic Mapping p 46 A86-33597
- Extended testing of a general contextual classifier using the massively parallel processor - Preliminary results and test plans --- for thematic mapping p 54 A86-33623
- Land use mapping using edge density texture measures on Thematic Mapper simulator data p 47 A86-33624
- SAR image segmentation using digitised field boundaries for crop mapping and monitoring applications p 7 A86-33625
- Physical interpretation of estuarine water color using vector analysis of satellite data p 43 A86-33630
- Spatial enhancement techniques for multichannel satellite imagery p 47 A86-33639
- Modified cubic convolution resampling for Landsat p 47 A86-33640
- Multi-crop area estimation and mapping on a microprocessor/mainframe network p 7 A86-33644
- Forestry information content of Thematic Mapper data p 8 A86-34741
- Problems with global mapping p 48 A86-35111
- Spectral characterization of biophysical characteristics in a boreal forest - Relationship between Thematic Mapper band reflectance and leaf area index for Aspen p 8 A86-35677
- Segmentation of a Thematic Mapper image using the fuzzy c-means clustering algorithm p 9 A86-35687
- Method for the quantitative estimation of convergence in mapping in the case of the interpretation of space photographs of oil-and-gas-bearing regions of Siberia p 23 A86-36505
- Landsat TM image forward/reverse scan banding Characterization and correction p 49 A86-36790
- Assessment and trends of Florida's marine fisheries habitat An integration of aerial photography and Thematic Mapper imagery p 34 A86-37013
- Analysis of data acquired by Shuttle Imaging Radar SIR-A and Landsat Thematic Mapper over Baldwin County, Alabama p 12 A86-37018
- Landsat MSS and airborne geophysical data combined for mapping granite in southwest Nova Scotia p 23 A86-37021
- Landsat Thematic Mapper geodetic accuracy - Implications for geocoded map compatibility p 18 A86-37024
- Measurement of Thematic Mapper data quality p 50 A86-37032
- Design of the European Space Agency Thematic Mapper processing chains p 51 A86-37864
- Use of Thematic Mapper data to assess water quality in Green Bay and central Lake Michigan p 43 A86-39004
- Remote sensing investigations of wetland biomass and productivity for global biosystems research [NASA-CR-176725] p 14 N86-23994
- Ducks Unlimited Joint Research Project [NASA-TM-88755] p 14 N86-25032
- A proposal for a project entitled Assessment of Forest Resources in Uruguay submitted to the United Nations Industrial Development Organization (UNIDO) [INPE-3828-NTE/255] p 15 N86-26666
- A multindex multitemporal approach to map crops in the early growing season: An application to two Italian irrigation districts: East Sesia and Grande Bonifiga Ferrarese --- flue gases [ICW-1611] p 15 N86-26674
- Research, investigations and technical developments: National mapping program, 1983-1984 [PB86-166097] p 17 N86-26675
- Department of Geology/NASA-GSFC geobotanical investigation [NASA-CR-177300] p 15 N86-27698

THERMAL MAPPING

- Monotemporal, multitemporal, and multiday thermal infrared data acquisition from satellites for soil and surface-material survey p 1 A86-30191
- Vegetation assessment using a combination of visible, near-IR and thermal-IR AVHRR data p 5 A86-33577
- The applicability of LOWTRAN 5 computer code to aerial thermographic data correction p 48 A86-34739
- Analysis of effective radiant temperatures in a Pacific Northwest forest using Thermal Infrared Multispectral Scanner data p 9 A86-36042
- Satellite thermal observation of oil slicks on the Persian Gulf p 33 A86-36048
- Agricultural applications for thermal infrared multispectral scanner data p 12 A86-37034
- THERMAL POLLUTION**
- Comprehensive integrated remote sensing for US Department of Energy applications [DE86-002101] p 17 N86-25036
- THERMISTORS**
- Development of a satellite-tracked oceanographic drifting buoy for the Brazilian Antarctic Program, part 1 [INPE-3793-PRE/888] p 36 N86-24166
- THERMOGRAPHY**
- The applicability of LOWTRAN 5 computer code to aerial thermographic data correction p 48 A86-34739
- TIDES**
- An atlas of original and mercator-transformed satellite-data images of the Alboran Sea, August-October 1983 [AD-A161898] p 36 N86-24170
- Objective analysis of tidal fields in the Atlantic and Indian Oceans [NASA-TM-87773] p 39 N86-26782
- TIMBER INVENTORY**
- Analysis of forest/structure using thematic mapper simulator data p 4 A86-33540
- California timber volume inventory using Landsat p 4 A86-33541
- Identifying deforestation in Brazil using multiresolution satellite data p 8 A86-34742
- Adding spatial considerations to the JABOWA model of forest growth p 11 A86-37014
- Predicting tree groundline diameter from crown measurements made on 35-mm aerial photography p 13 A86-39006
- Timber Resources Inventory and Monitoring Joint Research Project [NASA-TM-88754] p 14 N86-25863
- A proposal for a project entitled Assessment of Forest Resources in Uruguay submitted to the United Nations Industrial Development Organization (UNIDO) [INPE-3828-NTE/255] p 15 N86-26666
- TIMBER VIGOR**
- Evaluation of Landsat MSS bands and transformations for detecting heavy metal stress in forest-covered areas p 7 A86-33629
- TIME SERIES ANALYSIS**
- Sea level time series in the equatorial Pacific from satellite altimetry p 34 A86-38648
- TIROS N SERIES SATELLITES**
- The 1978 oceanic trilogy - Seasat, Nimbus-7, and TIROS-N p 27 A86-33482
- TOPEX**
- The Ocean Topography Experiment (TOPEX) - Some questions answered p 25 A86-32556
- TOPOGRAPHY**
- Topographic mapping from interferometric synthetic aperture radar observations p 18 A86-33516
- Topographic lineament domains of the Appalachians - Some new methods and techniques for paleostress analysis p 20 A86-33518
- Lithologic signatures in multi-channel SAR imagery p 45 A86-33522
- Accuracy estimate of geoid and ocean topography recovered jointly from satellite altimetry p 32 A86-35278
- Economical maintenance of a national topographic data base using Landsat images p 48 A86-36082
- Topographic mapping from interferometric synthetic aperture radar observations p 18 A86-36099
- Radar image simulation as a tool to analyze topographic effects on geometry and radiometry of radar imagery p 50 A86-37026
- Vegetation and environmental gradients of the Prudhoe Bay region, Alaska [AD-A162022] p 17 N86-24034
- Thematic mapper studies of Andean volcanoes [NASA-CR-176807] p 24 N86-25866
- The nature and origin of mineral coatings on volcanic rocks of the Black Mountain, Stonewall Mountain and Kane Springs Wash volcanic centers in southern Nevada [NASA-CR-176805] p 24 N86-25912
- Objective analysis of tidal fields in the Atlantic and Indian Oceans [NASA-TM-87773] p 39 N86-26782

TRACE ELEMENTS

- Investigation of the content of trace elements in sea aerosols and the surface microlayer off sea water p 32 A86-34754

TRACKING (POSITION)

- Navstar GPS (Global Positioning System) accuracy while surveying arrays of deep ocean transponders [AD-A163364] p 38 N86-26313
- A review of methods to track oil in arctic waters [AD-A164679] p 39 N86-26716

TRAJECTORY MEASUREMENT

- Investigation of ice dynamics in the marginal ice zone [AD-A164364] p 38 N86-25962

TRANSPONDERS

- Relative vertical positioning using ground-level transponders with the ERS-1 altimeter p 33 A86-35688
- Navstar GPS (Global Positioning System) accuracy while surveying arrays of deep ocean transponders [AD-A163364] p 38 N86-26313

TREES (PLANTS)

- Predicting tree groundline diameter from crown measurements made on 35-mm aerial photography p 13 A86-39006
- Identification of major backscattering sources in trees and shrubs at 10 GHz p 13 A86-39149
- Timber Resources Inventory and Monitoring Joint Research Project [NASA-TM-88754] p 14 N86-25863

TROPICAL METEOROLOGY

- Structural features of the easterly jet stream according to satellite data p 26 A86-33315
- Intraseasonal variations of OLR in the tropics during the FGGE year --- outgoing long wave radiation p 48 A86-36227
- Estimation of monthly rainfall from satellite-observed cloud amount in the tropical western Pacific p 43 A86-36234
- Proceedings of the First National Workshop on the Global Weather Experiment: Current Achievements and Future Directions, volume 2, part 2 [NASA-CR-176722] p 36 N86-24142
- Transient response to localized episodic heating in the tropics p 51 N86-27749

TROPICAL REGIONS

- The emergence of airborne video techniques as an alternative for accessing tropical environments - A historical perspective p 56 A86-37007

TROPICAL STORMS

- Seasat microwave wind and rain observations in severe tropical and midlatitude marine storms p 27 A86-33486
- Precipitation in tropical cyclones p 28 A86-33490

TSUNAMI WAVES

- Earthquake and tsunami data services and publications [PB86-156254] p 51 N86-25919

TURBULENCE

- Methods of obtaining offshore wind direction and sea-state data from X-band aircraft SAR (Synthetic Aperture Radar) imagery of coastal waters [AD-A165552] p 38 N86-26517

TURKEY

- The study of the natural geographic differences in the coastal areas of water covered parts of Marmara region in Turkey with the help of Landsat-4 MSS data using an unsupervised classification algorithm with Euclidean distance p 43 A86-37012

TYPHOONS

- Meteorological Satellite Center Technical Note, no. 13, 1986 [ISSN-0388-9653] p 40 N86-27694

U

U.S.S.R.

- Interpretation of ring structures on space images and their correlation with geophysical fields and crustal structure in the USSR p 19 A86-32681
- USSR report: Earth sciences [JPRS-UES-86-004] p 34 N86-23017

U.S.S.R. SPACE PROGRAM

- Agricultural and scientific space platforms --- Russian book p 1 A86-29843

ULTRAHIGH FREQUENCIES

- Wind dependence of L-band radar backscatter p 33 A86-35860

URUGUAY

- A proposal for a project entitled Assessment of Forest Resources in Uruguay submitted to the United Nations Industrial Development Organization (UNIDO) [INPE-3828-NTE/255] p 15 N86-26666

USER REQUIREMENTS

- Conceptual design study: Forest Fire Advanced System Technology (FFAST)
[JPL-PUBL-86-5] p 14 N86-25034
- ENVIROSAT-2000 report: Federal agency satellite requirements
[NASA-TM-88752] p 59 N86-26355

V

VAPORS

- An investigation of the marine boundary layer during cold air outbreak
[NASA-CR-177249] p 41 N86-27838

VEGETATION

- Satellite-derived leaf-area-index and vegetation maps as input to global carbon cycle models - A hierarchical approach p 2 A86-30194

- Estimation of the weight of vegetation using microwave transmission measurements p 3 A86-33524
- One step above ground truth - Airphoto keys for large-scale vegetation analysis p 3 A86-33538

- Modelling of backscatter from vegetation layers p 4 A86-33554

- Forestry information content of Thematic Mapper data p 8 A86-34741

- Use of SIR-A and Landsat MSS data in mapping shrub and intershrub vegetation at Koonamore, South Australia p 13 A86-39003

- Vegetation and environmental gradients of the Prudhoe Bay region, Alaska
[AD-A162022] p 17 N86-24034

- The nature and origin of mineral coatings on volcanic rocks of the Black Mountain, Stonewall Mountain and Kane Springs Wash volcanic centers in southern Nevada
[NASA-CR-176805] p 24 N86-25912

- Operational satellite support to scientific programs
[AD-A165081] p 59 N86-27412

VEGETATION GROWTH

- Scattering from a random layer embedded with dielectric needles --- for applications to coniferous vegetation p 10 A86-36045

- Regression models for vegetation radar-backscattering and radiometric emission p 10 A86-36046

- Distinguishing among tallgrass prairie cover types from measurements of multispectral reflectance p 10 A86-36047

- Evapotranspiration over an agricultural region using a surface flux/temperature model based on NOAA-AVHRR data p 10 A86-36237

- Adding spatial considerations to the JABOWA model of forest growth p 11 A86-37014

- Detection of biomass by an empiric albedo and spectral reflectance model in the Sahara Desert from Landsat-imagery p 11 A86-37015

- The tasseled cap - Size, shape and orientation changes due to soil background --- in soil brightness-plant greenness plane p 12 A86-37035

VEGETATIVE INDEX

- Diurnal patterns of bidirectional vegetation indices for wheat canopies p 1 A86-30192

- Vegetation index and possibility of complementary parameters from AVHRR/2 p 2 A86-30197

- Light interception and leaf area estimates from measurements of grass canopy reflectance p 4 A86-33557

- Reflectance modelling and the derivation of vegetation indices for an Australian semi-arid shrubland p 7 A86-34740

- Directional reflectance response in AVHRR red and near-IR bands for three cover types and varying atmospheric conditions p 13 A86-39146

VELOCITY DISTRIBUTION

- Objective analysis of tidal fields in the Atlantic and Indian Oceans
[NASA-TM-87773] p 39 N86-26782

VERTICAL DISTRIBUTION

- Remote sensing of vertical moisture profiles and cloud properties from simulated millimeter wave sounder and microwave imager data p 53 A86-33547

VERTICAL ORIENTATION

- Satellite-derived moisture profiles
[NOAA-NESDIS-24] p 44 N86-27703

VERY HIGH FREQUENCIES

- The fundamentals of microwave remote sensing
[SU-84] p 56 N86-23025

VERY LARGE SCALE INTEGRATION

- High speed image processing system with custom VLSI for DSP --- Digital Signal Processor p 54 A86-33641

VIDEO EQUIPMENT

- The emergence of airborne video techniques as an alternative for accessing tropical environments - A historical perspective p 56 A86-37007

VISIBLE INFRARED SPIN SCAN RADIOMETER

- Optimized retrievals of precipitable water fields from combinations of VAS satellite and conventional surface observations p 43 A86-36193

VISIBLE SPECTRUM

- Satellite remote sensing of atmospheric optical depth spectrum p 55 A86-36785

VOLCANOES

- Thematic mapper studies of Andean volcanoes
[NASA-CR-176807] p 24 N86-25866

- The nature and origin of mineral coatings on volcanic rocks of the Black Mountain, Stonewall Mountain and Kane Springs Wash volcanic centers in southern Nevada
[NASA-CR-176805] p 24 N86-25912

- Transport processes as manifested in satellite and lidar aerosol measurements p 17 N86-27788

VOLCANOLOGY

- Introductory analyses of SIR-B radar data for Hawaii p 21 A86-33551

VORTICES

- Near-surface water circulation in the sub-Arctic frontal zone (according to satellite data) p 25 A86-32676

- Some features of small-scale ocean eddies according to an analysis of satellite images p 25 A86-32677

W

WATER CIRCULATION

- Near-surface water circulation in the sub-Arctic frontal zone (according to satellite data) p 25 A86-32676

- Remote sensing and modeling of the dynamics of the western part of the Black Sea p 26 A86-32679

- Satellite imaging of coastal flow circulation in relation to numerical modelling p 31 A86-33631

- Optimal disposition of satellite-tracked drifting buoys in the South Atlantic p 31 A86-34488

WATER COLOR

- Ocean color measurements p 28 A86-33488

- Physical interpretation of estuarine water color using vector analysis of satellite data p 43 A86-33630

- Applicability of atmospheric correction algorithm for CZCS data to Japanese coastal area --- Coastal Zone Color Scanner p 31 A86-33632

WATER DEPTH

- Navstar GPS (Global Positioning System) accuracy while surveying arrays of deep ocean transponders
[AD-A163384] p 38 N86-26313

WATER POLLUTION

- Integrated global monitoring of the world ocean. Volumes 1, 2, & 3 --- Russian book p 24 A86-31350

- Environmental data sources for the Chesapeake Bay Area
[PB86-110640] p 35 N86-23211

- Comprehensive integrated remote sensing for US Department of Energy applications
[DE86-002101] p 17 N86-25036

WATER QUALITY

- Use of Thematic Mapper data to assess water quality in Green Bay and central Lake Michigan p 43 A86-39004

- Environmental data sources for the Chesapeake Bay Area
[PB86-110640] p 35 N86-23211

WATER RUNOFF

- Large area snowmelt runoff simulations based on Landsat-MSS data p 42 A86-33505

WATER VAPOR

- A model for the estimation of the surface fluxes of momentum, heat and moisture of the cloud topped marine atmospheric boundary layer from satellite measurable parameters
[NASA-CR-177283] p 41 N86-27837

WATER WAVES

- Observation of internal waves and seismic waves in the Sicilian Channel p 27 A86-33392

- Surface and internal ocean wave observations p 27 A86-33485

- Observations of the polar regions from satellites using active and passive microwave techniques p 28 A86-33489

- The spatial evolution of SAR derived wave spectra in the vicinity of Hurricane IVA p 30 A86-33602

- The SIR-B Extreme Waves Experiment in the southern oceans p 30 A86-33607

- Waves predicted by the Global Spectral Ocean Wave model off the west coast of Chile during the SIR-B mission p 30 A86-33608

- Simulations of SAR wave spectra using high spectral resolution estimates from the SCR and ROWS instruments p 30 A86-33611

- Directional ocean wave spectra obtained from the Shuttle Imaging Radar off the coast of Chile p 30 A86-33612

- An overview of the SAR internal wave signature experiment p 31 A86-33645

- SAR-observed internal wave signatures from SARSEX - Initial observations p 31 A86-33646

- SAR observed internal wave signatures from SARSEX-comparisons with SAR imaging models p 31 A86-33647

- Intensity modulation in SAR images of internal waves p 32 A86-35531

- Strategies for the calibration and operational use of the ERS-1 SAR wave mode
[JHU/APL/SDO-7565] p 35 N86-23207

- Management information (Wave Propagation Laboratory, Boulder, Colorado)
[PB86-139524] p 38 N86-25106

WATERFOWL

- Ducks Unlimited Joint Research Project
[NASA-TM-88755] p 14 N86-25032

WAVE PROPAGATION

- Management information (Wave Propagation Laboratory, Boulder, Colorado)
[PB86-139524] p 38 N86-25106

WAVE SCATTERING

- Open ocean radar sea scatter measurements p 25 A86-32599

WAVELENGTHS

- Wavelength intensity indices in relation to tree condition and leaf-nutrient content p 12 A86-37036

WEATHER

- Reduction of weather effects in the calculation of sea ice concentration from microwave radiances p 26 A86-33104

WEATHER FORECASTING

- Technological improvements to naval aviation weather support p 34 A86-37506

- Proceedings of the First National Workshop on the Global Weather Experiment: Current Achievements and Future Directions, volume 1
[NASA-CR-176720] p 36 N86-24120

- Federal agency satellite requirements
[AD-A165071] p 59 N86-27410

- NOAA satellite requirements forecast
[AD-A165244] p 40 N86-27414

- Satellite-derived moisture profiles
[NOAA-NESDIS-24] p 44 N86-27703

WETLANDS

- Remote sensing investigations of wetland biomass and productivity for global biosystems research
[NASA-CR-176725] p 14 N86-23994

WHEAT

- Diurnal patterns of bidirectional vegetation indices for wheat canopies p 1 A86-30192

- Effect of dew on canopy reflectance and temperature p 10 A86-36049

- Analysis of a resistance-energy balance method for estimating daily evaporation from wheat plots using one-time-of-day infrared temperature observations p 13 A86-39148

- Wheat area estimation using digital LANDSAT MSS data and aerial photographs
[INPE-3824-PRE/900] p 15 N86-26667

WIND (METEOROLOGICAL)

- Remote monitoring of processes that shape desert surfaces: The Desert Winds Project
[T186-900108] p 24 N86-25099

- Methods of obtaining offshore wind direction and sea-state data from X-band aircraft SAR (Synthetic Aperture Radar) imagery of coastal waters
[AD-A165552] p 38 N86-26517

WIND DIRECTION

- Oceanic surface winds p 27 A86-33484

- Methods of obtaining offshore wind direction and sea-state data from X-band aircraft SAR (Synthetic Aperture Radar) imagery of coastal waters
[AD-A165552] p 38 N86-26517

WIND EFFECTS

- Wind dependence of L-band radar backscatter p 33 A86-35860

- Remote monitoring of processes that shape desert surfaces: The Desert Winds Project
[T186-900108] p 24 N86-25099

WIND EROSION

- Remote monitoring of processes that shape desert surfaces: The Desert Winds Project
[T186-900108] p 24 N86-25099

WIND MEASUREMENT

- Seasat microwave wind and rain observations in severe tropical and midlatitude marine storms p 27 A86-33486

- Passive remote sensing of stratospheric and mesospheric winds p 53 A86-33545

- A median filter approach for correcting errors in a vector field p 29 A86-33601

- A simple, objective analysis scheme for scatterometer data --- Seasat A satellite observation of wind over ocean p 32 A86-35550

WIND VELOCITY

Studies of complex terrain wind flows using acoustic
sounder and optical cross-wind remote sensors
[DE86-002993] p 58 N86-25925

WIND VELOCITY

Open ocean radar sea scatter measurements
p 25 A86-32599

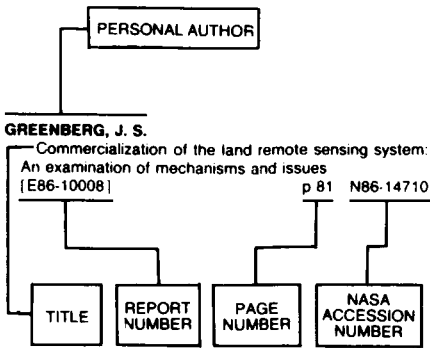
WIND VELOCITY MEASUREMENT

Oceanic surface winds p 27 A86-33484

WINTER

Aircraft and satellite passive microwave observations
of the Bering Sea ice cover during MIZEX West
p 32 A86-35683

Typical Personal Author Index Listing



Listings in this index are arranged alphabetically by personal author. The title of the document provides the user with a brief description of the subject matter. The report number helps to indicate the type of document listed (e.g., NASA report, translation, NASA contractor report). The page and accession numbers are located beneath and to the right of the title. Under any one author's name the accession numbers are arranged in sequence with the AIAA accession numbers appearing first.

A

AASE, J. K.
Development of agrometeorological crop model inputs from remotely sensed information p 6 A86-33579

ABDOU, I. E.
Nonparametric models and crop classification p 6 A86-33622

ABER, J. D.
Modeling the controls of forest productivity using canopy variables p 11 A86-37016

AHERN, F. J.
Forestry information content of Thematic Mapper data p 8 A86-34741

ALEKSEEV, A. S.
Technical and software facilities at a center for the processing of remote-sensing data p 48 A86-36511

ALEXANDER, D. P.
Hydrologic modeling using Landsat MSS data p 43 A86-37010

ALISHOUSE, J. C.
Sea surface temperature determinations p 28 A86-33487

ALLEY, R.
What are the best radar wavelengths, incidence angles and polarizations for geologic applications? A statistical approach p 21 A86-33592

ALLISON, D. E.
A model for the estimation of the surface fluxes of momentum, heat and moisture of the cloud topped marine atmospheric boundary layer from satellite measurable parameters [NASA-CR-177283] p 41 N86-27837
A model for the estimation of the surface fluxes of momentum, heat, and moisture of the cloud-topped marine atmospheric boundary layer from satellite measurable parameters [NASA-CR-177290] p 41 N86-27853

ALONSO, E. M. B.
Development of a satellite-tracked oceanographic drifting buoy for the Brazilian Antarctic Program, part 1 [INPE-3793-PRE/888] p 36 N86-24166
Comparison of Circulation estimates and winds based on shipboard and satellite-tracked buoy data in Bransfield Strait, 9-14 March, 1985, part 3 [INPE-3795-PRE/890] p 36 N86-24168

AMBROSIA, V. G.
Analysis of forest/structure using thematic mapper simulator data p 4 A86-33540

ANDERSON, J. M.
The applicability of LOWTRAN5 computer code to aerial thermographic data correction p 48 A86-34739

ANDERSON, L. A.
Navstar GPS (Global Positioning System) accuracy while surveying arrays of deep ocean transponders [AD-A163364] p 38 N86-26313

ANDERSON, S. J.
Remote sensing with the Jindalee skywave radar p 33 A86-36954

APEL, J. R.
Surface and internal ocean wave observations p 27 A86-33485
An overview of the SAR internal wave signature experiment p 31 A86-33645

ARANUVACHAPUN, S.
Satellite remote sensing of atmospheric optical depth spectrum p 55 A86-36785

ARMSTRONG, M. L.
Nonparametric models and crop classification p 6 A86-33622

ARNONE, R.
Contributions to the oceanography of the western Alboran Sea [AD-A162019] p 37 N86-24173

ASANUMA, I.
Satellite thermal observation of oil slicks on the Persian Gulf p 33 A86-36048

ASRAR, G.
Light interception and leaf area estimates from measurements of grass canopy reflectance p 4 A86-33557
Distinguishing among tallgrass prairie cover types from measurements of multispectral reflectance p 10 A86-36047

ATLAS, R.
GLAS experiments on the impact of FGGE satellite data on numerical weather prediction p 57 N86-24128
Simulation studies related to the design of post-FGGE observing systems p 57 N86-24160

AUMILLER, B.
Satellite-borne 90 GHz radiometer experiment (SABREX), phase A1 [DFVLR-MITT-85-13] p 57 N86-24000

AUSTIN, R. W.
Ocean color measurements p 28 A86-33488

AVDUEVSKII, V. S.
Agricultural and scientific space platforms p 1 A86-29843

AZZALI, S.
A multindex multitemporal approach to map crops in the early growing season: An application to two Italian irrigation districts: East Sesia and Grande Bonifiga Ferrarese [ICW-1611] p 15 N86-26674

B

BADHWAR, G. D.
Satellite-derived leaf-area-index and vegetation maps as input to global carbon cycle models - A hierarchical approach p 2 A86-30194
Estimation of biophysical properties of forest canopies through inversion of microwave scatterometer data p 4 A86-33542
Spectral characterization of biophysical characteristics in a boreal forest - Relationship between Thematic Mapper band reflectance and leaf area index for Aspen p 8 A86-35677
An information measure for class discrimination p 11 A86-36789

BAILEY, J.
Comparison of the Defense Meteorological Satellite Program (DMSp) and the NOAA Polar-orbiting Operational Environmental Satellite (POES) program [AD-A165118] p 59 N86-27413

BAKER, W. E.
GLAS experiments on the impact of FGGE satellite data on numerical weather prediction p 57 N86-24128

BANNINGER, C.
Comparison between Landsat MSS and Thematic Mapper data for geobotanical prospecting in the Spanish-Portuguese Pyrite Belt p 7 A86-33628
Evaluation of Landsat MSS bands and transformations for detecting heavy metal stress in forest-covered areas p 7 A86-33629

BARCALA, R.
Contributions to the oceanography of the western Alboran Sea [AD-A162019] p 37 N86-24173

BARKOV, N. I.
Ice shelves of Antarctica [PB86-106986] p 35 N86-23208

BARRICK, D. E.
Analysis and interpretation of altimeter sea echo p 27 A86-33483

BARTELS, K. I.
Lithologic signatures in multi-channel SAR imagery p 45 A86-33522

BARTLETT, D. S.
Assessing impacts of off-nadir observation on remote sensing of vegetation - Use of the Suits model p 1 A86-30193

BATISTA, G. T.
Wheat area estimation using digital LANDSAT MSS data and aerial photographs [INPE-3824-PRE/900] p 15 N86-26667

BAUMGARTNER, M. F.
Large area snowmelt runoff simulations based on Landsat-MSS data p 42 A86-33505
A stepwise hierarchical multi-binary approach in TM landuse classification p 46 A86-33597

BEAL, R. C.
The SIR-B Extreme Waves Experiment in the southern oceans p 30 A86-33607

BECK, F. B.
Design and benefits of a multibeam Earth Observing Radar p 29 A86-33591

BECKER, F.
A stable iterative procedure to obtain soil surface parameters and fluxes from satellite data p 8 A86-35678

BEFORT, W.
One step above ground truth - Airphoto keys for large-scale vegetation analysis p 3 A86-33538

BELIAEV, B. I.
Possibility of small-scale physiogeographical regionalization using space spectrometry data p 16 A86-30974

BERNARD, R.
Possible applications of the microwaves surface soil moisture remote sensing p 6 A86-33582
Evapotranspiration over an agricultural region using a surface flux/temperature model based on NOAA-AVHRR data p 10 A86-36237

BERNSTEIN, R. L.
Sea surface temperature from satellites: The impact of FGGE p 36 N86-24161

BEZDEK, J. C.
Segmentation of a Thematic Mapper image using the fuzzy c-means clustering algorithm p 9 A86-35687

BHADURI, L.
Wind dependence of L-band radar backscatter p 33 A86-35860

BIEHL, L. L.
Sun angle, view angle, and background effects on spectral response of simulated balsam fir canopies p 13 A86-39002

BILLINGSLEY, G. H.
Remote monitoring of processes that shape desert surfaces: The Desert Winds Project [T186-900108] p 24 N86-25099

BINNENKADE, P.
Semi-operational identification of agricultural crops from airborne SLAR-data p 12 A86-37025

BIRNIE, R. V.
Millimeter-wave backscatter from snowcover p 42 A86-33615

BISHOP, W. P.

Optimum management strategies for the NOAA (National Oceanic and Atmospheric Administration) polar-orbiting operational environmental satellites, 1985-2000. Volume 1
[AD-A165143] p 59 N86-28007

BLACK, P. G.

Seasat microwave wind and rain observations in severe tropical and midlatitude marine storms p 27 A86-33486

BLAKE, N.

ENVIROSAT-2000 report: Federal agency satellite requirements
[NASA-TM-88752] p 59 N86-26355

BLANCHARD, A. J.

Utilization of active microwave roughness measurements to improve passive microwave soil moisture estimates over bare soils p 8 A86-35679

BLANCHARD, B. J.

Utilization of active microwave roughness measurements to improve passive microwave soil moisture estimates over bare soils p 8 A86-35679

BLANCHARD, R. J.

Backscatter measurements from simulated resonant structures p 4 A86-33555

BLAZQUEZ, C. H.

Wavelength intensity indices in relation to tree condition and leaf-nutrient content p 12 A86-37036

BLOETSCHER, H.

Satellite-borne 90 GHz radiometer experiment (SABREX), phase A1
[DFVLR-MITT-85-13] p 57 N86-24000

BLOM, R.

What are the best radar wavelengths, incidence angles and polarizations for geologic applications? A statistical approach p 21 A86-33592

BLONDA, P. N.

Landsat TM image forward/reverse scan banding Characterization and correction p 49 A86-36790

BLUESTEIN, H. B.

Analysis of airborne Doppler lidar, Doppler radar and tall tower measurements of atmospheric flows in quiescent and stormy weather
[NASA-CR-3960] p 56 N86-23159

BOATRIGHT, J.

Vegetation assessment using a combination of visible, near-IR and thermal-IR AVHRR data p 5 A86-33577

BOATWRIGHT, G. O.

Overview and highlights of Early Warning and Crop Condition Assessment project p 5 A86-33576

BODANSKII, E. D.

Formation of a digital data base for automated forest mapping p 2 A86-32689

BODECHTEL, J.

MOMS-01 (Modular Optoelectronic Multispectral Scanner) for Earth observation: First results of STS-7 mission p 57 N86-24003

BOGOSLOVSKII, V. A.

Application of space imagery to the identification and geological-geophysical study of hidden plutons in early Proterozoic troughs p 20 A86-32682

BONN, F.

The fundamentals of microwave remote sensing [SU-84] p 56 N86-23025

BOREL, C. C.

Description of a databank of normalized radar cross section of terrain p 45 A86-33526

BOROVNIKOV, A. M.

Method for the quantitative estimation of convergence in mapping in the case of the interpretation of space photographs of oil-and-gas-bearing regions of Siberia p 23 A86-36505

BOS, H. J.

Map digitization offers new possibilities [NLR-MP-84061-U] p 51 N86-23028

BOTKIN, D. B.

Adding spatial considerations to the JABOWA model of forest growth p 11 A86-37014

BOYD, W. E.

Soil background effects on the spectral response of a three-component rangeland scene p 9 A86-36044

BRASS, J. A.

Analysis of forest/structure using thematic mapper simulator data p 4 A86-33540

BREED, C. S.

Remote monitoring of processes that shape desert surfaces: The Desert Winds Project [TI86-900108] p 24 N86-25099

BRINDT, L.

Direction dependent interpolation of aeromagnetic data p 23 A86-37009

BROWN, G. S.

Studies related to ocean dynamics. Task 3.2: Aircraft Field Test Program to investigate the ability of remote sensing methods to measure current/wind-wave interactions [NASA-CR-168349] p 38 N86-25100

BROWN, L.

Evidence of ongoing crustal deformation related to magmatic activity near Socorro, New Mexico p 18 A86-37797

BROWN, R. A.

A simple, objective analysis scheme for scatterometer data p 32 A86-35550

BROWN, R. J.

Microwave remote sensing of agricultural crops in Canada p 1 A86-30190
Integration of high and low resolution satellite data for crop condition assessment p 12 A86-37020

BRUCE, B.

A preliminary analysis of Landsat MSS and TM data in the Levack area, Sudbury, Canada p 20 A86-33519

BRUNFELDT, D. R.

Microwave emission from row crops p 9 A86-35681

BRYANT, N. A.

Landsat Thematic Mapper geodetic accuracy - Implications for geocoded map compatibility p 18 A86-37024

BUI, J. S.

Measurement of Thematic Mapper data quality p 50 A86-37032

BURNS, B. A.

Lithologic signatures in multi-channel SAR imagery p 45 A86-33522
SAR remote sensing during MIZEX 84 p 29 A86-33561

100 MHz dielectric constant measurements of snow cover Dependence on environmental and snow pack parameters p 42 A86-33613

BUTERA, M. K.

A correlation and regression analysis of percent canopy closure vs. TMS spectral response for selected forest sites in the San Juan National Forest, Colorado p 3 A86-33539

C

CALMANT, S.

The effective elastic lithosphere under the Cook-Austral and Society islands p 25 A86-32267

CAMP, D. B.

Physical oceanography report: Camp-based and helicopter-based STD data from the drifting ice station FRAM 3 [AD-A163097] p 37 N86-24181

CANNON, R. L.

Segmentation of a Thematic Mapper image using the fuzzy c-means clustering algorithm p 9 A86-35687

CARD, D. H.

Measurement of Thematic Mapper data quality p 50 A86-37032

CARDONE, V. J.

Oceanic surface winds p 27 A86-33484
Seasat microwave wind and rain observations in severe tropical and midlatitude marine storms p 27 A86-33486

CARLOTTO, M. J.

Techniques for multispectral image classification p 44 A86-32337

Surface material classification based on spectral shape p 6 A86-33598

Spatial enhancement techniques for multichannel satellite imagery p 47 A86-33639

CARLSON, T. N.

Preliminary assessment of soil moisture over vegetation [NASA-CR-177226] p 15 N86-27704

CARNES, J. G.

Spectral characterization of biophysical characteristics in a boreal forest - Relationship between Thematic Mapper band reflectance and leaf area index for Aspen p 8 A86-35677

CARR, J.

EOS radiometer concepts for soil moisture remote sensing [NASA-CR-177854] p 14 N86-23995

CARSEY, F. D.

Weddell-Scotia sea marginal ice zone observations from space, October 1984 p 26 A86-33105

CARVER, K.

Spaceborne Imaging Radar (SIR) project p 53 A86-33586

CARVER, K. R.

1985 International Geoscience and Remote Sensing Symposium (IGARSS '85), University of Massachusetts, Amherst, October 7-9, 1985, Digest. Volumes 1 & 2 p 52 A86-33501

CAUDILL, C. E.

Overview of the AgRISTARS research program. I p 2 A86-33503

CAVALIER, D. J.

Reduction of weather effects in the calculation of sea ice concentration from microwave radiances p 26 A86-33104

CAVALIERI, D. J.

Observations of the polar regions from satellites using active and passive microwave techniques p 28 A86-33489

Aircraft and satellite passive microwave observations of the Bering Sea ice cover during MIZEX West p 32 A86-35683

CAZENAVE, A.

The effective elastic lithosphere under the Cook-Austral and Society islands p 25 A86-32267

CHATTERJEE, B.

Automatic cloud classification p 46 A86-33534

CHEN, S. C.

Wheat area estimation using digital LANDSAT MSS data and aerial photographs [INPE-3824-PRE/900] p 15 N86-26667

CHENEY, R.

Sea level time series in the equatorial Pacific from satellite altimetry p 34 A86-38648

CHERNIN, V. M.

Choice of spectral bands for a spaceborne multispectral scanner p 55 A86-36514

CHESTERS, D.

Optimized retrievals of precipitable water fields from combinations of VAS satellite and conventional surface observations p 43 A86-36193

CHHIKARA, R. S.

Evaluation of crop acreage estimation methods using Landsat data as auxiliary input p 6 A86-33606

CHILTON, R. E.

Analysis of L-band multipolarization radar images for lava flow mapping p 21 A86-33593

CHOU, L. C.

Satellite cloud and precipitation analysis using a minicomputer [AD-A163821] p 58 N86-25084

CHOUDHURY, B. J.

Analysis of a resistance-energy balance method for estimating daily evaporation from wheat plots using one-time-of-day infrared temperature observations p 13 A86-39148

CHU, W. P.

SAGE observations of stratospheric nitrogen dioxide p 55 A86-36838

CIHLAR, J.

Microwave remote sensing of agricultural crops in Canada p 1 A86-30190

CLARK, D. K.

Ocean color measurements p 28 A86-33488

COAKLEY, J. A., JR.

Remote sensing of clouds p 52 A86-33533

COMPARD, S.

SPOT - A high-precision view of the earth p 52 A86-31222

CONRADSEN, K.

Statistical lineament analysis in South Greenland based on Landsat imagery p 22 A86-35676

CORNILLON, P.

Satellite observations of sea surface cooling by hurricanes p 32 A86-35545

COTTER, D.

ENVIROSAT-2000 report: Federal agency satellite requirements [NASA-TM-88752] p 59 N86-26355

Federal agency satellite requirements [AD-A165071] p 59 N86-27410

GOES (Geostationary Operational Environmental Satellite)-next overview p 59 N86-27411

Comparison of the Defense Meteorological Satellite Program (DMSP) and the NOAA Polar-orbiting Operational Environmental Satellite (POES) program [AD-A165118] p 59 N86-27413

NOAA satellite requirements forecast [AD-A165244] p 40 N86-27414

COTTER, D. J.

Operational satellite support to scientific programs [AD-A165081] p 59 N86-27412

CRACKNELL, A. P.

The estimation of atmospheric effects for SPOT using AVHRR channel-1 data p 47 A86-34738

CRAWFORD, H. S.

Estimation of the weight of vegetation using microwave transmission measurements p 3 A86-33524

- CURLIS, J. D.**
Geological mapping potential of computer-enhanced images from the Shuttle Imaging Radar - Lisbon Valley Anticline, Utah p 22 A86-36083
- CURRAN, P. J.**
Small format, oblique, colour aerial photography - An aid to the location of methane seepage p 11 A86-36783
- D**
- DAGGETT, P. H.**
Structure of the southern Rio Grande rift from gravity interpretation p 18 A86-37795
- DAMINOVA, T. A.**
Salyut-6 observation of color and brightness contrasts correlated with ocean-bottom relief p 26 A86-32678
- DANILOV, A. I.**
Optimal disposition of satellite-tracked drifting buoys in the South Atlantic p 31 A86-34488
- DAUGHTRY, C. S. T.**
Sun angle, view angle, and background effects on spectral response of simulated balsam fir canopies p 13 A86-39002
- DAVE, J. V.**
Segmentation of a Thematic Mapper image using the fuzzy c-means clustering algorithm p 9 A86-35687
- DAVIS, A. W.**
Reflectance modelling and the derivation of vegetation indices for an Australian semi-arid shrubland p 7 A86-34740
- DAWEI, L. I.**
A clustering algorithm for remote sensing multispectral data p 51 A86-37033
- DAWSON, G.**
Contributions to the oceanography of the western Alboran Sea [AD-A162019] p 37 N86-24173
- DE BOER, C.**
On-board data compression for advanced Landsat p 45 A86-32368
- DE LA TORRE, J. C.**
A measuring reference system to quantify the desertification process in a semiarid ecosystem based on Landsat MSS data p 16 A86-37011
- DEAN, K.**
Influence of the Yukon River on the Bering Sea [NASA-CR-177310] p 39 N86-26783
- DEBLONDE, G.**
Remote sensing of vertical moisture profiles and cloud properties from simulated millimeter wave sounder and microwave imager data p 53 A86-33547
- DELLWIG, L. F.**
Geological mapping potential of computer-enhanced images from the Shuttle Imaging Radar - Lisbon Valley Anticline, Utah p 22 A86-36083
- DEMENTEV, V. N.**
The use of remote-sensing data to predict regional and local oil-and-gas-bearing structures within the Dneprovsk-Donetsk paleorift p 23 A86-36508
Technical and software facilities at a center for the processing of remote-sensing data p 48 A86-36511
- DENNER, W. W.**
A study of sea ice kinematics and their relationship to arctic ambient noise. Part 3, Section 1: Ambient noise. Section 2: Ambient noise [AD-A165304] p 39 N86-26788
A study of sea ice kinematics and their relationship to arctic ambient noise. Part 3, section 3: Ambient noise [AD-A165305] p 40 N86-26789
- DERRYBERRY, B. A.**
Introductory analyses of SIR-B radar data for Hawaii p 21 A86-33551
- DESFOSSÉS, P.**
The fundamentals of microwave remote sensing [SU-84] p 56 N86-23025
- DIETERLE, D. A.**
A simulation analysis of the fate of phytoplankton within the mid-Atlantic bight [NASA-CR-177265] p 39 N86-26670
Satellite detection of phytoplankton export from the mid-Atlantic Bight during the 1979 spring bloom [NASA-TM-88782] p 41 N86-27699
- DOMIK, G.**
Radar image simulation as a tool to analyze topographic effects on geometry and radiometry of radar imagery p 50 A86-37026
- DOTT, M. S.**
A multindex multitemporal approach to map crops in the early growing season: An application to two Italian irrigation districts: East Sesia and Grande Bonifiga Ferrarese [ICW-1611] p 15 N86-26674
- DOVIK, R. J.**
Analysis of airborne Doppler lidar, Doppler radar and tall tower measurements of atmospheric flows in quiescent and stormy weather [NASA-CR-3960] p 56 N86-23159
- DUBOIS, J. M. M.**
The fundamentals of microwave remote sensing [SU-84] p 56 N86-23025
- DULEPOV, I. A.**
Combination of air and space remote-sensing methods and geological-geophysical methods for the purpose of oil and gas exploration in the southern Permsk region p 23 A86-36509
- E**
- EDWARDS, G. J.**
Wavelength intensity indices in relation to tree condition and leaf-nutrient content p 12 A86-37036
- EILTS, M. D.**
Analysis of airborne Doppler lidar, Doppler radar and tall tower measurements of atmospheric flows in quiescent and stormy weather [NASA-CR-3960] p 56 N86-23159
- EL NASHARTY, A. F.**
Application of spaceborne and airborne techniques in mineral exploration at Wadi El Allaqi area, Eastern Desert, Egypt p 23 A86-37865
- EL SHAZLY, E. M.**
Application of spaceborne and airborne techniques in mineral exploration at Wadi El Allaqi area, Eastern Desert, Egypt p 23 A86-37865
- ELACHI, C.**
Modelling of backscatter from vegetation layers p 4 A86-33554
Spaceborne Imaging Radar (SIR) project p 53 A86-33586
- ELMAN, R. I.**
Formation of a digital data base for automated forest mapping p 2 A86-32689
- ENGHETA, N.**
Modelling of backscatter from vegetation layers p 4 A86-33554
- ENGLÉ, S. W.**
The development of an MSS satellite imagery classification expert system p 46 A86-33596
- ENGMAN, E. T.**
Microwave backscatter and emission observed from Shuttle Imaging Radar B and an airborne 1.4 GHz radiometer p 53 A86-33584
- EOM, H. J.**
Scattering from a random layer embedded with dielectric needles p 10 A86-36045
Regression models for vegetation radar-backscattering and radiometric emission p 10 A86-36046
- EREMEEV, V. N.**
Optimal disposition of satellite-tracked drifting buoys in the South Atlantic p 31 A86-34488
- EROMENKO, V. I. A.**
Quantitative assessment of the information content of TV images of different scale on the example of disjunctives of Siberia p 23 A86-36506
- ERSHOV, O. A.**
Determination of sea spectral reflectance from airborne measurements p 26 A86-32683
- ESAIAS, W. E.**
Satellite detection of phytoplankton export from the mid-Atlantic Bight during the 1979 spring bloom [NASA-TM-88782] p 41 N86-27699
- ESKITE, W. H.**
Optimum management strategies for the NOAA (National Oceanic and Atmospheric Administration) polar-orbiting operational environmental satellites, 1985-2000. Volume 1 [AD-A165143] p 59 N86-28007
- EVERITT, J. H.**
Classification of south Texas farm and range resources using NOAA7 AVHRR satellite imagery p 5 A86-33558
- EYRE, J. R.**
Estimation of sea-surface temperature from AVHRR data Comments on the paper by Singh et al. (1985) p 31 A86-34743
- F**
- FEDOR, L. S.**
Surface and internal ocean wave observations p 27 A86-33485
Precipitation in tropical cyclones p 28 A86-33490
Measurement of sea ice backscatter characteristics at 36 GHz using the surface contour radar p 29 A86-33562
- FEDOROV, K. N.**
Near-surface water circulation in the sub-Arctic frontal zone (according to satellite data) p 25 A86-32676
- FEDOTOV, S. V.**
Probabilistic modeling of fields of atmospheric turbulence and sea roughness with reference to the study of complex systems p 33 A86-36480
- FERRARO, R. R., JR.**
Classification of geophysical parameters using passive microwave satellite measurements p 47 A86-33626
- FESTA, J. F.**
Heat budget and climatic atlas of the equatorial Atlantic Ocean during FGGE (First GARP Global Experiment, 1979 [PB86-111622] p 35 N86-23213
- FIEDLER, F.**
Contributions to the oceanography of the western Alboran Sea [AD-A162019] p 37 N86-24173
- FILHO, P. H.**
A proposal for a project entitled Assessment of Forest Resources in Uruguay submitted to the United Nations Industrial Development Organization (UNIDO) [INPE-3828-NTE/255] p 15 N86-26666
- FILY, M.**
Extracting sea ice data from satellite SAR imagery p 29 A86-33560
- FISCHER, J.**
On the information content of multispectral radiance measurements over an ocean [GKSS-85/E/43] p 40 N86-27697
- FISHER, L.**
NOAA satellite requirements forecast [AD-A165244] p 40 N86-27414
- FISHER, P. C.**
Structure of terrestrial impact craters from SIR-B radar data - Preliminary results p 21 A86-33552
- FISHER, T. A.**
Processing of multi-sensor remotely sensed data to a standard geocoded format p 50 A86-37019
- FISK, D. J.**
100 MHz dielectric constant measurements of snow cover Dependence on environmental and snow pack parameters p 42 A86-33613
- FLEMING, E. L.**
Characteristics of western region flash flood events in GOES imagery and conventional data [NOAA-TM-NESDIS-13] p 44 N86-26668
- FLOOD, W. A.**
Studies related to ocean dynamics. Task 3.2: Aircraft Field Test Program to investigate the ability of remote sensing methods to measure current/wind-wave interactions [NASA-CR-168349] p 38 N86-25100
- FOERSTNER, W.**
Examples of the automated derivation of digital surface models p 48 A86-35292
- FONG, Y.-S.**
Estimation of the location parameter of a multispectral distribution by a median operator p 49 A86-37006
- FORD, J. P.**
Forest discrimination with multipolarization imaging radar p 5 A86-33565
Forest discrimination with multipolarization imaging radar p 5 A86-33566
- FOWNE, J.**
Modeling the controls of forest productivity using canopy variables p 11 A86-37016
- FRANCIS, P. W.**
Thematic mapper studies of Andean volcanoes [NASA-CR-176807] p 24 N86-25866
- FRASER, R. S.**
Directional reflectance response in AVHRR red and near-IR bands for three cover types and varying atmospheric conditions p 13 A86-39146
- FREI, U.**
Landsat TM image forward/reverse scan banding Characterization and correction p 49 A86-36790
- FROST, V. S.**
Geological mapping potential of computer-enhanced images from the Shuttle Imaging Radar - Lisbon Valley Anticline, Utah p 22 A86-36083
- FUKAI, M.**
Research and development of the synthetic aperture radar transmitter and receiver subsystem design and some component test results p 54 A86-33636
- FUKUE, K.**
High accuracy clustering using residual image p 49 A86-37003
- FUKUSHIMA, H.**
Applicability of atmospheric correction algorithm for CZCS data to Japanese coastal area p 31 A86-33632
- FUNG, A. K.**
Scattering from a random layer embedded with dielectric needles p 10 A86-36045

FUSCO, L.

- Landsat TM image forward/reverse scan banding
Characterization and correction p 49 A86-36790

G

GADDIS, L. R.

- Preliminary geologic analyses of SIR-B radar data for Hawaii p 21 A86-33550
Introductory analyses of SIR-B radar data for Hawaii p 21 A86-33551
Analysis of L-band multipolarization radar images for lava flow mapping p 21 A86-33593

GALASSO, G. A.

- Sea ice dynamics and regional meteorology for the Arctic polynya experiment (APEX)-Bering Sea 1985 [PB86-148038] p 38 N86-25939

GALLAGHER, J. G.

- Millimeter-wave backscatter from snowcover p 42 A86-33615

GARCIA, R. R.

- Transient response to localized episodic heating in the tropics p 51 N86-27749

GARDNER, C. S.

- Remote sensing of atmospheric pressure and sea state using laser altimeters p 28 A86-33529

GARDNER, J. M.

- Wavelength intensity indices in relation to tree condition and leaf-nutrient content p 12 A86-37036

GASPAROVIC, R. F.

- An overview of the SAR internal wave signature experiment p 31 A86-33645
Intensity modulation in SAR images of internal waves p 32 A86-35531

GATSKOV, V. G.

- Combination of air and space remote-sensing methods and geological-geophysical methods for the purpose of oil and gas exploration in the southern Permsk region p 23 A86-36509

GATTO, L. W.

- Ice conditions on the Ohio and Illinois Rivers, 1972-1985 p 42 A86-33617

GAUTIER, C.

- Evolution of the net surface shortwave radiation over the Indian Ocean during summer MONEX (1979) - A satellite description p 26 A86-33120

GAVRISH, V. K.

- The use of remote-sensing data to predict regional and local oil-and-gas-bearing structures within the Dneprovsk-Donetsk paleorift p 23 A86-36508

GENTRY, R. C.

- Seasat microwave wind and rain observations in severe tropical and midlatitude marine storms p 27 A86-33486

GEOKHLANIAN, T. KH.

- Structural features of the easterly jet stream according to satellite data p 26 A86-33315

GERRITSEN, F. A.

- Map digitization offers new possibilities [NLR-MP-84061-U] p 51 N86-23028

GINZBURG, A. I.

- Near-surface water circulation in the sub-Arctic frontal zone (according to satellite data) p 25 A86-32676

GLOERSEN, P.

- Reduction of weather effects in the calculation of sea ice concentration from microwave radiances p 26 A86-33104

- Observations of the polar regions from satellites using active and passive microwave techniques p 28 A86-33489

- Aircraft and satellite passive microwave observations of the Bering Sea ice cover during MIZEX West p 32 A86-35683

GOKHMANN, B.

- Landsat Thematic Mapper geodetic accuracy - Implications for geocoded map compatibility p 18 A86-37024

GOLDFINGER, A. D.

- Strategies for the calibration and operational use of the ERS-1 SAR wave mode [JHU/APL/SDO-7565] p 35 N86-23207

GOLDSTEIN, R. M.

- Topographic mapping from interferometric synthetic aperture radar observations p 18 A86-33516
Topographic mapping from interferometric synthetic aperture radar observations p 18 A86-36099

GONZALEZ, F. I.

- Surface and internal ocean wave observations p 27 A86-33485

- The spatial evolution of SAR derived wave spectra in the vicinity of Hurricane IVA p 30 A86-33602

GORBUNOV, B. A.

- Statistical approach to the classification of objects on air and space remote-sensing images p 48 A86-36515

GORDON, D. K.

- A texture-enhancement procedure for separating orchard from forest in Thematic Mapper data p 2 A86-30198

GORDON, H. R.

- Ocean color measurements p 28 A86-33488

GRADY, L. T.

- Topographic lineament domains of the Appalachians - Some new methods and techniques for paleostress analysis p 20 A86-33518

GRAETZ, R. D.

- Reflectance modelling and the derivation of vegetation indices for an Australian semi-arid shrubland p 7 A86-34740

GRANT, L.

- Polarization photometer to measure bidirectional reflectance factor R(55 deg, 0 deg, 55 deg, 180 deg) of leaves p 9 A86-35748

GREEN, G. M.

- Use of SIR-A and Landsat MSS data in mapping shrub and intershrub vegetation at Koonamore, South Australia p 13 A86-39003

GREEN, W. B.

- Image processing system interfaces p 44 A86-32333

GREGORY, A. F.

- Economical maintenance of a national topographic data base using Landsat images p 48 A86-36082

GRENFELL, T. C.

- Multifrequency observations of brightness temperature of artificial new and young sea ice p 28 A86-33514

GRIEVE, R. A. F.

- Structure of terrestrial impact craters from SIR-B radar data - Preliminary results p 21 A86-33552

GRIFFIN, R. H.

- Remote sensing techniques for the detection of soil erosion and the identification of soil conservation practices p 3 A86-33506

GRIFFITH, C. G.

- Precipitation in tropical cyclones p 28 A86-33490

GRISWOLD, L.

- Practical photogrammetry from 35-mm aerial photography p 55 A86-36080

GRODY, N. C.

- Classification of geophysical parameters using passive microwave satellite measurements p 47 A86-33626

GROLIER, M. J.

- Remote monitoring of processes that shape desert surfaces: The Desert Winds Project [TI86-900108] p 24 N86-25099

GUINDON, B.

- Microwave remote sensing of agricultural crops in Canada p 1 A86-30190

GURETSKII, V. V.

- Optimal disposition of satellite-tracked drifting buoys in the South Atlantic p 31 A86-34488

H

HADDAD, K. D.

- Assessment and trends of Florida's marine fisheries habitat An integration of aerial photography and Thematic Mapper imagery p 34 A86-37013

HADY, M. A. A.

- Application of spaceborne and airborne techniques in mineral exploration at Wadi El Allaqi area, Eastern Desert, Egypt p 23 A86-37865

HAEFNER, H.

- Large area snowmelt runoff simulations based on Landsat-MSS data p 42 A86-33505

- Resource monitoring oriented remote sensing data processing capabilities p 16 A86-33643

HAGAN, G. F.

- Predicting tree groundline diameter from crown measurements made on 35-mm aerial photography p 13 A86-39006

HAJEK, B. F.

- Agricultural applications for thermal infrared multispectral scanner data p 12 A86-37034

HALEM, M.

- Simulation studies related to the design of post-FGGE observing systems p 57 N86-24160

HALEY, G. M.

- Multispectral change detection using difference classification and bitemporal classification p 49 A86-37004

HALL, F. G.

- Spectral characterization of biophysical characteristics in a boreal forest - Relationship between Thematic Mapper band reflectance and leaf area index for Aspen p 8 A86-35677

HALLIKAINEN, M.

- Remote sensing of snow water equivalent using Nimbus-7 SMMR data p 42 A86-33616

HAMZA, A.

- Remote sensing for developing countries - A case study of Tunisia p 15 A86-30195

HANCOCK, D. W., III

- Spectral measurements in support of SIR-B using the Surface Contour Radar p 30 A86-33609

HARALICK, R. M.

- Context classifier p 46 A86-33535

HARDISKY, M. A.

- Assessing impacts of off-nadir observation on remote sensing of vegetation - Use of the Suits model p 1 A86-30193

HARLOW, C. A.

- Methods of obtaining offshore wind direction and sea-state data from X-band aircraft SAR (Synthetic Aperture Radar) imagery of coastal waters [AD-A165552] p 38 N86-26517

HARRINGTON, R. F.

- An airborne multiple-beam 1.4 GHz pushbroom microwave radiometer p 6 A86-33583

HARRIS, B. A.

- Assessment and trends of Florida's marine fisheries habitat An integration of aerial photography and Thematic Mapper imagery p 34 A86-37013

HATCH, R. E.

- Overview of the AgRISTARS research program. I p 2 A86-33503

HAUSKA, H.

- Direction dependent interpolation of aeromagnetic data p 23 A86-37009

HAWKINS, J. D.

- Seasat microwave wind and rain observations in severe tropical and midlatitude marine storms p 27 A86-33486

HAXBY, W. F.

- Evidence for small-scale mantle convection from Seasat altimeter data p 25 A86-31976

HAYDN, R.

- MOMS-01 (Modular Optoelectronic Multispectral Scanner) for Earth observation: First results of STS-7 mission p 57 N86-24003

HEACOCK, E.

- Comparison of the Defense Meteorological Satellite Program (DMSP) and the NOAA Polar-orbiting Operational Environmental Satellite (POES) program [AD-A165118] p 59 N86-27413

HEAD, J. W.

- Structure of terrestrial impact craters from SIR-B radar data - Preliminary results p 21 A86-33552

HEBURN, G.

- Contributions to the oceanography of the western Alboran Sea [AD-A162019] p 37 N86-24173

HEILMAN, J. L.

- Soil background effects on the spectral response of a three-component rangeland scene p 9 A86-36044

HELM, P. J.

- Remote monitoring of processes that shape desert surfaces: The Desert Winds Project [TI86-900108] p 24 N86-25099

HERMAN, N.

- Spaceborne Imaging Radar (SIR) project p 53 A86-33586

HILL, C. L.

- Ducks Unlimited Joint Research Project [NASA-TM-88755] p 14 N86-25032

- Timber Resources Inventory and Monitoring Joint Research Project [NASA-TM-88754] p 14 N86-25863

HILLS, A.

- A technique for assessing the severity of terrain shadowing in mobile satellite service p 51 A86-39545

HINES, D. E.

- Spectral measurements in support of SIR-B using the Surface Contour Radar p 30 A86-33609

HIROSAWA, H.

- Terrain height measurement by synthetic aperture radar with an interferometer p 55 A86-34736

HLAVKA, C. A.

- Land use mapping using edge density texture measures on Thematic Mapper simulator data p 47 A86-33624

- Measurement of Thematic Mapper data quality p 50 A86-37032

HODGE, S. M.

- Radar sounding of ice masses containing liquid water p 30 A86-33619

HOFFER, R. M.

- Hierarchical classification of multitemporal/multispectral scanner data p 49 A86-37017

HOGE, F. E.

- High frequency sampling of the 1984 spring bloom within the mid-Atlantic Bight: Synoptic shipboard, aircraft, and in situ perspectives of the SEEP-I experiment [NASA-TM-88765] p 41 N86-27700

- HOLBEN, B.**
Identifying deforestation in Brazil using multiresolution satellite data p 8 A86-34742
Directional reflectance response in AVHRR red and near-IR bands for three cover types and varying atmospheric conditions p 13 A86-39146
- HOLT, B.**
Weddell-Scotia sea marginal ice zone observations from space, October 1984 p 26 A86-33105
- HORII, S.**
High speed image processing system with custom VLSI for DSP p 54 A86-33641
- HORLER, D. N. H.**
Forestry information content of Thematic Mapper data p 8 A86-34741
- HORNSBY, J. K.**
A preliminary analysis of Landsat MSS and TM data in the Leveck area, Sudbury, Canada p 20 A86-33519
- HOUSTON, A. G.**
Evaluation of crop acreage estimation methods using Landsat data as auxiliary input p 6 A86-33606
- HOVIS, W. A.**
Ocean color measurements p 28 A86-33488
- HOWARD, R. J.**
High resolution millimeter-wave imaging sensor p 54 A86-33590
- HOWLAND, W. G.**
Photogrammetry and remote sensing in periglacial geomorphology p 20 A86-33517
- HSU, L. C.**
The nature and origin of mineral coatings on volcanic rocks of the Black Mountain, Stonewall Mountain and Kane Springs Wash volcanic centers in southern Nevada [NASA-CR-176805] p 24 N86-25912
- HSU, S. A.**
Methods of obtaining offshore wind direction and sea-state data from X-band aircraft SAR (Synthetic Aperture Radar) imagery of coastal waters [AD-A165552] p 38 N86-26517
- HUANG, N. E.**
Studies related to ocean dynamics. Task 3.2: Aircraft Field Test Program to investigate the ability of remote sensing methods to measure current/wind-wave interactions [NASA-CR-168349] p 38 N86-25100
- HUETE, A. R.**
The tasseled cap - Size, shape and orientation changes due to soil background p 12 A86-37035
Separation of soil-plant spectral mixtures by factor analysis p 13 A86-39147
- HUH, O. K.**
Methods of obtaining offshore wind direction and sea-state data from X-band aircraft SAR (Synthetic Aperture Radar) imagery of coastal waters [AD-A165552] p 38 N86-26517
- HUSSEY, J.**
GOES (Geostationary Operational Environmental Satellite)-next overview p 59 N86-27411
- HUTSINPILLER, A.**
The nature and origin of mineral coatings on volcanic rocks of the Black Mountain, Stonewall Mountain and Kane Springs Wash volcanic centers in southern Nevada [NASA-CR-176805] p 24 N86-25912
- I**
- IAKOVLEV, S. G.**
Determination of the spectral characteristics of natural objects on test ranges, and aspects of the efficiency of space systems p 11 A86-36697
- IDSO, S. B.**
Detection and evaluation of plant stresses for crop management decisions p 5 A86-33578
Analysis of a resistance-energy balance method for estimating daily evaporation from wheat plots using one-time-of-day infrared temperature observations p 13 A86-39148
- IISAKA, J.**
Satellite thermal observation of oil slicks on the Persian Gulf p 33 A86-36048
- ILINA, E. B.**
Application of space imagery to the identification and geological-geophysical study of hidden plutons in early Proterozoic troughs p 20 A86-32682
- IMAI, H.**
On land-sea contrast in the Earth radiation budget p 40 N86-27695
- INGHAM, A. E.**
Position fixing afloat p 33 A86-36788
- INOSTROZAV, H. M.**
Comparison of Circulation estimates and winds based on shipboard and satellite-tracked buoy data in Bransfield Strait. 9-14 March, 1985, part 3 [INPE-3795-PRE/890] p 36 N86-24168
- IRVINE, D. E.**
The spatial evolution of SAR derived wave spectra in the vicinity of Hurricane IVA p 30 A86-33602
- ISAACS, R. G.**
Remote sensing of vertical moisture profiles and cloud properties from simulated millimeter wave sounder and microwave imager data p 53 A86-33547
- ISAACSON, D. L.**
The influence of observational interdependence on spectral reflectance relationships with plant and soil variables p 2 A86-30196
- ISAKOV, V. T.**
Salyut-6 observation of color and brightness contrasts correlated with ocean-bottom relief p 26 A86-32678
- ITTEN, K. I.**
Large area snowmelt runoff simulations based on Landsat-MSS data p 42 A86-33505
A stepwise hierarchical multi-binary approach in TM landuse classification p 46 A86-33597
Resource monitoring oriented remote sensing data processing capabilities p 16 A86-33643
- IVANCHENKO, G. N.**
Computer-aided interpretation of space images with the aim of structural analysis p 20 A86-32690
- IVANOV, L. M.**
Optimal disposition of satellite-tracked drifting buoys in the South Atlantic p 31 A86-34488
- IZRAEL, I. U. A.**
Integrated global monitoring of the world ocean. Volumes 1, 2, & 3 p 24 A86-31350
- IZUMI, I.**
Research and development of the synthetic aperture radar transmitter and receiver subsystem design and some component test results p 54 A86-33636
- J**
- JACK, J. W.**
Applications of sensor payloads p 56 A86-37343
- JACKSON, P. L.**
Verification of L-band SAR calibration p 54 A86-33634
- JACKSON, R. D.**
Detection and evaluation of plant stresses for crop management decisions p 5 A86-33578
Development of agrometeorological crop model inputs from remotely sensed information p 6 A86-33579
The tasseled cap - Size, shape and orientation changes due to soil background p 12 A86-37035
- JARMAN, J.**
ENVIROSTAT-2000 report: Federal agency satellite requirements [NASA-TM-88752] p 59 N86-26355
- JENSEN, J. R.**
Application of LANDSAT TM images to assess circulation and dispersion in coastal lagoons [NASA-CR-177315] p 44 N86-26665
- JOHNSON, D. E.**
Distinguishing among tallgrass prairie cover types from measurements of multispectral reflectance p 10 A86-36047
- JOHNSON, R. W.**
Assessing impacts of off-nadir observation on remote sensing of vegetation - Use of the Suits model p 1 A86-30193
- JOHNSON, TH.**
A stepwise hierarchical multi-binary approach in TM landuse classification p 46 A86-33597
- JOHNSON, W.**
Vegetation assessment using a combination of visible, near-IR and thermal-IR AVHRR data p 5 A86-33577
- JOLMA, P.**
Remote sensing of snow water equivalent using Nimbus-7 SMMR data p 42 A86-33616
- JONSSON, L.**
Satellite imaging of coastal flow circulation in relation to numerical modelling p 31 A86-33631
- JOO, H.**
Context classifier p 46 A86-33535
- JORDAN, T. H.**
Plate motions and deformations from geologic and geodetic data [NASA-CR-177299] p 18 N86-26741
Plate motions and deformations from geologic and geodetic data [NASA-CR-177313] p 19 N86-27833
- K**
- KALNAY, E.**
GLAS experiments on the impact of FGGE satellite data on numerical weather prediction p 57 N86-24128
- KANEMASU, E. T.**
Light interception and leaf area estimates from measurements of grass canopy reflectance p 4 A86-33557
Distinguishing among tallgrass prairie cover types from measurements of multispectral reflectance p 10 A86-36047
- KANUMA, A.**
High speed image processing system with custom VLSI for DSP p 54 A86-33641
- KASISCHKE, E.**
Verification of L-band SAR calibration p 54 A86-33634
- KASISCHKE, E. S.**
SAR-observed internal wave signatures from SARSEX - Initial observations p 31 A86-33646
SAR observed internal wave signatures from SARSEX-comparisons with SAR imaging models p 31 A86-33647
- KATS, I. A. G.**
Interpretation of ring structures on space images and their correlation with geophysical fields and crustal structure in the USSR p 19 A86-32681
- KAUPP, V. H.**
Preliminary analysis of SIR-B images for stereo applications p 45 A86-33515
Preliminary geologic analyses of SIR-B radar data for Hawaii p 21 A86-33550
Introductory analyses of SIR-B radar data for Hawaii p 21 A86-33551
Analysis of L-band multipolarization radar images for lava flow mapping p 21 A86-33593
- KAZANTSEV, V. A.**
Application of space imagery to the identification and geological-geophysical study of hidden plutons in early Proterozoic troughs p 20 A86-32682
- KAZMIN, A. S.**
Some features of small-scale ocean eddies according to an analysis of satellite images p 25 A86-32677
- KELLER, G. R.**
Structure of the southern Rio Grande rift from gravity interpretation p 18 A86-37795
- KELLEY, E. A., JR.**
Hydrographic data from the OPTOMA program, OPTOMA17: OPTOMA17 P, 21 July 1985, OPTOMA17 leg DI, 10-22 August 1985, OPTOMA17 leg DII, 23 August - 5 September 1985 [AD-A162067] p 37 N86-24176
- KIETZMANN, H.**
Satellite-borne 90 GHz radiometer experiment (SABREX), phase A1 [DFVLR-MITT-85-13] p 57 N86-24000
- KILLEEN, J. M.**
Distinguishing among tallgrass prairie cover types from measurements of multispectral reflectance p 10 A86-36047
- KIM, M.**
An improved hybrid classifier p 8 A86-34744
- KIMES, D.**
Directional reflectance response in AVHRR red and near-IR bands for three cover types and varying atmospheric conditions p 13 A86-39146
- KING, C.**
Studies of complex terrain wind flows using acoustic sounder and optical cross-wind remote sensors [DE86-002993] p 58 N86-25925
- KISELEVSKII, L. I.**
Possibility of small-scale physico-geographical regionalization using space spectrometry data p 16 A86-30974
- KITOV, A. D.**
The possibility of applying different types of image-analysis software to environment-protection problems p 16 A86-36513
- KJERFVE, B.**
Application of LANDSAT TM images to assess circulation and dispersion in coastal lagoons [NASA-CR-177315] p 44 N86-26665
- KLEMAS, V.**
Assessing impacts of off-nadir observation on remote sensing of vegetation - Use of the Suits model p 1 A86-30193
Remote sensing investigations of wetland biomass and productivity for global biosystems research [NASA-CR-176725] p 14 N86-23994
- KOBAYASHI, N.**
Terrain height measurement by synthetic aperture radar with an interferometer p 55 A86-34736
- KOGUT, J. A.**
Classification of geophysical parameters using passive microwave satellite measurements p 47 A86-33626
- KONDRATEV, K. IA.**
Environment and climate p 16 A86-38677
The effect of the atmosphere on the satellite remote sensing of earth resources p 56 A86-39969

KOO, J. Y.
An improved hybrid classifier p 8 A86-34744

KORONOVSKII, N. V.
Computer-aided interpretation of space images with the aim of structural analysis p 20 A86-32690

KORZH, V. D.
Investigation of the content of trace elements in sea aerosols and the surface microlayer off sea water p 32 A86-34754

KOVALENOK, V. V.
Salyut-6 observation of color and brightness contrasts correlated with ocean-bottom relief p 26 A86-32678

KOZHEVNIKOV, B. K.
Technical and software facilities at a center for the processing of remote-sensing data p 48 A86-36511

KOZODEROV, V. V.
The effect of the atmosphere on the satellite remote sensing of earth resources p 56 A86-39969

KUBO, M.
High speed image processing system with custom VLSI for DSP p 54 A86-33641

KUBOTA, I.
On land-sea contrast in the Earth radiation budget p 40 N86-27695

KULAKOV, A. P.
Investigation of the earth from space - A new contribution to the development of structural geomorphology p 22 A86-36504

KUMAR, R.
Wind dependence of L-band radar backscatter p 33 A86-35860

KUNIYASU, Y.
High speed image processing system with custom VLSI for DSP p 54 A86-33641

KUROCHKIN, V. S.
Combination of air and space remote-sensing methods and geological-geophysical methods for the purpose of oil and gas exploration in the southern Permsk region p 23 A86-36509

KUZMINA, N. P.
Some features of small-scale ocean eddies according to an analysis of satellite images p 25 A86-32677

L

LACKEY, J. G.
Comprehensive integrated remote sensing for US Department of Energy applications [DE86-002101] p 17 N86-25036

LAMBERT, S. J.
Stable-isotope studies of groundwaters in southeastern New Mexico [DE86-002590] p 43 N86-23027

LARSEN, S.
Evidence of ongoing crustal deformation related to magmatic activity near Socorro, New Mexico p 18 A86-37797

LARSON, R. W.
Lithologic signatures in multi-channel SAR imagery p 45 A86-33522
100 MHz dielectric constant measurements of snow cover Dependence on environmental and snow pack parameters p 42 A86-33613
Verification of L-band SAR calibration p 54 A86-33634

LATHROP, R. G., JR.
Use of Thematic Mapper data to assess water quality in Green Bay and central Lake Michigan p 43 A86-39004

LAUCHT, H.
MOMS-01 (Modular Optoelectronic Multispectral Scanner) for Earth observation: First results of STS-7 mission p 57 N86-24003

LAWRENCE, R. W.
An airborne multiple-beam 1.4 GHz pushbroom microwave radiometer p 6 A86-33583
Microwave backscatter and emission observed from Shuttle Imaging Radar B and an airborne 1.4 GHz radiometer p 53 A86-33584

LAZAREV, A. I.
Salyut-6 observation of color and brightness contrasts correlated with ocean-bottom relief p 26 A86-32678

LEE, D. C. L.
A proposal for a project entitled Assessment of Forest Resources in Uruguay submitted to the United Nations Industrial Development Organization (UNIDO) [INPE-3828-NTE/255] p 15 N86-26666

LEE, T.
Multisource data analysis in remote sensing and geographic information processing p 50 A86-37022

LEPPAERANTA, M.
Investigation of ice dynamics in the marginal ice zone [AD-A164364] p 38 N86-25962

LEVINE, D.
Electronically Steered Thinned Array Radiometer (ESTAR) system design, calibration, and sensitivity p 53 A86-33588

LEVY, G.
A simple, objective analysis scheme for scatterometer data p 32 A86-35550

LEWIS, J. K.
A study of sea ice kinematics and their relationship to arctic ambient noise. Part 3, Section 1: Ambient noise. Section 2: Ambient noise [AD-A165304] p 39 N86-26788
A study of sea ice kinematics and their relationship to arctic ambient noise. Part 3, section 3: Ambient noise [AD-A165305] p 40 N86-26789

LICHY, D.
ENVIROSAT-2000 report: Federal agency satellite requirements [NASA-TM-88752] p 59 N86-26355

LILLESAND, T. M.
Use of multitemporal spectral profiles in agricultural land-cover classification p 10 A86-36084
Use of Thematic Mapper data to assess water quality in Green Bay and central Lake Michigan p 43 A86-39004

LIPA, B. J.
Analysis and interpretation of altimeter sea echo p 27 A86-33483

LIPOVSCAK, B.
Automatic cloud classification p 46 A86-33534

LIRA, J.
A measuring reference system to quantify the desertification process in a semiarid ecosystem based on Landsat MSS data p 16 A86-37011

LIU, J.
Application of Shuttle imaging radar data for land use investigations p 51 A86-39150

LLEWELLYN-JONES, D. T.
ERS-1 - Our new window on the oceans for the 1990s p 34 A86-38718

LO, T. H. C.
Use of multitemporal spectral profiles in agricultural land-cover classification p 10 A86-36084

LONG, V. L.
Sea ice dynamics and regional meteorology for the Arctic polynya experiment (APEX)-Bering Sea 1985 [PB86-148038] p 38 N86-25939

LOZANO-GARCIA, D. F.
Hierarchical classification of multitemporal/multispectral scanner data p 49 A86-37017

LUNDGREN, J. C.
Evaluation of crop acreage estimation methods using Landsat data as auxiliary input p 6 A86-33606

LYBANON, M.
Ocean wave slope statistics from automated analysis of sun glitter photographs [AD-A161995] p 37 N86-24172

LYNN, D. W.
Monotemporal, multitemporal, and multirate thermal infrared data acquisition from satellites for soil and surface-material survey p 1 A86-30191

LYZENGA, D.
Simulations of SAR wave spectra using high spectral resolution estimates from the SCR and ROWS instruments p 30 A86-33611

LYZENGA, D. R.
SAR-observed internal wave signatures from SARSEX - Initial observations p 31 A86-33646
SAR observed internal wave signatures from SARSEX-comparisons with SAR imaging models p 31 A86-33647

M

MACDONALD, H. C.
Preliminary analysis of SIR-B images for stereo applications p 45 A86-33515
Preliminary geologic analyses of SIR-B radar data for Hawaii p 21 A86-33550
Introductory analyses of SIR-B radar data for Hawaii p 21 A86-33551
Analysis of L-band multipolarization radar images for lava flow mapping p 21 A86-33593

MACDONALD, R. B.
Satellite-derived leaf-area-index and vegetation maps as input to global carbon cycle models - A hierarchical approach p 2 A86-30194
Spectral characterization of biophysical characteristics in a boreal forest - Relationship between Thematic Mapper band reflectance and leaf area index for Aspen p 8 A86-35677

MACKENZIE, J. S.
Use of Seasat SAR imagery for geological mapping in a volcanic terrain - Askja Caldera, Iceland p 19 A86-30189

MACKINNON, D. J.
Remote monitoring of processes that shape desert surfaces: The Desert Winds Project [TI86-900108] p 24 N86-25099

MAGILL, K. E.
Application of LANDSAT TM images to assess circulation and dispersion in coastal lagoons [NASA-CR-177315] p 44 N86-26665

MAKALOVSKII, V. V.
Combination of air and space remote-sensing methods and geological-geophysical methods for the purpose of oil and gas exploration in the southern Permsk region p 23 A86-36509

MAKTAV, D.
The study of the natural geographic differences in the coastal areas of water covered parts of Marmara region in Turkey with the help of Landsat-4 MSS data using an unsupervised classification algorithm with Euclidean distance p 43 A86-37012

MANLEY, T. O.
Marginal ice zone experiment - 1984, physical oceanography report: USNS Lynch and helicopter-based STD data [AD-A163096] p 37 N86-24180
Physical oceanography report: Camp-based and helicopter-based STD data from the drifting ice station FRAM 3 [AD-A163097] p 37 N86-24181

MARGOLIS, J. S.
Passive remote sensing of stratospheric and mesospheric winds p 53 A86-33545

MARKS, B.
On-board data compression for advanced Landsat p 45 A86-32368

MARMOEJO, E.
Heat budget and climatic atlas of the equatorial Atlantic Ocean during FGGE (First GARP Global Experiment, 1979 [PB86-111622] p 35 N86-23213

MARTIN, S.
Weddell-Scotia sea marginal ice zone observations from space, October 1984 p 26 A86-33105

MARTINEC, J.
Large area snowmelt runoff simulations based on Landsat-MSS data p 42 A86-33505

MARTINKO, E. A.
Research on enhancing the utilization of digital multispectral data and geographic information systems in global habitability studies [NASA-CR-177294] p 17 N86-26669

MARUYAMA, T.
Estimation of monthly rainfall from satellite-observed cloud amount in the tropical western Pacific p 43 A86-36234

MASTIN, G. A.
Methods of obtaining offshore wind direction and sea-state data from X-band aircraft SAR (Synthetic Aperture Radar) imagery of coastal waters [AD-A165552] p 38 N86-26517

MATSON, M.
Hydrologic and land sciences applications of NOAA polar-orbiting satellite data p 43 N86-23993
NOAA Atlas: An atlas of satellite-derived Northern Hemispheric snow cover frequency p 44 N86-24075

MAUGHAN, P. M.
A multi-national consortium opportunity for remote sensing p 58 A86-34111

MCARDLE, R.
ENVIROSAT-2000 report: Federal agency satellite requirements [NASA-TM-88752] p 59 N86-26355

MCCAUL, E. W.
Analysis of airborne Doppler lidar, Doppler radar and tall tower measurements of atmospheric flows in quiescent and stormy weather [NASA-CR-3960] p 56 N86-23159

MCCAULEY, C. K.
Remote monitoring of processes that shape desert surfaces: The Desert Winds Project [TI86-900108] p 24 N86-25099

MCCAULEY, J. F.
Remote monitoring of processes that shape desert surfaces: The Desert Winds Project [TI86-900108] p 24 N86-25099

MCCLEAVE, E. P.
Sea surface temperature determinations p 28 A86-33487

MCCLEESE, D. J.
Passive remote sensing of stratospheric and mesospheric winds p 53 A86-33545

MCCORMICK, M. P.
SAGE observations of stratospheric nitrogen dioxide p 55 A86-36838
Transport processes as manifested in satellite and lidar aerosol measurements p 17 N86-27788

- MCELROY, J. H.**
The evolution of remote sensing science and applications p 58 A86-37002
- MCEWEN, R. B.**
Research, investigations and technical developments: National mapping program, 1983-1984 [PB86-166097] p 17 N86-26675
- MCINTOSH, R. E.**
Description of a databank of normalized radar cross section of terrain p 45 A86-33526
- MCKEE, B.**
Modified cubic convolution resampling for Landsat p 47 A86-33640
- MCNUTT, L.**
Weddell-Scotia sea marginal ice zone observations from space, October 1984 p 26 A86-33105
- MCPHERSON, R. D.**
Oceanic surface winds p 27 A86-33484
- MCROY, C. P.**
Influence of the Yukon River on the Bering Sea [NASA-CR-177310] p 39 N86-26783
- MEHTA, N. C.**
Satellite-derived leaf-area-index and vegetation maps as input to global carbon cycle models - A hierarchical approach p 2 A86-30194
- MEHTRE, B. M.**
Automatic cloud classification p 46 A86-33534
- MEIER, E. H.**
Resource monitoring oriented remote sensing data processing capabilities p 16 A86-33643
- MEISSNER, D.**
MOMS-01 (Modular Optoelectronic Multispectral Scanner) for Earth observation: First results of STS-7 mission p 57 N86-24003
- MELFI, S. H.**
Lidar observations of the planetary boundary layer p 29 A86-33532
- MENDEL, S. K.**
Machine processing of remotely sensed data - Quantifying global process: Models, sensor systems, and analytical methods; Proceedings of the Eleventh International Symposium, Purdue University, West Lafayette, IN, June 25-27, 1985 p 56 A86-37001
- MERCHANT, J. W.**
Research on enhancing the utilization of digital multispectral data and geographic information systems in global habitability studies [NASA-CR-177294] p 17 N86-26669
- MEYERS, M. B.**
A simulation analysis of the fate of phytoplankton within the mid-Atlantic bight [NASA-CR-177265] p 39 N86-26670
- MIKHALTSOV, E. G.**
Technical and software facilities at a center for the processing of remote-sensing data p 48 A86-36511
- MILBERT, D.**
Sea level time series in the equatorial Pacific from satellite altimetry p 34 A86-38648
- MILENOVA, L. I.**
Remote sensing and modeling of the dynamics of the western part of the Black Sea p 26 A86-32679
- MILLER, L.**
Sea level time series in the equatorial Pacific from satellite altimetry p 34 A86-38648
- MILLER, M. W.**
Commercial applications of the Navstar Global Positioning System p 54 A86-34112
- MINIELLY, N.**
Processing of multi-sensor remotely sensed data to a standard geocoded format p 50 A86-37019
- MITCHELL, L. P.**
'New opportunities in remote sensing' p 58 A86-34118
- MITCHELL, T. P.**
Relationships between surface observations over the global oceans and the southern oscillation [PB86-110038] p 35 N86-24112
- MO, T.**
Microwave backscatter and emission observed from Shuttle Imaging Radar B and an airborne 1.4 GHz radiometer p 53 A86-33584
- MOCCIA, A.**
An integrated approach to geometric precision processing of spaceborne high-resolution sensors p 55 A86-34737
- MOGNARD, N. M.**
Observations of the polar regions from satellites using active and passive microwave techniques p 28 A86-33489
- MOLINAN, R. L.**
Heat budget and climatic atlas of the equatorial Atlantic Ocean during FGGE (First GARP Global Experiment, 1979 [PB86-111622] p 35 N86-23213
- MONALDO, F. M.**
The spatial evolution of SAR derived wave spectra in the vicinity of Hurricane IVA p 30 A86-33602
Directional ocean wave spectra obtained from the Shuttle Imaging Radar off the coast of Chile p 30 A86-33612
- MONTGOMERY, D.**
NOAA satellite requirements forecast [AD-A165244] p 40 N86-27414
- MOOERS, C. N. K.**
Hydrographic data from the OPTOMA program, OPTOMA17: OPTOMA17 P, 21 July 1985, OPTOMA17 leg DI, 10-22 August 1985, OPTOMA17 leg DII, 23 August - 5 September 1985 [AD-A162067] p 37 N86-24176
- MOORE, H. D.**
Economical maintenance of a national topographic data base using Landsat images p 48 A86-36082
- MOORE, R. K.**
Identification of major backscattering sources in trees and shrubs at 10 GHz p 13 A86-39149
- MOREIRA, M. A.**
Wheat area estimation using digital LANDSAT MSS data and aerial photographs [INPE-3824-PRE/900] p 15 N86-26667
- MORGAN, P.**
Structure of the southern Rio Grande rift from gravity interpretation p 18 A86-37795
- MORRISON, D. B.**
Machine processing of remotely sensed data - Quantifying global process: Models, sensor systems, and analytical methods; Proceedings of the Eleventh International Symposium, Purdue University, West Lafayette, IN, June 25-27, 1985 p 56 A86-37001
- MOUGINIS-MARK, P. J.**
Preliminary geologic analyses of SIR-B radar data for Hawaii p 21 A86-33550
- MOWER, R. D.**
The emergence of airborne video techniques as an alternative for accessing tropical environments - A historical perspective p 56 A86-37007
- MUEKSCH, M. C.**
Detection of biomass by an empiric albedo and spectral reflectance model in the Sahara Desert from Landsat-imagery p 11 A86-37015
- MUNEYAMA, K.**
Satellite thermal observation of oil slicks on the Persian Gulf p 33 A86-36048
- MURTHY, N. N.**
Automatic cloud classification p 46 A86-33534
- MUSTARD, J. F.**
Spectroscopy of Moses Rock dike using remote sensing p 21 A86-33521
- MYHRE, D. L.**
Wavelength intensity indices in relation to tree condition and leaf-nutrient content p 12 A86-37036

N

- NACINI, E.**
An atlas of original and mercator-transformed satellite-data images of the Alboran Sea, August-October 1983 [AD-A161898] p 36 N86-24170
- NAKAHARA, S.**
Monthly maps of sea level anomalies in the Pacific, 1975-1981. Report on the IGOSS (Integrated Global Ocean Services System) Sea Level Pilot Project [AD-A163061] p 38 N86-25104
- NAKAZAWA, T.**
Intraseasonal variations of OLR in the tropics during the FGGE year p 48 A86-36227
- NARAYANAN, R. M.**
Description of a databank of normalized radar cross section of terrain p 45 A86-33526
- NEDOSHOVENKO, A. I.**
The use of remote-sensing data to predict regional and local oil-and-gas-bearing structures within the Dneprovsk-Donetsk paleo rift p 23 A86-36508
- NEFF, W.**
Studies of complex terrain wind flows using acoustic sounder and optical cross-wind remote sensors [DE86-002993] p 58 N86-25925
- NELSON, R.**
Identifying deforestation in Brazil using multiresolution satellite data p 8 A86-34742
- NICHOLS, J. D.**
Conceptual design study: Forest Fire Advanced System Technology (FFAST) [JPL-PUBL-86-5] p 14 N86-25034
- NICHOLSON, H. E.**
Technological improvements to naval aviation weather support p 34 A86-37506
- NILSSON, G.**
Statistical lineament analysis in South Greenland based on Landsat imagery p 22 A86-35676
- NISHIKOWA, K.**
Research and development of the synthetic aperture radar transmitter and receiver subsystem design and some component test results p 54 A86-33636
- NITTA, T.**
Estimation of monthly rainfall from satellite-observed cloud amount in the tropical western Pacific p 43 A86-36234
- NIXON, P. R.**
Spectral components analysis - A bridge between spectral observations and agrometeorological crop models p 7 A86-33627
- NOBLE, D. D.**
The nature and origin of mineral coatings on volcanic rocks of the Black Mountain, Stonewall Mountain and Kane Springs Wash volcanic centers in southern Nevada [NASA-CR-176805] p 24 N86-25912
- NOVAES, R. A.**
A proposal for a project entitled Assessment of Forest Resources in Uruguay submitted to the United Nations Industrial Development Organization (UNIDO) [INPE-3828-NTE/255] p 15 N86-26666
- NUESCH, D. R.**
Resource monitoring oriented remote sensing data processing capabilities p 16 A86-33643

O

- OCHOA, M. C.**
Agricultural applications for thermal infrared multispectral scanner data p 12 A86-37034
- OGISHIMA, T.**
Applicability of atmospheric correction algorithm for CZCS data to Japanese coastal area p 31 A86-33632
- OHNING, G.**
NOAA plans for remote sensing of the earth, oceans and atmosphere p 52 A86-33502
Operational satellite support to scientific programs [AD-A165081] p 59 N86-27412
- ONEILL, P. E.**
Passive microwave soil moisture research p 2 A86-33504
- ONSTOTT, R. G.**
100 MHz dielectric constant measurements of snow cover Dependence on environmental and snow pack parameters p 42 A86-33613
- OVERLAND, J.**
Oceanic surface winds p 27 A86-33484
- OZGA, M.**
USDA/SRS software for Landsat MSS-based crop-acreage estimation p 6 A86-33605

P

- PACHECODOSSANTOS, A.**
A proposal for a project entitled Assessment of Forest Resources in Uruguay submitted to the United Nations Industrial Development Organization (UNIDO) [INPE-3828-NTE/255] p 15 N86-26666
- PALAGIN, I. I.**
Probabilistic modeling of fields of atmospheric turbulence and sea roughness with reference to the study of complex systems p 33 A86-36480
- PALM, S. P.**
Lidar observations of the planetary boundary layer p 29 A86-33532
- PANASENKO, V. N.**
Aspects of the geological interpretation of geophysical fields and results of air and space remote-sensing observations of oil-and-gas-bearing territories p 23 A86-36510
- PANASENKO, V. V.**
Aspects of the geological interpretation of geophysical fields and results of air and space remote-sensing observations of oil-and-gas-bearing territories p 23 A86-36510
- PANGBURN, T.**
ENVIROSAT-2000 report: Federal agency satellite requirements [NASA-TM-88752] p 59 N86-26355
- PAPAS, C. H.**
Modelling of backscatter from vegetation layers p 4 A86-33554
- PARIS, J. F.**
Radar scatterometer probing of thick vegetation canopies p 3 A86-33523
- PARK, K. H.**
A non-stationary contextual classifier with improved accuracy p 47 A86-33621

- PARKS, G. S.**
High resolution millimeter-wave imaging sensor
p 54 A86-33590
- PARMENTER-HOLT, F.**
Hydrologic and land sciences applications of NOAA polar-orbiting satellite data
p 43 N86-23993
- PARRISH, J. B.**
Near infrared leaf reflectance modeling
p 4 A86-33556
- PARSONS, C. L.**
Design and benefits of a multibeam Earth Observing Radar
p 29 A86-33591
- PASQUARIELLO, G.**
Landsat TM image forward/reverse scan banding Characterization and correction
p 49 A86-36790
- PAUL, C.**
ENVIROSAT-2000 report: Federal agency satellite requirements
[NASA-TM-88752]
p 59 N86-26355
- PEASE, C. H.**
Sea ice dynamics and regional meteorology for the Arctic polynya experiment (APEX)-Bering Sea 1985
[PB86-148038]
p 38 N86-25939
- PECH, R. P.**
Reflectance modelling and the derivation of vegetation indices for an Australian semi-arid shrubland
p 7 A86-34740
- PELLETIER, R. E.**
Remote sensing techniques for the detection of soil erosion and the identification of soil conservation practices
p 3 A86-33506
Agricultural applications for thermal infrared multispectral scanner data
p 12 A86-37034
- PETERSON, D. L.**
Analysis of forest/structure using thematic mapper simulator data
p 4 A86-33540
- PETROVA, E. S.**
The use of remote-sensing data to predict regional and local oil-and-gas-bearing structures within the Dneprovsk-Donetsk paleorift
p 23 A86-36508
- PHILIPSON, W. R.**
A texture-enhancement procedure for separating orchard from forest in Thematic Mapper data
p 2 A86-30198
- PIATIBRAT, T. V.**
A histogram as the basis of the statistical classification of images
p 45 A86-32688
- PIATKIN, V. P.**
Certain transformations in a quantitative approach to image processing
p 48 A86-36517
- PIERSON, W. J., JR.**
Oceanic surface winds
p 27 A86-33484
- PIETERS, C. M.**
Spectroscopy of Moses Rock dike using remote sensing
p 21 A86-33521
- PIETRAFESA, L. J.**
High frequency sampling of the 1984 spring bloom within the mid-Atlantic Bight: Synoptic shipboard, aircraft, and in situ perspectives of the SEEP-1 experiment
[NASA-TM-88765]
p 41 N86-27700
- PINTER, P. J., JR.**
Detection and evaluation of plant stresses for crop management decisions
p 5 A86-33578
Development of agrometeorological crop model inputs from remotely sensed information
p 6 A86-33579
Effect of dew on canopy reflectance and temperature
p 10 A86-36049
- PISARUCK, M. A.**
Preliminary analysis of SIR-B images for stereo applications
p 45 A86-33515
- PITTS, D. E.**
Estimation of biophysical properties of forest canopies through inversion of microwave scatterometer data
p 4 A86-33542
- PLIUTA, V. E.**
Possibility of small-scale physiogeographical regionalization using space spectrometry data
p 16 A86-30974
- PLOKHENKO, IU. V.**
An algorithm for the identification of cloud cover and the estimation of spectral brightnesses of the cloudless atmosphere according to satellite scanning measurements of outgoing IR radiation
p 52 A86-33317
Experiments on the remote temperature sounding of the atmosphere on the basis of NOAA-satellite radiometer measurements
p 52 A86-33318
- POMALAZA-RAEZ, C. A.**
Estimation of the location parameter of a multispectral distribution by a median operator
p 49 A86-37006
- PONZONI, F. J.**
A proposal for a project entitled Assessment of Forest Resources in Uruguay submitted to the United Nations Industrial Development Organization (UNIDO)
[INPE-3828-NTE/255]
p 15 N86-26666
- PORCH, W. M.**
Studies of complex terrain wind flows using acoustic sounder and optical cross-wind remote sensors
[DE86-002993]
p 58 N86-25925
- POSCOLIERI, M.**
Lineament analysis in a test area of northern Mozambique
p 20 A86-33520
- POWELL, R. J.**
Relative vertical positioning using ground-level transponders with the ERS-1 altimeter
p 33 A86-35688
- PRAKASH, A.**
Modified cubic convolution resampling for Landsat
p 47 A86-33640
- PREVOST, C.**
Integration of high and low resolution satellite data for crop condition assessment
p 12 A86-37020
- PRICE, J. F.**
Satellite observations of sea surface cooling by hurricanes
p 32 A86-35545
- PYLE, T.**
NOAA satellite requirements forecast
[AD-A165244]
p 40 N86-27414
- R**
- RABIN, R.**
Analysis of airborne Doppler lidar, Doppler radar and tall tower measurements of atmospheric flows in quiescent and stormy weather
[NASA-CR-3960]
p 56 N86-23159
- RAFFY, M.**
A stable iterative procedure to obtain soil surface parameters and fluxes from satellite data
p 8 A86-35678
- RAMACHANDRA RAO, A.**
Hydrologic modeling using Landsat MSS data
p 43 A86-37010
- RAMSEY, A.**
Comparison of the Defense Meteorological Satellite Program (DMSP) and the NOAA Polar-orbiting Operational Environmental Satellite (POES) program
[AD-A165118]
p 59 N86-27413
- RANEY, R. K.**
SNR in SAR
p 54 A86-33633
- RANSON, K. J.**
Sun angle, view angle, and background effects on spectral response of simulated balsam fir canopies
p 13 A86-39002
- RAO, D. B.**
Objective analysis of tidal fields in the Atlantic and Indian Oceans
[NASA-TM-87773]
p 39 N86-26782
- RAPP, R. H.**
Gravity anomalies and sea surface heights derived from a combined GEOS 3/Seasat altimeter data set
p 33 A86-36096
The study of gravity field estimation procedures
[AD-A164564]
p 19 N86-26745
- RAWER, K.**
Problems with global mapping
p 48 A86-35111
- RAYNA, E.**
Estimation of biophysical properties of forest canopies through inversion of microwave scatterometer data
p 4 A86-33542
- REGINATO, R. J.**
Detection and evaluation of plant stresses for crop management decisions
p 5 A86-33578
Analysis of a resistance-energy balance method for estimating daily evaporation from wheat plots using one-time-of-day infrared temperature observations
p 13 A86-39148
- REILINGER, R.**
Evidence of ongoing crustal deformation related to magmatic activity near Socorro, New Mexico
p 18 A86-37797
- REUTOV, E. A.**
Determination of the moisture content of nonuniformly moistened soils with a surface transition layer on the basis of microwave spectroradiometry
p 2 A86-32684
- REYNALDES, T. E.**
Adding spatial considerations to the JABOWA model of forest growth
p 11 A86-37014
- REYNOLDS, M.**
Sea ice dynamics and regional meteorology for the Arctic polynya experiment (APEX)-Bering Sea 1985
[PB86-148038]
p 38 N86-25939
- RHO, J. K.**
A non-stationary contextual classifier with improved accuracy
p 47 A86-33621
- RICHARDS, J. A.**
Multisource data analysis in remote sensing and geographic information processing
p 50 A86-37022
- RICHARDSON, A. J.**
Diurnal patterns of bidirectional vegetation indices for wheat canopies
p 1 A86-30192
Classification of south Texas farm and range resources using NOAA7 AVHRR satellite imagery
p 5 A86-33558
Development of agrometeorological crop model inputs from remotely sensed information
p 6 A86-33579
Spectral components analysis - A bridge between spectral observations and agrometeorological crop models
p 7 A86-33627
- RIGTERINK, P. V.**
Detecting desert locust breeding grounds in the Sahel with satellite data
p 16 A86-32537
- RINGROSE, P. S.**
Use of Seasat SAR imagery for geological mapping in a volcanic terrain - Askja Caldera, Iceland
p 19 A86-30189
- RIPPLE, W. J.**
The influence of observational interdependence on spectral reflectance relationships with plant and soil variables
p 2 A86-30196
- ROBERTS, A.**
Practical photogrammetry from 35-mm aerial photography
p 55 A86-36080
- ROBINSON, W. D.**
Optimized retrievals of precipitable water fields from combinations of VAS satellite and conventional surface observations
p 43 A86-36193
- ROCK, B. N.**
Field and airborne spectral characterization of suspected damage in red spruce (*Picea rubens*) from Vermont
p 11 A86-37008
- ROGERS, D. C.**
A technique for assessing the severity of terrain shadowing in mobile satellite service
p 51 A86-39545
- ROLLIN, E. M.**
Estimation of atmospheric corrections from multiple aircraft imagery
p 49 A86-36784
- ROPELEWSKI, C. F.**
NOAA Atlas: An atlas of satellite-derived Northern Hemispheric snow cover frequency
p 44 N86-24075
- ROSE, A.**
Rectification of scanner images using prediction approaches
[SER-C-303]
p 57 N86-23992
- ROSS, D. B.**
Oceanic surface winds
p 27 A86-33484
- ROSSO, R.**
The ARGOS system for positioning and data collection by satellite - Characteristics and performance levels
p 56 A86-39559
- ROTHROCK, D. A.**
Weddell-Scotia sea marginal ice zone observations from space, October 1984
p 26 A86-33105
Extracting sea ice data from satellite SAR imagery
p 29 A86-33560
- RUF, C.**
Electronically Steered Thinned Array Radiometer (ESTAR) system design, calibration, and sensitivity
p 53 A86-33588
- RUFENACH, C. L.**
Surface and internal ocean wave observations
p 27 A86-33485
- RUMENINA, E. K.**
Remote sensing and modeling of the dynamics of the western part of the Black Sea
p 26 A86-32679
- RUSENOV, V. M.**
Remote sensing and modeling of the dynamics of the western part of the Black Sea
p 26 A86-32679
- RUZEK, M.**
Preliminary science results from the Shuttle Imaging Radar-B
p 50 A86-37027
- RYAN, T. W.**
Image segmentation algorithms
p 45 A86-32370
- S**
- SADER, S. A.**
Analysis of effective radiant temperatures in a Pacific Northwest forest using Thermal Infrared Multispectral Scanner data
p 9 A86-36042
- SAKATA, T.**
High accuracy clustering using residual image
p 49 A86-37003
- SALAMONOWICZ, P. H.**
Satellite orientation and position for geometric correction of scanner imagery
p 48 A86-36079
- SALBY, M. L.**
Transient response to localized episodic heating in the tropics
p 51 N86-27749
- SALO, S. A.**
Sea ice dynamics and regional meteorology for the Arctic polynya experiment (APEX)-Bering Sea 1985
[PB86-148038]
p 38 N86-25939

- SALTZMAN, B.**
Satellite oceanic remote sensing p 27 A86-33481
- SALVI, S.**
Lineament analysis in a test area of northern Mozambique p 20 A86-33520
- SALVINI, F.**
Topographic lineament domains of the Appalachians - Some new methods and techniques for paleostress analysis p 20 A86-33518
Slope-intercept-density plots - A new method for line detection in images p 46 A86-33600
- SALZER, D.**
Satellite-borne 90 GHz radiometer experiment (SABREX), phase A1 [DFVLR-MITT-85-13] p 57 N86-24000
- SANCHEZ, B. V.**
Objective analysis of tidal fields in the Atlantic and Indian Oceans [NASA-TM-87773] p 39 N86-26782
- SARKAR, A.**
Wind dependence of L-band radar backscatter p 33 A86-35860
- SASAKI, Y.**
Satellite thermal observation of oil slicks on the Persian Gulf p 33 A86-36048
- SASSER, J. H.**
A measuring reference system to quantify the desertification process in a semiarid ecosystem based on Landsat MSS data p 16 A86-37011
- SCARPACE, F. L.**
Use of multitemporal spectral profiles in agricultural land-cover classification p 10 A86-36084
- SCHENCK, L.**
What are the best radar wavelengths, incidence angles and polarizations for geologic applications? A statistical approach p 21 A86-33592
- SCHUIE, J. C.**
Microwave backscatter and emission observed from Shuttle Imaging Radar B and an airborne 1.4 GHz radiometer p 53 A86-33584
- SCHMID, R.**
Satellite-borne 90 GHz radiometer experiment (SABREX), phase A1 [DFVLR-MITT-85-13] p 57 N86-24000
- SCHMUGGE, T. J.**
Passive microwave soil moisture research p 2 A86-33504
Microwave backscatter and emission observed from Shuttle Imaging Radar B and an airborne 1.4 GHz radiometer p 53 A86-33584
- SCHOENENBERGER, J. G.**
The design, construction and early trials of a novel airborne surveillance radar p 25 A86-32635
- SCHOWENGERDT, R. A.**
Measurement of Thematic Mapper data quality p 50 A86-37032
- SCHRUMPF, B. J.**
The influence of observational interdependence on spectral reflectance relationships with plant and soil variables p 2 A86-30196
- SCHUELER, C.**
On-board data compression for advanced Landsat p 45 A86-32368
- SCHULTZ, H.**
A median filter approach for correcting errors in a vector field p 29 A86-33601
- SCHWALB, A.**
GOES (Geostationary Operational Environmental Satellite)-next overview [AD-A165080] p 59 N86-27411
- SCOTT, J. F.**
Spectral measurements in support of SIR-B using the Surface Contour Radar p 30 A86-33609
- SEIDEL, K.**
Large area snowmelt runoff simulations based on Landsat-MSS data p 42 A86-33505
- SHAFFER, L.**
ENVIROSAT-2000 report: Federal agency satellite requirements [NASA-TM-88752] p 59 N86-26355
International coordination of and contributions to environmental satellite programs [AD-A165142] p 60 N86-28016
- SHALYGIN, A. S.**
Probabilistic modeling of fields of atmospheric turbulence and sea roughness with reference to the study of complex systems p 33 A86-36480
- SHEFFNER, E.**
Multi-crop area estimation and mapping on a microprocessor/mainframe network p 7 A86-33644
- SHEMIKIN, L. M.**
Method for the quantitative estimation of convergence in mapping in the case of the interpretation of space photographs of oil-and-gas-bearing regions of Siberia p 23 A86-36505
- SHEN, S. S.**
An information measure for class discrimination p 11 A86-36789
- SHERMAN, J. W., III**
The 1978 oceanic trilogy - Seasat, Nimbus-7, and TIROS-N p 27 A86-33482
- SHIBAYAMA, M.**
Diurnal patterns of bidirectional vegetation indices for wheat canopies p 1 A86-30192
- SHIH, S.-F.**
Wavelength intensity indices in relation to tree condition and leaf-nutrient content p 12 A86-37036
- SHIMODA, H.**
High accuracy clustering using residual image p 49 A86-37003
- SHUCHMAN, R. A.**
SAR remote sensing during MIZEF 84 p 29 A86-33561
SAR-observed internal wave signatures from SARSEX - Initial observations p 31 A86-33646
SAR observed internal wave signatures from SARSEX-comparisons with SAR imaging models p 31 A86-33647
- SHULTS, S. S.**
Features of the geological application of space data p 19 A86-32680
- SHUTKO, A. M.**
Determination of the moisture content of nonuniformly moistened soils with a surface transition layer on the basis of microwave spectroradiometry p 2 A86-32684
- SIEBER, A. J.**
Forest signatures in imaging and non-imaging microwave scatterometer data p 9 A86-36037
- SILVER, G. L.**
Operational methods for data interpolation [DE85-016050] p 34 N86-15969
- SINGH, S. M.**
Vegetation index and possibility of complementary parameters from AVHRR/2 p 2 A86-30197
The estimation of atmospheric effects for SPOT using AVHRR channel-1 data p 47 A86-34738
- SINIAKOVICH, S. G.**
Possibility of small-scale physiogeographical regionalization using space spectrometry data p 16 A86-30974
- SKOU, N.**
Push-broom microwave radiometer systems for space applications p 53 A86-33589
Microwave radiometry for oil pollution monitoring, measurements, and systems p 32 A86-35682
- SLANEY, V. R.**
Landsat MSS and airborne geophysical data combined for mapping granite in southwest Nova Scotia p 23 A86-37021
- SLATER, P. N.**
Spectroradiometric considerations for advanced land observing systems [NASA-CR-177205] p 58 N86-27705
- SLIWINSKI, P.**
Satellite-borne 90 GHz radiometer experiment (SABREX), phase A1 [DFVLR-MITT-85-13] p 57 N86-24000
- SMITH, J. L.**
Predicting tree groundline diameter from crown measurements made on 35-mm aerial photography p 13 A86-39006
- SMOKTII, O. I.**
The effect of the atmosphere on the satellite remote sensing of earth resources p 56 A86-39969
- SPANNER, M. A.**
Analysis of forest/structure using thematic mapper simulator data p 4 A86-33540
- SPAYD, L. E., JR.**
Characteristics of western region flash flood events in GOES imagery and conventional data [NOAA-TM-NESDIS-13] p 44 N86-26668
- SPINIRNE, J. D.**
Lidar observations of the planetary boundary layer p 29 A86-33532
- SPRAY, L. A.**
Satellite cloud and precipitation analysis using a minicomputer [AD-A163821] p 58 N86-25084
- ST. MARTIN, J. W.**
A review of methods to track oil in arctic waters [AD-A164679] p 39 N86-26716
- STAENZ, K.**
A stepwise hierarchical multi-binary approach in TM landuse classification p 46 A86-33597
Resource monitoring oriented remote sensing data processing capabilities p 16 A86-33643
- STAGE, S. A.**
An investigation of the marine boundary layer during cold air outbreak [NASA-CR-177287] p 39 N86-26758
- An investigation of the marine boundary layer during cold air outbreak [NASA-CR-177249] p 41 N86-27838
- STANEV, E. V.**
Remote sensing and modeling of the dynamics of the western part of the Black Sea p 26 A86-32679
- STAROSTENKO, D. A.**
Formation of a digital data base for automated forest mapping p 2 A86-32689
- STAYLOR, W. F.**
Site selection and directional models of deserts used for ERBE validation targets [NASA-TP-2540] p 57 N86-23160
- STECH, J. L.**
Comparison of Circulation estimates and winds based on shipboard and satellite-tracked buoy data in Bransfield Strait, 9-14 March, 1985, part 3 [INPE-3795-PRE/890] p 36 N86-24168
- STEENROD, S. D.**
Objective analysis of tidal fields in the Atlantic and Indian Oceans [NASA-TM-87773] p 39 N86-26782
- STEGALL, M.**
On-board data compression for advanced Landsat p 45 A86-32368
- STEVEN, M. D.**
Estimation of atmospheric corrections from multiple aircraft imagery p 49 A86-36784
- STEVENSON, M. R.**
Development of a satellite-tracked oceanographic drifting buoy for the Brazilian Antarctic Program, part 1 [INPE-3793-PRE/888] p 36 N86-24166
Comparison of Circulation estimates and winds based on shipboard and satellite-tracked buoy data in Bransfield Strait, 9-14 March, 1985, part 3 [INPE-3795-PRE/890] p 36 N86-24168
- STRAHLER, A. H.**
California timber volume inventory using Landsat p 4 A86-33541
- STRAKHOVA, N. A.**
Application of space imagery to the identification and geological-geophysical study of hidden plutons in early Proterozoic troughs p 20 A86-32682
- STRAMMA, L.**
Satellite observations of sea surface cooling by hurricanes p 32 A86-35545
- STUMPF, R. P.**
Physical interpretation of estuarine water color using vector analysis of satellite data p 43 A86-33630
- STUTZMAN, W. L.**
Estimation of the weight of vegetation using microwave transmission measurements p 3 A86-33524
- SUDBIN, A. I.**
Determination of sea spectral reflectance from airborne measurements p 26 A86-32683
- SUGAI, M.**
High speed image processing system with custom VLSI for DSP p 54 A86-33641
- SULLIVAN, K.**
Structure of terrestrial impact craters from SIR-B radar data - Preliminary results p 21 A86-33552
- SUNDARA-RAJAN, A.**
Analysis of airborne Doppler lidar, Doppler radar and tall tower measurements of atmospheric flows in quiescent and stormy weather [NASA-CR-3960] p 56 N86-23159
- SUSSKIND, J.**
GLAS experiments on the impact of FGGE satellite data on numerical weather prediction p 57 N86-24128
Simulation studies related to the design of post-FGGE observing systems p 57 N86-24160
- SUTOVSKII, V. M.**
Estimation of the accuracy of the remote determination of ocean surface temperature on the basis of satellite measurements of outgoing thermal radiation in the 10.5-12.5 micron range p 27 A86-33320
- SWAIN, P. H.**
Approaches to computer reasoning in remote sensing and geographic information processing - A survey p 16 A86-33595
Multisource data analysis in remote sensing and geographic information processing p 50 A86-37022
- SWIFT, C. T.**
Observations of the polar regions from satellites using active and passive microwave techniques p 28 A86-33489
Electronically Steered Thinned Array Radiometer (ESTAR) system design, calibration, and sensitivity p 53 A86-33588
- SWIFT, R. N.**
Spectral measurements in support of SIR-B using the Surface Contour Radar p 30 A86-33609
High frequency sampling of the 1984 spring bloom within the mid-Atlantic Bight: Synoptic shipboard, aircraft, and in situ perspectives of the SEEP-1 experiment [NASA-TM-88765] p 41 N86-27700

T

- TACONET, O.**
Evapotranspiration over an agricultural region using a surface flux/temperature model based on NOAA-AVHRR data p 10 A86-36237
- TANAKA, K.**
Research and development of the synthetic aperture radar transmitter and receiver subsystem design and some component test results p 54 A86-33636
- TARANIK, J. V.**
The nature and origin of mineral coatings on volcanic rocks of the Black Mountain, Stonewall Mountain and Kane Springs Wash volcanic centers in southern Nevada [NASA-CR-176805] p 24 N86-25912
- TENG, X.**
Application of Shuttle imaging radar data for land use investigations p 51 A86-39150
- TEPLIAKOV, N. A.**
Choice of spectral bands for a spaceborne multispectral scanner p 55 A86-36514
- THEIS, S. W.**
Utilization of active microwave roughness measurements to improve passive microwave soil moisture estimates over bare soils p 8 A86-35679
- THOMPSON, D. R.**
SAR observed internal wave signatures from SARSEX-comparisons with SAR imaging models p 31 A86-33647
Intensity modulation in SAR images of internal waves p 32 A86-35531
- THORLEY, G.**
ENVIROSTAT-2000 report: Federal agency satellite requirements [NASA-TM-88752] p 59 N86-26355
- THYRSTED, T.**
Statistical lineament analysis in South Greenland based on Landsat imagery p 22 A86-35676
- TILLEY, D. G.**
Directional ocean wave spectra obtained from the Shuttle Imaging Radar off the coast of Chile p 30 A86-33612
- TILTON, J. C.**
Extended testing of a general contextual classifier using the massively parallel processor - Preliminary results and test plans p 54 A86-33623
- TIMCHALK, A.**
Satellite-derived moisture profiles [NOAA-NESDIS-24] p 44 N86-27703
- TINNEY, L. R.**
Comprehensive integrated remote sensing for US Department of Energy applications [DE86-002101] p 17 N86-25036
- TOM, V. T.**
Surface material classification based on spectral shape p 6 A86-33598
Spatial enhancement techniques for multichannel satellite imagery p 47 A86-33639
- TOWNSEND, W. F.**
The Ocean Topography Experiment (TOPEX) - Some questions answered p 25 A86-32556
- TRESHNIKOV, A. F.**
Optimal disposition of satellite-tracked drifting buoys in the South Atlantic p 31 A86-34488
Problems of the Arctic and the Antarctic, Collection of Articles, Volume 56, 1981 [PB86-107109] p 35 N86-23209
Problems of the Arctic and the Antarctic, collection of articles, vol. 57, 1981 [PB86-106994] p 37 N86-24182
- TRETIKOV, V. E.**
An algorithm for the identification of cloud cover and the estimation of spectral brightnesses of the cloudless atmosphere according to satellite scanning measurements of outgoing IR radiation p 52 A86-33317
Estimation of the accuracy of the remote determination of ocean surface temperature on the basis of satellite measurements of outgoing thermal radiation in the 10.5-12.5 micron range p 27 A86-33320
- TREVESE, D.**
Landsat TM image forward/reverse scan banding Characterization and correction p 49 A86-36790
- TREVISIOL, G.**
Design of the European Space Agency Thematic Mapper processing chains p 51 A86-37864
- TRIFONOV, V. G.**
Features of the geological application of space data p 19 A86-32680
- TRIVEDI, M. M.**
Segmentation of a Thematic Mapper image using the fuzzy c-means clustering algorithm p 9 A86-35687
- TRIVERO, P.**
Observation of internal waves and seismic waves in the Sicilian Channel p 27 A86-33392

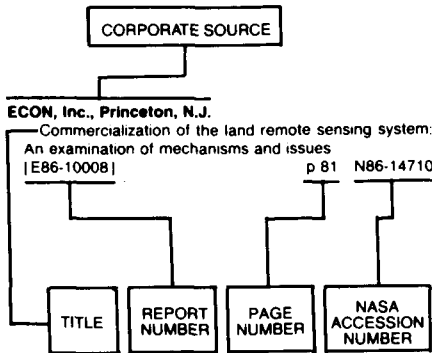
- TRIZNA, D. B.**
Open ocean radar sea scatter measurements p 25 A86-32599
- TROFIMOV, D. M.**
Application of space imagery to the identification and geological-geophysical study of hidden plutons in early Proterozoic troughs p 20 A86-32682
Problems and principles of the geological interpretation of remote-sensing data p 22 A86-36502
- TSUNEOKA, Y.**
Estimation of monthly rainfall from satellite-observed cloud amount in the tropical western Pacific p 43 A86-36234
- TUMOFEEV, I. U. M.**
Experiments on the remote temperature sounding of the atmosphere on the basis of NOAA-satellite radiometer measurements p 52 A86-33318
- U**
- UCCELLINI, L. W.**
Optimized retrievals of precipitable water fields from combinations of VAS satellite and conventional surface observations p 43 A86-36193
- UENK, D.**
Semi-operational identification of agricultural crops from airborne SLAR-data p 12 A86-37025
- UENO, Y.**
Research and development of the synthetic aperture radar transmitter and receiver subsystem design and some component test results p 54 A86-33636
- UHLIR, P.**
International coordination of and contributions to environmental satellite programs [AD-A165142] p 60 N86-28016
- ULABY, F. T.**
Microwave emission from row crops p 9 A86-35681
- USIKOV, D. A.**
A histogram as the basis of the statistical classification of images p 45 A86-32688
- USPENSKII, A. B.**
Experiments on the remote temperature sounding of the atmosphere on the basis of NOAA-satellite radiometer measurements p 52 A86-33318
Estimation of the accuracy of the remote determination of ocean surface temperature on the basis of satellite measurements of outgoing thermal radiation in the 10.5-12.5 micron range p 27 A86-33320
- USPENSKII, G. R.**
Agricultural and scientific space platforms p 1 A86-29843
- V**
- VAN KASTEREN, H. W. J.**
Semi-operational identification of agricultural crops from airborne SLAR-data p 12 A86-37025
- VAN ZYL, J. J.**
Modelling of backscatter from vegetation layers p 4 A86-33554
- VANDERBILT, V. C.**
Polarization photometer to measure bidirectional reflectance factor R(55 deg, 0 deg, 55 deg, 180 deg) of leaves p 9 A86-35748
- VARNADORE, M. S.**
NOAA Atlas: An atlas of satellite-derived Northern Hemispheric snow cover frequency p 44 N86-24075
- VASILKOV, A. P.**
Determination of sea spectral reflectance from airborne measurements p 26 A86-32683
- VASKOV, S. T.**
Technical and software facilities at a center for the processing of remote-sensing data p 48 A86-36511
- VETRELLA, S.**
An integrated approach to geometric precision processing of spaceborne high-resolution sensors p 55 A86-34737
- VIDAL-MADJAR, D.**
Possible applications of the microwaves surface soil moisture remote sensing p 6 A86-33582
Evapotranspiration over an agricultural region using a surface flux/temperature model based on NOAA-AVHRR data p 10 A86-36237
- VITIAZ, V. I.**
Quantitative assessment of the information content of TV images of different scale on the example of disjunctives of Siberia p 23 A86-36506
- VOGELMANN, J. E.**
Field and airborne spectral characterization of suspected damage in red spruce (*Picea rubens*) from Vermont p 11 A86-37008

W

- VOLKOV, A. M.**
Determination of the spectral characteristics of natural objects on test ranges, and aspects of the efficiency of space systems p 11 A86-36697
- W**
- WAGNER, C. A.**
Accuracy estimate of geoid and ocean topography recovered jointly from satellite altimetry p 32 A86-35278
- WAITE, W. P.**
Preliminary analysis of SIR-B images for stereo applications p 45 A86-33515
Preliminary geologic analyses of SIR-B radar data for Hawaii p 21 A86-33550
Introductory analyses of SIR-B radar data for Hawaii p 21 A86-33551
Analysis of L-band multipolarization radar images for lava flow mapping p 21 A86-33593
- WALKER, D. A.**
Vegetation and environmental gradients of the Prudhoe Bay region, Alaska [AD-A162022] p 17 N86-24034
- WALKER, R. E.**
Landsat Thematic Mapper geodetic accuracy - Implications for geocoded map compatibility p 18 A86-37024
- WALL, S. D.**
The SIR-C experiment - Measuring new variables from space with SAR p 50 A86-37028
- WALLACE, J. M.**
Relationships between surface observations over the global oceans and the southern oscillation [PB86-110038] p 35 N86-24112
- WALSH, E. J.**
Measurement of sea ice backscatter characteristics at 36 GHz using the surface contour radar p 29 A86-33562
Design and benefits of a multibeam Earth Observing Radar p 29 A86-33591
Spectral measurements in support of SIR-B using the Surface Contour Radar p 30 A86-33609
- WALSH, J. J.**
A simulation analysis of the fate of phytoplankton within the mid-Atlantic bight [NASA-CR-177265] p 39 N86-26670
Satellite detection of phytoplankton export from the mid-Atlantic Bight during the 1979 spring bloom [NASA-TM-88782] p 41 N86-27699
High frequency sampling of the 1984 spring bloom within the mid-Atlantic Bight: Synoptic shipboard, aircraft, and in situ perspectives of the SEEP-I experiment [NASA-TM-88765] p 41 N86-27700
- WANG, J. R.**
Passive microwave soil moisture research p 2 A86-33504
Microwave backscatter and emission observed from Shuttle Imaging Radar B and an airborne 1.4 GHz radiometer p 53 A86-33584
- WARREN, J. R.**
Conceptual design study: Forest Fire Advanced System Technology (FFAST) [JPL-PUBL-86-5] p 14 N86-25034
- WASH, C. H.**
Satellite cloud and precipitation analysis using a minicomputer [AD-A163821] p 58 N86-25084
- WEISER, R. L.**
Distinguishing among tallgrass prairie cover types from measurements of multispectral reflectance p 10 A86-36047
- WEISSEL, J. K.**
Evidence for small-scale mantle convection from Seasat altimeter data p 25 A86-31976
- WEN, C.-L.**
Structure of the southern Rio Grande rift from gravity interpretation p 18 A86-37795
- WESTMAN, W. E.**
Analysis of forest/structure using thematic mapper simulator data p 4 A86-33540
- WHITEHEAD, V. S.**
Overview and highlights of Early Warning and Crop Condition Assessment project p 5 A86-33576
Vegetation assessment using a combination of visible, near-IR and thermal-IR AVHRR data p 5 A86-33577
- WHITLEDGE, T. E.**
High frequency sampling of the 1984 spring bloom within the mid-Atlantic Bight: Synoptic shipboard, aircraft, and in situ perspectives of the SEEP-I experiment [NASA-TM-88765] p 41 N86-27700
- WICKLAND, D. E.**
Forest discrimination with multipolarization imaging radar p 5 A86-33565

- Forest discrimination with multipolarization imaging radar p 5 A86-33566
- WIEGAND, C. L.**
Diurnal patterns of bidirectional vegetation indices for wheat canopies p 1 A86-30192
Development of agrometeorological crop model inputs from remotely sensed information p 6 A86-33579
Spectral components analysis - A bridge between spectral observations and agrometeorological crop models p 7 A86-33627
- WILHEIT, T. T., JR.**
Aircraft and satellite passive microwave observations of the Bering Sea ice cover during MIZEX West p 32 A86-35683
- WILKES, Q.**
Comparison of the Defense Meteorological Satellite Program (DMSP) and the NOAA Polar-orbiting Operational Environmental Satellite (POES) program [AD-A165118] p 59 N86-27413
- WILLIAMS, D. L.**
Field and airborne spectral characterization of suspected damage in red spruce (*Picea rubens*) from Vermont p 11 A86-37008
- WILLIAMS, L. D.**
Millimeter-wave backscatter from snowcover p 42 A86-33615
- WILLIAMS, P. D. L.**
The design, construction and early trials of a novel airborne surveillance radar p 25 A86-32635
- WILSON, S. B.**
The applicability of LOWTRAN 5 computer code to aerial thermographic data correction p 48 A86-34739
- WILSON, W. J.**
High resolution millimeter-wave imaging sensor p 54 A86-33590
- WIRICK, C. D.**
High frequency sampling of the 1984 spring bloom within the mid-Atlantic Bight: Synoptic shipboard, aircraft, and in situ perspectives of the SEEP-I experiment [NASA-TM-88765] p 41 N86-27700
- WISE, D. U.**
Topographic lineament domains of the Appalachians - Some new methods and techniques for paleostress analysis p 20 A86-33518
- WITTE, F.**
Archimedes project remote sensing of oil spills North Sea experiment, October 1983. Report on DFVLR (Side-Looking Airborne Radar (SLAR) contribution [DFVLR-FB-85-54] p 35 N86-24002
- WITTMANN, P. A.**
Hydrographic data from the OPTOMA program, OPTOMA17: OPTOMA17 P, 21 July 1985, OPTOMA17 leg DI, 10-22 August 1985, OPTOMA17 leg DII, 23 August - 5 September 1985 [AD-A162067] p 37 N86-24176
- WOLZER, I.**
ENVIROSAT-2000 report: Federal agency satellite requirements [NASA-TM-88752] p 59 N86-26355
Federal agency satellite requirements [AD-A165071] p 59 N86-27410
- WOODCOCK, C.**
Variograms and spatial variation in remotely sensed images p 47 A86-33638
- WOODING, M. G.**
SAR image segmentation using digitised field boundaries for crop mapping and monitoring applications p 7 A86-33625
- WOODS, K. D.**
Adding spatial considerations to the JABOWA model of forest growth p 11 A86-37014
- WRIGHT, P. B.**
Relationships between surface observations over the global oceans and the southern oscillation [PB86-110038] p 35 N86-24112
- WRIGLEY, R. C.**
Measurement of Thematic Mapper data quality p 50 A86-37032
- WU, L. K.**
Identification of major backscattering sources in trees and shrubs at 10 GHz p 13 A86-39149
- WU, S. T.**
A preliminary report on the measurements of forest canopies with C-band radar scatterometer at NASA/NSTL p 3 A86-33525
Multipolarization SAR data for surface feature delineation p 46 A86-33594
- WU, S.-T.**
Analysis of data acquired by Shuttle Imaging Radar SIR-A and Landsat Thematic Mapper over Baldwin County, Alabama p 12 A86-37018
- WYRTKI, K.**
Monthly maps of sea level anomalies in the Pacific, 1975 1981. Report on the IGQSS (Integrated Global Ocean Services System) Sea Level Pilot Project [AD-A163061] p 38 N86-25104
- X**
- XIAO, J.**
Application of Shuttle imaging radar data for land use investigations p 51 A86-39150
- Y**
- YASUDA, Y.**
Satellite thermal observation of oil slicks on the Persian Gulf p 33 A86-36048
- YATES, H. W.**
Operational satellite support to scientific programs [AD-A165081] p 59 N86-27412
- YENTSCH, C. S.**
Ocean color measurements p 28 A86-33488
- Z**
- ZABELIN, V. A.**
Certain transformations in a quantitative approach to image processing p 48 A86-36517
Computer processing of spectrally superposed data p 49 A86-36518
- ZAMBRESKY, L. F.**
Waves predicted by the Global Spectral Ocean Wave model off the west coast of Chile during the SIR-B mission p 30 A86-33608
- ZBAR, F.**
NOAA satellite requirements forecast [AD-A165244] p 40 N86-27414
- ZEBKER, H.**
Modelling of backscatter from vegetation layers p 4 A86-33554
- ZEBKER, H. A.**
Topographic mapping from interferometric synthetic aperture radar observations p 18 A86-33516
Topographic mapping from interferometric synthetic aperture radar observations p 18 A86-36099
- ZIATKOVA, L. K.**
Methods of combined air and space remote-sensing studies of Siberia p 22 A86-36501
Combined structural and geomorphological methods for the processing of aerial and space photographic remote-sensing data with the aim of solving geological problems p 22 A86-36503
Methods for the remote sensing of transition zones of the junction of Siberian platforms and orogens p 23 A86-36507
- ZISK, S. H.**
Structure of terrestrial impact craters from SIR-B radar data - Preliminary results p 21 A86-33552
- ZLATOPOLSKII, A. A.**
Computer-aided interpretation of space images with the aim of structural analysis p 20 A86-32690
- ZOBRIST, A. L.**
Landsat Thematic Mapper geodetic accuracy - Implications for geocoded map compatibility p 18 A86-37024
- ZOOK, D. F.**
Backscatter measurements from simulated resonant structures p 4 A86-33555
- ZOUGH, R.**
Identification of major backscattering sources in trees and shrubs at 10 GHz p 13 A86-39149
- ZRNIC, D. S.**
Analysis of airborne Doppler lidar, Doppler radar and tall tower measurements of atmospheric flows in quiescent and stormy weather [NASA-CR-3960] p 56 N86-23159
- ZVEREV, A. T.**
Interpretation of ring structures on space images and their correlation with geophysical fields and crustal structure in the USSR p 19 A86-32681
- ZWALLY, H. J.**
Observations of the polar regions from satellites using active and passive microwave techniques p 28 A86-33488

Typical Corporate Source Index Listing



Listings in this index are arranged alphabetically by corporate source. The title of the document is used to provide a brief description of the subject matter. The page number and the accession number are included in each entry to assist the user in locating the abstract in the abstract section. If applicable, a report number is also included as an aid in identifying the document.

A

- Agricultural Research Center, Beltsville, Md.**
Microwave backscatter and emission observed from Shuttle Imaging Radar B and an airborne 1.4 GHz radiometer p 53 A86-33584
- Agricultural Research Service, Houston, Tex.**
Overview and highlights of Early Warning and Crop Condition Assessment project p 5 A86-33576
- Air Force Geophysics Lab., Hanscom AFB, Mass.**
Evidence of ongoing crustal deformation related to magmatic activity near Socorro, New Mexico p 18 A86-37797
- Alaska Univ., Anchorage.**
Influence of the Yukon River on the Bering Sea [NASA-CR-177310] p 39 N86-26783
- Applied Science Associates, Inc., Apex, N.C.**
Studies related to ocean dynamics. Task 3.2: Aircraft Field Test Program to investigate the ability of remote sensing methods to measure current/wind-wave interactions [NASA-CR-168349] p 38 N86-25100
- ARCO Oil and Gas Co., Dallas, Tex.**
Structure of the southern Rio Grande rift from gravity interpretation p 18 A86-37795
- Arizona Univ., Tucson.**
Measurement of Thematic Mapper data quality p 50 A86-37032
Spectroradiometric considerations for advanced land observing systems [NASA-CR-177205] p 58 N86-27705
- Arkansas Univ., Fayetteville.**
Preliminary geologic analyses of SIR-B radar data for Hawaii p 21 A86-33550
- Army Cold Regions Test Center, APO Seattle, Wash. 98733.**
Vegetation and environmental gradients of the Prudhoe Bay region, Alaska [AD-A162022] p 17 N86-24034

- Auburn Univ., Ala.**
Agricultural applications for thermal infrared multispectral scanner data p 12 A86-37034

B

- Bechtel National, Inc., San Francisco, Calif.**
Thematic mapper research in the Earth sciences: Tectonic evaluation of the Nubian Shield of northeastern Sudan/southeastern Egypt using thematic mapper imagery [NASA-CR-177311] p 24 N86-26740
- Bigelow Lab. for Ocean Sciences, West Boothbay Harbor, Maine.**
Ocean color measurements p 28 A86-33488
- Boston Univ., Mass.**
Variograms and spatial variation in remotely sensed images p 47 A86-33638
- Brown Univ., Providence, R. I.**
Spectroscopy of Moses Rock dike using remote sensing p 21 A86-33521
Structure of terrestrial impact craters from SIR-B radar data - Preliminary results p 21 A86-33552

C

- California Inst. of Tech., Pasadena.**
Modelling of backscatter from vegetation layers p 4 A86-33554
- California Univ., Santa Barbara.**
What are the best radar wavelengths, incidence angles and polarizations for geologic applications? A statistical approach p 21 A86-33592
- Clemson Univ., S.C.**
Seasat microwave wind and rain observations in severe tropical and midlatitude marine storms p 27 A86-33486
- Coast Guard, Washington, D.C.**
A review of methods to track oil in arctic waters [AD-A164679] p 39 N86-26716
- Colorado Univ., Boulder.**
Transient response to localized episodic heating in the tropics p 51 N86-27749
- Computer Sciences Corp., Beltsville, Md.**
Microwave backscatter and emission observed from Shuttle Imaging Radar B and an airborne 1.4 GHz radiometer p 53 A86-33584
- Cornell Univ., Ithaca, N.Y.**
Evidence of ongoing crustal deformation related to magmatic activity near Socorro, New Mexico p 18 A86-37797

D

- Delaware Univ., Newark.**
Assessing impacts of off-nadir observation on remote sensing of vegetation - Use of the Suits model p 1 A86-30193
Remote sensing investigations of wetland biomass and productivity for global biosystems research [NASA-CR-176725] p 14 N86-23994
- Department of Agriculture, Fort Worth, Tex.**
Remote sensing techniques for the detection of soil erosion and the identification of soil conservation practices p 3 A86-33506
- Department of Agriculture, Washington, D.C.**
Overview of the AgRISTARS research program. I p 2 A86-33503
- Deutsche Forschungs- und Versuchsanstalt fuer Luft- und Raumfahrt, Oberpfaffenhofen (West Germany).**
Satellite-borne 90 GHz radiometer experiment (SABREX), phase A1 [DFVLR-MITT-85-13] p 57 N86-24000
Archimedes project remote sensing of oil spills North Sea experiment, October 1983. Report on DFVLR (Side-Looking Airborne Radar (SLAR) contribution [DFVLR-FB-85-54] p 35 N86-24002

- Deutsche Geodaetische Kommission, Munich (West Germany).**
Rectification of scanner images using prediction approaches [SER-C-303] p 57 N86-23992
- Du Pont de Nemours (E. I.) and Co., Wilmington, Del.**
Modified cubic convolution resampling for Landsat p 47 A86-33640

E

- EG and G Energy Measurements, Inc., Las Vegas, Nev.**
Comprehensive integrated remote sensing for US Department of Energy applications [DE86-002101] p 17 N86-25036
- EG and G Washington Analytical Services Center, Inc., Pocomoke City, Md.**
Spectral measurements in support of SIR-B using the Surface Contour Radar p 30 A86-33609
- Energy, Mines and Resources Canada, Ottawa (Ontario).**
Structure of terrestrial impact craters from SIR-B radar data - Preliminary results p 21 A86-33552
- Environmental Research Inst. of Michigan, Ann Arbor.**
Simulations of SAR wave spectra using high spectral resolution estimates from the SCR and FROWS instruments p 30 A86-33611
Verification of L-band SAR calibration p 54 A86-33634

F

- Florida State Univ., Gainesville.**
A model for the estimation of the surface fluxes of momentum, heat and moisture of the cloud topped marine atmospheric boundary layer from satellite measurable parameters [NASA-CR-177283] p 41 N86-27837
- Florida State Univ., Tallahassee.**
An investigation of the marine boundary layer during cold air outbreak [NASA-CR-177287] p 39 N86-26758
An investigation of the marine boundary layer during cold air outbreak [NASA-CR-177249] p 41 N86-27838
A model for the estimation of the surface fluxes of momentum, heat, and moisture of the cloud-topped marine atmospheric boundary layer from satellite measurable parameters [NASA-CR-177290] p 41 N86-27853

G

- General Electric Co., Philadelphia, Pa.**
Modified cubic convolution resampling for Landsat p 47 A86-33640
- Geological Survey, Reston, Va.**
Remote monitoring of processes that shape desert surfaces: The Desert Winds Project [TI86-900108] p 24 N86-25099
Research, investigations and technical developments: National mapping program, 1983-1984 [PB86-166097] p 17 N86-26675
- Geological Survey, Tacoma, Wash.**
Observations of the polar regions from satellites using active and passive microwave techniques p 28 A86-33489
- GKSS-Forschungszentrum Geesthacht (West Germany).**
On the information content of multispectral radiance measurements over an ocean [GKSS-85/E/43] p 40 N86-27697

H

Hawaii Inst. of Geophysics, Honolulu.

Monthly maps of sea level anomalies in the Pacific, 1975-1981. Report on the IGOSS (Integrated Global Ocean Services System) Sea Level Pilot Project [AD-A163061] p 38 N86-25104

Hawaii Univ., Honolulu.

Preliminary geologic analyses of SIR-B radar data for Hawaii p 21 A86-33550

Houston Univ., Clear Lake, Tex.

Evaluation of crop acreage estimation methods using Landsat data as auxiliary input p 6 A86-33606

Hunter Coll., New York.

California timber volume inventory using Landsat p 4 A86-33541

I

Illinois Univ., Chicago.

Scattering from a random layer embedded with dielectric needles p 10 A86-36045
Regression models for vegetation radar-backscattering and radiometric emission p 10 A86-36046

Illinois Univ., Urbana.

Remote sensing of atmospheric pressure and sea state using laser altimeters p 28 A86-33529

Informatics General Corp., Moffett Field, Calif.

The development of an MSS satellite imagery classification expert system p 46 A86-33596

Institute for Land and Water Management Research, Wageningen (Netherlands).

A multiindex multitemporal approach to map crops in the early growing season: An application to two Italian irrigation districts: East Sesia and Grande Bonifica Ferrarese [ICW-1611] p 15 N86-26674

Instituto de Pesquisas Espaciais, Sao Jose dos Campos (Brazil).

Development of a satellite-tracked oceanographic drifting buoy for the Brazilian Antarctic Program, part 1 [INPE-3793-PRE/888] p 36 N86-24166

Comparison of Circulation estimates and winds based on shipboard and satellite-tracked buoy data in Bransfield Strait, 9-14 March, 1985, part 3 [INPE-3795-PRE/890] p 36 N86-24168

A proposal for a project entitled Assessment of Forest Resources in Uruguay submitted to the United Nations Industrial Development Organization (UNIDO) [INPE-3828-NTE/255] p 15 N86-26666

Wheat area estimation using digital LANDSAT MSS data and aerial photographs [INPE-3824-PRE/900] p 15 N86-26667

International Paper Co., Tuxedo Park, N.Y.

Timber Resources Inventory and Monitoring Joint Research Project [NASA-TM-88754] p 14 N86-25863

J

Jet Propulsion Lab., California Inst. of Tech., Pasadena.

Weddell-Scotia sea marginal ice zone observations from space, October 1984 p 26 A86-33105

Topographic mapping from interferometric synthetic aperture radar observations p 18 A86-33516

Radar scatterometer probing of thick vegetation canopies p 3 A86-33523

Passive remote sensing of stratospheric and mesospheric winds p 53 A86-33545

Modelling of backscatter from vegetation layers p 4 A86-33554

Near infrared leaf reflectance modeling p 4 A86-33556

Forest discrimination with multipolarization imaging radar p 5 A86-33565

Forest discrimination with multipolarization imaging radar p 5 A86-33566

Spaceborne Imaging Radar (SIR) project p 53 A86-33586

High resolution millimeter-wave imaging sensor p 54 A86-33590

What are the best radar wavelengths, incidence angles and polarizations for geologic applications? A statistical approach p 21 A86-33592

A median filter approach for correcting errors in a vector field p 29 A86-33601

Topographic mapping from interferometric synthetic aperture radar observations p 18 A86-36099

Field and airborne spectral characterization of suspected damage in red spruce (Picea rubens) from Vermont p 11 A86-37008

Landsat Thematic Mapper geodetic accuracy - Implications for geocoded map compatibility p 18 A86-37024

Preliminary science results from the Shuttle Imaging Radar-B p 50 A86-37027

The SIR-C experiment - Measuring new variables from space with SAR p 50 A86-37028

Conceptual design study: Forest Fire Advanced System Technology (FFAST) [JPL-PUBL-86-5] p 14 N86-25034

Johns Hopkins Univ., Laurel, Md.

Surface and internal ocean wave observations p 27 A86-33485

Strategies for the calibration and operational use of the ERS-1 SAR wave mode [JHU/APL/SDO-7565] p 35 N86-23207

Joint Publications Research Service, Arlington, Va.

USSR report: Earth sciences [JPRS-UES-86-004] p 34 N86-23017

K

Kansas State Univ., Manhattan.

Distinguishing among tallgrass prairie cover types from measurements of multispectral reflectance p 10 A86-36047

Kansas Univ., Lawrence.

Geological mapping potential of computer-enhanced images from the Shuttle Imaging Radar - Lisbon Valley Anticline, Utah p 22 A86-36083

Kansas Univ. Center for Research, Inc., Lawrence.

Identification of major backscattering sources in trees and shrubs at 10 GHz p 13 A86-39149

Research on enhancing the utilization of digital multispectral data and geographic information systems in global habitability studies [NASA-CR-177294] p 17 N86-26669

L

Lamont-Doherty Geological Observatory, Palisades, N. Y.

Marginal ice zone experiment - 1984, physical oceanography report: USNS Lynch and helicopter-based STD data [AD-A163096] p 37 N86-24180

Physical oceanography report: Camp-based and helicopter-based STD data from the drifting ice station FRAM 3 [AD-A163097] p 37 N86-24181

Lawrence Livermore National Lab., Calif.

Studies of complex terrain wind flows using acoustic sounder and optical cross-wind remote sensors [DE86-002993] p 58 N86-25925

Lockheed Engineering and Management Services Co., Inc., Houston, Tex.

Estimation of biophysical properties of forest canopies through inversion of microwave scatterometer data p 4 A86-33542

Vegetation assessment using a combination of visible, near-IR and thermal-IR AVHRR data p 5 A86-33577

Evaluation of crop acreage estimation methods using Landsat data as auxiliary input p 6 A86-33606

Spectral characterization of biophysical characteristics in a boreal forest - Relationship between Thematic Mapper band reflectance and leaf area index for Aspen p 8 A86-35677

An information measure for class discrimination p 11 A86-36789

Louisiana State Univ., Baton Rouge.

Methods of obtaining offshore wind direction and sea-state data from X-band aircraft SAR (Synthetic Aperture Radar) imagery of coastal waters [AD-A165552] p 38 N86-26517

Lunar and Planetary Inst., Houston, Tex.

Structure of the southern Rio Grande rift from gravity interpretation p 18 A86-37795

Thematic mapper studies of Andean volcanoes [NASA-CR-176807] p 24 N86-25866

M

Marine Research Inst., Helsinki (Finland).

Investigation of ice dynamics in the marginal ice zone [AD-A164364] p 38 N86-25962

Maryland Univ., College Park.

Department of Geology/NASA-GSFC geobotanical investigation [NASA-CR-177300] p 15 N86-27698

Massachusetts Inst. of Tech., Cambridge.

Plate motions and deformations from geologic and geodetic data [NASA-CR-177299] p 18 N86-26741

Remote sensing and oceanographic equipment technology: Some present systems and future needs, revised [PB86-156502] p 40 N86-26791

Plate motions and deformations from geologic and geodetic data [NASA-CR-177313] p 19 N86-27833

Massachusetts Inst. of Tech., Lexington.

Satellite-derived leaf-area-index and vegetation maps as input to global carbon cycle models - A hierarchical approach p 2 A86-30194

Massachusetts Univ., Amherst.

Observations of the polar regions from satellites using active and passive microwave techniques p 28 A86-33489

1985 International Geoscience and Remote Sensing Symposium (IGARSS '85), University of Massachusetts, Amherst, October 7-9, 1985, Digest, Volumes 1 & 2 p 52 A86-33501

Spaceborne Imaging Radar (SIR) project p 53 A86-33586

Electronically Steered Thinned Array Radiometer (ESTAR) system design, calibration, and sensitivity p 53 A86-33588

Messerschmitt-Boelkow-Blohm G.m.b.H., Ottobrunn (West Germany).

MOMS-01 (Modular Optoelectronic Multispectral Scanner) for Earth observation: First results of STS-7 mission p 57 N86-24003

Meteorological Satellite Center, Tokyo (Japan).

Meteorological Satellite Center Technical Note, no. 13, 1986 [ISSN-0388-9653] p 40 N86-27694

On land-sea contrast in the Earth radiation budget p 40 N86-27695

Miami Univ., Fla.

Ocean color measurements p 28 A86-33488

Mound Lab., Miamisburg, Ohio.

Operational methods for data interpolation [DE85-016050] p 34 N86-15969

N

National Academy of Sciences - National Research Council, Washington, D. C.

Proceedings of the First National Workshop on the Global Weather Experiment: Current Achievements and Future Directions, volume 1 [NASA-CR-176720] p 36 N86-24120

Proceedings of the First National Workshop on the Global Weather Experiment: Current Achievements and Future Directions, volume 2, part 2 [NASA-CR-176722] p 36 N86-24142

Earth science investigations in the United States Antarctic Research Program (USARP) for the period July 1, 1984 - June 30, 1985 [PB86-143773] p 58 N86-25076

National Aeronautics and Space Administration, Washington, D.C.

The Ocean Topography Experiment (TOPEX) - Some questions answered p 25 A86-32556

Overview of the AgRISTARS research program. I p 2 A86-33503

ENVIROSAT-2000 report: Federal agency satellite requirements [NASA-TM-88752] p 59 N86-26355

National Aeronautics and Space Administration. Ames Research Center, Moffett Field, Calif.

Analysis of forest/structure using thematic mapper simulator data p 4 A86-33540

The development of an MSS satellite imagery classification expert system p 46 A86-33596

Land use mapping using edge density texture measures on Thematic Mapper simulator data p 47 A86-33624

Multi-crop area estimation and mapping on a microprocessor/mainframe network p 7 A86-33644

Polarization photometer to measure bidirectional reflectance factor R(55 deg, 0 deg, 55 deg, 180 deg) of leaves p 9 A86-35748

Measurement of Thematic Mapper data quality p 50 A86-37032

National Aeronautics and Space Administration. Earth Resources Lab., Bay St. Louis, Miss.

Analysis of effective radiant temperatures in a Pacific Northwest forest using Thermal Infrared Multispectral Scanner data p 9 A86-36042

National Aeronautics and Space Administration. Goddard Space Flight Center, Greenbelt, Md.

Reduction of weather effects in the calculation of sea ice concentration from microwave radiances p 26 A86-33104

Observations of the polar regions from satellites using active and passive microwave techniques p 28 A86-33489

- Passive microwave soil moisture research p 2 A86-33504
- Lidar observations of the planetary boundary layer p 29 A86-33532
- Microwave backscatter and emission observed from Shuttle Imaging Radar B and an airborne 1.4 GHz radiometer p 53 A86-33584
- Electronically Steered Thinned Array Radiometer (ESTAR) system design, calibration, and sensitivity p 53 A86-33588
- Extended testing of a general contextual classifier using the massively parallel processor - Preliminary results and test plans p 54 A86-33623
- Identifying deforestation in Brazil using multiresolution satellite data p 8 A86-34742
- Aircraft and satellite passive microwave observations of the Bering Sea ice cover during MIZEX West p 32 A86-35683
- Optimized retrievals of precipitable water fields from combinations of VAS satellite and conventional surface observations p 43 A86-36193
- Field and airborne spectral characterization of suspected damage in red spruce (*Picea rubens*) from Vermont p 11 A86-37008
- Directional reflectance response in AVHRR red and near-IR bands for three cover types and varying atmospheric conditions p 13 A86-39146
- Analysis of a resistance-energy balance method for estimating daily evaporation from wheat plots using one-time-of-day infrared temperature observations p 13 A86-39148
- GLAS experiments on the impact of FGGE satellite data on numerical weather prediction p 57 N86-24128
- Simulation studies related to the design of post-FGGE observing systems p 57 N86-24160
- Objective analysis of tidal fields in the Atlantic and Indian Oceans [NASA-TM-87773] p 39 N86-26782
- Satellite detection of phytoplankton export from the mid-Atlantic Bight during the 1979 spring bloom [NASA-TM-88782] p 41 N86-27699
- National Aeronautics and Space Administration.**
Lyndon B. Johnson Space Center, Houston, Tex.
Satellite-derived leaf-area-index and vegetation maps as input to global carbon cycle models - A hierarchical approach p 2 A86-30194
- Estimation of biophysical properties of forest canopies through inversion of microwave scatterometer data p 4 A86-33542
- Structure of terrestrial impact craters from SIR-B radar data - Preliminary results p 21 A86-33552
- Overview and highlights of Early Warning and Crop Condition Assessment project p 5 A86-33576
- Vegetation assessment using a combination of visible, near-IR and thermal-IR AVHRR data p 5 A86-33577
- Evaluation of crop acreage estimation methods using Landsat data as auxiliary input p 6 A86-33606
- Spectral characterization of biophysical characteristics in a boreal forest - Relationship between Thematic Mapper band reflectance and leaf area index for Aspen p 8 A86-35677
- An information measure for class discrimination p 11 A86-36789
- National Aeronautics and Space Administration.**
Langley Research Center, Hampton, Va.
Assessing impacts of off-nadir observation on remote sensing of vegetation - Use of the Suits model p 1 A86-30193
- An airborne multiple-beam 1.4 GHz pushbroom microwave radiometer p 6 A86-33583
- Microwave backscatter and emission observed from Shuttle Imaging Radar B and an airborne 1.4 GHz radiometer p 53 A86-33584
- Design and benefits of a multibeam Earth Observing Radar p 29 A86-33591
- SAGE observations of stratospheric nitrogen dioxide p 55 A86-36838
- Site selection and directional models of deserts used for ERBE validation targets [NASA-TP-2540] p 57 N86-23160
- Transport processes as manifested in satellite and lidar aerosol measurements p 17 N86-27788
- National Aeronautics and Space Administration.**
National Space Technology Labs., Bay Saint Louis, Miss.
Remote sensing techniques for the detection of soil erosion and the identification of soil conservation practices p 3 A86-33506
- A preliminary report on the measurements of forest canopies with C-band radar scatterometer at NASA/NSTL p 3 A86-33525
- Multipolarization SAR data for surface feature delineation p 46 A86-33594
- Analysis of data acquired by Shuttle Imaging Radar SIR-A and Landsat Thematic Mapper over Baldwin County, Alabama p 12 A86-37018
- Agricultural applications for thermal infrared multispectral scanner data p 12 A86-37034
- Ducks Unlimited Joint Research Project [NASA-TM-88755] p 14 N86-25032
- Timber Resources Inventory and Monitoring Joint Research Project [NASA-TM-88754] p 14 N86-25863
- National Aeronautics and Space Administration.**
Wallops Flight Center, Wallops Island, Va.
Measurement of sea ice backscatter characteristics at 36 GHz using the surface contour radar p 29 A86-33562
- Design and benefits of a multibeam Earth Observing Radar p 29 A86-33591
- Spectral measurements in support of SIR-B using the Surface Contour Radar p 30 A86-33609
- High frequency sampling of the 1984 spring bloom within the mid-Atlantic Bight: Synoptic shipboard, aircraft, and in situ perspectives of the SEEP-I experiment [NASA-TM-88765] p 41 N86-27700
- National Aerospace Lab., Amsterdam (Netherlands).**
Map digitization offers new possibilities [NLR-MP-84061-U] p 51 N86-23028
- National Environmental Satellite Service, Suitland, Md.**
Characteristics of western region flash flood events in GOES imagery and conventional data [NOAA-TM-NESDIS-13] p 44 N86-26668
- National Environmental Satellite Service, Washington, D. C.**
Environmental data sources for the Chesapeake Bay Area [PB86-110640] p 35 N86-23211
- National Geophysical Data Center, Boulder, Colo.**
Earthquake and tsunami data services and publications [PB86-156254] p 51 N86-25919
- National Oceanic and Atmospheric Administration, Boulder, Colo.**
Surface and internal ocean wave observations p 27 A86-33485
- Measurement of sea ice backscatter characteristics at 36 GHz using the surface contour radar p 29 A86-33562
- Management information (Wave Propagation Laboratory, Boulder, Colorado) [PB86-139524] p 38 N86-25106
- National Oceanic and Atmospheric Administration, Miami, Fla.**
Seasat microwave wind and rain observations in severe tropical and midlatitude marine storms p 27 A86-33486
- Heat budget and climatic atlas of the equatorial Atlantic Ocean during FGGE (First GARP Global Experiment, 1979) [PB86-111622] p 35 N86-23213
- National Oceanic and Atmospheric Administration, Seattle, Wash.**
Surface and internal ocean wave observations p 27 A86-33485
- Relationships between surface observations over the global oceans and the southern oscillation [PB86-110038] p 35 N86-24112
- Sea ice dynamics and regional meteorology for the Arctic polynya experiment (APEX)-Bering Sea 1985 [PB86-148038] p 38 N86-25939
- National Oceanic and Atmospheric Administration, Washington, D. C.**
Ocean color measurements p 28 A86-33488
- Hydrologic and land sciences applications of NOAA polar-orbiting satellite data p 43 N86-23993
- NOAA Atlas: An atlas of satellite-derived Northern Hemispheric snow cover frequency p 44 N86-24075
- Federal agency satellite requirements [AD-A165071] p 59 N86-27410
- GOES (Geostationary Operational Environmental Satellite)-next overview [AD-A165080] p 59 N86-27411
- Operational satellite support to scientific programs [AD-A165081] p 59 N86-27412
- Comparison of the Defense Meteorological Satellite Program (DMSP) and the NOAA Polar-orbiting Operational Environmental Satellite (POES) program [AD-A165118] p 59 N86-27413
- NOAA satellite requirements forecast [AD-A165244] p 40 N86-27414
- Satellite-derived moisture profiles [NOAA-NESDIS-24] p 44 N86-27703
- Optimum management strategies for the NOAA (National Oceanic and Atmospheric Administration) polar-orbiting operational environmental satellites, 1985-2000. Volume 1 [AD-A165143] p 59 N86-28007
- International coordination of and contributions to environmental satellite programs [AD-A165142] p 60 N86-28016
- National Science Foundation, Washington, D.C.**
Ice shelves of Antarctica [PB86-106986] p 35 N86-23208
- Problems of the Arctic and the Antarctic, Collection of Articles, Volume 56, 1981 [PB86-107109] p 35 N86-23209
- Problems of the Arctic and the Antarctic, collection of articles, vol. 57, 1981 [PB86-106994] p 37 N86-24182
- Naval Ocean Research and Development Activity, Bay St. Louis, Miss.**
Proceedings of the Arctic Oceanography Conference and Workshop held at the Naval Ocean Research and Development Activity, NSTL, MS. on June 11-14, 1985 [AD-A162578] p 34 N86-23203
- Ocean wave slope statistics from automated analysis of sun glitter photographs [AD-A161995] p 37 N86-24172
- Contributions to the oceanography of the western Alboran Sea [AD-A162019] p 37 N86-24173
- Naval Postgraduate School, Monterey, Calif.**
Hydrographic data from the OPTOMA program, OPTOMA17: OPTOMA17 P, 21 July 1985, OPTOMA17 leg DI, 10-22 August 1985, OPTOMA17 leg DII, 23 August - 5 September 1985 [AD-A162067] p 37 N86-24176
- Satellite cloud and precipitation analysis using a minicomputer [AD-A163821] p 58 N86-25084
- Nevada Univ., Reno.**
The nature and origin of mineral coatings on volcanic rocks of the Black Mountain, Stonewall Mountain and Kane Springs Wash volcanic centers in southern Nevada [NASA-CR-176805] p 24 N86-25912
- Northeast Radio Observatory Corp., Westford, Mass.**
Haystack Observatory.
Structure of terrestrial impact craters from SIR-B radar data - Preliminary results p 21 A86-33552
- O**
- Oceanweather, Inc., White Plains, N.Y.**
Seasat microwave wind and rain observations in severe tropical and midlatitude marine storms p 27 A86-33486
- Office of Technology Assessment, Washington, D.C.**
Oil and gas technologies for the Arctic and deepwater [PB86-119948] p 24 N86-23030
- Ohio State Univ., Columbus.**
The study of gravity field estimation procedures [AD-A164564] p 19 N86-26745
- Oklahoma Univ., Norman.**
Analysis of airborne Doppler lidar, Doppler radar and tall tower measurements of atmospheric flows in quiescent and stormy weather [NASA-CR-3960] p 56 N86-23159
- Operations Research, Inc., Landover, Md.**
EOS radiometer concepts for soil moisture remote sensing [NASA-CR-177854] p 14 N86-23995
- P**
- Pacific Missile Test Center, Point Mugu, Calif.**
Navstar GPS (Global Positioning System) accuracy while surveying arrays of deep ocean transponders [AD-A163364] p 38 N86-26313
- Pennsylvania State Univ., University Park.**
Preliminary assessment of soil moisture over vegetation [NASA-CR-177226] p 15 N86-27704
- Purdue Univ., West Lafayette, Ind.**
Polarization photometer to measure bidirectional reflectance factor R(55 deg, 0 deg, 55 deg, 180 deg) of leaves p 9 A86-35748
- Structure of the southern Rio Grande rift from gravity interpretation p 18 A86-37795
- Sun angle, view angle, and background effects on spectral response of simulated balsam fir canopies p 13 A86-39002
- S**
- SACLANT ASW Research Center, La Spezia (Italy).**
An atlas of original and mercator-transformed satellite-data images of the Alboran Sea, August-October 1983 [AD-A161898] p 36 N86-24170
- Sandia National Labs., Albuquerque, N. Mex.**
Stable-isotope studies of groundwaters in southeastern New Mexico [DE86-002590] p 43 N86-23027

Science Applications International Corp., College Station, Tex.

A study of sea ice kinematics and their relationship to arctic ambient noise. Part 3, Section 1: Ambient noise. Section 2: Ambient noise
[AD-A165304] p 39 N86-26788

A study of sea ice kinematics and their relationship to arctic ambient noise. Part 3, section 3: Ambient noise
[AD-A165305] p 40 N86-26789

Scripps Institution of Oceanography, La Jolla, Calif.
Ocean color measurements p 28 A86-33488
Sea surface temperature from satellites: The impact of FGGE p 36 N86-24161

Sherbrooke Univ. (Quebec).
The fundamentals of microwave remote sensing
[SU-84] p 56 N86-23025

South Carolina Univ., Columbia.
Application of LANDSAT TM images to assess circulation and dispersion in coastal lagoons
[NASA-CR-177315] p 44 N86-26665

T

Technicolor Government Services, Inc., Moffett Field, Calif.
Analysis of forest/structure using thematic mapper simulator data p 4 A86-33540
Multi-crop area estimation and mapping on a microprocessor/mainframe network p 7 A86-33644
Measurement of Thematic Mapper data quality p 50 A86-37032

Texas Univ., Arlington.
Utilization of active microwave roughness measurements to improve passive microwave soil moisture estimates over bare soils p 8 A86-35679
Scattering from a random layer embedded with dielectric needles p 10 A86-36045

Texas Univ., El Paso.
Structure of the southern Rio Grande rift from gravity interpretation p 18 A86-37795

U

University of South Florida, St. Petersburg.
A simulation analysis of the fate of phytoplankton within the mid-Atlantic bight
[NASA-CR-177265] p 39 N86-26670

W

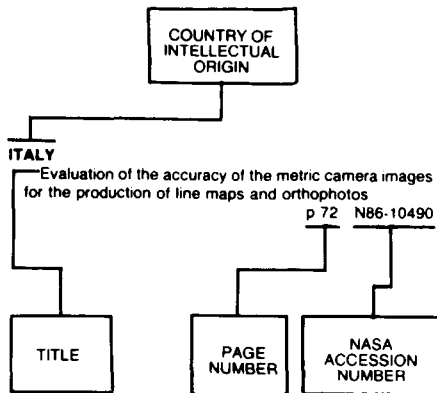
Washington Univ., Seattle.
Weddell-Scotia sea marginal ice zone observations from space, October 1984 p 26 A86-33105
Extracting sea ice data from satellite SAR imagery p 29 A86-33560
A simple, objective analysis scheme for scatterometer data p 32 A86-35550
Relationships between surface observations over the global oceans and the southern oscillation
[PB86-110038] p 35 N86-24112

Washington Univ., St. Louis, Mo.
Use of SIR-A and Landsat MSS data in mapping shrub and intershrub vegetation at Koonamore, South Australia p 13 A86-39003

Water Conservation Lab., Phoenix, Ariz.
Analysis of a resistance-energy balance method for estimating daily evaporation from wheat plots using one-time-of-day infrared temperature observations p 13 A86-39148

Wisconsin Univ., Madison.
Modeling the controls of forest productivity using canopy variables p 11 A86-37016

Typical Foreign Technology Index Listing



Listings in this index are arranged alphabetically by country of intellectual origin. The title of the document is used to provide a brief description of the subject matter. The page number and the accession number are included in each entry to assist the user in locating the citation in the abstract section.

BULGARIA

Remote sensing and modeling of the dynamics of the western part of the Black Sea p 26 A86-32679

C

CANADA

Microwave remote sensing of agricultural crops in Canada p 1 A86-30190
 A preliminary analysis of Landsat MSS and TM data in the Leveck area, Sudbury, Canada p 20 A86-33519
 SNR in SAR p 54 A86-33633
 Forestry information content of Thematic Mapper data p 8 A86-34741
 Practical photogrammetry from 35-mm aerial photography p 55 A86-36080
 Economical maintenance of a national topographic data base using Landsat images p 48 A86-36082
 Processing of multi-sensor remotely sensed data to a standard geocoded format p 50 A86-37019
 Integration of high and low resolution satellite data for crop condition assessment p 12 A86-37020
 Landsat MSS and airborne geophysical data combined for mapping granite in southwest Nova Scotia p 23 A86-37021
 The fundamentals of microwave remote sensing [SU-84] p 56 N86-23025

CHINA, PEOPLE'S REPUBLIC OF

A clustering algorithm for remote sensing multispectral data p 51 A86-37033
 Application of Shuttle imaging radar data for land use investigations p 51 A86-39150

D

DENMARK

Push-broom microwave radiometer systems for space applications p 53 A86-33589
 Statistical lineament analysis in South Greenland based on Landsat imagery p 22 A86-35676
 Microwave radiometry for oil pollution monitoring, measurements, and systems p 32 A86-35682

F

FINLAND

Remote sensing of snow water equivalent using Nimbus-7 SMMR data p 42 A86-33616
 Investigation of ice dynamics in the marginal ice zone [AD-A164364] p 38 N86-25962

FRANCE

SPOT - A high-precision view of the earth p 52 A86-31222
 The effective elastic lithosphere under the Cook-Austral and Society islands p 25 A86-32267
 Possible applications of the microwaves surface soil moisture remote sensing p 6 A86-33582
 A stable iterative procedure to obtain soil surface parameters and fluxes from satellite data p 8 A86-35678
 Evapotranspiration over an agricultural region using a surface flux/temperature model based on NOAA-AVHRR data p 10 A86-36237
 The ARGOS system for positioning and data collection by satellite - Characteristics and performance levels p 56 A86-39559

G

GERMANY, FEDERAL REPUBLIC OF

Problems with global mapping p 48 A86-35111
 Examples of the automated derivation of digital surface models p 48 A86-35292
 Forest signatures in imaging and non-imaging microwave scatterometer data p 9 A86-36037
 Detection of biomass by an empiric albedo and spectral reflectance model in the Sahara Desert from Landsat-imagery p 11 A86-37015

Rectification of scanner images using prediction approaches [SER-C-303] p 57 N86-23992
 Satellite-borne 90 GHz radiometer experiment (SABREX), phase A1 [DFVLR-MITT-85-13] p 57 N86-24000
 Archimedes project remote sensing of oil spills North Sea experiment, October 1983. Report on DFVLR (Side-Looking Airborne Radar (SLAR) contribution [DFVLR-FB-85-54] p 35 N86-24002
 MOMS-01 (Modular Optoelectronic Multispectral Scanner) for Earth observation: First results of STS-7 mission p 57 N86-24003
 On the information content of multispectral radiance measurements over an ocean [GKSS-85/E/43] p 40 N86-27697

I

INDIA

Remote sensing for developing countries - A case study of Tunisia p 15 A86-30195
 Automatic cloud classification p 46 A86-33534
 Wind dependence of L-band radar backscatter p 33 A86-35860

INTERNATIONAL ORGANIZATION

Landsat TM image forward/reverse scan banding Characterization and correction p 49 A86-36790

ITALY

Observation of internal waves and seismic waves in the Sicilian Channel p 27 A86-33392
 Lineament analysis in a test area of northern Mozambique p 20 A86-33520
 Slope-intercept-density plots - A new method for line detection in images p 46 A86-33600
 An integrated approach to geometric precision processing of spaceborne high-resolution sensors p 55 A86-34737
 Design of the European Space Agency Thematic Mapper processing chains p 51 A86-37864
 An atlas of original and mercator-transformed satellite-data images of the Alboran Sea, August-October 1983 [AD-A161898] p 36 N86-24170

J

JAPAN

Applicability of atmospheric correction algorithm for CZCS data to Japanese coastal area p 31 A86-33632
 Research and development of the synthetic aperture radar transmitter and receiver subsystem design and some component test results p 54 A86-33636
 High speed image processing system with custom VLSI for DSP p 54 A86-33641
 Terrain height measurement by synthetic aperture radar with an interferometer p 55 A86-34736
 Asian Conference on Remote Sensing, 5th, Kathmandu, Nepal, November 15-18, 1984, Proceedings p 55 A86-35425
 Satellite thermal observation of oil slicks on the Persian Gulf p 33 A86-36048
 Intraseasonal variations of OLR in the tropics during the FGGE year p 48 A86-36227
 Estimation of monthly rainfall from satellite-observed cloud amount in the tropical western Pacific p 43 A86-36234
 High accuracy clustering using residual image p 49 A86-37003
 Meteorological Satellite Center Technical Note, no. 13, 1986 [ISSN-0388-9653] p 40 N86-27694
 On land-sea contrast in the Earth radiation budget p 40 N86-27695

K

KOREA, (SOUTH)

A non-stationary contextual classifier with improved accuracy p 47 A86-33621

An improved hybrid classifier p 8 A86-34744

M

MEXICO

A measuring reference system to quantify the desertification process in a semiarid ecosystem based on Landsat MSS data p 16 A86-37011

N

NETHERLANDS

Semi-operational identification of agricultural crops from airborne SLAR-data p 12 A86-37025

Map digitization offers new possibilities [NLR-MP-84061-U] p 51 N86-23028

A multiindex multitemporal approach to map crops in the early growing season: An application to two Italian irrigation districts: East Sesia and Grande Bonifica Ferrarese [ICW-1611] p 15 N86-26674

S

SWEDEN

Satellite imaging of coastal flow circulation in relation to numerical modelling p 31 A86-33631

Direction dependent interpolation of aeromagnetic data p 23 A86-37009

SWITZERLAND

Large area snowmelt runoff simulations based on Landsat-MSS data p 42 A86-33505

A stepwise hierarchical multi-binary approach in TM landuse classification p 46 A86-33597

Resource monitoring oriented remote sensing data processing capabilities p 16 A86-33643

T

TURKEY

The study of the natural geographic differences in the coastal areas of water covered parts of Marmara region in Turkey with the help of Landsat-4 MSS data using an unsupervised classification algorithm with Euclidean distance p 43 A86-37012

U

U.S.S.R.

Agricultural and scientific space platforms p 1 A86-29843

Possibility of small-scale physiogeographical regionalization using space spectrometry data p 16 A86-30974

Integrated global monitoring of the world ocean. Volumes 1, 2, & 3 p 24 A86-31350

Near-surface water circulation in the sub-Arctic frontal zone (according to satellite data) p 25 A86-32676

Some features of small-scale ocean eddies according to an analysis of satellite images p 25 A86-32677

Saljut-6 observation of color and brightness contrasts correlated with ocean-bottom relief p 26 A86-32678

Features of the geological application of space data p 19 A86-32680

Interpretation of ring structures on space images and their correlation with geophysical fields and crustal structure in the USSR p 19 A86-32681

Application of space imagery to the identification and geological-geophysical study of hidden plutons in early Proterozoic troughs p 20 A86-32682

Determination of sea spectral reflectance from airborne measurements p 26 A86-32683

Determination of the moisture content of nonuniformly moistened soils with a surface transition layer on the basis of microwave spectroradiometry p 2 A86-32684

A histogram as the basis of the statistical classification of images p 45 A86-32688

Formation of a digital data base for automated forest mapping p 2 A86-32689

Computer-aided interpretation of space images with the aim of structural analysis p 20 A86-32690

Structural features of the easterly jet stream according to satellite data p 26 A86-33315

An algorithm for the identification of cloud cover and the estimation of spectral brightnesses of the cloudless atmosphere according to satellite scanning measurements of outgoing IR radiation p 52 A86-33317

Experiments on the remote temperature sounding of the atmosphere on the basis of NOAA-satellite radiometer measurements p 52 A86-33318

Estimation of the accuracy of the remote determination of ocean surface temperature on the basis of satellite measurements of outgoing thermal radiation in the 10.5-12.5 micron range p 27 A86-33320

Optimal disposition of satellite-tracked drifting buoys in the South Atlantic p 31 A86-34488

Investigation of the content of trace elements in sea aerosols and the surface microlayer off sea water p 32 A86-34754

Probabilistic modeling of fields of atmospheric turbulence and sea roughness with reference to the study of complex systems p 33 A86-36480

Methods of combined air and space remote-sensing studies of Siberia p 22 A86-36501

Problems and principles of the geological interpretation of remote-sensing data p 22 A86-36502

Combined structural and geomorphological methods for the processing of aerial and space photographic remote-sensing data with the aim of solving geological problems p 22 A86-36503

Investigation of the earth from space - A new contribution to the development of structural geomorphology p 22 A86-36504

Method for the quantitative estimation of convergence in mapping in the case of the interpretation of space photographs of oil-and-gas-bearing regions of Siberia p 23 A86-36505

Quantitative assessment of the information content of TV images of different scale on the example of disjunctives of Siberia p 23 A86-36506

Methods for the remote sensing of transition zones of the junction of Siberian platforms and orogens p 23 A86-36507

The use of remote-sensing data to predict regional and local oil-and-gas-bearing structures within the Dneprovsk-Donetsk paleorift p 23 A86-36508

Combination of air and space remote-sensing methods and geological-geophysical methods for the purpose of oil and gas exploration in the southern Permsk region p 23 A86-36509

Aspects of the geological interpretation of geophysical fields and results of air and space remote-sensing observations of oil-and-gas-bearing territories p 23 A86-36510

Technical and software facilities at a center for the processing of remote-sensing data p 48 A86-36511

The possibility of applying different types of image-analysis software to environment-protection problems p 16 A86-36513

Choice of spectral bands for a spaceborne multispectral scanner p 55 A86-36514

Statistical approach to the classification of objects on air and space remote-sensing images p 48 A86-36515

Certain transformations in a quantitative approach to image processing p 48 A86-36517

Computer processing of spectrally superposed data p 49 A86-36518

Determination of the spectral characteristics of natural objects on test ranges, and aspects of the efficiency of space systems p 11 A86-36697

Environment and climate p 16 A86-38677

The effect of the atmosphere on the satellite remote sensing of earth resources p 56 A86-39969

USSR report: Earth sciences [JPRS-UES-86-004] p 34 N86-23017

Ice shelves of Antarctica [PB86-106986] p 35 N86-23208

Problems of the Arctic and the Antarctic, Collection of Articles, Volume 56, 1981 [PB86-107109] p 35 N86-23209

Problems of the Arctic and the Antarctic, collection of articles, vol. 57, 1981 [PB86-106994] p 37 N86-24182

UNITED ARAB REPUBLIC

Application of spaceborne and airborne techniques in mineral exploration at Wadi El Allaqi area, Eastern Desert, Egypt p 23 A86-37865

UNITED KINGDOM

Use of Seasat SAR imagery for geological mapping in a volcanic terrain - Askja Caldera, Iceland p 19 A86-30189

Monotemporal, multitemporal, and multivariate thermal infrared data acquisition from satellites for soil and surface-material survey p 1 A86-30191

Vegetation index and possibility of complementary parameters from AVHRR/2 p 2 A86-30197

The design, construction and early trials of a novel airborne surveillance radar p 25 A86-32635

Millimeter-wave backscatter from snowcover p 42 A86-33615

SAR image segmentation using digitised field boundaries for crop mapping and monitoring applications p 7 A86-33625

The estimation of atmospheric effects for SPOT using AVHRR channel-1 data p 47 A86-34738

The applicability of LOWTRAN 5 computer code to aerial thermographic data correction p 48 A86-34739

Estimation of sea-surface temperature from AVHRR data Comments on the paper by Singh et al. (1985) p 31 A86-34743

Relative vertical positioning using ground-level transponders with the ERS-1 altimeter p 33 A86-35688

Small format, oblique, colour aerial photography - An aid to the location of methane seepage p 11 A86-36783

Estimation of atmospheric corrections from multiple aircraft imagery p 49 A86-36784

Satellite remote sensing of atmospheric optical depth spectrum p 55 A86-36785

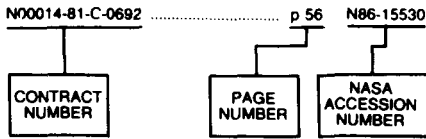
Position fixing afloat p 33 A86-36788

Applications of sensor payloads p 56 A86-37343

ERS-1 - Our new window on the oceans for the 1990s p 34 A86-38718

CONTRACT NUMBER INDEX

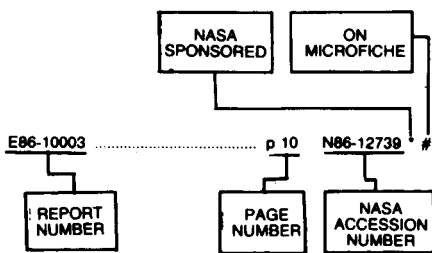
Typical Contract Number Index Listing



Listings in this index are arranged alphabetically by contract number. Under each contract number, the accession numbers denoting documents that have been produced as a result of research done under that contract are arranged in ascending order with the AIAA accession numbers appearing first. The accession number denotes the number by which the citation is identified in the abstract section. Preceding the accession number is the page number on which the citation may be found.

N00014-81-C-0692	p 56	N86-15530	NAS7-100	p 4	A86-33541
			NAS7-918	p 18	A86-37024
				p 14	N86-25034
			NAS8-34749	p 56	N86-23159
			NAS9-15421	p 10	A86-36045
			NAS9-15509	p 4	A86-33541
			NAS9-15800	p 6	A86-33606
			NAS9-16528	p 9	A86-35748
				p 13	A86-39002
			NA80RA-H-00002	p 38	N86-25104
			NA84AA-D-00046	p 40	N86-26791
			NCA2-IR-865-401	p 11	A86-37016
			NGL-17-004-024	p 17	N86-26669
			NOAA PROJECT 144-U824	p 43	A86-39004
			NOAA-NA-79SA00741	p 28	A86-33488
			NOAA-NA-80AAD00007	p 28	A86-33488
			NOAA-NA-84AAD00065	p 43	A86-39004
			NR PROJECT 083-165	p 32	A86-35545
			NR PROJECT 083-400	p 32	A86-35545
			NSF ATM-80-25329	p 36	N86-24120
				p 36	N86-24142
			NSF ATM-82-05817	p 26	A86-33120
			NSF DPP-82-07098	p 58	N86-25076
			NSF EAR-70-25371	p 18	A86-37795
			NSF ECS-82-13418	p 45	A86-33522
			NSF ECS-82-17191	p 9	A86-35687
			NSF ECS-84-00324	p 16	A86-33595
				p 50	A86-37022
			NSF IST-84-07860	p 9	A86-35687
			NSF OCE-82-02454	p 25	A86-31976
			NSF OCE-82-08927	p 25	A86-31976
			NSF OCE-82-14791	p 26	A86-33120
			NSG-5049	p 28	A86-33529
			NSG-5134	p 8	A86-35679
			NSG-5423	p 15	N86-27698
			N00014-76-C-0197	p 32	A86-35545
			N00014-78-C-0566	p 28	A86-33488
			N00014-80-C-0098	p 25	A86-31976
			N00014-81-C-0062	p 32	A86-35545
			N00014-81-C-0295	p 29	A86-33561
				p 42	A86-33613
			N00014-81-C-0692	p 30	A86-33611
				p 54	A86-33634
				p 31	A86-33646
				p 31	A86-33647
			N00014-83-C-0150	p 38	N86-26517
			N00014-83-C-0404	p 29	A86-33561
			N00014-84-C-0132	p 25	A86-31976
				p 37	N86-24180
				p 37	N86-24181
			N00014-85-C-0531	p 39	N86-26788
				p 40	N86-26789
			N00024-83-C-5301	p 31	A86-33647
			SBSA-56-84	p 23	A86-37009
			SBSA-63-83	p 23	A86-37009
			STU-83-4119	p 23	A86-37009
			USDA-53-9158-0-6362	p 4	A86-33541
			USDA-58-319T-3-0208X	p 2	A86-30198
			USGS-14-08-0001-20585	p 18	A86-37797
			W-7405-ENG-48	p 58	N86-25925
			644-11-00	p 14	N86-25034
			672-22-04-70	p 57	N86-23160
DAJA45-83-C-0034	p 38	N86-25962			
DE-AC04-76DP-00053	p 34	N86-15969			
DE-AC04-76DP-00789	p 43	N86-23027			
DE-AC08-83NV-10282	p 17	N86-25036			
DOC-MO-A01-78-004332	p 8	A86-35679			
ESA-5443/83/D/IM(SC)	p 50	A86-37026			
ESTEC-5538/83	p 35	N86-23207			
F19628-82-K-0022	p 33	A86-36096			
	p 19	N86-26745			
F19628-83-C-0027	p 53	A86-33547			
F19628-84-C-0134	p 53	A86-33547			
F19628-84-K-0018	p 45	A86-33526			
JPL-954946	p 22	A86-36083			
JPL-956427	p 13	A86-39003			
JPL-956515	p 13	A86-39003			
JPL-956925	p 21	A86-33550			
MOD-2205/24S	p 47	A86-34738			
NAGW-273	p 28	A86-33488			
NAGW-374	p 14	N86-23994			
NAGW-678	p 39	N86-26670			
NAGW-679	p 32	A86-35550			
NAG5-184	p 15	N86-27704			
NAG5-196	p 58	N86-27705			
NAG5-269	p 9	A86-35748			
NAG5-271	p 13	A86-39149			
NAG5-332	p 39	N86-26758			
	p 41	N86-27837			
	p 41	N86-27838			
	p 41	N86-27853			
NAG5-459	p 18	N86-26741			
	p 19	N86-27833			
	p 10	A86-36046			
NAG5-486	p 10	A86-36045			
NAG5-68	p 10	A86-36045			
NASA ORDER W-15084	p 27	A86-33485			
NASW-3389	p 18	A86-37795			
NASW-4048	p 21	A86-33521			
NAS1-67457	p 10	A86-36047			
NAS2-11101	p 7	A86-33644			
NAS5-22948	p 28	A86-33488			
NAS5-22963	p 28	A86-33488			
NAS5-25300	p 47	A86-33640			
NAS5-26247	p 28	A86-33488			
NAS5-27232	p 18	A86-37797			
NAS5-27339	p 18	A86-37797			
NAS5-28648	p 14	N86-23995			
NAS5-28741	p 44	N86-26665			
NAS5-28757	p 24	N86-26740			
NAS5-28759	p 24	N86-25866			
NAS5-28765	p 24	N86-25912			
NAS5-28769	p 39	N86-26783			
NAS6-2520	p 38	N86-25100			

Typical Report Number Index Listing



Listings in this index are arranged alpha-numerically by report number. The page number indicates the page on which the citation is located. The accession number denotes the number by which the citation is identified. An asterisk (*) indicates that the item is a NASA report. A pound sign (#) indicates that the item is available on microfiche.

ESA-86-96898	p 40	N86-27697	#	NASA-CR-176805	p 24	N86-25912	* #
ESA-86-96955	p 15	N86-26674	#	NASA-CR-176807	p 24	N86-25866	* #
GKSS-85/E/43	p 40	N86-27697	#	NASA-CR-177205	p 58	N86-27705	* #
HIG-84-3	p 38	N86-25104	#	NASA-CR-177214	p 14	N86-25034	* #
ICW-1611	p 15	N86-26674	#	NASA-CR-177226	p 15	N86-27704	* #
INPE-3793-PRE/888	p 36	N86-24166	#	NASA-CR-177249	p 41	N86-27838	* #
INPE-3795-PRE/890	p 36	N86-24168	#	NASA-CR-177265	p 39	N86-26670	* #
INPE-3824-PRE/900	p 15	N86-26667	#	NASA-CR-177283	p 41	N86-27837	* #
INPE-3828-NTE/255	p 15	N86-26666	#	NASA-CR-177287	p 39	N86-26758	* #
IR-6	p 38	N86-25962	#	NASA-CR-177290	p 41	N86-27853	* #
ISBN-3-7696-9353-1	p 57	N86-23992	#	NASA-CR-177294	p 17	N86-26669	* #
ISSN-0065-5325	p 57	N86-23992	#	NASA-CR-177299	p 18	N86-26741	* #
ISSN-0171-1342	p 35	N86-24002	#	NASA-CR-177300	p 15	N86-27698	* #
ISSN-0176-7739	p 57	N86-24000	#	NASA-CR-177310	p 39	N86-26783	* #
ISSN-0344-9629	p 40	N86-27697	#	NASA-CR-177311	p 24	N86-26740	* #
ISSN-0388-9653	p 40	N86-27694	#	NASA-CR-177313	p 19	N86-27833	* #
ISSN-0710-0868	p 56	N86-23025	#	NASA-CR-177315	p 44	N86-26665	* #
JHU/APL/SDO-7565	p 35	N86-23207	#	NASA-CR-177854	p 14	N86-23995	* #
JIMAR-84-0085	p 38	N86-25104	#	NASA-CR-3960	p 56	N86-23159	* #
JPL-PUBL-86-5	p 14	N86-25034	* #	NASA-TM-87773	p 39	N86-26782	* #
JPRS-UES-86-004	p 34	N86-23017	#	NASA-TM-88752	p 59	N86-26355	* #
KGRD-15-REV	p 51	N86-25919	#	NASA-TM-88754	p 14	N86-25863	* #
L-16041	p 57	N86-23160	* #	NASA-TM-88755	p 14	N86-25032	* #
LC-84-601115	p 24	N86-25099	#	NASA-TM-88765	p 41	N86-27700	* #
LDGO-85-7	p 37	N86-24180	#	NASA-TM-88782	p 41	N86-27699	* #
LDGO-85-8	p 37	N86-24181	#	NASA-TP-2540	p 57	N86-23160	* #
MITSG-85-21	p 40	N86-26791	#	NESDIS-ENVIRON-INVENT-3	p 35	N86-23211	#
MLM-3277	p 34	N86-15969	#	NLR-MP-84061-U	p 51	N86-23028	#
MR-6	p 24	N86-25866	* #	NOAA-DR-ERL-PMEL-12	p 35	N86-24112	#
NAS 1.15:87773	p 39	N86-26782	* #	NOAA-NESDIS-24	p 44	N86-27703	#
NAS 1.15:88752	p 59	N86-26355	* #	NOAA-TM-ERL-AOML-61	p 35	N86-23213	#
NAS 1.15:88754	p 14	N86-25863	* #	NOAA-TM-ERL-PMEL-64	p 38	N86-25939	#
NAS 1.15:88755	p 14	N86-25032	* #	NOAA-TM-NESDIS-13	p 44	N86-26668	#
NAS 1.15:88765	p 41	N86-27700	* #	NORDA-TN-315	p 37	N86-24173	#
NAS 1.15:88782	p 41	N86-27699	* #	NORDA-103	p 37	N86-24172	#
NAS 1.26:168439	p 38	N86-25100	* #	NPS63-85-003	p 58	N86-25084	#
NAS 1.26:176720	p 36	N86-24120	* #	NPS68-85-026	p 37	N86-24176	#
NAS 1.26:176722	p 36	N86-24142	* #	OPPORTUNITY-BRIEF-41	p 40	N86-26791	#
NAS 1.26:176725	p 14	N86-23994	* #	PB86-106986	p 35	N86-23208	#
NAS 1.26:176805	p 24	N86-25912	* #	PB86-106994	p 37	N86-24182	#
NAS 1.26:176807	p 24	N86-25866	* #	PB86-107109	p 35	N86-23209	#
NAS 1.26:177205	p 58	N86-27705	* #	PB86-110038	p 35	N86-24112	#
NAS 1.26:177214	p 14	N86-25034	* #	PB86-110060	p 35	N86-23211	#
NAS 1.26:177226	p 15	N86-27704	* #	PB86-111622	p 35	N86-23213	#
NAS 1.26:177249	p 41	N86-27838	* #	PB86-119948	p 24	N86-23030	#
NAS 1.26:177265	p 39	N86-26670	* #	PB86-139177	p 36	N86-24142	* #
NAS 1.26:177283	p 41	N86-27837	* #	PB86-139524	p 38	N86-25106	#
NAS 1.26:177287	p 39	N86-26758	* #	PB86-143773	p 58	N86-25076	#
NAS 1.26:177290	p 41	N86-27853	* #	PB86-148038	p 38	N86-25939	#
NAS 1.26:177294	p 17	N86-26669	* #	PB86-156254	p 51	N86-25919	#
NAS 1.26:177299	p 18	N86-26741	* #	PB86-156502	p 40	N86-26791	#
NAS 1.26:177300	p 15	N86-27698	* #	PB86-166097	p 17	N86-26675	#
NAS 1.26:177310	p 39	N86-26783	* #	PMT-C-TP-000037	p 38	N86-26313	#
NAS 1.26:177311	p 24	N86-26740	* #	REPT-86B0195	p 39	N86-26782	* #
NAS 1.26:177313	p 19	N86-27833	* #	SACLANTCEN-SR-89	p 36	N86-24170	#
NAS 1.26:177315	p 44	N86-26665	* #	SAIC-1-425-07-356-10-PT-3-SE	p 39	N86-26788	#
NAS 1.26:177854	p 14	N86-23995	* #	SAIC-1-425-07-356-10-PT-3-2	p 40	N86-26789	#
NAS 1.26:3960	p 56	N86-23159	* #	SAIC-85/1950-PT-3-SEC-3	p 40	N86-26789	#
NAS 1.60:2540	p 57	N86-23160	* #	SAIC-85/1950-PT-3	p 39	N86-26788	#
NASA-CR-168349	p 38	N86-25100	* #	SAND-85-1978C	p 43	N86-23027	#
NASA-CR-176720	p 36	N86-24120	* #	SER-C-303	p 57	N86-23992	#
NASA-CR-176722	p 36	N86-24142	* #	SU-84	p 56	N86-23025	#
NASA-CR-176725	p 14	N86-23994	* #				
AD-A161898	p 36	N86-24170	#				
AD-A161995	p 37	N86-24172	#				
AD-A162019	p 37	N86-24173	#				
AD-A162022	p 17	N86-24034	#				
AD-A162067	p 37	N86-24176	#				
AD-A162578	p 34	N86-23203	#				
AD-A163061	p 38	N86-25104	#				
AD-A163096	p 37	N86-24180	#				
AD-A163097	p 37	N86-24181	#				
AD-A163364	p 38	N86-26313	#				
AD-A163821	p 58	N86-25084	#				
AD-A164364	p 38	N86-25962	#				
AD-A164564	p 19	N86-26745	#				
AD-A164679	p 39	N86-26716	#				
AD-A165071	p 59	N86-27410	#				
AD-A165080	p 59	N86-27411	#				
AD-A165081	p 59	N86-27412	#				
AD-A165118	p 59	N86-27413	#				
AD-A165142	p 60	N86-28016	#				
AD-A165143	p 59	N86-28007	#				
AD-A165244	p 40	N86-27414	#				
AD-A165304	p 39	N86-26788	#				
AD-A165305	p 40	N86-26789	#				
AD-A165552	p 38	N86-26517	#				
AD-E301922	p 39	N86-26788	#				
AD-E301922	p 40	N86-26789	#				
AFGL-TR-85-0278	p 19	N86-26745	#				
ASCOT-85-2	p 58	N86-25925	#				
B8571449	p 51	N86-23028	#				
CONF-8503189-1	p 43	N86-23027	#				
CONF-8510222-1	p 17	N86-25036	#				
CRREL-85-14	p 17	N86-24034	#				
DE85-016050	p 34	N86-15969	#				
DE86-002101	p 17	N86-25036	#				
DE86-002590	p 43	N86-23027	#				
DE86-002993	p 58	N86-25925	#				
DFVLR-FB-85-54	p 35	N86-24002	#				
DFVLR-MITT-85-13	p 57	N86-24000	#				
EGG-10282-1096	p 17	N86-25036	#				
ERL-237	p 14	N86-25863	* #				
ERL-238	p 14	N86-25032	#				
ESA-CR(P)-2097	p 35	N86-23207	#				

SU-85

REPORT NUMBER INDEX

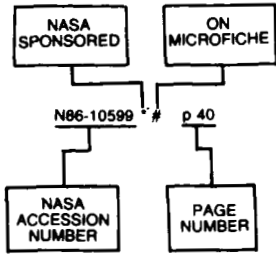
SU-85	p 56	N86-23025	#
TI86-900108	p 24	N86-25099	#
TR-410	p 38	N86-26517	#
TT-75-52081	p 35	N86-23208	#
TT-82-00-102	p 35	N86-23209	#
TT-82-00-104	p 37	N86-24182	#
UCID-20519	p 58	N86-25925	#
USCG-D-28-85	p 39	N86-26716	#
USGS-BULL-1634	p 24	N86-25099	#
USGS-OFR-85-304	p 17	N86-26675	#

ACCESSION NUMBER INDEX

OCTOBER 1986

EARTH RESOURCES / A Continuing Bibliography (Issue 51)

Typical Accession Number Index Listing



Listings in this index are arranged alpha-numerically by accession number. The page number listed to the right indicates the page on which the citation is located. An asterisk (*) indicates that the item is a NASA report. A pound sign (#) indicates that the item is available on microfiche.

A86-29843 #	p 1	A86-33502 #	p 52	A86-36047 * #	p 10	A86-39006 #	p 13
A86-30189 #	p 19	A86-33503 * #	p 2	A86-36048 #	p 33	A86-39146 * #	p 13
A86-30190 #	p 1	A86-33504 * #	p 2	A86-36049 #	p 10	A86-39147 #	p 13
A86-30191 #	p 1	A86-33505 #	p 42	A86-36079 #	p 48	A86-39148 * #	p 13
A86-30192 #	p 1	A86-33506 * #	p 3	A86-36080 #	p 55	A86-39149 * #	p 13
A86-30193 * #	p 1	A86-33514 #	p 28	A86-36082 #	p 48	A86-39150 #	p 51
A86-30194 * #	p 2	A86-33515 #	p 45	A86-36083 * #	p 22	A86-39545 #	p 51
A86-30195 #	p 15	A86-33516 * #	p 18	A86-36084 #	p 10	A86-39559 #	p 56
A86-30196 #	p 2	A86-33517 #	p 20	A86-36096 #	p 33	A86-39969 #	p 56
A86-30197 #	p 2	A86-33518 #	p 20	A86-36099 * #	p 18		
A86-30198 #	p 2	A86-33519 #	p 20	A86-36193 * #	p 43		
A86-30974 #	p 16	A86-33520 #	p 20	A86-36227 #	p 48	N86-15969 #	p 34
A86-31222 #	p 52	A86-33521 * #	p 21	A86-36234 #	p 43	N86-23017 #	p 34
A86-31350 #	p 24	A86-33522 #	p 45	A86-36237 #	p 10	N86-23025 #	p 56
A86-31976 #	p 25	A86-33523 * #	p 3	A86-36480 #	p 33	N86-23027 #	p 43
A86-32267 #	p 25	A86-33524 #	p 3	A86-36501 #	p 22	N86-23028 #	p 51
A86-32333 #	p 44	A86-33525 * #	p 3	A86-36502 #	p 22	N86-23030 #	p 24
A86-32337 #	p 44	A86-33526 #	p 45	A86-36503 #	p 22	N86-23159 * #	p 56
A86-32368 #	p 45	A86-33529 * #	p 28	A86-36504 #	p 22	N86-23160 * #	p 57
A86-32370 #	p 45	A86-33532 * #	p 29	A86-36505 #	p 23	N86-23203 #	p 34
A86-32537 #	p 16	A86-33533 #	p 52	A86-36506 #	p 23	N86-23207 #	p 35
A86-32556 * #	p 25	A86-33534 #	p 46	A86-36507 #	p 23	N86-23208 #	p 35
A86-32599 #	p 25	A86-33535 #	p 46	A86-36508 #	p 23	N86-23209 #	p 35
A86-32635 #	p 25	A86-33538 #	p 3	A86-36509 #	p 23	N86-23211 #	p 35
A86-32676 #	p 25	A86-33539 #	p 3	A86-36510 #	p 23	N86-23213 #	p 35
A86-32677 #	p 25	A86-33540 * #	p 4	A86-36511 #	p 48	N86-23992 #	p 57
A86-32678 #	p 26	A86-33541 * #	p 4	A86-36513 #	p 16	N86-23993 #	p 43
A86-32679 #	p 26	A86-33542 * #	p 4	A86-36514 #	p 55	N86-23994 * #	p 14
A86-32680 #	p 19	A86-33545 * #	p 53	A86-36515 #	p 48	N86-23995 * #	p 14
A86-32681 #	p 19	A86-33547 #	p 53	A86-36517 #	p 48	N86-24000 #	p 57
A86-32682 #	p 20	A86-33550 * #	p 21	A86-36518 #	p 49	N86-24002 #	p 35
A86-32683 #	p 26	A86-33551 #	p 21	A86-36697 #	p 11	N86-24003 #	p 57
A86-32684 #	p 2	A86-33552 * #	p 21	A86-36783 #	p 11	N86-24034 #	p 17
A86-32688 #	p 45	A86-33554 * #	p 4	A86-36784 #	p 49	N86-24075 #	p 44
A86-32689 #	p 2	A86-33555 #	p 4	A86-36785 #	p 55	N86-24112 #	p 35
A86-32690 #	p 20	A86-33556 * #	p 4	A86-36788 #	p 33	N86-24112 * #	p 57
A86-33104 * #	p 26	A86-33557 #	p 4	A86-36789 * #	p 11	N86-24128 * #	p 57
A86-33105 * #	p 26	A86-33558 #	p 5	A86-36790 #	p 49	N86-24142 * #	p 36
A86-33120 #	p 26	A86-33560 * #	p 29	A86-36838 * #	p 55	N86-24160 * #	p 57
A86-33315 #	p 26	A86-33561 #	p 29	A86-36954 #	p 33	N86-24161 * #	p 36
A86-33317 #	p 52	A86-33562 * #	p 29	A86-37001 #	p 56	N86-24166 #	p 36
A86-33318 #	p 52	A86-33565 * #	p 5	A86-37002 #	p 58	N86-24168 #	p 36
A86-33320 #	p 27	A86-33566 * #	p 5	A86-37003 #	p 49	N86-24170 #	p 36
A86-33392 #	p 27	A86-33576 * #	p 5	A86-37006 #	p 49	N86-24172 #	p 37
A86-33481 #	p 27	A86-33577 * #	p 5	A86-37007 #	p 56	N86-24173 #	p 37
A86-33482 #	p 27	A86-33578 #	p 5	A86-37008 * #	p 11	N86-24176 #	p 37
A86-33483 #	p 27	A86-33579 #	p 6	A86-37009 #	p 23	N86-24180 #	p 37
A86-33484 #	p 27	A86-33582 #	p 6	A86-37010 #	p 43	N86-24181 #	p 37
A86-33485 * #	p 27	A86-33583 * #	p 2	A86-37011 #	p 16	N86-24182 #	p 37
A86-33486 * #	p 27	A86-33584 * #	p 53	A86-37012 #	p 43	N86-25032 #	p 14
A86-33487 #	p 28	A86-33586 #	p 53	A86-37013 #	p 34	N86-25034 * #	p 14
A86-33488 * #	p 28	A86-33588 * #	p 53	A86-37014 #	p 11	N86-25036 #	p 17
A86-33489 * #	p 28	A86-33589 * #	p 53	A86-37015 #	p 11	N86-25076 #	p 58
A86-33490 #	p 28	A86-33590 * #	p 54	A86-37016 * #	p 11	N86-25084 #	p 58
A86-33501 * #	p 52	A86-33591 * #	p 29	A86-37017 #	p 49	N86-25099 #	p 24
				A86-37018 * #	p 12	N86-25100 * #	p 38
				A86-37019 #	p 50	N86-25104 #	p 38
				A86-37020 #	p 12	N86-25106 #	p 38
				A86-37021 #	p 23	N86-25863 * #	p 14
				A86-37022 #	p 50	N86-25866 * #	p 24
				A86-37024 * #	p 18	N86-25912 * #	p 24
				A86-37025 #	p 12	N86-25919 #	p 51
				A86-37026 #	p 50	N86-25925 #	p 58
				A86-37027 * #	p 50	N86-25939 #	p 38
				A86-37028 * #	p 50	N86-25962 #	p 38
				A86-37032 * #	p 50	N86-26313 #	p 38
				A86-37033 #	p 51	N86-26355 * #	p 59
				A86-37034 * #	p 12	N86-26517 #	p 38
				A86-37035 #	p 12	N86-26665 * #	p 44
				A86-37036 #	p 12	N86-26666 #	p 15
				A86-37343 #	p 56	N86-26667 #	p 15
				A86-37506 #	p 34	N86-26668 #	p 44
				A86-37795 * #	p 18	N86-26669 * #	p 17
				A86-37797 * #	p 18	N86-26670 * #	p 39
				A86-37864 #	p 51	N86-26675 #	p 17
				A86-37865 #	p 23	N86-26716 #	p 39
				A86-38648 #	p 34	N86-26740 * #	p 24
				A86-38677 #	p 16	N86-26741 * #	p 18
				A86-38718 #	p 34	N86-26745 #	p 19
				A86-39002 * #	p 13	N86-26758 * #	p 39
				A86-39003 * #	p 13	N86-26782 * #	p 39
				A86-39004 #	p 43	N86-26783 * #	p 39
						N86-26788 #	p 39

ACCESSION

N86-26789

N86-26789 # p 40
N86-26791 # p 40
N86-27410 # p 59
N86-27411 # p 59
N86-27412 # p 59
N86-27413 # p 59
N86-27414 # p 40
N86-27694 # p 40
N86-27695 # p 40
N86-27697 # p 40
N86-27698 * # p 15
N86-27699 * # p 41
N86-27700 * # p 41
N86-27703 # p 44
N86-27704 * # p 15
N86-27705 * # p 58
N86-27749 * # p 51
N86-27788 * # p 17
N86-27833 * # p 19
N86-27837 * # p 41
N86-27838 * # p 41
N86-27853 # p 41
N86-28007 # p 59
N86-28016 # p 60

AVAILABILITY OF CITED PUBLICATIONS

IAA ENTRIES (A86-10000 Series)

Publications announced in *IAA* are available from the AIAA Technical Information Service as follows: Paper copies of accessions are available at \$10.00 per document (up to 50 pages), additional pages \$0.25 each. Microfiche⁽¹⁾ of documents announced in *IAA* are available at the rate of \$4.00 per microfiche on demand. Standing order microfiche are available at the rate of \$1.45 per microfiche for *IAA* source documents and \$1.75 per microfiche for AIAA meeting papers.

Minimum air-mail postage to foreign countries is \$2.50. All foreign orders are shipped on payment of pro-forma invoices.

All inquiries and requests should be addressed to: Technical Information Service, American Institute of Aeronautics and Astronautics, 555 West 57th Street, New York, NY 10019. Please refer to the accession number when requesting publications.

STAR ENTRIES (N86-10000 Series)

One or more sources from which a document announced in *STAR* is available to the public is ordinarily given on the last line of the citation. The most commonly indicated sources and their acronyms or abbreviations are listed below. If the publication is available from a source other than those listed, the publisher and his address will be displayed on the availability line or in combination with the corporate source line.

Avail: NTIS. Sold by the National Technical Information Service. Prices for hard copy (HC) and microfiche (MF) are indicated by a price code preceded by the letters HC or MF in the *STAR* citation. Current values for the price codes are given in the tables on NTIS PRICE SCHEDULES.

Documents on microfiche are designated by a pound sign (#) following the accession number. The pound sign is used without regard to the source or quality of the microfiche.

Initially distributed microfiche under the NTIS SRIM (Selected Research in Microfiche) is available at greatly reduced unit prices. For this service and for information concerning subscription to NASA printed reports, consult the NTIS Subscription Section, Springfield, Va. 22161.

NOTE ON ORDERING DOCUMENTS: When ordering NASA publications (those followed by the * symbol), use the N accession number. NASA patent applications (only the specifications are offered) should be ordered by the US-Patent-Appl-SN number. Non-NASA publications (no asterisk) should be ordered by the AD, PB, or other *report* number shown on the last line of the citation, not by the N accession number. It is also advisable to cite the title and other bibliographic identification.

Avail: SOD (or GPO). Sold by the Superintendent of Documents, U.S. Government Printing Office, in hard copy. The current price and order number are given following the availability line. (NTIS will fill microfiche requests, as indicated above, for those documents identified by a # symbol.)

Avail: NASA Public Document Rooms. Documents so indicated may be examined at or purchased from the National Aeronautics and Space Administration, Public Document Room (Room 126), 600 Independence Ave., S.W., Washington, D.C. 20546, or public document rooms located at each of the NASA research centers, the NASA Space Technology Laboratories, and the NASA Pasadena Office at the Jet Propulsion Laboratory.

(1) A microfiche is a transparent sheet of film, 105 by 148 mm in size containing as many as 60 to 98 pages of information reduced to micro images (not to exceed 26.1 reduction).

- Avail: DOE Depository Libraries. Organizations in U.S. cities and abroad that maintain collections of Department of Energy reports, usually in microfiche form, are listed in *Energy Research Abstracts*. Services available from the DOE and its depositories are described in a booklet, *DOE Technical Information Center - Its Functions and Services* (TID-4660), which may be obtained without charge from the DOE Technical Information Center.
- Avail: Univ. Microfilms. Documents so indicated are dissertations selected from *Dissertation Abstracts* and are sold by University Microfilms as xerographic copy (HC) and microfilm. All requests should cite the author and the Order Number as they appear in the citation.
- Avail: USGS. Originals of many reports from the U.S. Geological Survey, which may contain color illustrations, or otherwise may not have the quality of illustrations preserved in the microfiche or facsimile reproduction, may be examined by the public at the libraries of the USGS field offices whose addresses are listed in this introduction. The libraries may be queried concerning the availability of specific documents and the possible utilization of local copying services, such as color reproduction.
- Avail: HMSO. Publications of Her Majesty's Stationery Office are sold in the U.S. by Pendragon House, Inc. (PHI), Redwood City, California. The U.S. price (including a service and mailing charge) is given, or a conversion table may be obtained from PHI.
- Avail: BLL (formerly NLL): British Library Lending Division, Boston Spa, Wetherby, Yorkshire, England. Photocopies available from this organization at the price shown. (If none is given, inquiry should be addressed to the BLL.)
- Avail: Fachinformationszentrum, Karlsruhe. Sold by the Fachinformationszentrum Energie, Physik, Mathematik GMBH, Eggenstein Leopoldshafen, Federal Republic of Germany, at the price shown in deutschmarks (DM).
- Avail: Issuing Activity, or Corporate Author, or no indication of availability. Inquiries as to the availability of these documents should be addressed to the organization shown in the citation as the corporate author of the document.
- Avail: U.S. Patent and Trademark Office. Sold by Commissioner of Patents and Trademarks, U.S. Patent and Trademark Office, at the standard price of 1.50 each, postage free.
- Avail: ESDU. Pricing information on specific data, computer programs, and details on ESDU topic categories can be obtained from ESDU International Ltd. Requesters in North America should use the Virginia address while all other requesters should use the London address.
- Other availabilities: If the publication is available from a source other than the above, the publisher and his address will be displayed entirely on the availability line or in combination with the corporate author line.

PUBLIC COLLECTIONS OF NASA DOCUMENTS

DOMESTIC: NASA and NASA-sponsored documents and a large number of aerospace publications are available to the public for reference purposes at the library maintained by the American Institute of Aeronautics and Astronautics, Technical Information Service, 555 West 57th Street, 12th Floor, New York, New York 10019.

EUROPEAN: An extensive collection of NASA and NASA-sponsored publications is maintained by the British Library Lending Division, Boston Spa, Wetherby, Yorkshire, England for public access. The British Library Lending Division also has available many of the non-NASA publications cited in *STAR*. European requesters may purchase facsimile copy or microfiche of NASA and NASA-sponsored documents, those identified by both the symbols # and * from ESA — Information Retrieval Service European Space Agency, 8-10 rue Mario-Nikis, 75738 CEDEX 15, France.

FEDERAL DEPOSITORY LIBRARY PROGRAM

In order to provide the general public with greater access to U.S. Government publications, Congress established the Federal Depository Library Program under the Government Printing Office (GPO), with 50 regional depositories responsible for permanent retention of material, inter-library loan, and reference services. At least one copy of nearly every NASA and NASA-sponsored publication, either in printed or microfiche format, is received and retained by the 50 regional depositories. A list of the regional GPO libraries, arranged alphabetically by state, appears on the inside back cover. These libraries are *not* sales outlets. A local library can contact a Regional Depository to help locate specific reports, or direct contact may be made by an individual.

STANDING ORDER SUBSCRIPTIONS

NASA SP-7041 and its supplements are available from the National Technical Information Service (NTIS) on standing order subscription as PB 86-903800 at the price of \$14.50 domestic and \$29.00 foreign. Standing order subscriptions do not terminate at the end of a year, as do regular subscriptions, but continue indefinitely unless specifically terminated by the subscriber.

ADDRESSES OF ORGANIZATIONS

American Institute of Aeronautics and
Astronautics
Technical Information Service
555 West 57th Street, 12th Floor
New York, New York 10019

British Library Lending Division,
Boston Spa, Wetherby, Yorkshire,
England

Commissioner of Patents and
Trademarks
U.S. Patent and Trademark Office
Washington, D.C. 20231

Department of Energy
Technical Information Center
P.O. Box 62
Oak Ridge, Tennessee 37830

ESA-Information Retrieval Service
ESRIN
Via Galileo Galilei
00044 Frascati (Rome) Italy

ESDU International, Ltd.
1495 Chain Bridge Road
McLean, Virginia 22101

ESDU International, Ltd.
251-259 Regent Street
London, W1R 7AD, England

Fachinformationszentrum Energie, Physik,
Mathematik GMBH
7514 Eggenstein Leopoldshafen
Federal Republic of Germany

Her Majesty's Stationery Office
P.O. Box 569, S.E. 1
London, England

NASA Scientific and Technical Information
Facility
P.O. Box 8757
B.W.I. Airport, Maryland 21240

National Aeronautics and Space
Administration
Scientific and Technical Information
Branch (NTT-1)
Washington, D.C. 20546

National Technical Information Service
5285 Port Royal Road
Springfield, Virginia 22161

Pendragon House, Inc.
899 Broadway Avenue
Redwood City, California 94063

Superintendent of Documents
U.S. Government Printing Office
Washington, D.C. 20402

University Microfilms
A Xerox Company
300 North Zeeb Road
Ann Arbor, Michigan 48106

University Microfilms, Ltd.
Tylers Green
London, England

U.S. Geological Survey Library
National Center – MS 950
12201 Sunrise Valley Drive
Reston, Virginia 22092

U.S. Geological Survey Library
2255 North Gemini Drive
Flagstaff, Arizona 86001

U.S. Geological Survey
345 Middlefield Road
Menlo Park, California 94025

U.S. Geological Survey Library
Box 25046
Denver Federal Center, MS 914
Denver, Colorado 80225

1. Report No. NASA SP-7041 (51)	2. Government Accession No.	3. Recipient's Catalog No.	
4. Title and Subtitle EARTH RESOURCES A Continuing Bibliography (Issue 51)		5. Report Date October 1986	6. Performing Organization Code
		8. Performing Organization Report No.	
7. Author(s)		10. Work Unit No.	
9. Performing Organization Name and Address National Aeronautics and Space Administration Washington, D.C. 20546		11. Contract or Grant No.	
		13. Type of Report and Period Covered	
12. Sponsoring Agency Name and Address		14. Sponsoring Agency Code	
		15. Supplementary Notes	
16. Abstract This bibliography lists 382 reports, articles and other documents introduced into the NASA scientific and technical information system between July 1 and September 30, 1986. Emphasis is placed on the use of remote sensing and geophysical instrumentation in spacecraft and aircraft to survey and inventory natural resources and urban areas. Subject matter is grouped according to agriculture and forestry, environmental changes and cultural resources, geodesy and cartography, geology and mineral resources, hydrology and water management, data processing and distribution systems, instrumentation and sensors, and economic analysis.			
17. Key Words (Suggested by Author(s)) Bibliographies Earth Resources Remote Sensors		18. Distribution Statement Unclassified - Unlimited	
19. Security Classif. (of this report) Unclassified	20. Security Classif. (of this page) Unclassified	21. No. of Pages 113	22. Price* A06/HC